NCRP REPORT No. 153

INFORMATION NEEDED TO MAKE RADIATION PROTECTION RECOMMENDATIONS FOR SPACE MISSIONS BEYOND LOW-EARTH ORBIT

NCRP

National Council on Radiation Protection and Measurements

NCRP REPORT No. 153

Information Needed to Make Radiation Protection Recommendations for Space Missions Beyond Low-Earth Orbit

Recommendations of the
NATIONAL COUNCIL ON RADIATION PROTECTION AND MEASUREMENTS

November 15, 2006

National Council on Radiation Protection and Measurements
7910 Woodmont Avenue, Suite 400 / Bethesda, MD 20814-3095

LEGAL NOTICE

This Report was prepared by the National Council on Radiation Protection and Measurements (NCRP). The Council strives to provide accurate, complete and useful information in its documents. However, neither NCRP, the members of NCRP, other persons contributing to or assisting in the preparation of this Report, nor any person acting on the behalf of any of these parties: (a) makes any warranty or representation, express or implied, with respect to the accuracy, completeness or usefulness of the information contained in this Report, or that the use of any information, method or process disclosed in this Report may not infringe on privately owned rights; or (b) assumes any liability with respect to the use of, or for damages resulting from the use of any information, method or process disclosed in this Report, *under the Civil Rights Act of 1964, Section 701 et seq. as amended 42 U.S.C. Section 2000e et seq. (Title VII) or any other statutory or common law theory governing liability.*

Disclaimer

Any mention of commercial products within NCRP publications is for information only; it does not imply recommendation or endorsement by NCRP.

Library of Congress Cataloging-in-Publication Data

National Council on Radiation Protection and Measurements.

Information needed to make radiation protection recommendations for space missions beyond low-Earth orbit.

p. cm. — (NCRP report ; no. 153)

Includes bibliographical references and index.

ISBN-13: 978-0-929600-90-1

ISBN-10: 0-929600-90-8

1. Space environment. 2. Astronauts—Protection. 3. Radiation—Safety measures—Research. 4. Radiation—Dosage—Measurement. 5. Space vehicles—Shielding (Radiation) I. National Council on Radiation Protection and Measurements.

TL1490.I54 2006

616.9'897--dc22

2006030291

[For detailed information on the availability of NCRP publications see page 407.]

Preface

This Report has been prepared at the request of the National Aeronautics and Space Administration (NASA). It is intended to provide guidance to NASA on information needed concerning exposure of NASA personnel to space radiations. The National Council on Radiation Protection and Measurements (NCRP) believes that this information should be obtained prior to future missions to the moon or deep space.

This endeavor is a continuation of NCRP Report No. 132, *Radiation Protection Guidance for Activities in Low-Earth Orbit*, that provided guidance to NASA on limitation of exposure to ionizing radiation in low-Earth orbit as encountered by NASA personnel on Space Transport Shuttle missions and the International Space Station. NCRP also provided recommendations on measurement of personnel radiation exposures and implementation of an operational radiation safety program for personnel in low-Earth orbit in Report No. 142, *Operational Radiation Safety Program for Astronauts in Low-Earth Orbit: A Basic Framework*.

This Report was drafted by NCRP Scientific Committee 1-7 on *Information Needed to Make Radiation Protection Recommendations for Travel Beyond Low-Earth Orbit*. Serving on Scientific Committee 1-7 were:

Lawrence W. Townsend, *Chairman*
University of Tennessee
Knoxville, Tennessee

Members

Gautam D. Badhwar*
Lyndon B. Johnson Space Center
National Aeronautics and Space Administration
Houston, Texas

Eleanor A. Blakely
Lawrence Berkeley National Laboratory
Berkeley, California

Leslie A. Braby
Texas A&M University
College Station, Texas

Francis A. Cucinotta
Lyndon B. Johnson Space Center
National Aeronautics and Space Administration
Houston, Texas

Stanley B. Curtis
Fred Hutchinson Cancer Research Center
Seattle, Washington

R.J. Michael Fry
Indiana University School of Medicine
Indianapolis, Indiana

Charles E. Land
National Cancer Institute
Bethesda, Maryland

Don F. Smart
Air Force Research Laboratory
Nashua, New Hampshire

NCRP Secretariat
William M. Beckner, *Consultant* (2004–2005)
Eric E. Kearsley, *Staff Scientist/Consultant* (1998–2001)
Cindy L. O'Brien, *Managing Editor*
David A. Schauer, *Executive Director*

The Council wishes to express its appreciation to the Committee members for the time and effort devoted to the preparation of this Report and to NASA for the financial support provided to enable NCRP to complete this effort.

NCRP and the members of Scientific Committee 1-7 wish to acknowledge the significant contributions of Dr. Gautam D. Badhwar, who died on August 28, 2001 in Houston, Texas. Dr. Badhwar was a major contributor to the galactic cosmic ray discussion in Section 3 of the Report. He was a Principal Investigator and Chief Scientist for Space Radiation at the NASA Johnson Space Center. Dr. Badhwar developed advanced instrumentation and made many measurements of the radiation environment to which astronauts are exposed in NASA missions and on the International Space Station. He also developed and tested new concepts and materials for shielding astronauts from space radiation. His many scientific accomplishments and his leadership at NASA are recognized with admiration by colleagues throughout the world, and his contributions to this NCRP Report are greatly appreciated.

Thomas S. Tenforde
President

*deceased

Contents

1. Executive Summary

The purpose of this Report is to identify and describe information needed to make radiation protection recommendations for space missions beyond low-Earth orbit (LEO). Current space radiation guidelines pertain only to missions in LEO and are not considered relevant for missions beyond LEO. Radiation protection in deep space is complicated because of the unique nature of the space radiation environment, which is unlike any radiation environment present on Earth or in LEO. The Executive Summary lists the major information that is needed. A summary of all needed information is included in Section 8.

1.1 Background

Astronauts on exploration missions of long duration beyond LEO face exposures to radiation levels that may easily exceed those routinely received by terrestrial radiation workers, or even those faced by crews in near-Earth spacecraft, such as the Space Transport Shuttle (STS) and International Space Station (ISS). Radiation fields encountered include the galactic cosmic radiation (GCR) background, sporadic solar-particle events (SPEs), energetic protons and electrons during traversals of the Van Allen radiation belts, and exposure to possible onboard radioactive sources used for power generation, propulsion, medical testing, and instrument calibration. Although it is true that crews on missions in LEO may be exposed to some extent to all of these radiation fields, they are not exposed to the full intensities of the GCR and SPE spectra because of the protection afforded by Earth's atmosphere and geomagnetic field, which tend to deflect protons and heavier ions at lower energies back into deep space thereby preventing them from reaching spacecraft in LEO. The degree of protection is a function of spacecraft orbital inclination and altitude. Orbits at higher inclinations, such as the 51.6 degree orbit of ISS are exposed to greater numbers of GCR particles because transmission through the magnetosphere is increased due to the reduced intensity and less favorable orientation of the magnetic field at these higher inclinations. However, significant shielding is provided by Earth's magnetic field and by shadow shielding from Earth itself. Hence, particle fluence rates from GCR and SPE sources are much lower in LEO than will be

encountered in missions beyond LEO, about a factor of three from ISS to deep space, where no protection from the magnetosphere or planetary bulk exists. Typically, astronauts and cosmonauts on ISS receive from 0.5 to 1.2 mSv d^{-1}, with ~75 % coming from GCR ions and 25 % coming from protons encountered in passages through the South Atlantic Anomaly region of the Van Allen belts. In deep space, radiation doses received by astronauts are expected to be higher (about a factor of two) than those measured in LEO. The main radiation sources of concern for missions beyond LEO are GCR and SPEs. Since spacecraft will be externally exposed to the full intensities of these sources, the radiation fields within the interior of the spacecraft are mitigated only by the shielding provided by the spacecraft structure. Properly describing how these radiation fields are altered by passage through the spacecraft structure is carried out using radiation transport codes, which model the atomic and nuclear interactions of these particles and describe the resulting composition and energy spectra of the radiation field constituents. Additional shielding is also provided by the body tissues overlying critical internal organs and must be accounted for as well. The biological effects of these unique radiation fields are not well known, nor are the associated radiation risks for late effects such as cancer induction. Unlike the situation for terrestrial exposures, the high costs of launching materials into space place limitations on spacecraft size and mass and preclude the purely engineering solution of providing as much additional shielding mass as is needed to reduce radiation exposures to some desired level. In addition, there are some model predictions which indicate that some types of shielding materials may give rise to secondary particle radiation fields that are more damaging than the unattenuated primary fields which produced them. Finally, in order to be effective in minimizing radiation exposure, the radiation protection program must include dosimetry instrumentation and data processing tools which can rapidly evaluate any realistic change in the exposure characteristics. This evaluation must include sufficient characterization of the radiation fields to allow determination of the radiation doses that would be received by astronauts, and to estimate the reduction in these doses that could be achieved by moving to areas of the spacecraft that provide different shielding.

The acceptable levels of risk for space exploration beyond LEO have not been defined at this time and need to be dealt with before sending manned missions to colonize the moon or to deep space such as a mission to Mars.

Other radiation health risks besides cancer are of concern for long-duration missions beyond LEO. Important questions related

to the addition of these risks and their possible impact on mortality and morbidity need to be addressed.

1.2 Space Radiation Environment

For exploratory missions beyond LEO, the main radiation-related concerns are chronic exposure to the ever-present GCR background, and acute exposure to sporadic SPEs. Both sources vary with the ~11 y solar cycle. The maximum intensity of the GCR spectrum occurs during the period of minimum solar activity. SPEs can occur at any time during the ~11 y long solar cycle, but are much more prevalent during periods of maximum solar activity, when the GCR intensity is reduced. The main concerns with GCR exposures to the human body are thought to be from late effects, such as the risk of cancer. In the case of SPEs, especially very large SPEs, the primary concern is the risk of acute effects. Most SPEs are relatively low in intensity and have spectra that are soft (*i.e.*, particle fluence rates decrease rapidly with increasing energy). Hence, they are of minor importance with regard to radiation protection since spacecraft structures can provide adequate shielding. Extremely-large SPEs, however, may occur several times (generally one to four times) during the solar cycle. In these events the fluence rates can be high and the spectra hard (*i.e.*, particle fluence rates decrease slowly with increasing energy). Increased shielding in the form of a storm shelter may be necessary to reduce radiation doses received by astronauts to acceptable levels from these events.

1.2.1 *Galactic Cosmic Radiation*

The assessment of radiation risk requires detailed knowledge of the composition and energy spectra of cosmic rays in interplanetary space, and their spatial and temporal variation. Current models are based on the standard diffusion-convection theory of solar modulation (Badhwar and O'Neill, 1992; Chen *et al.*, 1994a; Nymmik, 1996; 1997; Tylka *et al.*, 1997a); they are briefly discussed in Section 3. Typical uncertainties in the particle fluence rates predicted by the models are 15 %. Measurements of GCR fluence rates are ongoing using instrumented satellites outside of Earth's magnetosphere. Hence, refinements to the models are indicated as additional data become available.

1.2.2 *Solar-Particle Events*

For manned interplanetary missions there is concern that a large SPE could, in a short time period (hour or day), subject the spacecraft to substantially large numbers of protons with energies

above tens of megaelectron volts. Hence, doses from exposures to large SPEs could be large for crews and equipment that are not adequately protected. Large SPEs (~5×10^9 protons cm^{-2} at energies >30 MeV) occurred in November 1960, August 1972, and October 1989. Even larger events have occurred during the past 500 y (McCracken *et al*., 2001a). Estimates of absorbed doses from the largest of these events, the Carrington event of September 1859, exceed 1 Gy for bone marrow and 10 Gy for skin and ocular lens, for thinly-shielded spacecraft in deep space (Townsend *et al*., 2006). If it is assumed that the satellite energetic particle measurements acquired during the space era (1965 to the present) are representative of the SPE distributions to be encountered during missions beyond LEO, and utilize the Jet Propulsion Laboratory proton fluence model (Feynman *et al*., 1993) is used to estimate the probability of occurrence of a large event, then the probability of an event containing a >30 MeV fluence of ~5×10^9 protons cm^{-2} during a 2 y interplanetary mission near the solar cycle activity maximum is ~0.1. However, the ability to forecast large SPEs is poor. It is not currently possible to project the probability of SPEs 1 to 3 d in advance. The lack of a method to observe or account for interplanetary shocks and coronal mass ejections (CMEs) directed toward Earth is one of the major deficiencies of quantitative SPE predictions. When SPE predictions are issued and a significant event occurs, the observed fluence rate is generally, but not always, within an order of magnitude of the predicted peak particle fluence rate (Section 3). Prediction of an SPE's spectral characteristics has not proven to be reliable for large events. Similarly, the intensity-time fluence-rate profile predictions have not been adequate for large shock-dominated SPEs. Development of event-triggered methods of forecasting SPE doses over time using dosimeter measurements obtained early in the evolution of an event, coupled with Bayesian inference and artificial neural network methods, have met with some success (Hoff *et al*., 2003; Neal and Townsend, 2001; Townsend *et al*., 1999).

1.3 Space Radiation Physics and Transport

Whenever high-energy nuclei (protons, light ions, and heavier ions) pass through bulk materials, such as shielding or body tissues, they interact with the atoms and the atomic nuclei of the target materials. At the atomic level, interactions occur very frequently (~10^8 cm^{-1} of travel) and result in energy losses by the incident radiation fields as the atoms of the target materials are excited and ionized. However, the identities of the particles in the incident radiation fields are not altered by these atomic interactions. Nuclear

collisions on the other hand are much less frequent, occurring only once every few centimeters of travel. These collisions, however, can be violent and often result in the breakup of the incident and target nuclei. Hence, both the energy spectra and the actual composition of the transmitted radiation fields are altered. In addition, energetic neutrons are produced in large numbers by the nuclear collisions. The propagation of these radiation fields and their alterations by atomic and nuclear collisions are modeled using radiation transport codes. Clearly, an accurate description of these transported radiation fields requires accurate modeling methods for particle interactions and transport.

1.4 Space Dosimetry

Radiation exposures originate with different types of sources, each with distinct properties and variability. These sources include GCR, radiation from the sun including SPEs, protons and electrons in the trapped belts, and radiation from man-made sources intentionally included in the space vehicle. The onboard dosimetry system must be able to adequately characterize the exposure from all types of radiation and sources that are present. Both active and passive dosimetry systems will be needed. Instrumentation and techniques for some of these measurements exist, but several improvements are necessary to provide reliable dosimetry in these complex radiation fields.

1.5 Space Radiation Biology

Health effects of radiation exposures on humans during and after exploration missions beyond LEO are not completely known. Significant future research is needed to complete the estimation of these effects (Cucinotta, 2005; NCRP, 2000). The goal is to provide a consensus of radiation dose limits that will limit the risk of serious and persistent radiation effects from occupational radiation exposure in space to an acceptable level.

Historically, it has been assumed that major early effects of radiation exposure could be avoided simply by radiation shielding of the spacecraft. The focus, therefore, has been on estimating the risk of late radiation effects such as cancer and cataracts. However, the problem is broader and potentially includes both early and late radiation effects. The eminent problem of unpredictable large SPEs, and the potential of a rapid and progressive exposure to charged particles representing a wide array of atomic numbers, energies and dose rates (and any resulting secondary radiation cascades) is a daunting issue that requires extensive further study.

With what is known today, there are concerns about early effects on the brain and peripheral nervous system. There is concern about potential radiation damage to neural function, particularly in older individuals following exposure to low doses of high dose-rate radiation. Convincing evidence also is emerging for concern regarding the risk of cardiovascular disease. Defects in immunological function from exposure to low doses of high dose-rate radiation that contribute to life-shortening or diminished quality of life need further study. Biomarkers for identification of individuals at increased risk due to genomic predisposition, as well as radiation biodosimetry to estimate cumulative radiation doses may provide guidance for future individual mission worthiness. However, links between the appearance and abatement of some of the early biodosimetric markers and the risk of later medical consequences are uncertain. The combined effects of radiation exposure with other biophysical stressors, such as microgravity, exposure to ultraviolet (UV) light, or to microwaves have not been studied adequately.

1.6 Space Radiation Risk Assessment Methodology

On long-term missions outside Earth's magnetic field, three specific areas of radiation health risks can be identified as being of primary concern: (1) late effects (*e.g.*, cancer); (2) early effects due to acute, or at least short-term, exposures from large SPEs; and (3) possible effects (still to be identified) to the central nervous system (CNS) from the high-energy, high atomic number (Z) component of GCR. There is not enough information available to estimate the risk of other unknown potential late noncancer[1] radiation health risks. There are three factors that are important in their influence on the probability of noncancer effects occurring as a result of exposure to radiation in deep space: total dose, dose rate, and radiation quality. The importance of dose rate and radiation quality is different between ambient GCR and radiation from the SPEs. The radiation from GCR is continuous and varies in dose rate by perhaps a factor of two to three depending on the phase of the solar cycle, but does not reach what is considered to be a high dose rate. The highest dose rates in space occur during large SPEs. The dose rate and total dose depend on a number of factors that include the intensity of the disturbance on the sun, the longitude of the disturbance on the sun's disk relative to the position of the spacecraft, the condition of the interplanetary magnetic field between the sun

[1]The term noncancer refers to health effects other than cancer (*e.g.*, cataracts, cardovascular disease) that occur in the exposed individual.

and the spacecraft, and the amount of shielding provided by the spacecraft. Absorbed-dose rates as high as 1.4 Gy h^{-1} have been estimated for missions beyond LEO for an event similar to the large event of August 1972 (Parsons and Townsend, 2000). Regarding radiation quality, the spectrum of energies and linear energy transfers (LETs) of the heavy ions must be taken into account in the estimation of the risk of noncancer effects in deep space. The relative biological effectiveness (RBE) of neutrons, protons, carbon, neon and argon ions for the induction of noncancer effects was examined by ICRP (1989). Unfortunately, most of the data for noncancer effects have been obtained after exposure to acute high dose irradiation and there is no information about effects in humans of whole-body absorbed doses <1 Gy protracted over 1 to 2 y. The evidence, however, suggests that in most tissues, repair and recovery are efficient in reducing or eliminating the damage caused by radiation at the dose rates experienced in space. The equivalent dose[2] (in sievert) obtained using radiation weighting factors (w_R) derived from RBE information for late stochastic effects (*i.e.*, cancer and genetic effects), is not appropriate for use in describing the risk of early or late noncancer effects. The quantity gray equivalent[2] has been suggested as the analogy to equivalent dose when considering deterministic (see Glossary) noncancer effects (NCRP, 2000). As discussed in NCRP Reports No. 132, No. 137, and No. 142 (NCRP, 2000; 2001a; 2002) the organ dose equivalent[3] (in sievert), may be used as a surrogate for the equivalent dose when dealing with the space radiation environment. The effective dose[2] (in sievert) can be calculated by summing the products of the equivalent dose for each organ and the appropriate tissue weighting factor (w_T) from column three of Table 3.1 of NCRP Report No. 137 (NCRP, 2001a).

1.7 Major Information Needed

- Improve the accuracy and extend the range of energies and elemental species included in GCR models.

[2]The terms equivalent dose (H_T), effective dose (E), and gray equivalent (G_T) refer to quantities formulated for radiation protection purposes. The first two quantities apply to stochastic effects (*i.e.*, cancer and genetic effects), and the third applies to deterministic effects (see equivalent dose, effective dose, and gray equivalent in Glossary).

[3]The term organ dose equivalent ($\bar{H}_T$) refers to a quantity obtained by averaging or integrating over the quantity dose equivalent (H_T) that is measured or calculated at a number of points in an organ or tissue. For space radiations, $\bar{H}_T$ is used as the surrogate for equivalent dose (see organ dose equivalent and dose equivalent in Glossary).

- Develop SPE forecasting and prediction capabilities that are able to observe or account for interplanetary shocks and CMEs. These capabilities should include the ability to reliably predict the fluence spectra and time evolution of SPE.
- Develop realistic models of the largest expected SPE fluence rates, which may be encountered on exploratory missions. Assessments of their biological effects and shielding requirements need to be carried out.
- Develop and validate space radiation transport codes and nuclear cross-section models that treat all components of the primary and secondary spectra of the space radiation environment including protons, neutrons, light ions, heavy ions, mesons, and electromagnetic cascades.
- Improve existing nuclear interaction databases for properly assessing risk and concomitant shielding requirements, especially for neutrons and light ions.
- Determine the carcinogenic effect of protracted exposures of relevant energies of protons, neutrons and heavy ions.
- Determine the carcinogenic effects of heavy ions to provide data for determining quality factor values.
- Conduct experiments to underpin the risk estimates such as cell and molecular biology experiments using realistic cell and tissue models.
- Determine whether or not there is a significant risk of effects on the function of the CNS from space radiations.
- Determine the effect of protracted exposures of relevant energies of protons, neutrons and heavy ions on other tissues, such as the ocular lens, bone marrow, cardiovascular, and immune system.
- Develop methods of using experimental data for estimating risks of late and early effects in humans.
- Conduct studies of the effects of SPE dose rates on early radiation responses (*e.g.*, prodromal effects, such as nausea and vomiting) in order to determine the appropriate biological effectiveness factors to use in establishing gray equivalent limits to apply to organs and tissues for early effects.
- Evaluate biomarkers for their ability to detect adverse effects.
- Evaluate biomarkers to estimate cumulative doses.
- Assess countermeasures for their efficacy in preventing adverse effects.
- Develop radiation spectrometers which can accurately measure the fluence of indirectly ionizing particles in the presence of a fluence of directly ionizing particles.

2. Introduction

The purpose of this Report is to identify and describe information needed to make radiation protection recommendations for space missions beyond LEO. Current NCRP space radiation guidelines pertain only to missions in LEO and are not considered relevant for future missions beyond LEO. Radiation protection in deep space is complicated because of the unique nature of the space radiation environment which is unlike any radiation environment present on Earth or in LEO.

Astronauts on exploration missions of long duration beyond LEO face exposures to radiation levels that may easily exceed those routinely received by terrestrial radiation workers and those faced by crews in spacecraft in LEO. Radiation fields encountered in space travel include the ever-present GCR background, sporadic SPEs, energetic protons and electrons during traversals of the Van Allen radiation belts, and exposure to possible onboard radioactive sources used for power generation, propulsion, medical testing, and instrument calibration. The main radiation sources of concern for missions beyond LEO are GCR and SPEs. Since spacecraft will be externally exposed to the full intensities of these sources, radiation fields within the interior of the spacecraft are altered only by the shielding provided by the spacecraft structure. Proper descriptions of how these radiation fields are altered by passage through the spacecraft structure is accomplished using radiation transport codes, which model the atomic and nuclear interactions of these particles and describe the composition and energy spectra of the resulting radiation field. Additional shielding is also provided by the body tissues overlying critical internal organs and must be accounted for as well.

The biological effects of these unique radiation fields, especially the high atomic number, high-energy (HZE) component of GCR spectra, are not well known, nor are the associated radiation risks for late effects, such as cancer incidence and mortality.

Contributions to uncertainties in radiation risk from these particle sources may be significant. For the GCR spectrum, present uncertainties in the models appear to be ~15 %. For SPE spectra, the uncertainties may be much larger. Uncertainties in proton fluences measured by instruments onboard the Geostationary

Operational Environment Satellites (GOES) are probably less than a factor of two.[4] Absorbed doses and dose equivalents[5] calculated using the current generation transport codes appear to be uncertain by <25 %, but individual spectral components, especially secondary neutrons, are probably much more uncertain. In addition, the uncertainty increases as the shielding thickness increases. For thick shielding, the uncertainty resulting from radiation physics models is probably still less than a factor of two. None of the existing GCR codes, however, properly treat all of the components produced in the transported radiation fields, especially the three-dimensional nature of the secondary neutron and light ion fields produced by the nuclear fragmentation events involving the HZE particle components of the spectrum. Uncertainties in the biological risk due to the transmitted radiation fields present at critical body organs are possibly as large as a factor of four or more (NAS/NRC, 1996). There are no human data for risks from GCR particles. Human data for risks from protons exist from radiotherapy applications, but not for proton energies and dose rates found in space. The radiation fields that will be encountered in deep space, and their concomitant risks, depend upon the mission scenario under consideration. There are three mission scenarios that must be considered: (1) lunar surface missions, (2) transits to Mars, and (3) Mars surface missions.

For missions on the lunar surface, the concerns are mainly exposures resulting from large SPEs, especially near the period of maximum solar activity during the ~11 y solar cycle. Ions heavier than protons are present in the SPE spectra, but are not considered to be a hazard due to their soft spectra and low fluence rates. As the length of a lunar surface mission increases, however, chronic exposures to the background GCR environment may be of a magnitude to warrant concern. For either short- or long-duration missions, absorbed doses from large SPEs in excess of 1 Gy are possible if crews are in a thinly shielded area, but are easily reduced if adequate shielding (~20 g cm^{-2}) is provided. On the moon there is no atmosphere to provide shielding, but the moon's physical bulk does

[4]Zwickl, R.D. (1997). Personal communication (National Oceanic and Atmospheric Administration, Space Environment Center, Boulder, Colorado).

[5]The term dose equivalent refers to a measured or calculated value made at a point, accounting for the quality factor-linear energy transfer relationship for the biological effectiveness of the radiation types involved (see dose equivalent, quality factor, and linear energy transfer in Glossary).

provide some shadow shielding that reduces the incoming GCR particle fluence rates by approximately one-half.

For transits to Mars the main concerns are exposures from large SPEs and chronic exposures from both SPEs and the background GCR environment. Since transit times of approximately six months are thought to be necessary, effective doses as large as 1 Sv have been estimated from the GCR environment. Much of this effective dose comes from high-LET components of the spectrum, such as high-energy heavy ions (the so-called HZE particles) and the secondary radiations produced by their interactions in the spacecraft shielding and tissue overlying critical body organs. Typical shielding thicknesses for interplanetary spacecraft are likely to be ~20 g cm^{-2} or more of aluminum or other structural materials. Since GCR fluence rates are not correlated with solar activity, effective doses from GCR at solar maximum are likely to be ~40 % of the values at solar minimum. Doses from large SPEs, mainly from energetic protons with energies as large as several hundreds of megaelectron volts and higher, are likely to be well below any acute radiation syndrome response levels for spacecraft with ~20 g cm^{-2} or more of shielding.

For operations on the surface of Mars, the main sources of concern are chronic exposures to SPEs and the GCR environment. Acute exposures to SPE protons are unlikely because the overlying atmosphere of Mars (~16 to 20 g cm^{-2} carbon dioxide) provides substantial shielding for all surface operations, except those that might take place at high mountainous altitudes. Again, as was the case for the moon, the physical bulk of Mars and the Martian atmosphere will provide substantial shadow shielding and will reduce the incident GCR particle fluence rates by one-half. The overlying atmosphere on Mars will also provide some shielding against incident GCR particles. Unlike the moon, however, the radiation fields on the Martian surface will include a substantial component of secondary particles from interactions of the incident radiations with atmospheric constituents. Especially important will be secondary neutrons, which come from nuclear fragmentation interactions between the incident protons and heavy ions and the atmosphere, and from albedo neutrons emanating from the Martian soil. These neutron energies range from thermal up to hundreds of megaelectron volts or more.

3. Space Radiation Environment

The space radiation environment is mainly composed of the GCR background, sporadic SPEs, and energetic protons and electrons populating Earth's Van Allen radiation belts. For missions beyond LEO the main sources of concern are large but infrequent SPEs and the chronic background provided by the energetic heavy charged particles in the GCR spectrum consisting of all of the naturally-occurring elements. SPEs present both acute and chronic exposure concerns for manned missions. The GCR background will not give rise to early effects, but does present a chronic exposure concern and may cause unique biological responses in humans not easily replicated by standard x- or gamma-ray sources.

3.1 Galactic Cosmic Radiation

Exposure to GCR poses a serious hazard for long-duration space missions. Spacecraft shielding to reduce dose equivalents imposes a very stiff mass penalty, and thus a large increase in the mission cost. GCR radiation consists of particles of charge from hydrogen to uranium arriving from outside the heliosphere. These particles range in energy from ~10 MeV n^{-1} to ~10^{12} MeV n^{-1}, with fluence-rate peaks around 300 to 700 MeV n^{-1}. Because of the vast energy range, it is difficult to provide adequate shielding, and thus these particles provide a steady source of low dose-rate radiation.

Integrations of energy spectra show that ~75 % of the particles have energies below ~3 GeV n^{-1}. Under modest aluminum shielding, nearly 75 % of the dose equivalent is due to particles with energies <2 GeV n^{-1}. Thus, the most important energy range for risk estimation is from particles with energies below ~2 GeV n^{-1}, and nearly all of the risk is due to particles with energies <10 GeV n^{-1}. The local interstellar energy spectrum (outside the heliosphere) is a constant, but inside the heliosphere the spectrum and fluence of particles below ~10 GeV n^{-1} is modified by solar activity.

The assessment of radiation risk requires a detailed knowledge of the composition and energy spectra of GCR in interplanetary space, and their spatial and temporal variation.

3.1.1 *Galactic Cosmic Radiation Composition*

Table 3.1 summarizes the relative abundance of nuclei (hydrogen through nickel) at a few representative energies. The composition varies as a function of energy. The energy spectrum of iron nuclei, for example, is harder than that for helium nuclei, in that the iron to helium ratio increases with increasing energy above ~1 GeV n^{-1}. Since the high-energy particles are less efficiently stored in the Galaxy, the so-called secondary cosmic-ray nuclei (*e.g.*, lithium, beryllium and boron) have maximum abundance at energies of ~1 to 2 GeV n^{-1}, with the abundance decreasing at both lower and higher energies. These secondary cosmic-ray nuclei are produced by the fragmentation of heavier primary nuclei (*e.g.*, carbon, oxygen and iron) in collisions with interstellar gas.

3.1.2 *Solar Modulation*

The cyclic variation of the solar magnetic field and changes in the solar wind velocity cause modulation of the GCR spectrum within the heliosphere. Mewaldt *et al.*, (1988) suggested that the differential energy spectrum, $j(Z,\mathrm{E},t,r,\theta,\Phi)$, can be expressed in terms of separable functions:

$$j = j_0(Z,\mathrm{E})F_{\mathrm{t}}(Z,\mathrm{E},t)F_{\mathrm{r}}(Z,\mathrm{E},t)F_{\theta}(Z,\mathrm{E},t)F_{\Phi}(Z,\mathrm{E},t), \tag{3.1}$$

where $j_0(Z,\mathrm{E})$ is the local interstellar energy spectrum of particles with charge Z, and the four functions $F(Z,\mathrm{E},t)$ are the time, radial, heliolatitude and heliolongitude dependent functions, respectively. The angular terms are important for fairly low-energy particles. These terms are discussed below with the primary focus on the time-dependent term.

Figure 3.1 presents a highly schematic view of the main features of the heliosphere. The solar wind blowing radially outwards carries with it the heliospheric magnetic field (HMF). The rotation of the sun causes this field to have a spiral configuration in and away from the sun's equatorial plane. As the solar wind plows through the interstellar gas, the wind undergoes transition to a subsonic flow some distance from the sun. This is the heliospheric termination shock and is a likely acceleration site of the anomalous cosmic rays. It marks the boundary at which the characteristics of HMF are markedly different inside and outside. In the region outside, HMF becomes more tightly bound and has higher field strength than inside the termination shock. The outer portion of

TABLE 3.1—*Relative abundances of nuclei (hydrogen through nickel) at a few representative energies.*

Z	Element	0.2 GeV n^{-1}	1 GeV n^{-1}	5 GeV n^{-1}
1	H	2,200,000 ± 500,000	2,800,000 ± 500,000	4,600,000 ± 700,000
2	He	340,000 ± 80,000	250,000 ± 30,000	230,000 ± 30,000
3	Li	1,000 ± 60	1,400 ± 140	960 ± 100
4	Be	450 ± 50	730 ± 67	680 ± 53
5	B	2,100 ± 90	2,340 ± 102	1,600 ± 69
6	C	8,500 ± 290	7,100 ± 285	6,460 ± 258
7	N	1,940 ± 80	2,000 ± 82	1,610 ± 61
8	0	7,770 ± 280	6,430 ± 243	6,190 ± 217
9	F	183 ± 13	145 ± 11	115 ± 6
10	Ne	1,120 ± 60	1,050 ± 43	960 ± 35
11	Na	273 ± 34	224 ± 12	188 ± 8
12	Mg	1,430 ± 60	1,330 ± 54	1,260 ± 46
13	Al	252 ± 30	229 ± 12	207 ± 9
14	Si[a]	1,000	1,000	1,000
15	P	40 ± 7	47 ± 4	37 ± 2
16	S	164 ± 12	206 ± 11	190 ± 8
17	Cl	36 ± 5	45 ± 4	37 ± 2
18	Ar	63 ± 6	90 ± 7	68 ± 4
19	K	51 ± 6	66 ± 6	51 ± 4
20	Ca	135 ± 10	147 ± 10	119 ± 6
21	Sc	29 ± 5	33 ± 3	22 ± 2
22	Ti	107 ± 9	98 ± 8	74 ± 4
23	V	57 ± 6	44 ± 4	38 ± 3
24	Cr	109 ± 10	98 ± 4	83 ± 5
25	Mn	72 ± 12	55 ± 5	56 ± 4
26	Fe	602 ± 32	607 ± 34	685 ± 37
27	Co	2 ± 1	3 ± 1	4 ± 1
28	Ni	29 ± 4	27 ± 4	36 ± 3

[a]Relative abundances were scaled to silicon which was arbitrarily set equal to 1,000.

this region, the heliopause, eventually separates the interstellar gas from the solar wind. HMF is divided into hemispheres of opposite polarity by the wavy heliospheric neutral sheet. This sheet, rooted in the coronal magnetic field, is inclined to the sun's rotational equator by a few degrees during the minimum of the solar activity cycle. As the solar activity increases, the waviness of the heliospheric neutral sheet increases and eventually, near the solar activity maximum, this structure breaks down. Finally, near solar maximum, HMF reverses its polarity, followed by a gradual relaxation back to minimum activity to repeat the cycle approximately every 11 y, causing an effective 22 y solar magnetic cycle.

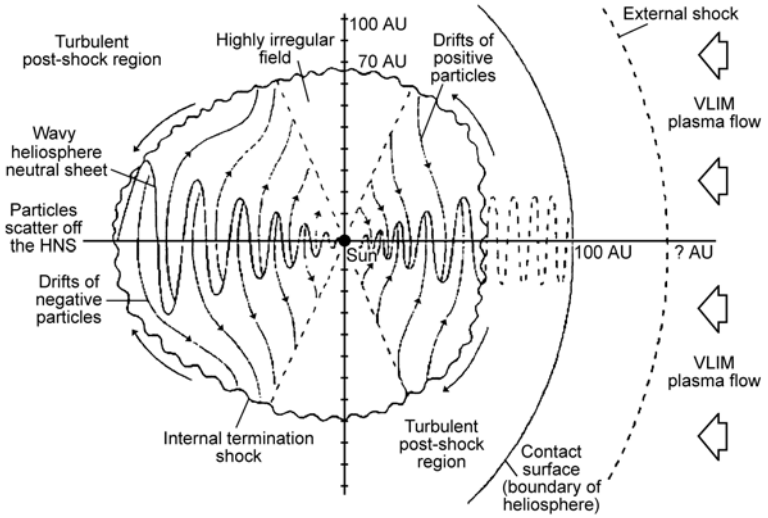

Fig. 3.1. A highly schematic view of the heliosphere with some of its main features (AU = astronomical unit; VLIM = limiting value) (Potgieter, 1995).

The present best estimates of the radius of the heliosphere are ~90 to ~160 astronomical units (AUs) (1 AU = 149,579,900 km or 92,955,825 miles). The modulation of cosmic rays as a function of position, energy and time is a complex function of outward convection by the solar wind, inward diffusion due to scattering by magnetic field irregularities, adiabatic cooling, field gradient, particle curvature and heliospheric neutral sheet drifts, and at lower energies, of shock acceleration. Due to HMF configuration, positively-charged particles will drift from the polar region towards the equatorial regions when HMF is directed outwards in the northern hemisphere of the heliosphere. After a polarity reversal, the drift velocity field reverses and cosmic rays will drift in along the wavy heliospheric neutral sheet and up towards the polar regions of the heliosphere. The heliosphere is transparent for particles >10 GeV n^{-1}. Below ~1 GeV n^{-1} it varies from semitransparent to totally opaque. This prevents us from observing the complete local interstellar energy spectrum.

Parker (1965) showed that the propagation of cosmic rays in the interplanetary medium is well described by the time-independent, spherically symmetric Fokker-Planck equation. The basic equation is:

$$\left(\frac{\partial U}{\partial t}\right) = \nabla(\kappa^{S} \cdot \nabla U) - \boldsymbol{V} \cdot \nabla U + \left(\frac{1}{3}\right)\nabla \cdot \boldsymbol{V}\,\frac{\mathrm{d}(\alpha \mathrm{E} U)}{\mathrm{dE}} = 0, \qquad (3.2)$$

where $\boldsymbol{V}_{sw} + \boldsymbol{V}_d = \boldsymbol{V}$, U is the density of cosmic rays, $\boldsymbol{V}_{sw}$ is the vector solar wind velocity, E is the kinetic energy of the particle, κ^s is the symmetric part of the diffusion tensor, $\boldsymbol{V}_d$ is the vector velocity resulting from particle gradient and curvature in the nonuniform HMF and is related to the anti-symmetric part of the diffusion tensor κ^a, and $\alpha = (E + 2m_p)/(E + m_p)$ where m_p is the proton rest mass energy. Using the assumptions of cosmic-ray fluence-rate isotropy and a spherically symmetric heliosphere, this equation was solved numerically (Fisk, 1971), and explains the variation of the cosmic-ray intensity over the solar activity cycle. Gleeson and Axford (1967) showed that the model had only three free parameters, the diffusion coefficient (κ), the solar wind velocity ($\boldsymbol{V}_{sw}$), and the radial extent of the heliosphere (r_B). Urch and Gleeson (1972) further showed that the full numerical solutions of the equation could be well represented in terms of the deceleration potential $\phi(r,t)$:

$$\phi(r,t) = \left(\frac{1}{3}\right)\int_{r}^{r_B} \frac{\boldsymbol{V}_{sw}(r',t)}{\kappa(r',t)}\, dr', \tag{3.3}$$

which is a very convenient parameter, usually given in units of megavolts. A number of studies using proton and helium data from 1965 to 1979 by Evenson *et al*. (1983) and Garcia-Munoz *et al*. (1986) have shown that a self-consistent proton and helium local interstellar energy spectrum together with ϕ describe their data very well. In these studies the diffusion coefficient was assumed to be of the separable form of:

$$\kappa(r,R,t) = \kappa_0 \beta \kappa_1(r) \kappa_2(R) \kappa(t), \tag{3.4}$$

where R is the rigidity (momentum per unit charge of the particle). The rigidity dependence of the diffusion coefficient, based on scattering data of SPEs and the power spectrum of magnetic field fluctuations, was taken to be $\kappa = \kappa_0 \beta R^{\delta}$ where $\delta = 1$ for $R > 0.3$ GV and $\delta = 0$ for $R < 0.3$ GV.

Webber and Yushak (1979) have shown that a similar situation exists for helium and iron spectra. In the particular case where κ is proportional to the particle rigidity, this modulation potential corresponds to a potential energy (Φ):

$$\Phi(r,t) = Ze\,\phi(r,t), \tag{3.5}$$

where Z is the particle charge. In this case, an approximation to the full numerical solution that is valid for energies above ~300 MeV n^{-1} is given by:

$$\frac{j(r,\mathrm{E})}{\mathrm{E}^2 - m_\mathrm{p}^2} = \frac{j_0(r_\mathrm{B},\mathrm{E}+\Phi)}{(\mathrm{E}+\Phi)^2 - m_\mathrm{p}^2}. \tag{3.6}$$

where $j(r,\mathrm{E})$ is the integral fluence of particles in the spectrum and j_0 is the local interstellar spectrum (LIS). This conventional model of solar modulation has, because of its simplicity, received wide acceptance. This standard convection-diffusion model of cosmic-ray modulation, however, does not account for either the observed charge dependence of the modulation or the observed dependence on the sign of HMF. However, these features can be incorporated into the model fairly easily, but only in *ad hoc* ways. Three-dimensional drift related models do account for these features (see reviews by Jokippi and Thomas, 1981; Kota and Jokippi, 1983; Potgieter, 1998). Further progress in understanding the relative importance of various mechanisms involved in the modulation process has been made with time-dependent models (Le Roux and Potgieter, 1990). However they require additional parameters that are difficult to obtain, and still do not explain the radial gradient. Further discussion is restricted to the standard model.

The standard model describes the differential fluence rate, $j(Z,\mathrm{E},t)$, at radial distance r in the heliosphere, in terms of the local LIS, $j_0(Z,\mathrm{E})$, which is time independent, and the modulation function $F_\mathrm{t}(Z,\mathrm{E},t)$, which is a function of $\phi(t)$. The solution, however, is not unique. A variety of combinations of $j_0(Z,\mathrm{E})$ and $\phi(t)$ lead to the same $j(Z,\mathrm{E},t)$. Since there are no measurements of LIS, different investigators have chosen different forms, with the constraint that the high-energy portion of the spectrum is the same as the near-Earth measured spectrum. Measurements on Voyager-2 that extend to 40.2 AU and on Pioneer-10 that extend to 56.2 AU are beginning to provide some real constraints on the lower energy portion of the local interstellar energy spectrum.

Until fairly recently, the most widely used model of GCR environment was the cosmic-ray effects of microelectronics (CREME-85) code developed at the Naval Research Laboratory (Adams, 1986; 1987). The problems with this code have been well documented and four new models that are much more accurate have recently been developed. All of the new models are based on the standard diffusion-convection theory of solar modulation (Badhwar and O'Neill, 1994; Chen *et al*., 1994a; Nymmik *et al*., 1992; Tylka *et al*., 1997a). They differ from each other primarily in their choice of the LIS, and the solar activity parameter used for prediction. Each of these models is briefly discussed below.

3.1.2.1 *Nymmik's Model*. The Nymmik (1996; 1997) model is sometimes referred to as the Moscow State University model. In the Nymmik model the LIS is expressed in terms of rigidity and is given by:

$$j_0(Z,\mathrm{E})\mathrm{dE} = j_0(Z,R)\left(\frac{\mathrm{d}R}{\mathrm{dE}}\right)\mathrm{dE} = \mathrm{C}\beta^{\alpha}R^{\gamma}\left(\frac{\mathrm{dE}}{\beta}\right), \tag{3.7}$$

where C, α, γ are constants that depend on the charge of the particle and are derived from fits to the experimental data, and β is the velocity of the particle as a fraction of the velocity of light. The modulated fluence rate near 1 AU in free space, $j_{Wn}(\mathrm{E},t)$, during the n^{th} solar cycle, at time t, with Wolf sunspot number W (averaged over 12 months) is given by:

$$j_{Wn}(Z,\mathrm{E},t) = \Psi_{Wn}(R,t)j_0(Z,\mathrm{E}), \tag{3.8}$$

where Ψ_{Wn} is the modulation function for the n^{th} solar cycle. The modulation function is not a solution to the diffusion-convection model, but is a product of two empirically derived functions. The first term is a function of the modulation parameter R_0 [nearly the same as the deceleration potential (ϕ)], and the second term a function of the sign of the particle charge. The modulation function is given by:

$$\Psi_{Wn} = \left(\frac{R}{R + R_0\{W[t - \Delta T(R,n,t)]\}}\right)\Delta(R,t), \tag{3.9}$$

where $\Delta(R,t) = 5.5 + 1.13\ (Z/|Z|)\ M(W,n)\ \phi(Z,R,\beta)$ and $M(W,n)$ is the magnitude of the polar magnetic field whose intensity and polarity are taken to be dependent on solar activity and on whether a given solar cycle is even or odd. The solar modulation parameter [R_0 (GV)] is calculated as:

$$R_0\{W[t - \Delta T(n,R,t)]\} = 0.37 + 3 \times 10^{-4} W^{1.45}[t - \Delta T(n,R,t)], \tag{3.10}$$

where the sunspot number W is calculated at earlier time. The time lag [$\Delta T(n,R,t)$] in months, is:

$$\Delta T(n,R,t) = 0.5(15 + 7.5\ R^{-0.45}) + 0.5(15 + 7.5\ R^{-0.75})\ \tau(W), \tag{3.11}$$

and

$$\tau(W) = (-1)^{\mathrm{n}}\frac{W(t-16) - W_{\mathrm{n}}^{\min}}{W_{\mathrm{n}}^{\min}}. \tag{3.12}$$

These features then describe the even-odd cycle of solar modulation and the hysteresis effect. The solar modulation function (ϕ) is given by:

$$\phi(R,t) = \left(\frac{\beta R}{R_0}\right) e^{-\frac{\beta R}{R_0}} . \quad (3.13)$$

This form is the same used by Badhwar *et al*. (1967), Hilderbrand and Silberberg (1966), and Silberberg (1966) based on Parker's model (Parker, 1965). The model provides a means of calculating the fluence rate and associated errors as a function of energy per nucleon (>10 MeV n^{-1}), given the solar cycle number and the 12 month average sunspot number. This model describes particles >10 MeV n^{-1} with a quoted error not to exceed 15 %, which is a factor of three better than the CREME-85 model.

3.1.2.2 *CREME-96 Model.* This model (Tylka *et al*. 1997a) is an update of the CREME-85 model that incorporated not only the GCR environment model, but also the geomagnetic transmission calculations (Smart *et al*., 1999a; 1999b). The GCR model in the CREME-96 code is essentially Nymmik's model.

3.1.2.3 *CHIME Model.* The CHIME model (Chen *et al*., 1994a) is based on the standard diffusion-convection theory of modulation. In this model the LISs were determined by requiring that the assumed GCR source spectra with a power law in energy is propagated through a weighted-slab of interstellar medium, and a path-length distribution function derived from matching the ratio of secondary nuclei (such as lithium, beryllium and B8) to primary nuclei (such as carbon, oxygen and iron) to observations. The derived LIS were then modulated using the deceleration potential (ϕ) and a numerical solution to the Fokker-Planck equation. The value of ϕ was derived using the IMP-8 helium fluence rate in the 25 to 93 MeV n^{-1} range. Thus the model requires the satellite observations and does not have predictive capabilities.

3.1.2.4 *Badhwar and O'Neill Model*. The Badhwar and O'Neill (1994) model is sometimes referred to as the Johnson Space Center model. This model is also based on the standard diffusion-convection theory. First, all of the data available at energies above ~10 GeV n^{-1} were fitted to a power law in energy per nucleon. This least squares fit established the high-energy portion of the LIS. These spectra were then matched to the LIS obtained by Tang (1990). These spectra were iterated with the solar modulation deceleration potential parameter (ϕ) to provide a self-consistent set

of LIS and ϕ such that the differential energy spectra of hydrogen, helium, oxygen and iron measured at nearly the same time, fitted well. The objective was to obtain a single value of ϕ that best described the measurements of hydrogen, helium, oxygen and iron simultaneously. Adams and Lee (1996) attempted to calculate simultaneously all elemental spectra from the LIS. They tried to derive a solution to the leaky-box cosmic-ray propagation model, but were not successful. Golden *et al*. (1995) examined the proton and helium measurements >400 MeV n^{-1} made from 1976 to 1993 by their magnetic spectrometer and found that the values of Φ derived from proton and helium data are different. In these calculations they assume a power law in rigidity of the LIS and used the force-field solution of Equation 3.5 to estimate Φ. However, they did not attempt to adjust the LIS so that the two species would give the same deceleration parameter. They fitted their derived parameter to the neutron monitor rate (x) as $\Phi = \Phi_0 + Ae^{Bx}$, and obtained values of Φ_0 that are different for hydrogen and helium. They concluded that the relation $\Phi = Ze\phi$ in Equation 3.5 was not satisfied. They did not take the even-odd solar cycle variability of ϕ into account. The raw data, however, are quite consistent with charge independence. This is supported by the analysis of the carbon, oxygen, neon, magnesium and iron data from the GEOTAIL satellite measurements (Kobayashi *et al*., 1998). The ϕ values were calculated using the force-field approximation and the high-energy data were tied to the data from Engelmann *et al*. (1990).

Figure 3.2 shows a comparison of LIS used in various models. The lowest value of adiabatic energy loss is ~200 MeV n^{-1}, and thus LIS < 200 MeV n^{-1} have no effect on the calculated spectra at 1 AU, as these particles are not observed at 1 AU. All of the available data on the differential energy spectra of hydrogen, helium, oxygen and iron were fitted to the LIS using the numerical solution of the Fokker-Planck equation to obtain ϕ(t). Figure 3.3 shows the fits to helium differential energy spectra at increasing levels of solar modulation. Figures 3.4 and 3.5 show fits to the hydrogen and helium differential energy spectra. The solid lines for oxygen and iron nuclei are model calculations (not fits), using the ϕ derived from proton and helium data. The agreement between the model and measurements is excellent. Figure 3.6 is a plot of ϕ(MV) as a function of time, derived from all observations from 1954 to 1989. It shows the even-odd cycle of modulation very clearly. In order to develop a predictive capability of GCR spectra at 1 AU, the relationships of ϕ(MV) to the Climax (Colorado) cosmic-ray neutron monitor counting rates and to the sunspot number were examined. Figure 3.7 shows the Climax (Colorado) cosmic-ray neutron monitor

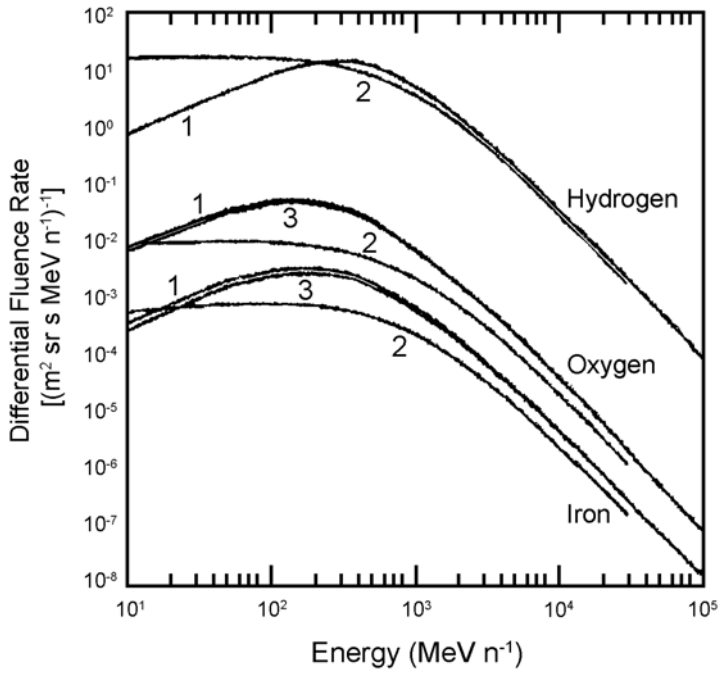

Fig. 3.2. Three calculations of LIS models [1 = Badhwar and O'Neill, 2 = Nymmik, and 3 = Johnson Space Center].

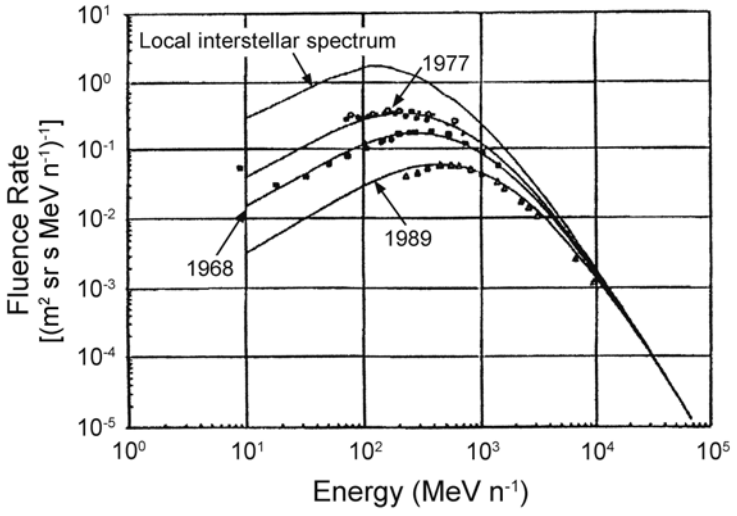

Fig. 3.3. Fits to helium differential energy spectra with increasing levels of solar modulation.

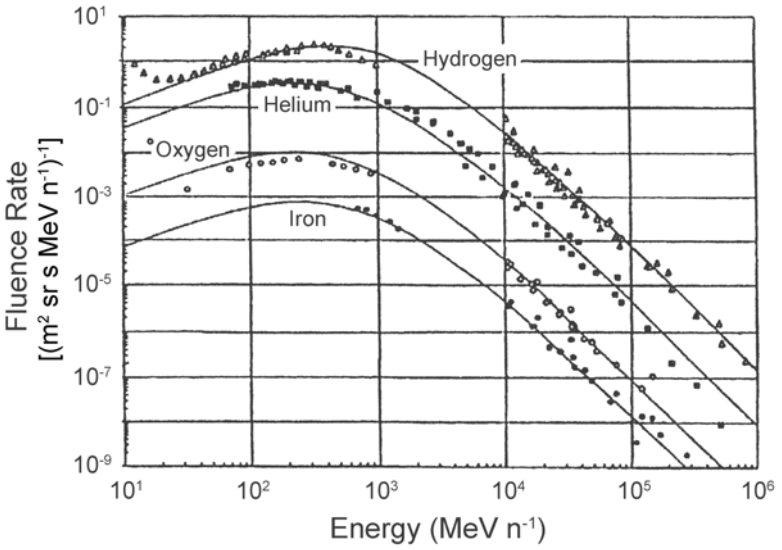

Fig. 3.4. Fit of the 1976 to 1977 hydrogen and helium energy spectra to the Fokker-Planck equation. Curves derived for oxygen and iron are shown.

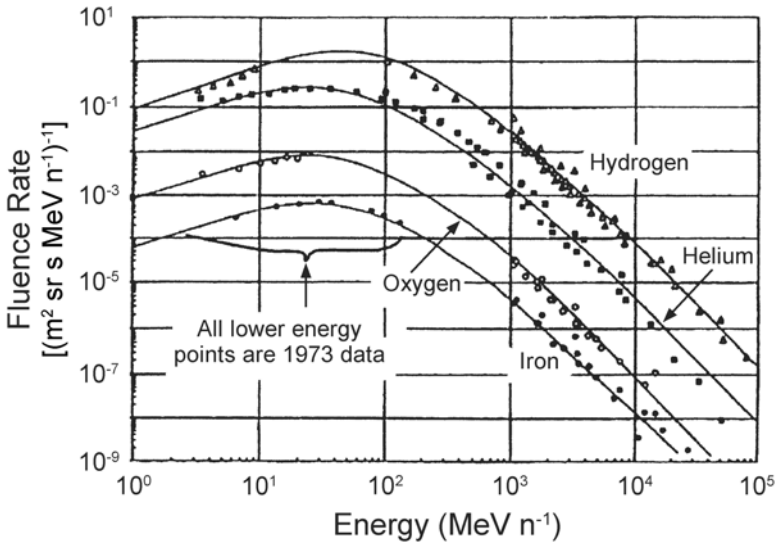

Fig. 3.5. Fits of the 1973 hydrogen and helium energy spectra to the Fokker-Planck equation. Curves derived from oxygen and iron are shown.

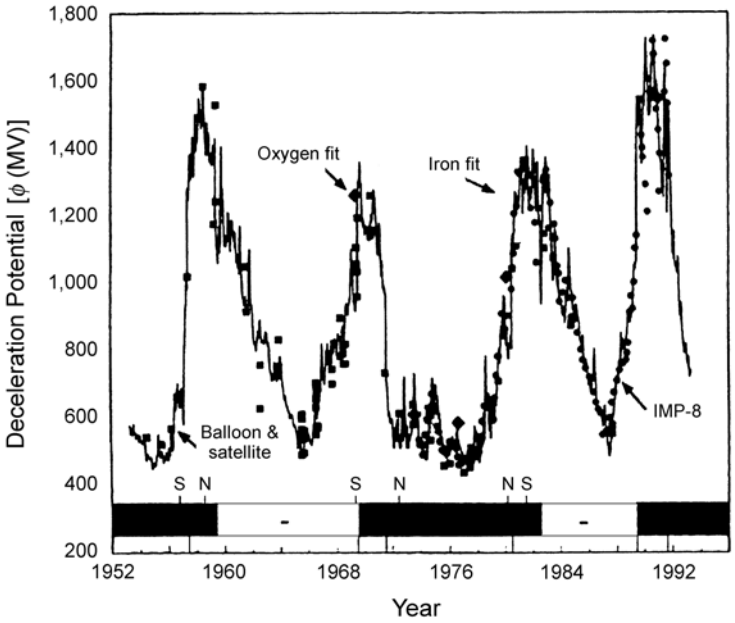

Fig. 3.6. Deceleration potential [ϕ(MV)] as a function of time.

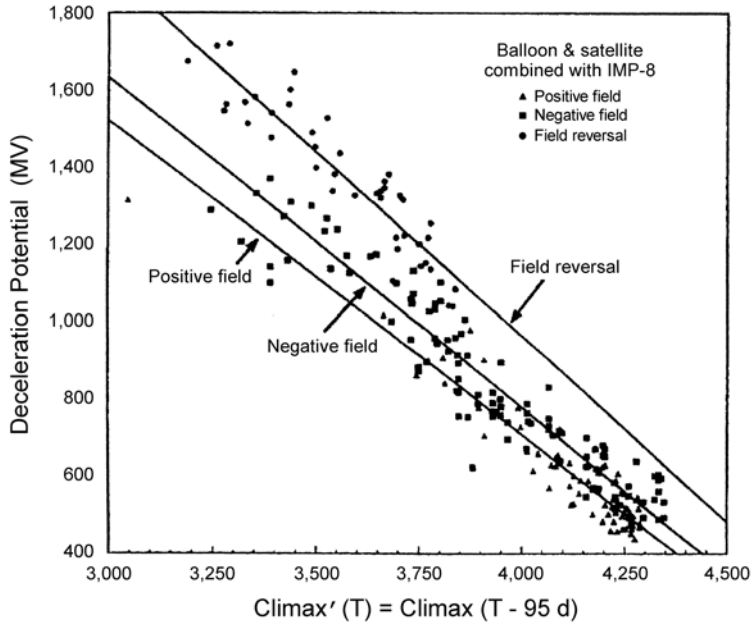

Fig. 3.7. Plot of derived deceleration potential, separated by HMF polarity versus neutron monitor rates.

counting rate data. The data very clearly separate into three very distinct regions: (1) when HMF is positive, (2) when HMF is negative, and (3) the transition region during which the polarity changes from one to the other. The solid lines are the regression fits. The best fits were obtained with an approximate three month (95 d) delay in cosmic-ray neutron monitor counting rate, and a nine month (270 d) delay in sunspot number. Using these regression equations ϕ(MV) was calculated as a function of time. The regression equations are given by:

$$\phi(t) = 3957.89 - 0.8124 \times \text{Climax rate } (t - 95 \text{ d}) \quad + \text{HMF}$$
$$\phi(t) = 4202.76 - 0.8563 \times \text{Climax rate } (t - 95 \text{ d}) \quad - \text{HMF}$$
$$\phi(t) = 4772.86 - 0.9526 \times \text{Climax rate } (t - 95 \text{ d}) \quad \text{field reversal}$$

and

$$\phi(t) = 439.89 + 3.0256 \times \text{sunspot number } (t - 270 \text{ d}) \quad + \text{HMF}$$
$$\phi(t) = 603.44 + 3.3101 \times \text{sunspot number } (t - 270 \text{ d}) \quad - \text{HMF}$$
$$\phi(t) = 895.25 + 3.3932 \times \text{sunspot number } (t - 270 \text{ d}) \quad \text{field reversal}$$

There are similarities between these ϕ and the R_0 (Equations 3.3 and 3.10) derived by Nymmik. The lowest value of R_0 is 370 MV, which is nearly the same as the lowest derived value for ϕ(400 MV). The best fit of ϕ as a function of sunspot number was obtained with a lag (delay) of about nine months (270 d). In Nymmik's model, the lag depends on rigidity and on whether it is an even or odd solar cycle, but is ~12 months for energies near those where the maximum fluence rates occur.

The Badhwar and O'Neill model gives root mean square errors of ~10 % for iron nuclei, nearly a factor of three smaller than the errors in the CREME-85 model. Figure 3.8 shows a comparison of the Badhwar and O'Neill model and Nymmik's model for predicting the IMP-8 oxygen data. Nymmik's model used the sunspot number, whereas Badhwar and O'Neill used the Climax cosmic-ray neutron monitor counting rates as predictors of solar activity. Both calculations fit the data within the respective quoted errors. The Climax cosmic-ray neutron monitor counting rates are a direct measure of higher-energy cosmic-ray particles, and thus should be a better indicator of cosmic-ray intensities than is the sunspot number. The data from the Climax cosmic-ray neutron monitor provide near term (three months) prediction capability. The sunspot number provides longer term (about nine months) prediction with somewhat larger errors.

Thus, standard diffusion-convection based models or their successors have provided phenomenological GCR environment descriptions possessing both short- and long-term prediction capabilities.

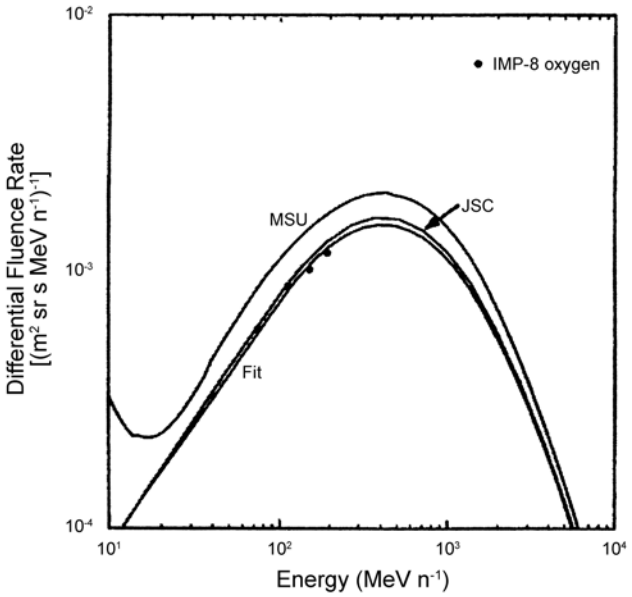

Fig. 3.8. A comparison of the Badhwar and O'Neill model [Johnson Space Center (JSC)] and Nymmik's model [Moscow State University (MSU)] for predicting the IMP-8 oxygen data.

These models have errors of <15 % in predicting the fluence rate in the energy region <5 GeV n^{-1} and this is the region in which solar modulation is most important, and which contributes essentially all of the absorbed dose and dose equivalent. Further improvements in characterizing cosmic-ray spectra can now be provided by the data from the Advanced Composition Explorer (ACE) launched in September 1997, and other missions such as ULYSSES, Solar Anomalous Magnetospheric Explorer, GEOTAIL (Kobayashi *et al*., 1998), and WIND. ACE, for example, has the capability to measure $>10^5$ oxygen and $>10^4$ iron nuclei in the energy range from ~100 to 1,000 MeV n^{-1} every 27 d solar rotation. Newer ACE measurements have recently led to improved model parameters (O'Neill, 2006).

Figures 3.9 and 3.10 show the integral and differential energy spectra of hydrogen, helium, oxygen and iron nuclei during the strongest observed cosmic-ray modulation (1989 to 1990) and weakest cosmic-ray modulation (1976 to 1977) during a solar cycle in the last 45 y. A very important question that bears on the design of spacecraft shielding is what are the likely maximum fluence rates which would be observed in an interplanetary environment? A possible answer to this can be seen from the relationship between $\phi(t)$ and the sunspot number. The lowest value of the sunspot number

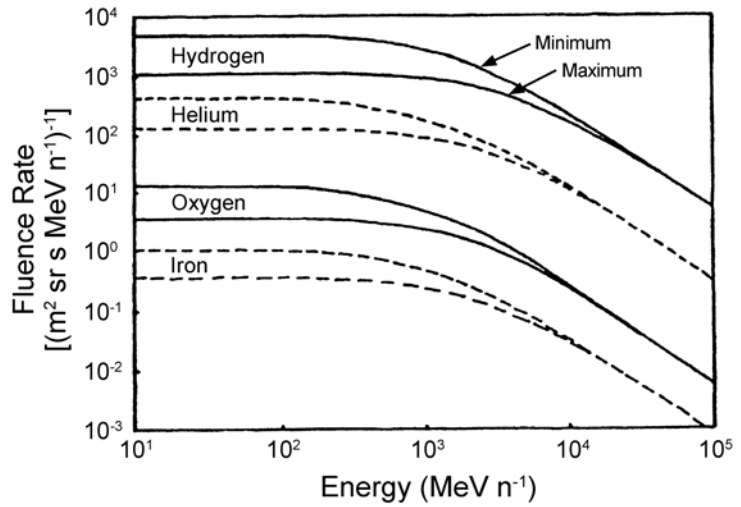

Fig. 3.9. Calculated integral energy spectra of hydrogen, helium, oxygen and iron for the 1976 to 1977 solar minimum and the 1989 to 1990 solar maximum.

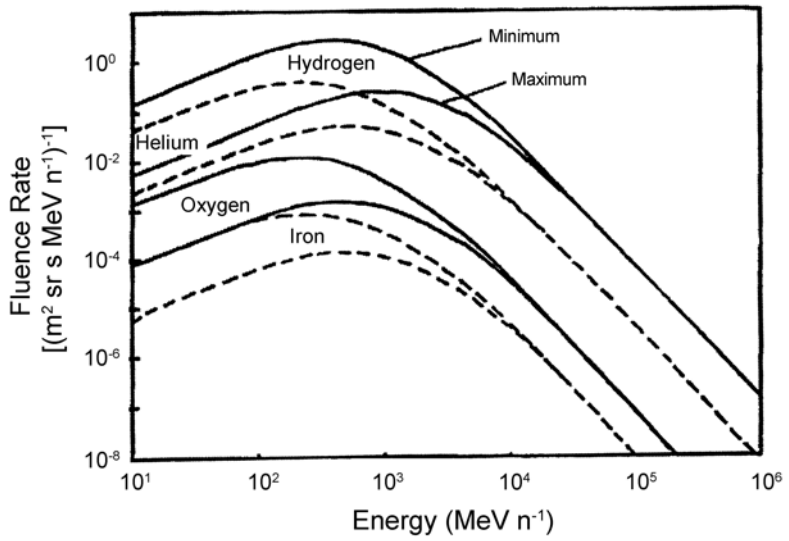

Fig. 3.10. Calculated differential energy spectra of hydrogen, helium, oxygen and iron for the 1976 to 1977 solar minimum and the 1989 to 1990 solar maximum.

in the 1954 to 1990 time period was around 20, when the lowest ϕ(MV) was ~400 MV. An extrapolation to sunspot number equals zero gives a value of ϕ of 370 MV. Thus, it is unlikely that fluence rates much larger than observed during the 1976 to 1977 solar minimum will be encountered. However, the next opportunity for such measurements will not occur until the expected solar minimum of 2020. Comments regarding the availability of alternative formalisms to those diffusion-convection models in the inner heliosphere have been made recently by O'Brien (2006).

3.1.3 *Radial Gradient of Cosmic-Ray Intensities*

The intensity of GCR fluence rates increases when moving radially outward from 1 AU to the boundary of the heliosphere (~90 to 160 AU). However, the gradient is relatively small, and can be ignored or taken into account fairly easily in the framework of the diffusion-convection model. For particles with energies >70 MeV n^{-1} the gradient is 2 to 3 AU^{-1} (McKibben,1987) and approaches ~12 % AU^{-1} for 300 MeV n^{-1} helium (Fujii and McDonald, 1997; McDonald *et al*., 1992). Thus, at the orbit of Mars the GCR fluence rate should only be ~5 % higher than the GCR fluence rate at 1 AU outside the influence of Earth's geomagnetic shield.

3.2 Solar-Particle Events

If adequate shielding is not available, large fluence rates of high-energy particles originating on or near the sun will pose the greatest radiation risk to space travelers outside the geomagnetosphere and, in any case, will impose important operational constraints on manned interplanetary space flight. Figure 3.11 illustrates the 175 MeV proton fluence rate observed at Earth from 1974 to 1994. The solar cycle modulation of GCR is clearly evident. Imposed on the GCR proton fluence rate are episodes when there are orders of magnitude increases in the observed fluence rate. These transient increases in the observed particle fluence rate are the result of energy releases into the solar corona where some of this energy has gone into the acceleration of energetic particles. As evident from Figure 3.11, these SPEs occur in many sizes and time scales. There is a general association of proton-event frequencies observed at Earth with the solar activity cycle, but it was the opinion of Shea and Smart (1990) that there was no repeatable systematic pattern in the proton-event occurrence in sequential solar cycles. Other researchers, however, such as Kurt and Nymmik

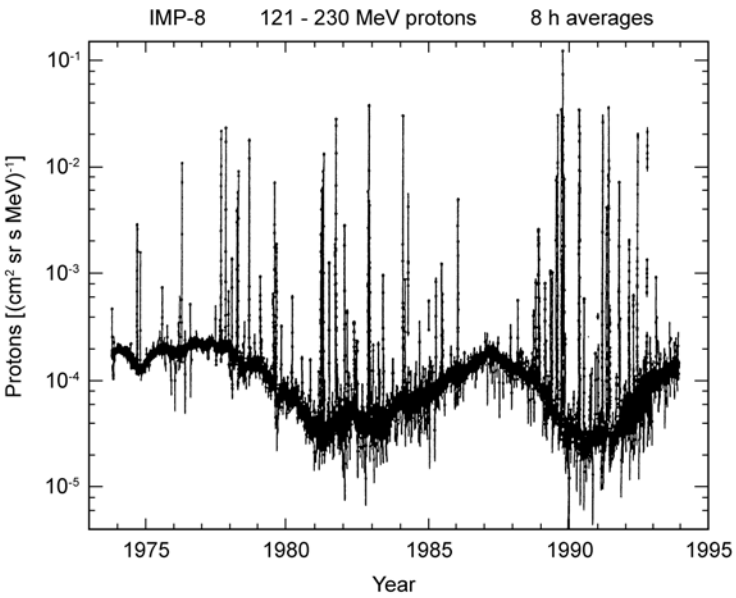

Fig. 3.11. The 121 to 230 (midpoint 175) MeV proton fluence rate observed at Earth from 1974 to 1994.[6]

(1997) and Nymmik (1996; 1997), have attempted to organize SPE frequency as a function of solar activity parameters.

3.2.1 *Solar-Particle Event Intensities*

For manned interplanetary missions the concern is that a very-large SPE could, in a short time period (hours or days), subject the vehicle to as much fluence at energies in the tens of megaelectron volts as a year of GCR exposure. There is a very small, but non-zero, possibility that an extraordinarily-large SPE would expose an interplanetary spacecraft to as much fluence at energies above tens of megaelectron volts as an entire solar cycle of exposure to GCR. SPEs of this magnitude (~5×10^9 cm^{-2}, ≥30 MeV) occurred in November 1960, August 1972, and October 1989.

Analysis of the existing record of SPEs measured by Earth-orbiting spacecraft for three solar cycles led Feynman *et al*. (1993) to conclude that solar-proton fluence during the active years

[6]Reames, D. Personal communication (National Aeronautics and Space Administration, Goddard Space Flight Center, Greenbelt, Maryland).

of the solar cycle is well approximated by a log-normal function. Other analysis of the same data using extreme value statistics (Xapsos *et al*., 1996) suggests that there may be two distributions. However, the application of either method gives similar results for the probability of a large fluence-rate value being encountered during a long-duration interplanetary mission. If it is assumed that the satellite energetic particle measurements acquired during the space era (1965 to the present) are truly representative of the SPE distribution encountered during missions beyond LEO, and the Jet Propulsion Laboratory (Feynman *et al*., 1993) particle fluence model is utilized to estimate the probability of occurrence of a very-large event, then the probability of an event containing a fluence of ~5×10^9 proton cm^{-2} at energies ≥30 MeV during a 2 y interplanetary mission near the solar cycle maximum is ~0.1 (Figure 3.12).

These types of models can be used to estimate probable exposure of a space vehicle on missions to the moon or Mars to an SPE during the solar active years for various mission durations. The Jet Propulsion Laboratory model is admittedly conservative since its intent was to insure that interplanetary vehicles would function for time periods of a decade or more in space (Feynman, 1997). Similar models for the heavy-ion component of the large SPEs observed

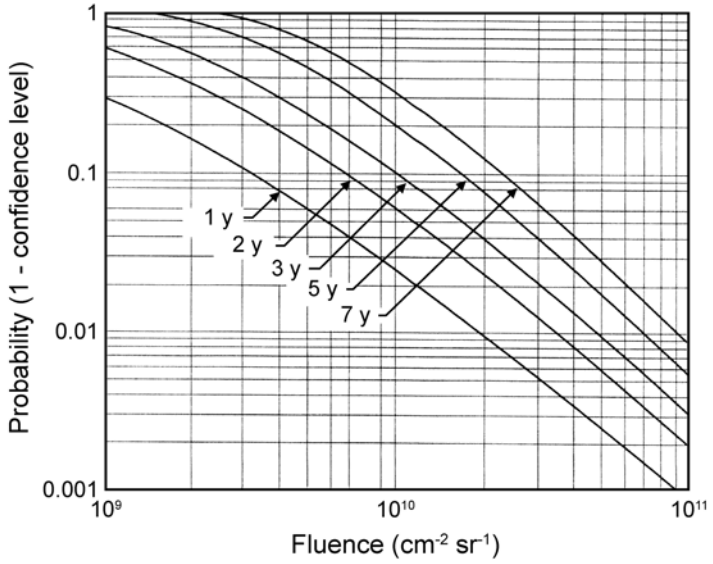

Fig. 3.12. The probable exposure to protons with energy ≥30 MeV during the solar active years for various exposure times in interplanetary space at 1 AU (Feynman *et al*., 1993).

during Solar Cycle 22, have been published by Tylka *et al*. (1997b; 1997c). These models can be used to estimate possible solar-particle exposure to interplanetary spacecraft from which risk assessments can be derived.

It had been previously suggested, as a result of the analysis of the SPEs observed in Solar Cycle 20, that there were ordinary and anomalously large events (King, 1974). Recent analysis of the fluence rate (Smart and Shea, 1997) and fluence data (Reedy, 1996) suggest that there may be two populations of SPEs. There may be one distribution of the most frequently occurring events, the events most likely to occur during a solar cycle. There may be a different distribution of extraordinarily-large and very-rare events, a class of events that may occur only about once a solar cycle or perhaps once in several solar cycles.

Estimates of the fluence distribution of SPEs over a very long period of time involve measuring the induced radioactivity in moon rocks and meteorites. Analyses of these data, combined with Earth measurements over the past four solar cycles, indicate that the very long-term SPE fluence distribution may be represented by a broken power law as illustrated in Figure 3.13 (see Reedy, 1996, for a review). The fluences of SPEs observed at Earth from 1954 through 1991 are in the left part of the figure. It is suggested that this distribution is representative of the most frequently occurring events. The right side of the figure shows the limits of the SPE fluences estimated from the analysis of induced radioactivity in moon rocks which encompasses a time span of perhaps one million years. The increasing slope of the fluence distribution for very-large events suggests that there may be limits to the acceleration process, and that extraordinarily-large events are very rare.

3.2.2 *Solar-Particle Event Spectra*

The SPE fluence as a function of energy is described by the particle spectrum. Many different spectral forms are used. The most commonly used spectral forms are a power law in energy or rigidity (rigidity is momentum per unit charge), an exponential form, or forms described by Bessel functions (McGuire and von Rosenvinge, 1984). Other forms used are a consequence of the expected results of shock-acceleration phenomena, which are not simple mathematical forms such as the Ellison and Ramaty (1985) shock-acceleration spectral form. More complex functional forms are being applied to better represent the particle spectrum, such as Weibull fits (Xapsos *et al*., 2000), and Bayesian statistics. Observed SPE integrated spectra acquired in 1978 by the ISSE-3 spacecraft instruments are displayed in Figure 3.14.

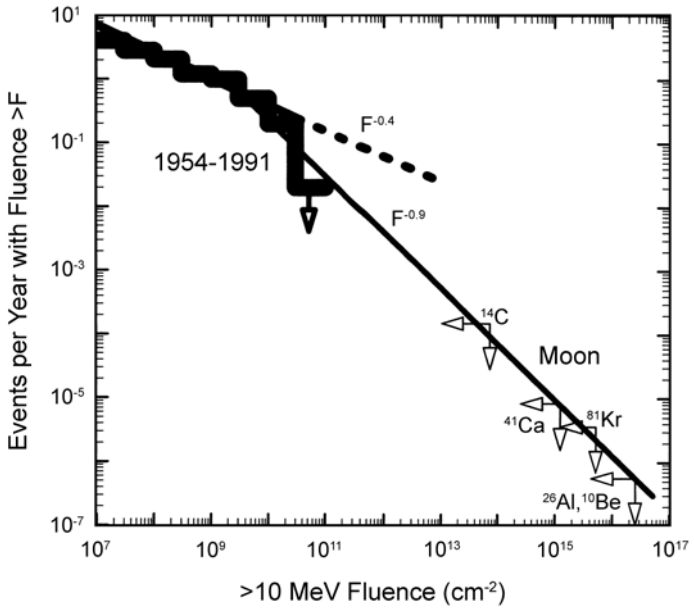

Fig. 3.13. The fluence distribution of Earth-sensed SPEs from 1954 to 1991 (heavy line) and the limits of the solar-proton fluences estimated from the analysis of induced radioactivity in moon rocks (adapted from Reedy, 1996).

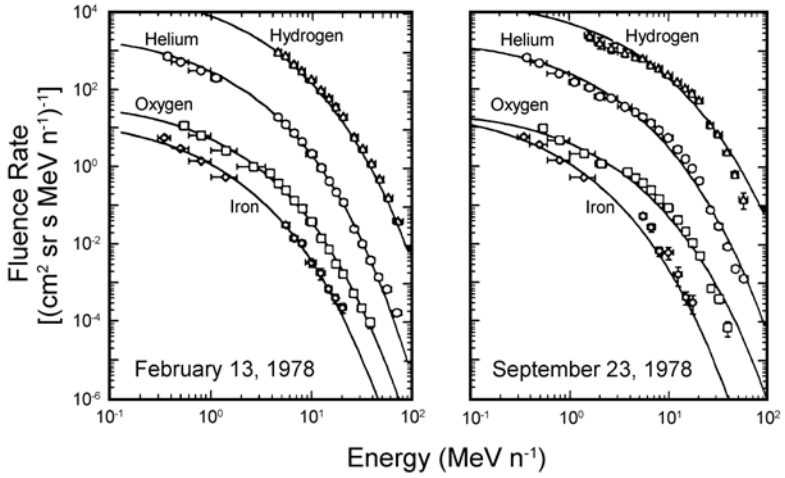

Fig. 3.14. Combined hydrogen, helium, oxygen and iron energy spectra for two large SPEs. The solid curves are fits to a stochastic particle acceleration model (adapted from Mazur *et al*., 1992).

The best recorded spectral information is for medium size SPEs. There are uncertainties associated with almost all of the very-large fluence-rate SPEs because many particle sensors saturate during the maximum fluence-rate phases of these events. The large fluence-rate SPEs do not appear to have a simple spectral form that is adequate to describe the particle fluence rate over five or more decades in particle energy (Figure 3.14). There are strong indications that these events have a complex spectral form that may be the result of intrinsic limiting features of the shock-acceleration process. The theoretical aspects of these limiting features are currently being investigated. The basic concept of the self-limiting features is that energetic protons, gyrating in a magnetic field, will generate hydromagnetic waves. As the proton fluence rate increases, the wave density will increase. Since the shock-acceleration scenarios are dependent on multiple scattering of the energetic particles through the shock front, as the wave density increases, there is an increasing probability that the particles will be scattered out of the acceleration region. It is possible that the streaming limit (Reames and Ng, 1998), a phenomenon where at high fluence-rate levels the proton self-generated waves affect particle acceleration and result in a flattening of the lower energy portion of the solar-particle spectrum (Reames, 1999a), biases the <100 MeV portion of the solar-proton spectrum, so that simple spectral forms are not truly representative of the entire energy range of the solar-proton fluence rate.

3.2.3 *Particle Sources*

There has been a dramatic change in perspective regarding the source of energetic particle events. In the past, the names solar cosmic rays and solar energetic particles were commonly used to describe transient increases in particle fluence rate that seemed to be associated with the occurrence of a solar flare. A new paradigm suggests that a source of the energetic ions observed in space is the result of acceleration of ions by interplanetary shocks generated by fast CMEs (see Reames, 1995a; 1999a for reviews).

Both the solar-flare scenario and the shock-acceleration scenario have enthusiastic advocates. Many of the large SPEs are associated with large solar flares. However, only about one-half of the SPEs observed at Earth can be unambiguously and confidently time-associated with specific solar flares. The intensity-time profiles of SPEs leave no doubt that interplanetary shocks accelerate ions.

In the following discussion the terms near-sun injection and extended interplanetary shock source are used to distinguish

between types of SPEs observed in interplanetary space. The near-sun injection will refer to the class of SPEs in which the intensity-time profile at the observer's position is dominated by the particle fluence rate injected near the sun onto the observer's interplanetary field line (Figure 3.15). This scenario represents the classic SPE illustrated by the October 24, 1989 event shown in Figure 3.16. This class of SPE often has relatively hard spectra (hard meaning more than an average number of particles at high energies). The extended interplanetary shock source will refer to the class of SPEs that does not conform to the classic intensity-time profile, but instead has a characteristic that the fluence rate continues to increase until a maximum fluence rate is observed as a powerful and fast interplanetary shock overtakes the observer, after which the fluence rate decreases. An example of this type of event is the March 1991 SPE as observed at Earth (Figure 3.17). This example is probably typical of this type of event with a relatively soft spectrum.

Historically, since large transient increases in particle fluence rate could often be associated with solar flares it was assumed that the solar-flare process was the source of energetic particles observed in space. The solar-flare acceleration process was assumed to be of an explosive nature, and it was further assumed that a full

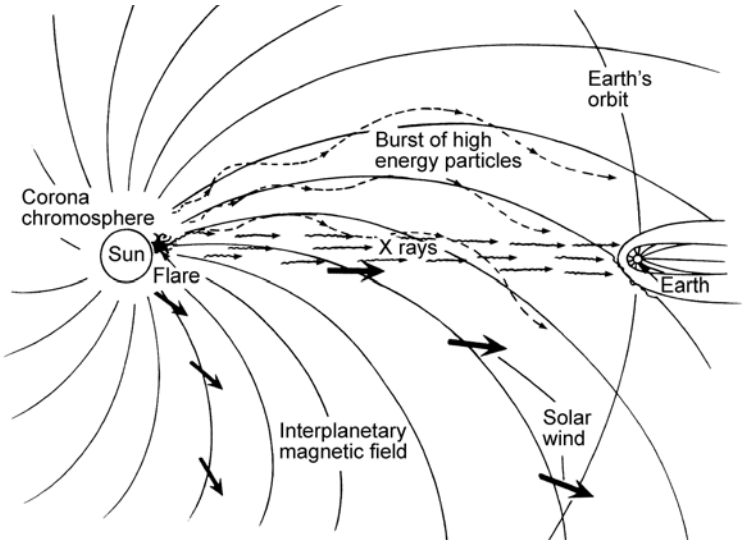

Fig. 3.15. Conceptual view of the basically Archimedean spiral geometry of the interplanetary magnetic field. The propagation of solar charged particles is controlled and organized by the interplanetary magnetic field.

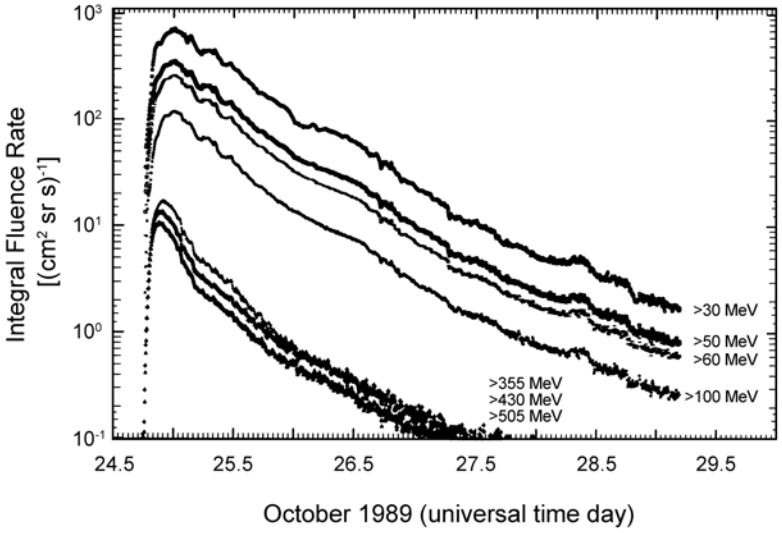

Fig. 3.16. The intensity-time profile of a classic SPE as observed at 1 AU. The intensity-time profile of this October 24, 1989 event observed at Earth is dominated by the near-sun injection of energetic particles onto the interplanetary magnetic field lines connected to Earth.

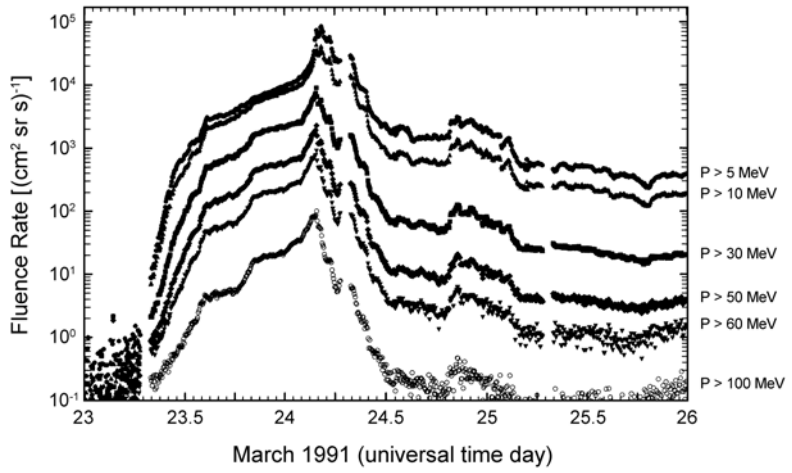

Fig. 3.17. The intensity-time profile of the extended interplanetary shock source class of an SPE. The maximum fluence rate was observed as the powerful fast interplanetary shock passed Earth on March 24, 1991.

spectrum of energetic particles would impact a location in space very soon after the initial particle acceleration. This presumption led to large dose estimates early in an SPE. Papers written in the 1960s and 1970s reflect this assumption (see for example Keller and Pruett, 1965). However, the measurements of large SPEs made during Solar Cycles 22 and 23 do not support the idea of an explosive impact of the full particle spectrum at a location in space.

In addition, papers written in the 1950s through the 1980s also reflect the assumption that SPEs were accelerated from the available material in or above the solar active region in which the flare occurred. During Solar Cycles 21 and 22, as measurement techniques improved, the elemental and isotopic composition of solar particles observed at various interplanetary spacecraft were found to be consistent with the particles having passed through <30 mg cm^{-2} of matter from the acceleration site to their detection location (Mason, 1987). Thus, the solar photosphere is eliminated as the source region of the particles observed in space since the elemental and isotopic composition of these solar energetic ions did not appear to have undergone fragmentation due to interaction with the significant mass of the solar atmosphere.

3.2.3.1 *Solar-Flare Particle Source*. In the current understanding of SPEs there are impulsive flares associated with SPEs which are the class of SPEs associated with impulsive solar x-ray events. The charge state of solar energetic ions provides information on their origin. The impulsive-flares associated SPEs have an elemental composition and charge state that is consistent with a multimillion degree hot ($\sim 2 \times 10^7$ °K) plasma source.

Extensive studies of these impulsive-flare associated SPEs by Cane *et al*. (1986) and Reames *et al*. (1994) showed that these events are generally small fluence and fluence-rate events measurable in space over a restricted heliolongitudinal range, about one radian of heliolongitudinal distance centered on the most favorable propagation path from the solar-flare location (Figure 3.15). The intensity-time profile of these impulsive-flare associated energetic particle events observed at Earth usually has the classic SPE profile since the solar-particle fluence rate observed is dominated by the near-sun particle injection and there is no extended interplanetary CME-shock source.

3.2.3.2 *Fast Interplanetary Shock Particle Source*. A new paradigm suggests that a source of the energetic ions observed in space is the result of acceleration associated with interplanetary shocks generated by fast (speeds in excess of the local Alfven speed in the

plasma) CMEs (see Reames, 1995a, for a review). It is hypothesized that the shock interaction accelerates some fraction of the ions in the solar corona or the local solar wind. The diffusive shock-acceleration scenario (Jones and Ellison, 1991; Lee, 1983; 1992; 1999; Lee and Ryan, 1986), a concept where particles near the shock are scattered back and forth across the shock by waves, gaining energy with each interaction, is favored as a mechanism for continuous acceleration of particles as the shock travels out from the sun. The accelerated particles stream away from the shock along the interplanetary magnetic field lines. The particle intensity-time profile will depend on how the observer is connected to the shock *via* the interplanetary magnetic field (Cane *et al*., 1988). As the shock approaches the observer, the observed fluence rate may increase. The magnitude of this increase is dependent on many parameters, not all of which are currently identified or understood. Some of these parameters are particle energy, the shock speed, and the turbulence in the plasma. In general, a low-energy (~1 MeV) fluence-rate maximum will be measured as the shock passes the observer.

Large SPEs seem to be associated with the occurrence of a fast CME or, in the absence of actual CME observations, CME proxies. This association is complicated by the fact that large fast CMEs also seem to have an association with big solar flares. The long-duration solar x-ray event is considered to be an excellent CME proxy. Figure 3.18 illustrates the fast CME associated with the October 24, 1989 SPE observed at Earth.

Particle fluence-rate enhancements associated with the passage of powerful and fast interplanetary shocks is a concept still being defined. A common misconception is that there will always be a fluence-rate enhancement with the passage of an interplanetary shock. This is true only at low energies (~1 MeV and below). At higher energies (≥30 MeV) it is the exception when a fluence-rate enhancement is observed with the passage of an interplanetary shock. Kallenrode (1993) and Kallenrode *et al*. (1993) examined the entire HELIOS particle database and found at 20 MeV that the correlation between the shock-jump plasma parameters and the fluence rate increase was approximately zero. The current theoretical modeling of the shock-acceleration phenomena has great difficulty in simulating acceleration of particles to high energies (Heras *et al*., 1995; Lario *et al*., 1998).

Finally, note that both of the above source mechanisms may play a role in the evolution of a single high-energy particle event. An example of this is the last significant particle event of Solar-Cycle 22, which began on February 20, 1994, and is shown in Figure 3.19. This is an event having both an initial near-sun injection

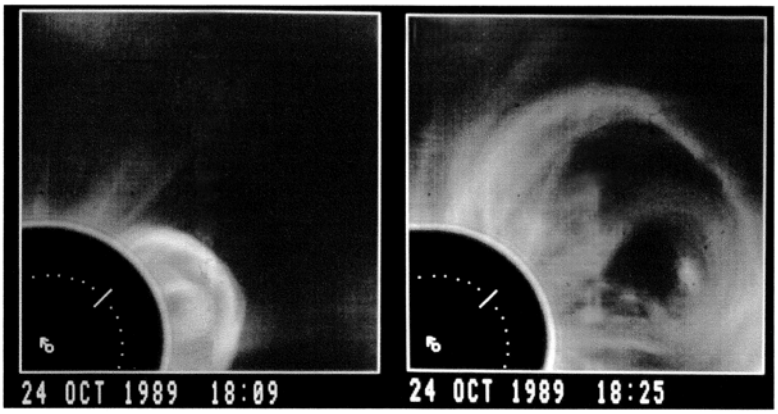

Fig. 3.18. The fast CME associated with the October 24, 1989 SPE observed at Earth.

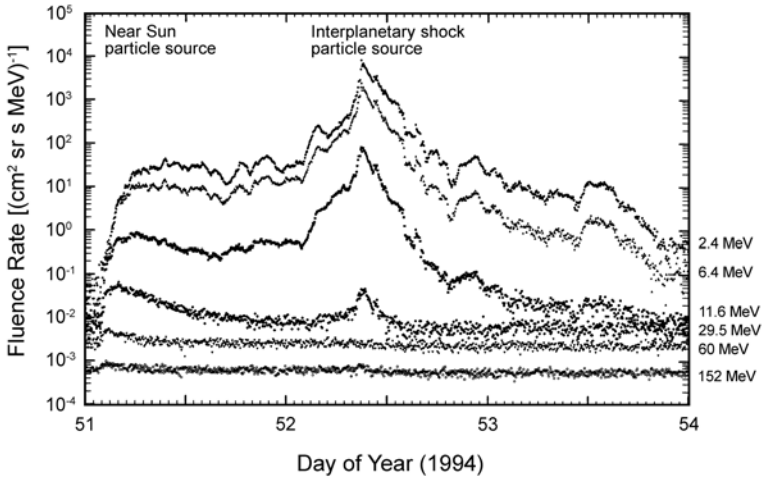

Fig. 3.19. The intensity-time profile of a composite SPE showing both the initial near-sun injection and the extended interplanetary shock-source fluence-rate profile.[7]

[7]Hundhauser, A. (1994). NASA solar maximum mission coronal image (High Altitude Observatory, Boulder, Colorado).

and a fluence-rate profile dominated by an extended interplanetary shock source.

3.2.4 *Solar-Particle Transport in the Inner Heliosphere*

The transport of solar particles in interplanetary space is controlled by the topology and characteristics of the interplanetary magnetic field. The topology of the magnetic field lines in interplanetary space is controlled by the flow speed of the ionized plasma and the rotation rate of the sun, resulting in the so-called Archimedean spiral configuration (Figure 3.15). SPEs observed in space resulting from solar activity at the probable foot point of an idealized Archimedean spiral interplanetary magnetic field line leading from the observer back to the sun are considered to be well-connected events. This means that the propagation path of the solar particles was probably along the interplanetary magnetic field lines with minimal scattering due to irregularities in the interplanetary magnetic field. This concept is often referred to as the favorable propagation path. The highest particle fluence-rate intensities are often observed along this favorable propagation path with lower fluence rates usually observed at heliocentric angular distances away from the favorable propagation path.

The particle fluence-rate longitudinal gradients in the inner heliosphere are variable, and local interplanetary conditions and structures greatly influence the time-intensity profiles observed. The average heliolongitudinal gradient of particle fluence rate is difficult to determine. However, the longitudinal proton fluence-rate gradient used in the U.S. Air Force (USAF) proton prediction system is a one order of magnitude decrease in fluence rate per radian of heliolongitudinal distance away from the most favorable propagation path (Smart and Shea, 1979; 1985).

There is a radial gradient in spacecraft observations of energetic particle fluence rate at different distances from the sun, which is most pronounced in the inner heliosphere. This gradient is the result of an initial near-sun particle injection and particle propagation away from the sun along the interplanetary field lines. The most extensive measurements are comparisons between the fluence rate measured by Earth-orbiting spacecraft and interplanetary spacecraft orbiting from 0.3 to 1 AU (primarily from the HELIOS spacecraft). There are less data available between 1 and 3 AU.

The form and magnitude of these radial gradients are the subject of controversy reflecting the difference between a solar-flare acceleration source and a CME-shock-acceleration source. In the

outer heliosphere, at distances of 5 AU and beyond, the particle fluence-rate profiles are dominated by major interplanetary shock structures.

3.2.4.1 *Characteristics of Solar Particles at 1 AU.* The majority of the solar-particle data that exist have been collected at Earth by ground-based sensors or by Earth-orbiting spacecraft. Prior to 1967, most of the solar-proton data were derived from analysis of the response of Earth's ionosphere to SPEs, therefore the spectral information derived lacks the accuracy of the spacecraft data. Most of the spacecraft data collected have been at energies <100 MeV. There is relatively good data coverage for energies in the range of 10, 30 and 60 MeV extending from 1967 to the present. These data are sufficient to derive meaningful statistics for modeling purposes. There is a serious deficiency in the fluence rate and spectral characteristics of SPEs at energies ≥100 MeV. *It is imperative that such data be available in order to provide reliable dose calculations for risk estimation*.

3.2.4.2 *Composition of Solar-Particle Events.* A recent quantification of SPEs classifies the particle emission by the associated solar x-ray emission as impulsive events or gradual events. The impulsive-flare events are those associated with impulsive solar x-ray events. The gradual events are those that seem to be associated with fast CMEs or with fast CME proxies. The composition of large or gradual SPEs appears to be relatively consistent with an ion selection process based on the first ionization potential of the elements in the solar corona or wind. The composition of impulsive or small SPEs is variable and has been separated into distinct composition groups (Table 3.2). From an astrophysical point of view the iron-rich and ^{3}He-rich events are extremely interesting, perhaps reflecting processes in the solar corona, but the particle fluence rate in these events is usually small. These types of events are less important from a radiation protection point of view because the energy per nucleon is low and even moderate shielding (such as the normal structure of a space vehicle) is likely to provide adequate crew protection.

The elemental composition of SPEs is important from a radiation protection viewpoint, since the composition is necessary for precise dose calculations. Large SPEs observed during the last two solar cycles have an elemental composition that is dominated by protons with the heavy-ion component being a small fraction of the proton fluence (Figure 3.14). The analyses of large SPEs (Mazur *et al*.,

TABLE 3.2—*Properties of impulsive and gradual SPEs characterized by the associated solar-flare x-ray emission (adapted from Reames, 1995b).*

	Impulsive X-Ray Event	Gradual X-Ray Event
	(associated particle event characteristics)	
Particles	Electron rich	Proton rich
^{3}He, ^{4}He	~1	~0.0005
Fe, O	~1	~0.1
H, He	~10	~100
Charge state of iron	~20	~14
Duration	Hours	Days
Heliolongitude range	<30° (generally well connected)	~180°
Associated solar radio type	III, V, (II)	II, IV
Associated solar x-ray emission	Impulsive	Gradual
CME association	—	96 %
Associated interplanetary shock	—	Yes
Events per year (at solar maximum)	~1,000	~10

1992; Reames, 1992) have shown that large events have an elemental composition that is relatively consistent (perhaps within a factor of three). Reames (1995b; 1998) concluded that in the energy range of ~1 to 20 MeV, the elemental composition ratios were relatively consistent, although there are event-to-event variations, particularly in the helium to hydrogen ratios. The ratio of the abundances of the elemental composition observed in large SPEs compared to the abundances of the elemental composition observed in the solar photosphere appears to be a function of the first ionization potential of the individual elements. Some researchers contend that large SPEs are a reasonable sample of the solar corona (Breneman and Stone, 1985; Mewaldt and Stone, 1989; Reames, 1998). The average elemental composition of large SPEs is given in Table 3.3.

TABLE 3.3—*Average relative element composition of large SPEs normalized to oxygen at 1,000 (adapted from Reames, 1999a).*

Mean Element	Z	First Ionization Potential	Solar Photosphere (O ≡ 1,000)	Solar Particle (O ≡ 1,000)
H	1	13.53	1,350,000	1,570,000 ± 220,000
He	2	22.46	132,000 ± 11,000	57,000 ± 3,000
C	6	11.22	479 ± 55	465 ± 9
N	7	14.48	126 ± 20	124 ± 3
O	8	13.55	1,000 ± 161	1,000 ± 10
Ne	10	21.47	162 ± 22	152 ± 4
Na	11	5.12	2.9 ± 0.2	10.4 ± 1.1
Mg	12	7.61	51 ± 6	196 ± 4
Al	13	5.96	4 ± 0.6	15.7 ± 1.6
Si	14	8.12	48 ± 5	152 ± 4
P	15	10.9	0.38 ± 0.04	0.64 ± 0.17
S	16	10.3	2 ± 7	31.7 ± 0.7
Cl	17	12.95	0.4 ± 0.3	0.24 ± 0.1
Ar	18	15.68	4.5 ± 1	3.3 ± 0.2
K	19	4.32	0.18 ± 0.55	0.55 ± 0.15
Ca	20	6.09	3.09 ± 0.14	10.6 ± 0.4
Ti	22	6.81	0.14 ± 0.02	0.34 ± 0.1
Cr	24	6.74	0.63 ± 0.04	2.1 ± 0.3
Fe	26	7.83	42.7 ± 3.9	134 ± 4
Ni	28	7.61	2.4 ± 0.05	6 ± 0.6

3.2.4.2.1 *Impulsive Solar-Particle Events.* The impulsive-flare-associated SPEs seem to be most closely related to the solar-flare particle acceleration process. Initially, these events were considered as composition anomalies since there were distinct differences from large SPEs. They were sometimes called ^{3}He-rich or iron-rich events. In general, the fluence rates in the impulsive events are orders of magnitude smaller than large or ordinary SPEs. The average elemental composition of impulsive SPEs is given in Table 3.4.

TABLE 3.4—*Relative elemental abundances in impulsive-flare associated SPEs normalized to oxygen at 1,000 (adapted from Reames, 1999b).*

Element	Z	Averaged Impulsive-Flare Associated (O ≡ 1,000)
H	1	~1,000,000
^{4}He	2	46,000 ± 4,000
C	6	434 ± 30
N	7	157 ± 18
O	8	1,000 ± 37
Ne	10	400 ± 28
Mg	12	408 ± 29
Si	14	352 ± 27
S	16	117 ± 15
Ca	20	88 ± 13
Fe	26	1,078 ± 46

3.2.4.2.2 *Long-Duration Solar-Particle Events*. The available data reflect the composition at relatively low energies (a few mega-electron volts to perhaps 10 MeV). The analysis of Mazur *et al*. (1992) suggested that there was relative consistency of the elemental composition during an event (up to energies of ~30 MeV). However, the latest analysis of the heavy-ion composition at high energies (≥100 MeV n^{-1}) for large fluence-rate events (Tylka *et al*., 1997c) suggests that the iron to oxygen ratio is a function of energy with variations larger than those reported by Mazur *et al*. (1992).

Calculations of the relative contributions to the total dose predicted behind nominal spacecraft shielding thickness indicate the proton component was the principal dose contributor for the large SPEs observed during the last four solar cycles, even if an iron-rich elemental composition was considered (Townsend *et al*., 1994).

3.2.4.3 *Solar-Particle Fluence-Rate Anisotropy.* The particle fluence-rate anisotropy is generally defined as the ratio of the maximum particle fluence rate divided by the average of the particle fluence rate in all directions. In the isotropic case, there is equal particle fluence rate from all directions. In the anisotropic case, there is an excess of particle fluence rate in one specific direction, generally along the interplanetary magnetic field direction. If it is assumed that the energetic charged particles are constrained to

travel along an interplanetary magnetic field line with little scattering across field lines, then the particle fluence-rate anisotropy also reflects the rate at which particles are injected onto the observer's interplanetary field line with respect to the rate at which the particle fluence rate is transported away from the observer. In the case where there is a near-sun injection of energetic charged particles, the particle fluence rate observed downstream will be initially anisotropic, with the degree of anisotropy decreasing as particles that have passed the observer scatter and are reflected back. In the case of extended interplanetary shock-dominated particle events, the relatively mild low-energy particle fluence-rate anisotropy is observed to change direction as the shock passes the spacecraft.

Particle fluence-rate anisotropy is a transient phenomenon, and at the energies important to dose calculations, at radial distances from the sun between Earth and Mars, a duration of a few hours is typical. In the example shown in Figure 3.20, there was no significant anisotropy remaining after 0.1 d. This figure illustrates the proton fluence-rate anisotropy at ~30 MeV observed by the HELIOS spacecraft at 0.95 AU during a large anisotropic SPE in June 1980 (day of year 173). The anisotropy amplitude (denoted by "A" in Figure 3.20) ranges from ~1 (extreme) to ~0.2 (low). An artifact of fitting a cosine function to coarsely sectored data results in anisotropies having values greater than one as shown in the first illustration of the figure.

3.2.5 *Extrapolation of Earth-Sensed Solar-Particle Events to Mars or Other Radial Distances*

The usual method for estimating the energetic proton environment for a Mars mission is to take the solar-proton observations at 1 AU and extrapolate them to other radial distances. In these extrapolations it is assumed that the proton fluence rate is confined to a magnetic fluence-rate tube and the volume of this tube will behave in the classical manner as the radial distance from the sun (which is designated as R) increases. From this purely geometrical argument, the peak fluence-rate extrapolations should behave as a function of R^{-3}, and the fluence extrapolations should behave as a function of R^{-2}. The limited experimental data of measuring the same event at different radial distances (Hamilton, 1977) generally confirm the utility of this type of radial extrapolation, however with a modified form of the power laws. The working group consensus recommendations for radial extrapolation documented in a Jet Propulsion Laboratory report edited by Feynman and Gabriel (1988) were:

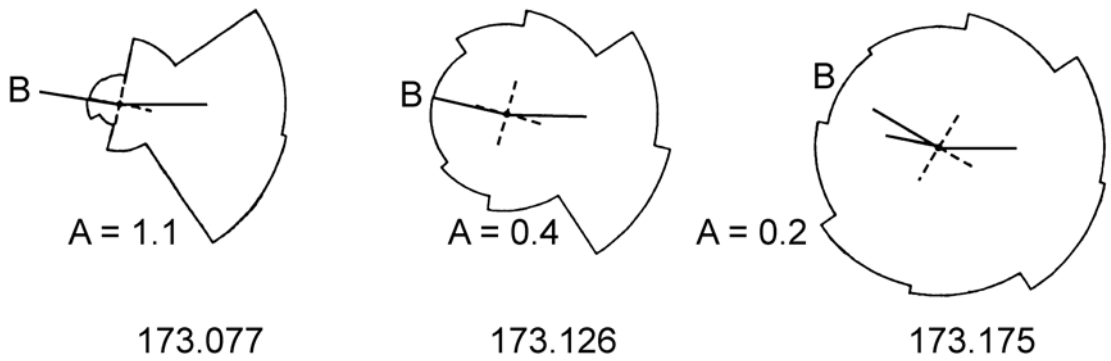

Fig. 3.20. The sectored proton fluence-rate anisotropy (A) at ~30 MeV measured by the HELIOS spacecraft during an anisotropic SPE observed by this interplanetary spacecraft in June 1980 (day of year 173). The distance of the sector envelope from the center indicates the relative directional particle fluence rate. The line labeled "B" indicates the magnetic field direction, and the line to the right of center indicates the direction toward the sun (adapted from Kunow, 1994).

- Fluence-rate extrapolations from 1 to >1 AU; use a functional form of $R^{-3.3}$ and expect variations ranging from R^{-4} to R^{-3}.
- Fluence-rate extrapolations from 1 to <1 AU; use a functional form of R^{-3} and expect variations ranging from R^{-3} to R^{-2}.
- Fluence extrapolations from 1 AU to other distances; use a functional form of $R^{-2.5}$ and expect variations ranging from R^{-3} to R^{-2}.

These generalizations only apply to well-connected solar-flare associated events (*i.e.*, the near-sun injection events). They do not always apply to the extended interplanetary shock source events.

There are a number of suggestions that the SPE profile observed at 1 AU may be dominated by the injection and release of particles from the acceleration source. The concept of scatter-free propagation was developed to explain the apparent lack of any significant diffusion in some of the observed solar-particle intensity-time profiles in the inner heliosphere. Scatter-free propagation means that apparently the charged particles travel along the interplanetary magnetic field lines with little scattering or cross field diffusion. Reames (1995b) and Reames *et al*. (1996), based on multi-spacecraft analysis of the fluence rate observed at different locations and radial distances in the inner heliosphere by the HELIOS spacecraft and Earth-orbiting spacecraft, have suggested the observed solar-particle fluence-rate profile may be dominated by the connection to the extended shock-acceleration source rather than by particle diffusion.

3.2.6 *Solar-Particle Event Prediction Capability*

Presently, the ability to forecast large SPEs in advance is quite limited. It will be very important to improve this ability before embarking on extended manned missions outside of the geomagnetosphere. The distinct possibility that a single SPE could expose an unshielded astronaut to potentially dangerous radiation levels, leads to a requirement for a storm shelter as part of an interplanetary space vehicle. The unpredictability of extremely-large SPE requires this storm shelter to be available on the time scale of an hour. The storm-shelter design should be able to reduce the dose to blood-forming organs experienced by an astronaut inside the shelter during an extremely-large SPE [3 σ larger than the average (Table 3.5)] to levels below the nausea threshold. The recommendation of the NASA Modeling and Analysis Working

TABLE 3.5—*The Nymmik solar-proton fluence classification (Nymmik, 1996; 1997).*

Class	Omnidirectional ≥30 MeV Fluence			
	Number (σ)[a]	Lower-Value Fluence (cm^{-2})	Mean-Value Fluence (cm^{-2})	Upper-Limit Fluence (cm^{-2})
Small	Average – 1 σ	$<2 \times 10^6$		
Normal	Average	2×10^6	$\sim 9 \times 10^6$	3.4×10^6
Large	Average + 1 σ	3.4×10^7	$\sim 1 \times 10^8$	5.3×10^8
Very large	Average + 2 σ	5.3×10^8	$\sim 2 \times 10^9$	8.3×10^9
Extremely large	Average + 3 σ	8.3×10^9	$\sim 2 \times 10^{10}$	

[a]Sigma (σ) is one standard deviation of the log-normal frequency distribution.

Group (Badhwar, 1997a) was that a prudent storm-shelter design should protect against >30 MeV omnidirectional free-space fluence of 8×10^9 proton cm^{-2}.

3.2.6.1 *Current Capabilities of Forecasting Solar-Particle Events Observed at Earth*. In the United States, the National Oceanic and Atmospheric Administration (NOAA) Space Environment Center (SEC) and USAF 55th Weather Squadron are responsible for providing space weather forecasts. NOAA SEC provides space weather forecasts to U.S. domestic civil and international users. The USAF 55th Weather Squadron serves specialized Department of Defense needs. Both centers share available data and both centers predict SPEs with approximately equal skill levels and success rates. SPE alerts are one of several products that NOAA currently provides to the National Aeronautics and Space Administration (NASA) Space Radiation Analysis Group.

When the available information indicates that conditions are favorable for the generation of an SPE, NOAA estimates the probability and the intensity of the event with the aid of a phenomenological model, PROTONS, first developed in 1972 and modified incrementally as experience accrued. The model is used if a sufficiently intense x-ray event is observed or if a significant radio burst is reported. Details of the model are described by Heckman (1993)

and Heckman *et al*. (1992). A list of products produced and distributed by NOAA is included in its *Products and Services User Guide* (NOAA, 1993).

The USAF objective is to predict solar-proton fluence rates that cause interference with USAF space systems or communications. Experience has shown that significant fluence rates of protons with energies ≥50 MeV are likely to cause interference in space systems (Wilkinson *et al*., 2000). The USAF 55th Weather Squadron does not attempt advance proton-event forecasting but operates in the reaction mode responding to a requirement to generate a system-specific forecast (the times when a specific system might expect interference from solar protons) within 15 min after the occurrence of a significant solar flare. The basic system is a phenomenology based model (Smart, 1988; Smart and Shea, 1979; 1985; 1992) of the expected behavior of the solar-proton fluence rates of various energies at Earth from a near-sun injection of solar particles at the position of the observed solar flare.

3.2.6.2 *Monitoring Information Currently Acquired for Proton-Event Forecasting*. The NOAA SEC Space Weather Operations in Boulder, Colorado receives data from the NOAA GOES spacecraft, the USAF global Solar Electro-optical Observing Network, and from other ground- and space-based assets, as available. The Solar Electro-optical Observing Network provides data on sunspot activity, flare locations, solar magnetic field maps, and radio wave spectra. GOES provides data on energetic charged particles and whole-disk solar x-ray fluence rates (x rays from the entire solar visible hemisphere). The data received, their source, accuracy and resolution, the average time available (coverage), and an explanation of some limitations of the data are described by Cliffswallow and Hirman (1992).

The NOAA PROTONS model uses as input:

- soft x-ray peak fluence rate and/or time-integrated power;
- location of observed flare (heliographic latitude and longitude);
- radio-burst data; and
- recent levels of solar activity in the same active region on the sun.

The USAF model uses as input:

- radio-burst data specifying the solar-flare peak power radio-emission spectra;

- location of observed flare (heliographic latitude and longitude). Solar radio peak or time-integrated power in the microwave frequencies monitored by the USAF solar radio network; or
- soft x-ray peak fluence rate, or time-integrated soft x-ray power.

3.2.6.3 *Limitations of the Prediction Capabilities.* Current SPE forecast methods rely on the concept of a solar-flare associated event and a subsequent near-sun injection of energetic particles that will be transported along the interplanetary magnetic field through space. The success of forecasts triggering on the big flare syndrome (Kahler, 1982), is probably due to the fact that solar-flare proton diagnostics are the same as the proxies for CMEs. The lack of a method to observe or account for interplanetary shocks and CMEs is one of the major deficiencies of quantitative SPE predictions.

NOAA SEC forecasters have some skill in predicting the likelihood of M- and X-class x-ray flare days in advance of the occurrence based on observations of an active region's history, size, complexity and recent changes. They are currently unable to project the probability of SPEs 1 to 3 d in advance. Heckman (1993) notes that NOAA SEC forecasters often significantly overestimate the probability of a proton event.

Currently an NOAA SEC forecast gives the probability for the occurrence of an SPE and an estimate of the peak particle intensity if an event occurs. When SPE predictions have been issued and a significant event occurred, the predicted peak particle fluence rate has been generally, but not always, within an order of magnitude of the observed fluence rate (Figure 3.21). Prediction of the SPE's spectral characteristics has not proven to be reliable for large events. Similarly, the intensity-time fluence-rate profile predictions have not been adequate for shock-dominated SPEs.

Recently developed event-triggered methods of forecasting doses over time from SPEs, using dosimeter measurements obtained early in the evolution of an event and coupled with Bayesian influence and artificial neural network methods, have met with some success (Hoff *et al*., 2003; Neal and Townsend, 2001; Townsend *et al*., 1999). These methods, however, can only be used after the SPE begins to arrive at the spacecraft.

3.2.6.4 *Forecasting Solar-Particle Events for Lunar Missions.* For lunar exploration, there is a need for reliable forecasts of safe periods, to be made at least 1 to 3 d in advance, in order to allow

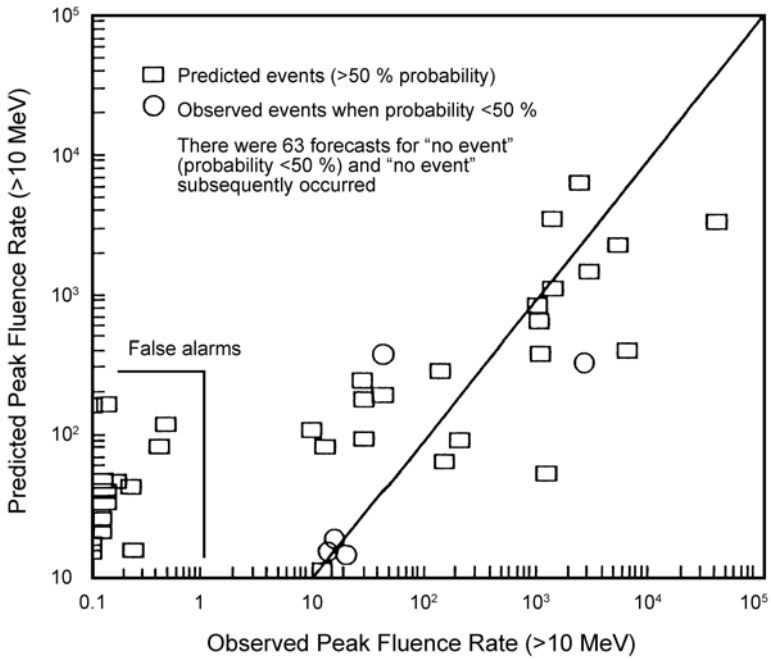

Fig. 3.21. Predicted peak particle fluence rate for SPEs in 1989 by the NOAA Space Environment Center PROTONS Model (Heckman *et al*., 1992). The diagonal line defines perfect forecasts.

astronauts to safely explore the surrounding terrain. If an SPE should occur, the particle fluence rate will envelope a lunar base without magnetic field attenuation. This increases the urgency of accurate forecasts of the time of arrival, rise time, peak fluence rate, and duration of each particle event (see Wilson *et al*., 1997a; 1997b, for details). It is essential to accurately forecast solar activity, specifically the probability of the occurrence on the sun of a fast CME within hours or days. A more specific need is to identify reliable diagnostics for the occurrence of solar activity associated with solar-particle acceleration and release into the interplanetary medium and to reliably predict the SPE characteristics at the position of the astronaut, specifically the fluence rate, fluence, composition, spectra, and time evolution. This requires the ability to predict the interplanetary particle source and transport. For successful forecasts that may impact the astronauts, there is a need for prediction algorithms for biologically effective energies.

3.2.6.5 *Considerations for Forecasting Solar-Particle Events for Space Missions to Mars*. As already indicated, the current SPE

forecast capability is inadequate for manned interplanetary missions. Essentially, the forecast centers operate in a reaction mode where there is some skill in forecasting SPEs that will affect Earth after the occurrence of a significant event on the sun that has the characteristics of solar-proton generating activity.

It is reasonable to assume that Earth-based solar monitoring network will support a Mars mission with SPE forecasts and alerts. However, there are substantial limitations. Earth will not always be in a position to watch critical regions of the sun which may be well connected to the spacecraft position or the position of Mars, or to monitor significant solar wind parameters which will pass by the spacecraft or planet. There may also be significant communication delays resulting from the large separation distances between the actual location of a spacecraft in transit to Mars and Earth.

For missions to Mars, there is a critical need to be able to accurately forecast solar events likely to accelerate and release a large fluence rate of solar particles onto the interplanetary magnetic field lines connected to the spacecraft position. During the interplanetary transit phase of such a mission, it will be necessary to forecast the probability of a fast CME in the next N hours or days and to reliably predict the SPE's characteristics at the position of the spacecraft, specifically the fluence rate, fluence, composition, spectra, and time evolution. For successful forecasts that may impact the astronauts, there is a need for prediction algorithms for biologically effective energies.

For Mars exploration, reliable forecasts that no significant SPE will occur in the next N days in the future, would allow astronauts to leave their home base to explore the surrounding terrain. The Mars surface radiation exposure will be less than the free-space exposure because the planetary mass and atmosphere will reduce the solid angle of incident charged particle radiation to slightly $<2\pi$ steradians. The ~16 g cm^{-2} of mass shielding (mainly CO_2) of the Martian atmosphere will offer some additional attenuation of the free-space solar-particle radiation (see Wilson *et al*., 1997a for a more detailed analysis). In some respects, the prediction of astronaut doses during Mars surface exploration is analogous to predicting the radiation dose for hypersonic high-altitude flight in Earth's upper polar atmosphere; the mass of the atmospheric shielding is of a similar magnitude.

For a manned mission to Mars there is a need for reliable information provided by onboard measurements of both particle fluence rate and radiation dose. This is needed both to verify the predicted SPE environment and to provide measurements of the actual radiation dose at the position of the spacecraft. The recent data from

the MARIE experiments onboard the Odyssey spacecraft provide a beginning to the generation of such a data set (Zeitlin *et al*., 2004).

There is a need to update the risk assessment of actual radiation hazards and mission impact at the position of an interplanetary spacecraft to Mars and to develop operational procedures to be implemented in the event of a large SPE.

3.2.7 *Worst-Case Solar-Particle Event Scenarios*

The database of actual solar-particle observations is limited to three solar cycles (Cycles 20, 21 and 22) of actual measurements in space. Solar Cycle 19 provided solar-proton information primarily inferred from the response of Earth's ionosphere to solar particles. The data for these four solar cycles (19 to 22) show a consistency in the number of SPEs per solar cycle. Smart and Shea (2002) note that if the current NOAA SEC event criteria of a ≥10 MeV proton fluence rate of ≥10 $(cm^2\ s\ sr)^{-1}$ is used, there have been ~75 proton events for each of the last four solar cycles. Furthermore there has been a consistent ratio of ~15 % of the events being ground-level events. These events contain ≥450 MeV protons that initiate nuclear cascades in the atmosphere capable of being detected by cosmic-ray neutron monitors at high latitudes. A statistical treatment of the ≥30 MeV fluence data by Nymmik (1993) suggests a fluence classification based on groups separated by one standard deviation of a log-normal distribution in fluence (Table 3.5) where the mean SPE fluence occurrence is normal. It is only the rare large events (3 σ greater than the average) that constitute a significant radiation hazard in space.

3.2.7.1 *Long-Term Record*. There are hints that the current space era observations may not be truly representative of the long-term population of SPEs in space. There are two additional solar cycles (Cycles 17 and 18) where surface cosmic-ray detectors responded to SPEs that generated muons with sufficient energy (≥4 GeV) to traverse Earth's atmosphere and be recorded by surface detectors. This class of SPEs has not occurred in the space era (Solar Cycles 20 to 23). An analysis by Smart and Shea (1991) evaluated the February 23, 1956 high-energy SPE, as the largest fluence-rate high-energy SPE in the modern era. However, they suggested that the largest fluence event of energetic particle measurement history in the tens of megaelectron volts range may have occurred in July 1946. The work of Goswami *et al*. (1988) suggests that the solar cycle averaged direct spacecraft measurement of the space

era may have had softer characteristic spectra than the spectra inferred from long-term (10^6 y average) induced radionuclides in lunar samples.

Upper limits can be placed on the maximum size SPE that may have occurred in the past. Examination of Figure 3.13 places limits on very high fluence events that may have occurred which induced radioactivity that would be detectable in moon rocks. Other limits can be found in ^{14}C and ^{10}Be records. Analysis of the ^{14}C record strongly suggests that there is no evidence of a single large SPE contribution (Lingenfelter and Hudson, 1980; Lingenfelter and Ramaty, 1970; Shea and Smart, 1992). Analysis of the record indicates that GCR is the major source of ^{10}Be in Earth's atmosphere, although there are some small anomalies in excess of the expected cosmic-ray production.

Recent work on the analysis of impulsive nitrate enhancements found in polar ice cores strongly suggests that these enhancements are a long-term record of SPEs (Dreschhoff and Zeller, 1990; Dreschhoff *et al*., 1997; Shea *et al*., 1999; Zeller and Dreschhoff, 1995). Recent attempts to calibrate these impulsive nitrate enhancements found in polar ice cores (McCracken *et al*., 2001a; 2001b) have resulted in a 450 y record of large fluence SPEs (those with a ≥30 MeV omnidirectional fluence exceeding 1×10^9 cm^{-2}) as illustrated in Figure 3.22.

This 450 y record indicates that events many orders of magnitude larger than those observed during the space era have not occurred in the last 450 y. Figure 3.22 indicates that SPEs larger than those observed in the contemporary space era are possible, however the largest event in the 450 y record, a ≥30 MeV omnidirectional fluence of 18×10^9 cm^{-2}, is only four to seven times larger than the largest fluence SPEs observed during the space era. Townsend *et al*. (2003; 2006) have estimated doses from this event, which is often referred to as the Carrington Flare (or Carrington Event) of 1859. The occurrence frequency of large fluence SPEs derived from this record is totally consistent with the contemporary space era occurrence frequency shown in Figure 3.13. This indicates that the modern era Earth-sensed proton-event frequency record is useful for predicting the SPE occurrence frequency to be expected during missions beyond LEO.

3.2.7.2 *Composite Events from the Modern Record*. Attempts to compile composite events from modern era solar-particle observations have been made, but there is no general consensus as to what constitutes reasonable and likely parameters to describe the event. Composite worst-case event with spectral, fluence rate, and fluence

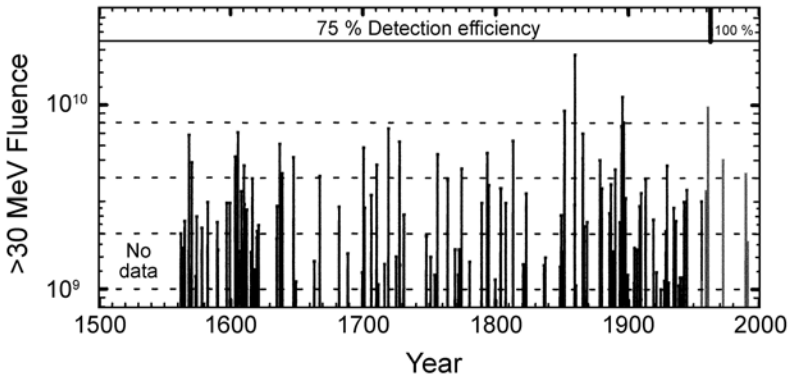

Fig. 3.22. A 450 y record of large fluence SPEs derived from impulsive nitrate precipitation events found in polar ice cores combined with the space era satellite sensed SPEs. (The detection threshold of SPEs by analysis of the $NO_{(Y)}$ precipitation events is a ≥30 MeV omnidirectional fluence of ~1×10^9 cm^{-2}) (McCracken *et al*., 2001c).

parameters might be constructed based on events observed during the space era. Townsend *et al*. (1992) and Wilson *et al*. (1990; 1991; 1997a; 1997b) have evaluated the predicted radiation dose from a composite extreme case event based on the spectral shape assumed appropriate for the February 1956 event and the fluence from the August 1972 event. They noted that this extreme case would generate a radiation environment such that 20 g cm^{-2} of aluminum would not reduce the predicted radiation dose to the annual limit of the current NCRP recommendations for flight in LEO. This extreme case was considered unrealistic by Feynman and Gabriel (1988). The consensus opinion reported was that the arbitrary scaling up of observed large events was not justified (Feynman and Gabriel, 1988). The NASA Modeling and Analysis Working Group (Badhwar, 1997a) specifically recommended against the procedure of scaling of the heavy-ion fluence rate by a linear proton fluence-rate ratio. Figure 3.23 illustrates the solar-particle integral omnidirectional fluence attributed to the very-large SPEs that have occurred in the last 50 y.

3.2.7.3 *Storm-Shelter Considerations*. The general nature of SPEs, and the distinct possibility that a single SPE could expose an unshielded astronaut to potentially dangerous radiation levels, leads to a requirement for a storm shelter as part of an interplanetary space vehicle. The unpredictability of extremely-large SPEs

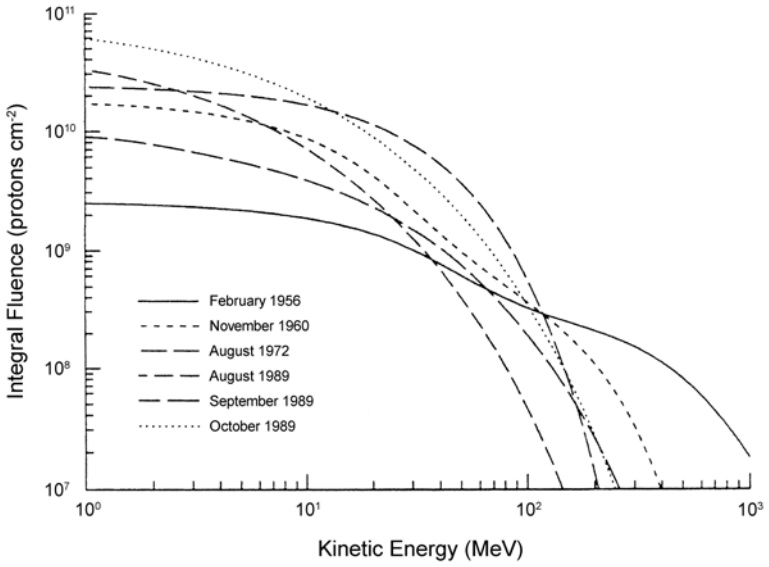

Fig. 3.23. Example of a large SPE integrated fluence spectra used in dose calculation (Wilson *et al*., 1997b).

requires this storm shelter to be available on the time scale of a few hours. Townsend *et al*. (1992) note that for nominal spacecraft shielding of 2 g cm^{-2} of aluminum, a large SPE such as August 1972 would generate sufficient radiation dose inside the spacecraft that the 30 d limit of the current NCRP recommendations (NCRP, 2000) for LEO flight would be exceeded in ~8 h. The storm-shelter design should be able to reduce the dose to blood-forming organs experienced by an astronaut inside the shelter during an extremely-large SPE (3 σ larger than the average) to tolerable levels (dose below the life threatening and the nausea thresholds). The recommendation that was reported in Badhwar (1997a) was that a prudent storm-shelter design should protect against >30 MeV omnidirectional free-space fluence of 8×10^9 proton cm^{-2}. The dose is also a function of the energetic particle spectral parameters as well as the radiation fluence. See the work of Townsend and Zapp (1999) for a discussion of the variability introduced by various assumptions about the solar-proton spectra.

Calculations by Wilson *et al*. (1999) suggested not using the actual fluence-rate and fluence observation of the August 1972 solar activity episode as a minimum design threshold for a storm shelter. Their calculations indicate that a shielding mass of 10 g cm^{-2} would attenuate the absorbed blood-forming organ dose

received from the observed free-space solar-proton fluence rate to the 30 d limit for LEO flight. They also note that additional radiation shielding benefit can be obtained by a choice of composite shielding material. Townsend *et al*. (1992) have calculated that a storm shelter of 20 g cm^{-2} of aluminum would reduce the dose from an August 1972 type of SPE to well below the 30 d limit. Wilson *et al*. (1999) further recommend that the storm-shelter design should have the capability of providing protection for a solar-particle fluence four times larger than the observed August 1972 fluence in the 70 to 100 MeV energy interval. This class of storm shelter would probably provide protection in the case of the largest SPE fluence illustrated in Figure 3.23, assuming normal spectral parameters.

3.2.8 *Recommendations for Research on Energetic Solar Particles*

Prediction of SPEs in support of manned space flight should be changed from the current criteria of predicting events having a peak proton fluence rate of ≥10 $(cm^2\ s\ sr)^{-1}$ at energies ≥10 MeV towards an orientation of predicting events during which the free-space absorbed dose would exceed 10 mGy. Since dose is also a function of the energetic particle spectral parameters as well as the particle fluence, there should be sufficient spectral information so that a reasonable dose computation can be made. A prediction of proton events with protons ≥30 MeV and fluences $>3 \times 10^6$ protons cm^{-2} (an energy content equivalent to ~10 mGy) would be more useful that the current >10 MeV peak fluence-rate predictions.

Research should be directed toward identifying and modeling the agents responsible for the acceleration of large fluences of energetic particles at biologically significant energies in space. There should also be research directed toward identifying precursors and unique signatures of fast CME and useful CME proxies. These would include possible techniques to improve the prediction and detection of the fast CME and associated interplanetary shock, the shock-Mach number (particularly at about five solar radii), and the shock shape and heliolongitudinal extent. Research directed toward a capability of remote sensing of fast interplanetary shocks and their speed (Alfven Mach number) and position in space with respect to a spacecraft will aid the prediction of solar-particle fluence rate expected from a specific interplanetary shock. The capability of modeling the connection from the observer to the shock front will improve the prediction capability. There is a definite need to model the acceleration of particles at the location of the shock

front including prediction of fluence rates and fluence changes as the shock approaches and passes Earth (or spacecraft).

There should be research directed toward identifying quiet periods when very reliable predictions of no significant SPEs can be made. These would be very useful for extravehicular activity or surface exploration on the moon or Mars.

4. Space Radiation Physics and Transport

4.1 Introduction

The physical description of the interactions of space radiations supports the understanding of the effects of radiation shielding, space radiation biology, and radiation dosimetry. Computer codes describing coupled proton, HZE, and neutron transport are used as shielding design tools for spacecraft and planetary habitats. The physical description of the interaction of space radiation with tissues, cells or biomolecules requires knowledge of the energy and isotopic distribution of primary and secondary charged particles and neutrons produced in atomic and nuclear collision processes in the transport of radiation through matter. These descriptions are augmented with stochastic models of particle track structure that describe the spatial distribution of excitations and ionizations in biomolecules for ions and secondary electrons (denoted delta rays) produced along an ion track. The development of design tools for shielding analysis and comparisons to dosimetry measurements utilize many of the same physical descriptions needed to support physical aspects of the radiation biology of heavy-ion beams. The broad energy range of GCR and SPEs and the large number of materials of interest in spacecraft structures, planetary atmospheres, and tissues require a robust description of the basic physical processes including the development of efficient computer models. In this Section current methods in radiation physics as applied to space radiation problems are reviewed and research areas where improvements are needed are discussed.

Several physical processes are involved in the transport of space radiations in materials. Energy loss and energy deposition processes dominate for thin shielding layers, while heavy-ion fragmentation dominates for intermediate shielding thicknesses. Particle production processes including neutrons and mesons and the electromagnetic cascades are involved in the evaluation of deep penetration problems such as a habitat on the surface of Mars. Physics models play important interpolation and extrapolation roles in space radiation studies, since the broad range of particle types and energies in space make the costs of experimental measurement of

all components prohibitive. Ground-based research focuses on the measurement of interaction cross sections and transport through materials of individual components of the space radiation environment. However, theoretical models are needed for extrapolating such results to all of the particles produced by GCR or SPEs including their temporal variations. Studies of potential risk mitigation including operational, shielding and biomedical approaches must rely on theoretical models that utilize radiation transport codes to make projections and to support design studies of such missions. Research aimed at optimizing the costs of radiation shielding through design studies and material selection could potentially provide a large cost advantage for exploration missions. However, the large uncertainties in current risk projection models (Cucinotta *et al*., 2001a; NAS/NRC, 1996; NCRP, 1997) preclude any final conclusions from design studies until a more complete understanding of space radiation biology is available (Section 6).

4.2 Radiation Transport in Shielding

Dominant physical processes in the transmission of high-energy nuclei through matter are energy loss through atomic and molecular collisions and the absorption and particle production from nuclear interactions with spacecraft materials and tissue. Materials with light constituent atoms, such as hydrogen, are the most efficient per unit mass of material at slowing down ions, attenuating heavy-ion projectiles through projectile fragmentation, and minimizing the buildup of neutrons and other target fragments produced directly from the shielding by nuclear interactions. Energy loss through ionization is proportional to the number of electrons per atom (Z) where Z is the atomic charge number and the energy loss per unit mass is proportional to ($Z/\rho A$) where ρ is the material density and A the atomic mass number. For heavy ions with high kinetic energies (>100 MeV n^{-1}) nuclear absorption by fragmentation is the dominant reaction mode (Hufner, 1985). The nuclear absorption cross section is approximately proportional to $A^{2/3}$ and fragmentation of GCR projectile nuclei is more efficient per unit mass for materials with light constituent atoms. At lower energies (<100 MeV n^{-1}) elastic scattering, compound nucleus formation or excitations of discrete nuclear levels that decay by gamma or particle emissions are dominant interaction modes. High-energy protons and neutrons interact through knockout and spallation reactions (Hufner, 1985). Such processes lead to a buildup of light particles ($Z \leq 2$) and the localized production near the primary track of heavy-ion target fragments with large values

of LET and short ranges (Cucinotta *et al*., 1996a; Wilson *et al*., 1991).

For GCR, materials such as aluminum (the most common spacecraft material) have relatively flat depth-dose (*i.e*., dose equivalent) responses due to the buildup of light particles in balance with the attenuation of heavy ions (Wilson *et al*., 1995a). Materials such as concrete or lead have a dose-equivalent response to GCR that is predicted to increase with shielding because of excessive production of neutrons and target fragments. The relationship between track structure and biological response must be understood in order to determine if risk is reduced through adding shielding materials such as aluminum. There is some doubt that practical shielding amounts offer any advantage from GCR (Wilson *et al*., 1995a). However, dose equivalents from SPEs are certainly reduced by shielding materials including aluminum, and can be optimized by using materials with high-Z to A ratios.

4.2.1 *Space Radiation Transport*

The description of the passage of high-energy nuclei through matter can be made using transport equations that treat the atomic and nuclear collisions. As an alternative, Monte-Carlo techniques can be used which sample from interaction processes for individual primaries or their secondaries to develop histories of charged particle passage and energy deposition in materials. Although used extensively for proton and neutron transport, the Monte-Carlo codes have only recently been developed for HZE transport (Pinsky *et al*., 2005; Townsend *et al*., 2002; 2005). The relevant transport equations are derived on the basis of conservation principles (Wilson *et al*., 2001) for the fluence-rate density $\phi_j(x,\boldsymbol{\Omega},\mathrm{E})$ of type j particles as:

$$\boldsymbol{\Omega}\cdot\nabla\phi_j(x,\boldsymbol{\Omega},\mathrm{E}) = \Sigma_k\int\sigma_{jk}(\boldsymbol{\Omega}\boldsymbol{\Omega}',\mathrm{E},\mathrm{E}')\phi_k(x,\boldsymbol{\Omega}',\mathrm{E}')\mathrm{d}\mathrm{E}'\,\mathrm{d}\boldsymbol{\Omega}' - \sigma_j(\mathrm{E})\phi_j(x,\boldsymbol{\Omega},\mathrm{E}), \qquad (4.1)$$

where $\sigma_j(\mathrm{E})$ and $\sigma_{jk}(\boldsymbol{\Omega},\boldsymbol{\Omega}',\mathrm{E},\mathrm{E}')$ are the media macroscopic cross sections. The $\sigma_{jk}(\boldsymbol{\Omega},\boldsymbol{\Omega}',\mathrm{E},\mathrm{E}')$ represent all those processes by which the type k particles moving in direction $\boldsymbol{\Omega}'$ with energy E' produce a type j particle in direction $\boldsymbol{\Omega}$ with energy E. The fluence-rate density $\phi_j(x,\boldsymbol{\Omega},\mathrm{E})$ is the main physical quantity used to determine the physical or biological response by folding it with an appropriate response function for the physical or biological system under study.

There may be several reactions which produce a particular product and the appropriate cross sections for Equation 4.1 are the inclusive ones. The total cross section $\sigma_j(E)$ with the medium for each particle type of energy E may be expanded as:

$$\sigma_j(E) = \sigma_j^{at}(E) + \sigma_j^{el}(E) + \sigma_j^{r}(E), \tag{4.2}$$

where the first term refers to collision with atomic electrons, the second term is for elastic nuclear scattering, and the third term describes nuclear reactions. The microscopic cross sections and mean energy transfer are ordered as follows:

$$\sigma_j(E) \sim 10^{-16}\ \text{cm}^2 \text{ for } \delta E_{at} \sim 10^2\ \text{eV}, \tag{4.3}$$

$$\sigma_j(E) \sim 10^{-19}\ \text{cm}^2 \text{ for } \delta E_{el} \sim 10^6\ \text{eV}, \tag{4.4}$$

and

$$\sigma_j(E) \sim 10^{-24}\ \text{cm}^2 \text{ for } \delta E_{r} \sim 10^8\ \text{eV}. \tag{4.5}$$

This ordering allows flexibility in expanding solutions to the Boltzmann equation as a sequence of physical perturbative approximations (Wilson *et al*., 2001). Many atomic collisions (~10^6) occur in a centimeter of ordinary matter, whereas ~10^3 nuclear coulomb elastic collisions occur per centimeter. In contrast, nuclear reactions are separated by a fraction to many centimeters depending on energy and particle type. For neutrons, $\sigma_n^{at}(E) \sim 0$ and the nuclear elastic process appears as the first-order perturbation. Mean-free paths for elastic scattering of neutrons may become quite small, especially at low energies in the resonance region (ICRU, 2000).

The solution of Equation 4.1 involves hundreds of multi-dimensional integro-differential equations which are coupled together by thousands of cross terms and must be solved self-consistently subject to boundary conditions ultimately related to the external environment and the geometry of the astronaut's body and/or a complex vehicle. A series of approximate solutions can be studied and indicates a high level of accuracy for most applications (Tweed *et al*., 2004; Wilson *et al*., 2001). The mean energy loss can be introduced in a continuous slowing down approximation, and straggling neglected for the broad energy spectra of the space radiation. The highly directional coulomb cross section for charged ions and nuclear elastic scattering for neutrons generally dominate

the second perturbation term. The angular dispersion and its effects on lateral beam spread and range straggling are important corrections in comparing to laboratory measurements. The nuclear elastic scattering is especially important to neutron fields and has been treated in the past using Monte-Carlo or multi-group methods (Hughes *et al*., 1997). The third perturbation term consists of complex energy and angle functions. Results from Monte-Carlo codes (Alsmiller *et al*., 1965) provided the basis for the generation of analytical techniques and the simplification of boundary conditions used in space shield code development (Wilson *et al*., 1991).

For transport of the GCR heavy ions ($A > 4$), the use of the continuous slowing down approximation in a marching procedure has been implemented in NASA's HZE transport code (Wilson *et al*., 1991). A full isotopic grid requires ~170 ions to represent GCR (Cucinotta *et al*., 2003), however a reduced isotopic grid of 59 ions is used more often (Wilson *et al*., 1995b) and is accurate for many applications. For mono-energetic beam transport, a Gaussian model of the fragment single differential cross section has been considered along with energy straggling using a Green's function approach (Tweed *et al*., 2004). For light particle transport, the broad redistribution in energy of the ions in collisions is considered in the marching procedure (Wilson *et al*., 1991). Angular effects for neutron transport are considered using a multi-group or Monte-Carlo transport models (Clowdsley *et al*., 2001; Hughes *et al*., 1997).

For determining the particle spectra, numerical techniques have been developed which allow for computationally efficient and accurate computer codes in the straight-ahead approximation (Wilson *et al*., 1995b). Complex spacecraft and organ geometry are described using ray-tracing distributions. Methods to include angular effects in transport processes relative to complex spacecraft geometries are not highly developed at this time. Monte-Carlo approaches exist to treat these problems for neutron and proton transport, however they have not been applied to the spacecraft problems with any degree of detail and have used a cylindrical shell approximation (Armstrong and Colborn, 2001). Efforts to extend Monte-Carlo codes, such as High Energy Transport Code and FLUctuating Kascade, to include HZE particle transport are nearing completion and will permit complex spacecraft geometries to be handled (Pinsky *et al*., 2005; Townsend *et al*., 2002; 2005). The Boltzmann equation methods of solution developed at Langley Research Center have considered bidirectional models for neutron transport problems, however new methods will be needed for full three-dimensional transport in a complex geometry.

4.2.2 *Transport Coefficients and Atomic Processes*

Transport coefficients describe the atomic (molecular) and nuclear processes by which the particle fields are modified by the presence of a material medium (Wilson *et al*., 2001). As such, basic atomic and nuclear theories provide the input to the transport code databases. The first-order physical perturbation on the right side of Equation 4.1 is the atomic (molecular) cross sections as noted in Equation 4.3 for which those terms in Equation 4.1 are expanded about the energy moments as:

$$S_n(E) = \sum_i \varepsilon_i^n \, \sigma_i(E), \tag{4.6}$$

where ε_i is based on the electronic excitation energy, and $\sigma_i(E)$ is the total atomic (molecular) cross section for delivering ε_i energy to the orbital electrons (including discrete and continuum levels). The first moment ($n = 1$) is the usual stopping power (see Glossary), and the usual continuous slowing down approximation is achieved by neglecting the higher-energy moments.

In Equation 4.6 specification of ε_i and $\sigma_i(E)$ requires a complete knowledge of the atomic (molecular) wave functions. Stopping power databases are derived semi-empirically as the Bethe reduction of Equation 4.6 in terms of mean excitation energies and various correction terms (Fano, 1963; Wilson *et al*., 1991). The stopping power (S) is adequately described by the Bethe-Bloch formula for most ion energies (Bichsel, 1992):

$$S = \frac{4\pi Z_p^2 \, Z_r N_T e^4}{mv^2}$$

$$\left[\ln\left(\frac{2\, mc^2\beta^2\gamma^2}{I}\right) - \beta^2 - \frac{C(\beta)}{Z_T} + Z_p L_1(\beta) + Z_p^2 \, L_2(\beta) + L_3(\beta)\right], \tag{4.7}$$

where e is the electronic charge, N_T is the density of target atoms, m is the mass of the electron, c is the speed of light, $\beta = v/c$, and I is the mean excitation energy. In Equation 4.7, the various correction terms are the shell correction $C(\beta)$, Barkas correction $L_1(\beta)$, Bloch term $L_2(\beta)$, and Mott and density corrections $L_3(\beta)$. The range of the ion is evaluated from the stopping power as:

$$R(E) = \int_0^E \frac{dE'}{S(E')} \, . \tag{4.8}$$

The second energy moment is related to energy or range straggling and provides corrections to the ion slowing down spectrum (Fano, 1963). Straggling has been well studied for ion beam applications with leading order and most higher-order correction terms well understood (Bichsel, 1992). For broad-beam conditions, GCR transport straggling effects are negligible, however they are important for laboratory studies with mono-energetic beams and for understanding radiation detector responses. The next physical perturbation term is the coulomb scattering by the atomic nucleus and is typically represented by Rutherford scattering modified by screening of the nuclear charge by the orbital electrons using the Thomas-Fermi distribution for the atomic orbits. The total nuclear coulomb cross section found by integrating over the scattering directions is related to the radiation length. The differential cross section is highly peaked in the forward direction, and only after many scatterings is significant beam divergence seen. Numerical solutions to the coulomb multiple-scattering problem have been investigated for many years (Fermi, 1940) and accurately describe experimental data with HZE (Wong *et al*., 1990) or proton beams (Carlsson and Rosander, 1973).

4.2.3 *Nuclear Interaction Cross Sections*

The extent of the nuclear interaction cross-section database required for the transport of cosmic rays spans most nuclear reaction physics from energies <10 MeV n^{-1} to energies above tens of GeV n^{-1}, including a large number of projectile and target material combinations. The types of cross sections required for transport involve total yields and multiplicities and inclusive secondary energy spectra for one-dimensional transport or inclusive double differential cross sections in angle and energy for three-dimensional transport. For Monte-Carlo simulations, exclusive cross sections are needed for computer algorithms; an enormous experimental task when considering the large number of projectile-target combinations, secondary multiplicities, etc., needed to transport all GCR particles and energies through spacecraft and tissues. Currently, event generators capable of providing particle yields, production angles, and energies of all secondary particles produced by these nuclear collisions are under refinement and have been introduced into Monte-Carlo codes (Miller and Townsend, 2004a; 2004b; 2005). Testing of the extended Monte-Carlo codes with laboratory beam data is underway (Townsend *et al*., 2005). Fortunately, physical considerations lead to great simplifications allowing inclusive cross sections to be appropriate for many applications. Table 4.1 shows reaction partners and secondaries of relevant reactions broken into

distinct reaction types or mechanisms. Low-energy evaporation products including heavy-ion target fragments are high-LET events. Knockout products from proton or neutron reactions and projectile fragments from GCR nuclei are typically of low- to moderate-LET, however their large ranges leads to radiation buildup through further reactions.

The abrasion-ablation models (Cucinotta *et al*., 1997; Hufner *et al*., 1975; Wilson *et al*., 1995b) are used to describe heavy-ion fragmentation cross sections. The description of nuclear reactions through abrasion (particle removal during ion to ion interaction) and ablation (nuclear de-excitation after the abrasion step) is illustrated in Figure 4.1, which shows the roles of projectile overlap, fireball formation in central regions, and the decay of the prefragment spectators. The individual steps of abrasion and ablation can be described in both semi-classical or quantum mechanical approaches. Nuclear database development has focused largely on quantum multiple scattering theories or Monte-Carlo approaches to nuclear reactions using an intra-nuclear cascade model. A starting point for formulating all reaction models is to consider the relationship between the phase space of final state momentum vectors, the transition matrix (T_{fi}) and the differential cross section ($\mathrm{d}\sigma$):

$$\mathrm{d}\sigma = \frac{(2\ \mathrm{p}\pi)^4}{\beta}\sum_{\mathrm{X}}\mathrm{d}\boldsymbol{p}\times\mathrm{d}\boldsymbol{p}_{\mathrm{F}^*}\sum_{n=1}\prod_{\mathrm{j}=1}^{n}(\mathrm{d}\boldsymbol{p}_{\mathrm{j}})\delta(\mathrm{E}_{\mathrm{i}}-\mathrm{E}_{\mathrm{f}})\delta(\boldsymbol{p}_{\mathrm{i}}-\boldsymbol{p}_{\mathrm{f}})\left|T_{\mathrm{fi}}\right|^2, \quad (4.9)$$

where β is the relative projectile-target velocity divided by the speed of light, $\boldsymbol{p}$ is the momentum of the particle, E is its energy, δ is the Dirac delta function, X represents the final target states (which are summed over), F* represents the prefragments formed in the projectile-target interaction, n is the number of nucleons knocked out of the projectile in the overlap region with the target, and i and f label the initial and final states, respectively. The prefragment decays through particle emission if sufficient energy is available and can be described by additional considerations on the phase space and transition matrix (Cucinotta *et al*., 1997).

The transition matrix in quantum theories provides first principles solution to the scattering problem. However, it must be treated approximately because of the complexity of its solution. For elastic scattering or excitation of discrete states, the relation between the transition matrix T_{fi} (or T-matrix) and the inclusive cross sections is trivial. For fragmentation reactions, where many particles are present in the final state, integrals become intractable and approximations are introduced. The multi-particle momentum integrals can be reduced to a computationally feasible form only

TABLE 4.1—*Reaction products in nuclear reactions important to space radiation studies.*

Reaction Type	Secondary	Mechanism	Comment
Nucleon-nucleus	Nucleon	Evaporation Knockout	Small range, high-LET Large range
		Elastic, quasi-elastic	
Nucleon-nucleus	Light particle (d,t,h,α)	Evaporation	High-LET, small range Large range
		Knockout, pickup	
Nucleon-nucleus	Heavy recoil	Elastic Fragmentation or spallation	High-LET, small range High-LET, small range
Nucleon-nucleus	Nucleon or light particle	Target or projectile knockout	Large range, low-LET Small range, high-LET
		Evaporation	
Nucleus-nucleus	Heavy ion	Projectile fragment	Large range, moderate-LET
Nucleus-nucleus	Heavy ion	Target fragment	Small range, high-LET
Nucleon or nucleus-nucleus	Pion, kaon, anti-nucleon, gamma	Projectile energy > 500 MeV n^{-1}	Deep penetration (>50 g cm^{-2})

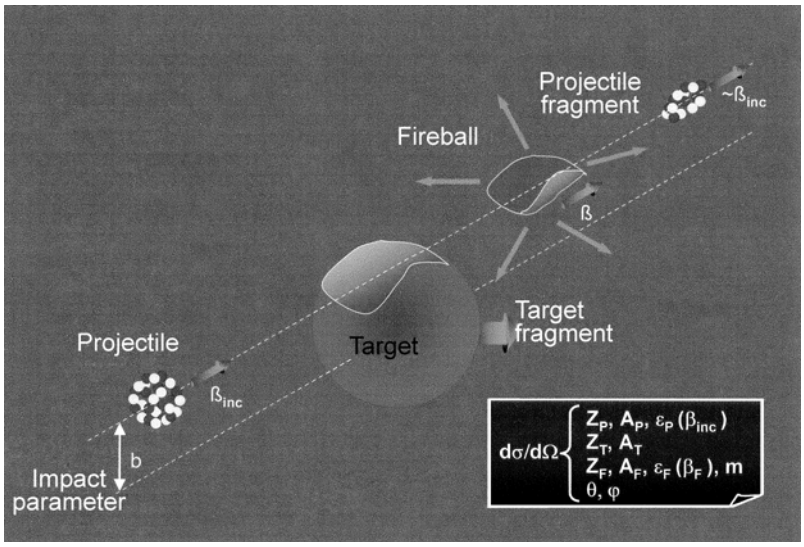

Fig. 4.1. Schematic diagram of a relativistic heavy-ion reaction showing the projectile and target fragments, and fireball and their dependence on the impact parameter.[8]

after theoretically studying the structure of the nucleus-nucleus T-matrix and introducing high-energy approximations such as the closure and Eikonal approximations.

The equations of motion for nuclear scattering are expressed in terms of the transition operator, which represents an infinite series for the multiple scattering of constituents of the projectile and target nucleon. The strong nature of the nuclear force requires a nonperturbative solution to the scattering problem. A T-matrix based on relativistic dynamics, or at the minimum employing relativistic kinematics, is required for high-energy space radiation databases, and production processes are naturally included in a relativistic theory. Relativistically covariant formulations of the T-matrix have been developed using meson exchange theories (Maung *et al*., 1996). The basic approach, in both relativistic and nonrelativistic multiple scattering theories, is to re-sum the multiple scattering series, which is expressed in terms of the irreducible and reducible exchange diagrams in a relativistic multiple scattering theory or the nuclear potential in a nonrelativistic multiple scattering theory, in terms of the T-matrix for projectile and target nuclei constituents.

[8]Schimmerling, W. Personal communication (National Aeronautics and Space Administration, Washington).

This avoids having to deal directly with the highly singular behavior of the nuclear potential at short distances, and instead the constituent transition matrix is used, which is known from experimental determinations. The integral equation approach is quite successful for studying elastic scattering where a one-body integral equation can be found after deriving an optical potential. For studying high-energy knockout and fragmentation reactions, the Eikonal approximation is accurate and leads to a reduction of the many component integral equation to a practical form after deriving a factorization approximation for many-particle removal (abrasion). Final state interactions between projectile fragments suggest the use of a Faddeev Type 3-body integral equation.

Monte-Carlo simulation techniques can be used to describe nuclear multiple scattering (Cugnon *et al*., 1981; Ferrari and Sala, 1996). However, many of the quantum aspects of the problem must be ignored including shell structure, the nuclear surface, and interference effects. Monte-Carlo approaches to reaction theories rely on phase space considerations and two-body cross sections as described above. Multiple scattering is treated in an algorithmic manner by sampling each nucleon over the possible energy and momentum transfers allowed by the two-body cross sections, often including Pauli blocking and other nuclear medium effects. Several models are used to couple to the intra-nuclear cascade including the pre-equilibrium models and the nuclear evaporation models (ICRU, 2000). One advantage is that all levels of scattering can be followed in the algorithm. Although continued improvement in nuclear reaction models are expected to support predictive capabilities, the need for experimental data on reaction cross sections is required for both improvement and validation of models. Total absorption plays a critical role in ensuring a reasonable solution to the Boltzmann equation, including the accuracy of particle conservation as a function of depth in the shield (Wilson *et al*., 1991). The total (TOT) cross section is found from the elastic amplitude $f(\mathbf{q})$ using the optical theorem (Wilson *et al*., 1991) as:

$$\sigma_{\mathrm{TOT}} = \frac{4\pi}{k}\mathrm{Im}f(\mathbf{q}=0). \tag{4.10}$$

The absorption (ABS) cross section is found by using:

$$\sigma_{\mathrm{TOT}} = \sigma_{\mathrm{ABS}} + \sigma_{\mathrm{EL}}, \tag{4.11}$$

where σ_{EL} is the elastic cross section. Formulae for these cross sections can be derived from microscopic theories of nuclear multiple scattering (Cucinotta *et al*., 1997). The absorption cross sections are accurately represented by energy dependent variants of the Bradt-Peters equation (Townsend and Wilson, 1986):

$$\sigma_{ABS} = \pi r_0^2 \, c_1(E)[A_p^{1/3} + A_T^{1/3} - c_2(E)]^2, \tag{4.12}$$

where r_0, $c_1(E)$, and $c_2(E)$ are parameters. Absorption cross sections have been studied both experimentally and theoretically and are known to within a few percent accuracy (Tripathi *et al*., 1997; 2001). Figure 4.2 show comparisons of calculated experimental data for absorption cross sections for proton and ^{12}C projectiles with ^{27}Al targets (Tripathi *et al*., 1997; 2001). Examples of fragmentation cross sections for ^{32}S and ^{56}Fe projectiles on ^{27}Al and ^{12}C targets, respectively, are shown in Figure 4.3 in comparison to the quantum multiple scattering fragmentation model. One feature of the elemental distribution of the fragments is the strong even-odd effect observed. The effect appears to be largest for intermediate mass projectiles (A = 20 to 40) and depends on the isospin of the projectile (Knott *et al*., 1996). Theoretical models provide a good representation of the even-odd effect if accurate nuclear de-excitation models are used (Cucinotta *et al*., 2003). Figure 4.4 shows measurements of double differential cross sections for proton and neutron production (ICRU, 2000) from proton bombardment of ^{12}C and ^{16}O targets. A larger database for cross sections for proton and neutron induced reactions now exists with recent surveys of such data provided in ICRU Report 63 (ICRU, 2000). Above kinetic energies of a few GeV n^{-1}, the quark-gluon-string model has been considered a nucleus-nucleus event generator.

The momentum distribution of projectile fragments can be described as a Gaussian distribution in the projectile rest frame with a small downshift in the average momentum from the projectiles velocity. The longitudinal momentum width is well described by (Goldhaber, 1974):

$$\sigma_L = \sigma_0 \left[\frac{n(A_P - n)}{A_P - 1}\right]^{1/2}, \tag{4.13}$$

where n is the number of nucleons removed from the projectile and σ_0 is approximately related to the Fermi momentum of the projectile (p_F) by $\sigma_0 = p_F/\sqrt{5}$. The functional form of the model of

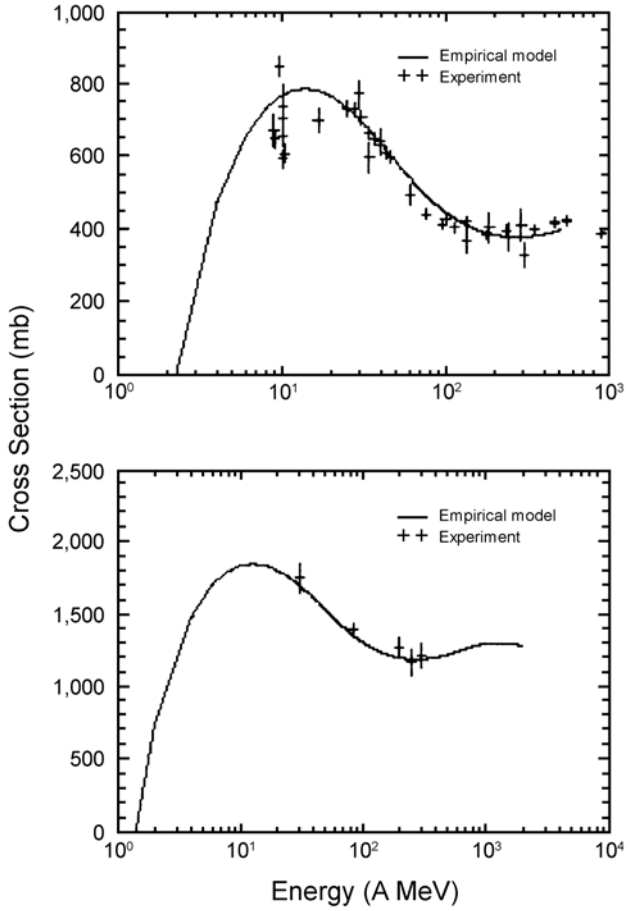

Fig. 4.2. (Top) reaction cross sections as a function of energy for $p + {}^{27}_{13}\mathrm{Al}$ collisions, and (bottom) reaction cross sections as a function of energy for ${}^{12}_{6}\mathrm{C} + {}^{27}_{13}\mathrm{Al}$ collisions (Tripathi *et al.*, 1997).

Equation 4.13 has been discovered in several distinct models (Hufner, 1985). However, it likely arises due to the large number of intermediate states in abrasion and ablation, such that the central limit theorem leads to a Gaussian form. The transverse width is approximately the same as the longitudinal width for heavier fragments. A small momentum downshift also occurs and is dependent on the fragment mass (Tull, 1990). Transformation of the Gaussian distribution to the laboratory rest frame reveals a narrow angular distribution for the projectile fragments that are strictly forward

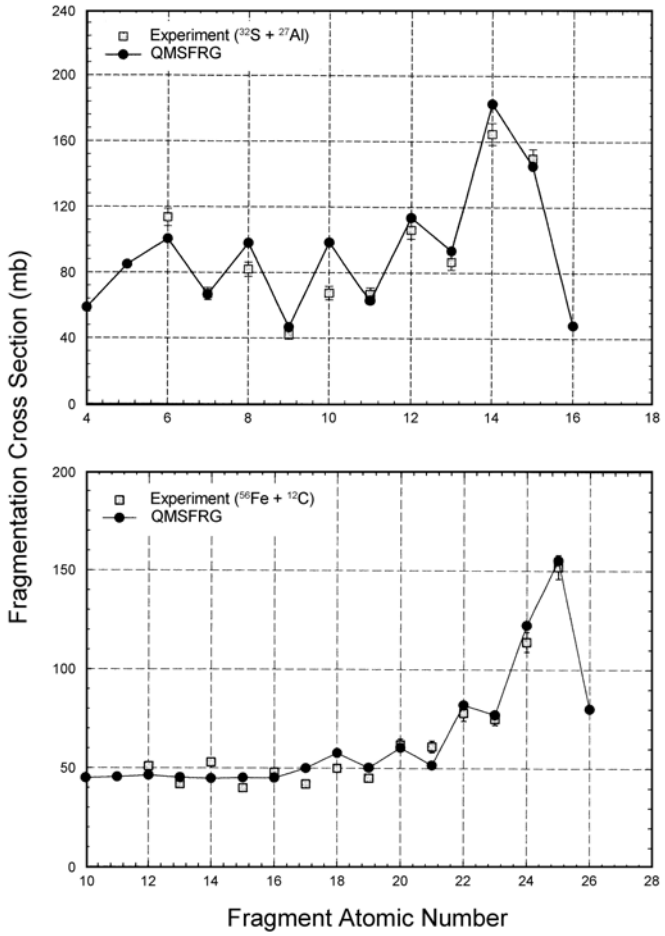

Fig. 4.3. Fragmentation cross sections for ^{32}S projectiles (1.2 GeV n^{-1}) on ^{27}Al targets (Brechtmann and Heinrich, 1988) and ^{56}Fe projectiles (1.05 GeV n^{-1}) on ^{12}C targets (Zeitlin *et al*., 1997) in comparison to the quantum multiple scattering fragmentation model (QMSFRG) model (Cucinotta *et al*., 2003).

peaked in a narrow cone (less than five degrees) (*i.e*., the physical reason for the success of the straight-ahead approximation). For lighter fragments the longitudinal and traverse widths diverge and the Gaussian model breaks down. This is due to the multiple sources for light particle production including projectile abrasion, projectile ablation, target abrasion, and target ablation, as well as a possible intermediate source due to the formation of an intermediate rapidity fireball in central collisions.

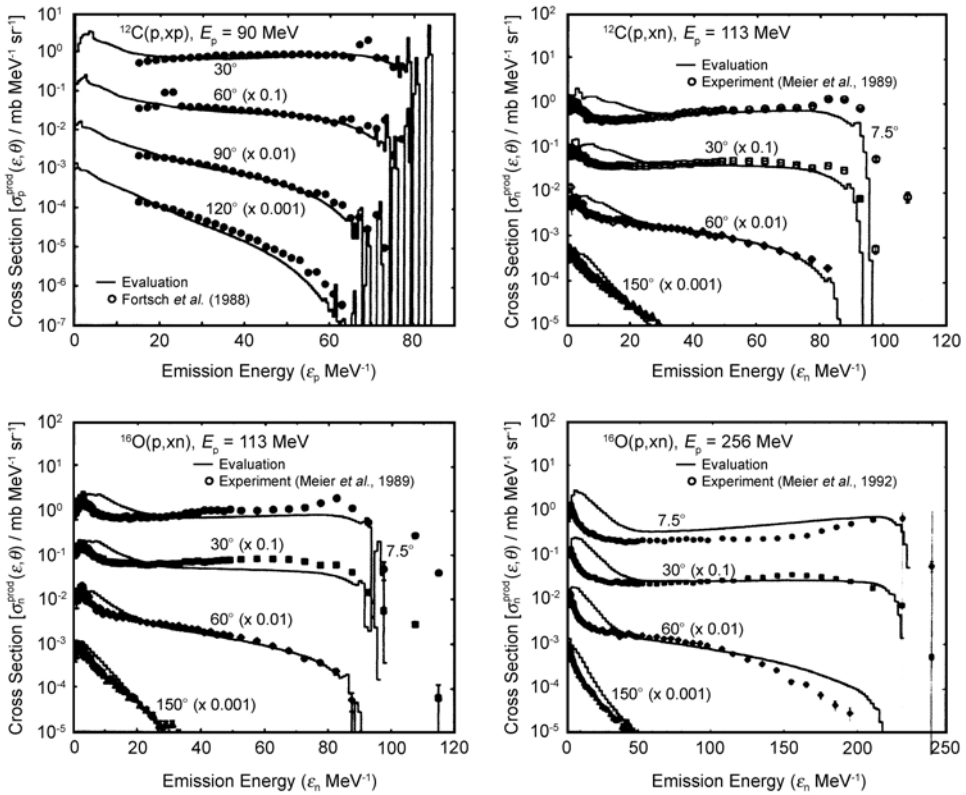

Fig. 4.4. Double differential cross sections for proton and neutron production from p-^{12}C or p-^{16}O reactions at several energies (ICRU, 2000).

4.2.4 *Survey of Existing Cross-Section Data*

For describing projectile fragmentation, total inclusive cross sections for fragmentation of the more abundant GCR nuclei are needed at several energies and for an array of targets of interest for spacecraft shielding and for transport in tissues. Fragments are produced in the forward direction in nearly velocity conserving interactions, however existing measurements of momentum widths and downshifts are sparse, and considerations of augmentation for other projectiles are warranted. Tests of the accuracy of this assumption would be to consider within radiation transport models a Gaussian distribution for the projectile fragments where several data sets for widths in downshifts have been made. A minimum data set would include elemental distributions for $Z_F > 2$, however isotopic cross sections would be more useful. For neutron, hydrogen and helium fragments, cross-section differentials in energy and angle are required. Older studies used chemical decay methods to extract fragmentation cross sections from target decays. However, these data are considered to be less accurate than the measurement of cross sections directly from projectile interactions with target atoms. Table 4.2 shows a recent survey of existing measurements for elemental distributions for fragments produced from GCR projectiles with charges from 10 to 26 showing the target mass projectile energy available. Cross sections for the carbon and oxygen nuclei are more numerous and have considered isotopic distributions rather than elemental ones (Olsen *et al*., 1983). Data sets for projectiles can be divided roughly into three types of studies, with the first including more than one beam energy over the full range of target masses important for spacecraft and planetary habitats. A second series of experiments have made complete measurements at one beam energy over the full range of target masses with supplemental data at other energies. Finally, other data sets consider measurements limited in target mass and energy spread. There is a shortage of data or absence of any data for several of the major GCR components such as helium, nitrogen, calcium, titanium and chromium. There are a reasonable number of projectile fragmentation data sets now available with the above noted exceptions. However, the projectile energy of the data are lacking with more data needed in the 0.1 to 0.4 GeV n^{-1} region and >1 GeV n^{-1}. Also cross-section data and multiplicities extending to lower fragment charge are needed. Issues related to the effects of the isotopic composition of fragments, especially for $Z_F = 2$ to 8 need to be addressed. The isotopic composition of GCR (Cucinotta *et al*., 2003; Webber *et al*., 1990a) need to be considered with the full grid of isotopes rather than reduced ones in order to eliminate unnecessary

TABLE 4.2—*Experimental data on fragmentation of Z = 10 to 26 projectiles on composite targets.*

Projectile	Energy (GeV n^{-1})	Targets	Z_F Range	Reference
^{20}Ne	0.6	H, C, Al, Cu, Sn, Pb	3 – 9	Zeitlin *et al.* (2001)
^{20}Ne		H, C		Webber *et al.* (1990b)
^{24}Mg	3.65	C, Al, Cu, Ag, Pb	6 – 11	Sampsonidis *et al*. (1995)
^{24}Mg	0.6	H, C	6 – 11	Webber *et al.* (1990b)
^{28}Si	14.5	H, C, Al, Cu, Ag, Pb	6 – 13	Brechtmann *et al.* (1989)
^{28}Si	0.45	H, C, Al, Cu, Ag, Pb	6 – 13	Flesch *et al.* (2001)
^{28}Si	0.6	H, C, Al, Cu, Ag, Pb	5 – 13	Zeitlin *et al.* (2002)
^{32}S	3.65	C, Al, Cu, Ag, Pb	7 – 15	Sampsonidis *et al*. (1995)
^{32}S	0.7	H, C, Al, Cu, Ag, Pb	6 – 15	Brechtmann and Heinrich (1988)
^{32}S	1.2	Al, Pb	6 – 15	Brechtmann and Heinrich (1988)
^{40}Ar	1.65	C, KCl	9 – 19	Tull (1990)
^{48}Ca	0.21	Be		Westfall *et al.* (1979)
^{56}Fe	1.09	H, C	12 – 25	Webber et al. (1990b)
^{56}Fe	1.55	H, C, Al, Cu, Pb	12 – 25	Cummings *et al.* (1990)
^{56}Fe	1.05	H, C, Al, Cu, Pb	12 – 25	Zeitlin *et al.* (1997)
^{56}Fe	0.66	H, C, Al, Cu, Ag	6 – 25	Flesch *et al.* (1999)
^{56}Fe	1.65	H, C, Al, Cu, Ag	6 – 25	Flesch *et al.* (1999)

error. The quality of existing data sets has also recently been examined. The iron fragmentation measurements of Zeitlin *et al*. (1997) have resolved discrepancies in older data sets. Energy spectra of heavy-ion target fragments from tissue components are also poorly known and are needed to define the LET spectra at the reaction site in tissue.

Light particle production (*e.g*., neutrons, protons, deuterons, tritons, helions, alpha particles, and mesons) in GCR is largely from primary proton and secondary proton and neutron induced reactions. Current transport codes predict 10 to 30 % of light particles are produced by alpha-particle and HZE-induced reactions depending on material type. However, these estimates are based on cross-section databases that have not received much study. A large number of measurements exist for proton and neutron production for proton and neutron induced reactions (ICRU, 2000). Most radiation transport codes have assumed only an evaporation component for deuteron, triton, helion and alpha-target fragments and neglected the importance of a fast knock-out component of these ions for GCR transport. These ions contribute substantially to the buildup effect in shielding due to their ranges which scale with the proton range as proton:deuteron:triton:helion:alpha to 1:2:3:3/4:1 and provide up to a 25 % increase in dose equivalent for aluminum shielding over the evaporation contribution alone (Cucinotta *et al*., 1996b). Direct knockout of high-energy tritons are especially of importance because of their large ranges in shielding. Knockout components will be sensitive to nuclear structure effects such as shell structure and clustering. For example, alpha knockouts should dominate for ^{12}C and ^{16}O projectile or targets, deuteron knockout for ^{14}N, and triton for ^{27}Al. The limited existing measurements of these cross sections suggest that double differential cross-section measurements at several proton energies on a wide range of targets are needed. Light particle production from composite projectiles provides an interesting effect where a substantial number of particles are produced with a higher velocity than that of the projectiles due to internal Fermi motion of the projectile. The effects of the Fermi boost on GCR transport have not been well studied (Shavers *et al*., 2001). These data could be supplemented with double differential cross sections for light particle production from several of the more abundant GCR nuclei (*e.g*., helium and oxygen).

For interaction cross-sections and radiation transport measurements, proton and heavy-ion accelerator facilities, which deliver ions in the energy range from 100 to 2,000 MeV n^{-1} are required. Radiation biology studies will require facilities in this energy

range, however they can also take advantage of lower energy facilities to isolate effects of dominant secondary charged particles and of neutrons. Figure 4.5 lists existing proton and heavy-ion accelerators with capabilities in the energy range of interest. The Alternating Gradient Synchrotron at Brookhaven National Laboratory has the capability for studies over the high-energy range of the GCR spectrum (>1,000 MeV n^{-1}). A new facility at Brookhaven National Laboratory, the NASA Space Radiation Laboratory (formerly known as the Boosters Application Facility) was completed in 2003 and provides the capabilities for the intermediate energy range (100 to 1,500 MeV n^{-1}) needed for science goals in space radiation research.

Optimal planning of future cross-section and thick target measurements should build on existing measurements. Variables

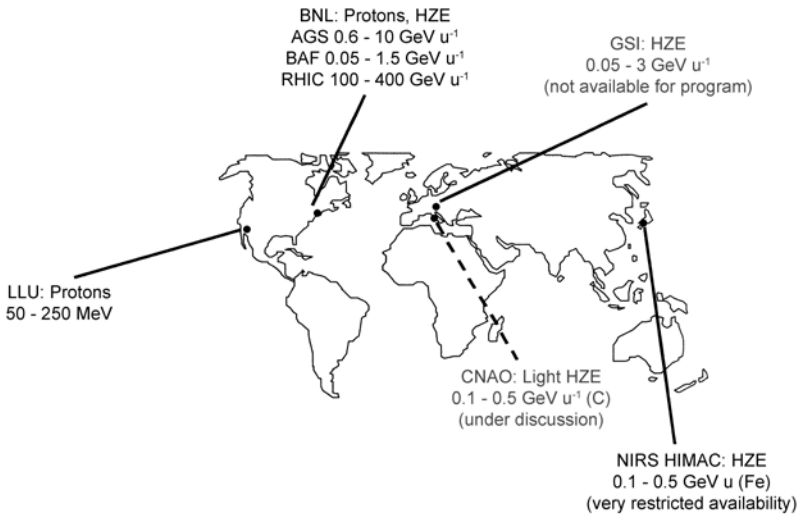

Fig. 4.5. Descriptions of worldwide accelerators available for proton and heavy-ion research [AGS = Alternating Gradient Synchrotron (Brookhaven National Laboratory, Upton, New York); BAF = Booster Applications Facility (Brookhaven National Laboratory, Upton, New York); BNL = Brookhaven National Laboratory (Upton, New York); CNAO = Centro Nazionale de Adroterapia Oncologica (Milan, Italy); GSI = Gesellschaft fur Schwerionenforschung (Darmstadt, Germany); HIMAC = Heavy Ion Medical Accelerator (Chiba, Japan); LLU = Loma Linda University Proton Therapy Accelerator (Loma Linda, California); NIRS = National Institute of Radiological Research (Chiba, Japan); and RHIS = Relativistic Heavy Ion Collator (Brookhaven National Laboratory, Upton, New York)].

for beam target selection include the number of projectiles, the number of projectile energies, and the number of target materials. Thick target measurements of fluence rates will be necessary including studies of multi-layered configurations. Needed cross-section measurements include inclusive double differential measurements in energy and angle, inclusive single differential measurements in energy, and total inclusive isotopic or elemental distributions. It has been estimated beam times of ~1 h per data point for small angle cross sections and fluences from iron fragments with 10 % accuracy (Wilson *et al*., 1997a). This value would change with angle and secondary energy as well as with the fragment mass and a range of 0.5 to 2 h per data point should be expected. New developments in charged particle detection methods could impact these estimates.

4.2.5 *Survey of Proton, Neutron, and High Atomic Number, High-Energy Transport Codes*

Much research has been invested in a large number of radiation transport codes that utilize distinct methods for a variety of applications. It is unlikely that space radiation problems can be handled with a one-size fits all approach. Therefore, the specific application will drive the methods to be used. One aspect of codes that can be standardized is the nuclear interaction models including developing methods of cross comparisons of distinct transport codes. Computational speeds are optimized if data libraries for cross sections are stored and called from data files in programs, rather than including the actual calculation procedure for cross sections within the transport code. Other considerations are the angular dependence of the reactions. For example, heavy ions >100 MeV n^{-1} travel predominantly in the forward direction and there is no need to evaluate angular deflections for isotropic fields in space. On the other hand, neutrons are created by several physical processes that have distinct angular production characteristics. The angular dependence of neutrons must be treated in the model. Light charged particles will behave intermediate to neutrons and heavy ions, and the role of angular deflections for space applications will require further study. In general, Monte-Carlo codes such as GEANT (Agostinelli *et al*., 2003), HETC (Armstrong and Colborn, 2001), and FLUKA (Fasso *et al*., 1997) have been used for accelerator studies and for atmospheric radiation and until recently were not yet fully developed for HZE transport calculations. Recent efforts to extend HETC and FLUKA to do HZE transport are nearing completion (Miller and Townsend, 2005; Pinsky *et al*., 2005;

Townsend *et al*., 2005). The NASA Code HZETRN has focused directly on the HZE transport problem (Tweed *et al*., 2004; Wilson *et al*., 1991; 1995b) and has been validated by space measurements in LEO where good agreement is found. Recent extensions of the code have added multi-group methods for bidirectional neutron transport (Clowdsley *et al*., 2000) and the addition of pion transport coupled to the GCR sources (Blattnig *et al*., 2004). However, no three-dimensional version of HZETRN currently exists.

4.3 Track Structure Models

The goal of track structure models is to provide a description of the position of excitation and ionization of target molecules from the passage of ions through a medium. Track structure descriptions are needed in theoretical models of biological responses, for understanding the extrapolation of limited radiation biology data to other radiation qualities, and for describing the response of radiation detectors to the variety of ions in space (Katz *et al*., 1971). Monte-Carlo track structure simulation codes have been used for studying the distribution and types of initial deoxyribonucleic acid (DNA) damage including models of single-strand break, double-strand breaks (DSB), base damage and clusters DNA damage (Goodhead and Nikjoo, 1989), or the description of the response of tissue equivalent proportional counters (TEPCs) (Nikjoo *et al*., 2002). Analytic models have also been used for a range of applications in particle detection and the theoretical description of radiation biology data. The assumptions of analytical models can be validated by more detailed Monte-Carlo simulations, and are useful for space radiation applications where the large number of particle types and energies place practical limitation on the use of Monte-Carlo simulations.

4.3.1 *Monte-Carlo Track Simulations*

Ionization and excitation processes caused by an ion's track and the electrons liberated by the primary ions lead to a stochastic process of biological events as particles pass through DNA, cells or tissues. Originating from the primary track are energetic secondary electrons (delta rays), which can traverse many cell layers from the track. Monte-Carlo methods have been developed over many years to consider these processes, but are rarely applied at high energies (>10 MeV n^{-1}). Simulation codes differ in interaction cross-section data used including treatments of liquid or gas phase cross sections. The cross sections needed for track simulation codes are the total, total elastic, total inelastic, ionization, and excitation cross sections.

Single and double differential cross sections are needed for production of electrons from the primary ion and for production from the secondary delta rays (Nikjoo *et al*., 1997). A review of the various track structure codes was made by Nikjoo *et al*. (1997), indicating a mature level of development. There are several codes available to consider electron tracks such as MOCA8B, OREC, and CPA100. For ion tracks, codes include PITS, NOREL (Semenenko *et al*., 2003), and DELTA, however the energy and charge range of many of these codes are limited to energies <10 MeV n^{-1} or require extensive computing times to sample high-energy delta rays produced by relativistic ions. There are few data at high-energies to validate the accuracy of the electron production cross sections, or effective charge assumptions used by these models (Rudd, 1997). Intercomparisons of codes for predicting the frequency distribution produced in biomolecules by ions and electrons have been made and indicate reasonable agreement between models (Nikjoo *et al*., 1997). Figure 4.6 illustrates the stochastic nature of the energy deposition showing a Monte-Carlo simulation of the energy transfer points made by a neon ion interacting with a spherical proportional volume of diameter 1 μm (Nikjoo *et al*., 2002).

4.3.2 *Analytic Track Structure Models*

A first-order numerical approach that relates LET, the basic physical parameter in conventional risk assessment, to track structure is to consider the relationship between the radial dose about the ion's track to the LET. The radial dose is the energy density distribution in a cylindrical shell of radius t, about the ion's path (Butts and Katz, 1967). LET is related to the radial dose by integrating the radial distribution over all radial distances up to the maximum allowable value (t_M):

$$\text{LET} = 2\pi \int_0^{t_M} t\,dt[D_\delta(t) + D_{\text{exc}}(t)] + \text{nuclear stopping.} \qquad (4.14)$$

In Equation 4.14 contributions from ionization are denoted here as D_δ, and excitations (D_{exc}) are considered in the radial distribution. The value of t_M defines the track width, and is a function of ion velocity, corresponding to the range of electrons with maximum energy ejected by the passing ion. The track width can extend well beyond 100 μm as the ion's velocity approaches the speed of light. The effects of nuclear stopping in radiation action are only important for very low-energy ions (<0.1 MeV n^{-1}). In the model of Kobetich and Katz (1968) the primary electron spectrum from

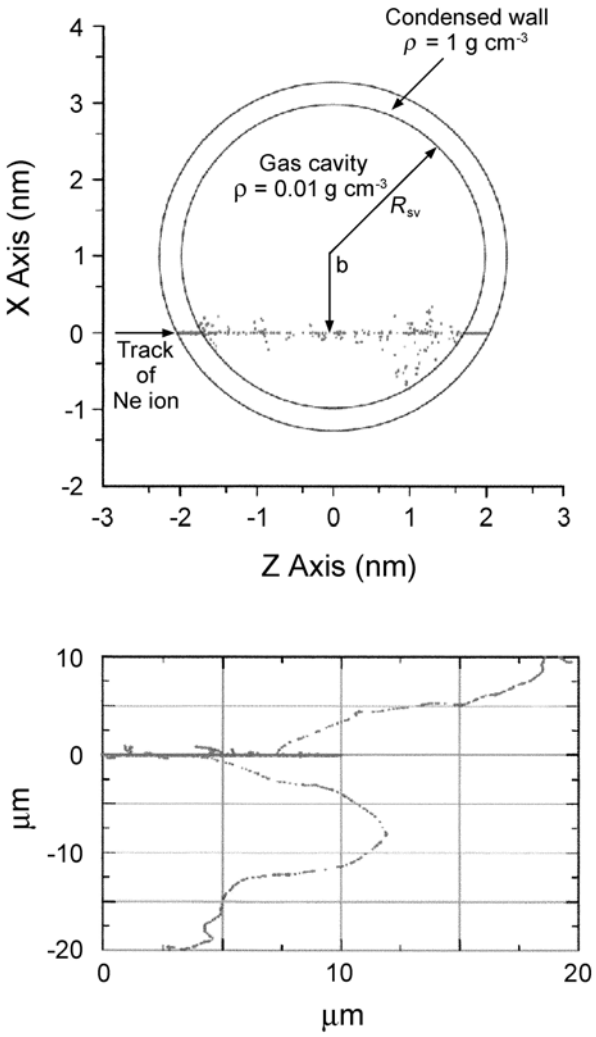

Fig. 4.6. An example of the energy transfer points produced by the passage of a high-energy neon ion through a walled proportional-counter chamber (top) and of the two-dimensional spatial distribution of two long-range delta rays (electrons) originating from the primary tract (bottom).

ion interactions with target atoms is folded with average transmission properties of electrons to obtain the spatial distribution of electron dose as a function of radial distance from the ion's path. The radial dose from ionization and delta-ray transport is described by:

$$D_{\delta}(t) = -\frac{1}{2\pi t}\sum_{i}\int \mathrm{d}\Omega\int \mathrm{d}\omega\frac{\partial}{\partial t}[\mathrm{E}(t,\omega)\,\eta(t,\omega)]\frac{\mathrm{d}n_{i}}{\mathrm{d}\omega\mathrm{d}\Omega}\,. \tag{4.15}$$

In Equation 4.15, ω is the initial electron energy, E is the residual energy of an electron with energy ω after traveling distance t, and $\eta(t,\omega)$ is the transmission probability that an electron with starting energy ω, penetrates a depth, t. Equation 4.15 includes an angular distribution for the number of primary electrons produced from target atom i (n_i) with energy, ω and solid angle Ω. The cross sections for electron production from protons are scaled to heavy ions using the effective charge. The angular distribution has important effects on the radial distribution both at large and small radial distances, and only a minor effect at intermediate values where a $1/t^2$ behavior holds. An *ansatz* (Brandt and Ritchie, 1974) can be used for the radial dependence of the excitation term, $D_{\mathrm{exc}}(t)$, as

$$D_{\mathrm{exc}}(t) = C_{\mathrm{exc}}(A,Z,\beta)\frac{\mathrm{e}^{-\frac{t}{2d}}}{t^{2}}\,, \tag{4.16}$$

with $d = \beta hc/4\pi\omega_{\mathrm{r}}$, c is the speed of light, β is the ion velocity divided by c, h is Planck's constant, $\omega_{\mathrm{r}} = 13$ eV for water, and C_{exc} is the normalization parameter. In Equation 4.16, the radial extension of excitations is confined to very small distances (<10 nm) as characterized by the parameter d (Brandt and Ritchie, 1974). Characteristics of the two components of the radial dose are illustrated in Figure 4.7, for two ions of LET close to 30 keV μm^{-1} (1 MeV protons and 300 MeV n^{-1} neon ions) (Cucinotta *et al*., 1999). The radial dose for the neon beam extends for many microns, while the low-energy proton beam deposits all of its energy within 0.1 μm of the track.

A second-order numerical approach to track structure, more closely related to the Monte-Carlo simulation, is to model the frequency distribution of energy imparted to a volume of biomolecular dimensions (Cucinotta *et al*., 2000). For high-energy ions, the frequency distribution can be described using the ion's impact parameter and distinguishing events where the ion passes through the volume (primary-ion events) and outside the volume (delta-ray events), and by determining the mean and variance of the energy imparted to the volume including corrections for delta ray escape out of the volume. The two components are weighted by considering the number of events as a function of impact parameter. Figure 4.8 shows calculations of the frequency distribution for energy imparted in a nucleosome for x rays, and iron ions using the analytic

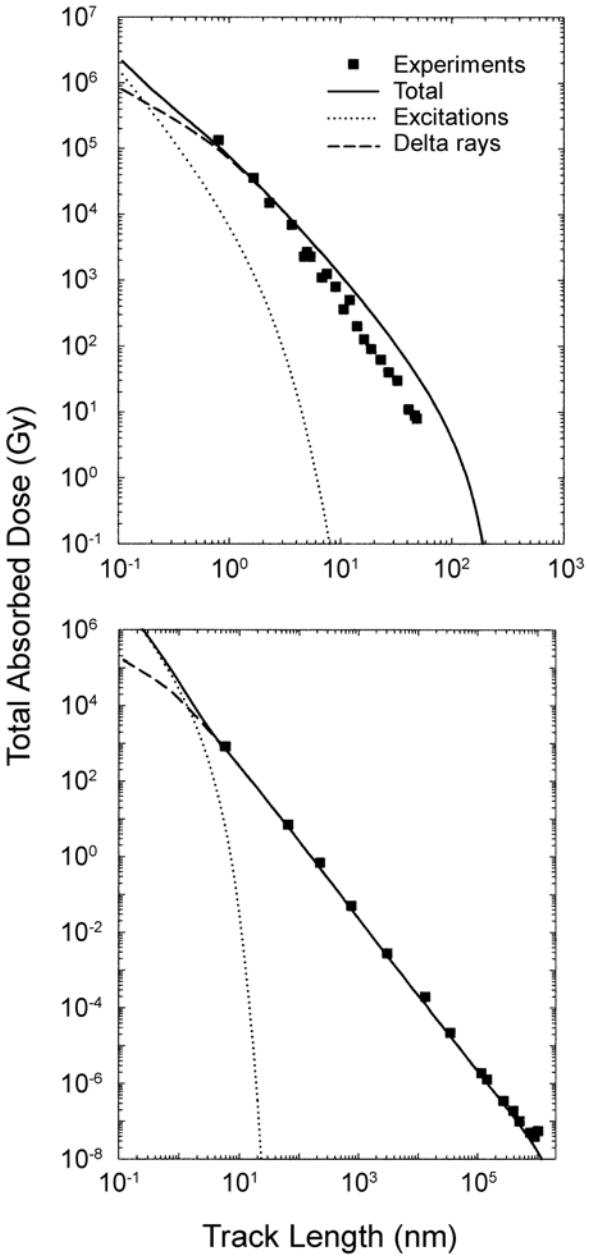

Fig. 4.7. Comparison of calculations of radial dose distributions to experiments for proton at 1 MeV (LET = 27 keV μm^{-1}) (top) and ^{20}Ne at 377 MeV n^{-1} (LET = 31 keV μm^{-1}) (bottom) (Cucinotta *et al*., 1999).

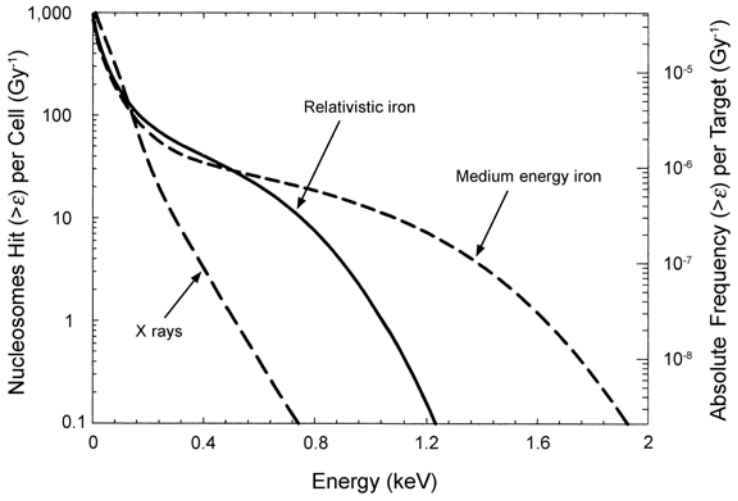

Fig. 4.8. Calculations of frequency distributions of energy deposition in a 10 × 5 nm target used to represent a nucleosome by x rays and different high-energy iron ions. The left ordinate shows the average number of events in the DNA structure in a typical mammalian cell, using the number of such targets given in Table 4.1. The right ordinate gives the absolute frequency in the DNA structure (Cucinotta *et al*., 2000).

model which agrees well with the PITS Monte-Carlo model. The results are normalized to the number of events per gray per target (left-hand axis) or the number of events per gray (right-hand axis). The frequency distributions demonstrate that there are energy deposition events in biomolecular targets that occur for high-LET radiation that are not possible with low-LET radiation, even at high doses (<100 Gy) (Goodhead and Nikjoo, 1989). Validations of theoretical predictions of track structure models is severely limited at this time, however the development of new experimental techniques in nanodosimetry could offer approaches for validation.

4.4 Validation of Radiation Transport Codes

An assessment of the accuracy of space radiation transport models for prediction of energy spectra of charged particles and neutrons can be made by comparisons to laboratory experiments with proton and heavy-ion beams or from spaceflight measurements. Spaceflight measurements involve many factors such that potential inadequacies in radiation transport models are difficult to isolate relative to possible inaccuracies in environmental or shielding models. Also, space validation is limited by the access to space and

current spacecraft materials, and may not be representative of model predictions for other material types such as those that occur on planetary surfaces or in advanced materials selection concepts. In this respect, laboratory validation is advantageous to test radiation transport computer codes and associated database models and to provide tests for studying material properties for reducing biological doses. Spaceflight measurements provide important tests of predictive capability of several factors and are needed for final validation of transport codes.

Tests of radiation transport codes with monoenergetic beams can be used to evaluate the accuracy of these codes. A minimal test of transport models is made by comparison to the Bragg ionization curve. More rigorous tests include the fluence distribution of particles along a water column or other target. Figures 4.9a and 4.9b show data and model comparisons for a neon beam using the Lawrence Berkeley Laboratory BEAM code (Wilson *et al.*, 1991). The off-axis distribution of dose or particle fluence provides a further test of the capability of a transport code. Figure 4.10 shows examples for proton beams comparing the traverse distribution measured experimentally with calculations from the LAHET code (ICRU, 2000; Siebers and Symons, 1997). Detailed beam characteristic data for fragment charges and energy or LET spectra from several HZE ions are clearly needed for benchmark studies in multi-layer material configurations representative of spacecraft structures of radiation transport codes.

Validation of the emerging Monte-Carlo codes High Energy Transport Code-Human Exploration and Development in Space and FLUKA using laboratory beam data for heavy-ion beams such as ^{56}Fe at energies representative of GCR particles (~1 GeV n^{-1}) have been undertaken. The initial results comparing fragment yields for thick targets of carbon and carbon epoxy materials appear to be promising (Townsend *et al.*, 2005).

4.4.1 *Flight Validation*

Measurements on NASA STS flights over many years and on the Russian space station Mir have allowed for a large number of comparisons of radiation transport codes to flight measurements. Passive measurements with CR-39® (PPG Industries, Inc., Pittsburgh, Pennsylvania) nuclear plastic detectors have limitations at both low-LET (<5 keV μm^{-1}) and for short tracks from target fragments or stopping GCR ions of high-LET values. The use of active dosimeters on STS flights has allowed for separation of GCR contributions from that of trapped protons, which was not possible with passive dosimetry (Badhwar and Cucinotta, 2000).

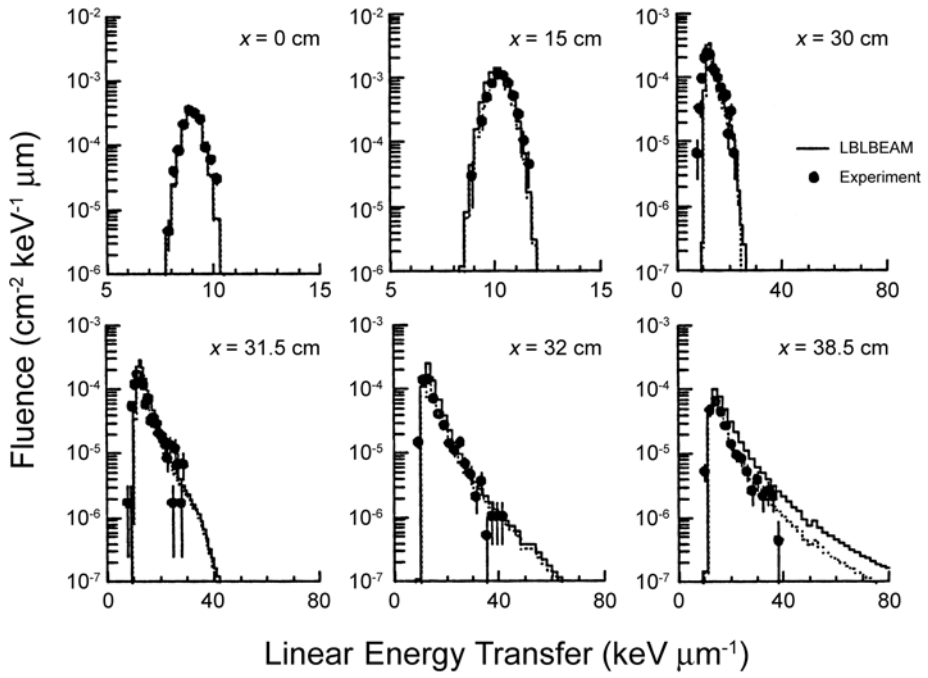

Fig. 4.9a. Differential fluence for carbon nuclei produced by neon nuclei incident on various thicknesses of water (Wilson *et al.*, 1991).

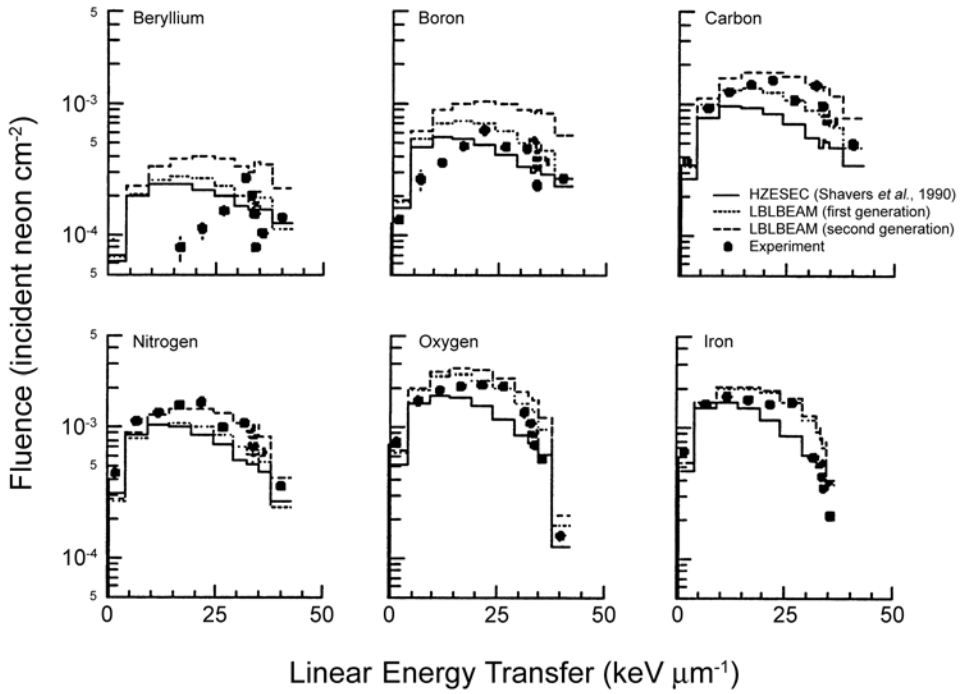

Fig. 4.9b. Integral fluence for all fragments produced by neon nuclei incident on various thicknesses of water as a function of water column thickness (Wilson *et al*., 1991).

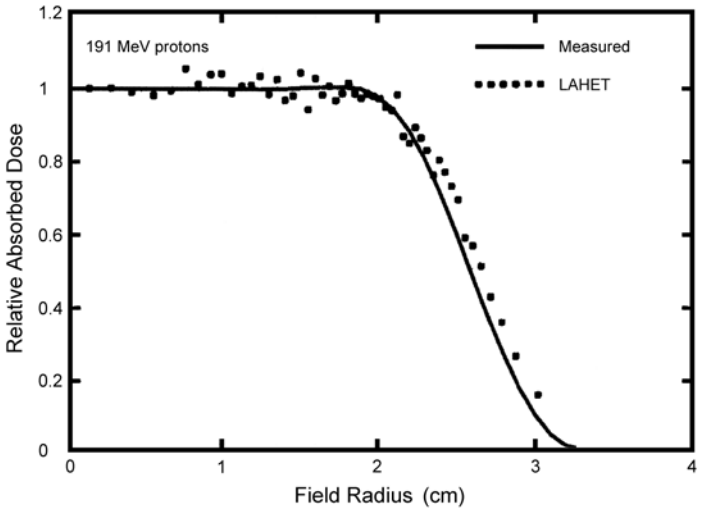

Fig. 4.10. Measured and computed traverse proton beam absorbed dose profiles at a depth of 5 cm for a 191 MeV incident proton beam. The collimator diameter was 5 cm, the beam was degraded with a 9.3 cm thick acrylic absorber, and the Bragg peak was spread out to 11 cm (90 % dose level in water). The profiles are normalized to one on the central axis (Siebers and Symons, 1997).

Measurements on STS flights by Badhwar (2000) were made with a cylindrical TEPC with a length to diameter ratio of one simulating a 2 μm diameter site that covered a lineal energy range of 0.25 to 1,250 keV μm^{-1} in 512 channels. Comparisons of space measurements using the TEPC to the HZETRN transport code for total absorbed dose and dose equivalent on several STS flights and Mir missions are shown in Table 4.3. The comparisons use the free-space GCR model of Badhwar and O'Neill (1992) and representations of the STS or Mir shielding distribution about the detectors. The root mean square error is found to be <15 % for the majority of the comparisons. In Table 4.4 comparisons between measurements with a human phantom torso to results from the HZETRN code using the computerized anatomical man model are shown (Badhwar *et al*., 2002). Agreement is excellent for the organ absorbed dose measurements, especially when the efficiency of the response of the thermoluminescent dosimeters (TLDs) to high-LET particles is considered. Further measurements of LET spectra and neutron fluence are needed at the organ level to fully validate the transport models. A comparison of the measurements of lineal energy spectrum on STS-56 with calculations using the HZETRN

TABLE 4.3—*Comparisons of TEPC measurements of the GCR absorbed dose and dose equivalent on several STS and Mir missions to HZETRN code with Badhwar and O'Neill (1992) GCR model.*

Mission	Date	Inclination	Altitude	Shielding	Absorbed Dose (mGy d^{-1})		Percent Difference	Dose Equivalent (mSv d^{-1})		Percent Difference
					Measured	Theory		Measured	Theory	
STS-40	1991	39	293	DLOC-2	0.052	0.048	7.7	0.13	0.16	–23.1
STS-49	1992	28.5	358	DLOC-2	0.05	0.048	4	0.127	0.155	–22
STS-51	1993	28.5	296	Payload bay	0.044	0.048	–9.1	0.144	0.154	–6.9
STS-57	1993	57	298	Payload bay	0.113	0.109	3.5	0.422	0.434	–2.8
STS-57	1993	57	298	DLOC-2	0.138	0.11	20.3	0.414	0.37	10.6
Mir-18	1995	51.6	390	P	0.142	0.141	0.7	0.461	0.526	–14.1
STS-81	1997	51.6	400	0-sphere	0.147	0.135	8.2	0.479	0.521	–8.8
STS-81	1997	51.6	400	Poly 3 inches	0.138	0.138	0	0.441	0.400	9.3
STS-81	1997	51.6	400	Poly 5 inches	0.129	0.118	8.5	0.316	0.368	–16.5
STS-81	1997	51.6	400	Poly 8 inches	0.128	0.113	11.7	0.371	0.323	12.9
STS-81	1997	51.6	400	Poly 12 inches	0.116	0.111	4.3	0.290	0.298	–2.8
STS-89	1998	51.6	393	0-sphere	0.176	0.148	15.8	0.561	0.614	–9.4
STS-89	1998	51.6	393	Al 3 inches	0.167	0.159	4.8	0.445	0.488	–9.7
STS-89	1998	51.6	393	Al 7 inches	0.149	0.161	–8.1	0.529	0.617	–16.6
STS-89	1998	51.6	393	Al 9 inches	0.171	0.162	5.3	0.492	0.541	–10

TABLE 4.4—*Comparisons of TLD measurements inside a human phantom torso on STS-91 to predictions from HZETRN code for absorbed doses in organs and tissues using the computerized anatomical man model.*

Phantom Data on STS-91 for Trapped and GCR (51.6 × 390 km)					
Organ	Measured (mGy)	Theory (mGy)	Theory[a] (mGy)	Percent Difference	Percent Difference[a]
Brain	2.23	2.42	2.26	–8.5	–1.4
Bone surface	2.16	2.36	2.21	–9.3	–2.1
Esophagus	1.71	1.79	1.67	–4.7	2.2
Lung	1.92	1.81	1.69	5.7	11.9
Stomach	2.05	2.08	1.94	–1.5	5.2
Liver	1.88	2.15	2.01	–14.4	–6.9
Spinal column	1.65	1.98	1.85	–20	–12.1
Bone marrow	1.75	1.98	1.85	–13.1	–5.7
Colon	1.71	1.9	1.78	–11.1	–3.8
Bladder	1.58	1.87	1.75	–18.4	–10.6
Gonad	1.75	1.85	1.73	–5.7	1.2
Skin (breast)	2.46	2.58	2.41	–4.9	2
Skin (abdomen)	2.35	2.58	2.41	–9.8	–2.6

[a]Includes a correction to TLD efficiency versus LET.

code and a track model of direct and indirect events is shown in Figure 4.11. Differences between y-spectra and LET-spectra arise due to the effects of straggling and delta rays including the wall effect. The region <0.2 keV μm^{-1} is shown to be dominated by indirect events from delta rays where the ion does not pass through the gas (Shinn *et al*., 1999).

Particle energy distributions measured on STS-48 are shown in Figure 4.12. Charged particle telescopes can provide measurements of the energy spectra of light particles from ~15 to 400 MeV for protons and other $Z = 1$ and $Z = 2$ ions from 5 to 70 MeV n^{-1}. These measurements are strictly secondary radiation due to Earth's geomagnetic cutoffs, which exclude particles below a few hundred MeV n^{-1} from entering the vehicle orbit. Excellent agreement with the HZETRN code for protons was observed. For deuteron spectra the agreement was satisfactory only when knockout

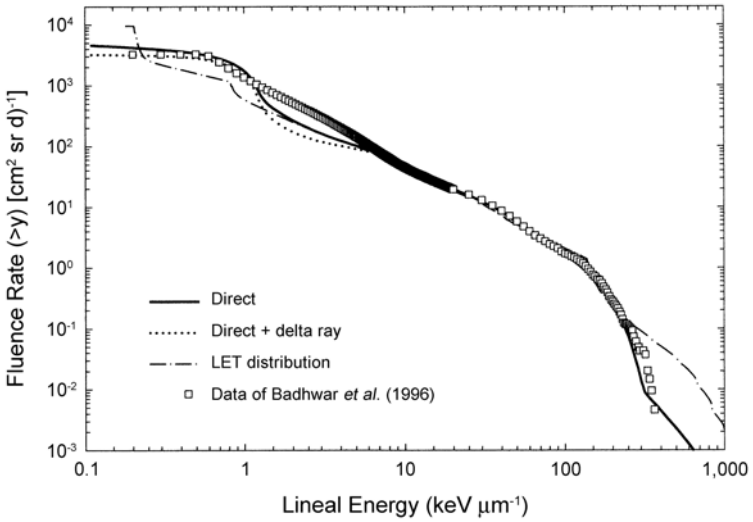

Fig. 4.11. Comparison of calculations of LET and lineal energy spectra to TEPC lineal energy spectra measurements from GCR and secondaries on STS-56 shuttle mission (Badhwar *et al*., 1996).

deuterons from proton and neutron induced reactions are included. For ^{3}He and ^{4}He the agreement was less satisfactory, and may point to a deficiency in the evaporation cross sections of the FLUKA model used by HZETRN.

4.4.2 *Mars Surface Validation*

There is a limitation in the use of LEO GCR measurements to validate models for deep-space mission exposure in that the comparisons are largely for aluminum shielding. Several other materials need to be tested for NASA mission scenarios including regolith on lunar or planetary surfaces or inside tissue. Also, there is a limitation in comparisons in LEO due to magnetic cutoffs where lower energy primary components contained in free space are not present. More recent measurements are being made with polyethylene spheres and others could be made on future space missions. On the surface of Mars other factors arise. Most notably models predict that 20 to 40 % of the dose equivalent will be from neutrons or secondary charged particles produced by neutrons. The undertaking of surface measurements on Mars prior to human exploration is warranted to confirm the ability of models to predict the surface environment. Recent measurements by the Odyssey spacecraft included neutron and gamma-ray spectrometry to verify the presence of water-ice at the northern and southern poles of Mars. Neutron

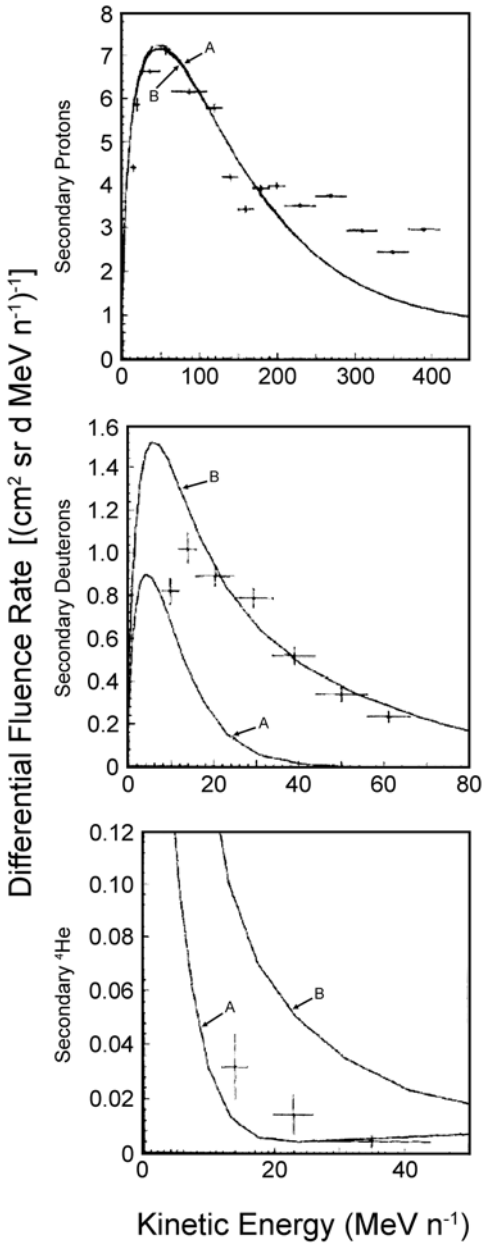

Fig. 4.12. Plot of the differential energy spectrum of secondary (top) protons, (center) deuterons, and (bottom) ^{4}He produced by GCR particles on STS-48 (September 11 and 12, 1981; 57° × 565 km). Curve A was calculated using the HZETRN model and Curve B was observed.

spectra on the Mars surface are predicted to be strongly dependent on the soil composition as shown in Figure 4.13 (Clowdsley *et al*., 2001). For a direct surface measurement, data on the directional composition of neutrons is needed and should be dependent on the soil composition including the presence of CO_2 or water frost.

4.5 Biophysics Models and Shielding Effectiveness

In the past, biological response has most often been defined using LET as the descriptive parameter of radiation quality. The accuracy of risk predictions using LET-dependent quality factors is of concern because of the small number of experiments available to determine radiation quality. Almost all biophysics models of energy deposition by heavy particles (Goodhead and Nikjoo, 1989; Katz *et al*., 1971) predict biological responses that are a function of ion charge and velocity and not unique to LET, especially at low particle fluence. Studies of shielding effectiveness with track structure models fitted to heavy-ion radiation biology data have allowed issues related to specification of radiation quality to be studied and have indicated important differences between the use of LET, or Z and β as descriptors of biological effects in assessing shielding materials (Wilson *et al*., 1995b).

For fixed-LET, ions of higher Z will have higher β and, therefore, wider tracks. Large track-width (>100 nm) ions will become less effective for DNA damage since on average less energy is deposited in the critical volume. The delta rays from higher-energy ions are also of higher energy, which are expected to be less effective in producing biological damage. For endpoints other than DNA damage other considerations may arise. For example, in studies of bystander effects the effect of track width could lead to an increased effect compared to particles with track widths <500 nm. For tissue damage, ion range is a consideration since the number of cells traversed is important. For low-Z ions, target fragments will have much higher ionization power than the primary ion and could dominate biological effects reducing the accuracy of LET as a descriptive variable. A dependence on both charge and energy, and not LET alone has been observed in several radiation biology experiments that have considered this effect in mammalian cells (Belli *et al*., 1991; Kiefer *et al*., 1996) and also in studies of inactivation or mutation in *E. Coli* and *B. Subtilis* (Cucinotta *et al*., 1997). There are very few experiments that have studied the possible variation of biological effects of fixed-LET values for distinct ion charge or velocity. Katz *et al*. (1971) noted that such effects are masked at high doses where on average more than one particle traverses a cell. Studies at high doses, where

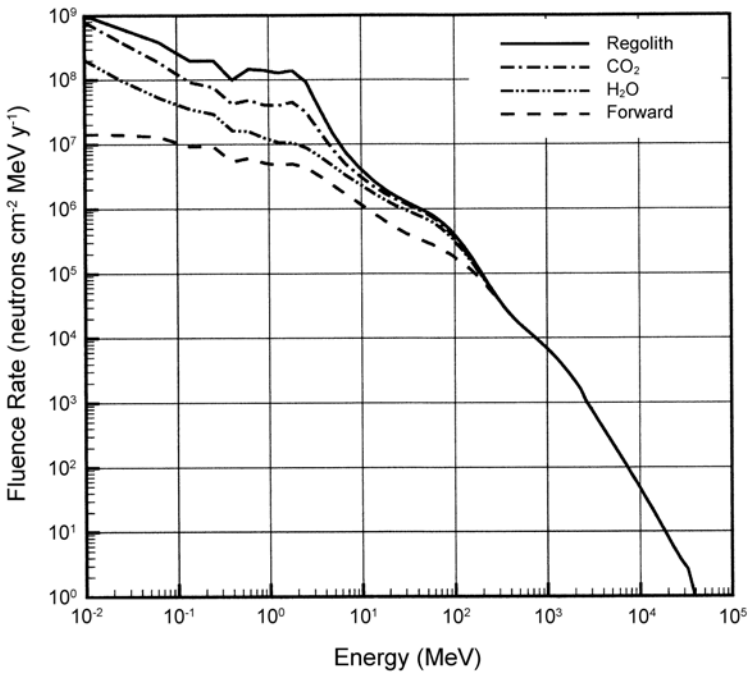

Fig. 4.13. Calculations of neutron energy spectra on surface of Mars that consider the soil composition of the Martian surface and the contribution of forward (from GCR interactions in the atmosphere) and backward neutrons (from the soil) (Clowdsley *et al*., 2001).

on average more than one particle traverses a cell, are predicted to mask this effect (Katz *et al*., 1971). Studies with space radiation transport codes show that estimating the effectiveness of spacecraft materials depends critically on the biological response model considered in the analysis (Wilson *et al*., 1995a). Studies of shielding effectiveness, using track structure approach fitted to available radiation biology data, suggest that shielding such as aluminum or other materials with higher mass constituents are ineffective in attenuating GCR dose equivalent, while water is marginally effective (Figure 4.14). This is largely due to the increased effectiveness of low-energy protons and alpha particles compared to relativistic ions of the same LET. Lower-*Z* materials, such as liquid hydrogen or carbon composites, are seen to be effective shields. This is in contrast to the attenuation in risk seen using quality factors where the attenuation is moderate for aluminum and significant for water. Design of spacecraft shielding for lunar and Mars missions is limited until the radiation biology of radiation quality is better understood.

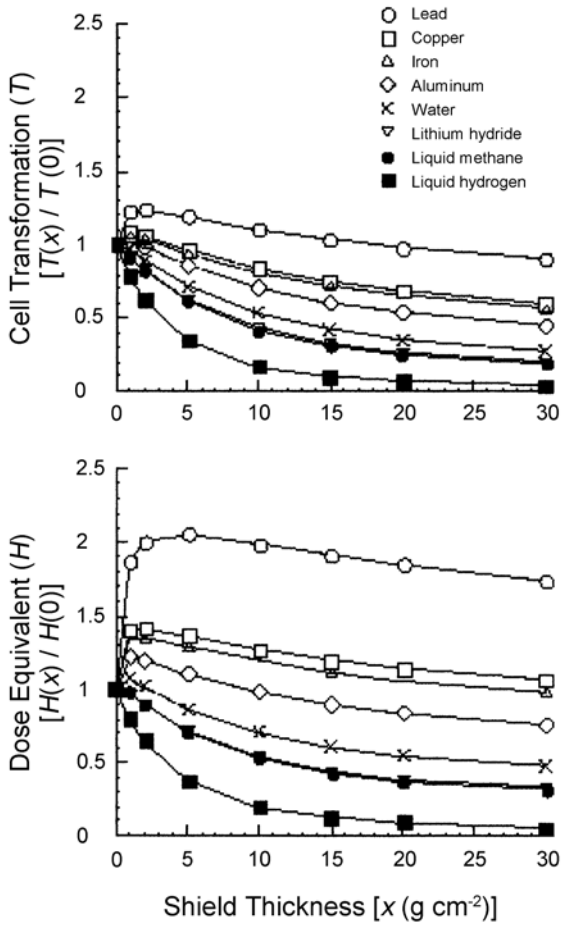

Fig. 4.14. The attenuation of dose equivalent and cell transformation for a 1 y GCR exposure at solar minimum behind various shield materials (Wilson *et al*. 2001).

5. Space Dosimetry

5.1 Introduction

Crew members on long-term space missions will be exposed to complex radiation fields resulting from a wide variety of radiation sources. In order to be effective in minimizing their radiation exposure, the radiation protection program must include dosimetry instrumentation and data processing tools which can evaluate changes in the radiation exposure characteristics, and make this evaluation in a time which is short compared to that which would lead to a significant increase in the projected crew member exposure for the mission. This evaluation must include sufficient characterization of the radiation field to allow determination of the absorbed dose and dose equivalent, and to estimate the reduction in dose equivalent that could be achieved by moving to areas of the spacecraft that provide different shielding. Radiation exposures on space missions originate from GCR, radiation from the sun including SPEs, and radiation from man-made sources intentionally included in the space vehicle. This Section outlines the properties that a dosimetry system must have in order to characterize crew exposure. Instrumentation and techniques for some of the needed measurements exist, but several improvements are necessary to provide reliable dosimetry for long-term space missions.

5.2 Radiation Environment

5.2.1 *Primary Radiations*

Outside the influence of Earth's magnetic field, the GCR fluence rate and spectrum vary slowly with time and are reasonably well known. The absorbed dose and dose equivalent (assuming that a definition of quality factor for each component of the radiation exists) due to the incident particles can be predicted in advance of the mission. However, GCRs produce a wide variety of fragmentation products when they interact with matter. The contribution to the absorbed dose produced by these secondary particles, particularly neutrons, depends in a complex way on the configuration of

the vehicle, the cross sections for producing secondary particles, and the cross sections for scattering and stopping the secondaries after they are produced. The absorbed dose and dose equivalent due to primary particles, charged fragmentation products, and secondary particles produced by uncharged fragmentation products, can be calculated at any point within the spacecraft using a model of the distribution of matter in the spacecraft, and validated radiation transport codes (Section 4). The accuracy of the results of these calculations is inherently less than the accuracy of data on the incident spectrum because of the uncertainties in fragmentation cross sections and approximations in the model of the distribution of matter in the space vehicle. Furthermore, changes that are made later in the physical configuration of equipment or supplies within the vehicle can significantly alter the scattering and attenuation of the radiation and have an effect on the dose-equivalent rate. In addition, evaluation of the health risks of the high-LET component of the radiation field involves large uncertainties (Section 6). Thus, although the spectrum of charged particles at a point can be calculated with modest accuracy, the conversion to dose equivalent requires use of quality factors that involve large uncertainties.

The absorbed-dose rate and quality of radiation from the sun are much more variable than GCR. The range of particle energies is somewhat less than for GCR, and the absorbed dose due to incident HZE particles of solar origin is generally negligible (Cleghorn and Badhwar, 1999). However, high-LET particles may still be produced by target atom fragmentation. A capability to calculate the expected dose rate and radiation quality of the particles reaching the crew based on observation of the sun would provide a valuable opportunity to plan the response to an SPE. However, sound radiation protection policy also requires that the onboard radiation protection system be able to measure the resulting dose rate and confirm the results of the calculations.

Radiation exposure from man-made sources is diverse, and could include sources used in instrumentation, possibly isotopic heat sources, and in some cases even small fission power sources. Such man-made sources would be expected to be engineered so that there would be very little radiation exposure under normal circumstances. However, the radiation protection and dosimetry system should be capable of dealing with a broad range of exposures which might occur as the result of an accident involving a radiation source, or changes in the configuration of the vehicle which do not involve the source directly.

5.2.2 *Secondary Particles*

Space radiations undergo a wide variety of atomic and nuclear interactions in irradiated material and produce three distinct classes of secondary radiation: additional heavy particles, photons and electrons. The heavy particles, including protons and neutrons, and high-energy photons are the result of target and projectile fragmentation, and their frequency and energy distributions are discussed in Section 4. Only a very small fraction of the energy transferred in a fragmentation event goes to photons so they deliver only a very small fraction of the total absorbed dose. The charged particles produced by fragmentation of incident particles have lower-Z, with velocity only slightly less than the incident particle. These fragments have lower stopping power than the particle that produced them, and longer range. The result is to increase the volume irradiated and decrease the mean absorbed dose in the irradiated volume, relative to that produced if the particle had not undergone a fragmentation event. Furthermore, lower stopping power can result in lower biological effectiveness per unit absorbed dose, so these fragmentation processes generally reduce the mean RBE of the resulting radiations. However, incident particle fragmentation also produces neutrons. These uncharged particles have relatively low interaction cross sections and long mean-free paths. When they do interact they may transfer a substantial fraction of their energy to a proton or heavier recoil nucleus. Recoil protons and nuclei have lower energies and potentially higher stopping powers than the particle that produced the neutron. Thus, this mechanism tends to distribute the energy over a large volume, reducing the dose at a point, but potentially increasing the biological effectiveness.

The products of target atom fragmentation frequently have higher-Z than the incident particle, as well as lower velocity, and consequently have much higher stopping power and shorter range. This process often increases the RBE of secondary particles relative to the incident particle. The overall effect of this is that a large fraction of the dose equivalent is produced by particles that deliver a very small fraction of the absorbed dose. In the case of measurements on the Mir Space Station, 65 % of the dose equivalent was delivered by the 15 % of the absorbed dose that was produced by particles with stopping power >10 keV μm^{-1} (Yasuda *et al*., 2000).

Energetic secondary electrons, commonly referred to as delta rays, are produced in large numbers as heavy ions interact with the electrons of the atoms they pass. These delta rays can have ranges which extend to much more than the diameter of a biological cell.

Their stopping power is low so they distribute some of the energy lost by the primary ion into a volume surrounding the path of the primary particle. Since the volume irradiated by delta rays significantly increases the number of cells that receive radiation damage, they may play a significant role in the biological effectiveness of HZE particles. The energy that delta rays deposit is included in the stopping power of the primary particle, so, if delta-ray equilibrium has been established, the absorbed dose can be calculated without referring specifically to the delta-ray component. However, the biological effectiveness may differ significantly from that delivered directly by the heavy particle. For example, the RBE for chromosome damage in rat tracheal epithelium exposed to 1 GeV n^{-1} iron ions is much less than the RBE for this endpoint when the tissue was exposed to radon alpha particles with similar stopping power, and thus LET (Brooks *et al*., 2001).

5.3 Measurement in Mixed Fields

Calculation of absorbed dose and evaluation of dose equivalent for a mixture of incident particles, secondary radiation, and man-made radiation is not difficult (although it may require a great deal of computer time). However, calculations can result in significant errors due to incomplete input data. For example, Figure 5.1 (Badhwar *et al*., 2001) shows a comparison of calculated and measured neutron fluence on the STS-57 mission. Comparisons of calculated and measured values of absorbed dose at different depths in spherical absorbers (Badhwar and Cucinotta, 2000) and of organ absorbed dose in a phantom (Badhwar, 2002) indicate that they differ by as much as 20 %. It appears that much of this error is due to models underestimating the contribution due to neutrons. Thus, calculations alone are generally not sufficient for a radiation protection program. In addition to other limitations, the sources of radiation, particularly the solar-particle fluence and man-made sources, may change unpredictably. Experimental evaluation of the absorbed dose and dose equivalent due to a complex radiation field requires measuring the charged particle fluence or other spectral information which can be used to deduce radiation quality. The interpretation of these measurements requires knowledge of the detector response for each component of the field and enough different detector types, with different response functions, so that the radiation spectrum can be derived unambiguously. Typically, detectors such as thin scintillators or TEPCs, which can characterize the stopping power of the particle and are sensitive to high-energy protons, will record some delta rays as distinct events. Such

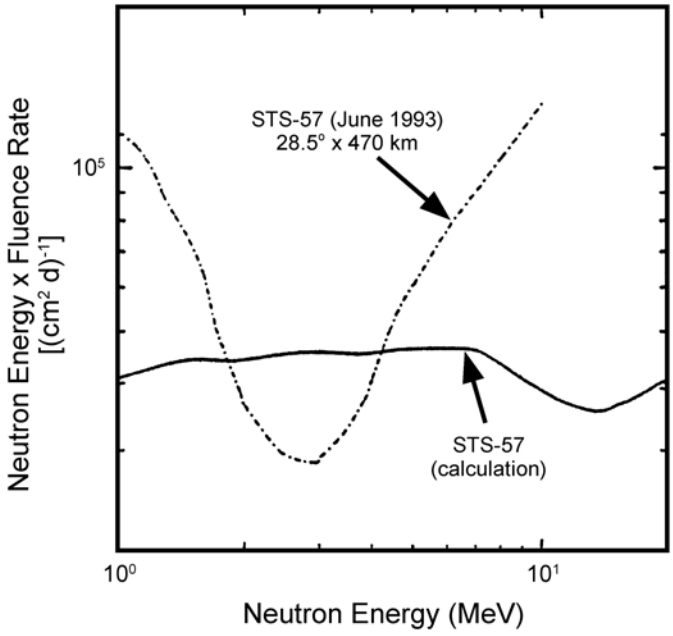

Fig. 5.1. Comparison of calculated versus measured neutron fluence for the STS-57 mission.

detectors will typically measure something related to a restricted LET for the primary radiation, a value less than the stopping power, due to escape of delta rays from the detector. Other spectrometers, such as charged particle telescopes, typically measure both the stopping power and the total energy of the incident particle. These data are used to determine the incident particle charge and velocity. These detectors will not detect delta rays separately from the primary radiation that produced them, and are not able to detect photons or neutrons. A third type of spectrometer, such as thick scintillator, measures only the total energy of the incident particle and cannot distinguish between particles with the same total energy but different stopping power and, therefore, different biological effectiveness. Furthermore, this third type of detector cannot distinguish between directly ionizing incident particles and the secondaries of neutrons or gamma rays. These detectors can be used to determine total absorbed dose, but cannot provide data for evaluating radiation quality. Other specialized detectors, such as neutron spectrometers, measure a component of the field, but must be used in coordination with additional detectors to attempt an evaluation of the total absorbed dose and dose equivalent.

The reason for these limitations on the information that can be derived from different types of detectors is simply that there is no difference between an incident proton and a recoil proton of the same energy, or between equal energy electrons produced as delta rays or photon secondaries. Small or thin detectors sample the energy transferred to a small volume. This is essentially the stopping power of the particle minus the energy transferred by the portion of each delta-ray track that lies outside the detector volume, and provides no information about the particle type or origin. Single detectors that are large enough to stop the primary particle, cannot distinguish between particles which have similar stopping power, such as electrons and protons. To distinguish different types of particles, a system which measures energy deposition in two or more detectors is required. This allows determination of the rate of change of stopping power and, therefore, the mass of the particle. However, charged particles produced as secondaries of indirectly ionizing radiation cannot be identified as such and those with short range may not be detected by such instruments.

Most of these differences in the response of different detector types do not affect the determination of the absorbed dose, but they make it difficult to determine the fluence spectrum and to determine the dose equivalent. Furthermore, they make it difficult to compare measurements with calculated absorbed dose distributions.

Radiation protection instrumentation must be adequate to deal with the consequences of accidental damage to any radioactive sources which may be present. The fluence of high-energy particles and secondary radiations will interfere with the conventional methods for characterizing the spread of contamination and changes in exposure rate which might occur as a result of such an accident.

5.4 Energy Deposition Patterns for Components of the Radiation Spectrum

The measurement of all of the components of the radiation spectrum in a spacecraft is difficult. The uncertainty in the biological consequences of the radiations involved adds another dimension to the problem. It is shown in Section 6 that an unambiguous relationship between charged particle stopping power and RBE does not exist. However, it has not been established that any other physical description of the radiation field will produce a more consistent relationship. Thus, NCRP has recommended continued use of the conventional procedure utilizing the quantity dose equivalent (NCRP, 2001a) for space radiation, rather than conversion to a particle fluence or a microdosimetry approach.

In order to determine the most effective way to measure and characterize the radiation fields encountered in space, the energy deposition characteristics of the components of those fields and the possible biological consequences of those characteristics must be evaluated. This includes the primary radiations and the secondary particles they produce when they interact with the spacecraft and its occupants. Furthermore, design of a dosimeter or spectrometer requires information on the range, stopping power, and secondary radiations which are likely to be produced by each incident radiation. Finally, when developing criteria for the design of instruments, data on energy deposition characteristics are useful for evaluating the potential biological significance of a specific group of particles and, therefore, the priority which should be given to measuring them accurately. That is, if particles of a particular type will contribute a negligible amount to the dose equivalent, the accuracy with which that contribution can be measured need not receive high priority in the design of the measurement system.

Radiation dose limits for the space environment are currently expressed in terms of effective dose and gray equivalent, using appropriate weighting factors for the type of radiation and the health effect of concern. Alternatives to this approach are possible, and a recent study (NCRP, 2001a) concluded that, when more biological data becomes available, significant improvements in the accuracy of risk estimates may be achieved by converting to a dosimetry system which is more directly related to the type and energy of the particles interacting with the biological targets.

Because the space radiation environment consists of such a wide range of incident particles, some of them with very high energies, a very wide range of energy deposition patterns can be produced. However, some of these energy deposition patterns occur during only a very small part of the total energy deposition of the primary particles. Table 5.1 lists the mass stopping power (in MeV cm^2 g^{-1}), range, and mean delta-ray penetration (radial dimension of the track) for three particle types which are of interest in space radiation. Table 5.2 gives an indication of the fraction of the absorbed dose and the fraction of the range of individual particles which occur in specific ranges of stopping power. Although a 100 MeV proton does deposit some of its energy at high-LET, that is between 10 and 80 keV μm^{-1} where the biological effectiveness is increasing, this is only 3.5 % of the total energy deposited and it occurs in just 0.3 % of the length of the proton track.

Incident high-energy protons would be expected to have low mean quality factors. However, the mean-free path for nuclear interactions is not large compared to the dimensions of space-craft

TABLE 5.1—*Summary of properties of some heavy charged particles in water.*

Energy (MeV n^{-1})	Proton		Helium		Iron		Delta-Ray Penetration[b] (μm)
	$dE/\rho dx$[a] (MeV cm^2 g^{-1})	Range (g cm^{-2})	$dE/\rho dx$ (MeV cm^2 g^{-1})	Range (g cm^{-2})	$dE/\rho dx$ (MeV cm^2 g^{-1})	Range (g cm^{-2})	
1	2.608×10^{2}	2.458×10^{-3}	1.03×10^{3}	2.71×10^{-3}	4.31×10^{4}	1.61×10^{-3}	0.1
10	4.56×10^{1}	1.23×10^{-1}	1.81×10^{-1}	1.24×10^{-1}	2.61×10^{4}	1.62×10^{-2}	2.86
100	7.29×10^{0}	7.72×10^{0}	2.90×10^{1}	7.76×10^{0}	4.97×10^{3}	6.30×10^{-1}	58.8
200	4.49×10^{0}	2.59×10^{1}	1.79×10^{1}	2.61×10^{1}	3.09×10^{3}	2.13×10^{0}	127
500	2.74×10^{0}	1.17×10^{2}	1.96×10^{1}	1.18×10^{2}	1.88×10^{3}	9.53×10^{0}	342
1,000	2.21×10^{0}	3.25×10^{2}	8.84×10^{0}	3.22×10^{2}	1.48×10^{3}	2.67×10^{1}	708

[a]$dE/\rho dx$ = mass stopping power.
[b]Chatterjee and Schaefer (1976).

TABLE 5.2—*Fraction of the absorbed dose and path length with specified stopping power.*

Stopping Power	1 – 10 keV μm^{-1}		10 – 80 keV μm^{-1}		80 – 120 keV μm^{-1}		>120 keV μm^{-1}	
Energy (MeV n^{-1})	Fraction of		Fraction of		Fraction of		Fraction of	
	Absorbed Dose	Path Length	Absorbed Dose	Path Length	Absorbed Dose	Path Length	Absorbed Dose	Path Length
Proton								
10	0.65	84	35	16	0.0045	0.0004	0	0
100	0.965	0.997	0.035	0.003	0.00045	0	0	0
500	0.992	0.9993	0.008	0.0002	0	0	0	0
Alpha								
10	0	0	0.85	0.96	0.075	0.025	0.075	0.015
100	0.80	0.945	0.185	0.0546	0.0075	0.0004	0.0075	0.0002
500	0.96	0.996	0.037	0.0037	0.0015	0	0.0015	0
Iron								
10	0	0	0	0	0	0	1	1
100	0	0	0	0	0	0	1	1
500	0	0	0	0	0	0	1	1

components and occupants. Many of the products of these interactions are low-energy, high-Z target fragments and neutrons. These charged particles and the charged secondary radiation produced by the neutrons have a much higher stopping power than the protons and result in a significantly higher mean quality factor.

The differences in charged particle tracks with the same stopping power can be visualized in Figures 5.2 and 5.3. Figure 5.2 shows segments of proton, alpha particle, and silicon ion tracks with the same initial stopping power of 50 keV μm^{-1}. These particles have markedly different velocities and, therefore, different delta-ray spectra. The tracks of the primary ions and delta rays are shown in these two dimensional projections of the three-dimensional tracks. Because of its low energy, the proton's stopping power increases rapidly and the particle stops in ~6 μm. Since the alpha particle and silicon ion have long ranges relative to the dimensions of this figure, and since their stopping powers are approximately equal, the total number of ionizations in the illustrated path segments are essentially the same. However, the spatial distribution

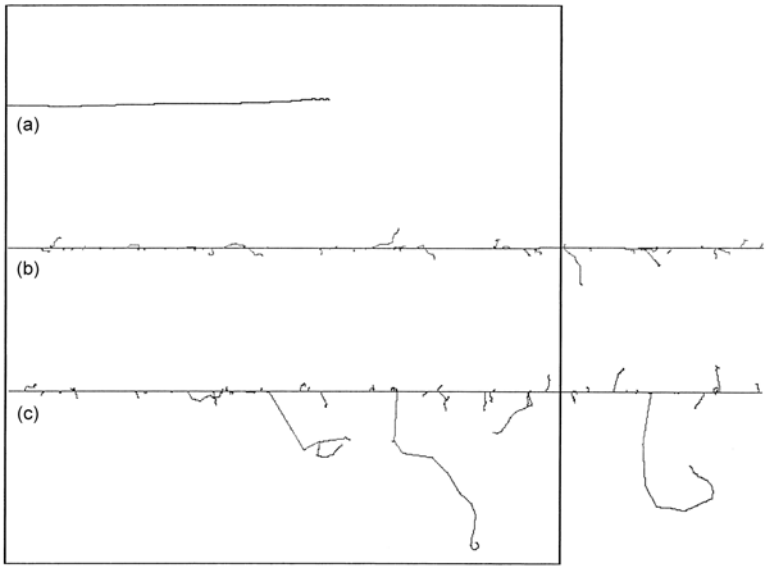

Fig. 5.2. Tracks of particles, with initial stopping power of 50 keV μm^{-1}, passing through water: (a) 0.35 MeV proton, (b) 11 MeV alpha particle and (c) 600 MeV n^{-1} ^{28}Si ion. The distance between the two vertical lines is 10 μm.

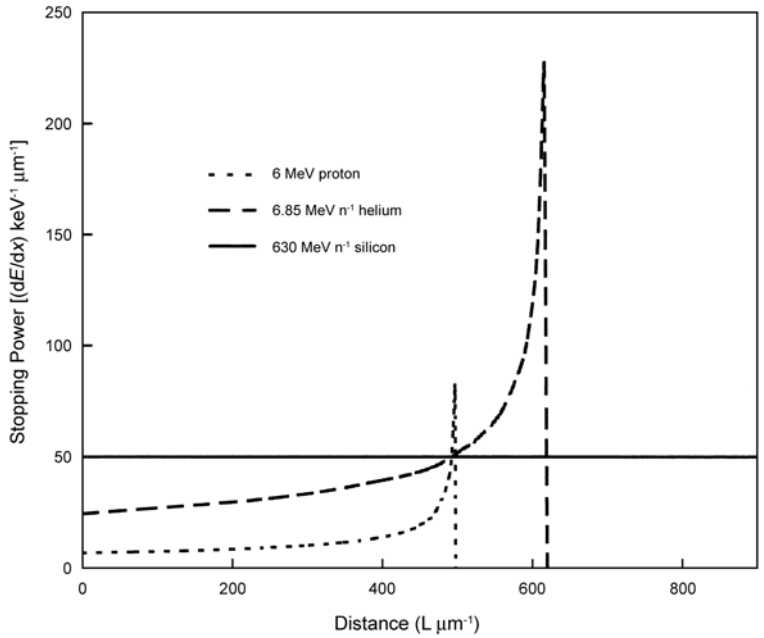

Fig. 5.3. Stopping power as a function of depth in water for a 6 MeV proton, 6.85 MeV n^{-1} helium ion, and 630 MeV n^{-1} silicon ion. These ions all have the same stopping power, 50 MeV μm^{-1}, at a depth of 500 µm, but their stopping powers below and above this depth are quite different.

of these ionizations is much different. Figure 5.3 shows how the stopping power changes along each particle's track as it approaches the point where the stopping powers are equal and then continues through the water absorber. The most obvious effect of these differences between tracks is that light ions produce only short segments of high-LET tracks. These deposit large amounts of energy in randomly distributed isolated cells, which happen to be at the end of the track. However, the HZE particles deposit similar large amounts of energy in large numbers of adjacent cells in a line.

5.4.1 *Clustering of Energy Deposition*

Many factors, including the random nature of the distance between successive interactions of a charged particle with the atoms of the medium, contribute to the clustering of energy deposition by ionizing radiations. However, the primary cause of clustering is the nature of the secondary electrons produced. A large

fraction of the ionization events produced by heavy charged particles produce electrons with sufficient energy to yield one or more additional ionizations. Most of these do not have enough energy to form a distinct track of their own, but deposit their energy in a very short distance. Thus, the ions they produce, plus the ionizations that started them, form small clusters along the track.

The higher-energy electrons with sufficient energy to form distinct tracks separated from the primary ion track are delta rays. The number of delta rays produced per unit of primary particle track depends on the stopping power and energy of the primary particle. The maximum energy and range of the delta rays depends on the velocity of the primary particle. However, electrons are easily scattered so the effective radius of the cylinder containing the delta-ray dose is significantly less than the path length of the most energetic delta rays. Several relationships have been developed to describe the absorbed dose due to delta rays as a function of distance from the primary track (Chatterjee and Holley, 1993; Katz *et al*., 1971; Varma *et al*., 1976). The fluence of delta rays a few micrometers from the primary ion track is relatively low, so the energy deposition is significant along the delta-ray tracks and zero elsewhere. Thus, the delta-ray tracks contribute to the clustering of radiation damage on the micrometer or smaller scale. Experimental measurements using a grid walled proportional counter at specific distances from 600 MeV n^{-1} iron ion tracks show that energy deposition in those volumes which receive a delta-ray track is similar to that produced by 170 keV x-ray irradiation (Metting *et al*., 1988). The dose mean lineal energy, one way of describing the clustering of energy deposition at the micrometer level, is 3 keV μm^{-1}. This is greater than the stopping power of a high-energy proton. About 87 % of the energy deposited by a proton with initial energy of 100 MeV is deposited while the stopping power is <3 keV μm^{-1}.

Unusually high values of local energy density can also be produced, in principal, by target atom fragmentation. When fragmentation occurs there are two or more charged particles both with lower velocity, and often with higher stopping power than the incident particle. Since the angle between the paths of the primary and fragment may be small both particles may pass through the same cell or subcellular region. The resulting high values of energy imparted will continue until the distance between the tracks becomes larger than the volume of interest. The fraction of a cell population experiencing this higher density of damage depends on the cell diameter as well as the angle between the primary and fragment and the mean-free path for fragmentation. Since the

mean-free path is generally large in terms of cellular dimensions, the fraction of cells receiving this type of energy deposition event is generally very small.

5.4.2 *Distribution of Affected Targets*

Radiation doses in space are generally low in the sense that the mean number of charged particle tracks through any individual target in a relevant time period (for example, one cell generation) is less than one. In this dose regime, a change in the dose does not affect the energy deposited in an individual target. It simply affects the fraction of the targets that receive a dose. If targets act entirely independently of each other with respect to the development of biological consequences following irradiation, the probability of a response must be proportional to the number of targets affected and, therefore, a linear function of absorbed dose (for a fixed radiation spectrum). The fraction of the population of targets which is affected depends on the mean energy per event in the target, as well as the absorbed dose, but does not depend on the charged particle track length except for very low-energy particles. However, the spatial distribution of the affected cells does depend strongly on the charged particle energy. A high-energy heavy-ion track will produce a long string of affected targets, surrounded by a cylindrical region containing randomly distributed targets affected by delta rays. For 100 MeV n^{-1} particles these strings of affected targets are several centimeters long and contain thousands of biological cells. Since, at a minimum, such a concentration of damaged targets would be likely to change the local environment of nearby, undamaged, cells and since there is some evidence that normal cells maintain a degree of cell-to-cell communication which alters their response to radiation induced damage (Azzam *et al*., 1998; Prise *et al*., 1998a). It appears unlikely that cells could respond in a truly independent fashion following this type of irradiation. Although there is little evidence for specific effects due to the spatial distribution of damaged cells in HZE irradiation (Section 6), such effects, if they occur, would be expected to be related to the range as well as the stopping power of the incident particle.

5.5 Charged Particle Equilibrium

Understanding of the biological effects of radiation is unavoidably linked to the concept of dosimetry. Many of the dosimetry concepts used to simplify the description of the radiation field, and to

characterize the radiation experimentally, rely on charged particle equilibrium at the point where the evaluation is to be made (Attix, 1986). However, the characteristics of the radiations encountered in space often make it difficult to achieve this condition. For example, in the low dose regime, as defined previously, there cannot be charged particle equilibrium at the cellular level because in the vicinity of a target there will be only a single line source of delta rays, with no opportunity to compensate for particles which stop in the site. The ranges of delta rays are typically no more than a few tens of micrometers, so the nonequilibrium resulting from delta-ray effects is limited to very small volumes, but may be an important factor in evaluating possible radiation effects models.

Charged particle and target atom fragmentation produce another component of the particle fluence which is often not in equilibrium. Changes in atomic composition will result in different fragmentation yields which will result in charged particle nonequilibrium for distances up to the maximum range of the charged particles produced. Since the range of charged particle fragments produced by cosmic rays is of the order of a few tens of centimeters, and there is a significant difference between atomic composition of the human body and surrounding materials, it is unlikely that strict charged particle equilibrium will occur inside the body.

Indirectly ionizing radiations, specifically neutrons and photons, have relatively long mean-free paths for transfer of energy back to directly ionizing particles. When these particles are produced in small isolated objects such as a detector or even a satellite, they produce almost no dose, because nearly all indirectly ionizing particles escape the system without transferring energy. However, as the system becomes larger, there is an increasing probability that, at any point, an indirectly ionizing particle from some other point will deposit energy. The absorbed dose at a location continues to increase with the size of the system until radiation equilibrium is achieved, when the location of interest is located several mean-free paths away from a discontinuity in the atomic composition. Since the range of neutrons produced in fragmentation processes may extend to many meters in typical materials, the absorbed dose that these fragmentation products produce will depend on the size of the space vehicle, and the position of the target within it. The range of these particles becomes a serious consideration for the design of habitations on planets without a thick atmosphere. Modest amounts of shielding will reduce the absorbed dose, but the absorbed dose which remains may be due primarily to neutron interactions and thus have a relatively high biological effectiveness.

5.6 Biological Significance

It is possible to devise many different ways of characterizing a radiation field in order to predict its biological effects. However, most of them are variations on one of three basic approaches which have been outlined previously (NCRP, 2001a). These include the traditional approach, where the absorbed dose and the mean quality factor (a function of the LET or radiation type) are evaluated separately. Another alternative is the evaluation of the total particle fluence spectrum at the point of interest, which would generally require measuring the spectrum at some other point and use of radiation transport codes to give the fluence of particles as a function of charge and velocity at the desired point. The third approach would be based on the energy deposition in small volumes as indicated by the lineal energy density. Some of the advantages and disadvantages of each of these approaches will be discussed in the following paragraphs.

5.6.1 *Fluence Spectra*

The most complete description of a radiation field is the fluence spectrum as a function of Z and energy. With these data, in principal, any other description of the radiation field (absorbed dose, LET, lineal energy) can be calculated. Furthermore, the spectrum that an incident radiation produces at any other point in a complex medium can be calculated using a suitable radiation transport method. There are limitations to the accuracy of both of these types of calculations due to the limitations of methods and cross-section data currently available, but the calculations are continuing to improve (Section 4).

The fluence approach is well suited to determining risk through the use of experimental animal data obtained using high-energy particle accelerators. These experiments are best conducted with a well defined beam of nearly monoenergetic particles with minimum absorbed dose due to fragmentation products. Generally several different types of particles can be obtained for different measurements, and particle energies can be specified with great accuracy. In such experiments the primary fluence is the basic dosimetry quantity measured. Furthermore, it is relatively simple to convert between absorbed dose and fluence in the monoenergetic particle beam. Thus, it is natural to express the risk of the observed endpoint in terms of the fluence as a function of particle type and energy.

Instruments for the measurement of the fluence spectrum of directly ionizing particles in free space have been developed and are currently used on ISS. However, by the nature of the technique used, these charged particle telescopes are insensitive to most indirectly ionizing radiation. Thus, they must be used to measure the incident radiation before fragmentation has occurred. Radiation transport codes must be relied upon to determine the absorbed dose and radiation quality at the biological target. Also, current designs have a limited angle of acceptance and limited data processing rate. Consequently, they may respond more slowly than some other instruments when an unexpected change in the radiation environment occurs.

A radiation protection system based on particle fluence would require additional detectors to measure man-made sources of indirectly ionizing radiation so that the charged particle spectra they produce could be calculated and added to the spectra of incident radiation and fragmentation products at the position of the biological target. Furthermore, when a specific type of radiation is being measured, corrections will have to be made to avoid including the component of that radiation which is actually a part of the cosmic-ray fragmentation spectrum. This creates very difficult measurement problems and can cause complex data management problems, but these problems may not be beyond the ability of technology.

5.6.2 *Energy Deposition in Small Volumes*

Measurement of energy deposition spectra in a specified volume representing a biological target (*e.g.*, a cell, chromosome, or even DNA strand size site) provides somewhat less information than measuring the particle fluence spectrum, but is easier in several respects. This technique, which generally utilizes tissue equivalent detectors, is sensitive to all types of radiation. Thus it can be used to characterize events caused by fragmentation products, man-made radiation, and the charged secondaries of indirectly ionizing radiation as well as incident HZE particles. The energy deposition spectra can be calculated from the charged particle fluence, but the reverse calculation is not possible. Thus, the energy deposition at some other location cannot be calculated from the spectrum measured at a point.

Instruments which measure the energy deposition in small tissue equivalent volumes and calculate the absorbed dose and an estimate of the dose equivalent, designated TEPC, are in routine use in the space program (Badhwar, 1997b; 2002). It has been proposed (ICRU, 1986) to define radiation protection quantities in

terms of lineal energy, however it is also possible to estimate quantities defined in terms of LET using lineal energy data. Most practical microdosimetry detectors use a solid wall and low-density gas. This results in a wall effect which shifts the spectrum to higher values of lineal energy than would be measured in a uniform medium (Braby *et al*., 1970; Dicello, 1992). The magnitude of this shift depends on the radiation spectrum (Braby and Ellett, 1972), and has not been fully characterized for high-energy particles. However, in many situations the effect, on the average, over the radiation spectrum is small compared to other uncertainties in calculating risk. These instruments respond rapidly to changes in dose rate, have nearly isotropic response, and detect all penetrating radiations, advantages which may offset the limitations of this approach.

There is a conceptual problem in basing a radiation protection system on energy deposition measurements. The value of the lineal energy is a function of the site size, especially for low-energy radiations (where some of the tracks may stop in the detector) or for very high energy, where delta-ray loss and straggling become important. There are many different biological structures, with a wide range of sizes, involved in biochemical processes which may contribute to the consequences of a radiation exposure. Thus, it is not possible to define the correct size site in which to measure lineal energy. Furthermore, no consensus has been reached about an acceptable site size for radiation protection purposes, although sites 1 or 2 μm in diameter are often used for practical reasons. As a practical matter, the size of the site may not be important in characterizing radiation in space since short tracks deposit such a small fraction of the absorbed dose and effects of delta-ray loss are partly compensated by wall effects.

5.6.3 *Absorbed Dose and Linear Energy Transfer*

The conventional system, using the average quantities absorbed dose and LET which are defined at a point, has the advantage of simplicity and established tradition. However, these quantities are not well suited to describing the radiation environment in space. Although the absorbed dose can be measured quite accurately, it does not typically describe the biological damage. When an HZE particle passes through a cell the energy deposited may correspond to 1 Gy or more, far higher than the absorbed dose for the entire mission. The reason is that these tracks are quite rare, and many cells with no energy deposited are averaged in to determine the mean absorbed dose.

Operationally, it is relatively easy to measure absorbed dose using a tissue equivalent ion chamber. However, no realistic method for measuring the LET for most radiations has been discovered. The best approach is the measurement of the lineal energy spectrum followed by the deconvolution of the track length and LET distributions, a technique that can be accomplished with TEPC data. However, this has been shown to differ significantly from the LET for many radiations where the charged particle path is too short, or the delta-ray range is too long for the measured energy deposition to represent the stopping power. For the space radiation environment, the fraction of the absorbed dose due to very short range particles is probably insignificant. However, a significant fraction of the absorbed dose is delivered by charged particles that can produce delta rays with ranges of several micrometers or more. Thus the mean lineal energy may be significantly less than the LET for this radiation environment. Experimental evidence suggests that the wall effect in the instruments in current use largely compensates for this effect. Delta-ray scattering in the walls of solid walled proportional counters results in an increase in the measured energy deposition relative to the lineal energy that would be measured in a uniform medium and the result is that values measured by typical instruments appear to be very near the LET values (Badhwar *et al*., 1994; Gersey *et al*., 2002).

5.7 Characterizing Biological Response

From the perspective of dosimetry, there are two possible approaches to experimental evaluation of the biological response to the space radiation environment. Experimental exposures, utilizing high-energy accelerators can be designed to simulate exposures in space by specifically including fragmentation products and other radiation components characteristic of a specific radiation exposure. Alternatively, measurements can be made for a limited number of beams which are carefully characterized, and the response to the mixed field can be calculated by summing the appropriately weighted responses.

Whether a pure beam or one with fragmentation is used, the exposures should be characterized by using all three dosimetry methods described earlier. This is not difficult in an experimental situation since the incident particle spectrum is fixed by the selection of accelerator operation parameters, and the fragmentation and lineal energy measurements are often made to characterize the irradiations.

Both of the irradiation approaches present experimental problems. Constructing the mixed field response from measurement of individual ion responses requires a large number of measurements for specific beam types and energies, plus a reliable method for interpolation to the intermediate values. It also requires a comprehensive knowledge of the spectrum which will actually be present in the space vehicle. This will require extensive calculations and validation measurements of primary particles, delta rays, and fragmentation products such as neutrons.

However, it is equally difficult to devise a simulated radiation spectrum for the interior of a space vehicle. Many different situations, characterized by different shielding depths and materials may be needed. It will be impossible to achieve secondary particle and radiation equilibrium for many experiments, because the available accelerator beam diameters cannot be made large enough. Furthermore, this approach requires new measurements for every new shielding design, since the effect of a new shielding combination cannot be determined unambiguously from the data for other combinations.

5.8 Measurement of Fluence

Instrumentation approaches are available to measure the fluence and energy spectra of almost any type of ionizing radiation. However, for indirectly ionizing radiations, it is generally necessary to convert the incident radiation to a charged secondary. In order to be useful in space, with the high fluence of high-energy directly ionizing radiation, special provisions must be made in the instrument in order to distinguish between the secondaries of indirectly ionizing radiations and the incident directly ionizing particles in order to avoid overestimating the fluence of indirectly ionizing radiation. The commonly utilized approaches to measuring fluence and spectra of these various types of radiation are described below.

5.8.1 *Directly Ionizing Particles*

The fluence of directly ionizing particles, the dominant part of the incident radiation in space, is easily measured. Almost any ionization detector will do. Pulse ion chambers, all types of solid-state detectors operated in the pulse mode, proportional counters and scintillators are common examples of active detectors. There are also many passive detectors which will be discussed later. In order to be useful in determining the fluence, the effective area of the

detector must be known and it must be sensitive to minimum stopping power protons as well as other particles. It is advantageous for such a detector to be thin, so that it will be equally efficient for low- and high-energy particles, but not so thin that straggling interferes with measuring energy loss. It may be useful for the detector response to be isotropic so that a single measurement gives the total fluence. A spherical proportional counter, or a set of three mutually orthogonal thin solid-state detectors, scintillators, or proportional counters connected to simple event counting electronics will closely estimate the true charged particle fluence. However, fluence alone is not sufficient for dosimetry. The spectrum of particle stopping powers is necessary to evaluate the absorbed dose at the location of the detector, and the spectrum of particle energies as a function of charge or mass is necessary in order to calculate the absorbed dose at other locations.

An approximation to the spectrum of stopping powers can be determined by adding some form of pulse height spectroscopy to almost any type of detector that can be used for fluence measurements. The added requirements are that the path length through the detector be known, and the detector output pulse should be a linear (or at least known) function of the energy deposited in the detector. A characteristic of this approach is that it inherently measures energy deposited rather than energy lost by the particle, so that it does not directly provide LET for evaluating the quality factor. Most solid detectors (*e.g.*, solid-state, scintillation) are not thin enough to satisfy cavity detector requirements, nor is secondary particle equilibrium established in the typical detector. Thus a dosimeter based on this approach will approximate the absorbed dose in the material of its construction, typically silicon, and the absorbed dose in tissue, which is determined by applying the ratio of stopping powers in tissue and the detector material, will have inherent errors as a function of incident particle energy. However, the errors are generally not large, and may be acceptable in the context of the space radiation environment.

A direct measurement of the stopping power and total energy of a particle is sufficient to determine the mass of the particle and provide the data needed for energy transport calculations. Over limited ranges of energies this can be accomplished by measuring energy deposited in a thin detector and in a very thick detector in coincidence (Knoll, 2000). The thin detector measures the incident particle stopping power, and the thick detector, which stops the incident particle, determines the total energy. Alternatively, two thin detectors separated by a known thickness of absorber can be used to determine stopping power and rate of change of stopping

power. The range of the incident particles found in space, equivalent to several inches in silicon, precludes use of a simple two detector approach. More involved detector assemblies, typically known as charged particle telescopes, are used for these radiations. In order to prevent errors due to particles leaving through the side of the detector stack, and to maximize the amount of information obtained when particles do escape, these instruments generally utilize a stack of thin and thick detectors, and an anticoincidence shield, or position sensitive detectors, to determine the trajectory of the primary particle. These instruments, when carefully employed, can discriminate between particles differing by a single atomic mass unit, and can resolve the energy spectrum of each type of incident charged particle, within the statistical limitations imposed by the relatively small solid angle that the detector accepts, and the available duration of the measurement. This means that they can distinguish between different particles with the same stopping power, a characteristic which is very important for evaluating the absorbed dose at other depths in an absorber such as the human body. However, this type of detector is inherently insensitive to indirectly ionizing radiation, and is also insensitive to directly ionizing particles with insufficient range to create two coincident events in successive detectors, typically protons with less than ~20 MeV or equivalent.

5.8.2 *Neutron and Photon Spectrometers*

Measurement of the fluence and energy spectra of indirectly ionizing radiation, specifically neutrons and photons, in the presence of high-energy directly ionizing particles is difficult. Various scintillators, proportional counters, and other detectors are commonly used to measure these energy spectra, but they function by measuring the energy deposited by secondary particles produced by specific interactions of the indirectly ionizing radiations. They also respond to the energy deposition by directly ionizing particles, and it can be extremely difficult to reliably separate the energy deposition events produced by the charged primary and secondary radiations. In the case of neutrons on Earth, it is common to utilize nuclear reactions that produce secondary particles with added energy [*e.g.*, $^{10}B(n,\alpha)^{7}Li$ and $^{3}He(n,p)^{3}H$ reactions] which allow separation of the neutron fluence from gamma-ray fluence over a limited range of neutron energies. However, these reactions do not produce energy deposition in the detector that is significantly different from the energy deposited by some primary charged particle events in space. Also, at high energies, protons

produce similar nuclear reactions, with essentially the same cross section, as neutrons. Thus these detectors are not sufficient to evaluate the neutron fluence generated by GCR.

The most direct way to discriminate between energy deposition by directly ionizing particles and secondaries of indirectly ionizing particles is to use a large detector (relative to the range of the secondaries from an indirectly ionizing particle) and an anticoincidence shield. If the shield completely covers the detector, and is not too thin, any directly ionizing particle that produces an event in the primary detector will also produce one in the shield. However, most secondary particles depositing energy in the main detector will not reach the anticoincidence shield. Thus the spectrum and fluence of indirectly ionizing radiation can be deduced from the spectrum of events which are not coincident with an event in the shield.

Unfortunately, it is very difficult to get perfect coverage with an anticoincidence detector. Various optical or electrical connections must be made to the primary detector and result in gaps in the shield. If neutrons are responsible for 1 % of the dose equivalent the neutron count rate in the detector will be ~1 % of the proton count rate. If 1 % of the surface of the detector is not covered by anticoincidence shield 1 % of the protons will not be properly identified thus the neutron fluence will be overestimated by a factor of two.

An alternative approach to identifying neutrons and measuring their energy takes advantage of the time required for high-energy neutrons to slow to thermal energies in a hydrogenous material (Feldman *et al*., 1991). The thermal neutron is then captured in a nuclear reaction that produces a prompt charged particle that can also be detected. The detector consists of a large volume of hydrogenous scintillator or similar material, which produces a signal proportional to the incident particle energy, and a thermal neutron detector. The size of detectors is chosen to efficiently produce signals in both detectors. Charged particles may also produce pulses in both detectors (depending on their path), but these pulses will be essentially simultaneous. Thus, neutrons can be identified by the time between the total energy pulse and the thermal capture pulse. This discrimination is very efficient at low-proton fluence rates, but some false neutron signals occur at high fluence rates due to chance coincidences in the thermalization time window.

Another approach to neutron spectroscopy is to measure the energy deposited by the recoil protons produced in a thin layer of hydrogenous material in contact with a solid-state detector. This also is sensitive to directly ionizing particles, but can be used with an anticoincidence shield.

5.8.3 *Passive Spectrometers*

Photographic emulsions and etchable track detectors can be used as passive particle spectrometers. Most of these materials have some sensitivity to neutrons as well as directly ionizing particles. Such detectors generally respond in proportion to the stopping power of the particle depositing energy, and it may be necessary to follow the particle through successive layers of detector in order to evaluate the initial energy. When this is done, it is often possible to discriminate between directly and indirectly ionizing particles based on the starting point of the track. Unfortunately, many of these detectors are insensitive to particles at high energy (low stopping power) and they integrate the fluence from the time they are produced until they are processed. This makes it difficult to use them for near real time health protection measurements.

Neutron activation of different materials is a standard technique for neutron spectroscopy in conventional environments, although the energy resolution is limited. Elements with a variety of threshold energies for neutron activation can be found. Periodic counting of the induced activity can be used to give a measure of the integrated fluence above the threshold energy. Differentiation of the count rate can give an indication of the instantaneous fluence rate. However, high-energy protons can produce nuclear reactions similar to those produced by neutrons, The energy thresholds for protons and neutrons are much different, but the energy spectra of protons in space include many particles which will trigger neutron-like events, resulting in an overestimate of the neutron fluence. Measurements of activation materials exposed on the long-duration exposure facility (Armstrong *et al*., 1996) showed that the proton induced activity in many materials exceeded the neutron induced activity by a large margin. Models of activation underestimated the actual activity by a factor of two, indicating significant potential for error when using activation to evaluate neutron absorbed dose.

5.9 Measurement of Absorbed Dose

Any detector that meets the Bragg-Gray cavity requirements will measure the absorbed dose at the effective center of the cavity. However, this may not be the same as the absorbed dose to a specific organ, or the mean absorbed dose to a person exposed to that radiation field. For most types of radiation on Earth, the approach is generally to establish secondary particle equilibrium in the detector, which makes it possible to relate the measured absorbed

dose to that which would occur in a phantom. Then either a small cavity ion chamber, another detector that satisfies cavity theory requirements, or a uniform (tissue equivalent) detector that satisfies the requirements for the application of the Fano theorem is used. However, the wide range of radiations encountered in space make it difficult to meet these requirements. In particular, the detector wall must be thick enough to produce secondary particle equilibrium, but thin enough that it does not modify the incident particle spectrum. The nature of the problem for the directly ionizing particles can be seen by comparing the range of the delta rays produced by high-energy particles with the range of the low-energy primary charged particles in Table 5.1. To meet the criteria for application of cavity theory the wall must be thick compared to the range of the delta rays, but thin compared to the range of the primaries, a combination which cannot be met. The situation becomes even more difficult when the indirectly ionizing secondaries must be considered. In order to meet the requirements of the Bragg-Gray cavity detector the cavity must be small compared to the range of the shortest range charged particles to be included in the absorbed dose measurement.

Several types of detectors can be used for dosimetry within the limitations imposed in trying to meet the above requirements.

5.9.1 *Ion Chambers*

One of the simplest devices for measuring absorbed dose in tissue is the tissue equivalent ion chamber. When used for a combination of radiations that allow a selection of wall thickness which will meet the requirements of the Fano theorem it can provide a measure of the absorbed dose. Even without maintaining tissue equivalence, if the cavity is small enough, the absorbed dose can be determined through application of the cavity theory, with suitable corrections for delta-ray effects (Attix, 1986). However, the usefulness of ion chambers is limited by their sensitivity. If it is assumed that the minimum current that can be measured reliably is 10^{-14} amps (lower current limits require rapidly escalating complexity and electronics costs) the volume of a detector required to detect a dose rate of 10 μGy h^{-1} is ~100 cm^3 at atmospheric pressure.

The conversion of current in an ion chamber to absorbed dose depends on knowledge of the mean energy required to form an ion pair in the gas used. This is known reliably for charged particles up to a few tens of MeV n^{-1}, but there is too little data to confirm the values extrapolated to much higher energies.

5.9.2 *Solid-State Detectors*

Directly ionizing particles produce electron-hole pairs in solid-state devices, similar to ion pairs in gases, and many types of semiconductor devices can collect this charge to produce a pulse height or current which is a measure of the energy deposited. Although there is continuing effort to develop organic semiconductors in order to make tissue equivalent solid-state detectors, such devices have not yet made it beyond the laboratory development stage. Most semiconductor dosimeters in use are made of silicon. In principle a very thin silicon detector surrounded by tissue equivalent material can be used as a Bragg-Gray cavity detector, and measure absorbed dose in tissue. However, in practice it is very difficult to make the detector thin enough. For space applications, where the majority of the absorbed dose is deposited by directly ionizing particles, thin, bare solid-state detectors are used to measure fluence and stopping power, while absorbed dose in tissue is estimated from these values. This approach is insensitive to neutrons, which do not produce useful charged secondary radiation in silicon, and nearly insensitive to photons because the detector cannot be thick enough to provide secondary particle equilibrium without being far too thick to accurately indicate charged particle stopping power.

Although the high density of silicon (compared to the gas used in an ion chamber) and the low mean energy required to produce an electron-hole pair make it possible to use much smaller solid-state detectors than ion chambers, there is a limit imposed by the stochastic nature of charged particle interactions, and the statistical reliability required of a measurement of absorbed dose. The fluence rate of GCR consisting of high-RBE particles is on the order of 2 cm^{-2} min^{-1}. Thus it requires almost 1 h to determine the fluence or dose rate of these particles with a relative standard deviation of 10 % using a 1 cm^2 detector. The time required for the measurement is inversely related to the surface area of the detector.

5.9.3 *Passive Detectors*

Traditionally, passive detectors have been favored as the dosimeter of record in conventional radiation protection environments because they are thought to be much less prone to failures which would result in underreporting of absorbed dose than are active dosimetry systems. In the case of the radiation environment in space and considering the characteristics of modern electronic systems, this difference in reliability may not be real, but passive dosimeters will probably continue to play a significant role in any

comprehensive dosimetry program. Passive dosimeters include nuclear emulsions, thermoluminescent and related materials, and etchable track materials.

One problem with the use of passive dosimeters on a long mission is that they integrate the absorbed dose until they are readout. Thus, they do not provide information on dose rate, or absorbed dose during a segment of the mission, unless a system for reading the detectors is included on the vehicle. Such a reader may not be excessively large nor require excessive power, but it may be larger than the typical charged particle spectrometer, and it will require significant crew time to readout a set of dosimeters. Those passive detectors which require chemical processing also introduce material handling and waste disposal complications.

5.9.4 *Thermoluminescent Dosimeters*

Thermoluminescent dosimeters (TLDs) and related materials rely on the ability of some doped crystalline materials to capture part of the energy deposited by ionizing radiation in stable traps. A signal which is proportional to the absorbed dose under some conditions can then be derived by heating the material or otherwise stimulating the emission of photons (or electrons in some cases) by the occupied traps. For the measurement of absorbed dose due to charged particles, the primary limitation of TLDs is that the most sensitive types under respond to high-LET radiation when calibrated with gamma rays. Furthermore, they are not tissue equivalent, as most are made of calcium or lithium fluoride, which results in an energy dependent calibration factor for the photon component of the radiation field. When neutron sensitivity is required, lithium fluoride detectors enriched in ^{6}Li are often used as the detection element in an albedo dosimeter, relying on thermal neutrons backscattered by the body of the badge wearer to produce a signal. This approach has an inherent energy dependence and requires calibration in the neutron spectrum that it will be used to measure; not a practical approach where the neutron spectrum may change from one SPE to the next due to changes in the incident particle spectrum.

5.9.5 *Photographic Emulsions and Etched Track Detectors*

These materials register individual tracks and are used to measure the stopping power spectrum and particle fluence. Some etched track materials are reasonably tissue equivalent and contain sufficient hydrogen to respond to fast neutrons, but both

systems have a minimum stopping power cutoff which depends on the specific material and processing method, but is generally too high to respond to high-energy protons, which are responsible for the majority of the absorbed dose in space. However, they can be used to detect protons near the ends of their tracks and fragmentation products. The absorbed dose due to low-LET radiation can also be determined by the general fogging of photographic film.

5.10 Linear Energy Transfer Spectrum

In order to evaluate the dose equivalent, it is necessary to evaluate the quality factor for the radiations depositing the energy, as well as the absorbed dose. In the case of the wide range of particle types and energies encountered in space, evaluation of the quality factor must be done through the relationship between the quality factor and LET. Since LET is a mean quantity defined at a point, it is impossible to measure it for a single particle track and, therefore, the spectrum cannot be measured. However, the stopping power averaged over a finite detector thickness can be measured, and this is usually an acceptable approximation to LET. This stopping power spectrum can be measured using a variety of different detectors. The spectrum recorded by the first detector of a charged particle telescope contains the information needed to calculate the stopping power spectrum. Similarly, a low-pressure proportional counter can be used to measure energy deposition in a short segment of a track.

For any energy deposition detector, the signal produced is the product of the stopping power and the path length in the detector modified by energy loss straggling and delta-ray effects. In order to approximate the stopping power distribution, the path-length distribution must be unfolded from the measurement. Two approaches are common. In charged particle telescopes, coincidence between two detectors is required in order to record an energy deposition event. By separating the detectors by a significant distance, the range of particle trajectories relative to normal incidence can be limited. In some cases two position sensitive detectors are used to define the trajectory of each particle recorded. This approach results in an anisotropic response which increases the exposure time required to obtain a given level of statistical precision, and requires multiple measurements if the incident field is anisotropic. The alternative, which is commonly used with spherical proportional counters, is to record all events which occur in a detector of known geometry (usually spherical), and then mathematically unfold the known path-length distribution. This results in an isotropic detector, but the unfolding process is very sensitive

to noise in the data, and this approach generally requires long exposures to obtain sufficient precision in the measured spectrum. The result of this unfolding, using the path-length distribution as an approximation to the detector response function, neglecting straggling and delta-ray loses, is generally an underestimate of LET in the space radiation environment.

Both of these measurement approaches are subject to a number of systematic differences between what is measured and the definition of LET. These differences are caused by energy loss straggling, changes in stopping power within the detector, and delta ray escape from the detector. The magnitude of each of these systematic errors depends on the size of the detector used, and on the characteristics of the radiation. The effect on dose equivalent is often less significant since the quality factor is constant for a wide range of low-LET where straggling effects are most significant (ICRP, 1991).

5.11 Measurement of Lineal Energy

An alternative to measuring absorbed dose and LET spectrum in order to evaluate dose equivalent is to measure the number and spectrum of energy depositions in a small detector simulating a tissue volume a few micrometers in diameter. The energy deposited divided by the mean chord length in the detector is known as the lineal energy, y, and can be used to calculate an approximation to the LET, as described above. Lineal energy spectra can be measured with a wide variety of detectors, the primary requirement being that the detector should be small, on the order of the size of biological cells or subcellular components. Various condensed phase detectors have been considered, but the only type of detector in common use for measuring lineal energy is the low-pressure proportional counter. Generally, these detectors are made of tissue equivalent plastic and filled with tissue equivalent gas, in order to take advantage of the Fano theorem, and are referred to as TEPCs. Since these detectors operate in the pulse mode they provide spectral data which can be used to estimate LET or can be used directly to estimate biological effectiveness, but since they are tissue equivalent, the sum of the energy deposited in events is the energy needed to calculate the absorbed dose, the equivalent of the charge collected in an ion chamber. Such a detector responds to all forms of ionizing radiation, neutrons and photons as well as directly ionizing particles. It is also subject to the same limitations related to establishing secondary particle equilibrium without distorting the incident spectrum as are all other cavity detectors.

The interpretation of the lineal energy spectrum in terms of the energy deposited in a subcellular volume assumes that the detector

is a part of a continuous medium of uniform density. In practice, the detectors are generally a low-pressure gas cavity in a tissue equivalent plastic medium. The resulting density difference, on the order of 10^5, makes it possible to use a solid walled detector to collect statistically significant event spectra at low doses. However, it also introduces some artifacts in the lineal energy spectrum, even though it does not distort the absorbed dose measurement in any way. The artifacts are due to the fact that some secondary charged particle tracks produced in the wall by a single primary particle enter the single large detector cavity, but would enter separate sites if the detectors were small. This results in reducing the number of small events (produced by single delta-ray tracks) and a small increase in the lineal energy value of the larger events. HZE tracks which pass just outside the cavity, in the wall, can result in large numbers of delta rays entering the cavity, resulting in an event which is much larger than would be produced by the small number of delta rays that would enter in a uniform medium. For primary particles which have long ranges compared to the site diameter, but produce delta rays which have ranges which are less than the site diameter, this wall effect, and the effect of delta ray escape from the detector are relatively small. In addition, the mean of the lineal energy is a reasonable estimate of the mean LET. For very high-energy particles which produce long-range delta rays (Table 5.1), the true lineal energy (measured with a detector that has the same density as the surrounding medium) is significantly less than the LET because the delta rays produced by primary particles that cross the detector deposit a significant fraction of their energy outside the detector, while the delta rays from primaries that miss the detector may still deposit a small amount of energy in it. In typical solid walled detectors this is at least partially offset by the wall effect which increases the large lineal energy values and eliminates some of the delta-ray events. Measurements of lineal energy for monoenergetic iron ions from 200 to 1,000 MeV n^{-1} (Gersey *et al*., 2002) clearly show the effects of delta ray escape and of the wall effect. For these monoenergetic particle beams it was found that dose mean lineal energy was always within 8 % of the LET. The mean quality factor, evaluated by substituting $f(y)$ for $f(L)$, was consistently high, by as much as 20 %. For typical radiation spectra in space the substitution of $f(y)$ for $f(L)$ appears to produce a good estimate of the dose equivalent. Dose equivalent calculated from measurements using solid walled TEPCs and LET spectra derived from assumed incident particle spectra are very similar (Badhwar *et al*., 1994), suggesting that delta-ray loss and the wall effect nearly cancel.

5.12 Rem Meters

For conventional radiation protection applications, a variety of instruments have been built which are intended to respond to neutron radiation in a way which simulates the dose equivalent. By using some combination of detectors, including neutron sensitive and neutron insensitive detectors, photon detectors, and charged particle detectors, it may be possible to devise a combination that responds to the space radiation environment in a way which is proportional to dose equivalent. There are two major problems with this approach in general. One is that such an instrument must be calibrated for the radiation spectrum to be measured, and may have significant errors in other radiation spectra. In the case of SPEs, the spectrum is not predictable, and such an instrument would have limited accuracy. The second problem is that the design of the instrument is tailored for the definition of dose equivalent, and there is no simple way to adapt it to changes in the definition. Since understanding of health risks may continue to evolve, this reduces the value of effort invested in devising a system with response tailored to current definitions.

5.13 Summary

The radiation environment inside a spacecraft operating outside Earth's magnetosphere will generally include charged particles originating as GCR and solar radiation, the charged and uncharged secondaries produced by inelastic interactions between these primary particles and the components of the craft, radiation from sources included in the spacecraft, and delta rays produced by the high-energy charged particles. This combination of radiations creates a wide range of energy deposition in individual cells or subcellular targets, and a wide range of spatial distributions of irradiated and unirradiated targets within tissues and organisms. These diverse energy deposition patterns produce a complex problem in relating energy deposition to biological consequences, and in predicting health risks. They also create a complex situation for evaluating absorbed dose and dose equivalent. In particular, the contribution of secondary neutrons to the absorbed dose depends on the size of the vehicle as well as the atomic composition of shielding and structural components. Current calculational methods underestimate the measured absorbed dose in such a situation by on the order of 20 %. Several techniques, including both active and passive dosimeters can be used in this radiation environment, but most can measure only certain components of the radiation field,

and those which can respond to all types of ionizing radiation and give an estimate of radiation quality (for example, TEPCs) have some limitations related to minimum event sizes and wall effects. Additional research and development are needed in a number of areas of dosimetry and instrumentation to:

- experimentally validate radiation transport and dosimetry models;
- evaluate the energy deposition in microscopic volumes in a uniform medium, and the effect of the wall on measurements made with TEPCs;
- study the effects of numerical and physical phantom configurations on the calculation and measurement of dose equivalent;
- develop radiation spectrometers that can accurately measure fluence of indirectly ionizing particles in the presence of a much higher fluence of directly ionizing particles; and
- improve data on neutron production in fragmentation processes and on neutron interaction cross sections for the purpose of absorbed dose calculation and detector design.

In order to provide the data needed to effectively evaluate risk of radiation exposures outside Earth's magnetosphere, future biological response studies should:

- be conducted with cells in three-dimensional organ culture, supported in a natural extracellular matrix or in suspension, in order to simulate the effects of the interaction of cell geometry and track structure; and
- specify lineal energy, absorbed dose, fluence, and spectrum for doses that lead to effects.

6. Space Radiation Biology

6.1 Introduction

Evaluation of potential health effects from radiation exposure during and after deep-space travel is important for the future of manned missions. The world's experience in human space flight is only about four decades old. To date, manned missions have been limited to near-Earth orbits, with the moon the farthest destination from Earth. Historical space radiation career exposures for astronauts from all NASA missions through December 1999 are summarized in Figure 6.1. The early Mercury, Gemini, STS, and Apollo missions involved total exposures of less than ~20 mSv (Cucinotta *et al*., 2002). With the advent of Skylab and Mir, total career exposure levels increased to a maximum of nearly 200 mSv. Missions beyond LEO, due to the requisite longer duration of the missions, may pose greater risks of exposure to complex radiation fields. It is

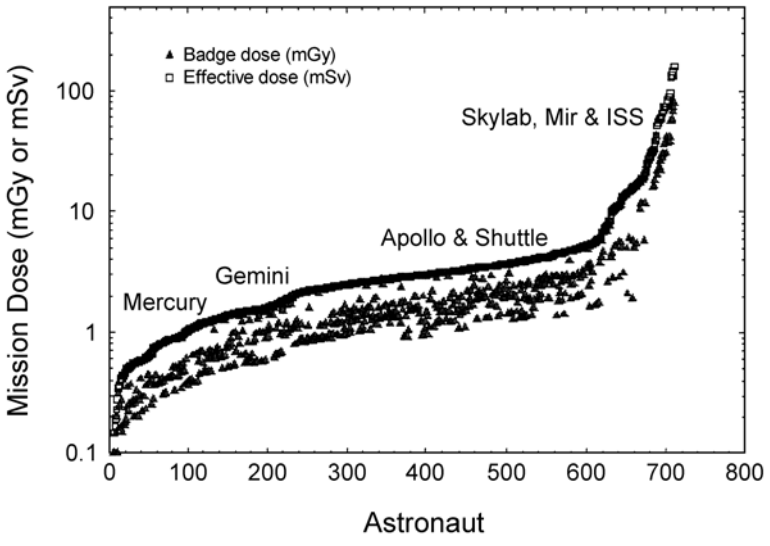

Fig. 6.1. Summary of space mission doses for astronauts from all NASA missions through December 1999 (Cucinotta *et al*., 2002).

not just the absorbed dose that is important but also the type of radiation contributing to the dose (Edwards, 2001). This point is emphasized in Figure 6.2, which presents the dependence of particle kinetic energy versus range in water for representative particles in space. The radiation quality or LET values of proton, carbon, argon and iron beams are shown over the tissue range that is significant to the exposure of the human skin, eye and brain. The LET of these particles ranges from <10 to >200 keV μm^{-1}. Protons are more prevalent and have relatively low-LET values, whereas the iron ions are relatively rare, but have high-LET values. Dose rates measured in LEO are of the order of fractions of 1 mSv d^{-1}, but as previous sections of this Report indicate, radiation dose rates will be higher beyond LEO on missions to Mars. Figure 6.2 demonstrates the complexity of the task of assessing the biological and clinical effects of space radiation.

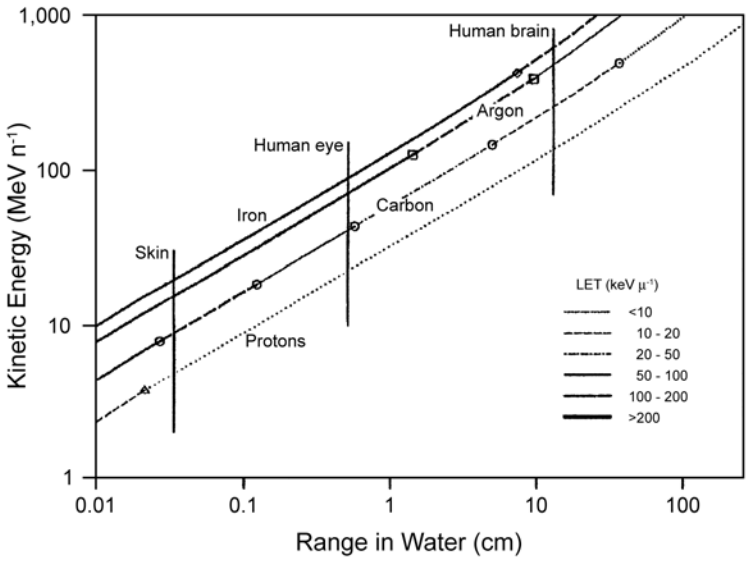

Fig. 6.2. Dependence of particle kinetic energy as a function of range in water for representative particles in space.[9]

[9]Heilbronn, L. Personal communication (Lawrence Berkeley National Laboratory, Berkeley, California).

Particle radiation fields have been graphically visualized in light-flash phenomena experienced by space travelers and evidence exists from accelerator-based human exposures with muons (McNulty, 1971; McNulty *et al*., 1976), pions (McNulty *et al*., 1975), helium ions (Tobias *et al*., 1971), carbon ions (McNulty *et al*., 1978) and nitrogen ions (Budinger *et al*., 1972). Visual phenomena have also been noted by human subjects on exposure to neutrons of several energies (Budinger *et al*., 1971; Charman *et al*., 1971; Fremlin, 1970). It may be too early in man's exploration of space for the evaluation of late tissue effects in large numbers of crew members, since a long follow-up period of astronauts or cosmonauts is not yet available. The first steps in such an evaluation are underway with bio- and physical-dosimetric measurements on both commercial flight personnel and international space crews who have experience in near-Earth orbits (De Angelis *et al*., 2001; George *et al*., 2001a; 2001b; Obe *et al*., 1997; Testard and Sabatier, 1999; Testard *et al*., 1996; Wolf *et al*., 1999a; 1999b; Yang *et al*., 1997).

The potential risks resulting from exposure to radiation in deep space are cancer, noncancer effects, and genetic effects (Blakely, 2000). These are primarily late tissue effects. The potential risk of early noncancer effects is most likely from exposure, without sufficient shielding, to a large SPE that could occur during an extravehicular activity. The highest potential dose would be to the skin and lens of the eye because of the abundance of low-energy protons. It is only during large SPEs, such as occurred in 1972, that the dose rate rises to above that which is considered a low dose rate based on biological effects (Parsons and Townsend, 2000).

In 1992 NASA approved the Longitudinal Study of Astronaut Health. In 2002, NASA's Chief Health and Medical Officer sought additional help from the NAS/NRC's Institute of Medicine (IOM) in assessing and improving the goal of evaluating effects of space flight on astronauts. Presently the IOM, through activities including studies and workshops undertaken at the National Academies under the standing Committee on Aerospace Medicine and the Medicine of Extreme Environments, provides NASA's Chief Health and Medical Officer independent technical advice relevant to aerospace medicine, including medical care of space travelers. A relatively recent review of the status of NASA's Longitudinal Study of Astronaut Health by IOM is available (Longnecker *et al*., 2004).

Both the Soviet and Russian space programs have provided evidence that living in space can produce profound physiological and clinical changes. These include bone demineralization, decreases in skeletal muscle mass, changes in blood volume and cranial fluid shifts, decreased or altered absorption of nutrients in

the gastrointestinal tract, disturbed fine motor control, increased risks of renal stones, anemia, and depressed immune system function (Nicogossian *et al*., 1993). It is likely that many of these effects are due to altered physiology under microgravity (Heer and Paloski, 2006). Several studies have been unable to support the hypothesis that astronauts are at an increased risk of cancer mortality compared to the U.S. population due to ionizing radiation exposures from space travel (Hamm *et al*., 1998; 2000; Peterson *et al*., 1993). However the relatively young age of the astronauts, the low doses of radiation during space flight, the modest interval between space flight and data analysis, and the small sample size of the astronaut corps all limit statistical confirmation.

To date, the only health detriment associated with ionizing radiation dose in space is cataract. There was a significant link between cataracts in astronauts who have flown high-inclination or lunar missions, where a higher fluence of heavy-ion radiation occurs (Cucinotta *et al*., 2001b). Ninety percent of 39 cataracts occurring after space flight were in astronauts on such missions (see further discussion in Section 6.2.1.1). Chromosome aberrations in astronauts and cosmonauts have been investigated as a method of individual biodosimetry for risk assessment after single and multiple flights (Durante *et al*., 2003; George *et al*., 2001c; 2004; Horstmann *et al*., 2005), but these studies are also limited by significant individual variability and inadequate statistics (Section 6.3.5.2.2).

A goal of manned space exploration is to ensure minimal risk to personnel. NASA has spent considerable research effort and resources to evaluate and to mitigate risk at all levels and to follow the goals of ALARA regarding radiation exposure. Early in the planning for space exploration the potential risks of radiation exposure were perceived to be important to investigate. The realization that information was lacking due to the unavailability of Earth-based, space-radiation sources with the closure of LBL-BEVALAC in Berkeley, California in 1993, led to NASA-funded programs to provide proton beams at the clinical radiotherapy accelerator facilities at the Loma Linda Medical Center in Loma Linda, California (Nelson *et al*., 2001) and the use of the Alternating Gradient Synchrotron and recently completed NASA Space Radiation Laboratory accelerator facility at Brookhaven National Laboratory, Brookhaven, New York to fill this need (Lowenstein, 2001).

NCRP Report No. 132 (NCRP, 2000) comprehensively reviewed available information on the biological effects of individual components of the space radiation environment with a focus on each of the radiation-types prevalent in near-Earth missions. A goal of this Report is to identify research needs for activities beyond LEO.

6.2 Late Radiation Effects

6.2.1 *Cataract*

6.2.1.1 *Incidence of Cataracts Among Astronauts and Cosmonauts*. The only reported health detriment among astronauts that has been associated with space radiation exposure is cataract formation (Cucinotta *et al*., 2001b). The human crystalline lens is known to be a radiosensitive tissue that responds with opacification in a delayed time course depending on the radiation type and exposure level. Cataracts are lesions that progressively increase, and can be defined in different ways, such as minor lesions not affecting sight, or as major lesions affecting vision. Historical data for the incidence of cataracts has been analyzed for 295 astronauts participating in NASA's Longitudinal Study of Astronaut Health based on individual occupational radiation exposure data (Cucinotta *et al*., 2001b). Eye examinations revealed 48 cases of lens opacification in the 295 astronauts, including one case of congenital cataract. The exposure histories were broken out to reveal the dose components from diagnostic x rays, aviation experience, and space travel. In this first analysis of space radiation exposure the contribution from individual radiation types in the space environment was not available. The astronauts were divided into two groups, a low dose group with doses <8 mSv (average 3.6 mSv), and a high dose group with lens doses >8 mSv (average 45 mSv). The probability of survival without cataract both as a function of age and time after first mission for NASA astronauts are depicted in Figures 6.3 and 6.4, respectively. This first epidemiological evidence for a late effect of space radiation exposure among astronauts strikingly showed that there was an increased risk of cataract formation at lens doses of >8 mSv, compared to exposures of <8 mSv (Cucinotta *et al*., 2001b). This suggested that relatively low doses of space radiation are correlated with an increased incidence and earlier appearance of cataract. It has not yet been determined which specific radiation component(s) is responsible for these observations. If a cataract is severe, it can affect vision unless surgically corrected with synthetic lens replacement, however this procedure is invasive and can have side effects. Stable vision during space flight has been reported in one astronaut with bilateral intraocular synthetic lenses (Mader *et al*., 1999). The lens, due to its ectodermal origin, may be considered a test model system for radiation effects in other cells of ectodermal origin for which there are not clear endpoints of low dose radiation effects.

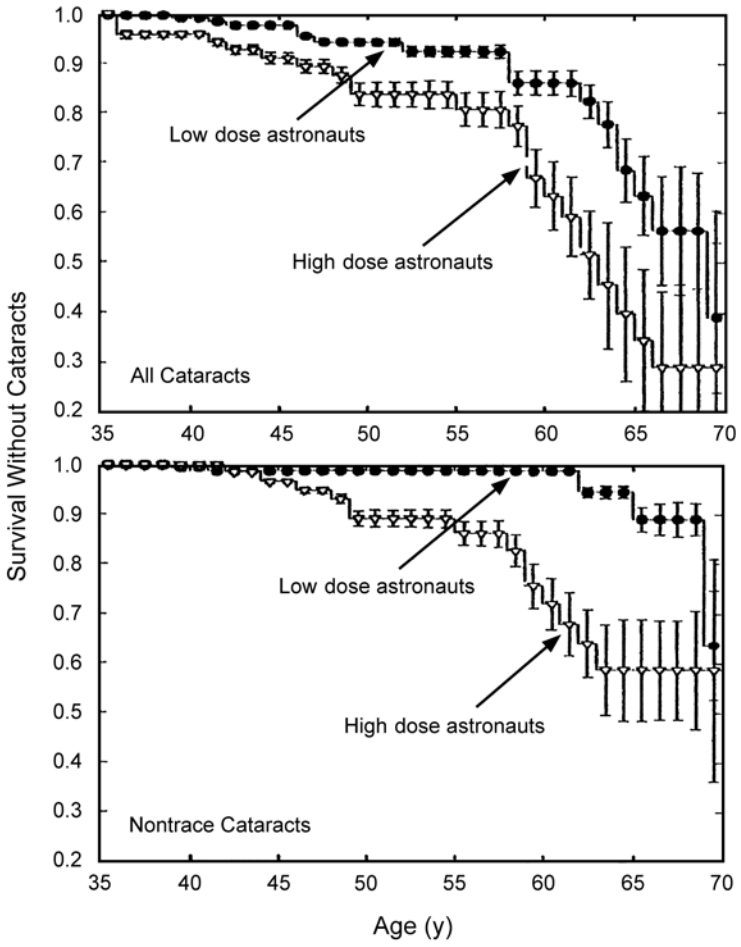

Fig. 6.3. Results for the probability of survival without cataracts as a function of age for NASA astronauts for the low-dose group (closed symbols) with lens doses <8 mSv (average 3.6 mSv) and the high-dose group (open symbols) with lens doses >8 mSv (average 45 mSv). Error bars indicate standard errors. The upper panel is for all cataracts and the lower panel is for nontrace cataracts. (Cucinotta *et al*., 2001b).

6.2.1.2 *Cataract Incidence in Patients Treated with Radiotherapy.* Human experience with radiation-induced cataracts is available from clinical radiotherapy for the treatment of cancer with x rays or radium plaques (Merriam and Focht, 1957; Nutting *et al*., 1999), with protons (Gragoudas *et al*., 1995), with helium ions (Meecham *et al*., 1994), or total body photon irradiation in preparation for bone-marrow transplantation (Belkacemi *et al*., 1996; Dunn *et al*.,

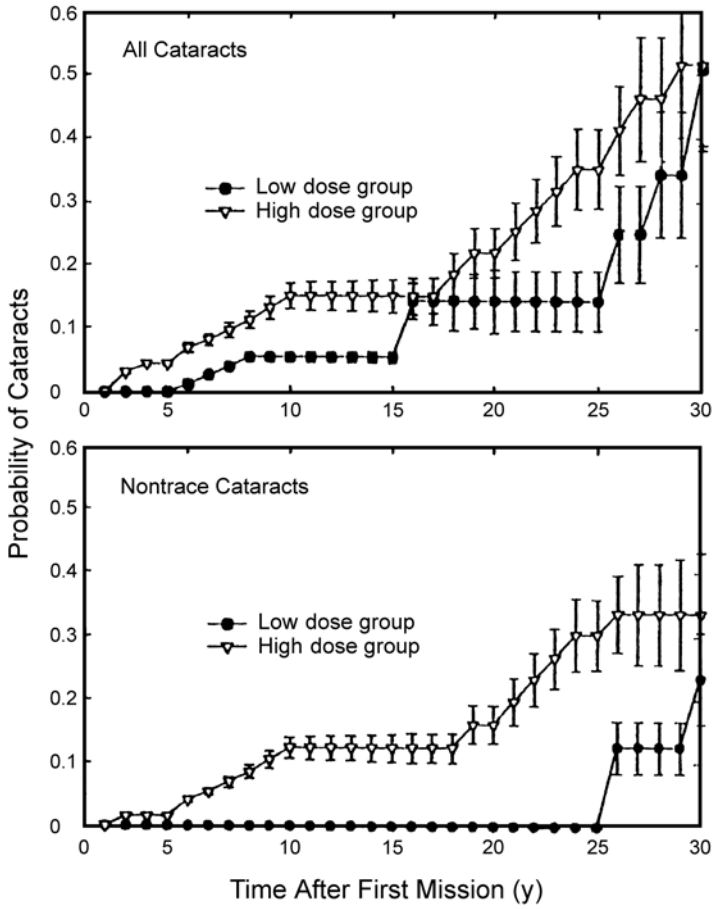

Fig. 6.4. Results for the probability of cataracts as a function of time after first space mission for NASA astronauts for the low-dose group (closed symbols) with lens doses <8 mSv (average 4.7 mSv) and the high-dose group (open symbols) with lens doses >8 mSv (average 45 mSv). Error bars indicate standard errors. The upper panel is for all cataracts, and the lower panel is for nontrace cataracts. Only cataracts occurring after a first space mission are included (Cucinotta *et al*., 2001b).

1993; Frisk *et al*., 2000; Thomas *et al*., 2001; van Kempen-Harteveld *et al*., 2002a; 2002b; Zierhut *et al*., 2000). In addition, there are analyses of cataract incidence among individuals exposed at Hiroshima and Nagasaki (Medvedovsky and Worgul, 1991; Otake and Schull, 1990), in radiotherapy patients exposed to fast neutrons (Roth *et al*., 1976), in cases of exposure of cyclotron- and

reactor-operators (ICRP, 1969) and in populations exposed to environmental radiation contamination (Junk *et al*., 1999). However, due to a number of reasons, none of the published data on humans allow a prediction of the risk of radiation-induced cataracts at doses in the millisievert range from chronic exposure to low dose protons or low fluence heavy-ion doses.

In vitro radiation studies using human lens cell models (Chang *et al*., 2000a) have suggested that molecular markers of radiation-stress can be measured at relatively lower doses of particles than previously documented *in vivo* (Chang *et al*., 2000b; McNamara *et al*., 2001). The *in vitro* models may also provide more specific evidence of the molecular mechanisms underlying the radiation damage that lead to the abnormal folding or aggregation of the crystalline proteins associated with cataract, and for potential countermeasures. Currently known countermeasures for cataract induction that require administration prior to radiation exposure include antioxidants (*e.g*., vitamins, especially C and E) (Bantseev *et al*., 1997; Jacques *et al*., 1997; Taylor *et al*., 2002) and sulfhydryl agents (Kador, 1983).

6.2.1.3 *Radiation-Induced Cataract in Animal Models*. There is a large literature on laboratory animal studies of cataract induction from individual components of space radiation (*e.g*., neutrons) (Abrosimova *et al*., 2000; Ainsworth, 1986; Bateman and Bond, 1967; Christenberry *et al*., 1956; Laporte and Delaye, 1987; Medvedovsky and Worgul, 1991; Merriam *et al*., 1984; Riley *et al*., 1991; Ross *et al*., 1990; Worgul, 1986; Worgul *et al*., 1996), high-energy particle beams such as protons (Lett *et al*., 1991), helium ions (Abrosimova *et al*., 2000), carbon ions (Abrosimova *et al*., 2000), neon ions (Abrosimova *et al*., 2000; Lett *et al*., 1980), argon ions (Abrosimova *et al*., 2000; Lett *et al*., 1980; Merriam *et al*., 1984; Worgul, 1986), and iron ions (Brenner *et al*., 1993; Jose and Ainsworth, 1983; Lett *et al*., 1991; Medvedovsky *et al*., 1994; Riley *et al*., 1991; Tao *et al*., 1994; Williams and Lett, 1994; Worgul, 1986; Worgul *et al*., 1993). This large database indicated an earlier appearance of cataracts, and at lower doses, than were observed from x rays. There are reports of an LET-dependence for cataract induction studies based on morphological endpoints in mice with photons, x rays, and various heavy particle beams with LET values <100 keV μm^{-1} (Yang and Ainsworth, 1987), but a small change in RBE for cataract induction in mice is reported at low doses (0.01 Gy) between argon ions at 88 keV μm^{-1} and iron ions at 190 keV μm^{-1} (Brenner *et al*., 1993). Particle-induced cataractogenesis studied in New Zealand white rabbits at 35 and

90 keV μm^{-1} showed that the rate of development of the early (acute) and intermediate (plateau) cataract stages increased with the LET of the incident radiation, and for a given intermediate level, the onset of late cataractogenesis occurred earlier the higher the LET (Keng *et al*., 1982).

The work of Worgul *et al*. (1996) provides evidence of higher RBE cataract induction in mice from neutrons, and from argon or iron ions. at very low doses (2 to 250 mGy) of 430 keV neutrons. More cataractogenesis studies with charged particle beams at very low doses are needed to confirm the risk due to exposure to very low-particle doses, and to investigate countermeasures.

Proton-induced cataractogenesis studies in nonhuman primates by Niemer-Tucker *et al*. (1999) have evaluated late ophthalmological complications after total body exposure. The data reveal increased cataract indices and shorter latencies with increasing dose from 0.31 to 7.5 Gy (Figure 6.5). Fedorenko *et al*. (1995) examined the dose-rate dependence of radiation induced lens opacities in mice after 4 Gy of very high-energy (645 MeV) protons and demonstrated dose rate sparing at 0.18 Gy min^{-1} versus 18 Gy min^{-1} (Figure 6.6).

6.2.1.4 *Genetic Susceptibility to Radiation-Induced Cataracts*. An important issue with regard to cataracts is the radiosensitivity or genetic background of the exposed individual. There are radiosensitive subsets of the human population represented by individuals with cancer-prone phenotypes (Hall and Angele, 1999), presumably due to inherent genetic deficiencies. One well-known but relatively rare autosomal recessive disorder is ataxia telangiectasia (Lavin and Shiloh, 1999). When there are mutations in both alleles of the ataxia telangiectasia mutated (ATM) gene, these homozygous individuals are radiosensitive. More commonly, 1 to 3 % of the human population are thought to be ATM heterozygotes with mutation in only one allele ($ATM^{+/-}$). Although phenotypically indistinguishable from the rest of the population, individuals heterozygous for the ATM gene may have an increased risk of cancer (Bay *et al*., 1999; Broeks *et al*., 2000). Three clinical reports indicate severe late radiation responses associated with defects in the ATM gene. In prostate cancer patients, Hall *et al*. (1998) found an association with the frequency of AT heterozygotes in 3 of 17 patients with severe late responses to radiation therapy compared to control patients without significant mutations in the ATM gene. In breast cancer patients there is conflicting evidence for this association. Iannuzzi *et al*. (2002) in a study of 46 early breast cancer patients treated with limited surgery and radiotherapy found that

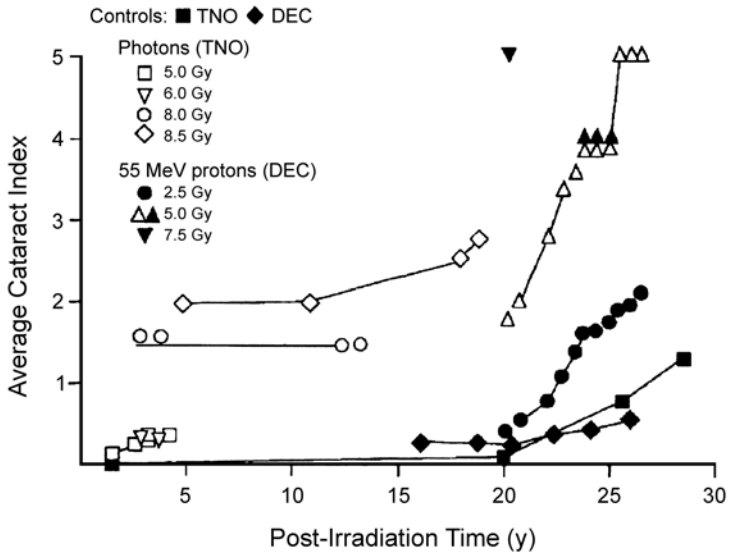

Fig. 6.5. Average cataract index as a function of time after exposure (Niemer-Tucker *et al*., 1999). Data are summarized from TNO (Netherlands Organization for Applied Scientific Research, Radiobiological Institute, Riijswijk, The Netherlands), and from a USAF Study [DEC (Delayed Effects Colony, USAF School of Aerospace Medicine, Brooks Air Force Base, Texas)]. The scoring system used (average cataract index) was the scoring system of Lett as published in Keng *et al*. (1982), where a cataract index of two does not affect vision.

possession of an AT mutation, particularly when two are present, may be predictive of an increase in subcutaneous late tissue effects after radiotherapy for breast cancer and may subsequently prove to be a relative contraindication to standard management with radiotherapy. In contrast, Bremer *et al*. (2003) collected DNA samples from 1,100 unselected breast cancer patients receiving adjuvant radiotherapy. Eleven patients were identified to be heterozygous for a pathogenic ATM gene mutation. Ten patients had received at least one course of radiotherapy. Median follow-up after completion of radiotherapy was 5.1 y (range 1.7 to 7.2). There was no evidence of increased radiation-induced early or late skin or subcutaneous reactions in patients treated with linac-based radiotherapy. The authors concluded that due to their increased cellular radiosensitivity, these patients may differentially benefit from radiotherapy and qualify for dose and volume reduction trials.

Two clinical reports indicate severe late radiation responses in ataxia telangiectasia heterozygotes with ATM during and after

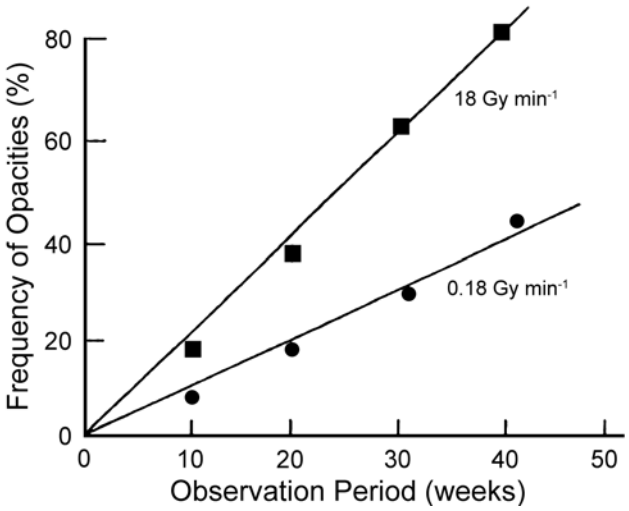

Fig. 6.6. Effect of dose rate on frequency of lens opacities in mice due to exposure to high-energy protons (Fedorenko *et al*., 1995).

cancer radiotherapy (Hall *et al*., 1998; Iannuzzi *et al*., 2002), when compared to the cohort of control patients with mutations in the ATM gene. Recently, results of radiation studies on ATM gene-deficient mice have indicated that ATM heterozygous mice are more sensitive to radiation-induced cataract than are their wild-type counterparts (Worgul *et al*., 2002). Worgul *et al*. (2002) found that the lenses of homozygous mice ATM-deficient were the first to opacify at any given dose, and more importantly that cataracts appeared earlier in the heterozygous versus the wild-type animals. It has been suggested that genetic screening of individuals for evidence of radiosensitive genes may become an important future criteria for selection of candidates for missions beyond LEO. However legal and ethical issues regarding the implementation of such an idea need further evaluation.

6.2.2 *Cancer*

Extensive literature on radiation carcinogenesis has been reviewed by the United Nations Scientific Committee on the Effects of Atomic Radiation (UNSCEAR, 2000). This Section briefly summarizes what is known about carcinogenesis following exposure to neutrons, gamma rays with a small neutron component, protons, and heavy charged particles. Very little data exist on human carcinogenesis from neutrons and charged particles, and

the data that do exist are primarily from studies of secondary cancers in radiotherapy patients treated with these radiations. The inherent limitations of epidemiology make it difficult to directly quantify health risks from most radiotherapy and other medical exposures (Sigurdson *et al*., 2002). While most epidemiological data are compatible with linear extrapolations from exposures at high doses or high dose rates of low-LET radiations down to low doses, they cannot entirely exclude other possibilities (Ron, 1998). There have been some attempts to estimate risks for fast neutrons with regard to solid cancers from the data of the atomic-bomb survivors (Kellerer and Walsh, 2001), but the conclusions that can be drawn are limited due to the deficiencies in available data. In addition, the neutron component is a small fraction of the total dose (RERF, 2005).

With regard to chronic occupational exposures to conventional low-LET radiations, to date there is no clear evidence of an increased cancer risk in medical radiation workers exposed under current occupational exposure (Yoshinaga *et al*., 2004). However, there are indications of excess leukemia, breast and skin cancer among technologists employed before 1950 when doses are assumed to have been higher than current levels (Mohan *et al*., 2003; Sigurdson *et al*., 2003). Analysis of the mortality experience among U.S. nuclear power industry workers after chronic low dose exposure to ionizing radiation displays a very substantial healthy worker effect, with a considerably lower cancer and noncancer mortality than the general population (Howe *et al*., 2004). Previous reports on the effects of low doses and low dose rates of external ionizing radiation and cancer mortality among nuclear workers in the United States (Gilbert *et al*., 1993), and in nuclear workers of the United States, United Kingdom, and Canada (Cardis *et al*., 1995) showed no evidence of an association between low-radiation dose and mortality from all causes or from all cancers. Epidemiological evaluation of cosmic radiation exposure and mortality or cancer risk among European airline flight crews (designated as radiation workers since 1996) have also not reported a clear cause-and effect-relationship between risk of any site-specific cancer and occupational exposure as a pilot or flight attendant (Langner *et al*., 2004; Sigurdson and Ron, 2004; Zeeb *et al*., 2003).

Therefore, for high-LET radiation the current situation is limited to extrapolating high-LET cancer risks to man from nonhuman experimental systems. This topic was recently reviewed in NCRP Report No. 150 (NCRP, 2005), where it was concluded that the animal data has provided information for the estimate of quality factors. Neutron results may also provide predictions of similar

risks from heavy-ion exposures in space flight. However, the very limited animal studies of adverse health effects from heavy-ion exposures warrant more research to validate the predictive potential of neutrons. There appears to be a RBE_{max} for experimental study of heavy-ion induction of Harderian gland tumors and it is comparable to that of the RBE for fission neutrons (Fry *et al*., 1983). If the RBE for fission neutrons is comparable to the RBE for heavy ions, perhaps the relative effects of heavy ions could be predicted from the effects of fission neutrons. Unfortunately, there are only limited data from studies of nonhuman experimental systems at low fluences from which to estimate the late effects of chronic exposures of high-LET radiations with confidence (Cucinotta *et al*., 2004). Recent rodent tumorigenesis data from studies with protons, iron ions, or protons and iron ions suggest that mean LETs of the primary cosmic rays may be insufficient to accurately evaluate the relative risks of each type of particle radiation in a field of mixed radiation qualities (Dicello *et al*., 2004).

6.2.2.1 *Neutron Carcinogenesis*. Neutrons are not a primary radiation in space, but rather a secondary radiation produced by the interaction of other radiations with matter. There is a wide range of neutron energies possible in these secondary radiation fields. Absorbed doses of secondary neutrons from GCR inside Mir and using the material of the ISS have been measured (Getselev *et al*., 2004). The neutron fluence rates in Mir covered the energy range from 0.1 to 500 MeV. Austrian measurements onboard Mir indicate neutron dose-equivalent rates between 31 to 41 μSv d^{-1}. The most biologically effective neutron energy range for experimental endpoints examined is between 0.2 to 0.5 MeV (Geard, 1996; ICRU, 1988; Schmid *et al*., 2003). However, there are not sufficient data for the appropriate neutron energies in space to estimate their risk. It would be reasonable to assume that the RBE for such neutrons would be significantly less than for fission neutrons.

6.2.2.2 *Cancer Risk from Protons and Heavy Ions*. The data for the induction of cancer in humans by protons or heavy ions is insufficient for the estimation of risks. Both ICRP (1991) and NCRP (1993) considered the radiation weighting factor (w_R) for protons to be greater than low-LET radiations for radiation protection purposes. ICRP (1991) chose a value of five, NCRP (1993) chose a value of two, with ICRP (2003) later also recommending a value of two. Based on second cancers in patients treated with protons, Schneider *et al*. (2002) concluded that the risk of cancer was comparable for protons and photons. Therefore, it is still important

to decide what the appropriate w_R for protons is even though the difference between one and two is small. Joseph R. Castro[10] reported a 0.7 % (3/425) secondary tumor incidence among 425 patients treated with helium ions with a 24 to 200 month follow-up (mean of 64 months). In a much smaller study of 92 patients treated with neon ions and a follow-up of 24 to 173 months (mean of 67 months), Castro found a secondary tumor incidence of 2.2 % (2/92). The sample size of both patient cohorts is inadequate for statistical analyses to allow conclusions other than noting a trend. Further analyses of data from radiotherapy patients in numerous proton facilities worldwide, and carbon ion patients treated in Japan and Germany should be helpful in estimating the w_R for protons and heavy ions.

6.2.2.3 *Breast Cancer Risk Due to Atomic-Bomb Exposure*. A recent updated incidence survey of breast cancer found in the Life Span Study (LSS) population confirms the finding of a linear and highly statistically significant radiation dose response (Land *et al*., 2003a). Figure 6.7 presents the estimated relative risk with 90 % confidence limits by mean estimated equivalent dose (w_R = 10) to breast tissue for consecutive dose intervals and fitted linear dose-response model stratified on city, age at the time of the bombings, attained age, and calendar time. Figure 6.8 presents the estimated excess relative risk (ERR) for female breast cancer per sievert by interval of attained age with fitted model (Tokunaga *et al*., 1994):

$$\mathrm{ERR}(H_T,A) = \alpha H_T^{\beta_1 A} , \tag{6.1}$$

where H_T is the equivalent dose in sieverts (w_R = 10) and A is attained age. The total number of cases is given above the upper confidence limit for each interval of attained age. A much lower, but marginally significant dose response was seen among women exposed at 40 y and older. Data such as these led to recommendations for gender and age differences in dose limits for space activities because the overall risks per unit dose for women are higher than for men, due to the greater probability of women developing some radiation-induced cancers, such as breast cancer (NCRP, 1989; 2000). As more epidemiological data become available from irradiated cohorts, there may be other tissues of the body vulnerable to radiation-induced cancer that may also restrict future career

[10]Castro, J.R. (2005). Personal communication (Lawrence Berkeley National Laboratory, Berkeley, California).

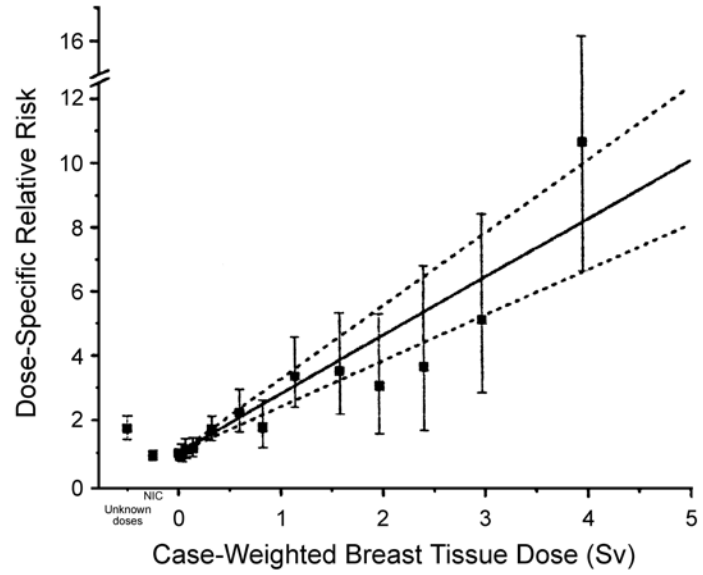

Fig. 6.7. Estimated relative risk of breast cancer, with 90 % confidence limits, by exposure status and equivalent dose in breast tissue, with fitted linear dose response for exposed subjects with dose estimates. All ages combined. The dashed lines indicate the 90 % confidence interval for the complete data set. The error bars are one standard deviation at each dose interval (NIC = not in city) (Land *et al*., 2003a).

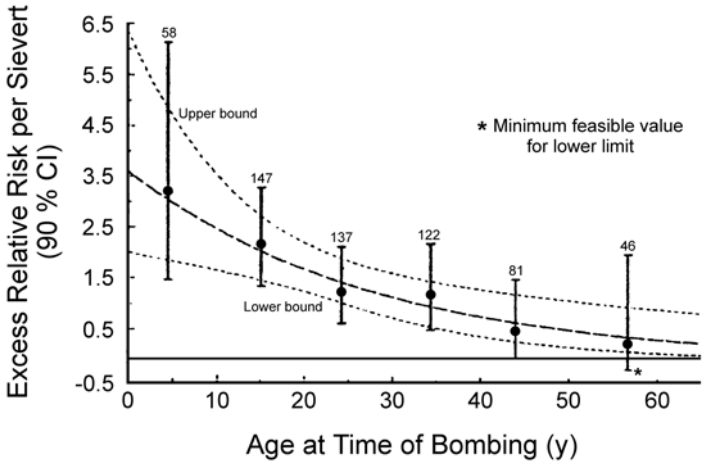

Fig. 6.8. Estimated ERR per sievert, by interval of age at the time of the bombings (ATB) (0 to 9, 10 to 19, 20 to 29, 30 to 39, 40 to 49, and ≥50) (see Equation 6.1). Estimates and 90 % confidence limits stratified on city, age ATB, attained age and period. Total number of cases appears above the upper confidence limit for each interval of age ATB (Tokunaga *et al*., 1994).

limits (Land, 1988). Recent changes in atomic-bomb survivor dosimetry have not significantly altered solid cancer mortality risk (Preston *et al*., 2004), but do indicate that it will be virtually impossible to make useful inference about the effects of neutron exposure on the cancer risk directly from the LSS data (Preston *et al*., 2004).

6.2.2.4 *Radiation-Induced Brain Tumors*. Experimental studies in laboratory animals (rats, monkeys and dogs) have examined the carcinogenic potential of charged-particle irradiation of the brain and found relatively high rates of tumor induction in the brain. This has not been seen in human clinical trials with charged-particle beams of protons, or carbon ions, and it is not known what species- or radiation-specific differences exist. Tumors of the brain and nervous system after conventional radiotherapy in childhood have been reported by Ron *et al*. (1988). Brain tumor inductions similar to those seen in laboratory animals with charged particles have been seen in humans after conventional radiotherapy (Cavin *et al*., 1990).

A very high incidence of pituitary tumors was found in 28 d old Long-Evans rats irradiated with deuterons (Van Dyke *et al*., 1959). All rats receiving doses of 13.6 Gy to the pituitary were found to have tumors at 2 y, many with two or three microtumors per gland. These rats have a high spontaneous incidence of pituitary tumors. Brain tumor-induction by short range (2.5 cm in unit density material) 55 MeV protons in Rhesus monkeys has also been reported (Dalrymple *et al*., 1994; Haymaker *et al*., 1972; Wood *et al*., 1986). In the Dalrymple study, 9 out of 72 monkeys who were adolescent at the time of exposure to 55 MeV proton doses of 4 to 8 Gy, developed grade IV astrocytoma or glioblastoma multiforme over a period of 14 months to 20 y after exposure. The monkeys were rotated during exposure, with the doses possibly being three to four times greater than the nominal surface dose of 4 to 8 Gy. The median latent period was 5 y. In the earlier Haymaker study, 21 monkeys received proton exposures (55 to 400 MeV), or x-ray exposures (2 MeV) ranging in dose from 2 to 8 Gy with the incidence of malignant glioma being 14 % among the animals that died 2 to 7 y after the exposure.

The monkey studies triggered a follow-up study with Fischer-344 rats irradiated with doses of 0 to 8.5 Gy of 55 MeV protons (Wood *et al*., 1994). A 2 y follow-up study revealed a linear dose-response for total head and neck tumor incidence. The exposed rats had a greater incidence of pituitary chromophobe adenomas and epithelial and mesothelial cell tumors than the unexposed controls, but the occurrence of malignant gliomas that was observed in the monkeys was absent in the rats. Experiments such as these suggest

that the induction of tumors by radiation is related to inherent susceptibility, and since the results are strain- and species-dependent, such results may not be useful for extrapolation of risks to humans.

Recent analysis of the LSS of the atomic-bomb survivors has demonstrated a significant dose-related excess of tumors of the CNS and the pituitary gland (Yonehara *et al*., 2004). Most of the individuals were estimated to have received brain doses of <100 mSv, and a significant number had brain doses of <5 mSv. Mengingoma was the most common tumor among clinically diagnosed tumors, followed by neuroepithelial tumor, schwannoma, and pituitary tumor. The overall incidence of these tumors increased initially with age, but declined among the elderly. For all age groups and for both genders, incidence increased over time. Meningiomas were more prevalent than neuroepithelial tumors in this Japanese population, but the characteristics of the tumors were consistent with being spontaneous. Yonehara *et al*. (2004) concluded that the increased incidence of CNS and pituitary tumors is likely attributable to the increased use of new diagnostic imaging techniques.

Estimates of charged particle integral fluences at the center of the human brain anticipated during space flight have been made by Craven and Rycroft (1994). They estimated absorbed dose rates for three scenarios: outside the magnetosphere without shielding, in polar orbit, and in the ISS orbit to be: 3, 1 and 0.3 mGy y^{-1}, respectively, corresponding to dose equivalent rates of 80, 25 and 8 mSv y^{-1}, and decreasing by roughly a factor of two behind 10 g cm^{-2} of aluminum. They concluded that behind 10 g cm^{-2} of aluminum, 3.4, 1.3, and 0.5 % of cell nuclei at the center of the brain will be traversed. In a similar approach, Curtis and colleagues (Curtis and Letaw, 1989; Curtis *et al*., 1998; 2000) made estimates of particle fluences and cell-hit frequencies for travel outside the magnetosphere during solar minimum as well as solar maximum. They concluded that for a 3 y mission to Mars at solar minimum (assuming the 1977 spectrum of GCR), 2 or 13 % of the critical sites of cells in the CNS would be directly hit at least once, by iron ions, depending on whether 60 m^2 or 471 m^2 is assumed as the critical cross-sectional area. They estimated that roughly 6 million out of some 43 million hippocampal cells and 55 thousand out of 1.8 million thalamus cell nuclei would be directly hit by iron ions at least once on such a mission for space travelers inside a simple pressure vessel, and that roughly 20 million out of 43 million hippocampal cells and 230 thousand out of 1.8 million thalamus cell nuclei would be directly hit by one or more particles with $Z > 15$ on such a mission.

6.2.2.5 *Particle-Radiation-Induced Harderian Gland Tumors*. For a long time the murine Harderian gland model and the rat skin (Burns and Albert, 1980) provided the only experimental animal radiation-induced tumor data *in vivo* available allowing a comparison of the effects of different particle beams. The Harderian gland lies behind the murine eye, but is not present in humans. Fry *et al*. (1983) reported RBE values of ~30 for induction of Harderian gland tumors by argon and iron ion beams, and lower RBE values with radiation beams of lower LET. Alpen *et al*. (1994) extended the study to include protons, niobium and lanthanum ions, as well as iron, neon and helium ions and ^{60}Co photons, extending the LET values up to 953 keV μm^{-1} (Figure 6.9). The results indicated that the RBE-LET relationship did indeed reach a plateau at ~100 to 200 keV μm^{-1}, and unlike the data for cell killing and mutations, did not decrease steeply at higher-LET values. An analysis of the Harderian tumor data using particle fluence rather than dose allowed a calculation of a risk coefficient that is a monotonic function of LET for the particles studied (Curtis *et al*., 1992). It was

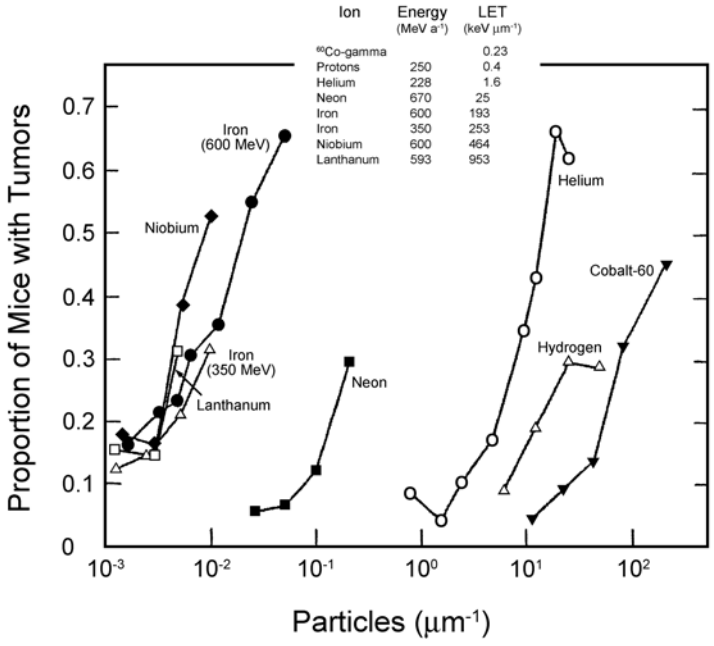

Fig. 6.9. Harderian gland tumor prevalence expressed as proportion of mice with tumors, plotted against the particle fluence. The abbreviation for the name of the ion is adjacent to the appropriate curve and the energy and LET of each ion are listed in the insert box (Alpen *et al*., 1993).

suggested that fluence-based risk coefficients for estimating the risk of cancer from exposure to radiations in space be used. This concept of a risk cross section or risk per particle fluence was further examined by Curtis who derived human cancer risk cross sections for low-LET radiation from the data with this approach from the atomic-bomb survivors (Curtis *et al*., 1995) (Figure 6.10). Both the fluence-based and microdosimetry event-based methodologies provide a way of dealing with the major objection to the conventional system: using LET alone as a universal physical descriptor of the radiation field to determine the biological effect. The fluence-based system allows for different values of the risk cross section for different particle types that have the same LET. This work led to NCRP Report No. 137 (NCRP, 2001a) which compared the conventional method of estimating risk from a mixed radiation field of low- and high-LET components with fluence- and event-related methodologies using risk cross section and a specific quality function. The result of the analysis where each of the approaches was applied to the same idealized shielding situation in space revealed that under the specified conditions the differences in the risk calculated by each method was less than a factor of two. In this NCRP Report it was concluded that when more fluence-based data become available and dosimetric techniques are refined, then the approach should be revisited. However, at this time, radiation risk estimates

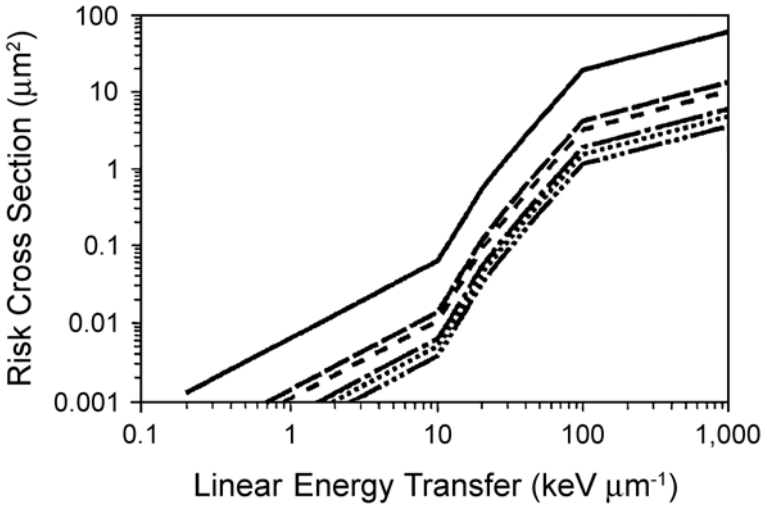

Fig. 6.10. The cancer risk cross sections for stomach (— — —), colon and lung (– – –), bone marrow (— - —), bladder and esophagus (— ••• —), breast (••••••), and total (———) as a function of LET (Curtis *et al*., 1995).

and radiation protection for work in space should continue to be based on the concepts of absorbed dose, quality factor, and dose equivalent (NCRP, 2001a). For these purposes, the organ dose equivalents should be estimated by averaging over the dose equivalents at representative points throughout each of the organs of interest and using $Q(L)$ defined by ICRU (1993) and NCRP (1993).

6.2.2.6 *Particle-Induced Skin Tumors*. Particle beam induction of rat skin tumors has been investigated (Burns and Albert, 1980; Burns *et al*., 1978; 1999; 2001; Heimbach *et al*., 1969). Figure 6.11 is a composite plot of the dose response for malignant and benign tumor induction at 1 y after exposure to ^{56}Fe, ^{20}Ne, or ^{40}Ar showing dose- and time-course differences in the yield depending on the particle. The effect of the 250 ppm dietary vitamin-A acetate on tumor induction was equivalent to lowering the ^{56}Fe LET effect to approximately that of neon ions. The antioxidant vitamins served as a countermeasure to the tumor induction, and this result is consistent with reports of vitamin mitigation of both UV- (Ayala and Soderberg, 2004) and ionizing radiation-induced cataract

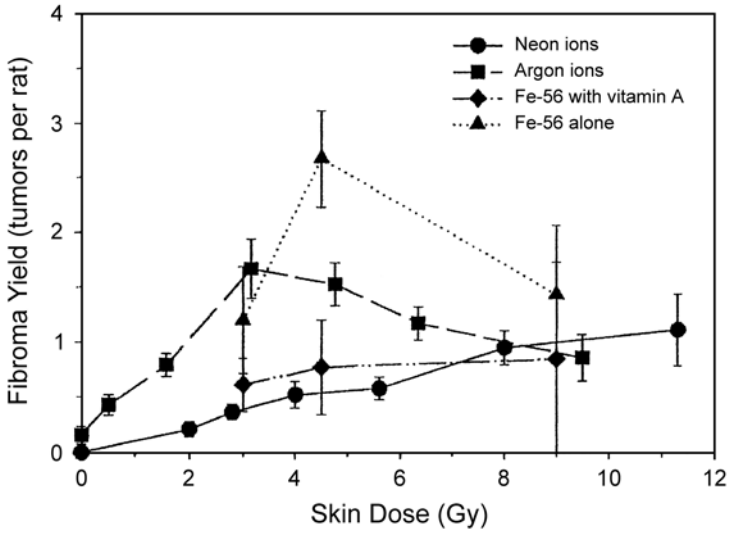

Fig. 6.11. Dose response for tumor induction for iron, argon and neon ions.[11]

[11]Burns, F.J. (2005). Personal communication (New York University School of Medicine, Tuxedo, New York).

(Karslioglu *et al*., 2004). The yield of skin fibromas as a function of time for a single 3 Gy fraction of ^{56}Fe ion radiation versus four fractions of the same radiation. and total absorbed dose delivered over a 10 d interval (a minimum of 2 d between fractions) has also shown that there are no significant differences in the single or fractionated dose regime.

6.2.2.7 *Particle-Induced Mammary Tumors*. The risk of mammary carcinomas in a Sprague-Dawley rat model irradiated whole-body with energetic iron ions, photons, or iron ions and photons at 60 d of age and followed to death in a series of three studies have been investigated by Dicello *et al*. (2004). The animals were continuously monitored for all disease and effects from the radiations and major tissues and tumors were archived. In the second part of the study reported separately, half of all animals were given Tamoxifen® (Bristol Myers Squibb Company, Princeton, New Jersey) to investigate the potential of this drug that is known to reduce the risk of mammary carcinomas. Figure 6.12 from the first study completed illustrates cumulative excess lifetime incidence of mammary tumors (both adenocarcinomas and benign fibro-adenomas) as a function of dose for photon-, proton- and iron-irradiated rats. The data suggest that iron ions are more efficient in inducing mammary tumors at lower doses in a nearly linear response up to 0.5 Gy with decreasing effects at higher doses, and reaching a maximum value nearly the same as that observed for animals irradiated with photons or protons. The curves for all three irradiated populations level at ~30 % excess incidence but in a different dose-dependent manner. Because of the high natural incidence of breast cancer in this animal model, the reduced slope of the data at higher doses for iron-irradiated animals is associated with the reduced population at risk and the increased risk of other lethal diseases was noted. Protons (250 MeV) were also apparently more effective than ^{60}Co-gamma rays.

6.2.2.8 *Cancer Countermeasures*. Kerwin and Seddon (2002) reported on eating in space from an astronaut's perspective. The goal of their work was to generate a diet that meets astronaut's nutrient requirements and satiates them. However, nutritional intervention is potentially a way to reduce some radiation risks, as well as the catabolic effects of prolonged inactivity and acute hypercortisolemia in microgravity (Paddon- Jones *et al*., 2005), and disruption of neurobehavioral functions (Rabin, 1982). Chemoprevention of cancers by antioxidant vitamins or Tamoxifen® has been

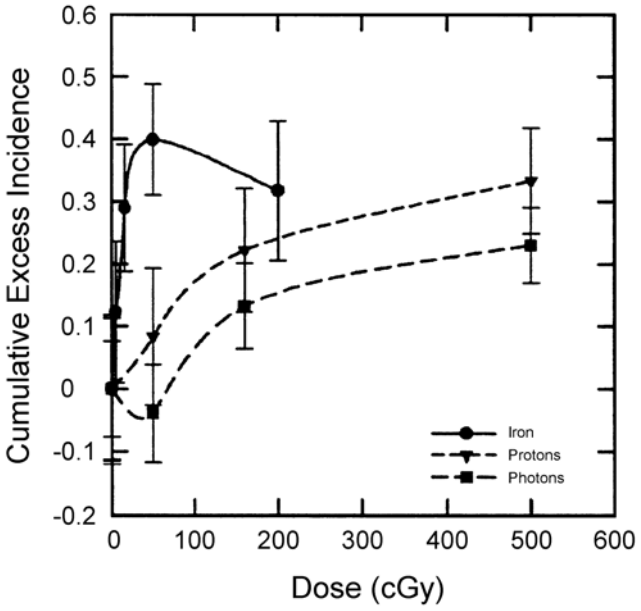

Fig. 6.12. Cumulative excess lifetime incidence of mammary tumors as a function of dose for photon-, proton- and iron-irradiated rats (Dicello *et al*., 2004).

mentioned above, but several other food or nutritional supplements have been shown to partially prevent the dose-dependent decrease in the serum or plasma levels of total antioxidants in animals exposed to alpha rays, protons, or HZE particles (Guan *et al*., 2004) and may affect cancer susceptibility (Weiss and Landauer, 2003). Some of those included in a review by Turner *et al*. (2002), include zinc (Leccia *et al*., 1999), selenomethionine (Kennedy *et al*., 2004), polyphenols (Parshad *et al*., 1998), thiols (Machlin and Bendich, 1987), fatty acids (Chang *et al*., 1998), yellow-green vegetables or fruits (Nagano *et al*., 2000), curcumin (Inano *et al*., 2000), restricted intake (Frame *et al*., 1998), or niacin-NAD (nicoinamide adenosine dinucleotide) (Gensler *et al*., 1999).

6.2.3 *Central and Peripheral Nervous System*

The possibility of radiation-induced effects on the CNS, especially by heavy ions is of concern. There are not sufficient data on the threshold doses for effects on the functions of the CNS despite a considerable number of relevant studies (Nelson and Tofilon, 2000), especially with regard to late radiation damage and its relationship to aging.

CNS consists of neurons differing markedly in size and number per unit area. There are several nuclei or centers that consist of closely packed neuron cell bodies (*e.g.*, the respiratory and cardiac centers in the floor of the fourth ventricle). In the cerebral cortex the large neuron cell bodies, such as Betz cells, are separated by a considerable distance. Of additional importance are the neuroglia, which are the supporting cells and consist of astrocytes, oligodendroglia, and microglia. These cells permeate and support the nervous tissue of the CNS, binding it together like a scaffold that also supports the vasculature. The most numerous of the neuroglia are Type I astrocytes, which make up about half the brain, greatly outnumbering the neurons. Neuroglia retain the capability of cell division in contrast to neurons and, therefore, the responses to radiation differ between the cell types. A third type of tissue in the brain is the vasculature which exhibits a comparable vulnerability for radiation damage to that found elsewhere in the body (Reinhold and Hopewell, 1980). Radiation-induced damage to oligodendrocytes and endothelial cells of the vasculature accounts for major aspects of the pathogenesis of brain damage that can occur after high doses of low-LET radiation.

6.2.3.1 *Low Linear Energy Transfer Radiation Effects on the Brain and Spinal Cord*. The CNS was previously considered a relatively radioresistant organ. The effects of high doses of low-LET radiation on the CNS are known reasonably well. The tolerance dose for early brain complications in adults usually does not develop if daily fractions of 2 Gy or less are administered with a total of up to 50 Gy, depending primarily on the volume irradiated, and secondarily on anatomical location in the human brain (Fabrikant *et al*., 1989; Kramer *et al*., 1972; Schultheiss *et al*., 1995). Neurocognitive effects are observed, however, at low doses (Schultheiss *et al*., 1995). Detailed information on the radiation tolerance of the human brain has been obtained from the localized use of protons and other charged particle beams for treatment of pituitary tumors (Kjellberg and Kliman, 1979; Linfoot, 1979), hormone-responsive metastatic mammary carcinoma (Tobias, 1979), brain tumors (Castro *et al*., 1985; Suit *et al*., 1982a), and intracranial arteriovenous malformations and other cerebrovascular diseases (Fabrikant *et al*., 1984; 1985; 1989; Kjellberg *et al*., 1983; Levy *et al*., 1989; Steinberg *et al*., 1990).

Mizumatsu *et al*. (2003) report extreme sensitivity of neurogenesis in adult mice to low doses of x rays. The pathogenesis of long-recognized radiation-induced cognitive injury is unknown, but may involve loss of neural precursor cells from the subgranular

zone (SGZ) of the hippocampal dentate gyrus and alterations in neurogenesis. Forty-eight hours after irradiation (2 to 10 Gy) proliferating neural precursor cells from the SGZ of the hippocampal dentate gyrus of the rat brain were reduced by 93 to 96 % and immature neurons were decreased by 40 to 60 % in a dose-dependent fashion (Figure 6.13). Not only is hippocampal neurogenesis ablated, but the remaining neural precursors adopt glial fates and transplants of nonirradiated rat neural precursor cells fail to differentiate into neurons in the irradiated hippocampus (Monje and Palmer, 2003). The inhibition of neurogenesis is accompanied by marked alterations in the neurogenic microenvironment, including disruption of the angiogenesis associated with adult neurogenesis and a marked increase in the number and activation status of microglia within the neurogenic zone. Cells in the dentate SGZ undergo dose-dependent apoptosis after low to moderate doses of x rays, and the production of new neurons in young adult male mice is reported to be significantly reduced by relatively low doses of x rays, with the change being dose dependent (Mizumatsu *et al*., 2003) (Figure 6.14). In contrast there were no apparent effects on the production of new astrocytes or oligodendrocytes. Measures of activated microglia indicated that changes in neurogenesis

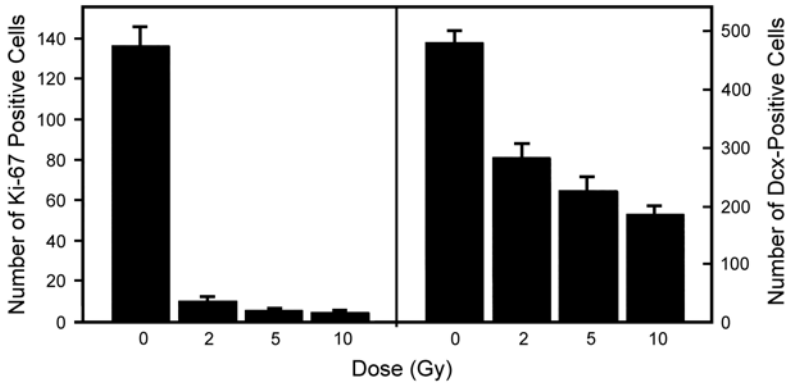

Fig. 6.13. Numbers of proliferating cells (left panel) and immature neurons (right panel) in the dentate SGZ are significantly decreased 48 h after irradiation. Antibodies against Ki-67 and Dcx were used to detect proliferating cells and immature neurons, respectively. Doses from 2 to 10 Gy significantly ($p < 0.05$) reduced the numbers of proliferating cells. Immature neurons were also reduced in a dose-dependent fashion ($p < 0.001$). Each bar represents an average of four animals; error bars, standard error (Mizumatsu *et al*., 2003).

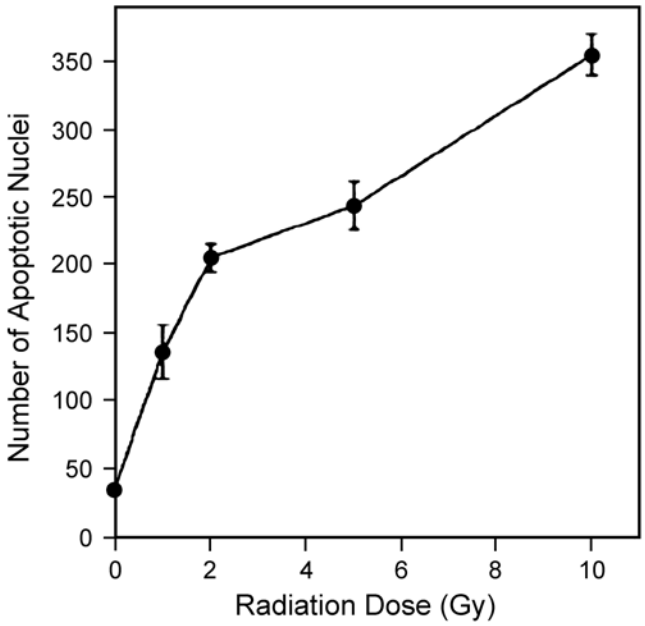

Fig. 6.14. Cells in the dentate SGZ undergo dose-dependent apoptosis after low to moderate doses of x rays. Apoptosis was quantified based on TUNEL (terminal deoxynucleotidyl transferase-mediated deoxyuridine triphosphate nick end labeling) labeling and morphological changes in irradiated cells in the SGZ regardless of cell type 12 h after irradiation. The steepest part of the response curve was dominated by loss of actively proliferating cells, whereas the shallower slope, >2 Gy, largely represented the response of immature neurons. Each datum point represents a mean of four to seven mice; error bars, standard error (Mizumatsu *et al*., 2003).

were associated with a significant dose-dependent inflammatory response even two months after irradiation. Countermeasures for these effects may involve replacement of the neural progenitor cell population, as well as drug-based manipulation of microenvironmental factors regulating microglial inflammation (Monje *et al*., 2003). Since there is a relationship emerging between hippocampal neurogenesis and associated memory formation, these studies suggest that precursor cell radiation response and altered neurogenesis may play a contributory if not causative role in radiation-induced cognitive impairment. Adult rat neural precursor cells from the hippocampus have demonstrated an acute dose-dependent apoptosis accompanied by an increase in reactive oxygen species (ROS) that persisted over a three to four week period (Limoli *et al*.,

2004). Relative ROS levels were increased at nearly all doses (1 to 10 Gy) of Bragg-peak 250 MeV protons at postirradiation times (6 to 24 h) compared to unirradiated controls (Giedzinski *et al*., 2005). The increase in ROS after proton irradiation was more rapid than that observed with x rays and showed a well-defined dose response at 6 and 24 h, increasing ~10 and 3 % Gy^{-1}, respectively. However, by 48 h postirradiation, ROS levels fell below controls and coincided with minor reductions in mitochondrial content. Use of the antioxidant alpha-lipoic acid (before or after irradiation) was shown to eliminate the radiation-induced rise in ROS levels. These results corroborate the earlier studies using x rays and provide further evidence that elevated ROS are integral to the radioresponse of neural precursor cells. Similar studies on the effects of space radiations on adult neurogenesis are needed. Studies of particle beam effects on *in vitro* neurogenesis are in progress and may also provide new information (Section 6.2.4.5).

6.2.3.2 *High Linear Energy Transfer Radiation Effects on the Spinal Cord and Brain*. Rat spinal cord radiation tolerance studies have also been completed with high doses of helium-, carbon-, neon-, and silicon ion beams (Leith *et al*., 1975a; 1975b; 1977; 1982a; Okada *et al*., 1998; Rodriguez *et al*., 1987; 1991); cellular changes, degeneration, paralysis and necrosis have been reported. Figure 6.15 illustrates the dose-effect response of the rat spinal cord to single and fractionated doses of helium ions, which show dose-sparing similar to other low-LET radiations. This implies that despite the sparseness of the fractionated data for the helium beams, there appears to be a reduced sparing effect with charged-particle radiation as the number of fractions was increased and the dose per fraction decreased (Rodriguez *et al*., 1991). This results in increased RBE values for the heavier charged particle beams (Table 6.1). A recent study using high-precision proton irradiation of relatively high doses to 20 mm sections of cord reported regional differences in radiosensitivity across the rat cervical spinal cord (Bijl *et al*., 2005). The results indicated, based on histology, that the lateral white matter is more radiosensitive than the central part of the white matter. The gray matter is highly resistant to radiation with no lesions observable in histology after 80 Gy.

Biochemical assessment of charged-particle radiation damage on rat spinal cord at 1 y after fractionated exposure to x rays, carbon and neon ions (Leith *et al*., 1982a) showed no correlation between the activity of alkaline phosphatase, an endothelial cell marker, and dose or radiation modality; activities of cyclic nucleotide phosphatase (CNP), and gamma-glutamyl transpeptidase

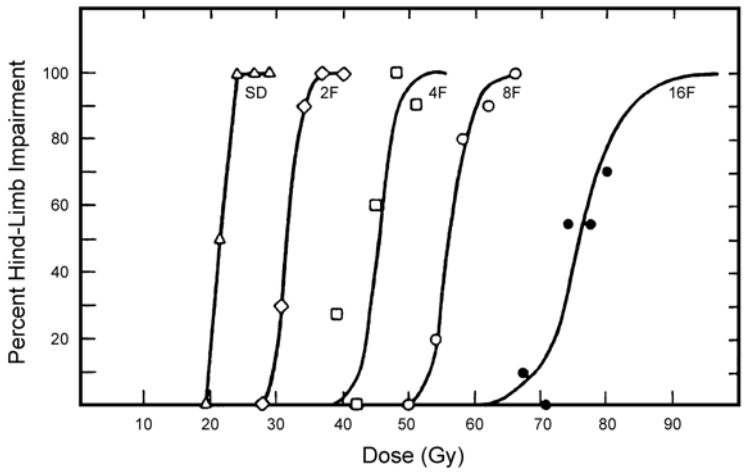

Fig. 6.15. Dose effect response of the rat spinal cord response to single (SD) and fractionated (F) doses of helium ions (Rodriguez *et al*., 1991).

(GGTP), however both showed a dose- and LET-dependence (CNP increased and GGTP decreased with dose). The GGTP data seemed to correlate to the ED_{50} data more closely than did the CNP data. The reduced GGTP data may reflect depletion of vascular endothelium, whereas increased CNP activity may reflect compensating increased myelin synthesis by oligodendrocytes (Rodriguez *et al*., 1991). Radiation damage by these enzyme endpoints could not be detected in the dose region below the threshold for paralysis.

Whereas the vasculature and the oligodendrocyte lineage have traditionally been considered the primary radiation targets in the CNS, recently it has been suggested that other phenotypes as well as critical cellular interactions may also be involved in determining the radioresponse of the CNS (Tofilon and Fike, 2000). These authors suggested that evidence is accumulating that in addition to acute cell death, radiation induces an intrinsic recovery/repair response in the form of specific cytokines and may initiate secondary reactive processes that result in the generation of persistent oxidative stress. These effects are discussed under Section 6.3.10.2.2

To address the hypothesis that the pathogenesis of heavy-ion particle radiations in space could impact the SGZ, a recent study irradiated female mice whole body with 1 GeV n^{-1} iron ion beams in a single dose of 0, 1, 2 or 3 Gy (Rola *et al*., 2004). Two months later mice were injected with bromodeoxyuridine (BrdU) to label proliferating cells. When the histology of the irradiated SGZ was

TABLE 6.1—*Summary of rat spinal cord response after charged particle irradiation (Rodriguez et al., 1991).*

Ion	Energy (MeV n^{-1})	Position	LET (keV μm^{-1})	Number of Fractions	ED_{50} (Gy)	RBE
Helium[a]	228	Plateau and distal peak	1.8	SD[b]	22.7 – 23.8	1.07
		Peak (4 cm)				
Helium[c]	228	Plateau	1.8	SD[b]	21.5	0.97
				2 FX	31.5	–
				4 FX	45	–
				8 FX	57	–
				16 FX	75.9	
Carbon[d]	400	Plateau	10	SD[b]	17.9	1.45
				4 FX	37.5	1.31
		Mid-peak (4 cm)	70	SD[b]	17.5	1.48
				4 FX	25.1	1.95
Neon[b]	670	Plateau	25	SD[b]	16.4	1.31
				4 FX	32.6	1.38
				8 FX	39.7	1.44
		Distal peak (4 cm)	150	SD[b]	15.2	1.41
				4 FX	23.1	1.95
				8 FX	<30.5	>1.95

Neon[d]	400	Plateau	35	SD[b]	17.5	1.46
				4 FX	27.2	1.80
		Mid-peak	130	SD[b]	13.8	1.86
				4 FX	22.5	2.18
Neon[d]	375	Plateau	33	SD[b]	17.8	1.30
Silicon[e]	670	Plateau	50	SD[b]	11.3	1.90

[a]Steinberg *et al*. (1990).
[b]SD = single dose; FX = fractions.
[c]Leith *et al.* (1982b).
[d]Leith *et al*. (1975a; 1981a).
[e]Rodriquez, A. Personal communication (Lawrence Berkeley Laboratory, University of California, Berkeley).

compared to the unirradiated controls, irradiated mice showed progressively fewer BrdU-positive cells as a function of dose. The progeny of the proliferating SGZ cells were visualized by doublecortin staining and were significantly reduced by irradiation. Histopathology indicated that the ^{56}Fe ions induced a chronic and diffuse astrocytosis and changes in pyramidal neurons in and around the hippocampal formation. This is the first evidence that high-LET radiation has deleterious effects on cells associated with hippocampal neurogenesis, and the work has been confirmed by Casadesus *et al*. (2005) who noted that these changes are consistent with those found in aged subjects, indicating that heavy-particle irradiation is a possible model for the study of aging.

This was followed up in 2005 with carbon ion studies (Rola *et al*., 2005). Mice were irradiated with 1 to 3 Gy of ^{12}C or ^{56}Fe ions and nine months later proliferating cells and immature neurons in the dentate SGZ were quantified. The results showed that reductions in these cells were dependent on the dose and LET. When compared with data for mice that were studied three months after ^{56}Fe-particle irradiation, the second study suggested that these changes are not only persistent but may worsen with time. Loss of precursor cells was also associated with altered neurogenesis and a robust inflammatory response. These results indicate that high-LET radiation has a significant and long-lasting effect on the neurogenic population in the hippocampus that involves cell loss and changes in the microenvironment.

6.2.3.3 *Radiation-Induced Neurocognitive Effects*. Radiotherapy applied to the CNS can cause neurological complications. These effects generally follow from extremely high doses below the threshold for necrosis, but also occasionally from relatively low doses (Goldberg *et al*., 1982; Keime-Guibert *et al*., 1998). There are three reports of loss of neurocognitive function in adulthood following brain irradiation of pediatric patients for tinea capitis (Ron et al., 1982; Yaar *et al*., 1982), or for cutaneous hemangioma (Hall *et al*., 2004). All three reports indicated that compared to unirradiated control subjects, low doses of ionizing radiation (25 to 130 cGy) to the brain in infancy or childhood influence cognitive abilities in adulthood assessed by a number of different indicators such as electroencephalogram tracings, scores on scholastic aptitude, intelligent quotients, psychologic tests, number of school grades completed or their risk for mental hospital admissions for certain disease categories. Over 11,000 irradiated children were studied in the largest study and they were compared to two nonirradiated tinea-free comparison groups that included either ethnic-,

sex- and age-matched individuals from the general population or siblings. While not all differences were statistically significant, there was a consistent trend for the irradiated subjects to exhibit signs of CNS impairment more often than either comparison group. Dementia has been reported following treatment of adult-brain tumors with radiotherapy administered alone or in combination with nitrosourea-based chemotherapy (Vigliani *et al*., 1999). In a retrospective clinical and pathological study of four patients who developed the syndrome of radiation-induced dementia, all patients were screened for a history of supratentorial irradiation, no evidence of symptomatic recurrent tumor, and no other cause of progressive cerebral dysfunction and dementia. The clinical picture after a course of cerebral conventional radiotherapy consisted of a progressive subcortical dementia occurring 3 to 12 months after a course of cerebral radiotherapy. Examination revealed early bilateral corticospinal tract involvement in all patients and dopa-resistant Parkinsonian syndrome in two. On computed tomography (CT) scan and magnetic resonance image (MRI) of the brain, the main features consisted of progressive enlargement of the ventricles associated with a diffuse hypodensity on CT, or a hyperintensity on MRI of the white matter best seen at T2-weighted images on MRI. The course was progressive over 8 to 48 months in three patients while one patient had stabilization of his condition for ~28 y. Treatment with corticosteroids or shunting did not produce sustained improvement and all patients eventually died. Pathological examination revealed diffuse white matter pallor with sparing of the arcuate fibers in all patients.

Despite a common pattern on gross examination, microscopic studies revealed a variety of lesions that took two basic forms: (1) a diffuse axonal and myelin loss in the white matter associated with tissue necrosis, particularly multiple small foci of necrosis disseminated in the white matter which appeared different from the usual radionecrosis; and (2) diffuse spongiosis of the white matter characterized by the presence of vacuoles that displaced the normally-stained myelin sheets and axons. Despite a rather stereotyped clinical and radiological course, the pathological substratum of radiation-induced dementia is not uniform. Whether the different types of white matter lesions represent the spectrum of a single pathological process or indicate that the pathogenesis of this syndrome is multifactorial with different target cells, remains to be seen (Vigliani *et al*., 1999).

In another study on 12 patients who developed delayed complications of whole-brain radiotherapy, that was given as sole treatment (four patients) or in combination with surgical resection

(eight patients) (De Angelis *et al*., 1989), it was reported that within 5 to 36 months (median, 14 months) all patients developed progressive dementia, ataxia, and urinary incontinence causing severe disability in all and leading to death in 7 of the 12. No patient had tumor recurrence when neurologic symptoms began. Cortical atrophy and hypodense white matter were identified by CT in all. Contrast-enhancing lesions were seen in three patients; two of the lesions yielded radionecrosis on biopsy. Autopsies on two patients revealed diffuse chronic edema of the hemispheric white matter in the absence of tumor recurrence. Corticosteroids and ventriculoperitoneal shunt offered significant but incomplete improvement in some patients. The total dose of whole-brain radiotherapy was 25 to 39 Gy, with daily fractions of 3 to 6 Gy being employed. It may be that these fractionation schedules, several of which are used commonly, predispose to delayed neurologic toxicity, and that more protracted schedules might lead to safer and efficacious treatment of good-risk patients with brain metastases. The incidence of whole-brain-induced dementia was only 1.9 % when radiotherapy was the sole treatment and was 5.1 % when given in combination with surgical resection.

6.2.3.4 *Radiation Effects on Retina*. An important unanswered question is whether neurons traversed by HZE particles and which survive, will develop changes as a late consequence of the damage they incurred. This question has been addressed using retinal photoreceptors, rods, as a surrogate for neurons in the CNS. There are several clinical reports of late retinal complications of conventional and proton radiation therapy for cancer therapy (Boozalis *et al*., 1987; Gordon *et al*.,1995; Takeda *et al*., 1999). The mechanisms responsible for late radiation effects to most tissues are unknown, but have long been thought to involve damage to the vessels, particularly to endothelial cells as a primary cause, since increased radiation dose to the optic nerve correlates with smaller numbers of endothelial cells (Levin *et al*., 2000). Retinal photoreceptor cell loss has also been reported (Cibis *et al*., 1955; Gragoudas *et al*., 1979), and the risk of neuropathy and maculopathy is reported to be enhanced among those with underlying vascular disorders (Gragoudas *et al*., 1999).

The retinas of primates exposed to ^{16}O ion beams have been examined by Bonney *et al*. (1974). Color photographs of the fundus and fluorescein angiograms were taken of the retinas prior to irradiation and up to five weeks postexposure. Animals were sacrificed at post-exposure intervals for histopathologic examination of the retinas. A series of animals were exposed to 200 kVp x rays and

examined on the same regime as the first series. The results indicate that ^{16}O ions had a higher quality factor than x rays, and a marked compression of the latency between exposure and onset of the retinal pathology. The early changes within the monkeys were retinal hemorrhages and altered capillary permeability, indicating that the oxygen nuclei irradiation, like other forms of irradiation, produces changes first in the retinal vasculature. At 5.5×10^7 particles cm^{-2}, and below, there was no evidence of changes in the angiograms. The histopathological evidence at 3.9×10^7 particles cm^{-2} indicates that some cellular alterations in the outer segments had occurred. A longer postexposure following of these animals might have revealed changes following a latent period. It would be useful to have these kinds of studies completed with ion beams of higher atomic number and at lower fluences, and to have longer follow-up data. Prompt visual observations of light flashes associated with exposure to radiations in space flight are described below in Section 6.3.4.

Lett *et al*. (1987; Williams and Lett, 1994; 1996) found changes in the DNA of retinal photoreceptor cells with time after irradiation. After exposure to low-LET radiation or HZE particles, the initial radiation-induced damage was repaired, but a subsequent breakdown of DNA occurred with age. Exposure to HZE particles resulted in secondary changes occurring at a younger age than after exposure to low-LET radiation. Loss of rods from rabbit retinas occurred with age but more markedly after exposure to irradiation, especially iron ions. Dose-response data are not available. This work should be repeated with more modern techniques and to include a dose response.

Mao *et al*. (2003) reported quantitative architectural and population changes in the rat retinal vasculature after high doses (8, 14, 20 or 28 Gy) of single or split doses of 100 MeV proton irradiation to the whole eye. Uniform progressive retinal growth was observed in the unirradiated, age-matched controls and in the retinas irradiated with 8 and 14 Gy, but not after 20 or 28 Gy, where there was a progressive time- and dose-dependent cell loss over 15 to 24 months.

While no reliable estimate of risk of important damage to the CNS from heavier charged particles can yet be given, there are enough data to indicate much more must be known before risk estimates of the effects of exposures in deep space can be made with any confidence. The accumulated evidence from the reported studies on DNA damage, loss of neurons, altered behavior, and motor function is sufficient to require a careful assessment of the total risk to the CNS from exposure to HZE particles.

6.2.4 *Behavioral Effects*

The study of behavioral effects due to exposure to low doses or low dose rates of radiation is complicated. The behavioral neurosciences literature is replete with examples of major differences in behavioral outcome depending on the animal species, strain or measurement method. For example, compared to unirradiated controls, x-irradiated mice show hippocampal-dependent spatial learning and memory impairments in the Barnes maze, but not the Morris water maze (Raber *et al*., 2004) which, however, can be used to demonstrate deficits in rats (Shukitt-Hale *et al*., 2000; 2003). Particle radiation studies of behavior have been accomplished with rats and mice, but with some differences in the outcome depending on the endpoint measured.

One human study of behavioral effects compared subclinical mental disorders with psychiatric and psychometric evaluations following either low doses of x rays (n = 109) or chemotherapy (n = 68) to patients treated 10 to 29 y earlier for tinea capitis (Omran *et al*., 1978), controlling for educational level and family psychiatric disorders. Despite the fact that the irradiated group manifested more psychiatric symptoms, had more deviant Minnesota Multiphasic Personality Inventory scores, were also judged more maladjusted from their profiles, and more frequently had a history of treated psychiatric disorders, the psychiatrist's overall rating of current psychiatric status showed only a borderline difference between the two groups among Caucasians and no differences among African-Americans.

6.2.4.1 *Iron Ion-Induced Sensorimotor Deficits*. Behavioral and brain neurochemical changes induced by exposure to ^{56}Fe (100 mGy, 600 MeV) resemble those associated with the aging process (Joseph *et al*., 1992; 1993). Low doses of ^{56}Fe ions in the 0.1 to 1 Gy range reduce performance as tested by the wire suspension test. This test, which assesses the time a rodent will or can hang on to a wire, is considered a measure of motor function. Enhancement of the K^+-evoked release of dopamine was significantly reduced in all irradiated groups, and paralleled the deficits observed in the wire suspension test. Deficits in nerve signal transduction involve alterations in the coupling/uncoupling of the ligand-receptor-G protein interface on the membrane surface which degrades its participation as part of the second messenger pathway (Joseph *et al*., 1994). It is important to point out that oxidative damage may be the common mechanism relating radiation effects to the aging process. Behavioral deficits are observed as early as 3 d after radiation exposure

and the neurochemical alterations (decreased dopamine release) are still found at 80 d post-exposure (Hunt *et al*., 1990). In contrast to the particle-induced deficits reported with rats on sensorimotor skills, tests of C57BL/6 mice whole-body irradiated with 0, 0.1, 0.5, or 2 Gy iron ions (1 GeV n^{-1}) and evaluated with open-field (a 20×40 cm plastic shoebox cage, with LED photosensors to detect activity), rotorad (rotating, textured nylon rod suspended 45 cm above a foam floor), or acoustic startle (a chamber with a constant white noise background with intermittent bursts of 120 dB sound) showed few significant effects during a two to eight week period immediately after radiation exposures (Pecaut *et al*., 2004). Mickley *et al*. (1988) compared behavioral performance of rats exposed to either electrons, bremsstrahlung, gamma rays, or fast neutrons and found that complex and physically demanding tasks are some of the most radiosensitive behavioral tasks. They also found that classic radioprotectant compounds (*e.g*., WR-2721)[12] proved effective as far as reducing the lethal effects of radiation, but unfortunately, most also potentiated the radiation's behavioral toxicity. In contrast, antihistamines under certain circumstances had the ability to reverse the radiation-induced performance deficits.

Exposure to ^{56}Fe particles may produce effects beyond that attributable to its LET (Hunt *et al*., 1989; Rabin *et al*., 1989). Learning that involves the dopaminergic nervous system [*e.g*., conditioned taste aversion (CTA)] was disrupted by exposure to iron while exposure to equal or higher doses of other types of radiation (*e.g*., gamma or neutrons) do not show a similar effect (Rabin *et al*., 1991). Subsequent work indicated that there was a high degree of specificity in the effects of the ^{56}Fe particles. Decrements were observed in muscarinic-stimulated low-K_m GTPase in striatum, but not in hippocampus, and ^{56}Fe particle irradiation did not affect a_1-adrenergic-stimulated low-K_m GTPase activity in brain tissue (Villalobos-Molina *et al*., 1994). Iron particles were also found to be potent modulators of thermoregulation (Kandasamy *et al*., 1994).

6.2.4.2 *Behavioral Deficits in Conditioned Taste Aversion Due to Particle Exposures*. It has been known for some time that changes in behavior of rodents could be detected after low doses of heavy ions (Hunt *et al*., 1989; Rabin *et al*., 1989; 1991; 1994; 2000). It has been found that low doses of ^{56}Fe ions can induce changes in dopaminergic function and that this, in turn, may alter a number of dopamine-mediated behaviors as discussed above, but also affect

[12]From the U.S. Army's drug development program (Walter Reed Army Medical Center, Washington).

CTA. The CTA test assesses the avoidance of normally acceptable food as a result of exposure to some toxic agent such as radiation (Riley and Tuck, 1985). The role of the dopaminergic system in radiation-induced changes in CTA is suggested by the fact that amphetamine-induced CTA, which depends on the dopaminergic system, is affected by radiation, whereas lithium chloride-induced CTA that does not involve the dopaminergic system is not affected by radiation. Rabin *et al*. (1989; 1991) have established that the degree of CTA due to radiation is LET-dependent (Figure 6.16) and that ^{56}Fe ions are the most effective of the various low- and high-LET radiations that have been tested. Doses of ~0.2 Gy of ^{56}Fe ions appear to have an effect on CTA.

6.2.4.3 *Iron Ion Effects on Operant Conditioning Task*. Recent studies by Rabin and colleagues (Rabin *et al*., 2003a) have examined the ability of rats to perform an operant order to obtain food reinforcement. Once the response was learned, the rats were placed on an ascending fixed-ratio (FR) schedule from FR-1 (every lever press is rewarded with a food pellet) through FR-35 (35 lever presses are required to produce one food pellet). In general, as the ratio increased, the rats increased their rate of responding. The rats exposed to 4 Gy of protons or 1 Gy of l GeV n^{-1} ^{56}Fe particles

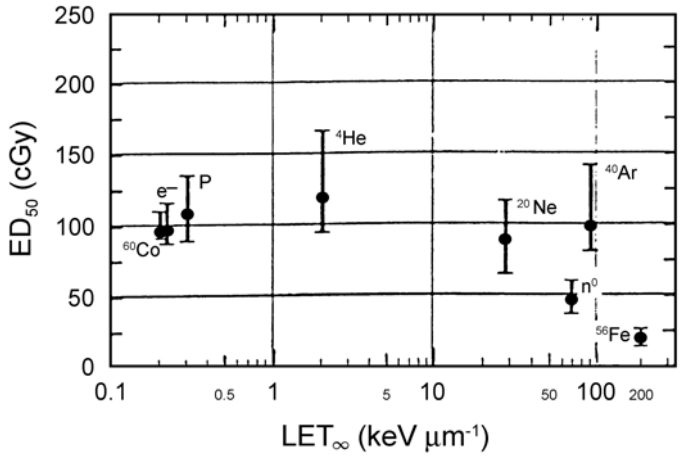

Fig. 6.16. ED_{50} for CTA as a function of LET for the following radiation sources: ^{40}Ar = argon ions, ^{60}Co = cobalt-60 gamma rays, e^- = electrons, ^{56}Fe = iron ions, ^{4}He = helium ions, n^0 = neutrons, ^{20}Ne = neon ions (Rabin *et al*., 1991).

responded similarly to controls, increasing their rate of responding as the ratio increased. However, rats exposed to 2 Gy of ^{56}Fe particles failed to increase their rate of responding at ratios greater than FR-20. These results indicated that rats exposed to 2 Gy of ^{56}Fe particles cannot respond appropriately to increasing work requirements. Additional experiments are necessary to determine the factors responsible for this deficit. A follow-up report by Rabin *et al*. (2005) indicated irradiation with 2 Gy ^{56}Fe particles produces a disruption of operant response in rats tested five and eight months after exposure, but maintaining the rats on a diet containing strawberry, but not blueberry, extract can prevent the disruption. When tested 13 and 18 months after irradiation, there were no differences in performance between the irradiated rats maintained on control, strawberry or blueberry diets. These observations suggest that the beneficial effects of antioxidant diets may be age dependent.

6.2.4.4 *Iron Ion Effects on Spatial Learning and Memory.* Investigations of the effects of exposure to ^{56}Fe particle irradiation on spatial learning and memory behavior and neuronal signaling have been performed in an attempt to determine the mechanisms involved in these deficits. Shukitt-Hale *et al*. (2000) used the Morris water maze one month after whole-body irradiation with 1.5 Gy of 1 GeV n^{-1} ^{56}Fe ions. Irradiated rats demonstrated cognitive impairment compared to the control group as seen in their increased latencies to find the hidden platform, particularly on the reversal day when the platform was moved to the opposite quadrant. The irradiated group used nonspatial strategies during the probe trials (swim with no platform) (*i.e*., less time spent in the platform quadrant, fewer crossings of and less time spent in the previous platform location, and longer latencies to the previous platform location). These findings are similar to those seen in aged rats, suggesting that an increased release of ROS may be responsible for the induction of radiation- and age-related cognitive deficits.

Denisova *et al*. (2002) exposed rats to 1.5 Gy of 1 GeV n^{-1} ^{56}Fe ions and tested their spatial memory in an eight-arm radial maze. Radiation exposure impaired the rats' cognitive behavior, since they committed more errors than control rats in the radial maze and were unable to adopt a spatial strategy to solve the maze. To determine whether these findings related to brain-region-specific alterations in sensitivity to oxidative stress, inflammation or neuronal plasticity, three regions of the brain, the striatum, hippocampus and frontal cortex that are linked to behavior, were isolated and compared to controls. Those that were irradiated were

adversely affected as reflected through the levels of dichlorofluorescein, heat shock, and synaptic proteins (*e.g.*, synaptobrevin and synaptophysin). Changes in these factors consequently altered cellular signaling (*e.g.*, calcium-dependent protein kinase C) and protein kinase A. These changes in brain responses significantly correlated with working memory errors in the radial maze. The results show differential brain-region-specific sensitivity induced by ^{56}Fe irradiation (Figure 6.17). These findings are similar to those seen in aged rats, suggesting that increased oxidative stress and inflammation may be responsible for the induction of both radiation and age-related cognitive deficits. These experiments warrant further evaluation of the behavioral and neurochemical effects of high-LET particles, as well as the exploration of potential nutritional modification (*e.g.*, antioxidants or anti-inflammatories) to offset the deleterious effects of heavy particles in space. Rabin *et al*. (2002) studied rats maintained on diets containing either 2 % blueberry or strawberry extract or a control diet for eight weeks prior to being exposed to 1.5 Gy of ^{56}Fe ions. Three days following irradiation, the rats were tested for the effects of irradiation on the

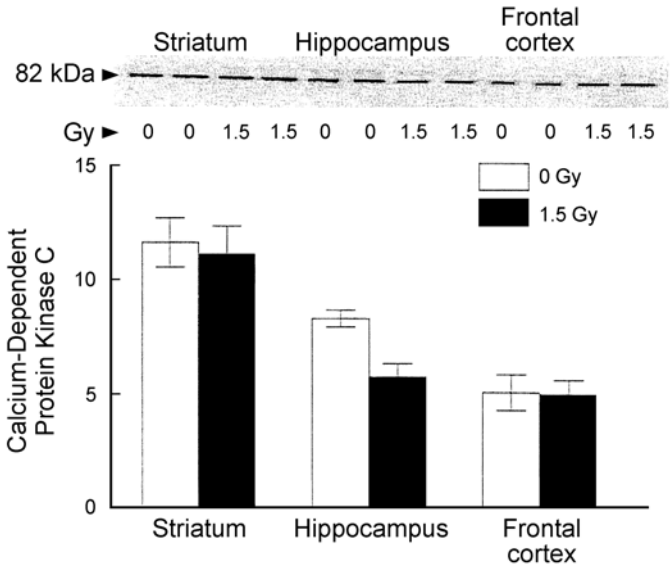

Fig. 6.17. Brain-region-specific calcium-dependent protein kinase C (α, β, γ) expression was assessed in control and irradiated rats using a standard Western immunoblotting procedure. Values are means ± SEM (Denisova *et al*., 2002).

acquisition of an amphetamine- or lithium-chloride-induced CTA. The rats maintained on the control diet failed to show the acquisition of a CTA following an injection of amphetamine. In contrast, the rats maintained on antioxidant diets (strawberry or blueberry extract) continued to show the development of an amphetamine-induced CTA following exposure to ^{56}Fe ions. Neither irradiation nor diet had an effect on the acquisition of a lithium chloride-induced conditioned taste aversion. The results are interpreted as indicating that oxidative stress following exposure to ^{56}Fe ions may be responsible for the disruption of the dopamine-mediated amphetamine-induced CTA in rats fed control diets, and that a reduction in oxidative stress produced by the antioxidant diets functions to reinstate the dopamine-mediated controlled taste aversion. A recent extension of this work with testing 12 months after exposure has been published (Rabin *et al*., 2005). The results indicated that the performance of the irradiated animals given blueberry extract did not differ from the irradiated animals fed the control diet, however both groups performed significantly poorer than the nonirradiated controls. There were no differences between the nonirradiated animals fed the control diet and the irradiated animals fed the strawberry diet, and their performance was significantly better compared to the irradiated rats fed the blueberry diet. The results indicate that diets containing strawberry extract provide significant radioprotection.

6.2.4.5 *Particle Effects on Nerve Cells In Vitro*. The effects of particle irradiation on retinal explants (Vazquez and Kirk, 2000) and primary cultures of mouse (Nojima *et al*., 2000) and rat brain cells *in vitro* (Mamoon, 1970) have been investigated in order to contribute further to understanding of fundamental mechanisms. Vazquez and Kirk (2000) exposed retinal explants from chick embryos to determine the dose response relationships for neurite outgrowth with morphometric techniques. Iron particles produced a dose-dependent reduction of the neurite outgrowth with a maximal effect at a dose of 1 Gy (Figure 6.18). Doses of 100 to 500 mGy induced reductions of the neurite outgrowth as compared to the control group. Neurite generation is a more sensitive parameter than neurite elongation, suggesting a different mechanism of radiation damage in the model. These results show that low doses or fluences of iron particles can impair retinal ganglion cells' capacity to generate neurites indicating the high neurotoxicity of iron ions. Nojima *et al*. (2000) irradiated primary mixed cultures of astrocytes and microglia from neonatal mice with high-energy carbon ions. Immunohistochemical staining showed that there was a

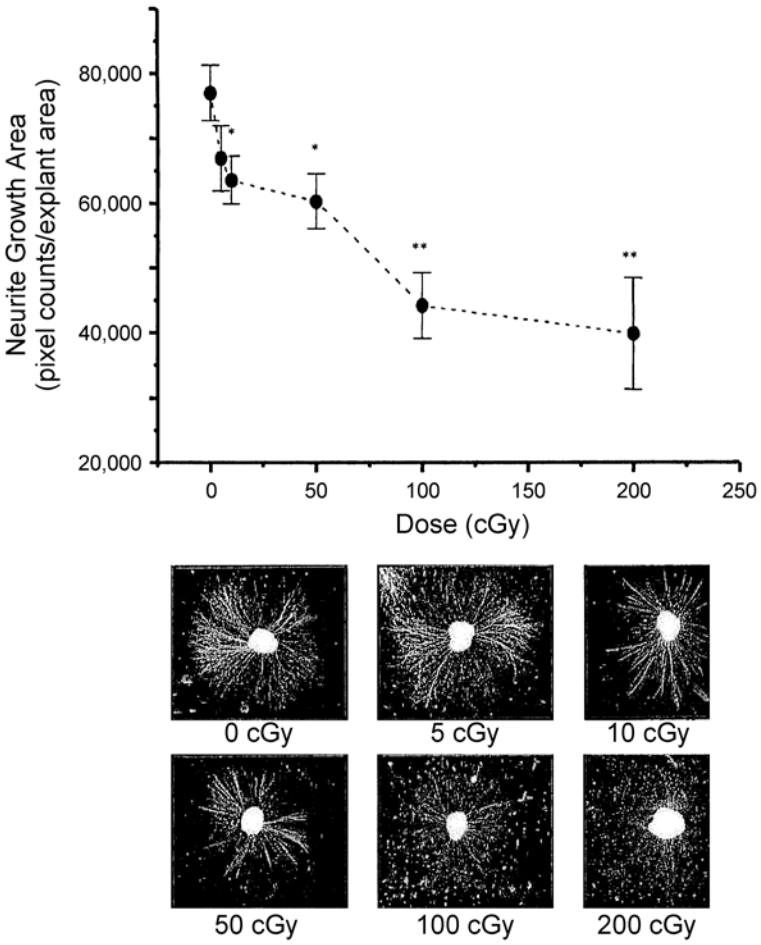

Fig. 6.18. *In vitro* dose-dependent neurotoxic effects of ^{56}Fe ions on retinal explants (adapted from Vazquez and Kirk, 2000).[13]

greater survival of astrocytes than microglia. Tagged with specific antibodies, astrocytes and microglia surviving after irradiation were counted by flow cytometry. Decreases in the number of microglia and astrocytes were detected at a dose of 2 Gy when day five cultures were irradiated with 13 keV μm^{-1} carbon ions. When the cultures were irradiated on day 10, the dose-dependent decrease of microglia was more prominent for 13 keV μm^{-1} compared to

[13]Vazquez, M.E. and Kirk, E. Personal communication (Brookhaven National Laboratory, Upton, New York).

70 keV μm^{-1} carbon ions. Astrocytes showed a marginal decrease at days 10 and 14. It appears that embryonic microglia are more sensitive than astrocytes to carbon ions and x rays, and that the radiosensitivity of microglia depends on both differentiation or proliferation status and radiation quality. The earlier histological studies of Kraft *et al*. (1979) examined pocket mice irradiated in the head region with 10, 1 or 0.1 Gy of Bragg-peak 400 MeV n^{-1} neon ions and observed that neuroglia cells suffered acute necrotic damage within a day of radiation exposure at doses of 10 and 1 Gy, but not at 0.1 Gy. These necrotic cells were noted to persist at reduced numbers by 3.5 d after the 0.1 Gy exposure, but were not noted 6 to 201 d after that dose.

To investigate effects of low dose heavy particle radiation on the CNS, mouse neonatal brain cells in culture were exposed to various heavy ions (Nojima *et al*., 2004). Doses varied from 0.05 Gy up to 2 Gy. The subsequent biological effects were evaluated by an induction of apoptosis and neuron survival focusing on comparing several animal strains, SCID, B6, B6C3F1, C3H, used for the brain cell culture. SCID was the most sensitive and C3H the least sensitive to particle radiation as evaluated by a 10 % apoptotic criterion. The LET dependency of SCID and B6 cells was compared by exposing them to different ions (hydrogen, carbon, neon, silicon, argon, and iron). No detectable LET dependency was observed in the high-LET (55 to 200 keV μm^{-1}) and low dose (<0.5 Gy) regions, however the survivability profiles of the neurons were different in the mouse strains for each ion.

Mamoon (1970) incubated small explants of neonatal rat cerebellum and midbrain embedded in plasma clots as a model of myelination response to radiation. Freshly dissected explants were irradiated with x rays (145 kV), deuteron (30 MeV), or helium ions (36 and 54 MeV) and examined at 15 d for evidence of myelin formation. At optimal growth conditions, 90 % of control explants had abundant myelination by this time. All the radiation types produced observable effects at 4 Gy and inhibition at 40 Gy. The ED_{50} for all the experiments was 17.27 ± 1.15 Gy with no statistically significant variation between different types of radiation.

The induction of apoptosis, TP53 expression, caspase activation and cell toxicity have been investigated after exposure of cells of the human neuronal progenitor cell line Ntera2 to low-LET radiation (gamma and x rays) (Guida *et al*., 2005). The data indicated that irradiation of Ntera2 cells quickly induced TP53 expression, followed in time by an increase in caspase activity, and ultimately resulted in the induction of apoptosis. Induction of apoptosis was dependent on dose, and the highest levels were measured 48 h after

exposure. For comparison, the level of apoptosis induced by high-LET particle radiation (1 GeV n^{-1} iron ions) was also determined and was found to be dependent on dose. RBE was estimated from the slopes of the dose-response curves for the induction of apoptosis. The RBE_{max} for apoptosis 48 h after exposure was at least 3.4. In short, exposure to high-LET radiation results in a more efficient and greater induction of apoptosis in human neuronal progenitor cells than low-LET radiation.

Radiation studies of the tolerance of rodent brains to particle beams have been examined by Manley (1988), Richards and Budinger (1988), and Rosander *et al*. (1987) who investigated the cellular response and cell population kinetics of the subependymal layer in the mouse with partial brain exposures of a single cortex to helium or neon ions. Both the irradiated and the unirradiated contralateral cortex showed similar disturbances of the cell and tissue kinetics in the subependymal layers. The irradiated hemisphere exhibited histological damage, whereas the unirradiated side appeared normal histologically. The decrease in labeling indices one week after exposure was dose- and ion-dependent. Analysis of cell kinetics one week after 10 Gy helium or neon suggests the presence of a progenitor subpopulation that is proliferating with a shorter cell-cycle time than normal. Comparison of the responses to the different charged particle beams indicates that neon ions are more effective in producing direct cellular damage than the helium ions, but the surviving proliferating cells several divisions later continue to maintain active cell renewal. *In vivo* surface coil proton magnetic resonance spectroscopy demonstrated changes in lipid and phosphatidylcholine peaks, and histology with Evans blue injections revealed blood-brain barrier alterations as early as 4 d after a high dose of 50 Gy. Using NMR imaging and spectroscopy, Richards and Budinger (1988) found that at 4 to 14 d post *in vivo* helium hemi-brain irradiation with 10, 20, 30 or 50 Gy, signal intensity and T1 relaxation time decreased on the irradiated side and increased on the nonirradiated side relative to nonirradiated control animals.

6.2.4.6 *Late-Appearing Brain Effects in Animals Irradiated with Particle Beams*. An early comparison was made of radiation necrosis and edema in canines, hemi-brain irradiated with either 225 MeV n^{-1} helium or 456 MeV n^{-1} neon ions using positron emission tomography (PET) and MRI (Brennan *et al*., 1993). The data reported are of interest, although the small number of animals and high doses (not relevant to spaceflight scenarios) limit the usefulness for extrapolation to humans. All of the dogs receiving 7.5 to

11 Gy of neon ions showed no signs of radiation injury up to 3 y after irradiation. Dogs receiving ≥13 Gy neon or helium ions succumbed to radiation necrosis and died 21 to 32 weeks after irradiation. The findings of imaging studies for all dogs that succumbed to radiation necrosis were normal until three to six weeks before death. The earliest CNS changes were seen as decreased metabolic activity in the cortex of the irradiated hemisphere with PET imaging or an increase in signal intensity in the periventricular white matter which are measures of the changes in the white matter. Changes in the white matter were consistently greater than those in the gray matter. The PET and MRI imaging and histopathological evidence indicated that both cellular and vascular mechanisms were involved in the radiation necrosis observed. MRI studies were also reported by Karger *et al*. (2002a; 2002b) in normal rat brain irradiated with carbon ions where similar results were found.

The understanding of late effects of particle irradiation of the adult brain has also recently been advanced by the publication of dose responses for late functional changes in the normal rat brain after single carbon ion Bragg-peak doses between 15.2 and 29.2 Gy evaluated by MRI (Karger *et al*., 2002b). Dose-response curves for late changes in the normal brain were measured using T1- and T2-weighted MRI. Tolerance doses were calculated at several effect probability levels and times after irradiation. The work was compared to earlier studies involving stereotactic irradiation of the right frontal lobe of rats using a linear accelerator and single doses between 26 and 50 Gy (Karger *et al*., 2002a). These doses are significantly higher than would occur during space travel, however no data are available at lower doses. The results of the carbon studies showed MRI changes were progressive in time up to 17 months and remained stationary after that time. At 20 months the tolerance doses at the 50 % effect probability level were 20.3 ± 2 and 22.6 ± 2 Gy for changes in T1- and T2-weighted images, respectively. RBE was calculated based on a previous animal study with photons. Using tolerance doses at the 50 % effect probability level, RBE values of 1.95 ± 0.20 and 1.88 ± 0.18 Gy were obtained for the T1- and T2-weighted MRI. A comparison with data in the literature for the spinal cord yielded good agreement, indicating that the RBE values for single-dose irradiations of the brain and the spinal cord are the same within the experimental uncertainty. However, it is not possible to extrapolate the effects observed to the much smaller particle doses expected in space in order to estimate risk. Unlike the clinical situation, most traversals of human brain tissue by heavy ions in space travel are expected to be composed of a distribution of different particle types, to be at low fluences, and to

involve very much smaller irradiated brain volumes. Further work is necessary to expand ongoing investigations of clinically-relevant effects from low fluences of the space radiation environment.

6.2.5 *Cardiovascular Disease*

6.2.5.1 *Radiation-Induced Vascular Changes*. Based on the experience of the atomic-bomb survivors' cohort it has become increasingly evident that this radiation-exposed population is susceptible, in addition to cancer, to chronic multifactorial diseases including coronary heart disease, essential hypertension and diabetes mellitus (Sankaranarayanan *et al*., 1999). These pathological effects can lead to noncancer mortalities (Kodama *et al*., 1996; Preston *et al*., 2003; Shimizu *et al*., 1999; Wong *et al*., 1999), and at radiation doses below those directly causing increased mortality, simply a reduced quality of life.

Vascular damage due to radiation exposure has been previously reported. Yang and Tobias (1984) irradiated 1 d old neonatal rats in the head region alone with either x rays or heavy ions to doses ranging from 0.5 to 8 Gy. Distinct petechial hemorrhages indicating vascular damage developed in the cerebral cortex within a few hours after irradiation, reached a maximum ~13 to 24 h, and decreased exponentially with time. No brain hemorrhage was found in neonatal rats 12 d after irradiation. These results indicated that a dose of a few gray of x rays can induce a significant number of hemorrhages in the young brain, and the number of lesions increased exponentially with dose. Heavy ions induced more hemorrhages than x rays for a given dose, and RBE for 670 MeV n^{-1} neon particles ranged from about two for low doses to about 1.4 for high doses. Histological examination of the hemorrhages revealed that a large number of red blood cells leaked from the blood vessels, indicating that the radiation-induced hemorrhages may be a result of some capillary membrane damages or reproductive death of blood vessel endothelial cells. The rapid onset of hemorrhage after irradiation suggests that membrane damage may be involved. Effects of negative pi mesons on vascular permeability of brain vessels in neonatal rats had previously been reported (Landolt *et al*., 1979). Dose-response relationships were developed for effects on vascular permeability in neonatal rats. The brains were removed and fixed in formalin 24 h after irradiation, and scored from zero to five by number and size of petechial hemorrhage. RBE was found to be 1.1 for peak and 0.6 for plateau negative pi mesons (peak to plateau ratio of 1.8 compared with 200 kV x rays). Interestingly, Yang and Tobias (1984) found that hesperetin, a compound of vitamin P, may reduce the formation of

brain hemorrhages in x-ray-irradiated rats. Neonatal rats that received a subcutaneous injection of 10 mg hesperetin (dissolved in propylene glycol) ~20 to 30 min before x-ray irradiation showed fewer hemorrhages in the brain than those rats that were only irradiated. Control animals receiving the same volume of propylene solution that was injected into rats but were not treated with hesperetin did not show the protection. Late effects of heavy charged particles or neutrons on the fine structure of the mouse coronary artery have been evaluated by Yang and Ainsworth (1982) and Yang *et al*. (1978), and revealed significantly altered tissue morphologies and damage compared to low-LET radiations. A single dose of only 0.2 Gy of ^{20}Ne ions produced significant damage to the smooth muscle cells in the coronary arteries. The major changes included medial smooth muscle degeneration, fibrosis, accumulation of debris, and extracellular matrix.

The development of late somatic lesions in most normal tissues of irradiated mammals has been suggested to be a result of vascular damage, although the true importance of vascular versus parenchymal cell changes is still not well understood (Hopewell, 1980). The heart muscle itself is very radioresistant, with anatomical changes not observed <100 Gy. In contrast, the capillaries have been found to be very sensitive to radiation with increased capillary permeability in human skin noted after 1 Gy (Neumayr and Thurnher, 1952).

Since 1899 radiation injury to blood vessels was recognized as one of the most common effects of therapeutic radiation on normal human tissues (Fajardo and Berthrong, 1988). Alterations in capillaries and arterioles are pathologic hallmarks of delayed damage in many mammalian tissues, primarily thought to be due to ischemia resulting from microvascular damage. The narrowest (and most prevalent element) of the vasculature is the most radiosensitive due to endothelial radiosensitivity and the fact that endothelial cells constitute the major component of the walls of the smallest vessels.

Vascular effects have also been evaluated at lower particle fluences. Dimitrievich *et al*. (1984) and Griem (1989; Griem *et al*., 1994) developed a tandem scanning confocal microscope to image the capillary network and the surrounding collagen architecture in the papillary dermis of the rabbit ear *in vivo* after exposure to single x-ray doses of 0.5 to 4 Gy. Serial observations of the micro-vasculature volume and vascular width have been digitally analyzed over a several week period after exposure. The 0.5 Gy dose shows transient increases in the width of the response that reach a maximum at 20 d postexposure, and persist out to 50 d. At 4 Gy the vessel width shrinks by 2 d after exposure. Particle beam effects on this endpoint are unknown.

6.2.5.2 *Radiation-Induced Atherosclerotic Effects*. Atherosclerosis is a multistep process involving injury to the endothelial lining of the arteries, infiltration of arterial intima with plasma lipoproteins, migration of smooth muscle cells from the media into the intima, proliferation of smooth muscle cells, and synthesis of connective tissue components. Monocytes in the peripheral blood become fat-filled foam cells through the uptake of low-density lipoproteins (LDL), and high LDL cholesterol is an important risk factor. Radiation-induced coronary disease in humans results in luminal narrowing (Stewart *et al*., 1995; Virmani *et al*., 1999). The morphological changes are different from typical atherosclerosis with more frequent medial destruction and greater adventitial fibrosis and thickening produced postradiation. These pathological findings are similar to the late radiation-induced tissue changes such as areas of necrosis, foam cell deposition, adventitial thickening and medial thinning and calcification, which were only observed in porcine arteries with a stent coated with a radionuclide.

Ionizing radiation is reported to accelerate aortic lesion formation in fat-fed mice *via* superoxide dismutase-inhibitable processes (Tribble *et al*., 1999) in a dose-dependent manner (Figure 6.19). The atherogenic effects of radiation appear to be particularly pronounced when the high-fat diet was introduced within 7 d after exposure to radiation. The mean lesion area was the same as that in the control, nonirradiated, high-fat-fed group if the high-fat diet was introduced 14 d after exposure. The primary mechanisms by which radiation promotes atherosclerosis have not been identified, but based on the premise that atherogenic effects of radiation may involve ROS-mediated promotion of lipoprotein oxidation and vascular inflammation, Tribble *et al*. (1999) demonstrated that overexpression of the anti-oxidant enzyme copper-zinc superoxide dismutase reduced radiation-induced atherosclerotic lesions, and aortic oxygen concentrations. Tribble *et al*. (2000) found evidence that ionizing radiation promotes changes in the artery wall that enhance the deposition of lipoprotein lipids. Using a trapped ligand methodology, they showed that LDL is degraded more readily in the irradiated aorta and that the enhanced degradation is affected by antioxidants, including alpha-tocopherol. These results show that LDL degradation products accumulate in the irradiated aorta, but the effect is inhibited by antioxidants which reduce the potential for LDL oxidation. The radiation used for these studies was ^{60}Co gamma rays at doses 2, 4 or 8 Gy. No data are available at lower photon doses, or for protons or HZE particles. Additional research is needed on the late radiation effects of low doses of radiation types prevalent in space on the pathophysiology of coronary

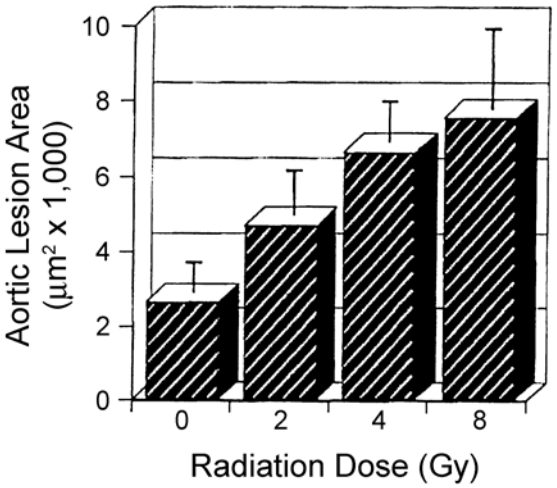

Fig. 6.19. Dose-dependent effects of ionizing radiation on aortic lesion formation in fat-fed mice (repeated-measures analysis of variance: $p = 0.02$) (Tribble *et al*., 1999).

artery disease, and the potential inhibition of these effects by antioxidants and low-fat diets.

Radiation induces several types of damage to the cardiovascular system (Basavaraju and Easterly, 2002). X rays induced changes in gene expression and distribution of atrial natiuretic peptide (ANP) in different anatomical regions of the heart after acute high doses (15 or 20 Gy) (Kruse *et al*., 2002). The ANP peptide is associated with a variety of morphological changes in the atria and venticles, eventually leading to impairment of cardiac function.

Circulating levels of ANP in the plasma may provide indications of early cardiac changes. No data exist on the effects of exposure to radiations in space on ANP plasma levels.

6.2.5.3 *Cardiovascular Disease in Radiotherapy Patients and Radiation Workers*. Several groups of radiation-exposed human populations have shown evidence of increased cardiovascular disease (CVD) after relatively high doses (5 to 50 Gy) of low-LET radiations, including radiotherapy patients with breast cancer (Seddon *et al*., 2002), head and neck cancer (Cheng *et al*., 1999; McGuirt *et al*., 1992), Hodgkin's disease (Thomson and Wallace, 2002), and testicular cancer (van den Belt-Dusebout *et al*., 2006). There is also an observable ERR for CVD among the atomic-bomb survivors (Wong *et al*., 1999) and Chernobyl workers (Ivanov *et al*., 2001). The effects of radiation on the long-term trends of the total serum cholesterol

levels of the Hiroshima and Nagasaki atomic- bomb survivors were examined using data collected in the adult Health Study over a 28 y period (1958 to 1986). The growth-curve method was used to model the longitudinal age-dependent changes. The mean growth curve of cholesterol levels for the irradiated subjects was significantly higher than for the unirradiated subjects, and that increase was greater for women than for men. No difference in dose response was detected between Hiroshima and Nagasaki. The maximum predicted increase at 1 Gy for women occurred at age 52 y for the 1930 cohort. The corresponding increase for men occurred at age 29 y for the 1940 cohort. The dose range of exposure for the Chernobyl workers and liquidators was 0.005 to 0.3 Sv. It has been estimated that the liquidators have an excess relative risk per unit dose (ERR Sv^{-1}) for CVDs of arteries, arterioles and capillaries of 0.54 (0.18, 0.91, 95 % CI) derived using an external control based on the mortality in the general population in Russia).

Newly discovered is the statistically significant dose risk of ischemic heart disease [ERR Gy^{-1} = 0.41, 95 % CI = (0.05; 0.78)] (Ivanov *et al*., 2006). Confirmation is provided for the existence of significant dose risks for essential hypertension [ERR Gy^{-1} = 0.36, 95 % CI = (0.005; 0.71)] and cerebrovascular diseases [ERR Gy^{-1} = 0.45, 95 % CI = (0.11; 0.80)]. In 1996 to 2000, the assessed ERR Gy^{-1} for cerebrovascular diseases was 0.22 with 95 % CI = (–0.15; 0.58). Special consideration is given to cerebrovascular diseases in the cohort of 29,003 emergency workers who arrived in the Chernobyl zone during the first year after the accident. The statistically significant heterogeneity of the dose risk of cerebrovascular diseases is shown as a function of the duration of stay in the Chernobyl zone: ERR Gy^{-1} = 0.89 for durations of less than six weeks, and ERR Gy^{-1} = 0.39 on average. The at-risk group with respect to cerebrovascular diseases are those who received external radiation doses >150 mGy in less than six weeks [RR = 1.18, 95 % CI = (1; 1.40)]. For doses >150 mGy, the statistically significant risk of cerebrovascular diseases as a function of averaged dose rate (mean daily dose) was observed: ERR per 100 mGy d^{-1} = 2.17 with 95 % CI = (0.64; 3.69). The duration of stay within the Chernobyl zone itself, regardless of the dose factor, had little influence on cerebrovascular disease morbidity: ERR $week^{-1}$ = –0.002, with 95 % CI = (–0.004; –0.001). The radiation risks in this large-scale cohort study were not adjusted for recognized risk factors such as excessive weight, hypercholesterolemia, smoking, alcohol consumption, and others. A systematic review of the 26 published epidemiological data <5 Sv however, has concluded that other than the atomic-bomb survivors, the U.S. radiological technologists, the

Three Countries Study, and the Study of Chernobyl emergency workers, no other published work has the statistical power to conclude a risk of circulatory diseases from ionizing radiations <4 Sv (McGale and Darby, 2005).

6.2.5.4 *Enhanced Long-Term Cardiovascular Disease-Related Inflammatory Responses in Atomic-Bomb Survivors*. Recent evidence points to significant increases in inflammatory activity demonstrable in long-term atomic-bomb survivors which may lead to increased risk of CVD and other noncancer diseases (Hayashi *et al*., 2003). The inflammatory markers C-reactive protein and interleukin-6 (IL-6) were increased 28 % in the plasma of atomic-bomb survivors after a 1 Gy exposure for C-reactive protein and 9.8 % for IL-6, after adjustments for other causative factors such as age, body mass index and history of myocardial infarction. The elevated levels of these proteins were associated with decreases in the percentages of CD4 (glycoprotein T-lymphocyte cell number) plus helper T-cells in peripheral blood lymphocyte populations, where CD4 is a T-lymphocyte cell marker. The association with increased CVD risk in this cohort is not proven, but appears likely. Clearly, information about the long-term effects of ionizing radiation on CVD in humans is needed.

6.2.5.5 *Countermeasures to Radiation-Induced Cardiovascular Disease*. Radioprotection of normal vascular endothelium with synthetic aminothiols (such as WR-2721 and WR-1065) has been reported (Mooteri *et al*., 1996; Warfield *et al*., 1990). Presumably the aminothiols are scavenging free radicals and aiding the repair of damaged macromolecules. Mooteri *et al*. (1996) have also suggested that endothelial cell division and morphology are affected by WR-1065. Drab-Weiss *et al*. (1998) have shown that WR-1065 attenuates the inhibition of DNA synthesis caused by lipopolysaccharide exposure by promoting DNA synthesis and lowering apoptosis in the endothelium. Vitamins E and C are also thought to be radioprotectors of the endothelium (Fajardo and Stewart, 1973). Treatment with certain growth factors such as fibroblast growth factor-2 can significantly decrease radiation-induced blood vessel stenosis (Fuks *et al*., 1994).

6.2.6 *Hereditary Effects*

6.2.6.1 *General Information*. There is considerable uncertainty in the estimate of radiation induced genetic effects in humans. No significant increase in genetic effects has been detected in the off-spring of the atomic-bomb survivors. Based on animal studies,

primarily mice, ICRP (1991) and NCRP (1993) estimate overall hereditary radiation induced effects to be 1×10^{-2} Sv^{-1}.

Hereditary effects connote those inherited from parent lines, and thus really reflect late effects on offspring due to irradiation of parental germ cells. Of concern for crew members who receive radiation doses during space flight is the risk of birth defects or increased incidence of disease in offspring that may result from damage to female or male germ cells. NCRP Report No. 98 (NCRP, 1989) recommends that counseling of crew members of hereditary risks in consideration of subsequent procreation be provided. A more detailed discussion of hereditary effects directed towards individuals engaged in space activities is provided in NCRP Report No. 132 (NCRP, 2000).

6.2.6.2 *Particle Studies on Germ Cells*. Little information exists on germ-cell mutations irradiated with the dose rates and types of radiation prevalent in space (Grahn, 1983). Wiley *et al*. (1994) analyzed embryonic effects transmitted by male mouse germ cells (sperm and sperm progenitor cells) surviving irradiation with low acute doses of high-energy iron ions. Previous low-LET radiation studies have determined a detection limit of sperm-transmitted effects of between 0.005 and 0.01 Gy, with a significant decrease in proliferation ratios occurring during postirradiation weeks four, six and seven. Figure 6.20 shows the number of type B spermatogonia as a function of dose of ^{56}Fe nuclei irradiation (Wiley *et al*., 1994). This was the first published account of highly radioresistant, mature sperm transmitting to the embryo an effect resulting from 0.01 to 0.05 Gy of irradiation. Since mature sperm are no longer connected by cytoplasmic bridges, sperm cells must be responding independently to the irradiation from ^{56}Fe nuclei. In the study as many as 10 times more elongated spermatids and mature sperm sustaining direct hits were observed to transmit lower proliferation ratios to their progeny embryos than was expected based on average cross-sectional area and particle fluence. However, without cytoplasmic bridges their responses could not be mediated by shared RNA and proteins. Epigenetic mechanisms cannot be ruled out. The authors concluded that amplification from secondary radiation produced in the mouse and/or from diffusible chemical products arising from hit sperm and adjacent cells contributed to the high incidence of transmitted effects on proliferation of embryonic cells. Cellular reprogramming appears to have occurred in F_3 mice with paternal F_0 low-LET radiation history, causing offspring with this radiation history to have altered responses to acute alpha-particle irradiation of somatic cells (Vance *et al*., 2002).

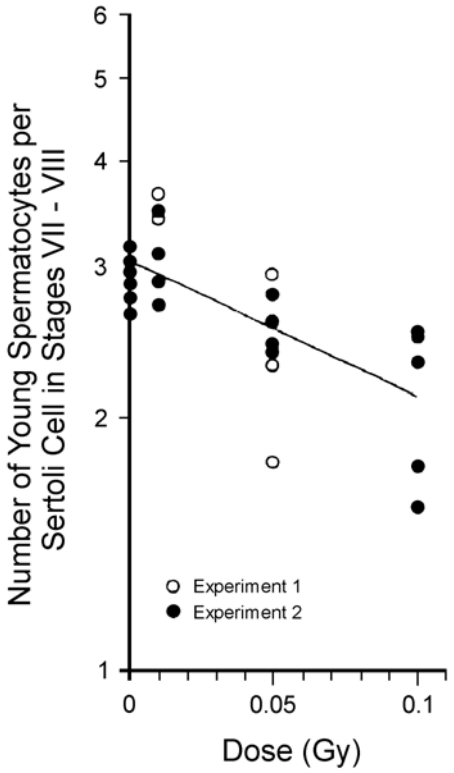

Fig. 6.20. The number of type B spermatogonia as a function of dose of ^{56}Fe nuclei irradiation (Wiley *et al*., 1994). The data show a highly significant dose-dependent killing of the type B spermatogonia ($p < 0.001$) with a D_0 value of 0.282 ± 0.075 Gy. The type B spermatogonia are the most radiosensitive stage of spermatogenesis, but more cells exhibited a biological response than the number of cells sustaining direct hits. The inactivation cross section is ~2 to 2.5 times the actual area that a single type B spermatogonium presents to the beam. The authors concluded that amplification from secondary radiation produced in the mouse and/or from diffusible chemical products arising from hit sperm and adjacent cells contributed to the high incidence of transmitted effects on proliferation of embryonic cells.

6.2.7 *Mutagenic Effects*

The enhanced mutagenic potential of charged particles compared to low-LET radiations has been recognized for many years (Chen *et al*., 1994b; Hei *et al*., 1988; Kronenberg, 1994). Belli *et al*.

(1989; 1991; 1993; 1998) however have pointed out that there is a LET range where low-LET protons are more effective than alpha particles. The broad range of hypoxanthine-guanine phosphoribosyl transferase (HPRT) mutation frequencies induced in primary human fibroblasts at various LET values by an assortment of particle beams is illustrated in Figures 6.21 and 6.22. It is also evident that the LET-RBE relationship may be different for individual genetic loci in human cells (Kronenberg and Little, 1989; Kronenberg *et al*., 1995). Using a novel nonessential human chromosome in a hamster background, complex multilocus deletions of several million base pairs within a single gene have been observed after exposure to a low-fluence of nitrogen ions or moderate doses of protons (Kraemer *et al*., 2000; Kronenberg *et al*., 1995; Waldren *et al*., 1998). Tables 6.2 and 6.3 summarize HPRT mutant spectra and the classification of partial deletion mutations in the HPRT locus after 1 Gy of iron ions (Wiese *et al*., 2001). Loss of heterozygosity mutations contribute markedly to the incidence of mutations at autosomal loci and can be up to 64 cM length at a model locus, TK1 (Wiese *et al*., 2001). In addition to the locus examined, the incidence of radiation-induced mutations is dependent on the genetic background of the cell at risk and on the mechanisms for mutation available at the locus of interest (Wiese *et al*., 2001). Loss of heterozygosity at an autosomal locus is one outcome of the repair of DNA double-strand breaks and can occur by deletion, mitotic recombination, or by chromosome loss followed by chromosome duplication. Wiese *et al*. (2001) reported that expression of mutant TP53 was associated with a small increase in mutation frequencies at a hemizygous locus, but the mutation spectra were unaffected at this locus. In contrast mutant-TP53-expressing human lymphoid cells were 30-fold more susceptible than the parent line that expressed wild-type TP53 to radiation-induced mutagenesis at the TK1 locus. Gene dosage analysis combined with microsatellite marker analysis showed that the increase in mutagenesis could be attributed in part to mitotic recombination. In general, longer loss of heterozygosity tracts were observed in mutants from the mutant TP53-expressing cells, than in mutants from the wild-type TP53-expressing cells.

HZE particle irradiation can induce dose-specific, tissue-specific, and p53-dependent mutagenesis in transgenic animals (Chang *et al*., 2001) as shown for mutant frequencies in mouse brain in Figure 6.23 at different times after a 1 Gy dose of ^{56}Fe ions. The delayed appearance of complex mutations is a hallmark of exposure to high-energy (1 GeV n^{-1}) iron ions reflecting persistent genomic instability (Evans *et al*., 2001).

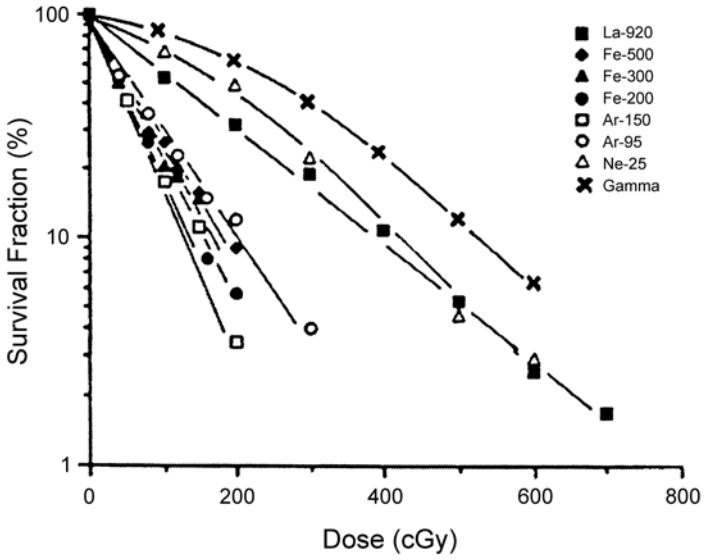

Fig. 6.21. Survival fractions (percent) of noted particle-irradiated human fibroblast cell lines as a function of dose for gamma rays and various heavy ions (Chen *et al*., 1994b).

Masumura *et al*. (2002) studied heavy-ion induced mutations in the gpt delta transgenic mouse, comparing mutation spectra by carbon ions, x- and gamma-ray radiation, and also found tissue-dependencies of mutation frequencies for all three radiation types. DNA sequence analysis revealed that carbon particles induced deletions that were mainly more than 1,000 base pairs in size, whereas gamma rays induced deletions of <100 base pairs, and base substitutions. X rays induced various-sized deletions and base substitutions. Masumura *et al*. (2002) concluded that carbon-ion beam irradiation is effective at inducing deletions *via* DNA double-strand breaks, but less effective than x- and gamma-ray irradiation at producing oxidative DNA damage by free radicals.

The effect of the radioprotector WR-1065 on the cytotoxic and mutagenic effects of ^{56}Fe ions has been investigated on both radioresistant and radiosensitive cells (Evans *et al*., 2002). WR-1065 provided no protection against the cytotoxic effects of exposure of either cell line to ^{56}Fe ions whether it was present during the exposure or when added after the exposure. In contrast, WR-1065 did provide protection against the cytotoxic effects of x rays when present during but not after the exposure (Evans *et al*., 1999). The activity of WR-1065 when added after exposure in certain types of cells (Evans *et al*., 2002; Grdina *et al*., 1985; 1991),

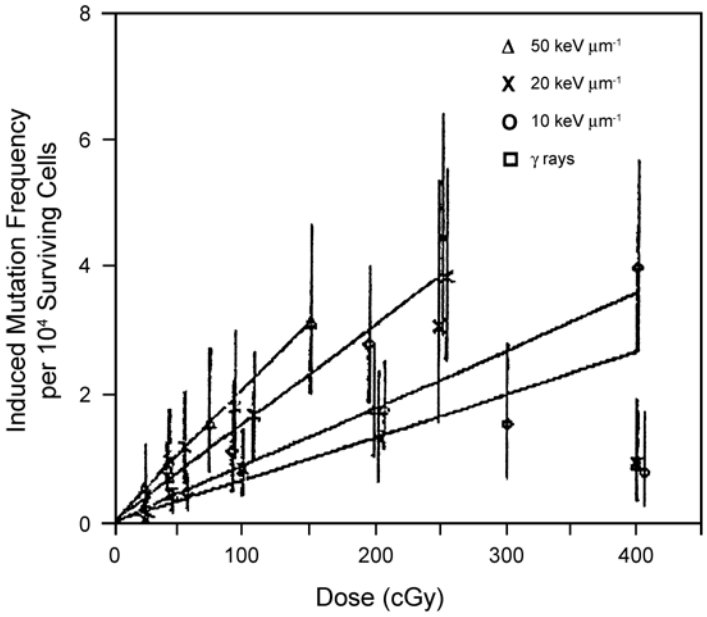

Fig. 6.22. HPRT mutation induction in primary human fibroblasts as a function of LET in accelerator studies with protons, deuterons or helium-3 ions (Hei *et al*., 1988).

TABLE 6.2—*Summary of HPRT mutant spectra (Kronenberg et al., 1995).*

Mutant Type	Iron Ions (1 Gy)	Spontaneous Mutants	
		Kronenberg *et al*. (1995)	Combined TK6 Data
Total deletion	19	2	13
Partial deletion or rearrangement	13	6	48
No detectable alteration	7	22	99
Total	39	30[a]	160[b]

[a]Spontaneous HPRT mutants from parallel control cultures.
[b]Spontaneous HPRT mutants from this series and other published TK6 (cell line derived from human lymphoblastoid tissue) data (Gennett and Thilly, 1988; Skopek *et al*., 1978; Whaley and Little, 1990).

TABLE 6.3—*Classification of partial deletion mutations HPRT locus (Kronenberg et al., 1995).*

	Iron-Induced Mutants	Spontaneous Mutants
5' terminal deletions	4	1
3' terminal deletions	6	3
Deletions with both termini within the locus	3	None
Complex rearrangement on Southern blotting	0	2
Total	13	6

as well as its protection when administered in the phosphorylated form (WR-2721) to normal but not tumor cells in humans (Yuhas, 1979; 1980) indicates its value when used for treatment after accidental exposures or as an adjuvant to radiation therapy or chemotherapy. Further research may prove useful. Two additional radioprotectors against charged particle induced mutations in human-hybrid cells have been reported; Rib-Cys (Lenarczyk *et al*., 2003) and ascorbate (Ueno *et al*., 2002; Waldren *et al*., 2004) which even could be effective when added after irradiation.

Mutational spectra in T-lymphocytes from Soviet cosmonauts who have completed spaceflights of 7 to 365 d have been analyzed using the clonal HPRT assay (Khaidakov *et al*., 1997). The doses received in space by the cosmonauts ranged from 4 to 127 mGy. Mutant frequencies were 2.4- to 5-fold higher than age-corrected values for healthy, unexposed subjects in western countries and exhibited an increased incidence of splicing errors, frameshifts, and complex mutations. Higher frequencies of contribution of adenine and thymine to guanine and cytosine transitions and guanine and cytosine to thymine and adenine transversions were also observed. It was concluded that the increased mutant frequencies and observed shifts in mutational spectra likely indicated a combination of potential influences, including environment, lifestyle, and occupational exposures. Further work that included comparisons with an unexposed cohort of Russian twins (Khaidakov *et al*., 1999) revealed that the distribution of mutations by class in the Russian twins data set was essentially similar to the background Western control, whereas cosmonaut samples demonstrated a significant excess of splice errors and complex mutations. The distribution of base substitutions showed similar trends in both the cosmonaut and Russian twin samples, which are quite distinct compared to

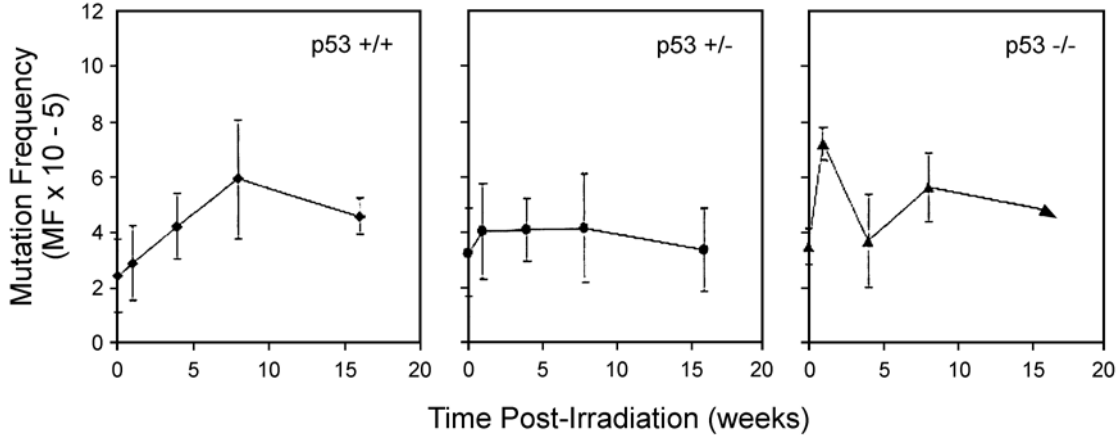

Fig. 6.23. Iron irradiation induced changes in lacZ mutant frequencies in the brain as a function of p53 genetic background after a single acute 1 Gy dose of ^{56}Fe ions (Chang *et al.*, 2001).

those seen in the Western control. In a recent follow-up study ~100 mutants collected from Russian twins reported in a previous study were sequenced and compared to an aged-matched Western mutant data set (Curry *et al*., 2000). The mutational spectrum of the Russian subjects was significantly different. Curiously, the younger Russian spectrum resembled that found in older individuals in the West. Specifically, adenine and thymine to guanine and cytosine transversions are significantly over-represented in the Russian twin spectrum as compared to the Western spectrum. Notably 42 % (23/55) of the base substitutions, almost double the expected value, have not been previously reported. The origin of this difference, whether related to genotoxic challenge, repair or avoidance, cannot be distinguished, but diet and other lifestyle factors clearly may be responsible. No correlations can be made with radiation exposure in space.

6.2.8 *Genomic Instability*

Another level of inheritance of radiation effects relates to genomic instability (Little, 1998; 2003a, 2003b; Morgan *et al*., 2002). Genomic instability is persistent, and transmissible genomic changes in the progeny of low- or high-LET-irradiated cells, as well as unirradiated, neighboring cells. Genomic instability is detected as an increased rate of acquisition of alterations in the mammalian genome, and includes such diverse biological endpoints as chromosomal destabilization, aneuploidy, micronucleus formation, sister chromatid exchange, gene mutation and amplifications, variations in colony size, reduced plating efficiency, and cellular transformation (Limoli *et al*., 2000a; 2000b). The major interest in genomic instability is the concern it may contribute to an increased risk of induced malignancies. This is not known at present, and more research is needed to clarify the mechanisms underlying this and other recent phenomena that may represent a paradigm shift in radiation biology away from the basic tenet that deposition of energy in irradiated targets is responsible for radiation's deleterious biological effects. It now appears that cellular exposure to radiation can initiate a process or processes that perpetuate the phenotypes of genomic instability indirectly *via* separate and distinct biochemical and molecular mechanisms.

Initial work to establish a clear dose response for the induction of genomic instability by low-LET radiations yielded conflicting results (Little *et al*., 1997). However, one study by Limoli *et al*. (1999) of the induction of chromosomal instability in clonal populations of human-hamster hybrid cells derived from single surviving

progenitors 20 generations after exposure has been completed with a range of low-LET radiation doses (0.1 to 10 Gy) and dose rates (0.092 to 17.45 Gy min^{-1}). In cells unsubstituted with BrdU, a dose response was found, where the probability of observing delayed chromosomal instability in any given clone was 3 % Gy^{-1} of x rays. For cells substituted with 25 to 66 % BrdU, a dose response was observed only at low doses (<1 Gy); at higher doses (>1 Gy) the incidence of chromosomal instability leveled off. There was an increase in the frequency and complexity of chromosomal instability per unit dose compared to cells unsubstituted with BrdU which suggests that DNA comprises at least one of the critical targets important for the induction of genomic instability. The frequency of chromosomal instability appeared to saturate around ~30 %, an effect that occurred at much lower doses in the presence of BrdU. Changing the alpha dose rate by a factor of 190 produced no significant differences in the frequency of chromosomal instability. Most other studies have not been able to demonstrate a dose response for ionizing radiation-induced chromosomal instability in other model systems.

This work has been extended to examine the induction of chromosomal instability by high-LET radiations using high-energy iron ions (1 GeV n^{-1}) and gold ions (11 GeV n^{-1}) (Limoli *et al*., 2000a). Dose-response data, with a particular emphasis at low doses (<1 Gy), indicated a frequency of 4 % Gy^{-1} for the induction of chromosomal instability in clones derived from single progenitor cells surviving exposure to iron ions. The induction of chromosomal instability by gold ions was less responsive, since the observed incidence of this phenotype varied from 0 to 10 % over 1 to 8 Gy (Figure 6.24). At the first mitosis after irradiation both iron and gold ions gave dose-dependent increases in the yield of chromosomal aberrations of both the chromosome- and chromatid-type, as well as shoulderless survival curves having $D_0 = 0.87$ and 1.1 Gy, respectively. Based on the present dose-response data, RBE of iron ions is 1.3 for the induction of chromosomal instability, and this indicates that heavy ions are only slightly more efficient than x rays at eliciting this delayed phenotype.

Even the traversal of a cell by a single charged particle has been shown to significantly increase its genomic instability. Using microbeam technology and an approach for immobilizing human T-lymphocytes, Kadhim *et al*. (2001) measured the effects of single alpha-particle traversals on the surviving progeny of cells. A significant increase in the proportion of aberrant cells was observed 12 to 13 population doublings after exposure, with a high level of chromatid-type aberrations, indicative of an unstable phenotype.

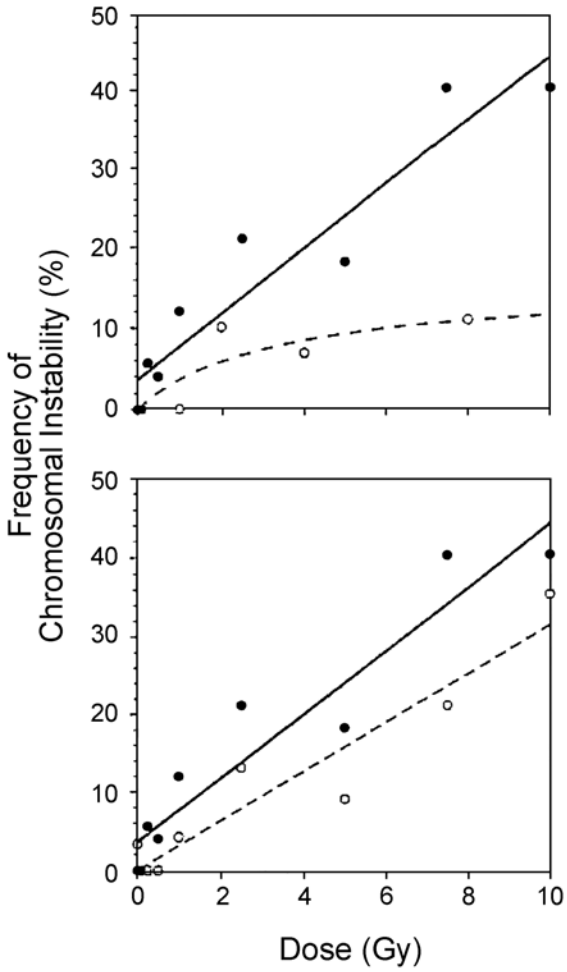

Fig. 6.24. Dose response for the induction of chromosomal instability by high-energy heavy ions: (top) GM10115 cells after exposures to 1 GeV n^{-1} iron (•) and 13 GeV n^{-1} gold (○), and (bottom) comparison between high 1 GeV n^{-1} iron (•) and low-LET x rays (○) radiation-induced chromosomal instability (Limoli *et al*., 2000a).

These data have important implications for likely risk associated with low fluence exposure *in vivo*. They suggest that a cell that has received only a single charged-particle traversal and survives may have a significantly increased probability of producing chromosomal changes in subsequent generations. Radioprotection of transgenerational genomic instability in murine oocytes irradiated

with 0.1 Gy of low-LET radiation has been demonstrated with pretreatment with the ceramide metabolite sphingosine 1-phosphate which mediates apoptosis (Morita *et al*., 2000).

6.2.8.1 *Genomic Instability in Humans.* There have been few human studies that specifically have looked for genomic instability in an exposed human population, and they have failed conclusively to find any excess levels of chromosome instability. Littlefield *et al*., (1997) observed transmissible chromosome complexes in lymphocytes of a Thorotrast® (van Heyden Company, Dresden-Radebeul, Germany) patient and concluded that they were the progeny of irradiated stem cells, and that the highly complex aberrations could be indicative of exposure to densely ionizing radiations.

Anderson *et al*. (2005) demonstrated a high proportion of complex aberrations with *in vivo* studies, many of which were nontransmissible in individuals with high-plutonium body burdens evaluated using meta-fluorescence *in situ* hybridization (mFISH), in addition to stable translocations. A second study, using single color fluorescence *in situ* hybridization (FISH) painting, also noted an increase in stable translocation (Tawn *et al*., 2006). This study failed to observe an elevation in stable complex aberrations, dicentrics or unstable complex aberrations in the plutonium-exposed groups. Differences between this study and the Anderson study may be due to differences in exposure profile and the sensitivity of the techniques employed to detect complex events.

Kodama *et al*. (2005) estimated cytogenetic instability *in vivo* using chromosomally marked clonal T-cell populations in atomic-bomb survivors >40 y postirradiation. The basic idea tested was that clonal translocations were derived from single progenitor cells that acquired an aberration, most likely after a radiation exposure, and then multiplied extensively *in vivo*, resulting in a large number of progeny cells that eventually comprise several percent of the total lymphocyte population. Therefore, if chromosome instability began to operate soon after a radiation exposure, an elevated frequency of additional but solitary chromosome aberrations in clonal cell populations would be expected. Instead, six additional translocations were found among 936 clonal cells examined with the G-band method (0.6 %); the corresponding value with multicolor FISH analysis was 1.2 % (4/333). Since these frequencies were no higher than 1.2 % (219/17,878 cells), the mean translocation frequency observed in control subjects using the G-band method, it was concluded that chromosome instabilities that could give rise to an increased frequency of persisting, exchange-type

aberrations were not commonly generated by radiation exposure. There are also limitations in the relevance of comparing protracted, mixed radiation-quality exposures during spaceflight to the acute, largely low-LET exposure of atomic-bomb survivors.

6.2.8.2 *Links of Genomic Instability with Other Phenomena*. Recent reviews of the radiation-induced genomic instability literature indicate that it may be linked or may have an early role in carcinogenesis (Huang *et al*., 2003), bystander effects and other nontargeted effects (Kadhim *et al*., 2004; Morgan, 2003; Nagar et al., 2003). A biological-based model that links genomic instability, bystander effects, and adaptive response has also been developed (Scott, 2004). The most convincing laboratory evidence is from Ponnaiya *et al*. (1997a) who have tested the hypothesis that individuals highly susceptible to induction of tumors by radiation should exhibit enhanced radiation-induced instability. BALB/c white mice are considerably more sensitive to radiation-induced mammary cancer than C57BL/6 black mice. In their study, primary mammary epithelial cell cultures from these two strains were examined for the delayed appearance of chromosomal aberrations after exposure to ^{137}Cs gamma radiation, as a measure of radiation-induced genomic instability. As expected, actively dividing cultures from both strains showed a rapid decline of initial asymmetrical aberrations with time postirradiation. However, after 16 population doublings, cells from BALB/c mice exhibited a marked increase in the frequency of chromatid-type breaks and gaps which remained elevated throughout the time course of the experiment (28 doublings). No such effect was observed for the cells of C57BL/6 mice; after the rapid clearance of initial aberrations, the frequency of chromatid-type aberrations in the irradiated population remained at or near those of nonirradiated controls. These results demonstrate a correlation between the latent expression of chromosomal damage *in vitro* and susceptibility for mammary tumors, and provide further support for the central role of radiation-induced instability in the process of tumorigenesis. Although the underlying mechanism of action still remains to be elucidated, these findings are pointing to a transmissible factor that could explain the high frequency of these effects, as well as the general lack of a well-defined dose response for nontargeted effects.

The radiation induction of genomic instability depends on the dose and radiation quality. There appears to be a low dose of low-LET radiation below which no additional genomic instability is induced. Low doses of both low- and high-LET radiation can induce

genomic instability and dose-rate effects of each are reported (Nagar *et al*., 2003) that may have significance in the estimation of radiation risk in space travel. Ponnaiya *et al*. (1997b) have studied progeny of either gamma- or neutron-irradiated human epithelial MCF-10A cells for chromosomal aberrations between 5 and 40 population doublings postirradiation. Exposure to either type of radiation resulted in an increase in chromatid-type gaps and breaks several doublings after the irradiation; no such effect was observed for chromosome-type aberrations. Neutron-irradiated cells showed consistently elevated frequencies of aberrations compared to nonirradiated controls at all times examined. Aberration frequencies for gamma-irradiated cells were not significantly different from controls until 20 to 35 population doublings postirradiation, where they increased twofold above background before returning to near control levels. These data represented the first evidence of chromosomal instability caused by neutron exposure, and have been confirmed by Kadhim *et al*. (1998). Results show that while either gamma rays or neutrons are capable of inducing similar types of delayed aberrations, the time course of their appearance can differ markedly.

On the other hand, Dugan and Bedford (2003) report that neither low- nor high-LET radiations induce chromosomal instability in low passage normal diploid human fibroblasts. This undermines the suggestion that instability is an initiating step in carcinogenesis if radiation cannot trigger chromosome instability in normal cells. A lack of a detectable transmissible chromosomal instability has also been reported after *in vivo* or *in vitro* exposure of mouse bone-marrow cells to ^{224}Ra alpha particles (Bouffler *et al*., 2001). In addition, there is no evidence that irradiation of the bone marrow in childhood cancer survivors resulted in instability being transmitted to their offspring (Tawn *et al*., 2005). However, contrasting results have been reported by others in normal human bone-marrow cells (Kadhim *et al*., 1995; 1992), normal human lymphocytes (Kadhim *et al*., 2001), and normal fibroblasts irradiated with HZE particles (Kadhim *et al*., 1998). In addition, Pirzio *et al*. (2004) have shown the karyotypic stability of human fibroblasts immortalized by expression of hTERT. The ectopic overexpression of telomerase however is associated with unusual spontaneous as well as radiation-induced chromosome stability. Long-term studies illustrated that human fibroblasts immortalized by telomerase show an unusual stability for chromosomes, both with and without exposure to ionizing radiation. These results confirm a role for telomerase in genome stabilization by a telomere-independent mechanism.

6.3 Early Radiation Effects

Early radiation effects include changes in gene activity, the induction of DNA damage and the initiation of the processing of the DNA damage. The damage may be repaired, rapidly in the case of exposure to low-LET radiation and largely without error, but slowly and with significant probability of misrepair after high-LET radiation. If the initial damage is sufficiently severe, cell death may occur. If cell loss exceeds a threshold, the level of which varies among tissues, the affected tissue may exhibit loss of function.

6.3.1 *Homeostasis*

Homeostasis is a concept based on the idea that numerous physiological systems within the body are controlled by direct and feedback regulation to maintain a normal, integrated state. Exposure to low levels of toxic chemicals can modify homeostasis, and in some cases has beneficial effects, such as increased resistance to related chemicals or stimulation of growth or development (Calabrese and Baldwin, 2002). It is known that ionizing radiations can disturb homeostatic regulation. Although the biological effects of ionizing radiation are predominantly harmful, low-to-intermediate doses have been observed in a number of species from plants to mammals to enhance growth and survival, augment the immune response, and increase resistance to the mutagenic and clastogenic effects of further radiation exposure (Upton, 2001). On the other hand, cancer cells are known to have defects in regulatory circuits in the extracellular matrix that govern normal cell proliferation and homeostasis (Hanahan and Weinberg, 2000).

High-LET radiations found in space are known to have greater effects compared to low-LET reference radiation and have demonstrated dependence on the quality of the radiation with maxima in the curves for each particle type often called hooks (Wulf *et al*., 1985). The RBE values for a number of biological endpoints (most of which are derived from *in vitro* or *in vivo* cell survival, molecular damage or mutation data in the laboratory) are widely accepted to demonstrate a maximum for many atomic nuclei in the LET range near 100 to 200 keV μm^{-1} (Blakely *et al*., 1984). There are notable exceptions such as a lower LET maximum near 80 keV μm^{-1} for some tissue-specific endpoints, such as those derived from lymphoid material, and a maximum of near 30 keV μm^{-1} for the effects of low-energy protons (Belli *et al*., 1989). Most of these RBE-LET experiments involved relatively high doses in the >2 to 20 Gy range. This work is reviewed in NCRP Report No. 132 (NCRP,

2000). Summarized below is an evaluation of early radiation effects that may be pertinent to space radiation exposures. This is followed by a description of some of the biological effects that can impact different kinds of homeostasis after exposure to relatively low doses of ionizing radiations for which further research is needed before the importance of its significance can be evaluated.

Although there are some forms of high-LET radiation damage that are qualitatively unique, for many biological indices, low- and high-LET radiation cause qualitatively identical changes in genetic and membrane cell targets, with differences only in the quantitative level of the effects. It is now recognized that biological targets and mechanisms of radiation damage and repair, as well as pathways underlying the effects of exposure to radiation of any quality can be different at low or high doses. There is an increased importance of membrane damage in the total damage after exposure to low doses of either low- or high-LET radiations compared to higher doses. This fact has changed the focus of radiation risk assessment to an understanding of the impact of relevant biology (Fry *et al*., 1998).

6.3.2 *Prodromal Effects of Radiation Exposure*

The term prodromal effect describes a transient period of anorexia, nausea and vomiting that generally develops within a few hours of radiation exposure and rarely exceeds 24 h with low-LET radiations (Fajardo *et al*., 2001). The time of onset, and both the severity and duration of symptoms are dose dependent and, therefore, can provide a rough indication of the dose. Figure 6.25 illustrates cumulative probability graphs for these prodromal symptoms. This work was performed at Oak Ridge Associated Universities from 1964 to 1975 (n = 502 patients, including therapy and accident situations). From these graphs the ED_{50} = 1.08 Gy for anorexia, ED_{50} = 1.58 Gy for nausea, and ED_{50} =2.40 Gy for emesis (Ricks and Lushbaugh, 1975). Useful information regarding the prodromal syndrome is also available in a software application (called Biodosimetry Assessment Tool) for management of radiation accidents that has been developed for post-exposure biodosimetry (Sine *et al*., 2001). Prodromal effects are not noted below low-LET radiation doses of 0.5 Gy (Mettler and Upton, 1995).

Until relatively recently little information has been available regarding prodromal effects of other radiation types. Rabin and colleagues (Rabin *et al*., 1992; 1994) have studied the dose response of 600 MeV n^{-1} ^{56}Fe-induced emesis in ferrets and compared it with the dose response from other radiation types. Over the dose range

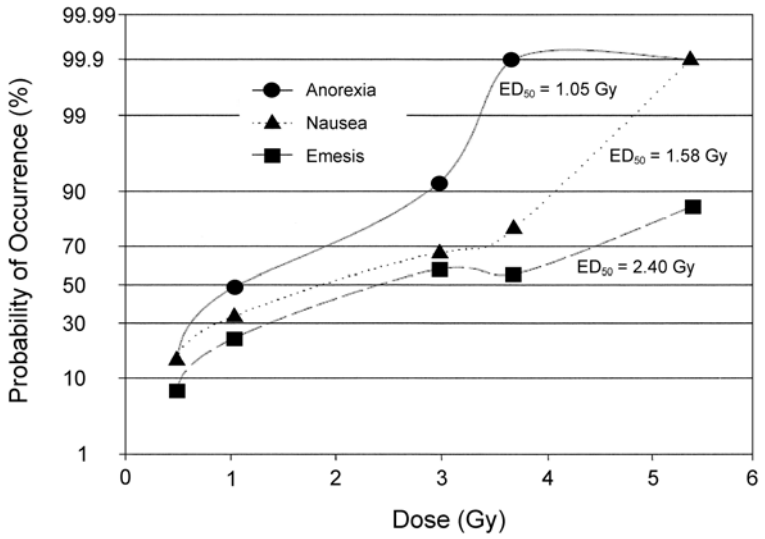

Fig. 6.25. Dose dependence of the probability of prodromal symptoms in humans based on data from radiation theory and accident patients (Ricks and Lushbaugh, 1975).

of 0.2 to 5 Gy, fission spectrum neutrons and high-energy iron ions were each more effective than ^{60}Co gamma rays in inducing emesis, and the effects of iron ions and fission neutrons could not be distinguished from each other. ^{60}Co gamma rays were significantly more effective in producing emesis than high-energy electrons or 200 MeV protons. Dose rates ranged from 0.1 to 1 Gy min^{-1}. The relative effectiveness of different types of radiation in producing emesis as a function of LET is presented in Figure 6.26. It was noted that the results were consistent with other behavioral toxicity in showing that LET was not a good predictor of the effect. The relatively large difference in LET between ^{56}Fe particles at ~190 keV μm^{-1}, and fission spectrum neutrons at ~65 keV μm^{-1} was not associated with any difference in the effectiveness with which the two types of radiation produced emesis. In contrast, the small differences in LET between ^{60}Co gamma rays at ~0.3 keV μm^{-1}, high-energy electrons at 0.2 keV μm^{-1}, and protons at ~0.3 keV μm^{-1} are associated with significant differences in the effectiveness with which these types of radiation cause vomiting in the ferret. Obviously the avoidance of vomiting is a high priority but little is known about the influence of proton dose rate. There is

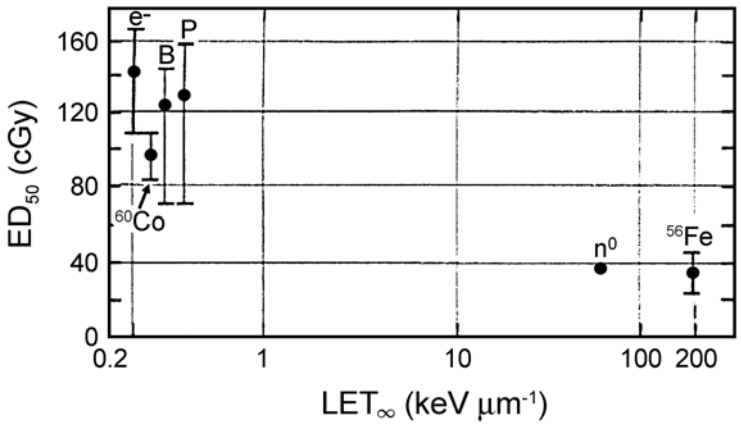

Fig. 6.26. LET dependence of relative behavioral effectiveness of radiation in producing emesis and or retching in ferrets; B = bremsstrahlung, P = protons, e^- = electrons, ^{60}Co = cobalt gamma rays, n^0 = neutrons, ^{56}Fe = iron ions.

no information about radiation-induced emesis in mixed radiation fields as would be found in deep space.

It is known from clinical radiotherapy that early symptoms including headache, nausea and vomiting and deterioration of pre-existing neurological signs following human brain treatment with relatively large dose fractions of conventional low-LET radiation can occur within hours after exposure. Experimental studies with animals have examined the initial response of the brain to whole-body or head-only gamma irradiation (Hong *et al*., 1995; Raju *et al*., 2000). Inflammatory gene products (which are probably responsible for clinically observed early symptoms of brain radiotherapy) are increased reaching a peak within 4 to 8 h after exposure. This effect was dose-dependent, however, and was not found <7 Gy, except for intercellular adhesion molecule-1, which was increased by doses as low as 2 Gy (Hong *et al*., 1995). The effects can be reduced by the use of steroids. Transcription factors associated with injury such as the DNA-binding activities of AP-1 (heterodimer formed by c-jun and c-fos), Sp-1 (an inhibitor of beta-like globin gene transcription during erythroid differentiation), p53 and nuclear factor kappa B are also increased in a time- and dose-dependent manner after exposure to asymptomatic doses (Raju *et al*., 2000). The ultimate consequences of these transient changes in gene expression are not known. Cytokines have been associated, however, with several pathologic conditions of the nervous system. Cytokine changes can also influence the proliferative characteristics of stem cells and

may be important to memory loss in other neurodegenerative disease. There is no published information on the effects of space radiations on gene expression of inflammatory gene products or DNA-binding transcription factors in the brain.

6.3.3 *Motor-Neural Effects*

There is biochemical evidence for LET-dependent premature aging and CNS degeneration (Joseph *et al*., 1992; 1993; 1994) and unique enhanced behavioral toxicity from particle radiation exposures (De Angelis *et al*., 1989; Hunt *et al*., 1989; 1990; Kastan *et al*., 1991) as discussed in Section 6.2.3. However, exposure to ordinarily available sources of penetrating radiations usually do not indicate sensory perception of irradiation. The retina is very sensitive to x and gamma rays (Section 6.3.4), and exposure to <1 R can cause an alteration in the absolute threshold to light sensation (Kameyama *et al*., 1956; Lipetz, 1955). Single millisecond pulses in excess of 400 Gy or pulse trains of <1 s duration elicited the corneal blinking reflex when delivered to the cornea of unanesthetized rabbits (Tobias, 1962). Radiation-induced stimulation of motility on exteriorized intestines of rats, rabbits and guinea pigs has been reported (Conard, 1951; 1956). In contrast, dose rates of 10 Gy min^{-1} of high-energy alpha particles failed to stimulate frog sciatic nerves, and persistent alterations of ionic balance in peripheral mammalian nerves follows only after irradiation by many thousands of gray (Bachofer and Gautereaux, 1959; Gaffey, 1962). Early performance decrement after radiation exposure is often produced by exposure to rapid, supra-lethal doses of ionizing radiation (Bogo, 1988). However, this appears to be species-dependent since nonhuman primates show more radiosensitivity to this endpoint than rodents (Bogo *et al*., 1987; Bruner, 1977); and dependent on the radiation quality (Bogo *et al*., 1989). Gauger *et al*. (1986) reported that movies of neurons exposed to particle radiation fields show a dendritic retraction phenomena in real time. All of this work has led to the conclusion that there are widely varying limits of excitability of nerve or of muscle action, that different radiation qualities are not equally effective at disrupting performance, and the data suggest that high-energy electrons potentially possible in space during solar events could disrupt behavior at lower doses than other radiations, regardless of the doses needed to produce early performance decrement. Fission neutrons were the least effective, and the work of Joseph *et al*. (1992) indicate high effectiveness for very low doses (<1 Gy) of iron ions. This work needs further research into dose-rate effects of the most effective beams for more nerve and muscle endpoints.

6.3.4 *Light Flashes*

Phosphene, the visual perception of flickering light, is considered a subjective sensation of light, since it can be caused simply by applying pressure on the eyeball. Phosphenes have also been reported by volunteers exposed to extremely low-frequency magnetic fields (internal induced fields ~1 to 1,000 mV m^{-1}) (Saunders, 2003). Phosphenes can be induced by transcranial magnetic stimulation to the human occipital cortex in the brain, or to the retina (Tenforde, 1996). X-ray exposures to the eye can induce phosphenes (Doly *et al*., 1978; 1980). The electrophysiological response of isolated albino rat retinas induced by x rays was found to be identical to the electrophysiological response produced by a visible light stimulation. To obtain the same electrophysiological response amplitude, the incident energy on the retina had to be ~5×10^6 times larger for x rays (E = 40 keV) than for visible light (Doly *et al*., 1980). The dose threshold for the detection of radiation by the dark-adapted human eye is a few thousandths of a milligray (Pape and Zakovsky, 1954). This is equivalent to an energy deposition of ~10^{10} ergs per cell, which implies that a single charged particle with sufficient range to traverse a sufficient number of rods and cones would be capable of causing a light flash (Todd *et al*., 1974).

Tobias (1952) predicted that space travelers whose retinas were traversed by a heavy cosmic-ray primary particle track would have several rods and cones activated producing a visual phenomenon of streaks or flashes of light. A number of astronauts who flew orbital missions in near-equatorial orbits below the Van Allen radiation zones failed to observe light flashes. But astronauts on Apollo missions IX through XV observed a series of light flashes and streaks when the interior of their spaceship was dark and regardless whether their eyes were open or closed. Fremlin (1970) suggested that the observed flashes were due to cosmic radiation or its Cerenkov radiation. However, Cerenkov radiation cannot be the only mechanism since slow particles also induce light (McNulty *et al*., 1978). Experiments to test a variety of radiations in producing visible phenomena have been carried out in the laboratory using accelerators (Budinger *et al*., 1972; 1976; 1977; Charman *et al*., 1971; Hoffman *et al*., 1977; McNulty, 1971; Osborne *et al*., 1975; Pinsky *et al*., 1974; Tobias *et al*., 1971). Several conclusions can be drawn from these studies:

- The diffuse ionization caused by 80 kV x rays does not produce discrete flashes but a dull glow, and the dose threshold for the x-ray phosphene is higher than that for high-energy neutrons.

- A fluence rate of 1.4×10^4 neutrons cm^{-2} s^{-1} produced 25 to 50 flashes in the subjects' view, probably due to 400 proton recoils per second in the vitreous fluid and ~40 spallation products per second in the eye.
- 1.5 GeV pi mesons to a total dose of 1,200 pions cm^{-2} or 0.02 mGy did not produce a visual effect, probably due to the fact that mesons do not ionize densely enough to cause flashes to be seen, and that Cerenkov radiation probably does not play a role in the production of flashes, however extremely relativistic muons did produce light flashes.
- High-energy helium ions produce streaks.
- The color of the light observed by the subjects was difficult to identify, but was considered to be gray, bluish or white light, consistent with the effects being due to direct interaction of the incoming radiation with the retinal photoreceptor cells.

As discussed above, loss of retinal photoreceptors has been reported to occur prematurely after heavy particle irradiation in rabbits (Williams and Lett, 1994).

There was an international effort spearheaded by Italian and Russian scientists to investigate the light flash phenomenon further, correlating measurements of the radiation environment and the nuclear abundance inside the ISS with the study of astronaut brain activity in space when subjected to cosmic rays as detected with light-excluding helmet equipment with particle detection equipment and recorded as a function of background fluence rate and orbit position. This study was called the Sileye-3/Alteino Experiment (Bidoli *et al*., 2002) and was completed on the Mir Space Station. The rates of occurrence of light flashes measured onboard the Mir Space Station as a function of particle rate for all particles and for relativistic nuclei inside and outside of the South Atlantic Anomaly have been reported by Bidoli *et al*. (2002).

The Anomalous Long-Term Effects in Astronauts (ALTEA) Alteino experiment has set the experimental baseline for providing information on the radiation environment onboard the ISS and on astronauts' brain electrophysiology during orbital flights (Narici *et al*., 2003; 2004). The concurrent acquisition of particle and electroencephalogram data will detect the number of particles traveling through each different region of the brain per unit time, perform nuclear discrimination, and calculate the amount of energy delivered to neural tissues. A parallel study called ALTEA-MICE will also be launched in the ISS to investigate the effects of heavy ions on the visual system of normal and mutant mice with visual defects (Sannita *et al*., 2004).

6.3.5 *Hematological Changes*

6.3.5.1 *Effects on Blood Cell Compartments*. Studies on the effects of whole-body proton irradiation on bone-marrow-derived cell types and the highly immunosuppressive cytokine transforming growth factor-β1 (TGF-β1) have been reported by Kajioka *et al*. (2000a). C57BL/6 female mice were irradiated with a single 3 Gy dose of either 250 MeV or mid-peak stopping protons of 149 MeV. Control animals were irradiated with 3 Gy ^{60}Co gamma rays. Animals were euthanized in a time course of 0.5, 4, 7, 10, 14, and 17 d after exposure. Highly significant decreases in white blood cell counts were noted as early as 12 h post-exposure in all irradiated groups, with means being only 32 to 35 % of those for nonirradiated controls (Figure 6.27). At this same point in time, significantly low numbers of lymphocytes (11 to 17 % of control), and monocytes (32 to 36 % of control) were present. The depression generally persisted until the end of the study. Collectively, the data show that dramatic and persistent changes occurred in all irradiated groups compared to the unirradiated controls, but that all irradiated groups gave similar results regardless of the radiation type.

In contrast, neutrophil levels tended to be erratic, and significant differences were observed among the irradiated groups on days four and seven. Eosinophils and basophils were noted only rarely in all four groups. Red blood cells counts, hematocrit and hemoglobin content were significantly decreased very early at 12 h only in the ^{60}Co irradiated mice but not the proton-irradiated animals. On days 4 to 17, however, these parameters were significantly decreased in all irradiated groups (both gamma and proton), with the lowest values observed on day four. Anemia is a common problem associated with irradiation of large body areas that include the bone marrow, and astronauts returning to Earth after even a few days in space often present with low red cell mass and symptomatic anemia (Alfrey *et al*., 1996). Thrombocyte counts fluctuated showing significant depression for all radiation groups on days 4 and 10 through 17, but normal levels on days 0.5 and 7. TGF-β1 levels in plasma were significantly elevated at 7 d post-exposure in mice irradiated with ^{60}Co gamma rays when compared to nonirradiated controls or to either of the proton-irradiated groups. However, by day 17 all irradiated groups had significantly lower levels of the cytokine than did the control animals.

An evaluation of the functional characteristics of leukocytes and circulating blood cell parameters after whole-body proton irradiation at varying doses and at low (0.01 Gy min^{-1}) and high (0.8 Gy min^{-1}) dose rates has been made by Pecaut *et al*. (2002). C57BL/6 mice were irradiated and euthanized at 4 d post-exposure

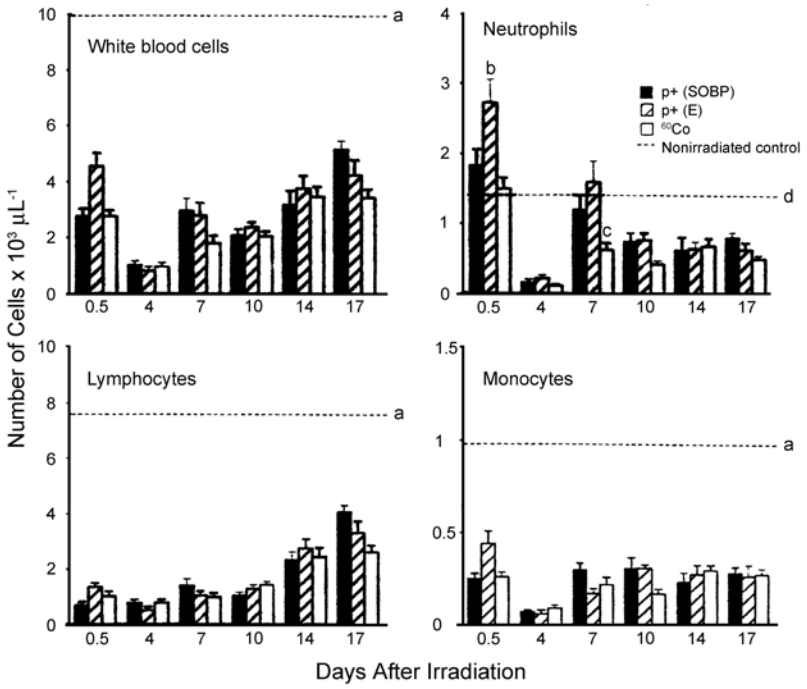

Fig. 6.27. Leukocytes in the blood with time after irradiation. Each bar represents the mean ± SEM. The dotted horizontal lines represent the means for nonirradiated controls; SEM values were ±0.55 (white blood cells), ±0.44 (lymphocytes), ±0.17 (neutrophils), and ±0.10 (monocytes). (a) $p < 0.05$ versus all irradiated groups at all time points except p + [E (entrance plateau of the Bragg curve)] on day four; (b) $p < 0.05$ versus p + [SOBP (spread-out Bragg peak)]; (c) $p < 0.05$ versus control; and (d) $p < 0.05$ versus ^{60}Co (Kajioka *et al*., 2000a).

for assay. Significant radiation dose-dependent decreases were observed in splenocyte responses to T and B cell mitogens when compared to sham-irradiated controls ($p < 0.001$). No sparing was observed when the dose rate was reduced to 0.01 Gy min^{-1} spontaneous blastogenesis, also significantly dose dependent, was increased in both blood and spleen ($p < 0.001$).

Early human lymphocyte depletion kinetics after acute high doses (>3 Gy) follow a single exponential, $L(t) = L_0\ e^{-K(D)t}$, where $K(D)$ is a rate constant, dependent primarily on the mean absorbed dose (D) (Goans *et al*., 1997). Within the first 8 h postaccident, $K(D)$

may be calculated using serial lymphocyte counts and used as a first approximation to guide initial medical management. Data are needed at protracted dose rates of protons.

Red blood cell counts, hemoglobin concentration, and hematocrit were decreased in a dose-dependent manner ($p < 0.05$), whereas thrombocyte numbers were only slightly affected. Comparison of proton- and gamma-irradiated groups (both receiving 3 Gy at high dose rate) showed a higher level of spontaneous blastogenesis in blood leukocytes and a lower splenocyte response to concanavalin A, following proton irradiation ($p < 0.05$). There were no dose-rate effects noted. Overall, the data demonstrate that the measurements in blood and spleen were largely dependent upon the total dose of proton radiation and that an 80-fold difference in the dose rate was not a significant factor. Some differences were found, however, between protons and gamma rays in the degree of change induced in some of the measurements.

The effects of single small doses of x rays upon murine hematopoietic stem cells have been studied to obtain a better estimate of the quasithreshold dose of the survival curve (Cronkite *et al*., 1987). The quasithreshold dose is small, of the order of 20 cGy. A dose fractionation schedule that does not kill or perturb the kinetics of hematopoietic cell proliferation was sought in order to investigate the leukemogenic potential of low-level radiation upon an unperturbed hematopoietic system. Doses used by others in past radiation leukemogenesis studies clearly perturbed hematopoiesis and killed a detectable fraction of stem cells. In contrast, Cronkite *et al*. (1987) reported that 1.25 cGy every day decreased the CFU-S content of bone marrow by the time 80 cGy were accumulated. Higher daily doses as used in published studies on radiation leukemogenesis produced greater effects; 2 cGy three times per week produced a modest decrease in the CFU-S content of bone marrow after an accumulation of 68 cGy. With 3 cGy three times per week an accumulation of 102 cGy produced a significant decrease in the CFU-S content of bone marrow. Dose fractionation at 0.5 and 1 cGy three times per week did not produce a CFU-S depression after accumulation of 17 and 34 cGy. Previous radiation leukemogenesis publications utilized single doses and chronic exposure schedules that probably significantly perturbed the kinetics of the hematopoietic stem cells. Whether radiation will produce leukemia in animal models with dose schedules that do not perturb kinetics of hematopoietic stem cells is still unknown.

Near-term effects of chronic, low daily-dose gamma-irradiation (3 to 128 mGy d^{-1}) on the blood-forming system of canines have been reported (Seed *et al*., 2002a). Change in hematopoietic capacity was

monitored along with time of exposure and cumulative radiation dose. The rate, magnitude and timing of suppression and accommodation were determined. The ability of periodic treatment with a lipopolysaccharide immunomodulator to alleviate the suppressive hematopoietic effects of chronic exposure was tested and the effects of other pharmacologics (amifostine, granulocyte colony-stimulating factor, cytokine) were evaluated based on evidence with rodent models.

Results indicated that low but significant suppression of blood leukocyte and platelet levels occurred at 3 mGy d^{-1}. As the dose rate increased from 3 to 128 mGy d^{-1}, the rate of suppression increased approximately eightfold, whereas the time to accommodate declined from 2,000 to ~150 d. Within the time frame required to reach the upper limit of 700 mGy, none of the dose rates examined elicited blood cell decrements large enough to severely compromise near-term immune function. Pharmacological intervention with lipopolysaccharide minimized hematopoietic suppression in only a small fraction of the treated animals that displayed distinctive long-term survival and pathology patterns.

Additional data (Seed *et al*., 2002b) suggest that the daily dose rate of 7.5 cGy d^{-1} represents a threshold below which the hematopoietic system can retain either partial or full trilineal cell-producing capacity (erythropoiesis, myelopoiesis and megakaryopoiesis) for extended periods of exposure (>1 y). Trilineal capacity was fully retained for several years of exposure at the lowest dose rate tested (0.3 cGy d^{-1}) but was completely lost within several hundred days at the highest dose rate (26.3 cGy d^{-1}). Retention of hematopoietic capacity under chronic exposure has been demonstrated to be mediated by hematopoietic progenitors with acquired radioresistance and repair functions, altered cytogenetics, and cell-cycle characteristics.

6.3.5.2 *Chromosome Aberrations in Lymphocytes*

6.3.5.2.1 *Technical issues with scoring radiation-induced aberrations*. A significant finding from work involving irradiation of individual cells is that radiation damage to DNA from ionizing radiations is clustered (Goodhead, 1994; Sutherland *et al*., 2000; 2002; Ward, 1994). There is a gradient of clustering that increases with increasing ionization density, and includes a large number of small DNA segments (Goodwin *et al*., 1994; Holley and Chatterjee, 1996; Lobrich *et al*., 1996; Newman *et al*., 1997; Rydberg, 1996).

DNA damage response proteins such as CDKN1A (p21Cip1) have been found to immediately localize to damage produced by

heavy-ion tracks (Jakob *et al*., 2002). CDKN1A foci arise rapidly at sites of localized DNA damage induced by heavy ions and are associated with the chromatin. The localization to the foci is not dependent on functional TP53, and occurs independently of the formation of the hMre11-rad50-NBS1 complex (Jakob *et al*., 2002).

Difficulty in correctly rejoining the breaks in damaged clusters may contribute to the high-RBE of high-LET radiation, and perhaps results in novel DNA lesions. This has been revealed at the genetic and chromosomal level by a number of recent technical advances in the identification of rearrangements between lesions (Boei and Natarajan, 1998; Grigorova *et al*., 1998; Knehr *et al*., 1999; Oberheitmann, 1997; Prasanna *et al*., 1997). As an example, Figure 6.28 presents the frequency of human fibroblast cells with damage to chromosome 4 by gamma rays, protons and iron particles (Yang, 1999). RBE for protons is close to one, while RBE for iron ions is 3.5 at low dose (<0.5 Gy) and 3.1 at higher doses.

Numerous cytogenetic assays have been proposed to measure individual doses, including conventional dicentric scoring, the conventional micronucleus scoring, the centromere micronucleus assay using p82H and an alpha AllCen-pancentromeric probe, and tricolor FISH with chromosome two, four and eight probes for the scoring of translocations. Thierens *et al*. (1999) evaluated these assays in the dose range from 0.1 to 2 Gy with ^{60}Co gamma rays and found that only the centromere micronucleus assay can combine high sensitivity with a reasonable scoring time for performing biodosimetry of relatively large populations. The induction of gene

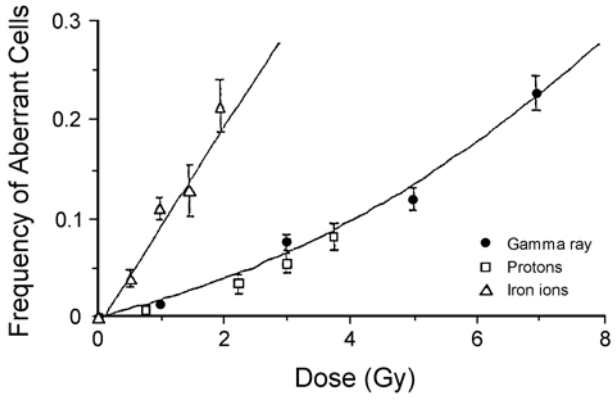

Fig. 6.28. Frequency of human fibroblast cells with damage to chromosome 4 by ^{60}Co gamma rays, 250 MeV protons, and 1 GeV n^{-1} iron particles (Yang, 1999). More complete data sets can be found in Wu *et al*. (1997).

expression as a monitor of exposure to ionizing radiation has also been proposed (Amundson *et al*., 2000; 2001a; 2001b). The combined use of multiple bioassay biodosimetric methods including cytogenetic, hematological and molecular markers has also been proposed (Blakely *et al*., 2001; 2003). Horneck (1998a) suggested monitoring of ionizing radiation exposure using *in situ* biomarkers for genetic (*e.g*., chromosomal aberrations in human lymphocytes, germ line minisatellite mutation rates) or metabolic changes in serum, plasma and blood (*e.g*., serum lipids, lipoproteins, lipid peroxides, melatonin, antibody titer) for individuals located in radiation environments including ISS. Based on methods and endpoints, biomarkers have been classified in a number of ways as either biomarkers of exposure, sensitivity or disease (Brooks, 1999). Durante (2005) in a recent review also distinguishes between biomarkers that are dose indicators versus those that are risk indicators. Chromosomal aberrations in peripheral blood lymphocytes are the only biomarker that can provide simultaneous information on absorbed dose and risk, and have been measured extensively in astronauts and cosmonauts during the past 10 y.

A major technical issue to using chromosomal aberrations for biodosimetry relates to selection of the optimal time course for examination of the maximum chromosomal damage after high-LET radiation exposure, which is different from the optimal post-exposure time after low-LET radiation exposure. Ritter *et al*. (1996) were the first to point out that after high-LET radiation (>100 keV μm^{-1}) aberration yields are higher in cells arriving late at the first mitosis (delayed by the enhanced high-LET radiation damage) than the yields measured in cells collected earlier. The differential time course of this phenomenon was further documented in hamster fibroblasts (Gudowska-Nowak *et al*., 2005; Ritter *et al*., 2002), human fibroblasts (Berger, 2001; Nasonova *et al*., 2004), and in human lymphocytes (Anderson *et al*., 2000; George *et al*., 2001b; Nasonova and Ritter, 2004). An illustration of how this effect impacts the estimated total yield of chromosomal damage induced in the first post-exposure cycle of V79 cells is summarized in Table 6.4. The enhanced cell-cycle progression delay of heavily-damaged cells after high-LET radiation is also evident when the aberration yields are scored by the premature chromosome condensation (PCC) technique in G_2-cells and compared to the yields found in metaphase (*e.g*., aberration yields in G_0 after repair) are much higher than in metaphase cells collected at 48 h (Durante *et al*., 1998). In summary it is recommended not to use a single sample time to quantify high-LET induced chromosome damage in metaphase cells.

TABLE 6.4—*Estimated total yield of chromosomal damage induced in the first cycle of V79 cells (Ritter et al., 2002).*

Radiation Type	Fluence (ions cm^{-2})	Absorbed Dose (Gy)	Aberrant Cells (%)	Undamaged Cells (%)	Lost Cells (%)	Aberrations in 100 Cells Exposed[a]						
						ctb	csb	dmin	dic	r	cte	Total Aberration
Ne ions[b]	1×10^6	0.62	12	39	49	7	7	4	6	1	5	30
Ne ions[b]	2×10^6	1.24	26	18	56	13	17	14	16	3	9	72
Ne ions[b]	4×10^6	2.48	34	13	53	32	43	27	26	8	20	156
Kr ions[c]	1×10^6	6.37	27	18	55	40	46	21	11	2	18	138
Kr ions[c]	2.5×10^6	15.93	34	10	56	68	72	41	15	7	28	231
Kr ions[c]	4×10^6	25.48	39	4	57	113	119	64	20	8	38	362
X rays												
X rays	–	2	30	54	16	11	13	6	7	2	3	42
X rays	–	4	47	35	18	13	26	17	24	6	2	88
X rays	–	7	66	10	24	19	41	53	52	11	6	182

[a]Abbreviated terms are: ctb = chromatid break; csb = chromosome break; dmin = double minute; dic = dicentric chromosome; r = ring chromosome; cte = chromatid exchange.

[b]10.6 MeV n^{-1}

[c]11.1 MeV n^{-1}

6.3.5.2.2 *Chromosome aberration studies in astronauts and cosmonauts*. Several types of chromosomal analyses have been used in published reports of radiation-induced chromosome damage in astronauts' lymphocytes from the Apollo missions (Kimzey *et al*., 1975), Gemini missions (Bender *et al*., 1967; 1968; Gooch and Berry, 1969), Skylab (Lockhart, 1977), and from Mir (Fedorenko *et al*., 2000; 2001; Obe *et al*., 1997; Sabatier *et al*., 1995; Testard *et al*., 1996; Yang *et al*., 1997). Lymphocytes from 17 astronauts with mission experience ranging from 0.5 to 18 months (8.4 months average) were examined by three of the groups of investigators, using either R-banding/Giemsa staining, fluorescence plus Giemsa staining, or FISH plus Giemsa staining. Results can be grouped into an analysis of lymphocytes from crew members who flew short missions lasting two to three weeks, or longer missions of 6 to 18 months duration. The observations from all three publications indicate that the short-duration missions resulted in no significant detectable differences in the aberrations measured after the flight, compared to the control blood samples. The number of breaks per aberrant metaphase was less than three, and no complex chromosomal rearrangements were detected from the short missions.

On longer missions, significant heterogeneity was observed among individuals. After six months in space, some damaged metaphases exhibited up to 19 breaks, and were described as rogue cells, after the definition of Awa and Neel (1986). Chromosome-type, but not chromatid-type, aberrations were significantly elevated after space flights when compared to preflight value. Sister chromatid exchanges were similar in pre- and post-flight measurements. The significance of these data is unknown. The restricted nature of these limited studies warrants further investigation. Analysis of physical dosimetry onboard Mir revealed considerable variation across the core module, but showed that the crew skin exposure rate was ~1.13 mSv d^{-1} (Badhwar, 2000; Badhwar *et al*., 1998). In separate studies, the incidence of cytogenetically abnormal rogue cells in peripheral blood did not correlate with exposure to low-LET ionizing radiations (Mustonen *et al*., 1998). Viral infections can also lead to chromosomal rearrangements and may be a confounder (Duensing and Munger, 2002; Fortunato and Spector, 2003; Fortunato *et al*., 2000; Neel, 1998).

Most pertinent to estimating the level of radiation exposure in space are the biodosimetric estimates that have been made of effects during airflight and in LEO. Cytogenetic investigations have been made on flight personnel (Heimers *et al*., 1995; Romano *et al*., 1997; Scheid *et al*., 1993). Many of these studies demonstrated increased dicentric and ring levels in peripheral blood lymphocytes,

but the studies suffered from the limitations of inadequate statistics, and inadequate dosimetric information on individual radiation exposures. A more comprehensive set of studies has been conducted on female cabin attendants with age- matched controls with desk jobs (Wolf *et al*., 1999a; 1999b). The results of measurements of the mean frequencies of dicentrics and ring chromosomes per 1,000 cells, as well as sister chromatid exchanges (SCEs) on the volunteers studied indicated that when compared with controls, cabin attendants have no elevation of the frequencies of dicentric and ring chromosomes and SCEs (Wolf *et al*., 1999a). However, an unexplained high frequency of multi-aberrant rogue cells was reported in both flight personnel and in controls. This inhomogeneous group was considered inadequate to make any conclusions regarding possible biological effects of radiation exposure during long-distance flights. The challenges of measuring biological dosimetry for astronauts have been reviewed by Testard and Sabatier (1999). Notably, they concluded that the scoring of dicentric chromosomes for biological dosimetry is suitable when samples could be obtained soon after acute exposure to nearly uniform whole-body irradiation, and in addition it provides the easiest, most sensitive and least expensive method of estimating radiation dose. However, this kind of biodosimetry on space missions lasting several months or more may not be reliable because of the large variability observed among individuals in the rate of loss of cells with dicentrics as pointed out by Straume and Bender (1997). On the other hand the frequency of reciprocal translocations is known to be relatively constant for up to 30 y after exposure (Awa *et al*., 1978). However, laboratory work on the lifetime persistence and clonality of chromosome aberrations in the peripheral blood of mice acutely exposed to ionizing radiation has indicated that the persistence of translocations is complicated by aging and clonal expansion, and that these factors must be considered when quantifying translocations at long times after exposure since there can be a loss of nonpersistent locations with time, and a gain of translocations by clonal expansion or aging (Fedorenko *et al*., 1999; Spruill *et al*., 2000).

Chromosome exchanges have been measured in the blood lymphocytes of eight crew members after their respective space missions using FISH with chromosome painting probes (George *et al*., 2001c) (Table 6.5). In agreement with the previous reports by Obe *et al*. (1997) and Testard *et al*. (1996), significant increases in chromosome aberrations were observed after the long-duration missions. The frequencies of exchanges were similar for a crew member whose samples were collected 9 and 114 d after a long-duration mission, and for another crew member whose values were

measured on the day of return and were compared to values measured 240 d after flight, indicating that the clearance of aberrations from the blood lymphocytes is insignificant over these periods. No increase in the frequency of simple reciprocal translocations was detected in a crew member after a flight lasting over four months, although the frequency of total and complex-type aberrations had increased significantly. Only one rogue cell was found among the analysis of 26,931 metaphase postflight samples from six astronauts after long-duration missions where the analysis involved only a fraction of the genome. Obe *et al*. (1997) and Testard *et al*. (1996) detected only two and five rogue cells in 5,317 and 9,984 metaphases, respectively, after long-duration missions, using techniques that involved assessment of the whole genome. The *in vivo* dose was derived from the frequencies of translocations and total exchanges using calibration curves. RBE was estimated by comparison with individually measured physical absorbed doses. The values for mean RBE were compared to the mean quality factor from direct measurements of the lineal energy spectra using a TEPC and radiation transport codes. The ratio of aberrations identified as complex was slightly higher after flight, which is thought to be an indication of exposure to high-LET radiation. The effects of the enhanced cell-cycle delay after high-LET radiation were evaluated by analyzing chromosome damage in PCC samples collected from two crew members before and after a short-duration mission. The yield of chromosome exchanges was slightly higher in PCC samples than in metaphase samples for one crew member after a 10 d mission. It is possible that the expression of complex chromosome damage after flight could be influenced by a complicated pattern of mitotic delay after exposure to the mixed radiation field in space and that the damage is, therefore, underestimated in metaphase analysis.

Recent chromosome aberration dosimetry on 39 cosmonauts after no missions, single or multiple space flights points to changes in the immune system under microgravity and/or adaptive response to space radiation, since there appears to be an increased radioresistance to chromosome aberrations after multiple space flights (Durante *et al*., 2003). Dicentrics measured in lymphocytes taken pre- (no missions in space) and postflight were compared for short-duration versus long-term flights. There were no statistically significant differences between the preflight background frequency in the short- and the long-term mission crew members. In cosmonauts returning from short-term flights, there was a slight increase in dicentrics that was just at the margin of significance ($p = 0.04$), presumably at the detection limit of the technique.

Table 6.5—*Frequencies of chromosome aberrations measured before and after space flight (George et al., 2001c).*

Crew Member	Sample Collection	Cells Scored	Chromosomes Analyzed	Apparent Simple Translocations		Complex Exchanges		No.	Total Exchanges Frequencies ± SD ($\times 10^{-3}$)	Total Exchanges Extrapolated to the Whole Genome (frequencies $\times 10^{-3}$)	Translocations Extrapolated to the Whole Genome (frequencies $\times 10^{-3}$)
				No.	Frequencies ± SD ($\times 10^{-3}$)	No.	Frequencies ± SD ($\times 10^{-3}$)				
1	Before flight	4,404	1 + 2	19	4.3 ± 1	1	0.2 ± 0.2	24	5.4 ± 1.1	18.9 ± 3.8	15 + 3.5
	10 d after flight	6,556	1 + 2	27	4.1 ± 0.8	7	1.1 ± 0.4	42	6.4 ± 1	22.4 ± 3.5	14.9 + 2.8
2	Before flight	1,892	1, 2 + 4	5	2.6 ± 1.2	1	0.5 ± 0.5	6	3.2 ± 13	7.6 ± 3.2	6.3 + 2.8
	12 d after flight	4,677	2 + 1	20	4.3 ± 1	2	0.4 ± 0.4	23	4.9 ± 1	17.1 ± 3.5	15 + 3.5
3	Before flight	3,995	2 + 4	4	1 ± 0.5	0	0	4	1 ± 0.5	3.8 ± 1.9	3.8 + 1.9
	Day of return	4,056	2 + 4	9	2.2 ± 0.7	2	0.5 ± 0.3	11	2.7 ± 0.8	10.3 ± 2.7	8.4 + 2.7
	240 d after flight	4,745	2 + 1	14	2.9 ± 0.8	2	0.4 ± 0.3	18	3.8 ± 0.9	13.3 ± 3.1	10.1 + 2.8
4	Before flight	3,792	2 + 4	12	3.2 ± 0.9	3	0.8 ± 0.5	17	4.5 ± 1.1	17.1 ± 4.2	12.2 + 3.4
	9 d after flight	4,843	2 + 4	30	6.2 ± 1.1	3	0.6 ± 0.4	38	7.8 ± 1.3	29.6 ± 4.9	23.6 + 4.2

	114 d after flight	3,604	2 + 4	20	5.5 ± 1.2	0	0	23	6.4 ± 1.3	24.3 ± 4.9	20.9 + 4.6
5	Before flight	742	2 + 4	3	4 ± 2.3	2	2.7 ± 1.9	5	6.7 ± 3	25.5 ± 11.4	15.2 + 8.7
	9 d after flight	2,630	2 + 4	19	7.2 ± 1.7	0	0	21	8 ± 1.7	30.4 ± 6.5	27.4 + 6.5
6	Before flight	2,852	2 + 4	7	2.4 ± 0.9	1	0.4 ± 0.4	8	2.8 ± 1	10.6 ± 3.8	9.1 + 3.4
	Day of return	4,672	2 + 4	26	5.6 ± 1.1	1	0.2 ± 0.2	30	6.4 ± 1.2	24.3 ± 4.6	21.3 + 4.2
	9 d after flight	3,147	2 + 4	13	4.1 ± 1.1	1	0.3 ± 0.3	19	6 ± 1.4	22.8 ± 5.3	15.6 + 4.2
7	Before flight	2,962	1, 2 + 5	5	1.7 ± 0.7	1	0.3 ± 0.3	7	2.4 ± 0.9	6.2 ± 2.3	4.4 + 1.8
	Day of return	4,287	1, 2 + 5	7	1.6 ± 0.6	1	0.2 ± 0.2	10	2.3 ± 0.7	6 ± 1.8	4.2 + 1.6
8	Before flight	712	1, 2 + 5	1	1.4 ± 1.4	0	0	1	1.4 ± 1.4	3.6 ± 3.6	3.6 + 3.6
	Day of return	2,529	1, 2 + 5	4	1.6 ± 0.8	0	0	4	1.6 ± 0.8	4.1 ± 2.1	4.1 + 2.1

In contrast, a highly statistically significant increase ($p < 0.001$) was measured in the pooled sample from 15 crew members returning from their first long-term flight. The mean absorbed dose in crew members of short- and long-term space flights was ~4.3 and 78 mGy, respectively. Using *in vitro* dose-response curves and in comparison to the published literature, the observed increase of dicentrics after long-term missions would correspond to a dose equivalent of ~0.2 Sv.

Analysis of the 12 cosmonauts involved in numerous long space missions, two of whom also participated in short missions over a period of 15 y provided a unique opportunity to evaluate the risk of dicentrics. The average time between two consecutive missions was ~2.5 y. The concept of cumulative absorbed dose is difficult to interpret with the measurement of dicentrics, since it is known that the yield of radiation-induced aberrations in lymphocytes declines after an acute exposure. Obe *et al*. (1999) estimated that assuming a half-life of 3 y for dicentrics in lymphocytes, ~50 % of the dicentrics from the first flight would be lost in the cosmonauts. Figure 6.29 presents detailed dicentric data from cosmonauts involved in multiple flights and indicates that the yield of dicentrics increases during the first mission, and declines with time after the first mission, but subsequent missions lead to less aberrations than the first mission. The time-course data in Figure 6.29 suggest a faster decline in the yield of dicentrics during the time interval between two missions than was estimated by Obe *et al*. (1999). It is also apparent that postflight samples after repeated flights present a smaller increase in aberrations than the first flight, and that the yield of stable translocations after repeated missions is similar to background levels, despite the increased total absorbed dose from multiple flights. The interpretation of these data is complex, and could relate to a number of factors, including the effects of microgravity on lymphocyte pools, declining survival of lymphocytes with chronic exposure, or adaptive responses related to a hormetic mechanism. When the yield of dicentrics in cosmonauts involved in multiple space flights is plotted versus the time in LEO, there is a pronounced inter-cosmonaut variability in the response after repeated space flight, and only a weak negative correlation of dicentrics with time in space that is not statistically significant. It is obvious that biodosimetry of this type in space travel will require much more basic research to clarify the combined mechanisms of action of the multiple stressors in space.

6.3.5.2.3 *Laboratory studies of particle-induced aberrations.* To clarify some of these ambiguities, comprehensive chromosome

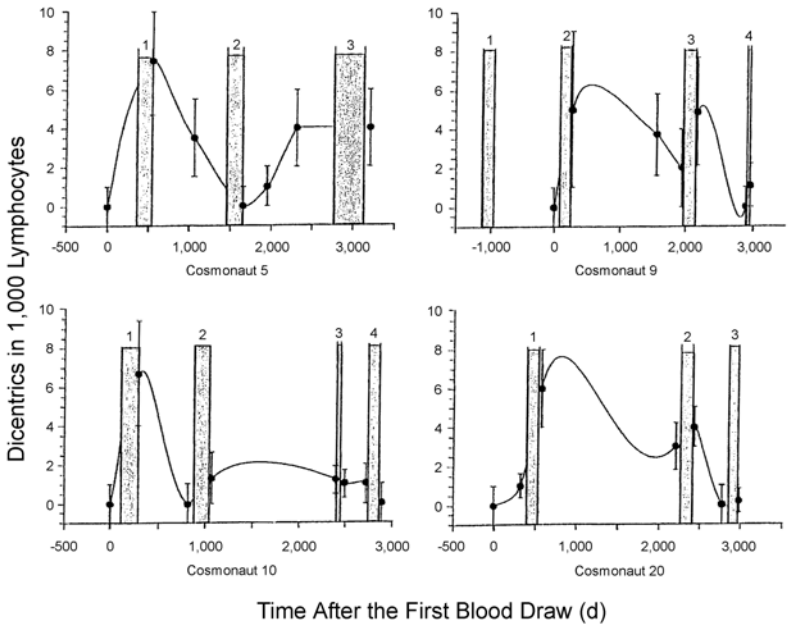

Fig. 6.29. Time course of dicentric yields in lymphocytes from four cosmonauts involved in multiple space flights (Durante *et al*., 2003).

aberration studies using human lymphocytes irradiated *in vitro* with a wide assortment of particle beams (protons to gold) and LET values (0.4 to 1,393 keV μm^{-1}) in the dose range of 0.075 to 3 Gy have been completed (George *et al*., 2003).

Comparisons were made for dose response curves for chromosome exchanges induced by 250 MeV n^{-1} protons at high (0.2 to 0.7 Gy min^{-1}) or low dose (0.075 Gy h^{-1}) rates and measured by PCC technique or in metaphase samples. Dose response curves for chromosome exchanges, measured at first mitosis postirradiation using FISH with whole chromosome probes, were fitted with linear or linear-quadratic functions (Figure 6.30). RBE was calculated from the initial slope of the dose response curve for chromosomal damage with respect to low dose-rate alpha particles. The RBE values, which ranged from ~1 to 26 for total exchanges, increased with LET, reaching a maximum at ~150 keV μm^{-1}, and decreased with further increases in LET. Complex-type exchanges for doses up to 1.5 Gy were only observed after exposure with carbon, argon and iron at 500 MeV n^{-1} and 1 GeV n^{-1}. No significant increase in complex damage was detected below ~200 mGy for metaphase analysis, indicating the possibility of a threshold for the induction

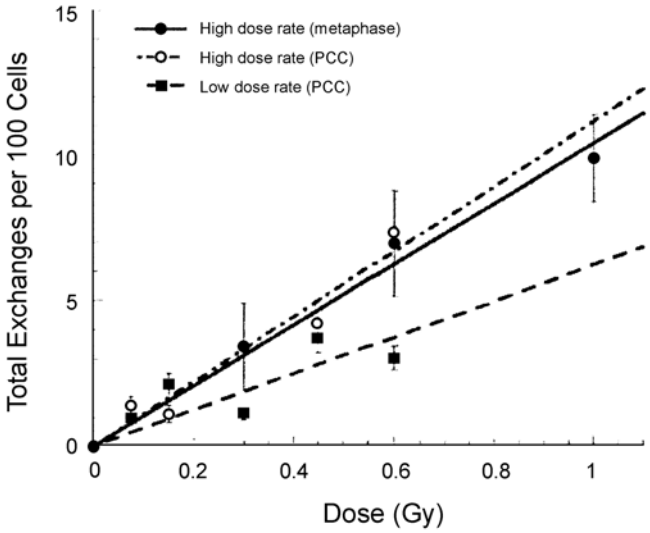

Fig. 6.30. Dose-response curves for whole genome equivalent yields of chromosome exchanges per 100 cells induced by 250 MeV n^{-1} protons delivered at high (0.7 Gy min^{-1}) or low (0.075 Gy h^{-1}) absorbed-dose rates and measured in interphase by PCC or metaphase at first division after *in vitro* exposure of human lymphocytes (George *et al*., 2003).

of complex type exchanges. RBE values for complex aberrations are undefined due to the lack of an initial slope for alpha particles. However, comparisons can be made of damage induced by 1 Gy of each particle studied. The effect of mitotic delay on RBE values was investigated by measuring chromosome aberrations in interphase after chemically-induced PCC, and values were threefold higher than metaphase analysis at the peak region of the curve, but frequencies of complex exchanges are similar in PCC and metaphase at LET values of 13 keV μm^{-1} and lower. However, the dose response for complex exchanges is linear quadratic with no apparent threshold when measured with the PCC technique. This result implicates a significant G2-M phase cell-cycle delay that hinders progression of many cells. These comprehensive studies confirm many previous investigations suggesting underestimation of chromosomal effects by high-LET radiations.

Separate *in vitro* studies have analyzed the true complexity of exchanges by analysis of chromosomes irradiated with either alpha particles or iron ions and compared then to low-LET radiation sources using mFISH (Anderson *et al*., 2002; Durante *et al*., 2002a). Both papers report that the high-LET radiations produced

more complex chromosome aberrations than the low-LET radiations. In the example of the mFISH analysis of iron ion irradiated cells, the data indicate that iron ions are more efficient than gamma rays per unit absorbed dose in the induction of chromosomal aberrations; they produce a high fraction of complex-type exchanges and aberrations. *In vitro* irradiation of human peripheral blood lymphocytes with accelerated iron ions (l GeV n^{-1}, 140 keV μm^{-1}) (Durante *et al*., 2002a) clearly shows (Figure 6.31) that a much higher fraction of cells have multiple aberrations after exposure to heavy ions, while more of the aberrant cells have only one aberration after exposure to low dose of gamma rays.

Alpha coefficients of the dose-response curves for total and simple exchanges measured in PCC or metaphase samples collected at one time after exposure, plotted as a function of LET, are shown in Figure 6.32 (George *et al*. 2003). Chromosome aberrations were investigated in human lymphocytes after *in vitro* exposure to ^{1}H-, ^{3}He-, ^{12}C-, ^{40}Ar-, ^{28}Si-, ^{56}Fe-, or ^{197}Au ion beams, with LET ranging from ~0.4 to 1,393 keV μm^{-1} in the dose range of 0.075 to 3 Gy. Dose-response curves for chromosome exchanges, measured at the

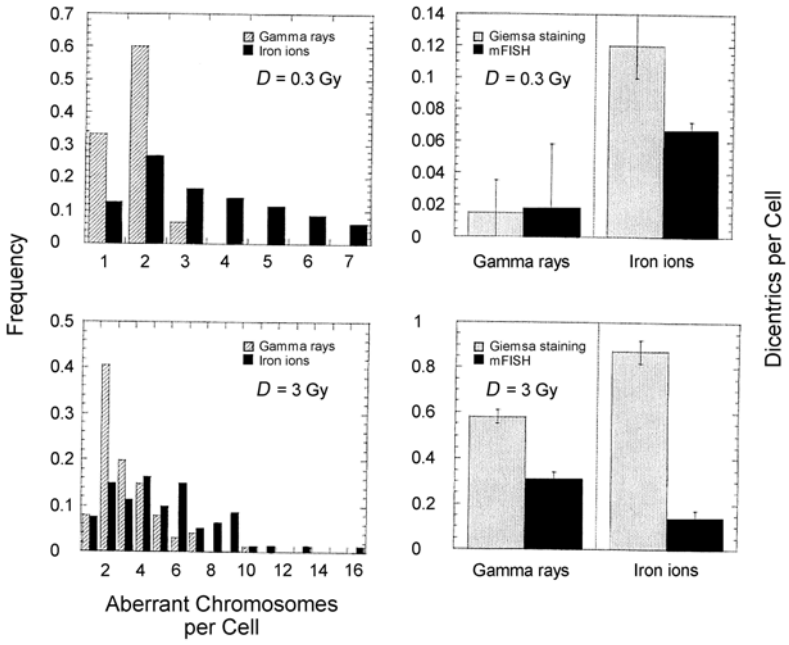

Fig. 6.31. mFISH chromosome analysis after heavy-ion exposure (Durante *et al*., 2002a).

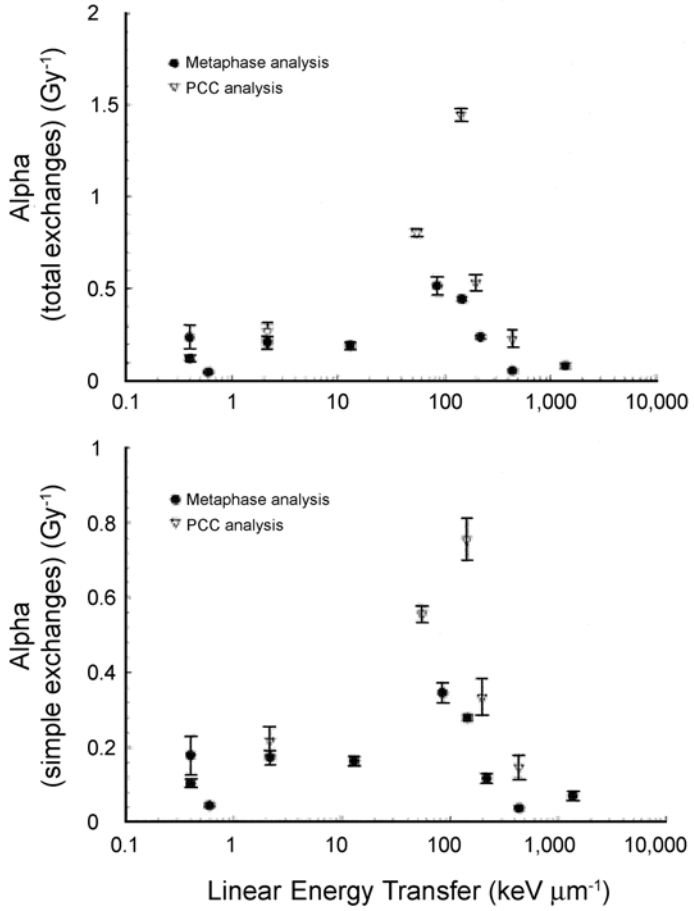

Fig. 6.32. Alpha coefficients of the dose-response curves for total and simple exchanges measured in PCC or metaphase samples that were collected at one time after *in vitro* exposure of human lymphocytes and plotted as a function of LET (George *et al*., 2003).

first mitosis postirradiation using FISH with whole-chromosome probes, were fitted with linear or linear-quadratic functions. RBE was estimated from the initial slope of the dose-response curve for chromosomal damage with respect to low or high dose-rate gamma rays. Estimates of RBE_{max} values for mitotic spreads, which ranged from near 0.7 to 11.1 for total exchanges, increased with LET, reaching a maximum at ~150 keV μm^{-1}, and decreased with further increase in LET. RBEs for complex aberrations were undefined due to the lack of an initial slope for gamma rays.

Additionally, the effect of mitotic delay on RBE values was investigated by measuring chromosome aberrations in interphase after chemically-induced PCC, and values were up to threefold higher than for metaphase analysis.

Chromosome aberrations after 1 GeV n^{-1} iron ion exposures measured in bone marrow, in the trachea, and in lung of Wistar rats have been shown to be induced by as low a dose as 0.5 Gy (Brooks *et al*., 2001). The frequency of chromosome aberrations induced by HZE particles was ~3.2 times higher than that observed after exposure to ^{60}Co gamma rays, but less than expected from radon alpha-particle studies. Microdosimetric calculations indicated that at least part of the cytogenetic damage measured was caused by the delta rays from the primary iron ions.

There is a major need to investigate the effects of exposure to low-LET radiations at lower doses, and dose rates, and over longer time scales.

6.3.5.2.4 *Potential link between chromosome aberrations and cancer risk*. The ultimate consequences to an individual who shows evidence of chromosomal rearrangements measured with biodosimetric assays is unknown. Recently, the presence of a correlative association between the frequency of chromosomal aberrations in peripheral blood lymphocytes and the risk of cancer has been suggested by epidemiological studies (Hagmar *et al*., 1998). This study involved a group of 3,541 healthy subjects from five European countries who were screened for chromosomal aberrations over a period of three decades. The subjects were divided into three categories (low, medium or high) based on percentiles of chromosomal aberration frequencies and were followed over time for cancer incidence or mortality. Both outcomes were significantly increased for the high-frequency group, in which the occurrence of cancer was more than double that of the subjects in the low-frequency group. Figure 6.33 shows the impact of the frequency of chromosomal aberrations on the survival analysis of incidence (in Nordic countries), and of mortality (in Italy). A linear relationship between stable chromosome translocations and cancer risk has also been demonstrated for the atomic-bomb survivors (Stram *et al*., 1993). The results suggest that the yield of chromosomal aberrations in lymphocytes is a relevant biomarker for cancer risk in humans, reflecting both the genotoxic effects of carcinogens and the individual cancer susceptibility. Chromosomal aberrations are early events in the pathway linking exposure to cancer. Therefore, intervention based on this biomarker offers a possible potential for prevention, especially for those at high risk. Anderson *et al*. (2003)

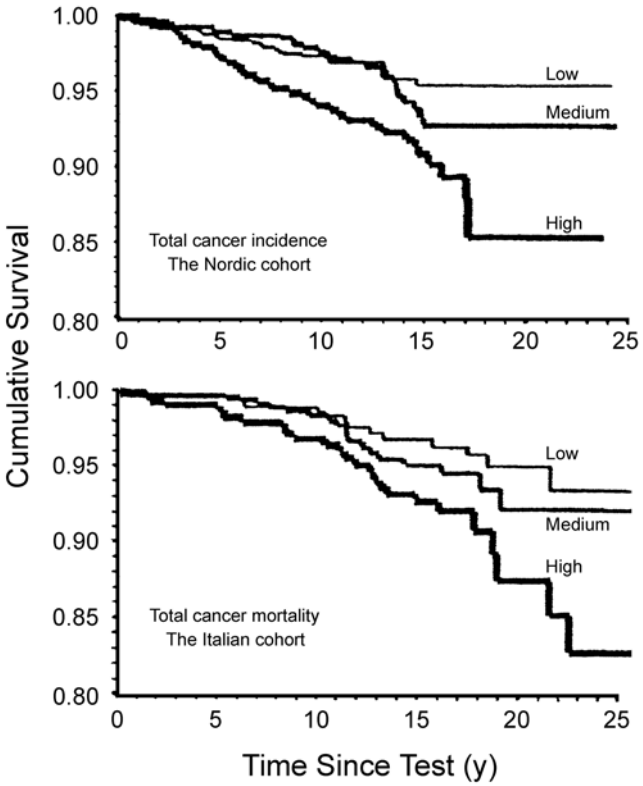

Fig. 6.33. Cohort study results of survival analyses of incidence (time from chromosomal aberration test to the first diagnosis of cancer) (Nordic countries) and mortality (time from chromosomal aberration test to death) (Italy) in the European Study Group on Cytogenetic Biomarkers and Health (Durante *et al*., 2001). Note that "time since test" refers to when the blood was drawn for the measurement of the chromosomal rearrangements. The three curves correspond to subjects classified as low chromosomal aberrations (1 to 33rd percentile), medium chromosomal aberrations (33 to 66th percentile), and high chromosomal aberrations (66 to 100th percentile).

have proposed a profile of damage that relies on the presence of insertions, a low frequency of stable simple reciprocal translocations of the type called 2B,[14] and significantly, the complexity of the damage initially induced. They suggest that the complexity of first- and second-division alpha-particle-induced nontransmissible complex aberrations reflects the structure of the alpha-particle track

[14]As originally defined by Gopinath and Burnham (1956).

and as a consequence adds radiation-quality specificity to the biomarker, increasing the signal:noise ratio of the characteristic 2B: insertion ratio.

Durante *et al*. (2001) have collected literature on space missions for information on the frequency of total chromosomal aberrations before and after flight (Fedorenko *et al*., 2001; George *et al*., 2001c; Obe *et al*., 1997; Testard *et al*., 1996; Yang *et al*., 1997) in order to estimate cancer risk. The data are summarized in Table 6.6. The algorithm of Schatzkin *et al*. (1990) was used to calculate the proportion of cases of a disease that is attributable to the intermediate endpoint, namely the attributable proportion. Evaluation of the attributable proportion considers the sensitivity of the assay and the relative risk. Durante *et al*. (2001) used this approach to estimate that the observed increase in chromosomal aberrations due to exposure to cosmic radiation is likely to increase the risk of cancer for astronauts 1.25 times (25 % increase). There are numerous uncertainties regarding this rough estimate of risk of cancer due to chromosomal aberrations. Peterson *et al*. (1993) have reported no increase in cancer risk in the small population of exposed astronauts.

6.3.6 *Other Tissue Effects*

6.3.6.1 *Skin Changes*. There are several issues regarding early skin changes due to radiation exposures in space. It is anticipated that shielding will prevent erythema and desquamation, however subclinical changes could predispose an individual to delayed wound healing. Recent studies with full-thickness human skin biopsy specimens obtained from cosmetic surgery have irradiated specimens with low doses of x rays down to 10 mGy (Goldberg *et al*., 2004). Gene expression changes in five core regulatory genes were assessed by real-time polymerase chain reaction, and results showed that low doses of radiation can produce changes in gene expression, though time- and dose-response relationships may be complex.

Mouse skin studies with low doses of iron ion beams investigating effects on laminin immunoreactivity have shown (Costes *et al*., 2000) that 1 h after exposure to 1 GeV n^{-1} iron ions over the dose range of 0.03 to 1.6 Gy, neither the visual appearance nor the mean pixel intensity of laminin in the basement membrane was altered compared to sham-irradiated tissue. However, the mean pixel intensity of laminin immmunoreactivity using several different antibodies was significantly decreased in epidermal basement membrane at 48 and 96 h after exposure to 0.8 Gy of iron ions. In

TABLE 6.6—*Results of cytogenetic analyses from different space missions (Durante et al., 2001).*

Space Mission	Number of Crew Members	Flight Duration (d)	Percentage of Aberrant Cells[a]		Frequency Ratio	Absorbed Dose (mGy)
			Before Flight	After Flight		
Mir 18 (Yang *et al.*, 1997)	2	115	4.4	8.9	2	42
ANTARES/ALTAIR (Testard *et al.*, 1996)	3	180	1.1	2	1.9	90
Mir/EUROMIR (Obe *et al.*, 1997)	6	120 – 198	0.6	2	3.5	61 – 101
Mir (Fedorenko *et al.*, 2001)	22	100 – 250	1.7	2.4	1.4	30 – 58
Shuttle/Mir (George *et al.*, 1999)	6	115 – 144	1.4	2.3	1.6	36 – 67
Total	39	100 – 250	1.8	3.5	2.1	30 – 101

[a]Percentages of aberrant cells, which include all types of aberrations, are evaluated as average values for the number of crew members specified in Column 2. Data from Yang *et al.* (1997) and George *et al.* (1999) were obtained using FISH with a combination of whole-chromosome probes specific for chromosomes 1, 2, 4 or 5, and then scaled to the whole genome. Data from Testard *et al.* (1996), Obe *et al.* (1997), and Fedorenko *et al.* (2001) were obtained from Giemsa-stained specimens. For after flight data (Column 5), sampling time after returning to Earth was between 0 and 180 d. The ratios of the fractions of aberrant cells (before and after flight) reported in Columns 4 and 5 are given in Column 6. Absorbed doses reported in Column 7 were measured by TLDs. In this column, dose ranges are reported when measured doses differed for the crew members studied.

contrast, collagen type IV, another component of the basement membrane, was unaffected. These studies demonstrate quantitatively that densely ionizing radiation elicits changes in skin microenvironments distinct from those induced by sparsely ionizing radiation.

There is a significant amount of literature on the early skin reactions of rodents to single and fractionated doses of various individual charged particle beams due to its significance in preclinical studies for heavy charged particle radiotherapy (Leith *et al*., 1975c; 1976; 1977; 1981b; 1982b). Skin RBE values for single dose fractions were 1.3 for helium peak ions, 1.5 for carbon peak ions, 1.7 for neon peak ions, and 1.9 for argon ions (Leith *et al*., 1975a). Human skin reactions were also scored in pilot studies with helium, carbon or neon ions (Blakely and Castro, 1994) and compared to an earlier analysis of RBE relative to dose per fraction by Field *et al*. (1976). The results indicated that skin reactions to stopping 400 MeV n^{-1} neon ions were comparable to fission neutron skin reactions for human, rat, pig and mouse skin.

6.3.6.2 *Endocrine/Hypothalamus*. The effects of radiation on endocrine function have been known for some time. Radiation-induced injury of the hypothalamic-hypophyseal axis can result in changes in endocrine homeostasis, as well as alteration of the morphologic integrity of most of the peripheral endocrine glands (Wigg *et al*., 1982). For example, therapeutic radiation doses as low as 0.4 Gy have led to adenomas or hyperplasias in the parathyroid gland that has a major role in calcium metabolism (Tezelman *et al*., 1995, Tisell *et al*., 1976; 1985). The exposure of atomic-bomb survivors who developed chief cell adenoma ranged from 0.01 to 5.6 Gy, with a mean absorbed dose of 0.4 Gy (Fujiwara *et al*., 1992).

Woodruff *et al*. (1984) reported pathologic changes in 15 autopsies performed on patients who had received highly-focused doses (56 to 116 Gy) of helium ion irradiation of the hypophysis for diabetic retinopathy or anterior lobe adenomas in six dose fractions. The autopsies performed 2.5 to 15 y after irradiation found fibrosis in all patients. In two patients the pituitary cells of the anterior lobe were processed with antibodies against TSH, ACTH, and growth hormone using the immunoperoxidase technique. The TSH-containing cells were more reduced in number than the ACTH- or growth hormone-containing cells. The endocrine organs under pituitary control showed varying degrees of atrophy, and clinical tests revealed progressive hypofunction. Hypothalamic-pituitary dysfunction following external beam irradiation is common but the reported incidence varies greatly, and patients must be

observed indefinitely for this possibility (Halberg, 1998). No information exists regarding endocrine function and homeostasis after chronic low dose-rate exposure to radiations found in space.

6.3.7 *Immune Deficiencies*

The immune system is affected by a number of stressors including exposure to radiation and microgravity. A brief description of the effects of radiation alone is provided.

The study of the effects of a total dose of 1.5 or 2 Gy of fractionated low-LET radiation at dose rates of 0.1 to 0.25 Gy administered over one week's time on the immune system is important, but its therapeutic value in inducing long-term remissions of tumors by stimulating the immune system has been controversial (Safwat, 2000). Numerous signs of immune system dysfunction in radiation-exposed populations have been reported. Since an impaired immune system promotes disease progression and initiation, both early and late effects of radiation on the immune system have been investigated. Kusunoki *et al*. (2001) found that the reduction in the phytohemagglutin response in heavily irradiated atomic-bomb survivors is dependent on a decrease in interleukin-2 (IL-2) producing CD4 T cells. When exogenous IL-2 was added to the peripheral blood lymphocytes of the heavily exposed individuals, the proliferative response to the mitogen was restored. In a follow-up study, the T cells of atomic-bomb survivors who received doses between <0.005 and 1 Gy were found to respond poorly to stimulation by *Staphylococcus aureus* toxins *in vitro*. The results clearly indicated that atomic-bomb irradiation led to an impairment of the ability of exposed individuals to maintain their native T-cell pools (Hayashi *et al*., 2003; Kusunoki *et al*., 2002a; 2002b).

Immunophenotyping of phytohemagglutin-activated mononuclear cells in Chernobyl liquidators who received between 150 to 500 mGy 13 y showed impaired T-cell function. Suppression of CD8+ T-cell propagation and augmentation of CD8+ T-cell propagation *in vitro* were both noted compared to control individuals (Kuzmenok *et al*., 2003). DNA synthesis in the mononuclear cells was markedly inhibited after activation for 3 d with suboptimal concentrations of phytohemagglutin, pokeweed mitogen and PMA. In contrast to control individuals, the monocytes of cleanup workers were able to stimulate the proliferation of T cells of healthy individuals but did not stimulate the proliferation of T cells of cleanup workers. Two recent papers have examined the acute effects of iron-particle radiation on immunity in population distributions (Pecaut *et al*., 2006), and with regard to leukocyte

activation, cytokines and adhesion (Gridley *et al*., 2006). Both papers indicate significant dose-dependent changes in cell-based immunity 4 d following single doses of 2 or 3 Gy, with fewer effects observed at 0.5 Gy

Kajioka *et al*. (1999) compared the effects of protons and ^{60}Co gamma radiation on cell-mediated and humoral immunological parameters. C57BL/6 mice were exposed to a single dose of 3 Gy protons (mid-peak of 3 cm 149 MeV protons) or gamma rays and intraperitoneally injected 1 d later with sheep red blood cells (sRBC). Subsets from each group were euthanized (along with non-irradiated controls with and without the sRBC injection) in a time course of 4, 10, 15 and 29 d after exposure. Body and relative spleen weights, leukocyte counts, spontaneous blastogenesis, lymphocyte populations, and anti-sRBC titers were evaluated. The data showed that whole-body irradiation with protons, or gamma rays at this relatively high dose resulted in marked, but transient immunosuppression in nearly all assays involving leukocyte populations as well as the spleen. On days 4 and 10 after irradiation B lymphocytes (CD19+) were the most radiosensitive, although reconstitution back to normal levels was observed by day 15. T cell (CD3+) and T helper cell (CD4+) recovery was evident by day 29, whereas the T cytotoxic cell (CD8+) count remained significantly below normal. Natural killer cells (NK1.1+) were relatively radioresistant. Anti-sRBC antibody production was slow and low titers were obtained after irradiation compared to the unirradiated controls. However, overall no significant differences were noted between the two types of radiation. Kajioka *et al*. (2000a) reported little differences with higher-energy protons at the entrance of the 250 MeV proton beam, compared to the mid 3 cm peak 149 MeV proton energy. Gridley *et al*. (2002a) reported on the dose and dose-rate effects of whole-body proton irradiation on leukocyte populations and lymphoid organs. C57BL/6 mice were exposed to the entry region of the proton Bragg curve to total doses of 0.5, 1.5, and 3 Gy, each delivered at a low dose rate of 1 cGy min^{-1} and high dose rate of 80 cGy min^{-1}. Nonirradiated and 3 Gy high dose rate gamma-irradiated groups were included as controls. At 4 d post-irradiation, highly significant radiation dose-dependent reductions were observed in the mass of both lymphoid organs and the numbers of leukocytes and T (CD3+), T helper (CD3+/CD4+), T cytotoxic (CD3+/CD8+), and B (CD19+) cells in both blood and spleen. A less pronounced dose effect was noted for natural killer (NK1.1+ NK) cells in spleen. Monocyte, but not granulocyte, counts in blood were highly dose-dependent. The numbers for each population generally tended to be lower with high dose rate than with low dose rate radiation; a

significant dose-rate effect was found in the percentages of T and B cells, monocytes, and granulocytes and in CD4+:CD8+ ratios. These data indicate that mononuclear cell response to the entry region of the proton Bragg curve is highly dependent upon the total dose and that dose-rate effects are evident with some cell types. Results from gamma- and proton-irradiated groups (both at 3 Gy high dose rate) were similar, although proton-irradiation gave consistently lower values in some measurements.

Gridley *et al*. (2002b), however, reported the effects of 0.1, 0.5, and 2 Gy iron ions on lymphoid cells and organs of C57B/6 mice at days 4 and 113 after whole-body exposure. The data collectively show that lymphoid cells and tissues are markedly affected by high-LET radiation at relatively low doses, that some changes persist long after exposure, and that different consequences may be induced by various densely-ionizing particles. The authors concluded that simultaneous exposure to multiple radiation sources could lead to a broader spectrum of immune dysfunction than currently anticipated.

There is a major need to investigate the effects of exposure to low-LET radiations at lower doses and dose rates. Few reports could be found on the effects of exposure to heavy particle beams on the immune system. This is a serious deficiency.

6.3.8 *Germ-Cell Sterility*

The literature (see review in NCRP, 2000) has indicated that human male germ cells are more sensitive to radiation-induced sterility than female germ cells. The recommended yearly and career limits provide protection from infertility in LEOs. Although there are protracted low dose data for low-LET radiations used in pediatric radiotherapy for cancer showing no significant increase in germ-line mutations or inherited genetic disease in their offspring (Boice *et al*., 2003; Rees *et al*., 2006), little information exists on the responses due to exposure of human germ cells to protracted doses of high-LET radiations expected for lunar and missions beyond LEO.

6.3.9 *Combined Stressors*

6.3.9.1 *Microgravity.* Without the effects of gravity, the human body experiences numerous physiological consequences that must be analyzed with the confounding additional stressors of launch and landing, as well as radiation exposure, and other environmental factors in space travel. Microgravity in space is known to affect

biological systems at a variety of levels (Vunjak-Novakovic *et al*., 2002), including loss of bone mass, muscle strength, and cardiovascular fitness in astronauts, even when they exercise regularly (Churchill, 1997; Hughes-Fulford and Lewis, 1996; Nicogossian *et al*., 1994). Microgravity also causes changes in plant cell growth and metabolism and in the swimming behavior of aquatic organisms (De Jong *et al*., 1996; Krikorian *et al*., 1992; Tripathy *et al*., 1996).

There are reports of changes in immune function of astronauts during space flight. In a review article Sonnenfeld and Shearer (2002) summarized information gleaned from both *in vitro* and *in vivo* studies. Early human studies have indicated that space flight changes human cell culture activities, such as leukocyte blastogenesis (Bechler *et al*., 1992; Cogoli, 1993; Cogoli *et al*., 1980; 1984), production of cytokines (Bechler *et al*., 1992; Talas *et al*., 1983), and signal transduction in leukocytes (Limouse *et al*., 1991; Schmitt *et al*., 1996). Studies on animal cell cultures have shown alterations in cytokine production (Chapes *et al*., 1992), and macrophage hematopoiesis and function (Armstrong *et al*., 1995). There is also a recent report of changes in neutrophil functions in astronauts (Kaur *et al*., 2004). The study indicated that neutrophil phagocytosis and oxidative functions are affected by factors associated with space flight and this relationship may depend on mission duration. Decreased nonMHC-restricted (CD56+) killer cell cytotoxicity has also been reported in astronauts after spaceflight (Mehta *et al*., 2001).

The effects of microgravity on leukocyte blastogenesis are very intriguing. Leukocytes from astronauts were placed in culture during a Space Shuttle mission and challenged with a mitogen to induce cell division (or blastogenesis). Blastogenesis of leukocytes is a requirement for a functional immune response. The leukocyte blastogenesis in flight was dramatically decreased compared to ground controls, or 1 g controls centrifuged in space flight. This was among the first demonstrations that microgravity could affect cell culture in space flight. However, when the cells were immobilized on beads, allowing lymphocytes undergoing division during blastogenesis to interact with accessory macrophages required for blastogenesis, the blastogenesis proceeded in a normal fashion. This led to the observation that factors that occur in space flight conditions other than microgravity, such as changes in shear stress and fluid dynamics that would interfere with interactions between cells, also play a role in the effects of space flight on leukocyte blastogenesis (see Sadhal, 2002 for an overview).

In space, a rotating bioreactor containing engineered cartilage was studied onboard Mir for a period of four months and an identical bioreactor was operated as a ground control (Freed *et al*., 1997). Constructs from the two groups had markedly different structure and function, and the observed differences were consistent with previous reports that musculoskeletal tissues remodel in response to physical forces and are adversely affected by space flight. Constructs grown on Mir (which floated freely in the bioreactor) tended to become more spherical whereas those grown on Earth settled, tumbled and collided with the vessel walls and maintained their discoid shape). A major limitation of this work was the lack of a 1 g control in space that would allow the separation of the effect of microgravity from other factors present during space flight. A fully automated cell culture unit for cell and tissue culture in microgravity at 1 g in space has been developed to overcome this issue (De Luis *et al*., 2002). The cell culture unit can accommodate diverse biological specimens in up to 24 individual culture chambers, each operated within a recirculation loop containing a gas exchanger, supply of medium and additives, a set of sensors, online sampling, and video microscopy. Ground testing in single-loop and single-event upsets prototype hardware have shown that diverse cell types can be cultured in the cell culture unit in a wide range of experimental conditions. There are commercial hardware choices from a NASA contractor for the study of biotechnology and bioprocessing in space (SHOT, 2006). These options should improve the acquisition of *in vitro* data on immune function as well as other biological endpoints.

In vivo studies of effects of microgravity on the immune system have not always yielded results similar to those data obtained *in vitro*. Talas *et al*. (1983) had cosmonauts in space flight obtain and culture leukocytes, and then challenge the cultures to produce interferon-α/β. The interferon production was greatly enhanced compared with controls. However, when the same cosmonauts who had donated the cells used for cultures in space had leukocyte samples challenged after they returned from space, interferon-α/β production was dramatically decreased compared with controls. The lymphocytes in culture would have experienced different fluid shear forces as well as a lack of neuroendocrine signals compared to the lymphocytes *in vivo* (Sonnenfeld and Shearer, 2002).

Early ground studies on immune function in mice maintained in an environment in which barometric pressure was altered in a similar way to space flight, revealed greater susceptibility to mengovirus infection than did mice maintained under normal barometric pressure conditions (Giron *et al*., 1967). Hind-limb unloading

(antiorthostatic 15 to 20 degree head-down tilt, with hypokinetic, and hypodynamic no-load suspension by raising the tail, or suspension with a harness) has been an effective model for some conditions that occur during space flight (Morey *et al*., 1979). With this model, muscle and bone changes occur that are similar to those after exposure to microgravity in the space flight environment. Involution of the thymus also occurs, but does not appear to have an effect on antibody production (Caren *et al*., 1980; Steffen and Musacchia, 1986).

Rats and mice have been used to investigate the effects of hind-limb unloading on cell-mediated immunity (Steffen *et al*., 1984). Interferon-α/β production was severely inhibited in rats and mice subjected to hind-limb unloading (Rose *et al*., 1984; Sonnenfeld *et al*., 1982). The mice required the head-down tilt for the inhibition effect to be seen, whereas the rats did not. The mice and rats regained the ability to produce interferon when they were allowed to recover in normal caging conditions. Interferon-γ production by spleen cells of hind-limb unloaded rats also was inhibited (Berry *et al*., 1991). Numerous studies have investigated how the hind-limb unloading model of microgravity affects the ability to combat infection. Evidence such as decreased production of superoxide and impaired killing of phagocytosed bacteria (Fleming *et al*., 1990), susceptibility to encephalomyocarditis virus D variant which correlated with the loss of interferon, and other pathogens (Belay *et al*., 2002; Gould and Sonnenfeld, 1987; Miller and Sonnenfeld, 1993; 1994) led to the conclusion that the hind-limb unloading model correlated to actual alterations in resistance to infection in space travel and can even lead to mortality. This is potentially a serious issue since threats to health normally combated by the immune system are enhanced in space flight due to a combination of enclosed environment and low gravity which can promote the growth of bacteria (Todd *et al*., 1999).

Sonnenfeld and Shearer have summarized effects of space flight on the immune system that have been observed from both studies *in vitro* and *in vivo* (Table 6.7) that followed the hind-limb unloading ground-based studies. The results of human studies are limited, but the data are also included in Table 6.7. Human ground-based models of space flight can mimic some of the conditions that occur during space flight, but none can re-create all space flight conditions. Delayed hypersensitivity skin test responses to common recall antigens which are a measure of cellular immune system function were determined during space flight and were found to be inhibited during short- and long-term space flights (Gmunder *et al*., 1994; Taylor and Janney, 1992). Recent studies in

TABLE 6.7—*Effects of space flight on the immune system (Sonnenfeld and Shearer, 2002).*

Effect	*In Vivo* or *In Vitro*
Leukocyte blastogenesis inhibited	Both
Thymic hypoplasia	*In vivo*
Cytokine production altered	Both
Leukocyte subset distribution altered	*In vivo*
Response to colony-stimulating factors inhibited	*In vivo*
Natural killer cell activity inhibited	*In vivo*
Delayed-type hypersensitivity inhibited	*In vivo*
Herpes viruses reactivated	*In vivo*
Immune responses of offspring of flown pregnant mice unaffected	*In vivo*

humans have investigated the effects of space flight on herpes virus and Epstein-Barr virus reactivation and have shown increases in urinary catecholamine excretion, an indicator of stress (Stowe *et al*., 2001a; 2001b). Persistent viruses have been associated with non-Hodgkin's lymphoma tumors (Vilchez *et al*., 2002) and raise concerns with regard to susceptibility of crew members to cancer. A short-term space flight study on the Space Shuttle showed no change in total immunoglobulin levels of astronauts compared with ground-based controls (Voss, 1984), but long-term space flight on a Soviet mission has indicated small increases in total immunoglobulin levels (Konstantinova and Fuchs, 1991). Significant levels of research on the effects of space flight on the antibody response to specific antigens have not yet been done, and are definitely needed to determine the true sensitivity of antibody responses to space flight conditions.

The combined stress of space flight and radiation exposure compound the complexities involved in the analysis of risk. Tables 6.8 and 6.9 from Horneck (1999) summarize the approaches that have been used to study the impact of microgravity on radiobiological processes by use of a 1 g centrifuge plus Biostack method, and the approaches that have been taken to study the impact of microgravity on radiobiological processes by use of a 1 g centrifuge plus additional radiation, respectively. Kiefer and Pross (1999) updated Horneck's (1988; 1992) comprehensive reviews of the results of these various approaches in an attempt to ascertain whether or not

TABLE 6.8—*Approach to study the impact of microgravity on radiobiological processes by use of a 1 × g centrifuge plus Biostack method (Horneck, 1999).*

Treatment	Space Parameter	Effects Caused By		
		Radiation	Microgravity	Interaction
Flight static	Microgravity, cosmic radiation	+	+ +	+ + +
Flight static + Biostack	HZE particles, microgravity, cosmic radiation	+ +	+ +	+ + + + +
Flight reference centrifuge	1 × g, cosmic radiation	+	–	–
Flight reference centrifuge + Biostack	HZE particles, 1 × g, cosmic radiation	+ +	–	–
Ground control	1 × g	–	–	–

TABLE 6.9—*Approaches to study the impact of microgravity on radiobiological processes using 1 × g centrifuge plus additional radiation (Horneck, 1999).*

Treatment	Space Parameter	Effects Caused By		
		Radiation	Microgravity	Interaction
Flight static	Microgravity, cosmic radiation	±	+ +	+ + +
Flight static and additional radiation	High-radiation dose, microgravity, cosmic radiation	+ +	+ +	+ + + + +
Flight reference centrifuge	1 × g, cosmic radiation	±	–	–
Flight reference centrifuge and additional radiation	High-radiation dose, 1 × g, cosmic radiation	+ +	–	–
Ground control	1 × g	–	–	–
Ground control and additional radiation	High-radiation dose, 1 × g	+ +	–	–

radiation effects are modified by microgravity (Table 6.10). This is an important aspect to estimating combined risks in space. In most cases, the biological samples were irradiated on the ground before the flight but in a few cases onboard radiation sources were used which mimic the real situation. The interactions were classified as additive (neither sensitization nor protection), synergistic (increased radiation effect under microgravity), or antagonistic (reduced radiation effect). Table 6.10 shows that the data are mixed in outcome, many merely additive effects, and some cases of synergistic actions were reported, and a few antagonistic situations. Most of the data in Table 6.10 have not been replicated, except for a few cases, namely, the induction of chromosomal aberrations in human lymphocytes (Bender *et al*., 1967), double-strand repair in yeast (Pross *et al*., 1994) and repair in bacteria and human fibroblasts (Horneck *et al*., 1996; 1997) in which a potentiation of radiation damage had originally been reported which could not be confirmed. It should be stated, however, that the techniques used to measure repair in these studies do not measure repair fidelity. Microgravity actually enhanced DNA repair for radiation-induced damage in the radioresistant bacterium *D. radiodurans* (Kobayashi *et al*., 1996). The first report of synergistic effects that was replicated was evidence for the developmental anomalies in the stick insect *C. morsus* (Bucker *et al*., 1986; Reitz *et al*., 1989; 1992). The development of the insect embryo is impaired by the action of particle radiation, and this effect is enhanced by microgravity. Separate studies not involving radiation exposure have confirmed that microgravity alone can interfere with fruit fly embryonic development (Vernos *et al*., 1989). Radiation combined with microgravity during space flight increased the frequency of developmental malformations in *D. melanogaster* after exposure to ^{85}Sr gamma rays (up to 14.32 Gy during space flight) (Browning, 1971). The anomalies included lethal mutations, visible mutations at specific loci, chromosome translocations and chromosome nondisjunctions. Synergism of space flight factors and radiation was observed in chromosome translocations and thorax deformations. Although the mechanism underlying the enhanced effects is unknown, it definitely appears that embryonic systems are susceptible to a synergistic interaction of radiation and microgravity. Except for the known enhanced effects of HZE radiations (Nagaoka *et al*., 1999), there is no evidence that microgravity in space flight enhances radiation-induced cell death, DNA replication or mutation frequency in *E. coli* (Harada *et al*., 1997; 1998a; 1998b), *B. subtilis* (Yatagai *et al*., 2000), *S. cerevisiae* (Fukuda *et al*., 2000), *D. Discoideum* (Harada

TABLE 6.10—*Radiation biology experiments in space (Kiefer and Pross, 1999).*

Test System, Year	Endpoint Studied	Mission, Duration	Irradiation	Effect
Human leukocytes, 1967	Chromosome deletion	Gemini 3, 5 h	^{32}P, 1.8 Gy in-flight	Synergistic
Human leukocytes, 1968	Chromosome deletion	Gemini 11, 72 h	^{32}P, 2.8 Gy in-flight	Additive
E. coli, 1971	Phage induction	Biosatellite II, 45 h	^{85}Sr, 17 Gy in-flight	Additive
Lettuce seeds, 1972	Chromosome aberration	Cosmos 368, 6 d	γ rays 100 Gy preflight	Additive
Hydrogenomonas eutrphia, 1972	Inactivation	Cosmos 368, 6 d	γ rays 60 Gy preflight	Additive
Saccharomyces ellipsoids, 1972	Inactivation	Cosmos 368, 6 d	γ rays 1.6 kGy preflight	Additive
Drosophila, 1974	Larvae mortality	Biosatellite II, 45 h	^{85}Sr, 8 Gy in-flight	Synergistic
Drosophila, 1974	Genetic effects in sperm	Biosatellite II, 45 h	^{85}Sr, 1.4 Gy in-flight	Synergistic
Neurospora, 1974	Inactivation mutagenesis	Biosatellite II, 45 h	^{85}Sr, 90 Gy in-flight	Antagonistic/additive
Rat, 1978	Hematopoetic system	Cosmos 690, 22 d	^{137}Cs, 8 Gy in-flight	Additive
Lettuce seeds, up to 1982	Chromosome aberration	Cosmos 782, 19 d	γ rays 150 Gy preflight	Synergistic

Lettuce seeds, up to 1982	Mutagenesis	Salyut 7, 72 d	γ rays 100 Gy preflight	Additive
Arabidopsis seeds, up to 1982	Mutagenesis	Soyuz/Salyut	γ rays 300 Gy pre postflight	Additive/synergistic
Carausius morosus, 1986	Development anomalies	Spacelab D1, 7 d	Cosmic HZE particles in-flight	Synergistic
S. cerevisiae rad 54–3, 1994	DSB repair	IML-1, 9 d	80 kV x rays, up to 140 Gy preflight	Synergistic
Deinococcus radiodurans, 1996	DNA repair	IML-2, 14 d	γ rays, up to 12 kGy preflight	Antagonistic
Bacillus subtilis HA 101, 1996	Survival/CFA	IML-2, Repair, 14 d	UV 254 nm, up to 335 J m^{-2} preflight	Additive
E. coli B/r, 1996	DSB repair	IML-2, Kinetics, 14 d	X rays 150 kV, 120 Gy preflight	Additive
E. coli PQ37, 1996	SOS-system	IML-2, Kinetics, 14 d	^{60}Co rays, 300 Gy preflight	Additive
Human fibroblasts, 1996	Single-strand break repair	IML-2, Kinetics, 14 d	X rays 300 kV, 5 and 10 Gy preflight	Additive
S. cerevisiae rad 54–3, 1998	DSB repair	X ray	80 kV x rays, up to 140 Gy preflight	Additive
S. cerevisiae rad 54–3, 1998	DSB repair	Beta ray	^{63}Ni particles, up to 160 Gy in-flight	Additive

et al., 1997; Takahashi *et al*., 1997), *C. elegans* (Nelson *et al*., 1994), or human cells (Horneck *et al*., 1995; Ishizaki *et al*., 2001).

Rats have been irradiated with doses of up to 8 Gy of ^{137}Cs gamma rays on day 10 of the 20 d space flight on the biosatellite Cosmos 690 to investigate combined effects of radiation and space flight. Endpoints investigated were mortality, mobility, weight, behavior, the hematopoietic system, metabolism, muscles, and tissue histologies. For the majority of endpoints the radiation effects were the same in microgravity as on Earth at 1 g (Gurovsky and Ilyin, 1978). However, after irradiation in-flight, the regeneration of the hematopoietic system was remarkably delayed compared to the animals irradiated on the ground (Gazenko *et al*., 1978). A recent report found impaired spatial learning in rats exposed to hypergravity in ground based studies (Mitani *et al*., 2004).

Several mechanisms have been proposed to explain the synergistic action of microgravity and radiation. Todd (1993) proposed involvement of the convection-free environment in space affecting molecular processes. Horneck (1999) suggested that at the cellular level there might be an impact on signal transduction, receptors, metabolic-physiological state, chromatin, or membrane structure. She also suggested that at the tissue and organ level, there is potential modification of self-assembly, intercellular communication, cell migration, pattern formation or differentiation. Further well-controlled studies are necessary to resolve specific mechanisms of action. Disruption of nutritional balance and intake during space flight could also play a role in space-flight-induced alterations of immunity (Sonnenfeld and Shearer, 2002) and may be a potential approach to countermeasures for adverse immune effects (Table 6.1). There are several recent reports of stress hormone related reactivation of latent viruses in astronauts including Epstein-Barr virus (Stowe *et al*., 2001a), herpes (Stowe *et al*., 2001b), and varicella zoster (Mehta *et al*., 2004). More research with adequate controls and high levels of reproducibility for significance testing is needed on the ground and in space flight to confirm that altered nutrition in space can boost the immune system against the rigors of radiation and other stressors encountered in space flight (Durante and Kronenberg, 2004).

6.3.9.2 *Ultraviolet Light*. Solar UV radiation has beneficial (*e.g*., stimulating vitamin D synthesis in human skin), as well as deleterious effects on the human body, including suppression of the immune system (Aubin, 2003; Schwarz, 2002), activation of viruses (Rooney *et al*., 1992; Zmudzka *et al*., 1996), induction of premature aging of the skin (Yin *et al*., 2001), and the induction of cataracts

(West *et al*., 1998) and cancer. Exposure to UV light in the range of 280 to 315 nm is a recognized causative agent for skin cancer. The potential carcinogenic effects of both long (>340 nm) and short (315 to 340 nm) wavelength UVA have been reported to induce squamous cell carcinoma in mice (Kelfkens *et al*., 1991; Sterenborg and van der Leun, 1990). Since DNA absorbs only very weakly in the UVA region where oxidative lesions would be formed, it is assumed that UVA produces effects on DNA *via* indirect mechanisms (Setlow *et al*., 1993).

The complete mechanisms underlying UV effects are not well understood, but it is known that UV radiation moderates the expression of cell adhesion proteins (Meineke *et al*., 2002) and many different genes (Cridland *et al*., 2001; Kaina *et al*., 1999; Libertin *et al*., 1994; Paunesku *et al*., 2000; Wang *et al*., 1999).

The highly mutagenic short-wavelength UVC and far-UVB (<295 nm) radiation are filtered out by the dissociation of ozone in the stratosphere and do not reach Earth's surface, so that the terrestrial sunlight UV spectrum consists of UVB (295 to 320 nm) and UVA (320 to 400 nm). High-UV fluence rates of both UVC radiation (<280 nm) and higher doses of UVB are estimated on the Martian surface in comparison to the surface of Earth (Cockell and Andrady, 1999; Cockell *et al*., 2000; Ronto *et al*., 2003).

Several types of countermeasures have been investigated for UV photohazards, beyond the protection that can be offered by shelters, including topical applications of vitamin E (Moison *et al*., 2002), and a-tocopherol, L-ascorbic acid, a-lipoic acid, glutathione ethylester, and N-acetylcysteine (Rijnkels *et al*., 2003), the ethanol extract of the flowers of the Prunus persica (Heo *et al*., 2001), and the sun protection offered by fabrics (Laperre and Gambichler, 2003).

6.3.9.3 *Electromagnetic Fields.* Electric and magnetic fields are created around any electrical device whenever electricity flows. The energy expended can range from microwaves emitted by cell phones, to radiowaves from radar aircraft tracking systems, to very low-frequency wavelengths from video displays on computers, to extremely low-frequency wavelengths from transmission and distribution power lines. Mobile phone use in the microwave range between 400 to 2,000 MHz has undergone extensive scrutiny. Recent reviews of epidemiological studies on cell phone users and other evidence have shown no direct relationship between the fields from wireless communication systems and cancer risk (Boice and McLaughlin, 2002; Moulder *et al*., 1999; Tenforde, 1998). Other effects of mobile phone radiofrequencies have been reported

on human brain activity and sleep variables (Hamblin and Wood, 2002), melatonin metabolite excretion (Burch *et al*., 2002; Preece *et al*., 1999), and visual memory (Lass *et al*., 2002).

The scientific evidence suggesting that electromagnetic exposures at frequencies <100 kHz or 60 mT pose any health risk is weak but further study is warranted (Ahlbom *et al*., 2001; Bailey, 2002). The strongest evidence comes from the association observed in human populations with two forms of cancer, childhood leukemia and chronic lymphocytic leukemia in occupationally exposed adults. There is no consistent *in vitro* or animal laboratory data to prove a cause and effect relationship of these cancers with electromagnetic exposures, despite the fact that DNA damage by such exposures have been reported to occur in a dose-dependent way *in vitro* in some studies (Ivancsits *et al*., 2002; 2003). A review of the available literature by the National Institute of Environmental Health Sciences (NIEHS, 2002) and the International Commission for Nonionizing Radiation Protection Standing Committee on Epidemiology (Ahlbom *et al*., 2001) concluded that electromagnetic exposure cannot be recognized at this time as entirely safe, because of weak scientific evidence that exposure may pose a leukemia hazard, but there is insufficient rationale to warrant aggressive regulatory setting of limits. Recent research in cognitive impairment (Li *et al*., 2002) and in neurodegenerative diseases (such as amyotrophic lateral sclerosis and Alzheimer's disease) (Feychting *et al*., 2003; Graves *et al*., 1999; Li and Sung, 2003) and cardiac diseases associated with heart rate variability and myocardial infarction (Bortkiewicz *et al*., 1996; Repacholi, 1998) have identified some interesting and novel findings that need further research. Studies in transformed breast cancer cells exposed to electromagnetic fields (EMFs) can overcome effects of melatonin and Tamoxifen® in regulating cell growth (Brainard *et al*., 1999; Kliukiene *et al*., 2003). Adverse reproductive outcomes have also been reported to show some correlation with electromagnetic exposure (Shaw, 2001). Radiofrequency fields can affect some cellular physiological functions, but the significance of such effects for human health is uncertain. Two recent monographs on the biological effects of EMFs (ICNIRP, 2003; McKinlay, 2004) may be consulted for additional information.

Of some concern is the complete lack of information in the public literature regarding nonionizing EMF exposures onboard spacecraft during space flight. Without this information there is no way to judge whether space travel entails a greater exposure to EMFs than one would experience occupationally on Earth, or whether it exceeds recommended exposure guidelines. Complex

EMFs onboard a space craft will likely be created by the large number of electrically-powered instruments and equipment required to maintain a viable environment in space. Although the health hazards of EMFs are still not fully evaluated, it would be prudent to devise methods to reduce exposures. It is recommended that area EMF monitors be used to evaluate these exposures and shielding methods be sought for crew members. Research is needed to investigate interactive effects between EMFs of varying levels, and other stressors in the space-craft environment.

6.3.9.4 *Space Environmental Toxins and Other Factors*. Astronauts living in habitats outside Earth's gravitational field and protective atmosphere may be exposed to potentially toxic contaminants possibly accumulating in their small living space. These contaminants may cause chronic low-level exposures, or higher accidental exposures. The response of the human to chemical contaminants and toxicants in gas, liquid or solid phase may be quite different with the altered physiological status caused by adaptations to microgravity. These concerns have spawned a new specialty called space toxicology which is concerned with investigating such effects with the ultimate goal of protecting the astronauts' health and well-being (Oberdorster *et al*., 1994). No literature could be found that reported on the investigation of combined radiation and chemical contaminant toxicity under microgravity, or on radiation in combination with increased vibration or noise.

6.3.10 *Low Dose Effects Needing Further Research*

6.3.10.1 *Hormesis and Low Dose Adaptive Effects*. Radiobiological evidence for hormesis [*i.e*., a biological phenomenon characterized by biphasic dose-response relationships displaying low-dose stimulation and high dose inhibition (Calabrese and Baldwin, 2002)] is based on radioadaptive response which has been convincingly demonstrated in cells *in vitro* in human lymphocytes from some but not all donors (Wolff, 1998). Questions remain as to how it affects humans (Johansson, 2003). Several reviews of radiation hormesis (Ducoff, 2002; Prekeges, 2003; Rozman and Doull, 2003; Sugahara *et al*., 2002) suggest that radiation stress is just one type of homeostatic exercise that makes organisms more fit for future biochemical-physiological-immunological-radiation challenges. More significantly, hormesis has suggested a reappraisal of the way risks are assessed (Calabrese and Baldwin, 2003b). Since there are examples indicating that some individuals may lack the capacity to produce the low dose stimulatory response to either chemical or

physical agents such as ionizing radiation (Calabrese and Baldwin, 2003a) there must also be an accounting for the differential susceptibility in high-risk groups in the hazard assessment process, whether it be due to developmental processes, aging, genetic background, gender, nutrition, disease, or health status. Recent understanding of the mechanisms of radiation damage and repair, and discoveries of induction of gene expression by radiation and other genotoxic agents by adaptive effects make it seem inevitable that under certain suitable conditions, irradiation can potentially produce beneficial effects (Ducoff, 2002). Since manifestation of these responses is highly variable, they cannot be incorporated into risk estimates at this time. Risk assessment of occupational radiation exposure in space will not be complete, however, without more basic research to define the impact of low dose exposures on several endpoints such as cancer induction and immune response.

6.3.10.2 *Bystander Effect and Low Dose Hypersensitivity.* After more than three decades of investigations, insight into the production of molecular lesions by energy absorption from ionizing radiations is available, as well as a somewhat limited understanding of how molecular lesions are expressed and modified biologically. The identification of the biological target of radiation damage has been dominated by the concept that it is the DNA of the genome. However, notable exceptions provide evidence for nonDNA targets (*e.g.*, Cramp and Walker, 1974) the most prominent of which is the cell membrane. Oxygen sensitizing processes have been found to be associated with damage to cell membranes independent of DNA damage. Some of these radiation-induced membrane changes have later been linked to apoptotic cell death (Radford, 1999). Implicit in the generalizations for both of these targets, however, has been the assumption that biological effects of radiation would occur only in cells actually exposed in the radiation field. It still appears to be true that for radiation protection purposes, radiation risks are based on organ doses and, therefore, any contributions from bystander effects do not alter risks estimates.

The relatively recent increase in the interest of the bystander effect, that is effects on unirradiated cells from radiation-exposed neighbors, has confounded and challenged radiation researchers. It has been difficult to understand fully how unirradiated cells could be affected. The bystander effect was first noted as the induction of SCE by extremely low doses of alpha particles (Nagasawa and Little, 1992). Sister chromatid exchanges were observed in ~30 % of the cells, even though <1 % of the cells' nuclei received a direct

nuclear hit by an alpha particle. Several other bystander endpoints have been reported including confirmation of increased SCEs (Deshpande *et al*., 1996), increased chromosomal instability (Lorimore *et al*., 1998), increased mutations (Nagasawa and Little, 1999; Zhou *et al*., 2000), increased number of micronuclei (Prise *et al*., 1998b), increased cell killing (Bishayee *et al*., 1999), increased *in vitro* neoplastic transformation (Sawant *et al*., 2001), and increased accumulations of DNA damage-inducible proteins (Azzam *et al*., 1998; 2001; Hickman *et al*., 1994). Bystander effects have been reported both in systems where irradiated cells are in obvious direct contact with one another, and also when cells are considerable distances apart from one another (Prise *et al*., 1998a). Bystander effects have been reported after cells were subjected to high-LET alpha-particle irradiation (Azzam *et al*., 1998; Belyakov *et al*., 2002; Deshpande *et al*., 1996; Lorimore *et al*., 1998; Nagasawa and Little, 1992; Prise *et al*., 1998a), as well as in low-LET alpha-irradiation studies (Mothersill and Seymour, 1998; Seymour and Mothersill, 2000). Most bystander studies have used a variety of cell types, but primarily established cell lines. The alpha-irradiation studies of Mothersill and Seymour (2000) also included immortalized human keratinocytes, as did the alpha-particle work of Hickman *et al*. (1994) with immortalized rat lung epithelial cells. Few epithelial cell studies of bystander effect could be found in the literature (Belyakov *et al*., 2002; 2005; 2006).

Several mechanisms by which damage signals may be transmitted from irradiated to nonirradiated bystander cells have been proposed involving reactive oxygen (Narayanan *et al*., 1997), extranuclear originating signaling (Deshpande *et al*., 1996), and secreted diffusible factors and gap junction-mediated intercellular communication. The role of cell communication in the mechanism has been controversial (Azzam *et al*., 1998; 2001; Mothersill and Seymour, 1997a; 1998). A recent review by Ballarini *et al.* (2002) of pertinent literature clearly implicates cellular communication in bystander effects, but notes features of the bystander effect are strongly dependent on different factors. These include:

- the way in which the radiation is delivered (conventional irradiation with low doses, irradiation with microbeams, or treatment with irradiated conditioned medium. Medium taken from irradiated epithelial cells reduced survival of unexposed fibroblasts, whereas medium from irradiated fibroblasts had no effect on unexposed epithelial cells (Mothersill and Seymour, 1997a). This latter observation implicates a second difference, namely;

- differences in the cell type (normal or cancerous, human or animal, epithelial or fibroblastic), and the cell-cycle stage;
- degree of cell-to-cell contact;
- in the case of irradiated conditioned medium, the number of irradiated cells and possibly the medium constituents affect bystander effects; and
- the particular endpoint being studied.

Cells are equipped with several systems that allow them to send or to respond to signals from other cells. These systems include molecular receptors, kinases, phosphatases, GTP-binding proteins, and several other molecules. Secreted factors can affect cells of the same type (autocrine signalling), or act on neighboring cells (paracrine signalling), or travel *via* the blood supply to affect distant target cells (endocrine signalling). Available *in vitro* data on bystander effects are thought to be associated mainly with paracrine and/or autocrine signaling (Ballarini *et al*., 2002). If cells are in close contact, gap-junctions seem to have a major role, whereas if the degree of contact is poor, the culture medium can be important. Inhibition of gap-junction activity in cells irradiated in close contact resulted in decreased levels of cell death (Mothersill and Seymour, 1997b), p53/p21 induction (Azzam *et al*., 1998), and gene mutations (Zhou *et al*., 2000). In contrast, a microbeam experiment performed with minimal cell-to-cell contact resulted in a random distribution of damaged cells over the entire surface of the culture dish (Belyakov *et al*., 2001), suggesting a major role of an extracellular factor released in the medium, rather than gap-junctions.

Information on radiation-induced bystander effects comes primarily from *in vitro* tissue culture experiments. It is not known what types of bystander effects might be observed in three-dimensional tissues or intact organisms, or how these effects might be modulated at doses <100 mGy. It is reported that a similar phenomenon, namely the production of clastogenic factors by irradiation of cells, can occur either *in vitro* or *in vivo* (Faguet *et al*., 1984). Lymphocytes cultured in medium containing plasma from irradiated individuals can result in significantly more chromosomal aberrations than in lymphocytes cultured with plasma from nonirradiated individuals. These effects can be extremely persistent in irradiated individuals with clastogenic activity persisting for several decades. Others have failed to find such effects (Leonard *et al*., 1998). It has been recently suggested that extracellular signaling through the microenvironment may link bystander effects, genomic instability, and carcinogenesis (Barcellos-Hoff and Brooks, 2001).

A significant hypersensitivity of V79 Chinese hamster cell survival at low doses (0.1 Gy) of high-energy (100 MeV n^{-1}) carbon ions at a LET of 27.5 keV μm^{-1} has been reported using a semi-automated cell detection system (Bohrnsen *et al*., 2002). This result is in contrast to the report of Marples *et al*. (1996) that showed a barely detectable hypersensitivity in the irradiation of V79 Chinese hamster cells with peak pions at an approximately equivalent LET of 35 keV μm^{-1}. Bohrnsen *et al*. (2002) speculate that the much more pronounced effect of carbon ions could possibly be due to the wider microscopic pattern of energy deposition from carbon particle tracks compared to pi mesons. Increased sensitivity at low doses of neutron irradiation at very low dose rates has also been reported (Dionet *et al*., 2000). The phenomenon of hypersensitivity occurs in most cell lines tested, and it is attractive to suggest that it is due to the bystander factor being produced at low doses in these cells. However, the data do not support this hypothesis and in fact suggest that hypersensitivity and bystander mechanisms are actually mutually exclusive (Mothersill *et al*., 2002). Most of the cells producing a bystander effect do not produce a hypersensitivity effect. Hypersensitivity is not found in normal epithelial cells having survival curves with small shoulders but, rather, is predominately found in radioresistant tumor cells having survival curves with large shoulders.

In summary, it is not always valid to extrapolate experimental results to low doses from studies at high doses. Biological responses vary with dose and LET, and have variable time-dependent effects after exposure (Skov, 1999). Unfortunately, as has been pointed out by Skov (1999), because of the scant knowledge of all of the relevant aspects at low doses, such as inducible-protective mechanisms, threshold, priming, dose-rate effects, and LET-dependent variables, it is not possible currently to draw conclusions for radiation protection. More basic research optimized technically to study effects of radiations found in space is needed on individual cells.

6.3.10.2.1 *Epigenetic effects*. Epigenetics is defined as the study of heritable changes of DNA that can regulate gene expression but do not involve changes in DNA sequence (Baylin and Herman, 2000). The genetic information provides the blueprint for the manufacture of all the proteins necessary to create living things, while the epigenetic information provides additional instructions on how, where, and when the genetic information should be used (Dunn *et al*., 2003). With the recent completion of the human genome sequencing project, the challenge now is to understand the regulation of gene function, which to a large extent is dependent on

epigenetic controls. Epigenetic changes which are often deregulated in cancer cells include modulation of chromatin structure, repression of transcription, genomic imprinting, inactivation of the X chromosome, and suppression of detrimental effects of repetitive and parasitic DNA sequences on genome integrity (Dunn *et al*., 2003). Modulators of DNA methylation and chromatin structure have a dramatic effect on gene expression, cellular proliferation, differentiation, and apoptosis, and these molecular pathways of epigenetic events are being exploited for therapeutic inventions (Kalebic, 2003). Aberrations in epigenetic machinery, either by genetic mutations, or by somatic changes such as viral infections, are associated with early alterations in chronic diseases such as immunodeficiency (Muegge *et al*., 2003).

6.3.10.2.2 *Cytokine activation leads to remodeling of the extracellular matrix*. The nonuniform ionization patterns associated with the signature track structure of each kind of charged particle results in differences in the induction of gene expression for low- and high-LET radiations (Woloschak and Chang-Liu, 1990) and differences in the activation of proteins in tissues and in the supporting microenvironment. This is exemplified by transforming growth factor beta 1 (TGFβ1), the activation of which is dependent on both radiation quality and dose (Barcellos-Hoff, 1993; 1998). TGFβ is the founding member of a large family of polypeptide growth factors that are abundant extracellularly in a latent form, and is one of the important regulators of the extracellular matrix. Latent TGF consists of a complex of TGF noncovalently associated with its processed N-terminal prosegment, called the latency-associated peptide (LAP). Release from the LAP is required for TGF to bind to its cell surface receptors. Activation releases TGF which then acts as the switch to initiate the response of tissue to damage in several physiological processes, such as inflammation, wounding and healing (Barcellos-Hoff, 1998). Using an immunostaining protocol to discriminate between latent and active TGF and neutralizing antibodies to confirm functional significance, Barcellos-Hoff *et al*. (1994) found that within 1 h after exposure to 5 Gy of sparsely ionizing radiation, there was increased TGF reactivity in the epithelium and stroma concomitant with decreased LAP immunoreactivity. This reciprocal shift in immunoreactivity is consistent with a process in which LAP is degraded after release of TGF, as would occur with activation. This activation persisted for >7 d after irradiation and included changes in Collagen III, a known target of TGF, suggesting there is a chronic stimulus for activation of TGF.

Administration of TGF neutralizing antibodies shortly before irradiation specifically inhibited the Collagen III changes. Ionizing radiation is the first exogenous stimulus known to cause activation of latent TGF *in situ* (Barcellos-Hoff *et al*., 1994). Several studies have now reported increased expression of TGF in irradiated tissues that develop fibrosis leading to the suggestion that TGF is an early radiation response that mediates late tissue reaction (Anscher *et al*., 1990; Canney and Dean, 1990). The mechanism of TGF activation by radiation is under investigation, but there is significant evidence that TGF may itself signal certain events through the generation of reactive oxygen (Shibanuma *et al*., 1991; Thannickal and Fanburg, 1995). It has been suggested that persistent disruption of the microenvironment in irradiated tissue compromises its ability to suppress carcinogenesis (Barcellos-Hoff, 2001). The fact that normal cells can exert epigenetic control on neoplastic behavior, and that by re-establishing appropriate interactions of normal cells with their microenvironment can reverse neoplastic behavior even in the presence of grossly abnormal genetic damage, can provide new strategies to prevent cancer (Weaver *et al*., 1997; Zutter *et al*., 1995).

Significant for space travel is the fact that stromal remodeling can be triggered by doses of HZE particles as low as 0.8 Gy (Ehrhart *et al*., 1997). In BALB/c mice receiving whole-body irradiation with 0.8 Gy of 600 MeV n^{-1} iron ions, Collagen III was induced in the adipose stroma within 1 d, continued to increase through day nine and was resolved by day 14. Immunoreactive tenascin was induced in the epithelium by day one, was evident at the epithelial-stromal interface by day five to nine and persisted as a condensed layer beneath the basement membrane through day 14. These findings parallel similar changes induced by alpha irradiation but demonstrate different onset and chronicity. In contrast, the integrity of the epithelial basement membrane, which was unaffected by sparsely ionizing radiation, was disrupted by iron-particle irradiation. Laminin immunoreactivity was mildly irregular at 1 h postirradiation and showed discontinuities and thickening from days one to nine with continuity being restored by day 14. High-LET radiation, like sparsely ionizing radiation, induces rapid remodeling of the stromal extracellular basement membrane, but also appears to alter the integrity of the epithelial basement membrane, which is an important regulator of epithelial cell proliferation and differentiation. The significance of these changes for cancer risk from iron ions remains to be determined, however nonmalignant human-mammary epithelial cells irradiated with as low as 0.25 Gy of gamma rays, reportedly gave rise to colonies

exhibiting decreased localization of E-cadherin, beta-catenin, and connexin-43, proteins necessary for the establishment of cellular polarity and communication (Park *et al*., 2003). Disrupted cell-cell communication, aberrant cell-extracellular matrix interactions, and loss of tissue-specific architecture observed in the daughters of irradiated nonmalignant human-mammary epithelial cells are characteristic of neoplastic progression. This illustrates a heritable, nonmutational mechanism whereby ionizing radiation compromises cell polarity and multicellular organization.

6.4 Summary of Current Space Radiation Biology

The probabilities of health effects due to radiation exposures of humans during and after exploration missions beyond LEO are not completely known presently. Research is needed to complete the estimation of these risks. This Section summarizes the biological and medical information that are available from flight and accelerator-based studies for radiations prevalent in space. In addition, brief summaries of radiation health effects from investigations with conventional radiations, but not yet completed with space radiations, have also been reviewed. New facts have emerged from the study of radiation-exposed populations that have added to understanding. The goal is to identify research needs for activities beyond LEO that could lead to recommendations for radiation dose limits that will prevent the risk of serious and persistent radiation effects from occupational radiation exposure in space.

As is the case for radiation workers on Earth, the aim is to prevent deterministic effects, and limit the risk of cancer to acceptable levels (NCRP, 1993). It is hoped that adequate shielding can do so, however not enough is known. For example, it is not known what special risks are posed by protracted exposures to heavy ions, neutrons and protons. Similarly, there is a need for better estimates of the risk of cataracts. The focus, therefore, has been on estimating the risk of late-appearing radiation effects such as cancer-induction, or radiation-induced cataract. An increased incidence of cataracts has been reported among astronauts, but more research is needed to understand which radiation type(s) is responsible, the dose-response relationship, and what can be done to prevent cataracts.

This Section broadens the problem of the estimation of both early and late radiation effects. The possibility of unexpected solar flares, and the potential of a rapid and progressive exposure to charged particles representing a wide array of atomic numbers, energies and fluences (and any resulting secondary radiation

cascades) is a daunting issue that requires extensive further study. Microgravity in space is well known to be associated with nausea in some individuals after short-duration spaceflight, and most individuals after long-duration spaceflight (Meck *et al*., 2001; Ziegler and Meck, 2001). With what is known today, however, there are no reported concerns among space-flight crew members regarding space radiation-induced early effects on the brain and peripheral nervous system, such as nausea or emesis. However, there are effects that have been reported in experimental animals on behavioral endpoints that are mediated by the peripheral nervous system that show increasing RBE with increasing LET. In contrast, behavioral effects mediated by the CNS, such as learning (CTA), that involve the dopaminergic nervous system are disrupted by exposure to iron ions, while exposure to equal or higher doses of other types of radiation (*e.g*., gamma rays or neutrons) do not show a similar effect. These adverse behavioral and neuronal effects are similar to those seen in aged animals, and the cognitive deficits are dependent on the individual dose response or age at exposure, and are unique to radiations found in space. The dependency of susceptibility for cancer induction on age at exposure is known for some types of cancer such as breast and thyroid. The concern here is that with increasing age there may also be more vulnerability to deficits in neural function from space radiation damage.

Convincing evidence also is emerging for concern regarding the risk of CVD, and defects in immunological function from protracted exposures to radiation that may contribute to life-shortening or diminished quality of life. Significant changes in the human cardiovascular (D'Aunno *et al*., 2003) and immune systems (Mills *et al*., 2001) correlate with time in space flight, presumably due to the stress of microgravity, but radiation exposure cannot be excluded and should be analyzed as a variable.

Biomarkers for identification of individuals at enhanced risk due to genetic predisposition, as well as radiation biodosimetry to estimate cumulative radiation exposures may provide guidance for future individual mission worthiness. However, links between the appearance and abatement of some of the early biodosimetric markers and the risk of later medical consequences are uncertain. An association of cancer incidence to persistent chromosome aberrations in peripheral lymphocytes has been reported.

The study of space radiation effects on various tissues of the body has revealed a previously unappreciated role for low dose tissue remodeling involving stromal cell populations as well as cytoskeletal rearrangements in individual cells. These epigenetic effects involve changes in protein expression independent of the

rapidly expanding work on direct radiation effects on gene expression. What is clear is that a different complement of genes and phosphorylated proteins is activated by exposure to low doses of conventional radiations, compared to the complement activated by higher doses of radiation (Coleman *et al*., 2005; Ding *et al*., 2005; Yang et al, 2006; Yin *et al*., 2003). The ultimate medical consequences of perturbations in both genetic and epigenetic endpoints, however, is completely unknown. The radiosensitivity of tissue-specific stem cells and endothelial cells remains a concern.

Extensive research exists on radiation effects of both male and female gametes with conventional radiations. The effects of exposure to high-energy iron ions has revealed a novel radiosensitivity for one stage of individual male gametes traversed by the iron ions, as well as significant effects to surrounding unirradiated cells. Hereditary effects from gametes irradiated with space radiations are completely unknown.

Physiological effects of space radiations on endocrine function have been known for some time. Radiation-induced injury of the hypothalamic-hypophyseal axis can result in changes in endocrine homeostasis, as well as alteration of the morphologic integrity of most of the peripheral endocrine glands. For example, therapeutic radiation doses of photons as low as 0.4 Gy have led to adenomas or hyperplasias in the parathyroid gland which has a major role in calcium metabolism. No information exists regarding endocrine function and homeostatis after chronic low dose-rate exposure to radiations found in space.

Some noninvasive biological countermeasures for an assortment of radiation effects hold promise for some diminution of specific kinds of radiation risk. Most notably, these include nutritional and biochemical neutralization of the oxidative consequences of radiation damage. Consumption of a low-fat diet rich in natural antioxidants may contribute to minimizing radiation effects for long space missions.

The combined effects of radiation exposure with other biophysical stressors, such as microgravity, exposure to UV light, or to microwaves are poorly understood. The data that exist indicate synergistic effects may well occur. Recent evidence on the biological significance of UVA exposure to skin and lens warrants further investigation.

Epidemiological data from atomic-bomb survivors indicate that there is an increased risk of breast cancer in women exposed to 1 Gy (Tokunaga *et al*., 1991; 1994). The radiosensitivity of the human breast also limits the total acceptable radiation exposure of female astronauts (NCRP, 2000), but as more epidemiological data

become available from irradiated cohorts, there may be other tissues of the body vulnerable to radiation-induced cancer that may also limit future career limits (Land, 1988).

6.5 Summary of Needed Space Radiation Biology Information

6.5.1 *Late Radiation Effects*

6.5.1.1 *Cancer Risk from Space Radiations*. A considerable number of questions and a significant degree of uncertainty remain regarding the risk of cancer and, in particular, the risk of solid tumors in humans from exposures to space radiations. Specific recommendations for research include obtaining experimental data to determine the carcinogenic effect of protracted exposures of relevant energies of protons, heavy ions, and neutrons. Animal studies should not be carried out without some confidence in how to extrapolate the risk data to humans (NCRP, 2005). Pilot studies using chromosome aberrations or other appropriate endpoints induced at low dose rates could provide a guide to the experimental design. A dual approach is suggested for providing risk estimates. First, the determination of equivalent doses for protons, neutrons and heavy ions, and their application to the most appropriate risk estimates for the effects of exposure of humans to gamma rays is needed, and secondly, the development of a risk model based on the mechanisms of radiation-induced cancer and the data with various components of the space radiation environment.

It is recommended that experiments be conducted to:

- determine the carcinogenic effects of space radiations in animals with a sufficient number of suitable heavy ions to provide data for determining an appropriate quality factor value for each;
- develop an alternative method for obtaining equivalent dose for neutrons in the 2 to 50 MeV range;
- determine the basis for the different initial slopes of the dose response curves for induction of cancer or surrogate markers for cancer by HZE particles and fragments;
- determine the number of cells at risk traversed by HZE particles and fragments and the resulting survival, and how these influence carcinogenic risk for particles of different energies;
- determine the influence of repair as well as damage processing on the probability of tumorigenesis by HZE particles;

- determine the role of delta rays in the induction of cancer by heavy ions;
- assess the importance of dose rate on the initial slope for cancer related endpoints for proton or HZE exposures; and
- develop methods using surrogate markers for cancer to extrapolate risk from experimental animal models to humans.

6.5.1.2 *Noncancer Risk from Space Radiations*. No excess incidence of late radiation effects has been revealed in studying lifetime space radiation exposures to date, except for cataract. However, there is significant need for more work.

It is recommended that experiments be conducted to:

- determine the effects of protracted exposures to low dose rates (<50 mSv y^{-1}) of protons, HZE particles, and neutrons of relevant energies in the 0.5 to 1.5 Sv range on the CNS, lens of the eye, vascular system throughout the body, hematopoietic and immune systems, gastrointestinal tract, gonadal cell populations, and fertility.

6.5.2 *Early Radiation Effects*

6.5.2.1 *Thresholds for Neurovestibular, Cardiac, Prodromal and Other CNS Effects.* It is recommended that:

- all available data from therapeutic uses of radiation be reexamined to estimate threshold doses for loss of balance, cardiac arrthymias, nausea, vomiting, and other CNS effects; and
- all radiation accident data be analyzed to determine if any behavioral changes can be expected from exposure to the highest doses likely to occur as a result of deep-space activities.

6.5.2.2 *Hematological, Dermal and Immune Issues*. It is recommended that experiments be conducted to:

- determine how to maintain the proliferative integrity of the hematopoietic, dermal and immune systems when exposed to low dose rates of protons, heavy ions and neutrons.

6.5.3 *Other Information Needed*

6.5.3.1 *Dose-Rate Issues*. It is recommended that experiments be conducted to:

- derive estimates of the dose, and in particular the dose rate over each hourly period for the worst-case SPE scenario that can be anticipated; and
- study the effects of the dose rate of protons and neutrons of relevant energies up to several hundred megaelectron volts. For initial estimates of risk and required shielding, these dose-rate studies could be carried out on cells *in vitro*, by determining cell survival and chromosome aberrations and mutation incidence for the purpose of establishing animal protocols.

6.5.3.2 *Combined Exposures/Stressors*. It is recommended that experiments be conducted to:

- evaluate the effects of combined exposures to protons and HZE particles; and
- acquire data and model effects from multiple stressors, including microgravity, UV, microwaves and hormonal stress cascades.

6.5.3.3 *Biomarkers*. It is recommended that experiments be conducted to:

- evaluate biomarkers for identification of individuals at increased risk due to genetic predisposition; and
- evaluate biomarkers to estimate cumulative doses.

6.5.3.4 *Countermeasures*. It is recommended that countermeasures be assessed for their efficacy in preventing adverse effects.

7. Space Radiation Risk Assessment Methodology

7.1 Introduction

On long-term missions outside Earth's magnetic field, three specific areas of radiation health risks can be identified as being of primary concern: (1) late effects (*e.g.*, cancer); (2) early (noncancer) effects due to acute, or at least short-term, exposures from large SPEs; and (3) possible effects (still to be identified) to the CNS from the HZE component of GCR. Risk assessment models play the important role of integration of experimental and theoretical knowledge of physics and biology into quantitative models to be used to project risks and assess risk mitigation concepts. New computational approaches to risk assessment that integrate molecular biology and genetics hold prospects for the future, however these have not replaced the traditional approaches that use epidemiological data and survival analysis for projecting long-term late effects. Each of these three areas of radiation health risk is discussed below. In addition, it is now recognized that point estimates of risk are inadequate and that uncertainty bounds in risk estimates are needed.

7.2 Late Radiation Effects

For projecting risks in LEO, NASA uses the model recommended by NCRP Report No. 132 (NCRP, 2000) for evaluating cancer risks. A review of the model is useful for discussing uncertainties of the point estimates and for discussing alternative approaches. The double detriment life-table is used to follow the age-specific mortality of a population over an entire lifespan and it allows for the description of competing risks between radiation and other causes of death (Bunger *et al.*, 1981). For a homogeneous population receiving an effective dose E, at age a_E, the probability of dying in the age-interval from a to $a + 1$ is described by the background mortality-rate for all causes of death except radiation-induced death $M(a)$, and the radiation cancer mortality rate $m(E,a_E,a)$, as:

$$q(E,a_{\mathrm{E}},a) = \frac{M(a) + m(E,a_{\mathrm{E}},a)}{1 + \frac{1}{2}[M(a) + m(E,a_{\mathrm{E}},a)]} . \tag{7.1}$$

The survival probability to live to age a, following an exposure E at age a_E, is:

$$s(E,a_{\mathrm{E}},a) = \prod_{u = a_{\mathrm{E}}}^{a-1} [1 - q(E,a_{\mathrm{E}},a)]. \tag{7.2}$$

The risk of radiation exposure-induced death (REID) is the lifetime risk that an individual in the population will die from a cancer caused by his or her radiation exposure, defined by (Vaeth and Pierce, 1990):

$$\mathrm{REID} = \sum_{a = a_{\mathrm{E}}}^{\infty} m(E,a_{\mathrm{E}},a)s(E,a_{\mathrm{E}},a). \tag{7.3}$$

A minimum latency time of 10 y is often used for low-LET radiation, however alternative assumptions for high-LET radiation need to be considered. The loss of life expectancy among radiation exposure-induced deaths (LLE_{REID}) is:

$$LLE_{\mathrm{REID}} = \frac{LLE}{\mathrm{REID}} , \tag{7.4}$$

where the average loss of life expectancy in the population is defined by:

$$LLE = \sum_{a = a_{\mathrm{E}}}^{\infty} S(a) - \sum_{a = a_{\mathrm{E}}}^{\infty} s(E,a_{\mathrm{E}},a), \tag{7.5}$$

where $S(a)$ is the survival probability to age a in the absence of exposure. The life-table and background cancer rates often employed are for the gender-specific average U.S. population. For projecting cancer risks in a healthy population such as the astronauts, other methods should be investigated.

The primary quantity in the model is the radiation-induced mortality rate (m), which should contain dependencies on radiation quality, dose rate, gender, age at exposure, and time since exposure. NCRP Report No. 132 (NCRP, 2000) used estimates from the LSS study (Pierce *et al*., 1996; Thompson *et al*., 1994) and applied a dose and dose-rate effectiveness factor (DDREF) and a LET-dependent quality factor [$Q(L)$], to consider other radiation types and dose rates. A mixture model is introduced for transferring risks from the

Japanese to the U.S. population under the assumption of a fractional likelihood, represented by the uncertain (*i.e.*, random) quantity ν, that the multiplicative risk model or additive risk model is the appropriate transfer model, such that the radiation mortality rate is (Cucinotta *et al.*, 2005; 2006):

$$m(E,a_{\mathrm{E}},a) = [\nu \mathrm{ERR}(a_{\mathrm{E}},a)M_{\mathrm{c}}(a) + (1-\nu)\mathrm{EAR}(a_{\mathrm{E}},a)]\frac{FLQ(L)}{\mathrm{DDREF}}, \quad (7.6)$$

where ERR and EAR are the excess relative risk and excess additive risk per sievert, respectively, $M_c(a)$ is the gender and age-specific cancer mortality rate in the U.S. population, and FLQ [the product of the tissue-weighted fluence (F), LET (L), and quality factor (Q)] is the organ dose equivalent. Equation 7.6 expresses the uncertain fractional division between the assumption of the multiplicative and additive risk models. For solid cancer it is assumed ν is uniformly distributed over the unit interval and for leukemia $\nu = 0$. Other weightings have been considered for several tissue sites including thyroid, breast and skin (Land *et al.*, 1980; Ron *et al.*, 1995). Equation 7.6 is a multiplicative model for the mortality rate, consisting of a product of several factors: the ERR or EAR, M_c, and the organ dose equivalent, which includes the quality factor dependence. The limiting behavior of the addition of many random variables is well known as the normal distribution. In contrast, the limiting behavior of the multiplication of many random factors will be a log-normal distribution. Equation 7.6 assumes each multiplicative factor is independent. This assumption may not be strictly valid because of the possibility of correlations between factors or nonadditivity of different radiation components since cells will be traversed by multiple particles and delta rays produced by ions passing through adjacent cells (Cucinotta *et al.*, 1999).

Estimating the uncertainties in the conventional model requires an evaluation of each set of coefficients that enter into the model. These include the uncertainties in the LSS data, transfer model, quality factors, DDREF, and physical models used to estimate organ doses and LET spectra. The baseline life-table and background cancer rates also introduce uncertainties into the calculation, especially for the astronaut population. Uncertainties in many of these coefficients have been evaluated and are described next. Monte-Carlo sampling can be used to propagate the overall uncertainty to form a statistical distribution of the risk calculation (NCRP, 1997). The uncertainties due to the basic assumptions of the model, such as the use of the linear-additivity model, and scaling of the effects of HZE ions to the LSS data including possible

differences in minimal latency times or plateau effects at longer times between gamma rays and HZE ions, have not been addressed. Also, for higher risk missions, such as a Mars mission, competing risks from nonradiation effects may constrain the upper bounds of a statistical distribution of radiation risks.

7.2.1 *Organ Dose Equivalents and Equivalent Doses for Late Effects*

As discussed in NCRP Reports No. 132, No. 137, and No. 142 (NCRP, 2000; 2001a; 2002), the *organ dose equivalent* may be used as a surrogate for the equivalent dose for the LEO space radiation environment. It is defined (ICRU, 1993) for a given organ or tissue as:

$$\overline{H}_{\mathrm{T}} = \overline{Q}D_{\mathrm{T}} = \frac{1}{m}\int_{m}\int Q(L)D(L)\mathrm{d}L\mathrm{d}m. \tag{7.7}$$

Here L is the linear energy transfer and $D(L)$ is the distribution in LET from the radiation environment in question between L and $L + \mathrm{d}L$. D_{T} is the mean tissue absorbed dose. The integration over the mass (m) of the organ can be approximated by averaging over a representative number of points within the organ. For example, for bone marrow, the mean has typically been obtained from 33 representative points in the marrow within a computerized male or female model. The calculated value is considered an acceptable approximation of the equivalent dose in the organ in question.

The function $Q(L)$ is given as follows:

$$\begin{aligned} Q(L) &= 1 \text{ for } L < 10 \text{ keV } \mu\mathrm{m}^{-1} \\ &= 0.32\ L - 2.2 \text{ for } 10 \le L \le 100 \text{ keV } \mu\mathrm{m}^{-1} \\ &= 300\ L^{-1/2} \text{ for } L > 100 \text{ keV } \mu\mathrm{m}^{-1}. \end{aligned} \tag{7.8}$$

7.2.2 *Procedure for Estimating Risk for Late Effects in Individual Organs*

The recommended procedure to estimate risk requires information in three distinct areas: (1) the spectral and time dependence of the radiation environment, (2) detailed solid-angle dependence of the available shielding (both spacecraft shielding as well as body self-shielding), and (3) the tissue or organ risk coefficients to be used. To calculate risk of cancers in specific organs, the shielding distributions for representative points within the organs must be

available for an appropriate averaging. The risk is calculated by multiplying the equivalent dose (as approximated in Equation 7.7) by the appropriate tissue-specific risk coefficient from the second column of Table 3.1 of NCRP Report No. 137 (NCRP, 2001a). If the incident spectra vary over time during the mission, the risk rates can be calculated at specific times and integrated over time to yield the risk for the total mission.

The total excess lifetime risk of mortality from all cancers can be determined by summing over all organs and is expressed:[15]

$$R = \Sigma_i R_i, \tag{7.9}$$

where:

$$R_i = \frac{k_{T,i}}{m} \int_m \int Q(L) D(L) \mathrm{d}L \, \mathrm{d}m, \tag{7.10}$$

and the summation is over all the organs where radiation risk of cancer exists.

The effective dose (E) can be calculated by summing the products of the equivalent dose for each organ and the appropriate w_T from column three of Table 3.1 of NCRP Report No. 137 (NCRP, 2001a).

If the ages and genders of the individual crew members are known, age- and gender-specific risk coefficients, k_T, A, G, can be used. Also, see appropriate approximations suggested for $k_{T,i}$ in Section 7.2.3.1.

7.2.3 *Uncertainties in the Risk from Late Effects*

Uncertainties exist for the three factors, $k_{T,i}$, $Q(L)$, and $D(L)$ in Equation 7.10.

7.2.3.1 *Uncertainties in the Low Linear Energy Transfer Risk Coefficients*. Risk of radiation-induced cancer has been extensively studied in a number of medically-, occupationally- and environmentally-irradiated populations, and in a large cohort of survivors of the atomic bombings of Hiroshima and Nagasaki. Because of these studies, and because it is often possible to estimate organ- and tissue-specific radiation dose with some precision, radiation-related cancer risk can be quantified. It is also estimated in considerable detail with respect to sex, age at exposure, attained age, and

[15]Strictly speaking, the risk of death from *all* cancers is: $R = 1 - \Pi (1 - R_i)$ but for small risk values ($R_i \ll 1$), R is very close to the sum of the individual risks ΣR_i.

cancer site. For example, the Radiation Effects Research Foundation (RERF) tumor registry report (Thompson *et al*., 1994) provided estimates of radiation-related cancer incidence risk in the atomic-bomb survivors for a total of 32 solid cancer sites and groups of sites. A companion report based on the RERF Leukemia Registry (Preston *et al*., 1994) gave estimates for subtypes of leukemia and lymphoma. For both solid and hematopoietic cancers, details of modification of dose response by sex, exposure age, attained age, and time since exposure were provided. An update of radiation-induced mortality in the RERF cohort has been published (Preston *et al*., 2003).

The site-specific data are available over the internet from the RERF (2006) website and can be used to calculate risk estimates, and the statistical uncertainties of these estimates, in the form of statistical likelihood distributions. A working group of the National Cancer Institute and the Centers for Disease Control and Prevention, charged with revising a 1985 report of the National Institutes of Health to provide radioepidemiological tables, has published tables of statistical uncertainty distributions for a total of 27 cancer sites and groups of sites, and an interactive computer program for estimating attributable risk, or probability of causation for individuals (Land *et al*., 2003b).

For most cancer sites, there is little evidence of variation in estimated ERR by exposure age >30 and by attained age >50 (*i.e*., age at observation for risk). This somewhat simplifies computation for many applications related to space flight in that, while separate estimates may be required for different cancer sites or groups of sites, a single site-specific estimate of ERR per unit dose of low-LET radiation is all that is required for estimation of excess lifetime risk for most sites, when exposure occurs at ages 30 or 40 and older. Tabular presentations of site-specific statistical uncertainty distributions (Land *et al*., 2003b) are given in Tables 7.1 through 7.9.

However, it is not only statistical uncertainty that is of concern. Site-specific cancer rates for the U.S. population are not identical to those in Japan and, for some sites, can vary between countries by as much as an order of magnitude. With the exceptions of female breast cancer and (to some extent) gastric cancer, little information on how best to transfer estimates of radiation-related cancer risk between populations with markedly different baseline rates is available. Because some rule must be used, there is considerable added uncertainty associated with transfer (Land, 2002; Land and Sinclair, 1991). Because there are few relevant data, quantification of this uncertainty is mainly subjective (Land *et al*., 2003b).

TABLE 7.1—*Computation of uncertainty distribution for ERR at 1 Sv. Sites for which lognormal theory could be used with confidence to approximate the likelihood profile distribution for log (α), and for which default values of γ and δ were not used (Land et al., 2003b).*[a]

Cancer Site	Log (α)	γ	δ	Var (Log α)	Cov (Log α, γ) (correlation)	Cov (Log α, δ) (correlation)	Var (γ) × 10^{-3}	Cov (γ, δ) × 10^{-3}	Var (δ)
All digestive Males	–1.590	–0.0477	–1.622	0.10621	0.001868 (0.314)	–0.020011 (–0.082)	0.3332	–7.395	0.56236
All digestive Females	–0.8614	–0.0477	–1.622	0.05018	0.001403 (0.343)	–0.001882 (–0.011)	0.3332	–7.395	0.56236
Stomach Females	–0.7998	–0.04723	–1.781	0.07512	0.001380 (0.279)	0.006263 (0.031)	0.3252	–7.185	0.54764
Liver Both sexes	–1.049	–0.05204	–1.579	0.17108	0.002291 (0.307)	–0.03610 (–0.115)	0.3255	–7.347	0.57368
Breast Females	0.02109	–0.03722	–2.006	0.05456	0.002586 (0.589)	–0.01907 (–0.107)	0.3530	–7.934	0.58018

[a]For exposure age $e \leq 30$ and attained age $a < 50$, log (ERR Sv^{-1}) is assumed to be normally distributed with mean log (α) and variance Var [log (α)]. For other values of e and a, the log scale mean and variance are:

Mean = log (α) + γ min [max (–15, e – 30), 0] + δ min [ln (a/50), 0];

Variance = var (log α) + 2 cov (log α, γ) min [max (–15, e – 30), 0] + 2 cov [log (α, δ)] min [ln (a/50), 0] + var (γ) min [max (–15, e – 30), 0]^2 + 2 cov (γ, δ) min [max (–15, e – 30), 0] min [ln (a/50), 0] + var (δ) min [ln (a/50), 0]^2.

TABLE 7.2—*Computation of uncertainty distribution for ERR at 1 Sv. Likelihood profile distributions for α, for exposure age e ≥ 30 and attained age a ≥ 50: Sites for which a lognormal approximation was not appropriate, and for which default values of γ and δ were used (Land et al., 2003b).*[a]

Profile Quantiles	Oral Cavity and Pharynx		Esophagus		Stomach	Colon		Rectum		Gall Bladder		Pancreas	
	Males	Females	Males	Females	Males	Males	Females	Males	Females	Males	Females	Males	Females
0.9975	0.8004	1.765	1.216	3.253	0.3802	1.531	1.671	0.4946	1.078	0.5258	1.114	0.7062	1.510
0.995	0.7321	1.619	1.117	2.919	0.3516	1.429	1.567	0.4675	1.022	0.4725	1.013	0.6401	1.379
0.9875	0.6404	1.423	0.9820	2.492	0.3137	1.289	1.423	0.3946	0.8701	0.4013	0.8761	0.5509	1.201
0.975	0.5694	1.271	0.8755	2.179	0.2846	1.177	1.308	0.3413	0.7581	0.3465	0.7677	0.4815	1.060
0.95	0.4962	1.113	0.7634	1.869	0.2545	1.058	1.185	0.2888	0.6467	0.2905	0.6538	0.4095	0.9117
0.875	0.3935	0.8909	0.6025	1.450	0.2112	0.8852	1.005	0.2178	0.4917	0.2128	0.4893	0.3083	0.6984
0.8413	0.3651	0.8288	0.5563	1.324	0.1967	0.8357	0.9537	0.1951	0.4396	0.1921	0.4442	0.2802	0.6378
0.5	0.2055	0.4755	0.2905	0.6759	0.1184	0.5405	0.6430	0.0812	0.1875	0.0756	0.1805	0.1227	0.2871
0.1587	0.0907	0.2136	0.0784	0.1779	0.0497	0.3020	0.3857	<0	<0	<0	<0	<0	<0
0.125	0.0739	0.1736	0.0545	0.1229	0.0369	0.2672	0.3523	<0	<0	<0	<0	<0	<0
0.05	0.0308	0.0724	<0	<0	0.0051	0.1694	0.2463	<0	<0	<0	<0	<0	<0
0.025	0.0082	0.0190	<0	<0	<0	0.1134	0.1849	<0	<0	<0	<0	<0	<0
0.0125	<0	<0	<0	<0	<0	0.0671	0.1336	<0	<0	<0	<0	<0	<0
0.005	<0	<0	<0	<0	<0	0.0176	0.0772	<0	<0	<0	<0	<0	<0
0.0025	<0	<0	<0	<0	<0	<0	0.0409	<0	<0	<0	<0	<0	<0

TABLE 7.2—*(continued)*.

Profile Quantiles	Respiratory, Nonlung		Urinary Tract		Bladder		Ovary	Male Genital	CNS		Residual Solid Cancers		Lymphoma[a]
	Males	Females	Males	Females	Males	Females			Males	Females	Males	Females	Both Sexes
0.9975	0.7400	1.716	1.480	3.561	1.561	3.887	2.02	1.51	0.9370	2.006	1.504	2.989	1.600
0.995	0.7009	1.619	1.396	3.354	1.474	3.577	1.86	1.44	0.8744	1.880	1.403	2.814	1.394
0.9875	0.5725	1.319	1.281	3.071	1.312	3.172	1.65	1.23	0.7444	1.618	1.267	2.575	1.134
0.975	0.4810	1.105	1.189	2.848	1.188	2.864	1.48	1.08	0.6491	1.424	1.160	2.385	0.9465
0.95	0.3930	0.9008	1.092	2.613	1.062	2.551	1.30	0.939	0.5553	1.230	1.048	2.185	0.7651
0.875	0.2755	0.6291	0.9489	2.273	0.8843	2.115	1.05	0.733	0.4295	0.9661	0.8887	1.893	0.5321
0.8413	0.2344	0.5366	0.9080	2.176	0.8311	1.987	0.982	0.667	0.3925	0.8862	0.8440	1.810	0.4742
0.5	0.0606	0.1377	0.6635	1.601	0.5388	1.282	0.576	0.3348	0.2057	0.4755	0.5859	1.315	0.1780
0.1587	<0	<0	0.4650	1.137	0.3091	0.7337	0.267	0.0670	0.0759	0.1772	0.3883	0.9148	0.0142
0.125	<0	<0	0.4380	1.073	0.2778	0.6587	0.230	0.0389	0.0600	0.1403	0.3626	0.8592	0.0032
0.05	<0	<0	0.3571	0.8820	0.1869	0.4414	0.117	<0	0.0189	0.0444	0.2871	0.6946	>0
0.025	<0	<0	0.3102	0.7698	0.1352	0.3176	0.0569	<0	0.00440	0.0101	0.2445	0.5986	>0
0.0125	<0	<0	0.2712	0.6759	0.0925	0.2159	<0	<0	<0	<0	0.2099	0.5187	>0
0.005	<0	<0	0.2285	0.5716	0.0457	0.1057	<0	<0	<0	<0	0.1726	0.4305	>0
0.0025	<0	<0	0.2011	0.5038	0.0173	0.0393	<0	<0	<0	<0	0.1492	0.3738	>0

[a]For exposure age $e < 30$ and/or attained age $a < 50$, α is multiplied by the uncertain age factor $f(e,a)$, which is assumed to be independent of α and lognormally distributed. The mean and variance of ln {[$f(e,a)$]}, which is assumed to be normally distributed, are as follows:

Mean = $-0.05255 \min[\max(-15, e-30), 0] - 1.626 \min[\ln(a/50), 0]$,

Variance = $0.0003261 \min[\max(-15, e-30), 0]^2 - 2 \times 0.007297 \min[\max(-15, e-30), 0] \min[\ln(a/50), 0] + 0.5648 \{\min[\ln(a/50), 0]\}^2$.

TABLE 7.3—*Computation of uncertainty distribution for ERR at 1 Sv. Likelihood profile distributions for α, for all exposure ages and attained ages: Sites for which a lognormal approximation was not appropriate for the statistical uncertainty distribution for α, and for which $\gamma = 0$ and $\delta = 0$ were assumed (Land et al., 2003b).*

Profile Quantiles	Lung		Female Genital Less Ovary
	Males	Females	
0.9975	1.114	3.449	0.172
0.995	1.053	3.307	0.136
0.9875	0.9680	3.109	0.0866
0.975	0.8987	2.948	0.0791
0.95	0.8237	2.775	0.0607
0.875	0.7112	2.516	0.0463
0.8413	0.6783	2.441	0.0030
0.5	0.4740	1.973	–0.189
0.1587	0.2953	1.563	–0.278
0.125	0.2681	1.504	–0.289
0.05	0.1885	1.323	>0
0.025	0.1408	1.214	>0
0.0125	0.1000	1.119	>0
0.005	0.0537	1.012	>0
0.0025	0.0239	0.9406	>0

TABLE 7.4—*Computation of uncertainty distribution for ERR at 1 Sv. Leukemia other than chronic lymphocytic, combined sexes: Likelihood profile distributions, by representative values for exposure age and time since exposure (Land et al., 2003b).*

Profile Quantiles	Exposure Age 20						Exposure Age 30					
	Time Since Exposure (y)						Time Since Exposure (y)					
	5	10	15	25	35	45	5	10	15	25	35	45
0.9975	72.69	29.87	13.54	3.967	1.671	0.8029	37.55	18.19	9.412	3.361	1.672	0.9342
0.995	65.99	27.68	12.71	3.744	1.538	0.7102	34.69	17.09	8.944	3.206	1.556	0.8387
0.9875	57.46	24.83	11.62	3.438	1.358	0.5913	30.97	15.62	8.311	2.991	1.400	0.7154
0.975	51.20	22.68	10.78	3.194	1.217	0.5038	28.16	14.49	7.816	2.818	1.277	0.6239
0.95	45.05	20.51	9.922	2.934	1.071	0.4180	25.33	13.33	7.299	2.633	1.149	0.5334
0.875	36.94	17.57	8.719	2.554	0.8658	0.3065	21.47	11.70	6.559	2.358	0.9676	0.4137
0.8413	34.80	16.76	8.385	2.445	0.8091	0.2778	20.42	11.25	6.350	2.278	0.9168	0.3820
0.5	23.55	12.35	6.481	1.784	0.4911	0.1352	14.65	8.662	5.121	1.789	0.6253	0.2185
0.1587	16.10	9.173	5.015	1.239	0.2730	0.0585	10.52	6.674	4.124	1.366	0.4060	0.1173
0.125	15.21	8.776	4.824	1.168	0.2480	0.0511	10.01	6.416	3.991	1.308	0.3786	0.1062
0.05	12.65	7.592	4.244	0.9509	0.1783	0.0320	8.481	5.633	3.580	1.127	0.2979	0.0755
0.025	11.25	6.925	3.907	0.8277	0.1428	0.0234	7.627	5.180	3.338	1.019	0.2535	0.0601
0.0125	10.14	6.380	3.627	0.7271	0.1161	0.0175	6.933	4.804	3.134	0.9281	0.2181	0.0486
0.005	8.959	5.788	3.315	0.6185	0.0898	0.0123	6.184	4.389	2.905	0.8259	0.1809	0.0374
0.0025	8.227	5.412	3.113	0.5503	0.0745	0.0095	5.709	4.120	2.754	0.7591	0.1581	0.0310

TABLE 7.5—*Computation of uncertainty distribution for ERR at 1 Sv. Acute lymphocytic leukemia, combined sexes: Likelihood profile distributions, by exposure age and time since exposure (Land et al., 2003b).*

Profile Quantiles	Exposure Age <20										Exposure Age ≥20
	Time Since Exposure (y)										Time Since Exposure (y)
	5	10	15	20	25	30	35	40	45	50	>5
0.9975	823.6	206.9	68.13	28.42	14.33	8.308	5.277	3.54	2.452	1.732	11.32
0.995	682.2	176.6	58.92	24.6	12.29	6.972	4.291	2.771	1.84	1.242	9.956
0.9875	521.1	140.8	47.85	19.97	9.787	5.358	3.138	1.91	1.189	0.7503	8.266
0.975	416.5	116.7	40.23	16.73	8.037	4.25	2.377	1.372	0.8066	0.4795	7.058
0.95	324.9	94.87	33.16	13.69	6.399	3.236	1.711	0.9272	0.5096	0.2825	5.900
0.875	221.3	68.87	24.52	9.91	4.382	2.041	0.9778	0.4755	0.2333	0.1151	4.419
0.8413	197.1	62.56	22.38	8.96	3.88	1.757	0.8142	0.3822	0.1807	0.0859	4.037
0.5	92.5	33.4	12.07	4.36	1.574	0.5685	0.2053	0.0742	0.0268	0.0097	2.114
0.1587	44.1	18.11	6.22	1.83	0.503	0.1345	0.0355	0.0093	0.0024	0.0006	0.9570
0.125	39.5	16.53	5.59	1.57	0.4105	0.104	0.0260	0.0064	0.0016	0.0004	0.8278
0.05	27.4	12.24	3.83	0.910	0.1975	0.0413	0.0085	0.0017	0.0003	0.0000	0.4797
0.025	21.8	10.1	2.93	0.610	0.1155	0.0210	0.0038	0.0007	0.0001	0.0000	0.3068
0.0125	17.7	8.49	2.25	0.409	0.0673	0.0107	0.0017	0.0003	0.0000	0.0000	0.1800
0.005	13.8	6.90	1.57	0.236	0.0323	0.0042	0.0005	0.0000	0.0000	0.0000	0.0601
0.0025	11.6	5.96	1.19	0.153	0.0180	0.0020	0.0002	0.0000	0.0000	0.0000	0.0000

TABLE 7.6—*Computation of uncertainty distribution for ERR at 1 Sv. Acute myelogenous leukemia, combined sexes: Likelihood profile distributions, by time since exposure (Land et al., 2003b).*

Profile Quantiles	Time Since Exposure (y)									
	5	10	15	20	25	30	35	40	45	50
0.9975	28.57	16.54	10.10	6.666	4.903	4.071	3.707	3.563	3.527	3.550
0.995	25.57	15.12	9.385	6.266	4.627	3.819	3.428	3.232	3.129	3.075
0.9875	21.79	13.28	8.443	5.729	4.253	3.478	3.057	2.802	2.626	2.493
0.975	19.05	11.91	7.727	5.314	3.959	3.210	2.771	2.479	2.261	2.085
0.95	16.40	10.55	7.001	4.884	3.651	2.931	2.477	2.157	1.907	1.701
0.875	12.96	8.719	5.997	4.277	3.208	2.530	2.067	1.722	1.450	1.228
0.8413	12.06	8.229	5.722	4.108	3.082	2.416	1.953	1.605	1.331	1.110
0.5	7.453	5.579	4.176	3.126	2.340	1.752	1.311	0.9810	0.7346	0.5499
0.1587	4.548	3.742	3.024	2.356	1.734	1.217	0.8329	0.5627	0.3776	0.2523
0.125	4.215	3.518	2.877	2.255	1.653	1.147	0.7734	0.5140	0.3390	0.2226
0.05	3.267	2.860	2.435	1.947	1.401	0.9314	0.5961	0.3745	0.2329	0.1440
0.025	2.765	2.497	2.183	1.768	1.252	0.8064	0.4978	0.3010	0.1800	0.1069
0.0125	2.374	2.206	1.976	1.618	1.126	0.7024	0.4188	0.2443	0.1408	0.0806
0.005	1.972	1.895	1.749	1.453	0.9829	0.5880	0.3354	0.1870	0.1029	0.0562
0.0025	1.728	1.700	1.603	1.345	0.8885	0.5146	0.2839	0.1531	0.0815	0.0430

TABLE 7.7.—*Computation of uncertainty distribution for ERR at 1 Sv. Chronic myelogenous leukemia: Likelihood profile distributions, by sex and time since exposure (Land et al., 2003b).*

Profile Quantiles	Time Since Exposure (y)									
	5	10	15	20	25	30	35	40	45	50
Males										
0.9975	134.6	34.15	14.49	7.474	4.262	2.573	1.606	1.023	0.6598	0.4290
0.995	120.7	30.82	12.86	6.480	3.588	2.091	1.254	0.7654	0.4720	0.2931
0.9875	103	26.62	10.82	5.242	2.762	1.519	0.8548	0.4875	0.2803	0.1620
0.975	90.12	23.56	9.337	4.355	2.187	1.138	0.6030	0.3230	0.1742	0.0943
0.95	77.60	20.58	7.899	3.506	1.655	0.8031	0.3954	0.1962	0.0978	0.0489
0.875	61.29	16.67	6.021	2.428	1.020	0.4363	0.1881	0.0815	0.0354	0.0154
0.8413	57.03	15.64	5.528	2.155	0.8702	0.3565	0.1470	0.0609	0.0253	0.0105
0.5	35.09	10.19	2.960	0.8598	0.2497	0.0725	0.0211	0.0061	0.0018	0.0005
0.1587	21.24	6.515	1.354	0.2548	0.0470	0.0086	0.0016	0.0003	0.0001	0.0000
0.125	19.66	6.071	1.182	0.2057	0.0350	0.0059	0.0010	0.0002	0.0000	0.0000
0.05	15.18	4.764	0.7191	0.0938	0.0119	0.0015	0.0002	0.0000	0.0000	0
0.025	12.81	4.038	0.5020	0.0532	0.0055	0.0006	0.0001	0.0000	0	0
0.0125	10.98	3.450	0.3518	0.0303	0.0025	0.0002	0.0000	0.0000	0	0
0.005	9.105	2.814	0.2193	0.0144	0.0009	0.0001	0.0000	0	0	0
0.0025	7.972	2.412	0.1523	0.0081	0.0004	0.0000	0.0000	0	0	0

TABLE 7.7.—*(continued).*

Profile Quantiles	Time Since Exposure (y)									
	5	10	15	20	25	30	35	40	45	50
Females										
0.9975	46.16	31.20	23.24	18.77	16.29	15.08	14.83	15.44	16.95	19.56
0.995	40.32	27.45	20.49	16.54	14.31	13.18	12.87	13.24	14.30	16.12
0.9875	33.14	22.87	17.14	13.83	11.91	10.87	10.48	10.58	11.13	12.10
0.975	28.06	19.63	14.79	11.92	10.22	9.259	8.804	8.728	8.957	9.443
0.95	23.24	16.55	12.55	10.12	8.630	7.733	7.231	7.003	6.973	7.086
0.875	17.18	12.64	9.728	7.851	6.625	5.813	5.265	4.886	4.614	4.411
0.8413	15.64	11.63	9.003	7.269	6.112	5.323	4.768	4.361	4.048	3.796
0.5	8.040	6.543	5.325	4.334	3.527	2.871	2.336	1.901	1.547	1.259
0.1587	3.697	3.385	3.000	2.500	1.919	1.393	0.9830	0.6838	0.4718	0.3239
0.125	3.239	3.027	2.729	2.289	1.736	1.231	0.8466	0.5729	0.3843	0.2563
0.05	2.005	2.020	1.948	1.686	1.212	0.7861	0.4901	0.2998	0.1815	0.1092
0.025	1.410	1.501	1.526	1.366	0.9354	0.5658	0.3280	0.1865	0.1048	0.0585
0.0125	0.9859	1.109	1.192	1.115	0.7207	0.4049	0.2181	0.1151	0.0601	0.0312
0.005	0.5983	0.7262	0.8444	0.8553	0.5006	0.2530	0.1229	0.0586	0.0277	0.0130
0.0025	0.3972	0.5123	0.6350	0.6968	0.3686	0.1702	0.0759	0.0333	0.0144	0.0062

TABLE 7.8—*Computation of uncertainty distribution for ERR at 1 Sv. Thyroid cancer, combined sexes: Lognormal theory geometric mean and geometric standard deviation by exposure age (Land et al., 2003b).*

Exposure Age	Geometric Mean	Geometric Standard Deviation
0	9.463	2.183
5	6.262	1.924
10	4.136	1.976
15	2.732	2.160
20	1.804	2.301
25	1.192	2.367
30	0.788	2.365
35	0.521	2.379
40	0.345	2.732
45	0.228	3.140
50	0.151	3.611

TABLE 7.9—*Computation of uncertainty distribution for ERR at 1 Sv. Likelihood profile distributions for nonmelanoma skin cancer, both sexes combined. Basal cell carcinoma: exposure ages 0 to 10, 20, 30, and 40 or older, and all attained ages; for intermediate ages at exposure, logarithms of specific quantiles are to be interpolated by age. Other nonmelanoma skin cancers: Combined sexes, all exposure ages and all attained ages (Land et al., 2003b).*

Profile Quantiles	Basal Cell Skin Cancer (by age at exposure)				Other Nonmelanoma Skin Cancer
	0 – 10	20	30	≥40	
0.9975	149.7	23.79	5.872	2.342	0.8243
0.995	129.1	21.34	5.360	2.095	0.7156
0.9875	104.3	18.26	4.687	1.773	0.5715
0.975	87.30	16.02	4.175	1.531	0.4613
0.95	71.53	13.84	3.655	1.288	0.3489
0.875	52.35	11.01	2.938	0.9613	0.1940
0.8413	47.61	10.27	2.742	0.8744	0.1519
0.5	25.22	6.441	1.645	0.4200	–0.0807
0.1587	13.14	3.970	0.8365	0.1495	<0
0.125	11.88	3.677	0.7399	0.1235	<0
0.05	8.467	2.837	0.4556	0.0579	<0
0.025	6.778	2.376	0.3132	0.0323	<0
0.0125	5.524	1.998	0.2125	0.0178	<0
0.005	4.295	1.576	0.1245	0.0078	<0
0.0025	3.584	1.301	0.0814	0.0041	<0

Another source of uncertainty associated with transfer of estimated risk from one population to another has to do with random and biased errors of dose reconstruction for the members of the population providing the dose-response data. For atomic-bomb survivor data, there is also uncertainty associated with the neutron weighting factor used for the mixed gamma neutron dose from the Hiroshima and Nagasaki bombs. The identical errors cannot be expected to apply to the second population, and some adjustment must be made. Some additional uncertainty, mainly subjective in nature, accrues to the transferred risk estimates (NCRP, 1997).

Most of the dose-response data on which radiation-related risk estimates depend come from populations, like the atomic-bomb survivors, exposed to acute radiation doses, and the greatest part of the information pertains to radiation doses of ~0.5 Sv and more. Most applications, on the other hand, are to populations exposed chronically, or to acute doses of 0.05 Sv or less. Experimental radiation studies generally suggest that, at least for cumulative doses exceeding 1 Sv, a reduction in estimated risk is appropriate for applications to chronic exposure. The epidemiological evidence, on the other hand, does not suggest a decrease in ERR Sv^{-1} at low acute doses for solid cancers generally, while a linear-quadratic model with a twofold reduction in ERR Sv^{-1} between acute doses of 1 and 0.1 Sv is suggested for leukemia. The curvilinearity of the leukemia dose response is the main epidemiological evidence in support of a reduced risk per unit dose at low and very low doses as suggested by experimental observations (NCRP, 1980), and radiation protection organizations such as the ICRP, NCRP and UNSCEAR have recommended that extrapolated dose-specific risk estimates be divided by a DDREF of two for chronic exposures and for acute doses <200 mSv (ICRP, 1991; NCRP, 1993; UNSCEAR, 1993). The recommended DDREF is no greater than two because a higher DDREF, in the context of a linear-quadratic dose response, would be statistically inconsistent with the LSS solid cancer data (Pierce and Preston, 2000). Accordingly, a DDREF would not necessarily be applied to the estimated linear-quadratic dose response for leukemia.

Implementation of a DDREF for chronic exposures can modify radiation-related risk estimates significantly, and there is much controversy and uncertainty about the DDREF value. Recent expressions of the uncertainty have assigned substantial probabilities to values near one, and to values greater than three or four (NAS/NRC, 2006; NCRP, 1997) and even some probability to values less than one (Grogan *et al*., 2001; Land *et al*., 2003b).

The possibility of a low dose or low dose-rate threshold, below which there is no radiation-related risk, cannot be ruled out on the basis of current knowledge. However, for the LSS a threshold >0.06 Sv can be ruled out (Pierce and Preston, 2000). There is ample evidence from radiation biology, and even epidemiology, suggesting that excess risk is proportional to radiation dose at nontrivial doses and dose rates. It is commonly thought that a mechanism by which ionizing radiation exposure contributes to radiation carcinogenesis is the induction of double-strand DNA breaks and more complex clustered DNA damage. Such events have been demonstrated by calculation (Brenner and Ward, 1992; Goodhead, 1994) and by experiment (Boudaiffa, 2000a; 2000b) to result from a single low-energy electron track produced by a photon interaction. At low doses and low dose rates, the occurrence of such events is proportional to radiation dose and to the number of cells irradiated.

Complete efficiency of repair of DSB and complex lesions at low doses and low dose rates would provide a strong argument for the existence of thresholds. However, in mammals, one of the mechanisms for repair of such lesions is nonhomologous end joining, which is known to be inefficient (Jeggo, 1998; Jeggo and Concannon, 2001). Somatic mutations resulting from mis-repaired DSB and complex lesions are thought to be contributors to the carcinogenic process (NCRP, 2001b).

Thus, while it is not possible to rule out the existence of a threshold dose below which radiation exposure does not contribute to carcinogenesis, the threshold hypothesis is at most a possibility, and not a particularly strong one, on the basis of current knowledge. Perhaps surprisingly, while the effect of a known threshold on radiation protection would be revolutionary, the influence on risk and uncertainty calculations of the uncertain *possibility* of a threshold at nontrivial doses and dose rates is minimal, considerably less than that of an assumed DDREF (Land, 2002). Therefore, in uncertainty calculations for the present Report, a threshold possibility will be ignored.

7.2.3.2 *Uncertainties in D(L).* It has been estimated that the uncertainty in the charged particle spectrum outside the spacecraft is ~10 % and increases at ~1 % per g cm^{-2} of material traversed (Cucinotta *et al.*, 2001a). For neutrons, the uncertainty was estimated at 25 % and increased at 2 % per g cm^{-2} of material traversed (Cucinotta *et al.*, 2001a). It is clear that for typical spacecraft shielding and body self-shielding thicknesses of <20 to 30 g cm^{-2}, the uncertainties in the physical parameters remain significantly less than a factor of two.

7.2.3.3 *Uncertainties in Q(L)*. It has long been recognized that *Q(L)* is only an approximation of the manner in which radiation risk is expected to vary with radiation quality. This subject has been discussed in some detail as it relates to space radiation risks in NCRP Report No. 137 (NCRP, 2001a). In that report a comparison was made between risks calculated by the conventional manner described above and two alternative methods, one based on particle fluences and one based on microdosimetric considerations. Calculations based on amorphous or stochastic track structure models (Cucinotta *et al*., 1999) were not considered in NCRP Report No. 137 (NCRP, 2001a). An example of a year's exposure to GCR was chosen behind shielding typical of a spacecraft flying outside the geomagnetosphere, and the cancer risk was calculated and compared using the three methodologies. Since it is convenient here to use the same formulation to explore the uncertainty, a brief review of the example follows.

The 1977 solar minimum differential fluence-energy spectra of GCR were assumed to be isotropically incident on a spherical aluminum shell of thickness 10 g cm^{-2}. This thickness is typical of that to be expected on a rather well-shielded spacecraft outside the magnetosphere. Placed at the center of the shell is a sphere of red bone marrow of radius 2.5 g cm^{-2}. This thickness was chosen so that secondary nuclear particles (including neutrons) would be roughly in equilibrium within a hydrogenous organic material as will be the case inside a human body. Spectra of all the primary and secondary charged particles found at the point at the center of the concentric spheres were used in the analysis. The spectra of all particles from protons to nickel were calculated with the computer code BRYNTRN/HZETRN (Shinn *et al*., 1992). From these spectra, various quantities of interest were calculated, such as the total yearly absorbed dose (0.19 Gy) and dose equivalent (0.67 Sv). The goal was to arrive at an excess risk of all cancers assuming a year's exposure from this highly idealized spherically symmetric environment. The result was an increased risk of cancer mortality of 2.7 % for a 1 y exposure and an mean quality factor of 3.5.

Uncertainty in the variation of risk with radiation quality is studied here by varying the quality factor as a function of LET. Equation 7.8 was modified to account for a reasonable upper and lower limit to the uncertainty. The factors chosen to multiply the quality factor to provide these limits were determined rather arbitrarily and are:

$$F_{\text{upper}} = 1.5 + 0.5 \log_{10} L \text{ for } L < 10 \text{ keV } \mu\text{m}^{-1}$$
$$= 2 \log_{10} L \text{ for } L = 10 \text{ keV } \mu\text{m}^{-1}, \quad (7.11)$$

$$F_{\text{lower}} = 0.9 - 0.1 \log_{10} L \text{ for } L < 10 \text{ keV } \mu\text{m}^{-1}$$
$$= 0.8 (\log_{10} L)^{-3} \text{ for } 10 \text{ keV } \mu\text{m}^{-1} < L \leq 100 \text{ keV } \mu\text{m}^{-1}$$
$$= 0.1 L \text{ for } L > 100 \text{ keV } \mu\text{m}^{-1}.$$

The quality factors, along with the curves multiplied by each of these two limiting factors, are shown in Figure 7.1. The results of the sensitivity calculations are that the upper limit risk is 8 % with an mean quality factor of 10.4, and the lower limit risk is 1.2 % with an mean quality factor of 1.5. Comparing this with the nominal value of 2.7 % and an mean quality factor of 3.5 leads to the conclusion that reasonable uncertainty in the variation of risk with radiation quality results in an uncertainty factor of 3 on the high side and 2.3 on the low side. That is, it is unlikely that the true risk is higher than the nominal risk by a factor of more than 3 or lower by a factor of >2.3 because of errors in the variation of risk with radiation quality [*i.e.*, the variation of $Q(L)$ with LET]. An alternative upper limit for Q was chosen such that it would be constant at a value of 60 above 100 keV μm^{-1}. This yielded a risk of 5.4 % and an mean quality factor of 7. Thus, this choice implies an uncertainty factor of two on the high side.

An alternative assessment of quality factor uncertainties was given by Cucinotta *et al*. (2001a) based on available radiation biology data for HZE ions. More recently, Cucinotta *et al*. (2006) have considered correlations in the uncertainties for quality factors when folded with LET-spectra by sampling over trial $Q(L)$ functions. In this approach each trial in the Monte-Carlo sampling chooses a new $Q(L)$ function, which is folded with model distributions for LET spectra. As in the above analysis, this approach recognizes that errors in the assignments of Q values are correlated by the nature of biophysical processes that determine biological effectiveness as a function of LET. The trial function used has a shape guided both by experimental data and biophysical models, and sample from distributions of parameters that enter into the functional form:

$$Q_{\text{trial}}(L) = \begin{cases} 1 & L < L_0 \\ AL - B & L_0 \leq L < L_m \\ \dfrac{C}{L_p} & L \geq L_m \end{cases}. \quad (7.12)$$

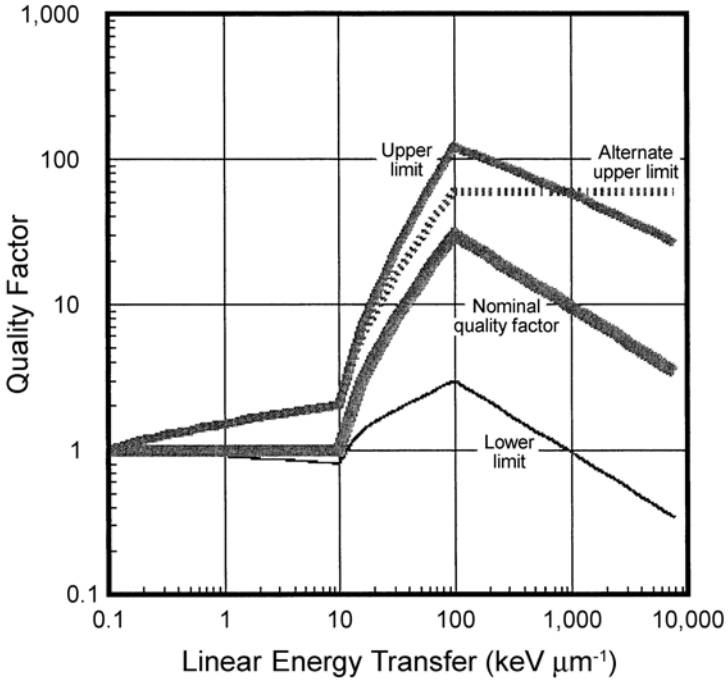

Fig. 7.1. Quality factors, along with the curves multiplied by each of the limiting factors described in Equation 7.11.

Once the parameters of the model, L_0, L_p, and L_m, along with the maximum value Q_m at L_m are defined, Equation 7.12 is used to solve for the values of the constants A, B and C. Note that the ICRP Publication 60 (ICRP, 1991) definition of *Q(L)* corresponds to L_0 = 10 keV μm^{-1}, L_m = 100 keV μm^{-1}, p = ½, and Q_m = 30 leading to A = 0.32, B = 2.2, C = 300. In the earlier ICRP Publication 26 definition of *Q(L),* L_0 = 3.5 keV μm^{-1}, L_m = 172.5 keV μm^{-1}, p = 0, and Q_m = 20. Often discussed issues in defining radiation quality dependence on LET are the value of the slope p that controls the decrease in $Q(L)$ above the maximum, the maximum value of $Q(L)$, the value of LET where the maximum occurs, L_m, and the minimum LET value where $Q(L)$ rises above unity, L_0. Track structure models suggest that each charge group would have distinct curves of similar shape to Equation 7.12 with hydrogen peaking at a much lower value of LET than for example iron ions. Based on track structure models it is expected that data sets that consider only a small number of ions would not be able to unfold a precise $Q(L)$ relationship. Another prediction of the track structure models of radiation

sensitivity is that the peak and maximum values of RBE will vary across tissues corresponding to the target size (*e.g.*, gene or chromosome region) causative of initiation or progression, and the related gamma-ray sensitivity. The parameter samplings are based on the following assumptions for probability distribution functions for parameters that enter in the function of Equation 7.12:

- L_0: the distribution has a peak of equal probability between 5 and 10 keV μm^{-1}, and falls to zero <1 keV μm^{-1}, and >15 keV μm^{-1}.
- L_p: distribution with equal probability for LET values between 75 and 150 keV μm^{-1}, and decreases to zero <50 keV μm^{-1} and >250 keV μm^{-1}.
- p: distribution with equal probability between $p = 1/2$ and 1, and a probability that decreases to zero at $p = 0$ and $p = 2$.
- Q_m: log-normal distribution with mean value of 30 and geometric standard deviation of 1.75.

The risk per 10 mGy versus LET that results from the model is shown in Figure 7.2. For chronic exposures, protraction effects including a so-called inverse dose-rate effect have been noted for high-LET radiation. Such effects have been studied in long-term exposures with neutrons in the mouse (NCRP, 1990), and in radon exposures to miners (NAS/NRC, 1999). The duration of a human mission to Mars would suggest that protraction effects would only contribute a minor uncertainty to the overall cancer risk projection.

7.2.3.4 *Overall Uncertainty in Risk Estimations*. Although no attempt is made here to perform a calculation in combining the uncertainties outlined above, it is clear that most of the uncertainty lies in the low-LET coefficients (k_T) and the LET-dependence of the quality factor [$Q(L)$] with the latter providing the major contribution. Thus, it can be concluded that the uncertainty in the biological parameters exceeds that in the physical parameters by a considerable margin. This conclusion is similar to that of Cucinotta *et al*. (2001a), who attributed roughly 5 % of the uncertainty to physics, 18 % to risk coefficient (*i.e.*, at low-LET), and 77 % to the quality factor for an aluminum shielding thickness of 20 g cm^{-2}.

7.3 Early Radiation Effects

Discussion of early radiation effects is based on the premise that cell killing is the central, if not the singular cause of the detectable noncancer effects in tissues and organs. Therefore, the response of

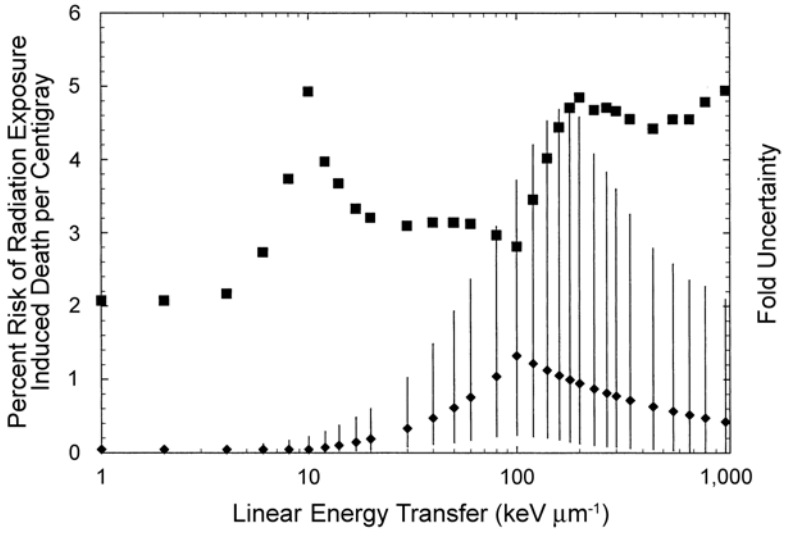

Fig. 7.2. Estimates of percent risk of REID per 10 mGy for males exposed (at low dose rates) at age 40 y as a function of LET (diamonds), 95 % confidence intervals, and the fold-uncertainty (squares) calculated as the ratio of the REID at the 97.5 to 50 % probability.

a tissue is determined by the characteristics of the survival of cells in the specific tissue. Because it requires sufficient cell killing for a change in the function or the morphology of an organ to be detected, a threshold dose must be exceeded after which the *severity* of the effect increases with increasing dose. Noncancer effects may occur early in tissues with a rapid cell turnover or later in tissues in which cell turnover is slower or the effect is complex.

Two factors are important in influencing the probability of noncancer effects occurring as a result of exposure to radiation in deep space. These are dose rate and radiation quality. The importance of these factors is different between ambient GCR radiation and radiation from SPEs.

7.3.1 *Dose Protraction and Dose Rate*

The radiation from GCR is continuous and varies in dose rate by perhaps a factor of two to three during a solar cycle, but does not reach a value considered to be a high dose rate. Organizations concerned with risk estimates and radiation protection differ in their definitions of a low dose rate. UNSCEAR (1993) suggested

0.1 mGy min^{-1} (144 mGy d^{-1}), ICRP (1991) suggested 0.1 Gy h^{-1} (2.4×10^3 mGy d^{-1}), and NCRP (1980) suggested 0.05 Gy y^{-1} (~0.1 mGy d^{-1}). In most biological test systems, lowering the dose rate decreases the biological effect (for the same dose) over a large range of dose rates, down to a limiting low dose rate, below which the biologic effect per unit dose does not change. The limiting dose rate is 5.2 Gy d^{-1} for cell inactivation (Bedford and Mitchell, 1973) and ~0.2 Gy d^{-1} for life shortening in mice (Sacher and Grahn, 1964). The dose rate of GCRs varies between 0.14 and 0.4 mGy d^{-1} over the solar cycle. The one tissue for which reduction in the dose rate does not reduce the effect is the testes where exposures to the same dose but a lower dose rate can be more effective in reducing sperm count or producing sterility than if the dose is delivered at a higher-dose rate (Meistrich and Samuels, 1985).

The highest dose rates in space occur during large SPEs. The dose rate and the total dose of radiation depend on a number of factors that include the intensity of the disturbance on the sun, the longitude of the disturbance on the sun's disk relative to the position of the spacecraft, the condition of the interplanetary magnetic field between the sun and the spacecraft, and the amount of shielding provided by the spacecraft. In addition, the intensity of individual SPEs varies greatly and it is not possible to predict the dose rate that might occur in the most intense event that might be encountered during a given mission to Mars. However, the analysis by Simonsen *et al*. (1993) based on the large SPE of October 1989 suggested that with 10 g cm^{-2} shielding, the dose rate would not exceed 400 mSv d^{-1}. More recently, Kim *et al*. (2006) have considered the dose rates for a large number of SPEs and found that when realistic spacecraft and tissue shielding are considered, dose rates for all SPEs over the last 60 y are <50 mGy h^{-1}. Typical examples of the dose rates of SPEs as a function of shielding and time are shown in Figure 7.3. An exception is during extravehicular activities in space or on the surface of the moon where higher-dose rates could occur. Risk assessment criteria necessary for mission design for a worse-case SPE must consider particle fluence rates, as well as total particle fluence and spectral characteristics.

7.3.2 *Radiation Quality*

The spectra of energies and LETs of protons, heavy ions, and neutrons have been discussed earlier and must be taken into account in the estimation of the risk of noncancer effects in deep space. The RBE values of neutrons, protons, carbon, neon and argon ions for the induction of noncancer effects have been examined

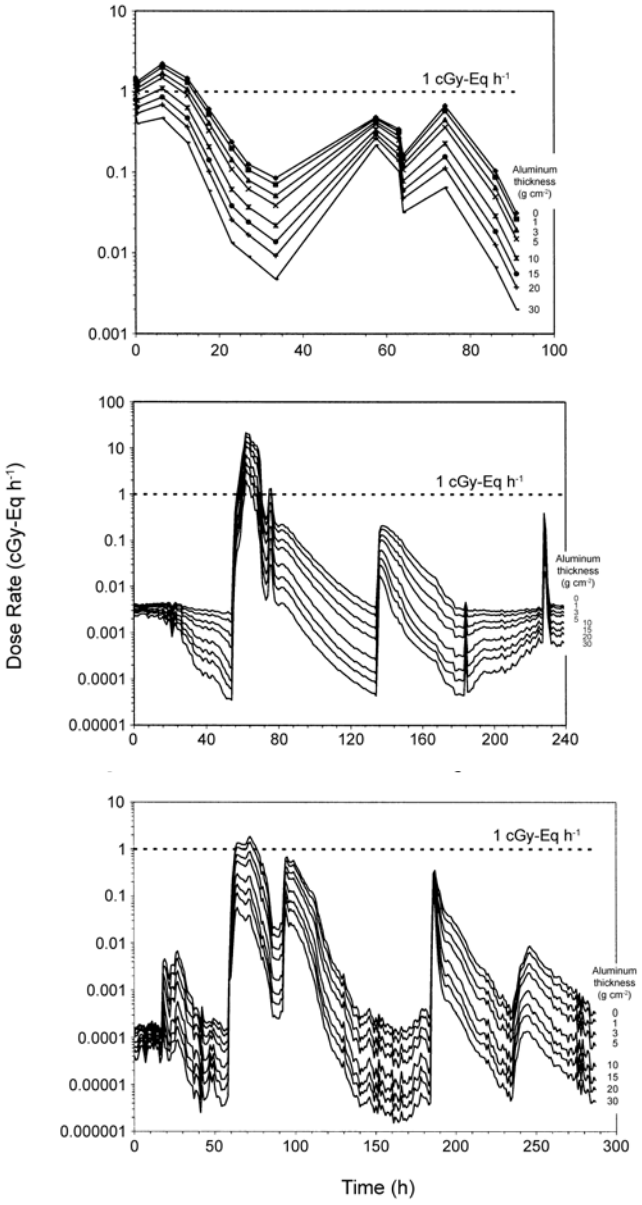

Fig. 7.3. Typical examples of the dose rate of SPEs under thicknesses of aluminum of 0 to 30 g cm^{-2} as a function of time in hours. (Top panel is November 1960 SPE, middle panel is August of 1972 SPE, and lower panel is October of 2003 SPE.)

by ICRP (1989). In the case of neutrons, ranging in energy from 5.6 to 22 MeV, the RBE values for early responses were between 1 and 6.6 and for late effects between 2.3 and 10. The limited data for protons and helium ions with energies >50 MeV n^{-1} indicated RBE values in the range of 1 to 1.5. The measured RBE values for heavy ions depend not only on the tissue exposed but also whether the exposure is in the plateau or peak region of the beam. For most tissues exposed in the plateau region, RBE ranged from one to three and in the extended peak region between six and eight. In these studies, various reference radiations were used. However, the choice of the reference radiation for studies of noncancer effects is not considered as important as for late effects. ICRU (1986) reported that at absorbed doses of ~1 Gy, the biological effectiveness of x and gamma rays does not change by >20 % over an energy range of 10 keV to 100 MeV. Unfortunately, most of the data for noncancer effects have been obtained after exposure to acute high dose irradiation and there is no information about effects in humans of whole-body doses of ~1 Gy protracted over 1 to 2 y. The evidence, however, suggests that in most tissues, repair and recovery from noncancer effects are efficient in reducing or eliminating the damage caused by radiation at the dose rates experienced in space.

For noncancer effects, RBE values will depend on the biological effect under consideration and the severity of the effect. Based on available data it is difficult to distinguish RBE values for blood-forming organs and skin damage, however for cataract higher RBE values occur, especially for cataract induced after longer latency times. Because the definition of a clinically significant cataract is obscured by the unidirectional nature of cataracts, this endpoint should be modeled distinctly from other noncancer effects. NCRP Report No. 132 (NCRP, 2000) noted that RBEs for noncancer effects should be determined at dose levels corresponding to the threshold for inducing the effect. At such doses, it is clear that RBEs for noncancer effects are lower than RBEs for late effects. Because of this, the dose equivalent, measured in sievert (Sv) and obtained using quality factors based on RBEs for stochastic effects, is not appropriate to be used for describing the risk of noncancer effects. A new quantity, the gray equivalent has been introduced and NCRP (2000) can be consulted for a further discussion of this subject. Several future considerations for improving noncancer risk assessments are warranted. These include expanding the database for RBEs as a function of radiation quality and dose rate. Also, models that include possible synergistic effects of microgravity and stress on early responses are needed.

7.4 Risk to the Central Nervous System

Since early in the history of spaceflight, it has been suggested that, for long flights outside the geomagnetosphere, the high-energy heavy-ion component of GCR, sometimes known as HZE particles (high-Z and energy), might cause a specific hazard to the CNS that has no counterpart from low-LET radiation (*e.g.*, NAS/NRC, 1973). However, the extent of any long-term damage from this source is still unknown. Calculations have been made of the probabilities that sensitive sites within the eye and brain would be hit by HZE particles during solar minimum (*i.e.*, when GCR intensities are maximum). For instance, the probability that an average neural cell (471 μm^2 area) would be hit by particles with charge $Z > 10$ during a 3 y mission was found to be 0.4 inside a typically shielded spacecraft and 0.1 that it would be hit by an iron ion (charge = 26) (Curtis *et al.*, 1998). An important task still remains to determine whether and to what extent such particle traversals contribute to functional degradation within the CNS. Section 6 reviews experimental behavioral data in animals placed in high-energy heavy-ion beams.

7.5 Alternative Cancer Projection Models

A fundamental problem in research for estimating radiation risks is the development of approaches to utilize data from cellular and animal models where studies as a function of radiation quality and dose rates are possible in order to estimate risk in humans, in whom data are not available. The models described above make use of quality factors and DDREFs to implement this requirement and, as noted above, no other considerations are made. Alternative approaches have been considered using more descriptive models of carcinogenesis in animals and humans. Carnes *et al.* (2003) studied the role of intrinsic and extrinsic causes of mortality and their variation across animal species as an approach to translate radiation data to humans. Issues related to extrapolating risks from non-human experimental systems to humans have been extensively discussed in NCRP Report No. 150 (NCRP, 2005). Survival theory and the Cox proportional hazard model were used. Estimates of the mean lifespan for intrinsic and extrinsic causes of death including solid tumors were used to scale life loss from radiation in mice and beagles, to life lost in humans. Figure 7.4 shows an example of the Carnes model (Carnes *et al.*, 2003) where data from $B6CF_1$ mice are used to predict survival after irradiation in the Japanese atomic-bomb survivors at several dose levels. The success of this

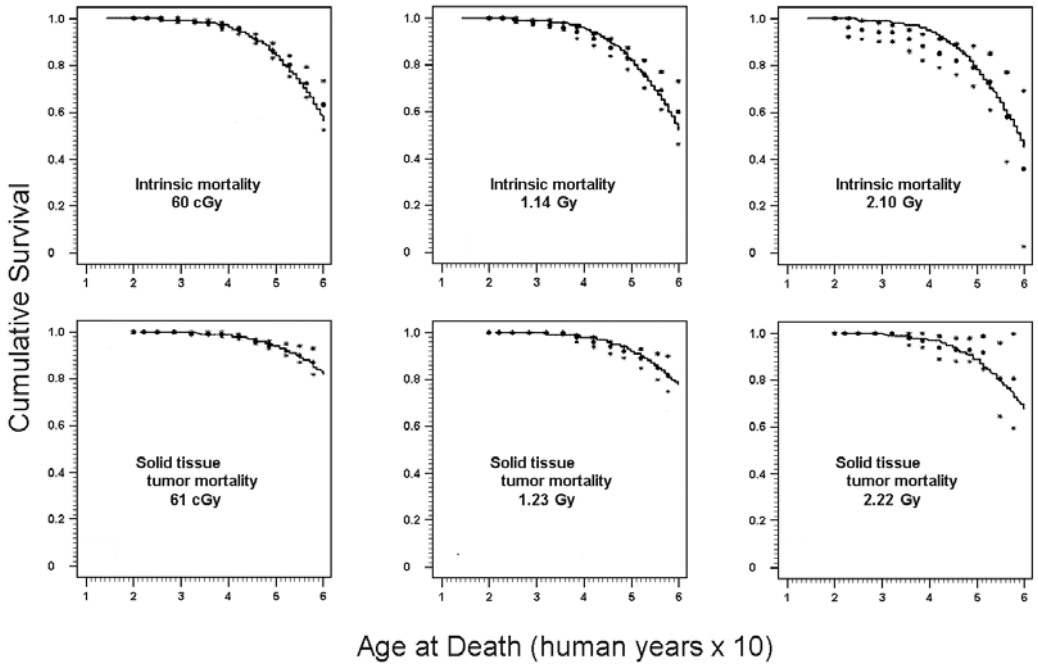

Fig. 7.4. Cumulative survivorship curves (scaled to human years) for irradiated $B6CF_1$ mice predicted from the dose-response model evaluated at the same total doses received by the atomic-bomb survivors, and the empirical survival curve (with 95 % confidence intervals) observed for representative dose groups of the atomic-bomb survivors (Carnes *et al*., 2003).

approach for gamma-ray exposures where the model is tested against the Japanese lifespan data provides confidence for other radiation types where animal data are available. More recently the model is being applied to animal carcinogenesis data for neutron irradiation. Data sets are not available for mice or other species following proton and HZE ions irradiation, and at this time consideration of radiation quality has not been implemented into the model other than fitting to neutron data sets.

The multi-stage models of carcinogenesis have had a long history in fitting carcinogenesis data among populations and for carcinogens such as radiation. Multi-stage models consider the processes of cancer initiation, promotion and progression in their application. These include models where the number of stages in carcinogenesis is treated as a free parameter in fits to data (Armitage and Doll, 1954; 2004), two-stage models where premalignant cells that have suffered one mutational event are given a growth advantage (Moolgavkar, 1991), and several variants of these approaches. As molecular biology and genetics approaches have made progress on the nature and number of steps in the formation of cancers, multi-stage models have been developed to incorporate such knowledge. Most recently models that investigate the relative roles of chromosomal instability relative to initiating mutational events have been developed (Nowak *et al*., 2002). For treating radiation induction of cancer, assumptions must be made on which stages are modified by radiation.

Although a complex task, it is believed that such knowledge will be useful in improving risk projections for radiation exposures in humans.

7.6 Computational Biology and Risk Assessment

Radiation biology has evolved in recent years with many experiments now describing cellular and tissue responses in terms of molecular interactions and genetics. To be fully utilized in risk assessment, mathematical or computational models of these approaches are needed to support the interpretation of results, and the extrapolation of data across radiation quality, dose, and dose rates. Over the course of several decades of research, the development of computation models for providing a comprehensive description of space radiation risks is a worthy goal. The modeling of surrogate endpoints such as gene mutation, chromosomal changes, or instability for cancer or other risks (Schatzkin *et al*., 1990; 1996) would be of particular value in improving the accuracy of risk assessments.

The modeling of DNA structures has been used in describing the ionization and excitation of DNA and local environment, and the early radiation chemistry of these processes (Nikjoo *et al*., 1999). More recently, stochastic track-structure models of DNA damage have been combined with computer descriptions of large-scale structures of chromosomes using random walk models, models of large-scale DNA loops, and treatment confinement of each human chromosome into the nuclear volume (Sachs *et al*., 1995). These models are used in stochastic Monte-Carlo simulations of the distribution of DNA fragments and form the basis for models of DNA damage processing or geometrical model of the formation of chromosomal aberrations (Ballarini and Ottolenghi, 2004; Holley *et al*., 2002). These models have not treated DNA damage repair and the subsequent biological events in any substantive manner.

Biochemical kinetics approaches are needed to extend physical models of DNA damage and structures to the description of radiation biology experiments that describe DNA repair and signal transduction pathways by radiation. In the application of mathematical descriptions of the metabolic pathways, radiation acts as a perturbation of these systems leading to protective signal transduction processes, and also potentially aberrant events. In this approach, DNA damage serves as a substrate for modulation of protein levels, interactions, and signaling processes. Because a fundamental theoretical description of complex cellular control systems does not exist, the use of biochemical kinetics can be described as phenomenological. However, biochemical kinetics models of molecular radiation biology will allow the results of these experiments to be extrapolated to other dose, dose rate, and radiation quality regimes and for testable predictions to be developed. Two early seminal works on metabolic control systems are those of Koshland *et al*. (1966) and Monod *et al*. (1963), which highlighted the role of the specificity of enzymatic binding. This is especially important because of the large number of molecular species within cells, which operate under nonequilibrium modes. The specificity of enzyme binding is due, in part, to their unique molecular structures and is also favored by the compartmental structure of cells. This specificity allows phenomenological models to work with much success, which is surprising because of the complex heterogeneous processes occurring within cells and since a fundamental theoretical description of such phenomena has not been developed. The work of Monod *et al*. (1963) developed the description of allosteric regulation (regulation through conformational changes in proteins) of the metabolic controls of many cellular responses.

Goldbeter and Koshland (1981) developed mathematical descriptions of protein regulation by covalent modification. These works predicted the important role of kinases in cellular controls including their potential to act as switches, positive or negative feedback controls, and in molecular cascades and, in fact, anticipated the importance of the dysfunction of kinase pathways in human diseases. New approaches in systems biology are of interest for integrating biology data into models of health risks (Alberghina and Westerhoff, 2005).

8. Summary of Information Needed

Listed below is a summary of the information needed by major subject area. Additional details are provided in each section. The major information needed is also summarized in Section 1, and included here for completeness.

8.1 Space Radiation Environment

- Develop SPE forecasting and prediction capabilities that are able to observe or account for interplanetary shocks and CMEs. These capabilities should include the ability to reliably predict the fluence spectra and time evolution of an SPE.
  - Prediction of SPEs in support of manned space flight should be changed from the current criterion of predicting events having a peak proton fluence rate of ≥ 10 $(cm^2\ s\ sr)^{-1}$ at energies ≥ 10 MeV towards a method of predicting events for which the free-space dose would exceed some biological threshold. Since the radiation dose is also a function of the energetic particle spectral parameters as well as the particle fluence, there needs to be sufficient spectral information so that a reasonable dose estimate can be made. For example, predictions of ≥ 30 MeV proton events with fluences $>3 \times 10^6$ protons cm^{-2} (an energy content equivalent to ~10 mGy absorbed dose) would be more useful than the current >10 MeV peak fluence-rate predictions.
  - Identify and model the agents responsible for the acceleration of large fluences of energetic particles at biologically significant energies in space. There should also be research directed toward identifying precursors and unique signatures of fast CMEs and useful CME proxies. These would include techniques to improve the prediction and detection of fast CMEs and associated interplanetary shock, the shock-Mach number (particularly at about five solar radii), and the shock shape and heliolongitudinal extent. Research directed toward a capability

of remote sensing of fast interplanetary shocks and their speed and position in space with respect to a spacecraft will aid the prediction of solar-particle fluence rate expected from a specific interplanetary shock. A capability of modeling the connection from the observer to the shock front will improve the prediction capability. There is also a definite need to model the acceleration of particles at the location of the shock front including prediction of fluence rates and fluence changes as the shock approaches and passes Earth (or spacecraft).

- Develop realistic models of the largest expected SPE fluence rates, which may be encountered on exploratory missions. Assessments of their potential biological effects and shielding requirements need to be carried out.
  - As a complement to the development of worst-case fluence-rate models, research directed toward identifying quiet periods, when very reliable predictions of no significant SPEs can be made, should also be carried out. Developing this capability would be very useful for planning extravehicular activities or surface exploration on the moon or Mars.
- Continue to improve the accuracy and extend the range of energies and elemental species included in the GCR environmental models.

8.2 Space Radiation Physics and Transport

- Develop and validate space radiation transport codes and nuclear cross-section models that treat all components of the primary and secondary spectra of the space radiation environment including protons, neutrons, light ions, heavy ions, mesons, and electromagnetic cascades. It is unlikely that space radiation problems can be handled with a one-size fits all approach and the specific application will drive the method to be used.
  - Develop methods of incorporating angle and energy distributions of neutrons and light ions, especially for applications on the surfaces of the moon and Mars.
  - Add methods to treat meson and electromagnetic cascades coupled to GCR primaries to space radiation transport codes that also include heavy ions.
  - Conduct intercomparisons of space radiation transport code predictions from applicable deterministic and

Monte-Carlo transport codes for a variety of relevant space radiation protection scenarios.

- Perform assessments of the accuracy of space radiation transport codes for prediction of energy spectra of charged particles and neutrons by comparisons to laboratory experiments with proton and heavy-ion beams and from spaceflight measurements. Tests of radiation transport codes with monoenergetic beams can be used to evaluate the accuracy of these codes. Laboratory beam validation is advantageous for validating radiation transport computer codes and associated database models and to provide tests for studying material properties for reducing biological doses. Spaceflight measurements provide important tests of predictive capability of several factors and are needed for final validation of the transport codes.

• Improve existing nuclear interaction databases for properly assessing risk and concomitant shielding requirements, especially for neutrons and light ions. For describing projectile fragmentation, cross sections for fragmentation of the more abundant GCR nuclei are needed at several energies and for an array of targets of interest for spacecraft shielding and for transport in tissues.

- Develop models to accurately predict neutron and light ion (hydrogen and helium isotopes) spectra from nucleon-nucleus and nucleus-nucleus collisions of GCR ions on relevant target atoms.
- Develop models or databases for meson production and meson-nucleus interactions.
- Develop high-energy heavy-ion (HZE particle) event generators that properly treat all secondary particle types, energies and directions of travel from nuclear collisions for use in the Monte-Carlo transport codes.

There is a shortage or absence of data for several of the major GCR components such as helium, nitrogen, calcium, chromium and titanium. There are a reasonable number of projectile fragmentation data sets now available with the above noted exceptions, however the projectile energy coverage of the data are lacking with more data needed in the 0.1 to 0.4 GeV n^{-1} region and >1 GeV n^{-1}. Although several data sets exist for iron beams, there is a paucity of data for iron at energies >2 GeV n^{-1}. Also cross-section data and multiplicities extending to lower fragment charges and masses are needed. Many of the earlier cross-section measurements only

extend down to approximately half of the incident beam charge or mass numbers. Based on existing measurements of interaction cross sections for major contributors of GCR and the wide range of materials to be characterized for missions beyond LEO, physics measurements recommended for improving radiation transport codes are:

- light particle spectra (Z = 1, 2) from proton interactions on a variety of targets typical of shielding materials (*e.g.*, carbon, oxygen, aluminum, calcium, iron). This should include double differential cross sections over energies up to the beam energy at several beam energies (0.25 to 2 GeV);
- fragmentation parameters for all secondary ions from a variety of GCR projectiles over a full range of targets (*e.g.*, hydrogen, carbon, aluminum, copper, and lead);
- measurements of thick target yields of ions and neutrons for a variety of GCR projectiles (*e.g.*, helium, oxygen, iron). Targets should include single elements (*e.g.*, carbon, aluminum), H_2O, multi-layered materials, and composites such as *in situ* materials similar to lunar regolith and Martian soil; and
- spaceflight measurements using composite materials of varying composition using particle spectrometers or proportional counters.

8.3 Space Dosimetry

Additional research and development are needed in a number of specific areas of space radiation dosimetry and instrumentation. These include:

- Develop radiation spectrometers which can accurately measure fluence of indirectly ionizing particles (neutrons) in the presence of much higher fluence of directly ionizing particles.
- Experimentally validate radiation transport and dosimetry models.
- Evaluate the energy deposition in microscopic volumes in a uniform medium, and of the effect of the wall on measurements made with TEPC.
- Study the effects of numerical and physical phantom configurations on the calculation and measurement of organ dose.

- Improve data on neutron production in fragmentation processes and on neutron interaction cross sections for the purpose of dose calculation and detector design.
- In order to provide the data needed to effectively evaluate risk of radiation exposures outside Earth's magnetosphere, future biological response studies should specify lineal energy as well as dose, fluence and spectrum for the radiation exposures leading to observed effects.

8.4 Space Radiation Biology

8.4.1 *Late Radiation Effects*

- *Cancer*. It is recommended that experiments be conducted to:
  - determine the carcinogenic effects of space radiations in animals with a sufficient number of suitable heavy ions to provide data for determining an appropriate quality factor value for each;
  - develop an alternative method for obtaining an equivalent dose for neutrons in the 2 to 50 MeV range;
  - determine the basis for the different initial slopes of the dose response curves for induction of cancer or surrogate markers for cancer by HZE particles and fragments;
  - determine the number of cells at risk traversed by HZE particles and fragments and the resulting survival, and how these influence carcinogenic risk for particles of different energies;
  - determine the influence of repair as well as damage processing on the probability of tumorigenesis by HZE particles;
  - determine the role of delta rays in the induction of cancer by heavy ions;
  - assess the importance of dose rate on the initial slope for cancer related endpoints for proton or HZE exposures; and
  - develop methods using surrogate markers for cancer to extrapolate risk from experimental animal models to humans.
- *Noncancer*. It is recommended that experiments be conducted to:
  - determine the effects of protracted exposures to low dose rates (<50 mSv y^{-1}) of protons, HZE particles, and neutrons of relevant energies in the 0.5 to 1.5 Sv range on

the CNS, lens of the eye, vascular system throughout the body, hematopoietic and immune systems, gastrointestinal tract, gonadal cell populations, and fertility.

8.4.2 *Early Radiation Effects*

- *Thresholds for Neurovestibular, Cardiac, Prodromal and Other CNS Effects.* It is recommended that:
  - all available data from therapeutic uses of radiation be reexamined to estimate threshold doses for loss of balance, cardiac arythmias, nausea, vomiting, and other CNS effects; and
  - all radiation accident data be analyzed to determine if any behavioral changes can be expected from exposure to the highest doses likely to occur as a result of deep-space activities.
- *Hematological, Dermal and Immune Issues*. It is recommended that experiments be conducted to:
  - determine how to maintain the proliferative integrity of the hematopoietic, dermal and immune systems when exposed to low dose rates of protons, heavy ions and neutrons.

8.4.3 *Other Information Needed*

- *Dose-Rate Issues*. It is recommended that experiments be conducted to:
  - derive estimates of the dose, and in particular the dose rate over each hourly period for the worst-case SPE scenario that can be anticipated; and
  - study the effects of the dose rate of protons and neutrons of relevant energies up to several hundred megaelectron volts. For initial estimates of risk and required shielding, these dose-rate studies could be carried out on cells *in vitro*, by determining cell survival and chromosome aberrations and mutation incidence for the purpose of establishing animal protocols.
- *Combined Exposures/Stressors*. It is recommended that experiments be conducted to:
  - evaluate the effects of combined exposures to protons and HZE particles; and
  - acquire data and model effects from multiple stressors, including microgravity, UV, microwaves and hormonal stress cascades.

- *Biomarkers*. It is recommended that experiments be conducted to:
  - evaluate biomarkers for identification of individuals at increased risk due to genetic predisposition; and
  - evaluate biomarkers to estimate cumulative doses.
- *Countermeasures*. It is recommended that countermeasures be assessed for their efficacy in preventing adverse effects.

8.5 Space Radiation Risk Assessment Methodology

- Several future considerations for improving noncancer risk assessments are warranted. These include expanding the database for RBEs as a function of radiation quality and dose rate, and developing models that include possible synergistic effects of microgravity and stress on early responses.
- To be fully utilized in risk assessment, mathematical models of molecular interactions and genetics are needed to support the interpretation of results, and the extrapolation of data across radiation quality, dose, and dose rates. The modeling of surrogate endpoints for cancer or other risks will be of particular value in improving the accuracy of risk assessments.

Appendix A

Summary Tables of Literature by Radiation Type[16]

TABLE A.1—*Neutron irradiation experiments.*

Discipline	Biological Models		Radiation Type and Energies	Selected References
Cytogenetic damage	*In vitro*	Human diploid fibroblast	2.2 MeV	Kadhim *et al.* (1998)
	In vitro	Murine spleen cells	1 MeV	Bouffler *et al.* (1996)
Genomic instability	*In vitro*	Mammalian cells	2.3 MeV	Trott *et al.* (1998)
Gene expression		MCF-7	Fission neutrons	Balcer-Kubiczek *et al.* (1995)
	In vitro	Syrian hamster embryo cells	Fission neutrons	Woloschak and Chang-Liu (1990)

[16]This listing does not include all relevant publications but is included to inform the reader of representative work.

TABLE A.1—*(continued)*.

Discipline	Biological Models		Radiation Type and Energies	Selected References
Mutation frequency and spectrum	*In vitro*	Human lymphoblastoid cells	4.2 MeV	Kronenberg (1991)
	In vitro	Murine hematopoietic cells	4.2 MeV	Harper *et al*. (1997)
Behavior cataractogenesis	*In vivo*	Mice, rats, guinea pigs, and rabbits	Fast neutrons	Abrosimova *et al*. (2000) Ainsworth (1986) Bateman and Bond (1967) Christenberry *et al*. (1956) Laporte and Delaye (1987) Medvedovsky and Worgul (1991) Mickley *et al*. (1988) Riley *et al*. (1991) Ross *et al*. (1990) Worgul (1986) Worgul *et al*. (1996)
Hypersensitivity	*In vitro*	Human melanoma cells	14 MeV	Dionet *et al*. (2000)

Multi-organ pathogenesis	*In vivo*	Mice	Fission neutrons	Carnes *et al*. (2002)
Reproduction	*In vivo*	Mice	7 MeV fast neutrons	Pampfer and Streffer (1988) Pampfer *et al*. (1992)
Prodromal effects	*In vivo*	Ferrets	Fission neutrons	Rabin *et al*. (1992)

TABLE A.2—*Proton and alpha particle irradiation experiments.*

Discipline	Biological Models		Radiation Type and Energies	Selected References
Cytogenetic damage	*In vitro*	CHO cells	^{238}Pu alpha	Little *et al*. (1997)
	In vitro		250 MeV protons	George *et al*. (2003) Yang (1999)
	In vitro	Human lymphocytes	^{238}Pu alpha	Anderson *et al*. (2000; 2002; 2003)
	In vitro /in vivo	Mouse/human bone marrow	3.3 MeV alpha	Kadhim *et al*. (1992; 1994; 1995; 1998; 2001) Lorimore *et al*. (1998)
	In vitro	Human lymphocytes (dose, dose rate, and shielding effects)	250 MeV protons	Durante *et al*. (1998) George *et al*. (2002)
	In vitro	Human diploid fibroblast	3.3 MeV alpha	Kadhim *et al*. (1998)
Bystander effects – cytogenetic	*In vitro*	Cultured fibroblasts	^{238}Pu alpha	Deshpande *et al*. (1996) Nagasawa and Little (1992; 1999) Narayanan *et al*. (1997)
Bystander effects – mutation induction	*In vitro*	CHO cells	^{238}Pu alpha	Nagasawa and Little (1999)

	In vitro	Human hamster hybrid	Microbeam alpha	Zhou *et al*. (2000; 2004)
Bystander effects – micronucleus	*In vitro*	Human fibroblasts	X ray or alpha	Belyakov *et al*. (1999) Prise *et al*. (1998a)
Bystander effects – cell killing		Three-dimensional tissue cultures	Beta from tritium ^{3}H	Bishayee *et al*. (1999)
Bystander effects – transformation	*In vitro*	Hamster cells	Microbeam alpha	Sawant *et al*. (2001)
Bystander-ROS	*In vitro*	Fibroblasts	Alpha	Narayanan *et al*. (1997)
Bystander effects – inducible proteins	*In vitro*	Immortalized	Alpha	Azzam *et al*. (1998; 2001) Hickman *et al*. (1994)
Incomplete chromosome exchanges (FISH)	*In vitro*	Normal human lymphocytes and fibroblasts	250 MeV protons	Wu *et al*. (1997)
Genomic instability	*In vitro*	Human and murine Hematopoietic stem cells	Alpha	Kadhim *et al*. (1998) Wright (1998)
	In vitro	Human lymphoid cells	Alpha	Kadhim *et al*. (2001)
Metastatic potential	*In vivo*	Mouse osteosarcomas	190 MeV protons	Ogata *et al*. (2005)

TABLE A.2—*(continued)*.

Discipline	Biological Models		Radiation Type and Energies	Selected References
	In vitro	Hamsters	Alpha	Little *et al*. (1997)
	In vitro	Hamster and V79	Alpha	Manti *et al*. (1997)
	In vitro	Mammalian cells	Alpha	Deshpande *et al*. (1996)
	In vitro	Human bronchial epithelial cells	^{238}Pu alpha	Kennedy *et al*. (1996)
	In vitro	Human mammary epithelial cells	Alpha	Durante *et al*. (1996)
Cataractogenesis	*In vitro*	Human lens epithelial cells	55 MeV protons	Chang *et al*. (2005)
Immune response and cytokine production	*In vivo*	C57Bl6	250 MeV protons	Gridley *et al*. (2002a) Kajioka *et al*. (1999; 2000a; 2000b) Pecaut *et al*. (2001; 2002)
Immune responses with or without aluminum shielding	*In vivo*	C57Bl6	250 MeV protons	Pecaut *et al*. (2003a)

Hematological response	*In vivo*	C57Bl6	250 MeV protons	Gridley *et al*. (2001)
Mutation frequency and spectrum	*In vitro*	Human lymphoid cell line	55 MeV protons	Gauny *et al*. (2001) Nagasawa and Little (1999) Zhou *et al*. (2000)
Transformation	*In vitro*	Mammalian cells	3.7 MeV alpha	Yang *et al*. (2000)
Behavior	*In vivo*	Rats	155 MeV protons	Rabin *et al*. (1991)
Neuronal/CNS effects	*In vivo*	Rhesus monkeys	55 MeV protons	Wood *et al*. (1986)
Cataractogenesis	*In vivo*	Rhesus monkeys	32 – 2,300 MeV protons	Lett *et al*. (1991)
	In vitro	Human lens epithelial cells	55 MeV protons	Chang *et al*. (2000a) McNamara *et al*. (2001)
Carcinogenesis	*In vivo*	Harderian gland in mice	55 MeV protons	Alpen *et al*. (1994)
	In vivo	Mammary tumorigenesis in Sprague-Dawley rats	250 MeV protons	Dicello *et al*. (2004)
	In vivo	Skin	Protons	Burns *et al*. (1978) Heimbach *et al*. (1969)

TABLE A.3—*Helium, neon and carbon ion irradiation experiments*.

Discipline	Biological Models		Radiation Type and Energies	Selected References
Cytogenetic damage	*In vitro*	Human fibroblasts	Helium, neon (120 keV μm^{-1})	Goodwin *et al*. (1994; 1996) Holley and Chatterjee (1996) Lobrich *et al*. (1996) Newman *et al*. (1997) Rydberg (1996)
	In vitro	Human skin fibroblasts	X rays or 195 MeV n^{-1} carbon	Nasonova *et al*. (2004)
	In vitro	Human skin fibroblasts	10.7 MeV n^{-1} neon	Martins *et al*. (1993)
	In vitro	V79	100 MeV n^{-1} carbon	Bohrnsen *et al*. (2002)
		Human lymphocytes	Carbon, neon (0.3 – 140 keV μm^{-1})	Durante *et al*. (1998)
			Helium, carbon, silicon, iron, gold (0.4 – 1,393 keV μm^{-1})	George *et al*. (2003)
Chromosome instability-Hprt mutations	*In vitro*	Chinese hamster cells	Helium, carbon, nitrogen (20 – 360 keV μm^{-1})	Govorun *et al*. (2002)

Incomplete chromosome exchanges (FISH)			290 MeV n^{-1} carbon	Wu *et al*. (1997)
Vascular effects	*In vivo*	Neonatal rats	670 MeV n^{-1} neon	Yang and Tobias (1984)
	In vivo	Rats	290 MeV n^{-1} carbon	Okada *et al*. (1998)
Transformation	*In vitro*	Hamster 10T1/2	474 MeV n^{-1} carbon, 425 MeV n^{-1} neon	Yang *et al*. (1980; 1985)
Behavior	*In vivo*	Rats	165 MeV n^{-1} helium, 522 MeV n^{-1} neon	Rabin *et al*. (1991)
	In vivo	Rats – thermoregulation	522 MeV n^{-1} neon (~28 keV μm^{-1}), 165 MeV n^{-1} helium (~2 keV μm^{-1})	Kandasamy *et al*. (1994)
CNS/neuronal effects	*In vivo*	Rabbits	230 MeV n^{-1} helium	Lo *et al*. (1989; 1991a)
	In vivo	Rabbits, mice	Neon (35 keV μm^{-1})	Cox and Kraft (1984)
	In vivo/ in vitro	Mouse brains	230 MeV n^{-1} helium, 425 MeV n^{-1} neon	Manley (1988) Richards and Budinger (1988) Rosander *et al*. (1987)

TABLE A.3—*(continued)*.

Discipline	Biological Models		Radiation Type and Energies	Selected References
	In vivo	Rat brains	205 MeV n^{-1} carbon	Karger *et al*. (2002a; 2002b)
	In vivo	Dog hemibrains	456 MeV n^{-1} neon, 225 MeV n^{-1} helium	Brennan *et al*. (1993)
	In vitro	Neonatal rat explants	36 MeV n^{-1}, 54 MeV n^{-1} helium	Mamoon (1970)
	In vivo	Mouse brains	Helium (6 keV μm^{-1}), carbon (80 keV μm^{-1}), neon (150 keV μm^{-1})	Kraft and Cox (1986)
	In vivo	Rat spinal cords	400 MeV n^{-1} neon, carbon, 225 MeV n^{-1} helium, 230 kV n^{-1} x rays	Leith *et al*. (1975a; 1975b; 1982a) Okada *et al*. (1998) Rodriguez *et al*. (1987; 1991)
	In vitro	Mouse brain cells	290 MeV n^{-1} carbon	Nojima *et al*. (2000)
	In vivo	Mice	400 MeV n^{-1} neon	Kraft *et al*. (1979)

	In vitro	Mouse astrocytes and microglia	Carbon	Nojima *et al*. (2000)
Cataractogenesis			300 MeV n^{-1}, ^{137}Cs helium, carbon	Abrosimova *et al*. (2000)
	In vivo	Rabbits	400 MeV n^{-1} neon	Abrosimova *et al*. (2000) Lett *et al*. (1980)
	In vitro	Human lens epithelial cells	32 MeV n^{-1} helium	Chang *et al*. (2000a)
Carcinogenic potential	*In vivo*	Rat skins	Neon (25 keV μm^{-1})	Burns *et al*. (1991; 1994) Felber *et al*. (1994)
	In vivo	Mouse fibrosarcoma	290 MeV n^{-1} carbon	Ando *et al*. (1999)
	In vivo	Harderian gland in mice	228 MeV n^{-1} helium	Alpen *et al*. (1993)
Metastatic potential	*In vivo*	Mouse osteosarcomas	290 MeV n^{-1} carbon	Ogata *et al*. (2005)
Vascular/cardiovascular effects	*In vivo*	Neonatal rats	670 MeV n^{-1} neon	Yang and Tobias (1984)
Hypersensitivity	*In vitro*	V79	100 MeV n^{-1} carbon	Bohrnsen *et al*. (2002)

TABLE A.4—*Silicon, argon and gold ion irradiation experiments.*

Discipline	Biological Models		Radiation Type and Energies	Selected References
Cytogenetic damage	*In vitro*	Human fibroblasts	400 MeV n^{-1} argon (120 keV μm^{-1})	Goodwin *et al*. (1996)
	In vitro	Hamster fibroblasts	11.4 MeV n^{-1} argon	Nasonova *et al*. (2001) Ritter *et al*. (1992; 1996)
	In vitro	Hamster fibroblasts V79	550 MeV n^{-1} argon, 100 MeV n^{-1} silicon	Furusawa *et al*. (2002)
	In vitro	Human skin fibroblasts	10.5 MeV argon	Martins *et al*. (1993)
	In vitro	V79	Argon (1,233 keV μm^{-1})	Nasonova *et al*. (2001)
		Human lymphocytes	10 GeV n^{-1}, 550 MeV n^{-1} argon	George *et al*. (2003)
Genomic instability	*In vitro*		11 GeV n^{-1} gold (1,450 keV μm^{-1})	Limoli *et al*. (2000a; 2000b)
Mutation frequency and spectrum	*In vitro*	Human skin fibroblasts	330 MeV n^{-1} argon (150 keV μm^{-1}) 600 MeV n^{-1} lanthanum (920 keV μm^{-1})	Tsuboi *et al*. (1992)

	In vitro	Human lymphoblastoid cells	470 MeV n^{-1} argon (95 – 97 keV μm^{-1}) 456 MeV n^{-1} silicon (61 keV μm^{-1})	Kronenberg and Little (1989a; 1989b)
Transformation	*In vitro*	Mammalian cells	670 MeV n^{-1} silicon 320 MeV n^{-1} silicon 330 MeV n^{-1} argon	Yang *et al*. (1985)
Behavior	*In vivo*	Rats	670 MeV n^{-1} argon	Rabin *et al*. (1991; 1994)
	In vivo	Rats – thermoregulation	670 MeV n^{-1} argon (~85 keV μm^{-1})	Kandasamy *et al*. (1994)
CNS/neuronal effects	*In vivo*	Mice	570 MeV n^{-1} argon	Philpott *et al*. (1985)
	In vivo	Mouse brains	Argon (650 keV μm^{-1})	Kraft and Cox (1986)
	In vivo	Rabbit retinas	530 MeV n^{-1} argon	Williams and Lett (1994)
	In vivo	Rabbits, mice	570 MeV n^{-1} argon (90 keV μm^{-1})	Cox and Kraft (1984)
Retinal effects	*In vivo*	Rabbits	530 MeV n^{-1} argon	Williams and Lett (1994)

TABLE A.4—*(continued)*.

Discipline	Biological Models		Radiation Type and Energies	Selected References
Cataractogenesis	*In vivo*	Rabbits, mice	570 MeV n^{-1} argon	Abrosimova et al. (2000) Brenner *et al*. (1991) Lett *et al*. (1980) Merriam *et al*. (1984) Worgul (1986)
Carcinogenesis	*In vivo*	Rat skins	Argon (125 keV μm^{-1})	Burns *et al*. (1991; 1994)
	In vivo	Harderian gland	570 MeV n^{-1} argon	Fry *et al*. (1983)
Immune responses	*In vivo*	C57Bl.6	1.2 GeV n^{-1} silicon (42 keV μm^{-1})	Gridley *et al*. (2002b)

TABLE A.5—*Iron, lead and chromium ion irradiation experiments.*

Discipline	Biological Models		Radiation Type and Energies	Selected References
DNA damage and repair	*In vitro*	Human fibroblasts	250 – 600 MeV n^{-1} iron	Rydberg *et al*. (1994) Rydberg (1996)
		Mammalian fibroblasts	600 MeV n^{-1} iron	Metting *et al*. (1988)
Cytogenetic damage	*In vitro*	Rat tissues (lung, trachea, bone marrow)	1 GeV n^{-1} iron	Brooks *et al*. (2001)
	In vitro	Hamster fibroblasts V79	115 MeV n^{-1} iron	Furusawa *et al*. (2002)
	In vitro	Human lymphocytes	1 GeV n^{-1}, 100 MeV n^{-1}, 200 MeV n^{-1} iron	Durante *et al*. (1998; 2002a) George *et al*. (2003) Horstmann *et al*. (2004)
	In vitro	Human lymphocytes	0.5 GeV n^{-1}, 5 GeV n^{-1} iron	Loucas *et al*. (2004)
	In vivo	Mouse lymphocytes	1 GeV n^{-1} iron	Tucker *et al*. (2004)

TABLE A.5—*(continued)*.

Discipline	Biological Models		Radiation Type and Energies	Selected References
	In vivo	Micronucleus	1 GeV n^{-1} iron	Chang *et* al. (2000a)
Chromosome aberrations and shielding	*In vitro*	Human fibroblasts	1 GeV n^{-1} iron	Antonelli *et al*. (2004)
	In vitro	Human lymphocytes	200 MeV n^{-1}, 500 MeV n^{-1} iron	Durante *et al*. (2002b; 2004) Grossi *et al*. (2004)
Incomplete chromosome exchanges (FISH)	*In vitro*	Human cells	1 GeV n^{-1} iron	George *et al*. (2001b) Wu *et al*. (1997; 2003)
Genomic instability	*In vitro*	Human lymphoid cell lines	1 GeV n^{-1} iron	Evans *et al*. (2001; 2002; 2003)
		Immortalized human bronchial epithelial cells	1 GeV n^{-1} iron	Hei *et al*. (1998) Suzuki *et al*. (2001)

	In vitro	Human lymphoid cells	1 GeV n^{-1} iron	Grosovsky *et al*. (2001)
Mutation frequency and spectrum	*In vitro*	Human lymphoblastoid cell lines	600 MeV n^{-1} iron	Kronenberg *et al*. (1995)
	In vitro	Human skin fibroblasts	300 MeV n^{-1} iron (500 keV μm^{-1}), 400 MeV n^{-1} iron (300 keV μm^{-1}), 600 MeV n^{-1} iron (200 keV μm^{-1})	Tsuboi *et al.* (1992)
	In vitro	Mammalian hybrid cells	1 GeV n^{-1} iron	Kronenberg *et al*. (1995) Waldren *et al*. (1998)
	In vitro	Human–hamster hybrid cells	1 GeV n^{-1} iron	Lenarczyk *et al*. (2003)
	In vitro	Human lymphoblastoid TK6 and WTK1 cell lines	1 GeV n^{-1} iron	Wiese *et al*. (2001)
	In vivo	LacZ transgenics	1 GeV n^{-1} iron	Chang *et al*. (2001)

TABLE A.5—*(continued)*.

Discipline	Biological Models		Radiation Type and Energies	Selected References
Transformation	*In vitro*	Mammalian cells	600 MeV n^{-1}, 400 MeV n^{-1}, 300 MeV n^{-1} iron	Yang *et al*. (1985; 1996)
		Immortalized human bronchial epithelial cells	1 GeV n^{-1} iron	Hei *et al*. (1998) Suzuki *et al*. (2001)
DNA damage responsive proteins	*In vitro*		3.1 MeV n^{-1} lead (12,600 keV μm^{-1}), 3.7 MeV n^{-1} chromium (3,270 keV μm^{-1})	Jakob *et al*. (2002)
Behavior	*In vivo*	Rats	600 MeV n^{-1}, 1 GeV n^{-1} iron	Denisova *et al*. (2002) Joseph *et al*. (1992; 1993; 1994) Rabin *et al*. (2000; 2003b) Shukitt-Hale *et al*. (2000)
	In vivo	Rats – thermoregulation	600 MeV n^{-1} iron (~190 keV μm^{-1})	Kandasamy *et al*. (1994)

	In vivo	Rats – GTPase in striatum	600 MeV n^{-1} iron	Villalobos-Molina *et al*. (1994)
	In vivo	Rat dopaminergic systems	600 MeV n^{-1}, 1 GeV n^{-1} iron	Hunt *et al*. (1989; 1990) Rabin *et al*. (1989) Riley and Tuck (1985)
	In vivo	Rat amphetamine – induced taste aversion	1 GeV n^{-1} iron	Rabin *et al*. (2003b)
	In vivo	Cognition	1 GeV n^{-1} iron	Shukitt-Hale *et al*. (2003)
	In vivo	Rat – age and diet countermeasures	1 GeV n^{-1} iron	Rabin *et al*. (2005)
	In vivo	C57Bl6 mice	1 GeV n^{-1} iron	Pecaut *et al*. (2004)
CNS/neuronal effects	*In vivo*	Rabbit retinas	465 MeV n^{-1} iron	Williams and Lett (1994; 1996)
	In vivo	Mouse brains	600 MeV n^{-1} iron (180 keV μm^{-1})	Kraft and Cox (1986)
	In vivo	Hippocampal neurogenesis	1 GeV n^{-1} iron	Rola *et al*. (2004)

TABLE A.5—*(continued)*.

Discipline	Biological Models		Radiation Type and Energies	Selected References
	In vitro	Neurite retraction/ outgrowth	1 GeV n^{-1} iron	Vazquez and Kirk (2000)
Cataractogenesis	*In vivo*	Rats	450 MeV n^{-1} iron	Worgul *et al*. (1993)
	In vivo	Mice	600 MeV n^{-1} iron	Medvedovsky *et al*. (1994) Tao *et al*. (1994)
	In vivo	Rats	600 MeV n^{-1} iron	Brenner *et al*. (1993)
	In vivo	Rats	460 MeV n^{-1} iron (460 keV μm^{-1})	Wu *et al*. (1994)
	In vivo	Monkeys	460 MeV n^{-1} iron	Lett *et al*. (1991)
	In vivo	New Zealand rabbits	460 MeV n^{-1} iron	Riley *et al*. (1991) Worgul (1986)

	In vitro	Human lens epithelial cells	1 GeV n^{-1} iron	Chang *et al*. (2005)
Retinal effects	*In vivo*	Rabbits	465 MeV n^{-1} iron	Williams and Lett (1994; 1996)
Carcinogenesis	*In vivo*	Harderian gland in rodents	350 MeV n^{-1}, 600 MeV n^{-1} iron	Alpen *et al*. (1994) Fry *et al*. (1983)
	In vivo	Mammary tumorigenesis in Sprague-Dawley rats	1 GeV n^{-1} iron	Dicello *et al*. (2004)
	In vivo	Rat skins	1 GeV n^{-1} iron	Burns *et al*. (2001)
Immune responses	*In vivo*	C57Bl.6	1 GeV n^{-1} iron	Gridley *et al*. (2002b)
Vascular/ cardiovascular effects	*In vivo*	Neonatal rats	600 MeV n^{-1} iron	Yang and Tobias (1984)
Epigenetic effects	*In vivo*	Mice mammary/skin tissue	1 GeV n^{-1}, 600 MeV n^{-1} iron	Costes and Barcellos-Hoff (2002) Costes *et al*. (2000; 2004)
Prodromal effects	*In vivo*	Ferrets	600 MeV n^{-1} iron	Rabin *et al*. (1992)
Oxidative stress and dietary supplement	*In vivo*	Sprague-Dawley rats	1 GeV n^{-1}, 5 GeV n^{-1} iron	Guan *et al*. (2004)

TABLE A.6a—*Human studies.*

Biological Endpoint	Radiation Source	Selected References
Cataractogenesis	Radiotherapy – x rays	Nutting *et al*. (1999)
	Radiotherapy – protons	Gragoudas *et al*. (1995)
	Radiotherapy – helium	Meecham *et al*. (1994)
	Hiroshima/Nagasaki	Medvedovsky and Worgul (1991) Otake and Schull (1990)
	Environmental contamination	Junk *et al*. (1999)
	Cyclotron and reactor experience	ICRP (1969)
	Space exposure	Cucinotta *et al*. (2002) Mader *et al*. (1999) Rastegar *et al*. (2002)
Carcinogenic potential	Fast neutrons from Atomic-Bomb Survivor Study	Kellerer and Walsh (2001; 2002) Tokunaga *et al*. (1994)
	Atomic-Bomb Survivor Study	Preston *et al*. (2004)
	Neutron therapy patients	Sigurdson *et al*. (2002)
	Airline cabin attendants in Europe	Zeeb *et al*. (2003)

	Protons/photons	Schneider *et al*. (2002)
Neuronal/CNS effects	Radiotherapy – helium	Castro *et al*. (1985)
	Radiotherapy – protons	Kjellberg and Kliman (1979) Kjellberg *et al*. (1983) Linfoot (1979) Suit *et al*. (1982a; 1982b) Tobias (1979)
Cerebral vascular effects	Radiotherapy – protons and helium	Fabrikant *et al*. (1984; 1985; 1989) Kjellberg *et al*. (1983) Levy *et al*. (1989; 1990; 1992) Lo and Fabrikant (1991) Lo *et al*. (1989; 1991a; 1991b; 1992) Rodriguez *et al*. (1991) Steinberg *et al*. (1990)
Cytogenetic effects	Flight crew	De Angelis *et al*. (2001) Heimers *et al*. (1995) Romano *et al*. (1997) Scheid *et al*. (1993) Wolf *et al*. (1999a; 1999b)
	Atomic-Bomb Survivor Study	Awa *et al*. (1978) Stram *et al*. (1993)

TABLE A.6a—*(continued)*.

Biological Endpoint	Radiation Source	Selected References
	Astronauts after long-term low-Earth missions, carbon-treated cancer patients, and patients before and after radiotherapy	Durante *et al*. (2004)
	Astronauts	Fedorenko *et al*. (2000; 2001) George *et al*. (2001c; 2004) Obe *et al*. (1997) Sabatier *et al*. (1995) Testard and Sabatier (1999) Testard *et al*. (1996) Yang *et al*. (1997)
Light flashes	Apollo astronauts	Tobias *et al*. (1971)
	Accelerator studies – nitrogen and neutrons	Budinger *et al*. (1972)
Mutation in T-lymphocytes	Soviet cosmonauts	Curry *et al*. (2000) Khaidakov *et al*. (1997; 1999)
Hereditary effects	Atomic-Bomb Survivor Study	Neel (1998)
	Space exposure	Jennings and Santy (1990)

CVD	Atomic-Bomb Survivor Study cohort	Sankaranarayanan *et al*. (1999) Wong *et al*. (1999)
	Chernobyl workers	Ivanov *et al*. (2001)
	Three Mile Island	Talbott *et al*. (2000)
	Oak Ridge Laboratory (1943 – 1972)	Richardson and Wing (1999)
	Medical radiation exposure	Gofman (1999)
Noncancer effects	Atomic-Bomb Survivor Study cohort	Shimizu *et al*. (1999)
	Astronauts – fluid balance and kidney function	Drummer *et al*. (2004)
Immune deficiencies	Atomic-Bomb Survivor Study	Hayashi *et al*. (2003) Kusunoki *et al*. (2001; 2002a; 2002b)
	Space flight	Sonnenfeld (1998; 2001) Sonnenfeld and Shearer (2002) Stowe *et al*. (200la; 2001b; 2003)
	Chernobyl	Kuzmenok *et al*. (2003)
Second cancers/genomic instability	Radiotherapy – x rays	Sigurdson *et al*. (2003)

TABLE A.6b—*Flight experiments.*

Discipline	Biological Model		Mission (duration)	Dates	Selected References
Immune responses	*In vivo*	C57BL/6	Space Shuttle Explorer – 12 d	December 5, 2001	Gridley *et al*. (2003) Pecaut *et al*. (2003b)

Glossary

absorbed dose (*D*): The quotient of $d\bar{\varepsilon}$ by dm, where $d\bar{\varepsilon}$ is the mean energy imparted to matter of mass dm (*i.e.*, $D = d\bar{\varepsilon}/dm$). The unit for D is joule per kilogram (J kg^{-1}) with the special name gray (Gy).

albedo neutrons: Secondary neutrons produced by interactions of galactic cosmic radiation and the atmosphere, and reflected back into space.

alpha particles: Nuclei of helium atoms consisting of two protons and two neutrons in close association. They have a net charge of +2 and can therefore be accelerated in large electrical devices similar to those used for protons, and they are also emitted during the decay of some radioactive isotopes.

anisotropy: The ratio of the maximum to the average particle fluence rate distribution as a function of angle.

anomalous cosmic ray: Component perhaps of a different origin than that of the high-energy cosmic rays. The peak in the energy spectrum at solar maximum is ~10 MeV m^{-1}.

ansatz: An assumed form for a mathematical statement that is not based on any underlying theory or principle.

Archimedean spiral: A mathematical curve resulting from a linear angular rotation with increasing distance.

as low as reasonably achievable (ALARA**):** A principle of radiation protection philosophy that requires that exposures to ionizing radiation should be kept as low as reasonably achievable, economic and social factors being taken into consideration. The protection from radiation exposure is ALARA when the expenditure of further resources would be unwarranted by the reduction in exposure that would be achieved. In the case of space activities, ALARA applies to actions taken to keep all doses to the astronauts as low as reasonably achievable, balancing the mission objectives with practical dose reduction steps.

astronomical unit (AU**):** The average distance from the sun to Earth, 150×10^6 km.

bremsstrahlung: Secondary photon radiation produced by deceleration of charged particles.

bystander effect: The effect detected in cells not traversed by a particle.

chromosphere: The portion of the solar atmosphere between the photosphere and the corona. The portion of the solar atmosphere in which color can be distinguished.

cornea: The transparent epithelial structure forming the anterior part of the external covering of the eye.

corona: The portion of the solar atmosphere above the chromosphere.

coronal mass ejection (CME): A transient outflow of plasma from or through the solar corona which may be associated with the generation of solar-particle events.

cosmic-ray modulation: The variation of the observed cosmic-ray intensity as a function of the solar cycle. The cosmic-ray intensity is observed to vary approximately inversely with the solar activity cycle.

delta ray: Electrons stripped from atoms as a charged particle passes through matter.

deterministic effects: Effects for which the severity varies with dose and for which a threshold usually exists (*e.g.*, cataracts and skin burns).

detriment: Health detriment is the sum of the probabilities of all the components of health effects. These include in addition to fatal cancer the probability of heritable effects and the probability of morbidity from nonfatal cancer.

dose: A general term used when the context is not specific to a particular dose quantity. When the context is specific, the name or symbol for the quantity is used [*i.e.*, absorbed dose (D), mean absorbed dose (D_T), dose equivalent (H), effective dose (E), equivalent dose (H_T), or organ dose equivalent $\overline{H}_T$].

dose equivalent (H): The product of the absorbed dose (D) at a point and the quality factor (Q) at that point for the radiation type (*i.e.*, $H = DQ$). The unit of H is J kg^{-1} with the special name sievert (Sv).

dose limit: A limit on radiation dose that is applied for exposure to individuals or groups of individuals in order to prevent the occurrence of radiation-induced deterministic effects or to limit the probability of radiation related stochastic effects to an acceptable level. For astronauts working in low-Earth orbit, unique dose limits for deterministic and stochastic effects have been recommended by NCRP.

dose rate: Dose delivered per unit time. Can refer to any dose quantity (*e.g.*, absorbed dose, dose equivalent).

dose-response model: A mathematical formulation of the way in which the effect, or response, depends on dose.

dosimeter: A radiation detection device worn or carried by an individual to monitor the individual's radiation exposure. For space activities, a device worn or carried by an astronaut in-flight.

effective dose (E): The sum over specified tissues of the products of the equivalent dose in a tissue (H_T) and the tissue weighting factor for that tissue or organ (w_T) (*i.e.*, $E = \sum_T w_T H_T$). Effective dose (E) applies only to stochastic effects. The unit is the joule per kilogram (J kg^{-1}) with the special name sievert (Sv).

electrons: Small negatively charged particles that can be accelerated to high energy and velocity close to the speed of light.

electron volt (eV): A unit of energy = 1.6×10^{-12} ergs = 1.6×10^{-19} J; 1 eV is equivalent to the energy gained by an electron in passing

through a potential difference of 1 V; 1 keV = 1,000 eV; 1 MeV = 1,000,000 eV.

equivalent dose (H_T): The product of the mean absorbed dose in an organ or tissue and the radiation weighting factor (w_R) of the radiation type of interest. For external exposure w_R applies to the radiation type incident on the body.

erythema: A redness of the skin.

excess relative risk (ERR)**:** An expression of excess risk relative to the underlying (baseline) risk; if the excess equals the baseline the relative risk is two.

exposure: A measure of the ionization produced in air by x or gamma radiation. Exposure is the sum of electric charges on all ions of one sign produced in air when all electrons liberated by photons in a volume of air are completely stopped, divided by the mass of the air in the volume. The unit of exposure in air is the roentgen (R) or in SI units it is expressed in coulombs (C), $1\ R = 2.58 \times 10^{-4}\ C\ kg^{-1}$.

acute exposure: Radiation exposure of short duration.

chronic exposure: Radiation exposure of long duration, because of fractionation or protraction.

extravehicular activity: Any activity undertaken by the crew outside a space vehicle.

favorable propagation path: A concept suggesting that the Archimedean spiral path from the earth to the sun would connect to a specific solar longitude. It is based on the concept that charged particles travel along the interplanetary magnetic field which is transported out from the sun. For an idealized constant speed solar wind flow, if the interplanetary magnetic field is frozen in the plasma, then the result would form an Archimedean spiral.

first ionization potential: The energy required to remove the first electron from an electrically neutral atom. (The ionization potential is usually given in electron volts.)

fluence (Φ): The quotient of dN by da, where dN is the number of particles incident on a sphere of cross-sectional area da (*i.e.*, $\Phi = dN/da$). The unit for fluence is m^{-2}, commonly given in cm^{-2}. In this Report, distributions of fluence are also noted variously as a function of one or more other variables [*e.g.*, $\Phi(L,t)$, the distribution of fluence as a function of linear energy transfer (L) and time (t)].

fluence rate: The quotient of $d\Phi$ by dt, where $d\Phi$ is the increment of the fluence in the time interval dt. The unit for fluence rate is $m^{-2}\ s^{-1}$.

fractionation: The delivery of a given total dose of radiation as several smaller doses, separated by intervals of time.

galactic cosmic radiation (GCR)**:** The charged-particle radiation outside the magnetosphere comprised of 2 % electrons and positrons, and 98 % nuclei, the latter component consisting (by fluence) of 87 % protons, 12 % helium ions, and 1 % high atomic number, high-energy (HZE) particles.

gamma rays: Short-wavelength electromagnetic radiation of nuclear origin (approximate range of energy: 10 keV to 9 MeV).

Geostationary Operational Environmental Satellite (GOES): A satellite in geosynchronous orbit used for monitoring protons. The satellite travel at the same angular speed above the equator as Earth's rotation and therefore appears stationary when observed from Earth's surface.

gray (Gy): The International System (SI) unit of absorbed dose of radiation, 1 Gy = 1 J kg^{-1}.

gray equivalent (G_T)**:** The product of D_T and R_i, where D_T is the mean absorbed dose in an organ or tissue and R_i is a recommended value for relative biological effectiveness for deterministic effects for a given particle type i (*i.e.*, $G_T = R_i \times D_T$). An R_i value applies to the particle type incident on the body.

gray equivalent (Gy-Eq): The name for the unit of the quantity gray equivalent (G_T) (NCRP, 2000), 1 Gy-Eq = 1 J kg^{-1}.

heavy charged particles: Atomic and subatomic charged particles with masses substantially heavier than that of an electron.

heavy ions: Nuclei of elements heavier than helium such as nitrogen, carbon, boron, neon, argon or iron which are positively charged due to some or all of the planetary electrons having been stripped from them.

heliocentric: A measurement system with its origin at the center of the sun.

heliolongitude: Imaginary lines of longitude on the sun measured east (left) or west (right) of the central meridian (imaginary north-south line through the middle of the visible solar disk) as viewed from Earth. The left edge of the solar disk is 90°E and the right edge is 90°W.

heliosphere: The immense negative bubble containing the solar system, solar wind, and entire solar magnetic field. It extends beyond the orbit the Pluto.

high atomic number, high-energy (HZE) particles: Heavy ions having an atomic number greater than that of helium (such as nitrogen, carbon, boron, neon, argon or iron ions that are positively charged) and having high kinetic energy.

incidence: The rate of occurrence of a disease, usually expressed in number of cases per million.

interplanetary magnetic field: The magnetic field in interplanetary space. The interplanetary magnetic field is transported out from the sun via the solar wind.

interplanetary shocks: An abrupt change in velocity or density that is moving faster than the wave propagation speed in interplanetary space.

ionization: The process by which a neutral atom or molecule acquires a positive or negative charge through the loss or gain of an orbital electron.

latent period: Period or state of seeming inactivity between time of exposure of tissue to an injurious agent and an observed response (also time to response or induction period).

lifetime risk: The lifetime probability of dying of a specific disease.

light ions: Nuclei of hydrogen and helium which are positively charged due to some or all of the planetary electrons having been stripped from them.

lineal energy (y): The quotient of ε by $\bar{\ell}$, where ε is the energy imparted to the matter in a given volume by a single (energy deposition) event and $\bar{\ell}$ is the mean chord length of that volume (*i.e.*, $y = \varepsilon / \bar{\ell}$). The unit for lineal energy is J m^{-1}, commonly given in keV μm^{-1}.

linear energy transfer (LET**):** Average amount of energy lost per unit of particle track length and expressed in keV μm^{-1}.

low-LET: Radiation having a low-linear energy transfer; for example, electrons, x rays, and gamma rays.

high-LET: Radiation having a high-linear energy transfer; for example, protons, alpha particles, heavy ions, and interaction products of fast neutrons.

linear-quadratic model (also linear-quadratic dose-response relationship): expresses the incidence of (*e.g.*, mutation or cancer) as partly directly proportional to the dose (linear term) and partly proportional to the square of the dose (quadratic term). The linear term will predominate at lower doses, the quadratic term at higher doses.

lognormal: If the logarithms of a set of values are distributed according to a normal distribution the values are said to have a lognormal distribution, or be distributed log normally.

mass stopping power: (see ***stopping power***).

mean absorbed dose (D_T): The mean absorbed dose in an organ or tissue, obtained by integrating or averaging absorbed doses at points in the organ or tissue.

mean-free path: The average distance between scattering events in interplanetary particle propagation. Also, the average distance between particle collisions with nuclei, atoms or molecules in a material.

Mir: The Russian (previously Soviet) orbital space station.

neutrons: Particles with a mass similar to that of a proton, but with no electrical charge. Because they are electrically neutral, they cannot be accelerated in an electrical field.

noncancer: Health effects other than cancer (*e.g.*, cataracts, cardovascular disease) that occur in the exposed individual.

organ dose equivalent ($\bar{H}_T$): The mean dose equivalent for an organ or tissue, obtained by integrating or averaging dose equivalents at points in the organ or tissue. It is the practice in the space radiation protection community to obtain point values of absorbed dose (D) and dose equivalent (H) using the accepted quality factor-LET relationship [$Q(L)$], and then to average the point quantities over the organ or tissue of interest by means of computational models to obtain the organ

dose equivalent ($\bar{H}_T$). For space radiations, NCRP adopted the organ dose equivalent as an acceptable approximation for equivalent dose (H_T) for stochastic effects.

photosphere: The portion of the sun visible in white light. Also the limit of seeing down through the solar atmosphere in white light.

prevalence: The number of cases of a disease in existence at a given time per unit of population, usually per 100,000 persons.

protons: The nucleus of the hydrogen atom. Protons are positively charged.

protraction: Extending the length of exposure, for example, the continuous delivery of a radiation dose over a longer period of time.

quality factor (Q): The factor by which absorbed dose (D) at a point is modified to obtain the dose equivalent (H) at the point (*i.e.*, $H = Q\ D$), in order to express the effectiveness of an absorbed dose (in inducing stochastic effects) on a common scale for all types of ionizing radiation. There is a specified dependence [$Q(L)$] of the quality factor (Q) as a function of the unrestricted linear energy transfer (L) in water at the point of interest.

quasithreshold dose: The dose at which the extrapolated straight portion of the dose-response curve intercepts the dose axis at unity survival fraction.

radiation:

1. The emission and propagation of energy through space or through matter in the form of waves, such as electromagnetic, sound, or elastic waves.
2. The energy propagated through space or through matter as waves; radiation or radiant energy, when unqualified, usually refers to electromagnetic radiation; commonly classified by frequency—Hertzian, infrared, visible, ultraviolet, x and gamma rays.
3. Corpuscular emission, such as alpha and beta particles, or rays of mixed or unknown type, such as cosmic radiation.

background radiation: The amount of radiation to which a member of the population is exposed from natural sources, such as terrestrial radiation from naturally-occurring radionuclides in the soil, cosmic radiation originating in outer space, and naturally-occurring radionuclides in the soil, cosmic radiation originating in outer space, and naturally-occurring radionuclides deposited in the human body. The natural background radiation received by an individual depends on geographic location and living habits. In the United States, the background radiation is on the order of 1 mSv y^{-1}, excluding indoor radon which amounts to ~2 mSv y^{-1} on average.

ionizing radiation: Any electromagnetic or particulate radiation capable of producing ions, directly or indirectly, in its passage through matter.

radiation quality: A general term referring to the spatial distribution of absorbed dose. For example, an exposure to neutron radiation may be quantitatively the same as an exposure to gamma rays, in the sense

that, for large volumes of tissue on the order of 1 cm^3, the absorbed energy is the same, yet at resolutions of a few micrometers the ionizing events will be more uniformly dispersed for the gamma-ray radiation than for the neutron radiation, producing quantitatively different biological effects (see ***relative biological effectiveness***).

radiation weighting factor (w_R): A factor used to allow for differences in the biological effectiveness between different radiations when calculating equivalent dose (H_T) (see ***equivalent dose***). These factors are independent of the tissue or organ irradiated.

regolith: A layer of loose, heterogeneous material covering solid rock.

relative biological effectiveness (RBE): A factor used to compare the biological effectiveness of absorbed doses from different types of ionizing radiation, determined experimentally. RBE is the ratio of the absorbed dose of a reference radiation (usually taken as 250 kVp x rays) to the absorbed dose of the radiation in question required to produce an identical biological effect in a particular experimental organism or tissue.

rigidity: The momentum of a charged particle per unit charge. Determines the curvature of the particle's trajectory in a magnetic field. Two particles with different charge but the same rigidity will travel along a path having the same curvature in a given magnetic field.

risk: The probability of a specified effect or response occurring.

absolute risk: Expression of excess risk due to exposure as the arithmetic difference between the risk among those exposed and that obtaining in the absence of exposure.

annual risk: The risk in a given year from an earlier exposure. The annual risk (average) from an exposure is the lifetime risk divided by the number of years of expression.

lifetime risk: The total risk in a lifetime resulting from an exposure(s). It is equal to the average annual risk times the period of expression.

relative risk: An expression of excess risk relative to the underlying (baseline) risk; if the excess equals the baseline risk the relative risk is two.

risk coefficient: The increase in the annual incidence or mortality rate per unit dose: (1) absolute risk coefficient is the observed minus the expected number of cases per person year at risk for a unit dose; (2) the relative risk coefficient is the fractional increase in the baseline incidence or mortality rate for a unit dose.

risk cross section: The probability of a particular excess cancer mortality per particle fluence (excluding delta rays).

risk estimate: The number of cases (or deaths) that are projected to occur in a specified exposed population per unit dose for a defined exposure regime and expression period; number of cases per person-gray or, for radon, the number of cases per person cumulative working level month.

roentgen: A unit of radiation exposure. Exposure in SI units is expressed in C kg^{-1} of air.

secondary radiation: Radiation resulting from absorption of other radiation in matter; may be either electromagnetic or particulate.

sievert (Sv): The special name for the unit of effective dose (E), equivalent dose (H_T), dose equivalent (H), and organ dose equivalent ($\overline{H}_T$), 1 Sv = 1 J kg^{-1}.

solar cycle: The solar-activity cyclic behavior, usually represented by the number of sunspots visible on the solar photosphere. The average length of solar cycles since 1900 is 11.4 y.

solar flare: The name given to the sudden release of energy (often $>10^{32}$ ergs) in a relatively small volume of the solar atmosphere. Historically, an optical brightening in the chromosphere, now expanded to cover almost all impulsive radiation from the sun.

solar maximum: The period of the 11 y solar cycle during which the solar wind is at its most intense resulting in lower levels of galactic cosmic radiation about Earth.

solar minimum: The portion of the 11 y solar cycle during which the solar wind is at its least intense resulting in higher levels of galactic cosmic radiation about Earth.

solar-particle event (SPE): An eruption at the sun that releases a large number of particles (primarily protons) over the course of hours or days.

solar wind: The plasma flowing into space from the solar corona. The ionized gas carrying magnetic fields can alter the intensity of the interplanetary radiation.

spallation: A nuclear reaction in which light particles are ejected as a result of bombardment, for example, by high-energy protons.

stochastic effects: Effects, the probability of occurrence which, rather than their severity, is a function of radiation dose without threshold (*e.g.*, cancer).

stopping power (lineal stopping power): The quotient of the energy lost (dE) by a charged particle in traversing a distance (dx) in a material. Can also be expressed as mass stopping power by dividing the lineal stopping power by the density (ρ) of the material.

tissue weighting factor (w_T): A factor representing the ratio of risk of stochastic effects attributable to irradiation of a given organ or tissue to the total risk when the whole body is irradiated uniformly. The factor is independent of the type of radiation or energy of the radiation.

vitreous: The semifluid, transparent substance which lies between the retina and the lens of the eye.

Symbols, Abbreviations and Acronyms

ACE	Advanced Composition Explorer
ALTEA	Anomalous Long-Term Effects in Astronauts study
ANP	atrial natiuretic peptide
ATM	ataxia telangiectasia mutated
AU	astronomical unit
BrdU	bromodeoxyuridine
CME	coronal mass ejection
CNP	cyclic nucleotide phosphatase
CNS	central nervous system
CREME-85	cosmic-ray effects of microelectronics code
CREME-96	update of CREME-85
CT	computed tomography
CTA	conditioned taste aversion
CVD	cardiovascular disease
DDREF	dose and dose-rate effectiveness factor
DNA	deoxyribonucleic acid
DSB	double-strand break
E	energy
E	effective dose
EAR	excess additive risk
ED_{50}	dose to cause 50 % of the population to have the effect (*e.g.*, nausea)
ELF	extremely-low frequency
EMF	electromagnetic field
ERR	excess relative risk
FISH	fluorescence *in situ* hybridization
FLUKA	Monte-Carlo computer code
FR	fixed-ratio
GCR	galactic cosmic radiation
GGTP	gamma-glutamyl transpeptidase
GOES	Geostationary Operational Environment Satellites
G_T	gray equivalent
HMF	heliospheric magnetic field
HPRT	hypoxanthine-guanine phosphoribosyl transferase
H_T	equivalent dose
$\overline{H}_T$	organ dose equivalent
HZE	high atomic number, high energy
HZETRN	HZE transport computer code

IL-2	interleukin-2
IL-6	interleukin-6
ISS	International Space Station
LAP	latency-associated peptide
LDL	low-density lipoproteins
LEO	low-Earth orbit
LET	linear energy transfer
LIS	local interstellar energy spectrum
LSS	Life Span Study
mFISH	meta-fluorescence *in situ* hybridization
MRI	magnetic resonance imaging
n	nucleon
PCC	premature chromosome condensation
PET	positron emission tomography
RBE	relative biological effectiveness
REID	radiation exposure-induced death
ROS	reactive oxygen species
SCE	sister chromatid exchange
SD	single dose
SEC	Space Environment Center (NOAA)
SGZ	subgranular zone
SPE	solar-particle event
sRBC	sheep red blood cells
STS	Space Transport Shuttle
TEPC	tissue equivalent proportional counter
TGF	transforming growth factor
TLD	thermoluminescent dosimeter
UV	ultraviolet
w_R	radiation weighting factor
w_T	tissue weighting factor

References

ABROSIMOVA, A.N., SHAFIRKIN, A.V. and FEDORENKO, B.S. (2000). "Probability of lens opacity and mature cataracts due to irradiation at various LET values," Aviakosm Ekolog Med. **34**, 33–41.

ADAMS, J.H., JR. (1986). *Cosmic Ray Effects of Microelectronics, Part IV*, NRL-MR-5901 (U.S. Naval Research Laboratory, Washington).

ADAMS, J.H., JR. (1987). *Cosmic Ray Effects of Microelectronics, Part IV*, NRL-MR-5901, rev. (U.S. Naval Research Laboratory, Washington).

ADAMS, J.H., JR. and LEE, J. (1996). "A model of the primary cosmic ray spectra," Radiat. Meas. **26**, 467–470.

AGOSTINELLI, S., ALLISON, J., AMAKO, K., APOSTOLAKIS, J., ARAUJO, H., ARCEL, P., ASAI, M., AXEN, D., BANERJEE, S., BARRAND, G., BEHNERL, F., BELLAGAMBA, L., BOUDREAU, J., BROGLIA, L., BRUNENGO, A., BURKHARDT, H., CHAUVIE, S., CHUMA, J., CHYTRACEK, R., COOPERMAN, G., COSMO, G., DEGTYARENKO, P., DELL'ACQUA, A., DEPAOLA, G., DIETRICH, D., ENAMI, R., FELICIELLO, A., FERGUSON, C., FESEFELDT, H., FOLGER, G., FOPPIANO, F., FORTI, A., GARELLI, S., GIANI, S., GIANNITRAPANI, R., GIBIN, D., GOMEZ CADENAS, J.J., GONZALEZ, I., GRACIA ABRIL, G., GREENIAUS, G., GREINER, W., GRICHINE, V., GROSSHEIM, A., GUATELLI, S., GUMPLINGER, P., HAMATSU, R., HASHIMOTO, K., HASUI, H., HEIKKINEN, A., HOWARD, A., IVANCHENKO, V., JOHNSON, A., JONES, F.W., KALLENBACH, J., KANAYA, N., KAWABATA, M., KAWABATA, Y., KAWAGUTI, M., KELNER, S., KENT, P., KIMURA, A., KODAMA, T., KOKOULIN, R., KOSSOV, M., KURASHIGE, H., LAMANNA, E., LAMPEN, T., LARA, V., LEFEBURE, V., LEI, F., LIENDL, M., LOCKMAN, W., LONGO, F., MAGNIK, S., MAIRE, M., MEDERNACH, E., MINAMIMOTO, K., MORA DE FREITAS, P., MORITA, Y., MURAKAMI, K., NAGAMATU, M., NARTALLO, R., NIEMINEN, P., NISHIMURA, T., OHTSUBO, K., OKAMURA, M., O'NEALE, S., OOHATA, Y., PAECH, K., PERL, J., PFEIFFER, A., PIA, M.G., RANJARD, F., RYBIN, A., SADILOV, S., DI SALVO, E., SANTIN, G., SASAKI, T., SAVVAS, N., SAWADA, Y., SCHERER, S., SEI, S., SIROTENKO, V., SMITH, D., STARKOV, N., STOECKER, H., SULKIMO, J., TAKAHATA, M., TANAKA, S., TCHERNIAEV, E., SAFAI TEHRANI, E., TROPEANO, M., TRUSCOTT, P., UNO, H., URBAN, L., URBAN, P., VERDERI, M., WALKDEN, A., WANDER, W., WEBER, H., WELLISCH, J.P., WENAUS, T., WILLIAMS, D.C., WRIGHT, D., YAMADA, T., YOSHIDA, H. and ZSCHIESCHE, D. (2003). "Geant4—a simulation toolkit," Nucl. Inst. Meth. Phys. Res. A **506**, 250–303.

AHLBOM, I.C., CARDIS, E., GREEN, A., LINET, M., SAVITZ, D. and SWERDLOW, A. (2001). "Review of the epidemiologic literature on EMF and health," Environ. Health Perspect. **109** (Suppl. 6), 911–933.

AINSWORTH, E.J. (1986). "Early and late mammalian responses to heavy charged particles," Adv. Space Res. **6**, 153–165.

ALBERGHINA, L. and WESTERHOFF, H.V., Eds. (2005). *Systems Biology. Definitions and Perspectives, Topics in Current Genetics*, Vol. 13 (Springer-Verlag, New York).

ALFREY, C.P., UDDEN, M.M., LEACH-HUNTOON, C.S., DRISCOLL, T., PICKETT, M.H. (1996). "Control of red blood cell mass in spaceflight," J. Appl. Physiol. **81**, 98–104.

ALPEN, E.L., POWERS-RISIUS, P., CURTIS, S.B. and DEGUZMAN, R. (1993). "Tumorigenic potential of high-*Z*, high-LET charged-particle radiations," Radiat. Res. **136**, 382–391.

ALPEN, E.L., POWERS-RISIUS, P., CURTIS, S.B., DEGUZMAN, R. and FRY, R.J.M. (1994). "Fluence-based relative biological effectiveness for charged particle carcinogenesis in mouse Harderian gland," Adv. Space Res. **14**, 573–581.

ALSMILLER, R.G., JR., IRVING, D.C., KINNEY, W.E. and MORAN, H.S. (1965). "The validity of the straight ahead approximation in space vehicle shielding design studies," pages 177 to 181 in *Second Symposium on Protection Against Radiations in Space*, Reetz, A., Jr., Ed., NASA-SP-71 (National Technical Information Service, Springfield, Virginia).

AMUNDSON, S.A., DO, K.T., SHAHAB, S., BITTNER, M., MELTZER, P., TRENT, J. and FORNACE, A.J., JR. (2000). "Identification of potential mRNA biomarkers in peripheral blood lymphocytes for human exposure to ionizing radiation," Radiat. Res. **154**, 342–346.

AMUNDSON, S.A., BITTNER, M., MELTZER, P., TRENT, J. and FORNACE, A.J., JR. (2001a). "Induction of gene expression as a monitor of exposure to ionizing radiation," Radiat. Res. **156**, 657–661.

AMUNDSON, S.A. and FORNACE, A.J., JR. (2001b). "Gene expression profiles for monitoring radiation exposure," Radiat. Prot. Dosim. **97**(1), 11–16.

ANDERSON, R.M., MARSDEN, S.J., WRIGHT, E.G., KADHIM, M.A., GOODHEAD, D.T. and GRIFFIN, C.S. (2000). "Complex chromosome aberrations in peripheral blood lymphocytes as a potential biomarker of exposure to high-LET alpha-particles," Int. J. Radiat. Biol. **76**, 31–42.

ANDERSON, R. M., STEVENS, D.L. and GOODHEAD, D.T. (2002). "M-FISH analysis shows that complex chromosome aberrations induced by alpha-particle tracks are cumulative products of localized rearrangements," Proc. Natl. Acad. Sci. USA, **99**, 12167–12172.

ANDERSON, R.M., MARSDEN, S.J., PAICE, S.J., BRISTOW, A.E., KADHIM, M.A., GRIFFIN, C.S. and GOODHEAD, D.T. (2003). "Transmissible and nontransmissible complex chromosome aberrations

characterized by three-color and mFISH define a biomarker of exposure to high-LET alpha particles," Radiat. Res. **159**, 40–48.

ANERSON, R.M., TSEPENKO. V.V., GASTEVA, G.N., MOLOKANOV, A.A., SEVANKAEV, A.V. and GOODHEAD, D.T. (2005). "mFISH analysis reveals complexity of chromosome aberrations in individuals occupationally exposed to internal plutonium: A pilot study to assess the relevance of complex aberrations as biomarkers of exposure to high-LET α particles," Radiat. Res. **163**, 26–35.

ANDO, K., KOIKE, S., OHIRA, C., CHEN, Y.J., NOJIMA, K., ANDO, S., OHBUCHI, T., KOBAYASHI, N., SHIMIZU, W. and URANO, M. (1999). "Accelerated reoxygenation of a murine fibrosarcoma after carbon-ion radiation," Int. J. Radiat. Biol. **75**, 505–512.

ANSCHER, M.S., CROCKER, I.R. and JIRTLE, R.L. (1990). "Transforming growth factor-beta 1 expression in irradiated liver," Radiat. Res. **122**, 77–85.

ANTONELLI, F., BELLI, M., CAMPA, A., CHATTERJEE, A., DINI, V., ESPOSITO, G., RYDBERG, B., SIMONE, G. and TABOCCHINI, M.A. (2004). "DNA fragmentation induced by Fe ions in human cells: Shielding influence on spatially correlated damage," Adv. Space Res. **34**, 1353–1357.

ARMITAGE, P. and DOLL, R. (1954). "The age distribution of cancer and multi-stage theory of carcinogenesis," Br. J. Cancer **8**, 1–12.

ARMITAGE, P. and DOLL, R. (2004). "The age distribution of cancer and multi-stage theory of carcinogenesis. 1954," Int. J. Epidemiol. **33**, 1174–1179.

ARMSTRONG, A. and COLBORN, B.L. (2001). "Predictions of secondary neutrons and their importance to radiation effects inside the International Space Station," Radiat. Meas. **33**, 229–234.

ARMSTRONG, J.W., GERREN, R.A. and CHAPES, S.K. (1995). "The effect of space and parabolic flight on macrophage hematopoiesis and function," Exp. Cell Res. **216**, 160–168.

ARMSTRONG, T.W., COLBORN, B.L., HARMON, B.A. and LAIRD, C.E. (1996). "Predictions of the nuclear activation of materials on LDEF produced by the space radiation environment and comparison with flight measurements," Radiat. Meas. **26**, 765–777.

ATTIX, F.H. (1986). *Introduction to Radiological Physics and Radiation Dosimetry* (John Wiley and Sons, Inc., New York).

AUBIN, F. (2003). "Mechanisms involved in ultraviolet light-induced immunosuppression," Eur. J. Dermatol. **13**, 515–523.

AWA, A.A. and NEEL, J.V. (1986). "Cytogenetic "rogue" cells: What is their frequency, origin, and evolutionary significance?" Proc. Natl. Acad. Sci. USA **83**, 1021–1025.

AWA, A.A., SOFUNI, T., HONDA, T., ITOH, M., NERIISHI, S. and OTAKE, M. (1978). "Relationship between the radiation dose and chromosome aberrations in atomic bomb survivors of Hiroshima and Nagasaki," J. Radiat. Res. (Tokyo) **19**, 126–140.

AYALA, M.N. and SODERBERG, P.G. (2004). "Vitamin E can protect against ultraviolet radiation-induced cataract in albino rats," Ophthalmic Res. **36**, 264–269.

AZZAM, E.I., DE TOLEDO, S.M., GOODING, T. and LITTLE, J.B. (1998). "Intercellular communication is involved in the bystander regulation of gene expression in human cells exposed to very low fluences of alpha particles," Radiat. Res. **150**, 497–504.

AZZAM, E.I., DE TOLEDO, S.M. and LITTLE, J.B. (2001). "Direct evidence for the participation of gap junction-mediated intercellular communication in the transmission of damage signals from alpha-particle irradiated to nonirradiated cells," Proc. Natl. Acad. Sci. USA **98**, 473–478.

BACHOFER, C.S. and GAUTEREAUX, M.E. (1959). "X-ray effects on single nerve fibers," J. Gen. Physiol. **42**, 723–735.

BADHWAR, G.D., Ed. (1997a). *Impact of Solar Energetic Particle Events for Design of Human Missions* (Center for Advanced Studies, Houston, Texas).

BADHWAR, G.D. (1997b). "The radiation environment in low-Earth orbit," Radiat. Res. **148**, S3–S10.

BADHWAR, G.D. (2000). "Radiation measurements in low Earth orbit: U.S. and Russian results," Health Phys. **79**, 507–514.

BADHWAR, G.D. (2002). "Shuttle radiation dose measurements in the International Space Station orbits," Radiat. Res. **157**, 69–75.

BADHWAR, G.D. and CUCINOTTA, F.A. (2000), "A comparison of depth dependence of dose and linear energy transfer spectra in aluminum and polyethylene," Radiat. Res. **153**, 1–8.

BADHWAR, G.D. and O'NEILL, P.M. (1992). "An improved model of galactic cosmic radiation for space exploration missions," Nucl. Tracks Radiat. Meas. Int. J. Radiat. Instrum. **20**, 403–410.

BADHWAR, G.D. and O'NEILL, P.M. (1994). "Long-term modulation of galactic cosmic radiation and its model for space exploration," Adv. Space Res. **14**, 749–757.

BADHWAR, G.D., DENNY, C.L., DENNIS, B.R. and KAPLON, M.F. (1967). "Measurements of the low-energy cosmic radiation during the summer of 1966," Phys. Rev. **163**, 1327–1342.

BADHWAR, G.D., CUCINOTTA, F.A, BRABY, L.A. and KONRADI, A. (1994). "Measurements on the shuttle of the LET spectra of galactic cosmic radiation and comparison with the radiation transport model," Radiat. Res. **139**, 344–351.

BADHWAR, G.D., CUCINOTTA, F.A. and KONRADI, A. (1996). "Shuttle measurements of galactic cosmic radiation LET spectra," Adv. Space Res. **18**(12), 159–165

BADHWAR, G.D., ATWELL, W., CASH, B., PETROV, V.M., AKATOV, Y.A., TCHERNYKH, I.V., SHURSHAKOV, V.A. and ARKHANGELSKY, V.A. (1998). "Radiation environment on the Mir orbital station during solar minimum," Adv. Space Res. **22**, 501–510.

BADHWAR, G.D., KEITH, J.E. and CLEGHORN, T.F. (2001). "Neutron measurements onboard the space shuttle," Radiat. Meas. **33**, 235–241.

BADHWAR, G.D., ATWELL, W., BADAVI, F.F., YANG, T.C. and CLEGHORN T.F. (2002). "Space radiation absorbed dose distribution in a human phantom," Radiat. Res. **157**, 76–91.

BAILEY, W.H. (2002). "Health effects relevant to the setting of EMF exposure limits," Health Phys. **83**, 376–386.

BALCER-KUBICZEK, E.K., YIN, J., LIN, K., HARRISON, G.H., ABRAHAM, J.M. and MELTZER, S.J. (1995). "P53 mutational status and survival of human breast cancer MCF-7 cell variants after exposure to x rays or fission neutrons," Radiat. Res. **142**, 256–262.

BALLARINI, F. and OTTOLENGHI, A. (2004). "A model of chromosome aberration induction and chronic myeloid leukaemia incidence at low doses," Radiat. Environ. Biophys. **43**, 165–171.

BALLARINI, F., BIAGGI, M., OTTOLENGHI, A. and SAPORA, O. (2002). "Cellular communication and bystander effects: A critical review for modelling low-dose radiation action," Mutat. Res. **501**, 1–12.

BANTSEEV, V., BHARDWAJ, R., RATHBUN, W., NAGASAWA, H. and TREVITHICK, J.R. (1997). "Antioxidants and cataract (Cataract induction in space environment and application to terrestrial aging cataract)," Biochem. Mol. Biol. Int. **42**, 1189–1197.

BARCELLOS-HOFF, M.H. (1993). "Radiation-induced transforming growth factor beta and subsequent extracellular matrix reorganization in murine mammary gland," Cancer Res. **53**, 3880–3886.

BARCELLOS-HOFF, M.H. (1998). "How do tissues respond to damage at the cellular level? The role of cytokines in irradiated tissues," Radiat Res. **150** (Suppl. 5), S109–S120.

BARCELLOS-HOFF, M.H. (2001). "It takes a tissue to make a tumor: Epigenetics, cancer and the microenvironment," J. Mammary Gland Biol. Neoplasia. **6**, 213–221.

BARCELLOS-HOFF, M.H. and BROOKS, A.L. (2001). "Extracellular signaling through the microenvironment: A hypothesis relating carcinogenesis, bystander effects, and genomic instability," Radiat. Res. **156**, 618–627.

BARCELLOS-HOFF, M.H., DERYNCK, R., TSANG, M.L. and WEATHERBEE, J.A. (1994). "Transforming growth factor-beta activation in irradiated murine mammary gland," J. Clin. Invest. **93**, 892–899.

BASAVARAJU, S.R. and EASTERLY, C.E. (2002). "Pathophysiological effects of radiation on atherosclerosis development and progression, and the incidence of cardiovascular complications," Med. Phys. **29**, 2391–2403.

BATEMAN, J.L. and BOND, V.P. (1967). "Lens opacification in mice exposed to fast neutrons," Radiat. Res. **7** (Suppl.), 239–249.

BAY, J.O., UHRHAMMER, N., PERNIN, D., PRESNEAU, N., TCHIRKOV, A., VUILLAUME, M., LAPLACE, V., GRANCHO, M., VERRELLE, P., HALL, J. and BIGNON, Y.J. (1999). "High incidence of cancer in a

family segregating a mutation of the ATM gene: Possible role of ATM heterozygosity in cancer," Hum. Mutat. **14**, 485–492.

BAYLIN, S.B. and HERMAN, J.G. (2000). "DNA hypermethylation in tumorigenesis: Epigenetics joins genetics," Trends Genet. **16**, 168–174.

BECHLER, B., COGOLI, A., COGOLI-GREUTER, M., MULLER, O., HUNZINGER, E. and CRISWELL, S.B. (1992). "Activation of microcarrier-attached lymphocytes in microgravity," Biotechnol. Bioeng. **40**, 991–996.

BEDFORD, J.S. and MITCHELL, J.B. (1973). "Dose-rate effects in synchronous mammalian cells in culture," Radiat. Res. **54**, 316–327.

BELAY, T., AVILES, H., VANCE, M., FOUNTAIN, K. and SONNENFELD, G. (2002). "Effects of the hindlimb-unloading model of spaceflight conditions on resistance of mice to infection with Klebsiella pneumoniae," J. Allergy Clin. Immunol. **110**, 262–268.

BELKACEMI, Y., OZSAHIN, M., PENE, F., RIO, B., LAPORTE, J.P., LEBLOND, V., TOUBOUL, E., SCHLIENGER, M., GORIN, N.C. and LAUGIER, A. (1996). "Cataractogenesis after total body irradiation," Int. J. Radiat. Oncol. Biol. Phys. **35**, 53–60.

BELLI, M., CHERUBINI, R., FINOTTO, S., MOSCHINI, G., SAPORA, O., SIMONE, G. and TABOCCHINI, M.A. (1989). "RBE-LET relationship for the survival of V79 cells irradiated with low energy protons," Int. J. Radiat. Biol. **55**, 93–104.

BELLI, M., CERA, F., CHERUBINI, R., IANZINI, F., MOSCHINI, G., SAPORA, O., SIMONE, G., TABOCCHINI, M.A. and TIVERON, P. (1991). "Mutation induction and RBE-LET relationship of low-energy protons in V79 cells," Int. J. Radiat. Biol. **59**, 459–465.

BELLI, M., CERA, F., CHERUBINI, R., HAQUE, A.M., IZNZINI, F., MOSCHINI, G., SAPORA, O., SIMONE, G., TABOCCHINI, M.A. and TIVERON, P. (1993). "Inactivation and mutation induction in V79 cells by low energy protons: Re-evaluation of the results at the LNL facility," Int. J. Radiat. Biol. **63**, 331–337.

BELLI, M., CERA, F., CHERUBINI, R., DALLA VECCHIA, M., HAQUE, A.M., IANZINI, F., MOSCHINI, G., SAPORA, O., SIMONE, G., TABOCCHINI, M.A. and TIVEON, P. (1998). "RBE-LET relationships for cell inactivation and mutation induced by low energy protons in V79 cells: Further results at the LNL facility," Int. J. Radiat. Biol. **74**, 501–509.

BELYAKOV, O.V., PRISE, K.M., TROTT, K.R. and MICHAEL, B.D. (1999). "Delayed lethality, apoptosis and micronucleus formation in human fibroblasts irradiated with x-rays or alpha-particles," Int. J. Radiat. Biol. **75**, 985–993.

BELYAKOV, O.V., MALCOLMSON, A.M., FOLKARD, M., PRISE, K.M. and MICHAEL, B.D. (2001). "Direct evidence for a bystander effect of ionizing radiation in primary human fibroblasts," Br. J. Cancer **84**, 674–679.

BELYAKOV, O.V., FOLKARD, M., MOTHERSILL, C., PRISE, K.M. and MICHAEL, B.D. (2002). "Bystander-induced apoptosis and premature

differentiation in primary urothelial explants after charged particle microbeam irradiation," Radiat Prot Dosim. **99**, 249–251.

BELYAKOV, O.V., MITCHELL, S.A., PARIKH, D., RANDERS-PEHRSON, G., MARINO, S.A., AMUNDSON, S.A., GEARD, C.R. and BRENNER, D.J. (2005). "Biological effects in unirradiated human tissue induced by radiation damage up to 1 mm away," Proc. Natl. Acad. Sci. USA **102**, 14203–14208.

BELYAKOV, O.V., FOLKARD, M., MOTHERSILL, C., PRISE, K.M. and MICHAEL, B.D. (2006). "Bystander-induced differentiation: A major response to targeted irradiation of a urothelial explant model," Mutat. Res. **597**, 43–49.

BENDER, M.A., GOOCH, P.C. and KONDO, S. (1967). "The Gemini-3 S-4 spaceflight-radiation interaction experiment," Radiat. Res. **31**, 91–111.

BENDER, M.A., GOOCH, P.C. and KONDO, S. (1968). "The Gemini XI S-4 spaceflight-radiation interaction experiment: The human blood experiment," Radiat. Res. **34**, 228–238.

BERGER, S. (2001). "Investigations of the biological effects of heavy ions on human skin fibroblasts with special respect to chromosomal damage," Ph.D. Thesis (University of Mainz, Germany).

BERRY, W.D., MURPHY, J.D., SMITH, B.A., TAYLOR, G.R. and SONNENFELD, G. (1991). "Effect of microgravity modeling on interferon and interleukin responses in the rat," J. Interferon Res. **11**, 243–249.

BICHSEL, H. (1992). "Stopping power and ranges of fast ions in heavy elements," Phys. Rev. A. **46**, 5761–5773.

BIDOLI, V., CASOLINO, M., DE PASCALE, M.P., FURANO, G., MINORI, M., MORSELLI, A., NARICI, L., PICOZZA, P., REALI, E., SPARVOLI, R., FUGLESANG, C., SANNITA, W., CARLSON, P., CASTELLINI, G., GALPER, A., KOROTKOV, M., POPOV, A., NAVILOV, N., AVDEEV, S., BENGHIN, V., SALNITSKII, V., SHEVCHENKO, O., BOEZIO, M., BONVICINI, W., VACCHI, A., ZAMPA, G., ZAMPA, N., MAZZENGA, G., RICCI, M., SPILLANTINI, P. and VITTORI, R. (2002). "The Sileye-3/Alteino experiment for the study of light flashes, radiation environment and astronaut brain activity on board the International Space Station," J. Radiat. Res. (Tokyo) **43** (Suppl.), S47–S52.

BIJL, H.P., VAN LUIJK, P. COPPES, R.P., SCHIPPERS, J.M., KONINGS, A.W. and VAN DER KOGEL, A.J. (2005). "Regional differences in radiosensitivity across the rat cervical spinal cord," Int. J. Radiat. Oncol. Biol. Phys. **61**, 543–551.

BISHAYEE, A., RAO, D.V. and HOWELL, R.W. (1999). "Evidence for pronounced bystander effects caused by nonuniform distributions of radioactivity using a novel three-dimensional tissue culture model," Radiat. Res. **152**, 88–97.

BLAKELY, E.A. (2000). "Biological effects of cosmic radiation: Deterministic and stochastic," Health Phys. **79**, 495–506.

BLAKELY, E.A. and CASTRO, J.R. (1994). "Assessment of acute and late effects to high-LET radiation," pages 149 to 157 in *Proceedings of National Institute of Radiological Sciences: International Seminar on the Application of Heavy Ion Accelerator to Radiation Therapy of Cancer*, NIRS-M-103/HIMAC-008 (National Institute of Radiological Research, Chiba, Japan).

BLAKELY, E.A., NGO, F.Q.H., CURTIS, S B. and TOBIAS, C.A. (1984). "Heavy-ion radiobiology: Cellular studies," Adv. Radiat. Biol. **11**, 295–389.

BLAKELY, W.F., PRASANNA, P.G., GRACE, M.B. and MILLER, A.C. (2001). "Radiation exposure assessment using cytological and molecular biomarkers," Radiat. Prot. Dosim. **97**, 17–23.

BLAKELY, W.F., MILLER, A.C., GRACE, M.B., MCLELAND, C.B., LUO, L., MUDERHWA, J.M., MINER, V.L. and PRASANNA, P.G.S. (2003). "Radiation biodosimetry: Applications for spaceflight," Adv. Space Res. **31**, 1487–1493.

BLATTNIG, S.R., NORBURY, J.W., NORMAN, R.B., WILSON, J.W. SINGLETERRY, R.C., JR. and TRIPATHI, R.K. (2004). *MESTRN: A Deterministic Meson-Muon Transport Code for Space Radiation*, NASA/TM-2004-212995 (National Aeronautics and Space Administration, Washington).

BOEI, J.J. and NATARAJAN, A.T. (1998). "Combined use of chromosome painting and telomere detection to analyse radiation-induced chromosomal aberrations in mouse splenocytes," Int. J. Radiat. Biol. **73**, 125–133.

BOGO, V. (1988). "Early behavioral toxicity produced by acute ionizing radiation," Fundam. Appl. Toxicol. **11**, 578–579.

BOGO, V., HILL, T.A. and NOLD, J. (1987). "Motor performance effects of propylene glycol dinitrate in the rat," J. Toxicol. Environ. Health **22**, 17–27.

BOGO, V., ZEMAN, G.H. and DOOLEY, M. (1989). "Radiation quality and rat motor performance," Radiat. Res. **118**, 341–352.

BOHRNSEN, G., WEBER, K.J. and SCHOLZ, M. (2002). "Measurement of biological effects of high-energy carbon ions at low doses using a semi-automated cell detection system," Int. J. Radiat. Biol. **78**, 259–266.

BOICE, J.D., JR. and MCLAUGHLIN, J.K. (2002). *Epidemiologic Studies of Cellular Telephones and Cancer Risk – A Review*, SSI Report 2002(16) (Swedish Radiation Protection Authority, Stockholm, Sweden).

BOICE, J.D., JR., TAWN, E.J., WINTHER, J.F., DONALDSON, S.S., GREEN, D.M., MERTENS, A.C., MULVIHILL, J.J., OLSEN, J.H., ROBISON, L.L. and STOVALL, M. (2003). "Genetic effects of radiotherapy for childhood cancer," Health Phys. **85**, 65–80.

BONNEY, C.H., BECKMAN, F.N. and HUNTER, D.M. (1974). "Retinal change induced in the primet (Macaca mulatta) by oxygen nuclei radiation," Life Sci. Space Res. **12**, 31–42.

BOOZALIS, G.T., SCHACHAT, A.P. and GREEN, W.R. (1987). "Subretinal neovascularization from the retina in radiation retinopathy," Retina **7**, 156–161.

BORTKIEWICZ, A., ZMYSLONY, M., GADZICKA, E. and SZYMCZAK, W. (1996). "Evaluation of selected parameters of circulatory system function in various occupational groups exposed to high frequency electromagnetic fields. II. Electrocardiographic changes," Med. Pr. **47**, 241–252.

BOUDAIFFA, B., HUNTING, D., CLOUTIER, P., HUELS, M.A. and SANCHE, L. (2000a). "Induction of single- and double-strand breaks in plasmid DNA by 100–1500 eV electrons," Int. J. Radiat. Biol. **76**, 1209–1221.

BOUDAIFFA, B., CLOUTIER, P., HUNTING, D., HUELS, M.A. and SANCHE, L. (2000b). "Resonant formation of DNA strand breaks by low-energy (3 to 20 eV) electrons," Science **287**, 1603–1604.

BOUFFLER, S.D., MEIJNE, E.I., HUISKAMP, R. and COX, R. (1996). "Chromosomal abnormalities in neutron-induced acture myeloid leukemias in CBA/H mice," Radiat. Res. **146**, 349–352.

BOUFFLER, S.D., HAINES, J.W., EDWARDS, A.A., HARRISON, J.D. and COX, R. (2001). "Lack of detectable transmissible chromosomal instability after *in vivo* or *in vitro* exposure of mouse bone marrow cells to ^{224}Ra alpha particles," Radiat. Res. **155**, 345–352.

BRABY, L.A. and ELLETT, W.H. (1972). "Ionization in solid- and grid-walled detectors," Radiat. Res. **51**, 569–580.

BRABY, L.A., ROESCH, W.C. and GLASS, W.A. (1970). "Energy deposition spectra of ^{14}C beta radiation in a uniform medium," Radiat. Res. **43**, 499–503.

BRAINARD, G.C., KAVET, R. and KHEIFETS, L.I. (1999). "The relationship between electromagnetic field and light exposures to melatonin and breast cancer risk: A review of the relevant literature," J. Pineal Res. **26**, 65–100.

BRANDT, W. and RITCHIE, H.R. (1974). "Primary processes in the physical stage," pages 20 to 29 in *Physical Mechanisms in Radiation Biology*, Cooper, R.D. and Woods, R., Eds. (National Technical Information Service, Springfield, Virginia).

BRECHTMANN, C. and HEINRICH, W. (1988). "Fragmentation cross sections of ^{32}S at 0.7, 1.2, and 200 GeV/nucleon," Z. Phys. A. **331**, 463–472.

BRECHTMANN, C., HEINRICH, W. and BENTON, E.V. (1989). "Fragmentation cross sections of ^{28}Si at 14.5 GeV/nucleon," Phys. Rev. C Nucl. Phys. **39**, 2222–2226.

BREMER, M., KLOPPER, K., YAMINI, P., BENDIX-WALTES, R., DORK, T. and KARSTENS, J.H. (2003). "Clinical radiosensitivity in breast cancer patients carrying pathogenic ATM gene mutations: No observation of increased radiation-induced acute or late effects," Radiother. Oncol. **69**, 155–160.

BRENEMAN, H.H. and STONE, E.C. (1985). "Solar coronal and photospheric abundances from solar energetic particle measurements," Astrophys. J. **299**, L57–L61.

BRENNAN, K.M., ROOS, M.S., BUDINGER, T.F., HIGGINS, R.J., WONG, S.T. and BRISTOL, K.S. (1993). "A study of radiation necrosis and edema in the canine brain using positron emission tomography and magnetic resonance imaging," Radiat. Res. **134**, 43–53.

BRENNER, D.J. and WARD, J.F. (1992). "Constraints on energy deposition and target size and multiply damaged sites associated with DNA double-strand breaks," Int. J. Radiat. Biol. **61**, 737–748.

BRENNER, D.J., MEDVEDOVSKY, C., HUANG, Y., MERRIAM, G.R., JR. and WORGUL, B.V. (1991). "Accelerated heavy particles and the lens. VI. RBE studies at low doses," Radiat. Res. **128**, 73–81.

BRENNER, D.J., MEDVEDOVSKY, C., HUANG, Y. and WORGUL, B.V. (1993). "Accelerated heavy particles and the lens. VIII. Comparisons between the effects of acute low doses of iron ions (190 keV/microns) and argon ions (88 keV/microns)," Radiat. Res. **133**, 198–203.

BROEKS, A., URBANUS, J.H., FLOORE, A.N., DAHLER, E.C., KLIJN, J.G., RUTGERS, E.J., DEVILEE, P., RUSSELL, N.S., VAN LEEUWEN, F.E. and VAN'T VEER, L.J. (2000). "ATM-heterozygous germline mutations contribute to breast cancer-susceptibility," Am. J. Hum. Genet. **66**, 494–500.

BROOKS, A.L. (1999). "Biomarkers of exposure, sensitivity and disease," Int. J. Radiat. Biol. **75**, 1481–1503.

BROOKS, A., BAO, S., RITHIDECH, K., COUCH, L.A. and BRABY, L.A. (2001). "Relative effectiveness of HZE iron-56 particles for the induction of cytogenetic damage *in vivo*," Radiat. Res. **155**, 353–359.

BROWNING, L.S. (1971). "Genetic effects of the space environment on the reproductive cells of *Drosophilia* adults and pupae," pages 55 to 78 in *The Experiments of Biosatellite II*, Deserres, F.J., Reynolds, O.E. and Sanders, J.F., Eds., NASA Special Publication 204 (National Technical Information Service, Springfield, Virginia).

BRUNER, A. (1977). "Immediate dose-rate effects of ^{60}Co on performance and blood pressure in monkeys," Radiat. Res. **70**, 378–390.

BUCKER, H., FACIUS, R., HORNECK, G., REITZ, G., GRAUL, E.H., BERGER, H., HOFFKEN, H., RUTHER, W., HEINRICH, W., BEAUJEAN, R. and ENGE, W. (1986). "Embryogenesis and organogenesis of Carausius morosus under spaceflight conditions," Adv. Space Res. **6**, 115–124.

BUDINGER, T.F., BICHSEL, H. and TOBIAS, C.A. (1971). "Visual phenomena noted by human subjects on exposure to neutrons of energies less than 25 million electron volts," Science **172**, 868–870.

BUDINGER, T.F., LYMAN, J.T. and TOBIAS, C.A. (1972). "Visual perception of accelerated nitrogen nuclei interacting with the human retina," Nature **239**, 209–211.

BUDINGER, T., TOBIAS, C., SCHOPPER, E., SCHOTT, J., HUESMAN, R., UPHAM, F., WIESKAMP, T., KUCALA, L., GOULDINGS, F.,

LANDIS, D., WALTON, J. and WALTON, R. (1976). "Quantitative observation of light flash sensations experiment MA-106," pages 13-11 to 13-17 in *Apollo-Soyuz Test Project: Preliminary Science Report*, NASA-TM-X-58173 (National Technical Information Service, Springfield, Virginia).

BUDINGER, T., TOBIAS, C., HUESMAN, R., UPHAM, F., WIESKAMP, T., SCHOTT, J. and SCHOPPER, E. (1977). "Light flash observations," pages 193 to 209 in *Apollo-Soyuz Test Project: Volume 1, Astronomy, Earth Atmosphere and Gravity Field, Life Sciences, and Materials Processing*, NASA SP-412 (National Technical Information Service, Springfield, Virginia).

BUNGER, B.M., COOK, J.R. and BARRICK, M.K. (1981). "Life table methodology for evaluating radiation risk: An application based on occupational exposures," Health Phys. **40**, 439–455.

BURCH, J.B., REIF, J.S., NOONAN, C.W., ICHINOSE, T., BACHAND, A.M., KOLEBER, T.L. and YOST, M.G. (2002). "Melatonin metabolite excretion among cellular telephone users," Int. J. Radiat. Biol. **78**, 1029–1036.

BURNS, F.J. and ALBERT, R.E. (1980). "Dose response for skin tumors induced by single and split doses of argon ions," in *Biological and Medical Research with Accelerated Heavy Ions at the Bevalac*, Tobias, C.A. and Pirruccello, M.C., Eds. (Lawrence Berkeley Laboratory, University of California, Berkeley, California).

BURNS, F.J., STRICKLAND, P., VANDERLAAN, M. and ALBERT, R.E. (1978). "Rat skin tumor incidence following single and fractionated exposures to proton radiation," Radiat. Res. **74**, 152–158.

BURNS, F.J., HOSSELET, S., JIN, Y., DUDAS, G. and GARTE, S.J. (1991). "Progression and multiple events in radiation carcinogenesis of rat skin," J. Radiat. Res. (Tokyo) **32** (Suppl. 2), 202–216.

BURNS, F.J., JIN, Y., GARTE, S.J. and HOSSELET, S. (1994). "Estimation of risk based on multiple events in radiation carcinogenesis of rat skin," Adv. Space Res. **14**, 507–519.

BURNS, F.J., ZHAO, P., HIZ, Z., CHEN, S. and ROY, N. (1999). "High-LET radiation-induced malignant and benign tumors in rat skin," pages 109 to 119 in *Risk Evaluation of Cosmic-Ray Exposure in Long-Term Manned Space Mission*, Fujitaka, K., Majima, H., Ando, K., Yasuda, H. and Suzuki, M., Eds. (Kodansha Scientific Ltd., Tokyo).

BURNS, F.J., ZHAO, P., XU, G., ROY, N. and LOOMIS, C. (2001). "Fibroma induction in rat skin following single or multiple doses of 1.0 GeV/nucleon ^{56}Fe ions from the Brookhaven Alternating Gradient Synchrotron (AGS)," Phys. Med. **17** (Suppl. 1), 194–195.

BUTTS, J.J. and KATZ, R. (1967). "Theory of RBE for heavy ion bombardment of dry enzymes and viruses," Radiat. Res. **30**, 855–871.

CALABRESE, E.J. and BALDWIN, L.A. (2002). "Defining hormesis," Hum. Exp. Toxicol. **21**, 91–97.

CALABRESE, E.J. and BALDWIN, L.A. (2003a). "Toxicology rethinks its central belief," Nature **421**, 691–692.

CALABRESE, E.J. and BALDWIN, L.A. (2003b). "Hormesis: The dose-response revolution," Ann. Rev. Pharmacol. Toxicol. **43**, 175–197.

CANE, H.V., MCGUIRE, R.E. and VON ROSENVINGE, T.T. (1986). "Two classes of solar energetic particle events associated with impulsive and long duration soft x-ray flares," Astrophys. J. **301**, 448–459.

CANE, H.V., REAMES, D.V. and VON ROSENVINGE, T.T. (1988). "The role of interplanetary shocks in the longitude distribution of solar energetic particles," J. Geophys. Res. **93**, 9555–9567.

CANNEY, P.A. and DEAN, S. (1990). "Transforming growth factor beta: A promotor of late connective tissue injury following radiotherapy?" Br. J. Radiol. **63**, 620–623.

CARDIS, E., GILBERT, E.S., CARPENTER, L., HOWE, G., KATO, I., ARMSTRONG, B.K., BERAL, V., COWPER, G., DOUGLAS, A., FIX, J., FRY, S.A., KALDOR, J., LAVE, C., SALMON, L., SMITH, P.G., VOELZ, G.L. and WIGGS, L.D. (1995). "Effects of low doses and dose rates of external ionizing radiation: Cancer mortality among nuclear industry workers in three countries," Radiat. Res. **142**, 117–132.

CAREN, L.D., MANDEL, A.D. and NUNES, J.A. (1980). "Effect of simulated weightlessness on the immune system in rats," Aviat. Space Environ. Med. **51**, 251–255.

CARLSSON, J. and ROSANDER, K. (1973). "Effects of multiple scattering on proton beams in radiotherapy," Phys. Med. Biol. **18**, 633–640.

CARNES, B.A., GAVRILOVA, N. and GRAHN, D. (2002). "Pathology effects at radiation doses below those causing increased mortality," Radiat. Res. **158**, 187–194.

CARNES, B.A., GRAHN, D. and HOEL, D. (2003). "Mortality of atomic bomb survivors predicted from laboratory animals," Radiat. Res. **160**, 159–167.

CASADESUS, G., SHUKITT-HALE, B., STELLWAGEN, H.M., SMITH, M.A., RABIN, B.M. and JOSEPH, J.A. (2005). "Hippocampal neurogenesis and PSA-NCAM expression following exposure to ^{56}Fe particles mimics that seen during aging in rats," Exp. Gerontol. **40**, 249–254.

CASTRO, J.R., CHEN, G.T. and BLAKELY, E.A. (1985). "Current considerations in heavy charged-particle radiotherapy: A clinical research trial of the University of California Lawrence Berkeley Laboratory, Northern California Oncology Group, and Radiation Therapy Oncology Group," Radiat. Res. **8** (Suppl.), S263–S271.

CAVIN, L.W., DALRYMPLE, G.V., MCGUIRE, E.L., MANERS, A.W. and BROADWATER, J.R. (1990). "CNS tumor induction by radiotherapy: A report of four new cases and estimate of dose required," Int. J. Radiat. Oncol. Biol. Phys. **18**, 399–406.

CHANG, W.L., CHAPKIN, R.S. and LUPTON, J.R. (1998). "Fish oil blocks azotymethane-induced rat colon tumorigenesis by increasing cell differentiation and apoptosis rather than decreasing cell proliferation," J. Nutr. **128**, 491–497.

CHANG, P.Y., TOROUS, D., LUTZE-MANN, L. and WINEGAR, R. (2000a). "Impact of p53 status on heavy-ion radiation-induced micronuclei in circulating erythrocytes," Mutat. Res. **466**, 87–96.

CHANG, P.Y., BJORNSTAD, K.A., CHANG, E., MCNAMARA, M., BARCELLOS-HOFF, M.H., LIN, S.P., ARAGON, G., POLANSKY, J.R., LUI, G.M. and BLAKELY, E.A. (2000b). "Particle irradiation induces FGF2 expression in normal human lens cells," Radiat. Res. **154**, 477–484.

CHANG, P.Y., KANAZAWA, N., LUTZE-MANN, L. and WINEGAR, R.A. (2001). "p53 deficiency alters the yield and spectrum of radiation-induced lacZ mutants in the brain of transgenic mice," Mutagenesis **16**, 7–15.

CHANG, P.Y., BJORNSTAD, K.A., ROSEN, C.J., MCNAMARA, M.P., MANCINI, R., GOLDSTEIN, L.E., CHYLACK, L.T. and BLAKELY, E.A. (2005). "Effects of iron ions, protons and x rays on human lens cell differentiation," Radiat. Res. **164**, 531–539

CHAPES, S.K., MORRISON, D.R., GUIKEMA, J.A., LEWIS, M.L. and SPOONER, B.S. (1992). "Cytokine secretion by immune cells in space," J. Leukoc. Biol. **52**, 104–110.

CHARMAN, W.N., DENNIS, J.A., FAZIO, G.G. and JELLEY, J.V. (1971). "Visual sensations produced by single fast particles," Nature, **230**, 522–524.

CHATTERJEE, A. and HOLLEY, W.R. (1993), "Computer simulation of initial events in the biochemical mechanisms of DNA damage," Adv. Radiat. Biol. **17**, 181–226.

CHATTERJEE, A. and SCHAEFER, H.J. (1976). "Microdosimetric structure of heavy ion tracks in tissue," Radiat. Environ. Biophys. **13**, 215–227.

CHEN, J., CHENETTE, D., CLARK. R., GARCIA-MUNOZ, M., GUZIK, T.K., PYLE, K.R., SNAG, Y. and WEFEL, P.J. (1994a). "A model of galactic cosmic rays for use in calculating linear energy transfer spectra," Adv. Space. Res. **14**, 765–769.

CHEN, D.J., TSUBOI, K., NGUYEN, T. and YANG, T.C. (1994b). "Charged-particle mutagenesis II. Mutagenic effects of high energy charged particles in normal human fibroblasts," Adv. Space Res. **14**, 347–354.

CHENG, S.W., WU, L.L., TING, A.C., LAU, H., LAM, L.K. and WEI, W.I. (1999). "Irradiation-induced extracranial carotid stenosis in patients with head and neck malignancies," Am. J. Surg. **178**, 323–328.

CHRISTENBERRY, K.W., FURTH, J., HURST, G.S., MELVILLE, G.S. and UPTON, A.C. (1956). "The relative biological effectiveness of neutrons, x-rays, and gamma rays for the production of lens opacities: Observations on mice, rats, guinea-pigs, and rabbits," Radiology **67**, 686–696.

CHURCHILL, S.E. (1997). *Fundamentals of Space Life Sciences* (Krieger Publishing, Malabar, Florida).

CIBIS, P.A., NOELL, W.K. and EICHEL, B. (1955). "Ocular effects produced by high-intensity x-radiation," AMA Arch. Opthalmol. **53**, 651–663.

CLEGHORN, T.F. and BADHWAR, G.D. (1999). "Comparison of the SPE model with proton and heavy ion data," Radiat. Meas. **30**, 251–259.

CLIFFSWALLOW, W. and HIRMAN, J. (1992). "U.S. space weather real-time observing and forecasting capabilities," pages 185 to 200 in *Solar Terrestrial Predictions IV, Vol. 1*, Hruska, J., Shea, M.A., Smart, D.F. and Heckman, G., Eds. (U.S. Department of Commerce, National Oceanic and Atmospheric Administration, Boulder, Colorado).

CLOWDSLEY, M.S., HEINBOCKEL, J.H., KANEKO, H., WILSON, J.W., SINGLETERRY, R.C. and SHINN, J.L. (2000). "A comparison of the multigroup and collocation methods for solving the low-energy Boltzmann equation," Can. J. Phys. **78**, 45–56.

CLOWDSLEY, M.S., WILSON, J.W., KIM, M.H., SINGLETERRY, R.C., TRIPATHI, R.K., HEINBOCKEL, J.H., BADAVI, F.F. and SHINN, J.L. (2001). "Neutron environments on the Martian surface," Phys. Med. **17** (Suppl.), 94–96.

COCKELL, C.S. and ANDRADY, A.L. (1999). "The Martian and extraterrestrial UV radiation environment–1. Biological and closed-loop ecosystem considerations," Acta. Astronaut **44**, 53–62.

COCKELL, C.S., CATLING, D.C., DAVIS, W.L., SNOOK, K., KEPNER, R.L., LEE, P. and MCKAY, C.P. (2000). "The ultraviolet environment of Mars: Biological implications past, present, and future," Icarus **146**, 343–359.

COGOLI, A. (1993). "The effect of hypogravity and hypergravity on cells of the immune system," J. Leukoc. Biol. **54**, 259–268.

COGOLI, A., VALLUCHI-MORF, M., MUELLER, M. and BRIEGLEB, W. (1980). "Effect of hypogravity on human lymphocyte activation," Aviat. Space Environ. Med. **51**, 29–34.

COGOLI, A., TSCHOPP, A. and FUCHS-BISLIN, P. (1984). "Cell sensitivity to gravity," Science **225**, 228–230.

COLEMAN, M.A., YIN, E., PETERSON, L.E., NELSON, D., SORENSEN, K., TUCKER, J.D. and WYROBEK, A.J. (2005). "Low-dose irradiation alters the transcript profiles of human lymphoblastoid cells including genes associated with cytogenetic radioadaptive response," Radiat. Res. **164**, 369–382.

CONARD, R.A. (1951). "Effect of x-irradiation on intestinal motility of the rat," Am. J. Physiol. **165**, 375–385.

CONARD, R. (1956). "Some effects of ionizing radiation on the physiology of the gastrointestinal tract: A review," Radiat. Res. **5**, 167–188.

COSTES, S. and BARCELLOS-HOFF, M.H. (2002). "Radiation quality and tissue-specific microenvironments following exposure to 1 GeV/amu Fe," Adv. Space Res. **30**, 865–870.

COSTES, S., STREULI, C.H., and BARCELLOS-HOFF, M.H. (2000). "Quantitative image analysis of laminin immunoreactivity in skin

basement membrane irradiated with 1 GeV nucleon^{-1} iron particles, Radiat. Res. **154**(4), 389–397.

COSTES, S.V., DAELEMANS, D. CHO, E.H., DOBBIN, Z., PAVLAKIS, G. and LOCKETT, S. (2004). "Automatic and quantitative measurement of protein-protein colocalization in live cells," Biophys. J. **86**, 3993–4003.

COX, A.B. and KRAFT, L.M. (1984). "Quantitation of heavy ion damage to the mammalian brain: Some preliminary findings," Adv. Space Res. **4**, 247–250.

CRAMP, W.A. and WALKER, A. (1974). "The nature of the new DNA synthesized by DNA-membrane complexes isolated from irradiated E. coli," Int. J. Radiat. Biol. Relat. Stud. Phys. Chem. Med. **25**, 175–187.

CRAVEN, P.A. and RYCROFT, M.J. (1994). "Fluxes of galactic iron nuclei and associated HZE secondaries, and resulting radiation doses, in the brain of an astronaut," Adv. Space Res. **14**, 873–878.

CRIDLAND, N.A., MARTIN, M.C., STEVENS, K., BALLER, C.A., PEARSON, A.J., DRISCOLL, C.M. and SAUNDERS, R.D. (2001). "Role of stress responses in human cell survival following exposure to ultraviolet C radiation," Int. J. Radiat. Biol. **77**, 365–374.

CRONKITE, E.P., BOND, V.P., CARSTEN, A.L., INOUE, T., MILLER, M.E. and BULLIS, J.E. (1987). "Effects of low level radiation upon the hematopoietic stem cell: Implications for leukemogenesis," Radiat. Environ, Biophys. **26**, 103–114.

CUCINOTTA, F.A. (2005). "Introduction," Radiat. Res. **164**, 453.

CUCINOTTA, F.A., WILSON, J.W., SHINN, J.L., BADAVI, F.F. and BADHWAR, G.D. (1996a). "Effects of target fragmentation on evaluation of LET spectra from space radiations: Implications for space radiation protection studies," Radiat. Meas. **26**, 923–934.

CUCINOTTA, F.A., TOWNSEND, L.W., WILSON, J.W., SHINN, J.L., BADHWAR, B.D. and DUBEY, R.R. (1996b). "Light ion component of the galactic cosmic rays: Nuclear interactions and transport theory," Adv. Space Res. **17**, 77–86.

CUCINOTTA, F.A, WILSON, J.W., SHAVERS, M.R. and KATZ, R. (1997). *Calculation of Heavy Ion Inactivation and Mutation Rates in Radial Dose Model of Track Structure*, NASA-TP-3630 (National Aeronautics and Space Administration, Washington).

CUCINOTTA, F.A., NIKJOO, H. and GOODHEAD, D.T. (1999). "Applications of amorphous track models in radiation biology," Radiat. Environ. Biophys. **38**, 81–92.

CUCINOTTA, F.A., NIKJOO, H. and GOODHEAD, D.T. (2000). "Model for radial distribution of frequency distribution for energy imparted in nanometer volumes from HZE particles," Radiat. Res. **153**, 459–468.

CUCINOTTA, F.A., SCHIMMERLING, W., WILSON, J.W., PETERSON, L.E., BADHWAR, G.D., SAGANTI, P.B. and DICELLO, J.F. (2001a). "Space radiation cancer risks and uncertainties for Mars missions," Radiat. Res. **156**, 682–688.

CUCINOTTA, F.A., MANUEL, F.K., JONES, J., ISZARD, G., MURREY, J., DJOJONEGRO, B. and WEAR, M. (2001b). "Space radiation and cataracts in astronauts," Radiat. Res. **156**, 460–466.

CUCINOTTA, F.A., BADHWAR, G.D., SAGANTI, P.B., SCHIMMERLING, W., WILSON, J.W., PETERSON, L.E. and DICELLO, J.F. (2002). *Space Radiation Cancer Risk Projections for Exploration Missions: Uncertainty Reduction and Mitigation*, NASA/TP-2002-210777 (Center for AeroSpace Information, Hanover, Maryland).

CUCINOTTA, F.A., SAGANTI, P.B., HU, X., KIM, M.H.Y., CLEGHORN, T.F., WILSON, J.W., TRIPATHI, R.K. and ZEITLIN, C.J. (2003). *Physics of the Isotopic Dependence of Galactic Cosmic Ray Fluence Behind Shielding*, NASA/TP-2003-210792 (National Technical Information Service, Springfield, Virginia).

CUCINOTTA, F.A, SCHIMMERLING, W., WILSON, J.W., PETERSON, L.E., SAGANTI, P.B. and DICELLO, J.F. (2004). "Uncertainties in estimates of the risks of late effects from space radiation," Adv. Space Res. **34**, 1383–1389.

CUCINOTTA, F.A., KIM, M.H.Y. and REN, L. (2005). *Managing Lunar and Mars Mission Radiation Risks. Part 1: Cancer Risks, Uncertainties, and Shielding Effectiveness*, NASA/TP-2005-213164 (Center for AeroSpace Information, Hanover, Maryland).

CUCINOTTA, F.A., KIM, M.Y. and REN, L. (2006). "Evaluating shielding effectiveness for reducing space radiation cancer risks," Radiat. Meas. (in press).

CUGNON, J., MIZUTANI, T., VANDERMEULEN, J. (1981). "Equilibration in relativistic nuclear collisions. A Monte Carlo calculation," Nucl. Phys. A. **352**, 505–534.

CUMMINGS, J.R., BINNS, W.R., GARRAND, T.L., ISRAEL, M.H., KLARMANN, J., STONE, E.C. and WADDINGTON, C.J. (1990). "Determination of the cross sections for the production of fragments with relativistic nucleus-nucleus interactions I. Measurements," Phys. Rev. C Nucl Phys. **42**, 2508–2529.

CURRY, J., KHAIDAKOV, M. and GLICKMAN, B.W. (2000). "Russian mutational spectrum differs from that of their Western counterparts," Hum. Mutat. **15**, 439–446.

CURTIS, S.B. and LETAW, J.R. (1989). "Galactic cosmic rays and cell-hit frequencies outside the magnetosphere," Adv. Space Res. **9**, 293–298.

CURTIS, S.B., TOWNSEND, L.W., WILSON, J.W., POWERS-RISIUS, P., ALPEN, E.L. and FRY, R.J.M. (1992). "Fluence-related risk coefficients using the Harderian gland data as an example," Adv. Space Res. **12**, 407–416.

CURTIS, S.B., NEALY, J.E. and WILSON, J.W. (1995). "Risk cross sections and their application to risk estimation in the galactic cosmic-ray environment," Radiat. Res. **141**, 57–65.

CURTIS, S.B., VAZQUEZ, M.E., WILSON, J.W., ATWELL, W., KIM, M. and CAPALA, J. (1998). "Cosmic ray hit frequencies in critical sites in the central nervous system," Adv. Space Res. **22**, 197–207.

CURTIS, S.B., VAZQUEZ, M.E., WILSON, J.W., ATWELL, W. and KIM, M.H. (2000). "Cosmic ray hits in the central nervous system at solar maximum," Adv. Space Res. **25**, 2035–2040.

DALRYMPLE, G.V., LEICHNER, P.K., HARRISON, K.A., COX, A.B., HARDY, K.A., SALMON, Y.L. and MITCHELL, J.C. (1994). "Induction of high grade astrocytoma (HGA) by protons: Molecular mechanisms and RBE considerations," Adv. Space Res. **14**, 267–270.

D'AUNNO, D.S., DOUGHERTY, A.H., DEBLOCK, H.F. and MECK, J.V. (2003). "Effect of short- and long-duration spaceflight on QTc intervals in healthy astronauts," Am. J. Cardiol. **91**, 494–497.

DE ANGELIS, L.M., DELATTRE, J.Y. and POSNER, J.B. (1989). "Radiation-induced dementia in patients cured of brain metastases," Neurology **39**, 789–796.

DE ANGELIS, G., CALDORA, M., SANTAQUILANI, M., SCIPIONE, R. and VERDECCHIA, A. (2001). "Health risks from radiation exposure for civilian aviation flight personnel: A study of Italian airline crew members," Radiat. Res. **156**, 689–694.

DE JONG, H.A., SONDAG, E.N., KUIPERS, A. and OOSTERVELD, W.J. (1996). "Swimming behavior of fish during short periods of weightlessness," Aviat. Space Environ. Med. **67**, 463–466.

DE LUIS, J., VUNJAK-NOVAKOVIC, G. and SEARBY, N. (2002). "Design and testing of the ISS cell culture unit, Rio de Janeiro," in *Proceedings of the 51st Congress of the International Astronautical Federation* (International Astronautical Federation, Paris).

DENISOVA, N.A., SHUKITT-HALE, B., RABIN, B.M. and JOSEPH, J.A. (2002). "Brain signaling and behavioral responses induced by exposure to ^{56}Fe-particle radiation," Radiat. Res. **158**, 725–734.

DESHPANDE, A., GOODWIN, E.H., BAILEY, S.M., MARRONE, B.L. and LEHNERT, B.E. (1996). "Alpha-particle-induced sister chromatid exchange in normal human lung fibroblasts: Evidence for an extranuclear target," Radiat. Res. **145**, 260–267.

DICELLO, J.F. (1992). "HZE cosmic rays in space. Is it possible that they are not the major radiation hazard?" Radiat. Prot. Dosim. **44**, 253–257.

DICELLO, J.F., CHRISTIAN, A., CUCINOTTA, F.A., GRIDLEY, D.S., KATHIRITHAMBY, R., MANN, J., MARKHAM, A.R., MOYERS, M.F., NOVAK, G.R., PIANTADOSI, S., RICART-ARBONA, R., SIMONSON, D.M., STRANDBERG, J.D., VAZQUEZ, M., WILLIAMS, J.R., ZHANG, Y., ZHOU, H. and HUSO, D. (2004). "*In vivo* mammary tumourigenesis in the Sprague-Dawley rat and microdosimetric correlates," Phys. Med. Biol. **49**, 3817–3830.

DIMITRIEVICH, G.S., FISCHER-DZOGA, K. and GRIEM, M.L. (1984). "Radiosensitivity of vascular tissue. I. Differential radiosensitivity of capillaries: A quantitative in vivo study," Radiat. Res. **99**, 511–535.

DING, L.H., SHINGYOJI, M., CHEN, F., HWANG, J.J., BURMA, S., LEE, C., CHENG, J.F. and CHEN, D.J. (2005). "Gene expression profiles of normal human fibroblasts after exposure to ionizing radiation: A comparative study of low and high doses," Radiat. Res. **164**, 17–26.

DIONET, C., TCHIRKOV, A., ALARD, J.P., ARNOLD, J., DHERMAIN, J., RAPP, M., BODEZ, V., TAMAIN, J.C., MONBEL, I., MALET, P., KWIATKOWSKI, F., DONNARIEIX, D., VEYRE, A. and VERRELLE, P. (2000). "Effects of low-dose neutrons applied at reduced dose rate on human melanoma cells," Radiat. Res. **154**, 406–411.

DOLY, M., ISABELLE, D.B., TETEFORT, A., GAILLARD, G. and MEYNIEL, G. (1978). "Mechanism of formation of phosphenes by action of x-rays," Life Sci. Space Res. **16**, 113–118.

DOLY, M., ISABELLE, D.B., VINCENT, P., GAILLARD, G. and MEYNIEL, G. (1980). "Mechanism of the formation of x-ray-induced phosphenes. I. Electrophysiological investigations," Radiat. Res. **82**, 93–105.

DRAB-WEISS, E.A., HANSRA, I.K., BLAZEK, E.R. and RUBIN, D.B. (1998). "Aminothiols protect endothelial cell proliferation against inhibition by lipopolysaccharide," Shock **10**, 423–429.

DRESCHHOFF, G.A.M. and ZELLER, E.J. (1990). "Evidence of individual solar proton events in antarctic snow," Solar Phys. **127**, 337–346.

DRESCHHOFF, G.A.M., SHEA, M.A., SMART, D.F. and MCCRACKEN, K.G. (1997). "Evidence for historical solar proton events from NO(x) precipitation in polar ice cores," pages 89 to 92 in *Proceedings of the 25th International Cosmic Ray Conference* (World Scientific, Hackensack, New Jersey).

DRUMMER, C., CIRILLO, M. and DE SANTO, N.G. (2004). "History of fluid balance and kidney function in space," J. Nephrol. **17**, 180–186.

DUCOFF, H.S. (2002). "Radiation hormesis: Incredible or inevitable?" Korean J. Biol. Sci. **6**, 187–193.

DUENSING, S. and MUNGER, K. (2002). "The human papillomavirus type 16 E6 and E7 oncoproteins independently induce numerical and structural chromosome instability," Cancer Res. **62**, 7075–7082.

DUGAN, L.C. and BEDFORD, J.S. (2003). "Are chromosomal instabilities induced by exposure of cultured normal human cells to low- or high-LET radiation?" Radiat. Res. **159**, 301–311.

DUNN, J.P., JABS, D.A., WINGARD, J., ENGER, C., VOGELSANG, G. and SANTOS, G. (1993). "Bone marrow transplantation and cataract development," Arch. Ophthalmol. **111**, 1367–1373.

DUNN, B.K., VERMA, M. and UMAR, A. (2003). "Epigenetics in cancer prevention: Early detection and risk assessment: Introduction," Ann. NY Acad. Sci. **983**, 1–4.

DURANTE, M. (2005). "Biomarkers of space radiation risk," Radiat. Res. **164**, 467–473.

DURANTE, M. and KRONENBERG, A. (2005). "Ground-based research with heavy ions for space radiation protection," Adv. Space Res. **35**, 180–184.

DURANTE, M., GROSSI, G.F. and YANG, T.C. (1996). "Radiation-induced chromosomal instability in human mammary epithelial cells," Adv. Space Res. **18**, 99–108.

DURANTE, M., FURUSAWA, Y., GEORGE, K., GIALANELLA, G., GRECO, O., GROSSI, G., MATSUFUJI, N., PUGLIESE, M. and YANG, T.C. (1998). "Rejoining and misrejoining of radiation-induced chromatin breaks. IV. Charged particles," Radiat. Res. **149**, 446–454.

DURANTE, M., BONASSI, S., GEORGE, K. and CUCINOTTA, F.A. (2001). "Risk estimation based on chromosomal aberrations induced by radiation," Radiat. Res. **156**, 662–667.

DURANTE, M., GEORGE, K., WU, H. and CUCINOTTA, F.A. (2002a). "Karyotypes of human lymphocytes exposed to high-energy iron ions," Radiat. Res. **158**, 581–590.

DURANTE, M., GIALANELLA, G., GROSSI, G., PUGLIESE, M., SCAMPOLI, P., KAWATA, T., YASUDA, N. and FURUSAWA, Y. (2002b). "Influence of the shielding on the induction of chromosomal aberrations in human lymphocytes exposed to high-energy iron ions," J. Radiat. Res. (Tokyo) **43** (Suppl.) S107–S111.

DURANTE, M., SNIGIRYOVA, G., AKAEVA, E., BOGOMAZOVA, A., DRUZHININ, S., FEDORENKO, B., GRECO, O., NOVITSKAYA, N., RUBANOVICH, A., SHEVCHENKO, V., VON RECKLINGHAUSEN, U. and OBE, G. (2003). "Chromosome aberration dosimetry in cosmonauts after single or multiple space flights," Cytogenet. Genome Res. **103**, 40–46.

DURANTE, M., ANDO, K., FURUSAWA, Y., OBE, G., GEORGE, K. and CUCINOTTA, F.A. (2004). "Complex chromosomal rearrangements induced *in vivo* by heavy ions," Cytogenet. Genome Res. **104**, 240–244.

EDWARDS, A.A. (2001). "RBE of radiations in space and the implications for space travel," Phys. Med. **17** (Suppl. 1), 147–152.

EHRHART, E.J., SEGARINI, P., TSANG, M.L., CARROLL, A.G. and BARCELLOS-HOFF, M.H. (1997). "Latent transforming growth factor beta1 activation *in situ*: Quantitative and functional evidence after low-dose gamma-irradiation," FASEB J. **11**, 991–1002.

ELLISON, D.C. and RAMATY, R. (1985). "Shock acceleration of electrons and ions in solar flares," Astrophys. J. **298**, 400–408.

ENGELMANN, J.J., FERRANDO, P., SOUTOUL, A., GORET, P., JULIUSSON, E. KOCH-MIRAMOND, L., LUND, N., MASSEE, P., PETERS, B., PETROU. N. and RASMUSSEN, I.L. (1990). "Charge composition and energy spectra of cosmic-ray nuclei for elements from Be to Ni. Results from HEAO-3-C2," Astron. Astrophys. **233**, 96–111.

EVANS, H.H., HORNG, M.F., RICANATI, M. and MCCOY, E.C. (1999). "Differential antimutagenicity of WR-1065 added after irradiation in L5178Y cell lines," Radiat. Res. **151**, 391–397.

EVANS, H.H., HORNG, M.F., RICANATI, M., DIAZ-INSUA, M., JORDAN, R. and SCHWARTZ, J.L. (2001). "Diverse delayed effects in human lymphoblastoid cells surviving exposure to high-LET ^{56}Fe particles or low-LET ^{137}Cs gamma radiation," Radiat. Res. **156**, 259–271.

EVANS, H.H., EVANS, T.E. and HORNG, M.F. (2002). "Antimutagenicity of WR-1065 in L5178Y cells exposed to accelerated ^{56}Fe ions," Radiat. Res. **158**, 110–114.

EVANS, H.H., HORNG, M.F. RICANATI, M., DIAZ-INSUA, M., JORDAN, R. and SCHWARTZ, J.L. (2003). "Induction of genomic instability in TK6 human lymphoblasts exposed to ^{137}Cs gamma radiation: Comparison to the induction by exposure to accelerated ^{56}Fe particles," Radiat. Res. **159**, 737–747.

EVENSON, P., GARCIA-MUNOZ, M., MEYER, P., PYLE, K.R. and SIMPSON, J.A. (1983). "A quantitative test of solar modulation theory: The proton, helium, and electron spectra from 1965 through 1979," Astrophys. J. Lett **275**, L15–L18.

FABRIKANT, J.I., LYMAN, J.T. and HOSOBUCHI, Y. (1984). "Stereotactic heavy-ion Bragg peak radiosurgery for intra-cranial vascular disorders: Method for treatment of deep arteriovenous malformations," Br. J. Radiol. **57**, 479–490.

FABRIKANT, J.I., LYMAN, J.T. and FRANKEL, K.A. (1985). "Heavy charged-particle Bragg peak radiosurgery for intracranial vascular disorders," Radiat. Res. **8** (Suppl.), S244–S258.

FABRIKANT, J.I., FRANKEL, K.A., PHILIPS, M.H. and LEVY, R.P. (1989). "Stereotactic heavy charged-particle Bragg peak radiosurgery for intracranial arteriovenous malformation," pages 389 to 409 in *Cerebral Vascular Diseases of Childhood and Adolescence*, Edwards, M.S.B. and Hoffman, H.J., Eds. (Williams and Wilkins, Baltimore).

FAGUET, G.B., REICHARD, S.M. and WELTER, D.A. (1984). "Radiation-induced clastogenic plasma factors," Cancer Genet. Cytogenet. **12**, 73–83.

FAJARDO, L.F. and BERTHRONG, M. (1988). "Vascular lesions following radiation," Pathol. Annu. **23**, 297–330.

FAJARDO, L.F. and STEWART, J.R. (1973). "Pathogenesis of radiation-induced myocardial fibrosis," Lab. Invest. **29**, 244–257.

FAJARDO, L.F., BERTHONG, M. and ANDERSON, R.E. (2001). *Radiation Pathology* (Oxford University Press, New York).

FANO, U. (1963). "Penetration of protons, alpha particles, and mesons," pages 1 to 66 in *Annual Review of Nuclear Science, Volume 13*, Segre, E., Ed. (Annual Review, Inc., Palo Alto, California).

FASSO, A., FERRARI, A., RANFT, J. and SALA, P.R. (1997). "New developments in FLUKA modelling of hadronic and EM interactions," pages 32 to 43 in *Proceedings of the 3rd Workshop on Simulating Accelerator Radiation Environments*, Hirayama, H., Ed., KEK Proceedings 97-5 (High Energy Accelerator Research Organization, Tsukuba).

FEDORENKO, B.S., ABROSIMOVA, A.N. and SMIRNOVA, O.A. (1995). "The effect of high-energy accelerated particles on the crystalline lens of laboratory animals," Phys. Part. Nucl. **26**, 573–588.

FEDORENKO, B.S., PETROV, V. and DRUZHININ, S. (1999). "Chromosome damages in cosmonauts' blood lymphocytes as a measure of radiation effect," pages 187 to 194 in *Fundamentals for the Assessment of*

Risks from Environmental Radiation, Proceedings of the NATO Advanced Research Workshop, Baumstark-Khan, C., Kozubek, S. and Horneck, G., Eds. (Springer-Verlag, New York).

FEDORENKO, B.S., SHEVCHENKO, V.A., SNIGIREVA, G.P., DRUZHININ, S.V., REPINA, L.A., NOVITSKAIA, N.N. and AKATOV, I.A. (2000). "Cytogenetic studies of blood lymphocytes of cosmonauts after long-term, space flights," Radiat. Biol. Radioecol. **40**, 596–602.

FEDORENKO, B., DRUZHININ, S., YUDAEVA, L., PETROV, V., AKATOV, Y., SNIGIRYOVA, G., NOVITSKAYA, N., SHEVCHENKO, V. and RUBANOVICH, A. (2001). "Cytogenetic studies of blood lymphocytes from cosmonauts after long-term space flights on Mir station," Adv. Space Res. **27**, 355–359.

FELBER, M., BURNS, F.J. and GARTE, S.J. (1994). "DNA fingerprinting analysis of radiation-induced rat skin tumors," Cancer Biochem. Biophys. **14**, 163–170.

FELDMAN, W.C., AUCHAMPAUGH, G.F. and BYRD, R.C. (1991). "A novel fast-neutron detector for space applications," Nucl. Inst. Methods A **306**, 350–365.

FERMI, E. (1940). *Summer Lectures* (University of Chicago, Chicago).

FERRARI, A. and SALA, P. (1996). *GEANT Hadronic Event Generators: A Comparison at the Single Interaction Level*, ATLAS Internal Note PHYS-No-086 (European Organization for Nuclear Research, Geneva).

FEYCHTING, M., JONSSON, F., PEDERSEN, N.L. and AHLBOM, A. (2003). "Occupational magnetic field exposure and neurodegenerative disease," Epidemiology **14**, 413–419; discussion 427–418.

FEYNMAN, J. (1997). "Proton fluence prediction models," pages 457 to 469 in *Solar-Terrestrial Predictions-V*, Heckman, G., Marubashi, K., Shea, M.A., Smart, D.F. And Thompson, R., Eds. (RWC, Tokyo Hiraiso Solar Terrestrial Research Center, Hitachinaka, Ibaraki, Japan).

FEYNMAN, J. and GABRIEL, S., Eds. (1988). *Interplanetary Particle Environment*, JPL 88-28 (Jet Propulsion Laboratory, California Institute of Technology, Pasadena, California).

FEYNMAN, J., SPITALE, G., WANG, J. and GABRIEL, S. (1993). "Interplanetary proton fluence model," J. Geophys. Res. **98**, 13281–13294.

FIELD, S.B., MORGAN, R.L. and MORRISON, R. (1976). "The response of human skin to irradiation with x-rays or fast neutrons," Int. J. Radiat. Oncol. Biol. Phys. **1**, 481–486.

FISK, L.A. (1971). "Solar modulation of galactic cosmic rays," J. Geophys. Res. **76**, 221–226.

FLEMING, S.D., ROSENKRANS, C.F., JR. and CHAPES, S.K. (1990). "Test of the antiorthostatic suspension model on mice: Effects on the inflammatory cell response," Aviat. Space Environ. Med. **61**, 327–332.

FLESCH, F., HIRZEBRUCH, S.E., HUNTRUP, G., ROCHER, H., STREIBEL, T., WINKEL, E. and HEINRICH, W. (1999). "Fragmentation cross section measurements of iron projectiles using CR-39 plastic nuclear track detectors," Radiat. Meas. **31**, 533–536.

FLESCH, F., IANCU, G., HEINRICH, W. and YASUDA, H. (2001). "Projectile fragmentation of silicon ions at 490 MeV," Radiat. Meas. **34**, 237–240.

FORTSCH, S.V., COWLEY, A.A., PILCHER, J.V., WHITTAL, D.M., LAWRIE, J.J., VAN STADEN J.C. and FRIEDLAND, E. (1988). "Continuum yields from ^{12}C(p,p') at incident proton energies of 90 and 200 MeV," Nucl. Phys. A **485**, 258–270.

FORTUNATO, E.A. and SPECTOR, D.H. (2003). "Viral induction of site-specific chromosome damage," Rev. Med. Virol. **13**, 21–37.

FORTUNATO, E.A., DELL'AQUILA, M.L. and SPECTOR, D.H. (2000). "Specific chromosome 1 breaks induced by human cytomegalovirus," Proc. Natl. Acad. Sci. USA **97**, 853–858.

FRAME, L.T., HART, R.W. and LEAKEY, J.E. (1998). "Caloric restriction as a mechanism mediating resistance to environmental disease," Environ. Health Perspect. **106** (Suppl. 1), 313–324.

FREED, L.E., LANGER, R., MARTIN, I., PELLIS, N.R. and VUNJAK-NOVAKOVIC, G. (1997). "Tissue engineering of cartilage in space," Proc. Natl. Acad. Sci. USA **94**, 13885–13890.

FREMLIN, J.H. (1970). "Cosmic ray flashes," New Scientist **47**, 42.

FRISK, P., HAGBERG, H., MANDAHL, A., SODERBERG, P. and LONNERHOLM, G. (2000). "Cataracts after autologous bone marrow transplantation in children," Acta. Paediatr. **89**, 814–819.

FRY, R.J.M., POWERS-RISIUS, P., ALPEN, E.L., AINSWORTH, E.J. and ULLRICH, R.L. (1983). "High-LET radiation carcinogenesis," Adv. Space Res. **3**, 241–248.

FRY, R.J.M., GROSOVSKY, A., HANAWALT, P.C., JOSTES, R.F., LITTLE, J.B., MORGAN, W.F., OLEINICK, N.L. and ULLRICH, R.L. (1998). "The impact of biology on risk assessment: Workshop of the National Research Council's Board on Radiation Effects Research. July 21-22, 1997, National Academy of Sciences, Washington, DC," Radiat. Res. **150**, 695–705.

FUJII, Z. and MCDONALD, F.B. (1997). "The radial intensity gradients of galactic cosmic rays (1972–1995) in the heliosphere," J. Geophys. Res. **102**, 24201–24208.

FUJIWARA, S., SPOSTO, R., EZAKI, H., AKIBA, S., NERIISHI, K., KODAMA, K., HOSODA, Y. and SHIMAOKA, K. (1992). "Hyperparathyroidism among atomic bomb survivors in Hiroshima," Radiat. Res. **130**, 372–378.

FUKS, Z., PERSAUD, R.S., ALFIERI, A., MCLOUGHLIN, M., EHLEITER, D., SCHWARTZ, J.L., SEDDON, A.P., CORDON-CARDO, C. and HAIMOVITZ-FRIEDMAN, A. (1994). "Basic fibroblast growth factor protects endothelial cells against radiation-induced programmed cell death *in vitro* and *in vivo*," Cancer Res. **54**, 2582–2590.

FUKUDA, T., FUKUDA, K., TAKAHASHI, A., OHNISHI, T., NAKANO, T., SATO, M. and GUNGE, N. (2000). "Analysis of deletion mutations of the *rpsL* gene in the yeast Saccharomyces cerevisiae detected after

long-term flight on the Russian space station Mir," Mutat. Res. **470**, 125–132.

FURUSAWA, Y., AOKI, M. and DURANTE, M. (2002). "Simultaneous exposure of mammalian cells to heavy ions and x-rays," Adv. Space Res. **30**, 877–884.

GAFFEY, C. (1962). "Response of sciatic nerve to high energy radiation," in *Proceedings of the International Symposium on the Response of the Nervous System to Ionizing Radiation*, Haley, T.J. and Snider, R.S., Eds. (Academic Press, Inc., New York).

GARCIA-MUNOZ, M., MEYER, P., PYLE, K.R., SIMPSON, J.A. and EVENSON, P.A. (1986). "The dependence of solar modulation on the sign of cosmic ray particle charge," J. Geophys. Res. **91**, 2858–2866.

GAUGER, G.E., TOBIAS, C.A., YANG, T. and WHITNEY, M. (1986). "The effect of space radiation on the nervous system," Adv. Space Res. **6**, 243–249.

GAUNY, S., WIESE, C. and KRONENBERG, A. (2001). "Mechanisms of mutagenesis in human cells exposed to 55 MeV protons," Phys. Med. **17** (Suppl. 1), 235–237.

GAZENKO, O.G., ADAMOVICH, B.A., GRIGORIEV, Y.G., DRUZHININ, Y.P., ILYIN, E.A. and POPOV, V.I. (1978). "Radiobiological experiment aboard the biosatellite Cosmos-690," Aviat. Space Environ. Med. **49**, 42–46.

GEARD, C.R. (1996). "Neutron induced recoil protons of restricted energy and range and biological effectiveness," Health Phys. **70**, 804–811.

GENNETT, I.N. and THILLY, W.G. (1988). "Mapping the large spontaneous endpoints in the human hprt gene," Mutat. Res. **201**, 149–160.

GENSLER, H.L., WILLIAMS, T., HUANG, A.C. and JACOBSON, E.L. (1999). "Oral niacin prevents photocarcinogenesis and photoimmunosuppression in mice," Nutr. Cancer **34**, 36–41.

GEORGE, K., DURANTE, M., ZAPP, N., WU, H. and YANG, T.C. (1999). "Biodosimetry results from crewmembers of MIR spaceflights," page 302 in Radiation Research, Proceedings of the 11th International Congress of Radiating Research, Vol. 1, Moriarty, M., Mothersill, C. and Seymour, C., Eds. (Allen Press, Lawrence, Kansas).

GEORGE, K., WU, H., WILLINGHAM, V. and CUCINOTTA, F.A. (2001a). "The effect of space radiation on the induction of chromosome damage," Phys. Med. **17** (Suppl. 1), 222–225.

GEORGE, K., WU, H., WILLINGHAM, V., FURUSAWA, Y., KAWATA, T. and CUCINOTTA, F.A. (2001b). "High- and low-LET induced chromosome damage in human lymphocytes: A time-course of aberrations in metaphase and interphase," Int. J. Radiat. Biol. **77**, 175–183.

GEORGE, K., DURANTE, M., WU, H., WILLINGHAM, V., BADHWAR, G. and CUCINOTTA, F.A. (2001c). "Chromosome aberrations in the blood lymphocytes of astronauts after space flight," Radiat. Res. **156**, 731–738.

GEORGE, K., WILLINGHAM, V., WU, H., GRIDLEY, D., NELSON, G. and CUCINOTTA, F.A. (2002). "Chromosome aberrations in human

lymphocytes induced by 250 MeV protons: Effects of dose, dose rate and shielding," Adv. Space Res. **30**, 891–899.

GEORGE, K., DURANTE, M., WILLINGHAM, V., WU, H., YANG, T.C. and CUCINOTTA, F.A. (2003). "Biological effectiveness of accelerated particles for the induction of chromosomal damage measured in metaphase and interphase human lymphocytes," Radiat. Res. **160**, 425–435.

GEORGE, K., DURANTE, M., WILLINGHAM, V. and CUCINOTTA, F.A. (2004). "Chromosome aberrations of clonal origin are present in astronauts' blood lymphocytes," Cytogenet. Genome Res. **104**, 245–251.

GERSEY, B.B., BORAK, T.B., GUETERSLOH, S.B., ZEITLIN, C., MILLER, J., HEILBRONN, L., MURAKAMI, T. and IWATA, Y. (2002). "The response of a spherical tissue-equivalent proportional counter to iron particles from 200 – 1000 MeV/nucleon," Radiat. Res. **157**, 350–360.

GETSELEV, I., RUMIN, S., SOBOLEVSKY, N., UFIMTSEV, M. and PODZOLKO, M. (2004). "Absorbed dose of secondary neutrons from galactic cosmic rays inside the International Space Station," Adv. Space Res. **34**, 1429–1432.

GIEDZINSKI, E., ROLA, R., FIKE, J.R. and LIMOLI, C.L. (2005). "Efficient production of reactive oxygen species in neural precursor cells after exposure to 250 MeV protons," Radiat. Res. **164**, 540–544.

GILBERT, E.S., CRAGLE, D.L. and WIGGS, L.D. (1993). "Updated analyses of combined mortality data for workers at the Hanford Site, Oak Ridge National Laboratory, and Rocky Flats Weapons Plant," Radiat. Res. **136**, 408–421.

GIRON, D.J., PINDAK, F.F. and SCHMIDT, J.P. (1967). "Effect of a space cabin environment on viral infection," Aerosp. Med. **38**, 832–834.

GLEESON, L.J. and AXFORD, W.I. (1967). "Cosmic rays in the interplanetary medium," Astrophys. J. **149**, L115–L118.

GMUNDER, F.K., KONSTANTINOVA, I., COGOLI, A., LESNYAK, A., BOGOMOLOV, W. and GRACHOV, A.W. (1994). "Cellular immunity in cosmonauts during long duration spaceflight on board the orbital MIR station," Aviat. Space Environ. Med. **65**, 419–423.

GOANS, R.E., HOLLOWAY, E.C., BERGER, M.E. and RICKS, R.C. (1997) "Early dose assessment following severe radiation accidents," Health Phys. **72**, 513–518.

GOFMAN, J.W. (1999). *Radiation from Medical Procedures in the Pathogenesis of Cancer and Ischemic Heart Disease: Dose-Response Studies with Physicians per 100,000 Population* (Committee for Nuclear Responsibility, San Francisco).

GOLDBERG, I.D., BLOOMER, W.D. and DAWSON, D.M. (1982). "Nervous system toxic effects of cancer therapy," J. Am. Med. Assoc. **247**, 1437–1441.

GOLDBERG, Z., SCHWIETERT, C.W., LEHNERT, B., STERN, R. and NAMI, I. (2004). "Effects of low-dose ionizing radiation on gene

expression in human skin biopsies," Int. J. Radiat. Oncol. Biol. Phys. **58**, 567–574.

GOLDBETER, A. and KOSHLAND, D.E., JR. (1981). "An amplified sensitivity arising from covalent modification in biological systems," Proc. Natl. Acad. Sci. USA **78**, 6840–6844.

GOLDEN, R.L., PARADIS, P.J., STOCHAJ, S.J., MAUGER, B.G., HORAN, S., BADWHAR, G.D., DANIEL, R.R., LACY, J.L., STEPHENS, S.A., ZIPSE, J.E., KIMBELL, B.L., WEBBER, W.R., BASINI, G., BONGIORNO, F., BRANCACCIO, F.M., RICCI, M., ORMES, J.F., SEO, E.S., STREITMATTER, R.E., PAPINI, P., SPILLANITINI, S., BRUNETTI, M.T., CODINO, A., GRIMANI, C., MENICHELLI, M., SALVATORI, I., DE PASCALE, M.P., MORSELLI, A., PICOZZA, P., CIRCELLA, M., CAFAGNA, F., BELOTTI, R., DEMARZO, C.N., SPINELLI, P., HOF, M., SIMON, M., MITCHELL, J.W., BARBIER, L.M., AVERSA, F., BARBIELLINI, G., VACCHI, A., FRATNIK, F., BRAVAR, U., SCHIAVON, P.M., COLAVITA, A. and ZAMPA, N. (1995). "Solar modulation of hydrogen and helium cosmic ray nuclei spectra above 400 MeV/nucleon, from 1976 to 1993," pages 828 to 831 in Proceedings of the 24th International Cosmic Ray Conference, 4 (University of Rome, Rome).

GOLDHABER, A.S. (1974). "Statistical models of fragmentation," Phys. Lett. B **53B**, 303–308.

GOOCH, P.C. and BERRY, C.A. (1969). "Chromosome analyses of Gemini astronauts," Aerosp. Med. **40**, 610–614.

GOODHEAD, D.T. (1994). "Initial events in the cellular effects of ionizing radiations: Cluster damage in DNA," Int. J. Radiat. Biol. **65**, 7–17.

GOODHEAD, D.T. and NIKJOO, H. (1989). "Track structure analysis of ultrasoft x-rays compared to high- and low-LET radiations," Int. J. Radiat. Biol. **55**, 513–529.

GOODWIN, E.H., BLAKELY, E.A. and TOBIAS, C.A. (1994). "Chromosomal damage and repair in G1-phase Chinese hamster ovary cells exposed to charged-particle beams," Radiat. Res. **138**, 343–351.

GOODWIN, E.H., BAILEY, S.M., CHEN, D.J. and CORNFORTH, M.N. (1996). "The effect of track structure on cell inactivation and chromosome damage at a constant LET of 120 keV/micrometer," Adv. Space Res. **18**, 93–98.

GOPINATH, D.M. and BURNHAM, C.R. (1956). "A cytogenetic study in maize of deficiency-duplication produced by crossing interchanges involving the same chromosomes," Genetics **41**, 382–395.

GORDON, K.B., CHAR, D.H. and SAGERMAN, R.H. (1995). "Late effects of radiation on the eye and ocular adnexa," Int. J. Radiat. Oncol. Biol. Phys. **31**, 1123–1139.

GOSWAMI, J.N., MCGUIRE, R.E., REEDY, R.C., LAL, D. and JHA, R. (1988). "Solar flare protons and alpha particles during the last three solar cycles," J. Geophys. Res. **93**, 7195–7205.

GOULD, C.L. and SONNENFELD, G. (1987). "Enhancement of viral pathogenesis in mice maintained in an antiorthostatic suspension

model: Coordination with effects on interferon production," J. Biol. Regul. Homeost. Agents **1**, 33–36.

GOVORUN, R.D., KOSHLAN, I.V., KOSHLAN, N.A., KRASAVIN, E.A. and SHMAKOVA, N.L. (2002). "Chromosome instability of hprt-mutant subclones induced by ionising radiation of various LET," Adv. Space Res. **30**, 885–890.

GRAGOUDAS, E.S., ZAKOV, N.Z., ALBERT, D.M. and CONSTABLE, I.J. (1979). "Long-term observations of proton-irradiated monkey eyes," Arch. Ophthalmol. **97**, 2184–2191.

GRAGOUDAS, E.S., EGAN, K.M., WALSH, S.M., REGAN, S., MUNZENRIDER, J.E. and TARATUTA, V. (1995). "Lens changes after proton beam irradiation for uveal melanoma," Am. J. Ophthalmol. **119**, 157–164.

GRAGOUDAS, E.S., LI, W., LANE, A.M., MUNZENRIDER, J. and EGAN, K.M. (1999). "Risk factors for radiation maculopathy and papillopathy after intraocular irradiation," Ophthalmology **106**, 1571–1577; discussion 1577–1578.

GRAHN, D. (1983). "Genetic risks associated with radiation exposures during space flight," Adv. Space Res. **3**, 161–170.

GRAVES, A.B., ROSNER, D., ECHEVERRIA, D., YOST, M. and LARSON, E.B. (1999). "Occupational exposure to electromagnetic fields and Alzheimer disease," Alzheimer Dis. Assoc. Disord. **13**, 165–170.

GRDINA, D.J., NAGY, B., HILL, C.K., WELLS, R.L. and PERAINO, C. (1985). "The radioprotector WR1065 reduces radiation-induced mutations at the hypoxanthine-guanine phosphoribosyl transferase locus in V79 cells," Carcinogenesis **6**, 929–931.

GRDINA, D.J., CARNES, B.A., GRAHN, D. and SIGDESTAD, C.P. (1991). "Protection against late effects of radiation by S-2-(3-aminopropylamino)-ethylphosphorothioic acid," Cancer Res. **51**, 4125–4130.

GRIDLEY, D.S., PECAUT, M.J., MILLER, G.M., MOYERS, M.F. and NELSON, G.A. (2001). "Dose and dose rate effects of whole-body gamma-irradiation: II. Hematological variables and cytokines," In Vivo **15**, 209–216.

GRIDLEY, D.S., PECAUT, M.J., DUTTA-ROY, R. and NELSON, G.A. (2002a). "Dose and dose rate effects of whole-body proton irradiation on leukocyte populations and lymphoid organs: Part I," Immunol. Lett. **80**, 55–66.

GRIDLEY, D.S., PECAUT, M.J. and NELSON, G.A. (2002b). "Total-body irradiation with high-let particles: Acute and chronic effects on the immune system," Am. J. Physiol. Regul. Integr. Comp. Physiol. **282**, R677–R688.

GRIDLEY, D.S., NELSON, G.A., PETERS, L.L., KOSTENUIK, P.J., BATEMAN, T.A., MORONY, S., STODIECK, L.S., LACEY, D.L., SIMSKE, S.J. and PECAUT, M.J. (2003). "Genetic models in applied physiology: Selected contribution: Effects of spaceflight on immunity in the C57BL/6 mouse. II. Activation, cytokines, erythrocytes, and platelets," J. Appl. Physiol. **94**, 2095–2103.

GRIDLEY, D.S., DUTTA-ROY, R., ANDRES, M.L., NELSON, G.A. and PECAUT, M.J. (2006). "Acute effects of iron-particle radiation on immunity," *Part II: Leukocyte activation, cytokines and adhesion*, Radiat. Res. **165**, 78–87.

GRIEM, M.L. (1989). "Early response of blood vessels to radiation," page 346 in *Prediction of Response to Radiation Therapy, Proceedings of the American Association of Physicists in Medicine Symposium*, Orton, C.G., Ed., **7** (American Association of Physicists in Medicine, College Park, Maryland).

GRIEM, M.L., ROBOTEWSKYJ, A. and NAGEL, R.H. (1994). "Potential vascular damage from radiation in the space environment," Adv. Space Res. **14**, 555–563.

GRIGOROVA, M., BRAND, R., XIAO, Y. and NATARAJAN, A.T. (1998). "Frequencies and types of exchange aberrations induced by x-rays and neutrons in Chinese hamster splenocytes detected by FISH using chromosome-specific DNA libraries," Int. J. Radiat. Biol. **74**, 297–314.

GROGAN, H.A, SINCLAIR, W.K. and VOILLEQUE, P.G. (2001). "Risk of fatal cancer from inhalation of 239,240-plutonium by humans: A combined four-method approach with uncertainty evaluation," Health Phys. **80**, 447–461.

GROSOVSKY, A., BETHEL, H., PARKS, K., RITTER, L., GIVER, C., GAUNY, S., WIESE, C. and KRONENBERG, A. (2001). "Genomic instability in human lymphoid cells exposed to 1 GeV/amu Fe ions," Phys. Med. **17** (Suppl. 1), 238–240.

GROSSI, G., DURANTE, M., GIALANELLA, G., PUGLIESE, M., SCAMPOLI, P., FURUSAWA, Y., KANAI, T. and MATSUFUJI, N. (2004). "Chromosomal aberrations induced by high-energy iron ions with shielding," Adv. Space Res. **34**, 1358–1361.

GUAN, J., WAN, X.S., ZHOU, Z., WARE, J., DONAHUE, J.J., BIAGLOW, J.E. and KENNEDY, A.R. (2004). "Effects of dietary supplements on space radiation-induced oxidative stress in Sprague-Dawley rats," Radiat. Res. **162**, 572–579.

GUDOWSKA-NOWAK, E., KLECZKOWSKI, A., NASONOVA, E., SCHOLZ, M. and RITTER, S. (2005). "Correlation between mitotic delay and aberration burden, and their role for the analysis of chromosomal damage," Int. J. Radiat. Biol. **81**, 23–32.

GUIDA, P. VAZQUEZ, M.E. and OTTO, S. (2005). "Cytotoxic effects of low- and high-LET radiation on human neuronal progenitor cells: Induction of apoptosis and TP53 gene expression," Radiat. Res. **164**, 545–551.

GUROVSKY, N. and ILYIN, V. (1978). "Soviet bio-satellites in the Cosmos-series: The main results of the 8-year program," Aviat. Space Environ. Med. **49**, 1355–1356.

HAGMAR, L., BONASSI, S., STROMBERG, U., BROGGER, A., KNUDSEN, L.E., NORPPA, H. and REUTERWALL, C. (1998). "Chromosomal aberrations in lymphocytes predict human cancer: A report

from the European Study Group on Cytogenetic Biomarkers and Health (ESCH)," Cancer Res. **58**, 4117–4121.

HALBERG, F.E. (1998). "Pituitary tumors," in *Textbook of Radiation Oncology*, Leibel, S.A. and Phillips, T.L., Eds. (Elsevier, New York).

HALL, J. and ANGELE, S. (1999). "Radiation, DNA damage and cancer," Mol. Med. Today **5**, 157–164.

HALL, E.J., SCHIFF, P.B., HANKS, G.E., BRENNER, D.J., RUSSO, J., CHEN, J., SAWANT, S.G. and PANDITA, T.K. (1998). "A preliminary report: Frequency of A-T heterozygotes among prostate cancer patients with severe late responses to radiation therapy," Cancer J. Sci. Am. **4**, 385–389.

HALL, P., ADAMI, H.O., TRICHOPOULOS, D., PEDERSEN, N.L., LAGIOU, P., EKBOM, A., INGVAR, M., LUNDELL, M. and GRANATH, F. (2004). "Effect of low doses of ionising radiation in infancy on cognitive function in adulthood: Swedish population based cohort study," Br. Med. J. **328**, 19.

HAMBLIN, D.L. and WOOD, A.W. (2002). "Effects of mobile phone emissions of human brain activity and sleep variables," Int. J. Radiat. Biol. **78**, 659–669.

HAMILTON, D.C. (1977). "The radial transport of energetic solar flare particles from 1 to 6 AU," J. Geophys. Res. **82**, 2157–2169.

HAMM, P.B., BILLICA, R.D., JOHNSON, G.S., WEAR, M.L. and POOL, S.L. (1998). "Risk of cancer mortality among the Longitudinal Study of Astronaut Health (LSAH) participants," Aviat. Space Environ. Med. **69**, 142–144.

HAMM, P.B., NICOGOSSIAN, A.E., POOL, S.L., WEAR, M.L. and BILLICA, R.D. (2000). "Design and current status of the longitudinal study of astronaut health," Aviat. Space Environ. Med. **71**, 564–570.

HANAHAN, D. and WEINBERG, R. A. (2000). "The hallmarks of cancer," Cell **100**, 57–70.

HARADA, K., OBIYA, Y., NAKANO, T., KAWASHIMA, M., MIKI, T., KOBAYASHI, Y., WATANABE, H., OKAICHI, K., OHNISHI, T., MUKAI, C. and NAGAOKA, S. (1997). "Cancer risk in space due to radiation assessed by determining cell lethality and mutation frequencies of prokaryotes and a plasmid during the Second International Microgravity Laboratory (IML-2) Space Shuttle experiment," Oncol. Rep. **4**, 691–695.

HARADA, K., NAGAOKA, S., MOHRI, M., OHNISHI, T. and SUGAHARA, T. (1998a). "Lethality of high linear energy transfer cosmic radiation to Escherichia coli DNA repair-deficient mutants during the 'SL-J/FMPT' space experiment," FEMS Microbiol. Lett. **164**, 39–45.

HARADA, K., SUGAHARA, T., OHNISHI, T., OZAKI, Y., OBIYA, Y., MIKI, S., MIKI, T., IMAMURA, M., KOBAYASHI, Y., WATANABE, H., AKASHI, M., FURUSAWA, Y., MIZUMA, N., YAMANAKA, H., OHASHI, E., YAMAOKA, C., YAJIMA, M., FUKUI, M., NAKANO, T., TAKAHASHI, S., AMANO, T., SEKIKAWA, K., YANAGAWA, K. and NAGAOKA, S. (1998b). "Inhibition in a microgravity environment of

the recovery of Escherichia coli cells damaged by heavy ion beams during the NASDA ISS phase I program of NASA Shuttle/Mir mission no. 6," Int. J. Mol. Med. **1**, 817–822.

HARPER, K., LORIMORE, S.A. and WRIGHT, E.G. (1997). "Delayed appearance of radiation-induced mutations at the hprt locus in murine hemopoietic cells," Exp. Hematol. **25**, 263–269.

HAYASHI, T., KUSUNOKI, Y., HAKODA, M., MORISHITA, Y., KUBO, Y., MAKI, M., KASAGI, F., KODAMA, K., MACPHEE, D.G. and KYOIZUMI, S. (2003). "Radiation dose-dependent increases in inflammatory response markers in A-bomb survivors," Int. J. Radiat. Biol. **79**, 129–136.

HAYMAKER, W., RUBINSTEIN, L.J. and MIQUEL, J. (1972). "Brain tumors in irradiated monkeys," Acta. Neuropathol. (Berl) **20**, 267–277.

HECKMAN, G. (1993). "Prediction of solar particle events for exploration class missions," pages 89 to 100 *Biological Effects and Physics of Solar and Galactic Cosmic Radiation, Part B,* Swenberg, C.E., Horneck, G. and Stassinopoulos, E.G., Eds. (Plenum Press, New York).

HECKMAN, G.R., KUNCHES, J.M. and ALLEN, J.H. (1992). "Prediction and evaluation of solar particle events based on precursor information," Adv. Space Res. **12**, 313–320.

HEER, M. and PALOSKI, W.H. (2006). "Space motion sickness: Incidence, etiology and countermeasures," Autono. Neurosci. **129**, 77–79.

HEI, T.K., CHEN, D.J., BRENNER, D.J. and HALL, E.J. (1988). "Mutation induction by charged particles of defined linear energy transfer," Carcinogenesis **9**, 1233–1236.

HEI, T.K., PIAO, C.Q., WU, L.J., WILLEY, J.C. and HALL, E.J. (1998). "Genomic instability and tumorigenic induction in immortalized human bronchial epithelial cells by heavy ions," Adv. Space Res. **22**, 1699–1707.

HEIMBACH, R.D., BURNS, F.J. and ALBERT, R.E. (1969). "An evaluation by alpha-particle Bragg peak radiation of the critical depth in the rat skin for tumor induction," Radiat. Res. **39**, 332–344.

HEIMERS, A., SCHRODER, H., LENGFELDER, E. and SCHMITZ-FEUERHAKE, I. (1995). "Chromosome aberration analysis in aircrew members," Radiat. Prot. Dosim. **60**, 171–175.

HEO, M.Y., KIM, S.H., YANG, H.E., LEE, S.H., JO, B.K. and KIM, H.P. (2001). "Protection against ultraviolet B- and C-induced DNA damage and skin carcinogenesis by the flowers of Prunus persica extract," Mutat. Res. **496**, 47–59.

HERAS, A.M., SANAHUJA, B., LARIO, D., SMITH, Z.K., DETMAN, T. and DRYER, M. (1995). "Three low-energy particle events: Modeling the influence of the parent interplanetary shock," Astrophys. J. **445**, 497–508.

HICKMAN, A.W., JARAMILLO, R.J., LECHNER, J.F. and JOHNSON, N.F. (1994). "Alpha-particle-induced p53 protein expression in a rat lung epithelial cell strain," Cancer Res. **54**, 5797–5800.

HILDERBRAND, B and SILBERBERG, R. (1966). "Modulation of generically related galactic cosmic rays," Phys. Rev. **141**, 1248–1260.

HOFF, J.L. TOWNSEND, L.W. and HINES, J.W. (2003). "Prediction of energetic solar particle event dose-time profiles using artificial neural networks," IEEE Trans. on Nucl. Sci. **50**, 2296–2300.

HOFFMAN, R.A., PINSKY, L.S., OSBORNE, W.Z. and BAILEY, J.V. (1977). "Visual light flash observations on Skylab 4," pages 127 to 130 in *Biomedical Results from Skylab*, NASA SP-377, Johnston, R.S. and Dietlein, L.F., Eds. (U.S. Government Printing Office, Washington).

HOLLEY, W.R. and CHATTERJEE, A. (1996). "Clusters of DNA induced by ionizing radiation: Formation of short DNA fragments. I. Theoretical modeling," Radiat. Res. **145**, 188–199.

HOLLEY, W.R., MIAN, I.S., PARK, S.J., RYDBERG, B. and CHATTERJEE, A. (2002). "A model for interphase chromosomes and evaluation of radiation-induced aberrations," Radiat. Res. **158**, 568–580.

HONG, J.H., CHIANG, C.S., CAMPBELL, I.L., SUN, J.R., WITHERS, H.R. and MCBRIDE, W.H. (1995). "Induction of acute phase gene expression by brain irradiation," Int. J. Radiat. Oncol. Biol. Phys. **33**, 619–626.

HOPEWELL, J.W. (1980). "The importance of vascular damage in the development of late radiation effects in normal tissues," pages 449 to 460 in *Radiation Biology in Cancer Research*, Meyn, R.E. and Withers, H.R., Eds. (Raven Press, New York).

HORNECK, G. (1988). "Impact of space flight environment on radiation response," in *Terrestrial Space Radiation and its Biological Effects*, McCormack, P.D., Swenberg, C.E. and Bucker, H., Eds. (Plenum Press, New York).

HORNECK, G. (1992). "Radiobiological experiments in space: A review," Nucl. Tracks Radiat. Meas. **20**, 185–205.

HORNECK, G. (1998). "Biological monitoring of radiation exposure," Adv. Space Res. **22**, 1631–1641.

HORNECK, G. (1999). "Impact of microgravity on radiobiological processes and efficiency of DNA repair," Mutat. Res. **430**, 221–228.

HORNECK, G., RETTBERG, P., SCHAFER, M., ZIMMERMANN, H., RINK, H., BAUMSTARK-KHAN, C. and KOZUBEK, S. (1995). "Enzymatic repair of radiation-induced DNA damage under microgravity," pages 1195 to 1198 in *Proceedings of the 10th International Congress of Radiation Research, Volume 2*, Hagen, U., Harder, D., Jung, H. and Streffer, C., Eds. (Universitatsdruckerei, Wurzburg).

HORNECK, G., RETTBERG, P., BAUMSTARK-KHAN, C., RINK, H., KOZUBEK, S., SCHAFER, M. and SCHMITZ, C. (1996). "DNA repair in microgravity: Studies on bacteria and mammalian cells in the experiments REPAIR and KINETICS," J. Biotechnol. **47**, 99–112.

HORNECK, G., RETTBERG, P., KOZUBEK, S., BAUMSTARK-KHAN, C., RINK, H., SCHAFER, M. and SCHMITZ, C. (1997). "The influence of microgravity on repair of radiation-induced DNA damage in bacteria and human fibroblasts," Radiat. Res. **147**, 376–384.

HORSTMANN, M., DURANTE, M. and OBE, G. (2004). "Distribution of breakpoints and fragment sizes in human chromosome 5 after heavy-ion bombardment," Int. J. Radiat. Biol. **80**, 437–443.

HORSTMANN, M., DURANTE, M., JOHANNES C., PIEPER, R. and OBE, G. (2005). "Space radiation does not induce a significant increase of intrachromosomal exchanges in astronauts' lymphocytes," Radiat. Environ. Biophys. **44**, 219–224.

HOWE, G.R., ZABLOTSKA, L.B., FIX, J.J., EGEL, J. and BUCHANAN, J. (2004). "Analysis of the mortality experience amongst U.S. nuclear power industry workers after chronic low-dose exposure to ionizing radiation," Radiat. Res. **162**, 517–526.

HUANG, L., SNYDER, A.R. and MORGAN, W.F. (2003). "Radiation-induced genomic instability and its implications for radiation carcinogenesis," Oncogene **22**, 5848–5854.

HUFNER, J. (1985). "Heavy fragments produced in proton-nucleus and nucleus-nucleus collisions at relativistic energies," Phys. Rep. **125**, 129–185.

HUFNER, J., SCHAFER, K. and SCHURMANN, B. (1975). "Abrasion-ablation in reactions between relativistic heavy ions," Phys. Rev. C **12**, 1888–1898.

HUGHES, H.G., PRAEL, R.E. and LITTLE, R.C. (1997). *MCNPX – The LAHET/MCNP Code Merger*, LA-UR-97-4891 (Los Alamos National Laboratory, Los Alamos, New Mexico).

HUGHES-FULFORD, M. and LEWIS, M.L. (1996). "Effects of microgravity on osteoblast growth activation," Exp. Cell Res. **224**, 103–109.

HUNT, W.A., JOSEPH, J.A. and RABIN, B.M. (1989). "Behavioral and neurochemical abnormalities after exposure to low doses of high-energy iron particles," Adv. Space Res. **9**, 333–336.

HUNT, W.A., DALTON, T.K., JOSEPH, J.A. and RABIN, B.M. (1990). "Reduction of 3-methoxytyramine concentrations in the caudate nucleus of rats after exposure to high-energy iron particles: Evidence for deficits in dopaminergic neurons," Radiat. Res. **121**, 169–174

IANNUZZI, C.M., ATENCIO, D.P., GREEN, S., STOCK, R.G. and ROSENSTEIN, B.S. (2002). "ATM mutations in female breast cancer patients predict for an increase in radiation-induced late effects," Int. J. Radiat. Oncol. Biol. Phys. **52**, 606–613.

ICNIRP (2003). International Commission on Non-Ionizing Radiation Protection. *Exposure to Static and Low Frequency Electromagnetic Fields, Biological Effects and Health Consequences (0-100 kHz)*, Matthes, R., McKinlay, A.F., Bernhardt, J.H., Vecchia, P. and Veyret, B., Eds (Earthprint, Ltd., Hertfordshire, United Kingdom).

ICRP (1969). International Commission on Radiological Protection. *Radiation Cataract in Man: Radiosensitivity and Spatial Distribution of Dose*, Appendix 1, ICRP Publication 14 (Elsevier Science, New York).

ICRP (1989). International Commission on Radiological Protection. *RBE for Deterministic Effects,* ICRP Publication 58, Ann. ICRP **20**(4) (Elsevier Science, New York).

ICRP (1991). International Commission on Radiological Protection. *1990 Recommendations of the International Commission on Radiological Protection*, ICRP Publication 60, Ann. ICRP **21**(1–3) (Elsevier Science, New York).

ICRP (2003). International Commission on Radiological Protection. *Relative Biological Effectiveness (RBE), Quality Factor (Q), and Radiation Weighting Factor (w_R)*, ICRP Publication 92, Ann. ICRP **33**(4) (Elsevier Science, New York).

ICRU (1986). International Commission on Radiation Units and Measurements. *The Quality Factor in Radiation Protection*, ICRU Report 40 (Oxford University Press, Cary, North Carolina).

ICRU (1988). International Commission on Radiation Units and Measurements. *Determination of Dose Equivalent from External Radiation Sources – Part 2*, ICRU Report 43 (Oxford University Press, Cary, North Carolina).

ICRU (1993). International Commission on Radiation Units and Measurements. *Quantities and Units in Ionizing Radiation Protection Dosimetry*, ICRU Report 51 (Oxford University Press, Cary, North Carolina).

ICRU (2000). International Commission on Radiation Units and Measurements. *Nuclear Data for Neutron and Proton Radiation Therapy and for Radiation Protection,* ICRU Report 63 (Oxford University Press, Cary, North Carolina).

INANO, H., ONODA, M., INAFUKU, N., KUBOTA, M., KAMADA, Y. OSAWA, T., KOBAYASHI, H. and WAKABAYASHI, K. (2000). "Potent preventive action of curcumin on radiation-induced initiation of mammary tumorigenesis in rats," Carcinogenesis **21**, 1835–1841.

ISHIZAKI, K., NISHIZAWA, K., KATO, T., KITAO, H., HAN, Z.B., HIRAYAMA, J., SUZUKI, F., CANNON, T.F., KAMIGAICHI, S., TAWARAYAMA, Y., MASUKAWA, M., SHIMAZU, T. and IKENAGA, M. (2001). "Genetic changes induced in human cells in space shuttle experiment (STS-95)," Aviat. Space Environ. Med. **72**, 794–798.

IVANCSITS, S., DIEM, E., PILGER, A., RUDIGER, H.W. and JAHN, O. (2002). "Induction of DNA strand breaks by intermittent exposure to extremely-low-frequency electromagnetic fields in human diploid fibroblasts," Mutat. Res. **519**, 1–13.

IVANCSITS, S., DIEM, E., JAHN, O. and RUDIGER, H.W. (2003). "Intermittent extremely low frequency electromagnetic fields cause DNA damage in a dose-dependent way," Int. Arch. Occup. Environ. Health **76**, 431–436.

IVANOV, V.K., GORSKI, A.I., MAKSIOUTOV, M.A., TSYB, A.F. and SOUCHKEVITCH, G.N. (2001). "Mortality among the Chernobyl emergency workers: Estimation of radiation risks (preliminary analysis)," Health Phys. **81**, 514–521.

IVANOV, V.K., MAKSIOUTOV, M.A., CHEKIN, S.Y., PETROV, A.V., BIRYUKOV, A.P., KRUGLOVA, Z.G., MATYASH, V.A., TSYB, A.F., MANTON, K.G. and KRAVCHENKO, J.S. (2006). "The risk of

radiation-induced cerebrovascular disease in Chernobyl emergency workers," Health Phys. **90**, 199–207.

JACQUES, P.F., TAYLOR, A., HANKINSON, S.E., WILLETT, W.C., MAHNKEN, B., LEE, Y., VAID, K. and LAHAV, M. (1997). "Long-term vitamin C supplement use and prevalence of early age-related lens opacities," Am. J. Clin. Nutr. **66**, 911–916.

JAKOB, B., SCHOLZ, M. and TAUCHER-SCHOLZ, G. (2000). "Immediate localized CDKN1A (p21) radiation response after damage produced by heavy-ion tracks," Radiat. Res. **154**, 398–405.

JAKOB, B., SCHOLZ, M. and TAUCHER-SCHOLZ, G. (2002). "Characterization of CDKN1A (p21) binding to sites of heavy-ion-induced damage: Colocalization with proteins involved in DNA repair," Int. J. Radiat. Biol. **78**, 75–88.

JEGGO, P.A. (1998). "Identification of genes involved in repair of DNA double-strand breaks in mammalian cells," Radiat. Res. **150** (Suppl. 5), S80–S91.

JEGGO, P.A. and CONCANNON, P. (2001). "Immune diversity and genomic stability: Opposite goals but similar paths," J. Photochem. Photobiol. B. **65**, 88–96.

JENNINGS, R.T. and SANTY, P.A. (1990). "Reproduction in the space environment: Part II. Concerns for human reproduction," Obstet. Gynecol. Surv. **45**, 7–17.

JOHANSSON, L. (2003). "Hormesis, an update of the present position," Eur. J. Nucl. Med. Mol. Imaging **30**, 921–933.

JOKIPPI, J.R. and THOMAS, B.T. (1981). "Effect of drifts on the transport of cosmic rays modulated by a wavy interplanetary current sheet," Astrophys. J. **243**, 1115–1122.

JONES, F.C. and ELLISON, D.C. (1991). "The plasma physics of shock acceleration," Space Sci. Rev. **58**, 259–346.

JOSE, J.G. and AINSWORTH, E.J. (1983). "Cataract production in mice by heavy charged argon, neon, and carbon particles," Radiat. Res. **94**, 513–528.

JOSEPH, J.A., HUNT, W.A., RABIN, B.M. and DALTON, T.K. (1992). "Possible "accelerated striatal aging" induced by ^{56}Fe heavy-particle irradiation: Implications for manned space flights," Radiat. Res. **130**, 88–93.

JOSEPH, J.A., HUNT, W.A., RABIN, B.M., DALTON, T.K. and HARRIS, A.H. (1993). "Deficits in the sensitivity of striatal muscarinic receptors induced by ^{56}Fe heavy-particle irradiation: Further "age-radiation parallels," Radiat. Res. **135**, 257–261.

JOSEPH, J.A., VILLALOBOS-MOLINA, R., RABIN, B.M., DALTON, T.K., HARRIS, A. and KANDASAMY, S. (1994). "Reductions of ^{56}Fe heavy-particle irradiation-induced deficits in striatal muscarinic receptor sensitivity by selective cross-activation/inhibition of second-messenger systems," Radiat. Res. **139**, 60–66.

JUNK, A.K., KUNDIEV, Y., VITTE, P. and WORGUL, B.V., Eds. (1999). *Ocular Radiation Risk Assessment in Populations Exposed to*

Environmental Radiation Contamination (Kluwer Academic Publishers, Boston).

KADHIM, M.A., MACDONALD, D.A., GOODHEAD, D.T., LORIMORE, S.A., MARSDEN, S.J. and WRIGHT, E.G. (1992). "Transmission of chromosomal instability after plutonium alpha-particle irradiation," Nature **355**, 738–740.

KADHIM, M.A., LORIMORE, S.A., HEPBURN, M.D., GOODHEAD, D.T., BUCKLE, V.J. and WRIGHT, E.G. (1994). "Alpha-particle-induced chromosomal instability in human bone marrow cells," Lancet **344**, 987–988.

KADHIM, M.A., LORIMORE, S.A., TOWNSEND, K.M., GOODHEAD, D.T., BUCKLE, V.J. and WRIGHT, E.G. (1995). "Radiation-induced genomic instability: Delayed cytogenetic aberrations and apoptosis in primary human bone marrow cells," Int. J. Radiat. Biol. **67**, 287–293.

KADHIM, M.A., MARSDEN, S.J. and WRIGHT, E.G. (1998). "Radiation-induced chromosomal instability in human fibroblasts: Temporal effects and the influence of radiation quality," Int. J. Radiat. Biol. **73**, 143–148.

KADHIM, M.A., MARSDEN, S.J., GOODHEAD, D.T., MALCOLMSON, A.M., FOLKARD, M., PRISE, K.M. and MICHAEL, B.D. (2001). "Long-term genomic instability in human lymphocytes induced by single-particle irradiation," Radiat. Res. **155**, 122–126.

KADHIM, M.A., MOORE, S.R. and GOODWIN, E.H. (2004). "Interrelationships amongst radiation-induced genomic instability, bystander effects, and the adaptive response," Mutat. Res. **568**, 21–32.

KADOR, P.F. (1983). "Overview of the current attempts toward the medical treatment of cataract," Ophthalmology **90**, 352–364.

KAHLER, S.W. (1982). "The role of the big flare syndrome in correlations of solar energetic proton fluxes and associated microwave burst parameters," J. Geophys. Res. **87**, 3439–3448.

KAINA, B., HAAS, S., GROSCH, S., GROMBACHER, T., DOSCH, J., BISWAS, T., BOLDOGH, I., MITRA, S. and FRITZ, G. (1999). "Inducible responses and protective functions of mammalian cells upon exposure to UV light and ionizing radiation," pages 289 to 300 in *Fundamentals for the Assessment of Risks from Environmental Radiation*, Baumstark-Khan, C., Kozubek, S. and Horneck, G., Eds. (Kluwer Academic Publishers, Boston).

KAJIOKA, E.H., GHEORGHE, C., ANDRES, M.L., ABELL, G.A., FOLZ-HOLBECK, J., SLATER, J.M., NELSON, G.A. and GRIDLEY, D.S. (1999). "Effects of proton and gamma radiation on lymphocyte populations and acute response to antigen," In Vivo **13**, 525–533.

KAJIOKA, E.H., ANDRES, M.L., MAO, X.W., MOYERS, M.F., NELSON, G.A. and GRIDLEY, D.S. (2000a). "Hematological and TGF-beta variations after whole-body proton irradiation," In Vivo **14**, 703–708.

KAJIOKA, E.H., ANDRES, M.L., LI, J., MAO, X.W., MOYERS, M.F., NELSON, G.A., SLATER, J.M. and GRIDLEY, D.S. (2000b). "Acute

effects of whole-body proton irradiation on the immune system of the mouse," Radiat. Res. **153**, 587–594.

KALEBIC, T. (2003). "Epigenetic changes: Potential therapeutic targets," Ann. NY Acad. Sci. **983**, 278–285.

KALLENRODE, M.B. (1993). "Shocks as mechanism for the acceleration and propagation of energetic particles," Adv. Space Res. **13**, 341–350.

KALLENRODE, M.B., WIBBERENZ, G., KUNOW, H., MULLER-MELLIN, R., STOLPOVSKII, V. and KONTOR, N. (1993). "Multi-spacecraft observations of particle events and interplanetary shocks during November-December 1982," Solar Phys. **147**, 377–410.

KAMEYAMA, M., KOBAYASHI, M., MOTOKAWA, K. and UMETSU, J. (1956). "The effect of a small dose of roentgen rays upon the human body as revealed by the method of electric flicker," Tohoku. J. Exp. Med. **64**, 151–159.

KANDASAMY, S.B., RABIN, B.M., HUNT, W.A., DALTON, T.K., JOSEPH, J.A. and HARRIS, A.H. (1994). "Exposure to heavy charged particles affects thermoregulation in rats," Radiat. Res. **139**, 352–356.

KARGER, C.P., DEBUS, J., PESCHKE, P., MUNTER, M.W., HEILAND, S. and HARTMANN, G.H. (2002a). "Dose-response curves for late functional changes in the normal rat brain after single carbon-ion doses evaluated by magnetic resonance imaging: Influence of follow-up time and calculation of relative biological effectiveness," Radiat. Res. **158**, 545–555.

KARGER, C.P., MUNTER, M.W., HEILAND, S., PESCHKE, P., DEBUS, J. and HARTMANN, G.H. (2002b). "Dose-response curves and tolerance doses for late functional changes in the normal rat brain after stereotactic radiosurgery evaluated by magnetic resonance imaging: Influence of end points and follow-up time," Radiat. Res. **157**, 617–625.

KARSLIOGLU, I., ERTEKIN, M.V., KOCER, I., TAYSI, S., SEZEN, O., GEPDIREMEN, A. and BALCI, E. (2004). "Protective role of intramuscularly administered vitamin E on the levels of lipid peroxidation and the activities of antioxidant enzymes in the lens of rats made cataractous with gamma-irradiation," Eur. J. Ophthalmol. **14**, 478–485.

KASTAN, M.B., ONYEKWERE, O., SIDRANSKY, D., VOGELSTEIN, B. and CRAIG, R.W. (1991). "Participation of p53 protein in the cellular response to DNA damage," Cancer Res. **51**, 6304–6311.

KATZ, R., ACKERSON, B., HOMAYOONFAR, M. and SCHARMA, S.C. (1971). "Inactivation of cells by heavy ion bombardment," Radiat. Res. **47**, 402–425.

KAUR, I., SIMONS, E.R., CASTRO, V.A., OTT, C.M. and PIERSON, D.L. (2004). "Changes in neutrophil functions in astronauts," Brain Behav. Immun. **18**, 443–450.

KEIME-GUIBERT, F., NAPOLITANO, M. and DELATTRE, J.Y. (1998). "Neurological complications of radiotherapy and chemotherapy," J. Neurol. **245**, 695–708.

KELFKENS, G., DE GRUIJL, F.R. and VAN DER LEUN, J.C. (1991). "Tumorigenesis by short-wave ultraviolet A: Papillomas versus squamous cell carcinomas," Carcinogenesis **12**, 1377–1382.

KELLER, F.L. and PRUETT, R.G. (1965). "The effect of charged-particle environments on manned military space systems," pages 265 to 286 in *Second Symposium on Protection Against Radiations in Space*, NASA SP-71, Reetz, A., Jr., Ed. (U.S. Government Printing Office, Washington).

KELLERER, A.M. and WALSH, L. (2001). "Risk estimation for fast neutrons with regard to solid cancer," Radiat. Res. **156**, 708–717.

KELLERER, A.M. and WALSH, L. (2002). "Solid cancer risk coefficient for fast neutrons in terms of effective dose," Radiat. Res. **158**, 61–68.

KENG, P.C., LEE, A.C., COX, A.B., BERGTOLD, D.S. and LETT, J.T. (1982). "Effects of heavy ions on rabbit tissues: Cataractogenesis," Int. J. Radiat. Biol. Relat. Stud. Phys. Chem. Med. **41**, 127–137.

KENNEDY, C.H., MITCHELL, C.E., FUKUSHIMA, N.H., NEFT, R.E. and LECHNER, J.F. (1996). "Induction of genomic instability in normal human bronchial epithelial cells by ^{238}Pu alpha-particles," Carcinogenesis **17**, 1671–1676.

KENNEDY, A.R., WARE, J.H., GUAN, J., DONAHUE, J.J., BIAGLOW, J.E., ZHOU, Z., STEWART, J., VAZQUEZ, M. and WAN, X.S. (2004). "Selenomethionine protects against adverse biological effects induced by space radiation," Free Radic. Biol. Med. **36**, 259–266.

KERWIN, J. and SEDDON, R. (2002). "Eating in space—from an astronaut's perspective," Nutrition **18**, 921–925.

KHAIDAKOV, M., YOUNG, D., ERFLE, H., MORTIMER, A., VORONKOV, Y. and GLICKMAN, B.W. (1997). "Molecular analysis of mutations in T-lymphocytes from experienced Soviet cosmonauts," Environ. Mol. Mutagen, **30**, 21–30.

KHAIDAKOV, M., CURRY, J., WALSH, D., MORTIMER, A. and GLICKMAN, B.W. (1999). "Study on genotoxic effects of the space environment: A comparison between experienced cosmonauts and unexposed Russian twins," Mutat. Res. **430**, 337–342.

KIEFER, J. and PROSS, H.D. (1999). "Space radiation effects and microgravity," Mutat. Res. **430**, 299–305.

KIEFER, J., BRENDAMOUR, M. and STOLL, U. (1996). "Heavy ion action on biological systems," Nucl. Instrum. Meth. Phys. Res. B **107**, 292–298.

KIM, M.Y., WILSON, J.W. and CUCINOTTA, F.A. (2006). "A solar cycle statistical model for the projection of space radiation environment," Adv. Space Res. **37**, 1741–1748.

KIMZEY, S.L., FISCHER, C.L., JOHNSON, P.C., RITZMANN, S.E. and MENGEL, C.E. (1975). "Hematology and immunology studies," pages 197 to 226 in *Biomedical Results of Apollo*, Johnston, R.S., Dietlein, L.F. and Berry, C.A., Eds., NASA SP-368 (NASA Center for AeroSpace Information, Hanover, Maryland).

KING, J.H. (1974). "Solar proton fluences for 1977–1983 space missions," J. Spacecraft **11**, 401–408.

KJELLBERG, R.N. and KLIMAN, B. (1979). "Life-time effectiveness; a system of therapy for pituitary adenomas, emphasizing Bragg peak proton hypophysectomy," pages 269 to 288 in *Recent Advances in the Diagnosis and Treatment of Pituitary Tumors*, Linfoot, J.A., Ed. (Raven Press, New York).

KJELLBERG, R.N., HANAMURA, T., DAVIS, K. R., LYONS, S.L. and ADAMS, R.D. (1983). "Bragg-peak proton-beam therapy for arteriovenous malformations of the brain," N. Engl. J. Med. **309**, 269–274.

KLIUKIENE, J., TYNES, T. and ANDERSEN, A. (2003). "Follow-up of radio and telegraph operators with exposure to electromagnetic fields and risk of breast cancer," Eur. J. Cancer Prev. **12**, 301–307.

KNEHR, S., HUBER, R., BRASELMANN, H., SCHRAUBE, H. and BAUCHINGER, M. (1999). "Multicolour FISH painting for the analysis of chromosomal aberrations induced by 220 kV x-rays and fission neutrons," Int. J. Radiat. Biol. **75**, 407–418.

KNOLL, G.E. (2000). *Radiation Detection and Measurement*, 3rd ed. (John Wiley and Sons, New York).

KNOTT, C.N., ALBERGO, S., CACCIA, Z., CHEN, C., COSTA, S., CRAWFORD, H.J., CRONQVIST, M., ENGELAGE, J., FERRANDO, P., FONTE, R., GREINER, L., GUZIK, T.G., INSOLIA, A., JONES, F.C., LINDSTROM, P.J., MITCHELL, J.W., POTENZA, R., ROMANSKI, J., RUSSO, G.V., SOUTOUL, A., TESTARD, O., TULL, C.E., TUVE, C., WADDINGTON, C.J., WEBBER, W.R. and WEFEL, J.P. (1996). "Interactions of relativistic neon to nickel projectiles in hydrogen, elemental production cross sections," Phys. Rev. C. Nucl. Phys. **53**, 347–357.

KOBAYASHI, Y., KIKUCHI, M., NAGAOKA, S. and WATANABE, H. (1996). "Recovery of Deinococcus radiodurans from radiation damage was enhanced under microgravity," Biol. Sci. Space **10**, 97–101.

KOBAYASHI, M., DOKE, T, KAKUCHI, J., TOKAYOSHI, H., TAKASHIMA, T., TAKKKEHANA, N., HIDEKAZU, S., NOBUYUKI, H., KOJI, K. and WILKEN, B. (1998). "The relationship between corotating energetic ion enhancements and solar wind speed at 1 AU," J. Phys. Soc. Japan **67**, 3991–3996.

KOBETICH, E.J. and KATZ, R. (1968). "Energy deposition by electron beams and δ rays," Phys. Rev. **170**, 391–396.

KODAMA, K., FUJIWARA, S., YAMADA, M., KASAGI, F., SHIMIZU, Y. and SHIGEMATSU, I. (1996). "Profiles on non-cancer diseases in atomic bomb survivors," World Health Stat. Q. **49**, 7–16.

KODAMA, Y., OHTAKI, K., NAKANA, M. HAMASAKI, K. AWA, A.A., LAGARDE, F. and NAKAMURA, N. (2005). "Clonally expanded T-cell populations in atomic bomb survivors do not show excess levels of chromosome instability," Radiat. Res. **164**, 618–626.

KONSTANTINOVA, I.V. and FUCHS, B.B. (1991). *The Immune System in Space and Other Extreme Conditions* (Harwood Academic Publishers, Philadelphia).

KOSHLAND, D.E., JR., HY, G. and FILMER, D. (1966). "Comparison of experimental binding data and theoretical models in proteins containing subunits," Biochemistry **5**, 365–385.

KOTA, J. and JOKIPII J.R. (1983). "Effects of drift on the transport of cosmic rays. VI – A three-dimensional model including diffusion," Astrophys. J. **265**, 573–581.

KRAEMER, S.M., KRONENBERG, A., UENO, A. and WALDREN, C.A. (2000). "Measuring the spectrum of mutation induced by nitrogen ions and protons in the human-hamster hybrid cell line A(L)C," Radiat. Res. **153**, 743–751.

KRAFT, L.M. and COX, A.B. (1986). "Morphometric studies of heavy ion damage in the brains of rodents," Adv. Space Res. **6**, 251–256.

KRAFT, L.M., KELLY, M.A., JOHNSON, J.E., JR., BENTON, E.V., HENKE, R.P., CASSOU, R., HAYMAKER, W., PHILPOTT, D.E., VOGEL, F.S. and ZEMAN, W. (1979). "Effects of high-LET neon (^{20}Ne) particle radiation on the brain, eyes and other head structures of the pocket mouse: A histological study," Int. J. Radiat. Biol. Relat. Stud. Phys. Chem. Med. **35**, 33–61.

KRAMER, S., SOUTHARD, M.E. and MANSFIELD, C.M. (1972). "Radiation effects and tolerance of the central nervous system," pages 332 to 345 in *Radiation Effects and Tolerance, Normal Tissue, Volume 6, Frontiers of Radiation Therapy and Oncology*, Vaeth, J.M., Meyer, J.L. and Hinkelbein, W., Eds. (Karger Publishing, San Francisco).

KRIKORIAN, A.D., LEVINE, H.G., KANN, R.P. and O'CONNER, S.A. (1992). "Effects of spaceflight on growth and cell division in higher plants," in *Advances in Space Biology and Medicine, Volume 2* Bonting, S.L., Ed. (Elsevier, New York).

KRONENBERG, A. (1991). "Perspectives on fast-neutron mutagenesis of human lymphoblastoid cells," Radiat. Res. **128** (Suppl. 1), S87–S93.

KRONENBERG, A. (1994). "Mutation induction in human lymphoid cells by energetic heavy ions," Adv. Space Res. **14**, 339–346.

KRONENBERG, A. and LITTLE, J.B. (1989a). "Locus specificity for mutation induction in human cells exposed to accelerated heavy ions," Int. J. Radiat. Biol. **55**, 913–924.

KRONENBERG, A. and LITTLE, J.B. (1989b). "Molecular characterization of thymidine kinase mutants of human cells induced by densely ionizing radiation," Mutat. Res. **211**, 215–224.

KRONENBERG, A., GAUNY, S., CRIDDLE, K., VANNAIS, D., UENO, A., KRAEMER, S. and WALDREN, C.A. (1995). "Heavy ion mutagenesis: Linear energy transfer effects and genetic linkage," Radiat. Environ. Biophys. **34**, 73–78.

KRUSE, J.J., STROOTMAN, E.G., BART, C.I., VISSER, A., LEER, J.W. and WONDERGEM, J. (2002). "Radiation-induced changes in gene expression and distribution of atrial natriuretic peptide (ANP) in different anatomical regions of the rat heart," Int. J. Radiat. Biol. **78**, 297–304.

KUNOW, H. (1994). "Angular distributions of energetic charged particles observed with the HELIOS-1 and -2 between 0.3 and 1 AU and their relevance to manned interplanetary space missions," Adv. Space Res. **14**, 599–610.

KURT, V. and NYMMIK, R.A. (1997). "Distribution of solar cosmic ray events over proton fluences," Cosmic Res. **35**, 559–569.

KUSUNOKI, Y., HAYASHI, T., MORISHITA, Y., YAMAOKA, M., MAKI, M., BEAN, M.A., KYOIZUMI, S., HAKODA, M. and KODAMA, K. (2001). "T-cell responses to mitogens in atomic bomb survivors: A decreased capacity to produce interleukin 2 characterizes the T cells of heavily irradiated individuals," Radiat. Res. **155**, 81–88.

KUSUNOKI, Y., HIRAI, Y., HAKODA, M. and KYOIZUMI, S. (2002a). "Uneven distributions of naive and memory T cells in the CD4 and CD8 T-cell populations derived from a single stem cell in an atomic bomb survivor: Implications for the origins of the memory T-cell pools in adulthood," Radiat. Res. **157**, 493–499.

KUSUNOKI, Y., YAMAOKA, M., KASAGI, F., HAYASHI, T., KOYAMA, K., KODAMA, K., MACPHEE, D.G. and KYOIZUMI, S. (2002b). "T cells of atomic bomb survivors respond poorly to stimulation by Staphylococcus aureus toxins *in vitro*: Does this stem from their peripheral lymphocyte populations having a diminished naive CD4 T-cell content?" Radiat. Res. **158**, 715–724.

KUZMENOK, O., POTAPNEV, M., POTAPOVA, S., SMOLNIKOVA, V., RZHEUTSKY, V., YARILIN, A.A., SAVINO, W. and BELYAKOV, I.M. (2003). "Late effects of the Chernobyl radiation accident on T cell-mediated immunity in cleanup workers," Radiat. Res. **159**, 109–116.

LAND, C.E. (1988). "New understanding from epidemiology—the next 25 years," Health Phys. **55**, 269–278.

LAND, C.E. (2002). "Uncertainty, low-dose extrapolation and the threshold hypothesis," J. Radiat. Prot. **22**, A129–A135.

LAND, C.E. and SINCLAIR, W.K. (1991). "The relative contributions of different organ sites to the total cancer mortality associated with low-dose radiation exposure," pages 31 to 57 in *Risks Associated With Ionising Radiations*, Ann. ICRP **22**(1) (Elsevier Science, New York).

LAND, C.E., BOICE, J.D., JR., SHORE, R.E., NORMAN, J.E. and TOKUNAGA, M. (1980). "Breast cancer risk from low-dose exposure to ionizing radiation: Results of parallel analysis of three exposed populations of women," J. Natl. Cancer Inst. **65**, 353–376.

LAND, C.E., TOKUNAGA, M., KOYAMA, K., SODA, M., PRESTON, D.L., NISHIMORI, I. and TOKUOKA, S. (2003a). "Incidence of female breast cancer among atomic bomb survivors, Hiroshima and Nagasaki, 1950–1990," Radiat Res. **160**, 707–717.

LAND, C.E., GILBERT, E., SMITH, J., HOFFMAN, F.O., APOSTOIAE, I., THOMAS, B. and KOCHER, D. (2003b). *Report of the NCI-CDC Working Group to Revise the 1985 NIH Radioepidemiological Tables*,

NIH Publication No. 03-5387 (U.S. Department of Health and Human Services, Washington).

LANDOLT, R., ARN, D., BLATTMANN, H., CORDT, I. and FRITZ-NIGGLI, H. (1979). "Effect of negative pi mesons on vascular permeability of brain in neonatal rats," Radiat. Environ. Biophys. **16**, 303–308.

LANGNER, I., BLETTNER, M., GUNDESTRUP, M., STORM, H., ASPHOLM, R., AUVINEN, A., PUKKALA, E., HAMMER, G.P., ZEEB, H., HRAFNKELSSON, J., RAFNSSON, V., TULINIUS, H., DE ANGELIS, G., VERDECCHIA, A., HALDORSEN, T., TVETEN, U., ELIASCH, H., HAMMAR, N. and LINNERSJO, A. (2004). "Cosmic radiation and cancer mortality among airline pilots: Results from a European cohort study (ESCAPE)," Radiat. Environ. Biophys. **42**, 247–256.

LAPERRE, J. and GAMBICHLER, T. (2003). "Sun protection offered by fabrics: On the relation between effective doses based on different action spectra," Photodermatol. Photoimmunol. Photomed. **19**, 11–16.

LAPORTE, D. and DELAYE, M. (1987). "Neutron scattering by calf lens cytoplasm. A comparison between two models of cataract," Eur. Biophys. J. **14**, 441–447.

LARIO, D., SANAHUJA, B. and HERAS, A.M. (1998). "Energetic particle events: Efficiency of interplanetary shocks as 50 keV < E < 100 MeV proton accelerators," Astrophys. J. **509**, 415 – 434.

LASS, J., TUULIK, V., FERENETS, R., RIISALO, R. and HINRIKUS, H. (2002). "Effects of 7 Hz-modulated 450 MHz electromagnetic radiation on human performance in visual memory tasks," Int. J Radiat. Biol. **78**, 937–944.

LAVIN, M.F. and SHILOH, Y. (1999). "Primary immunodeficency diseases, a molecular and genetic approach," pages 306 to 323 in *Ataxia-Telangiectasia (A-T),* Ochs, H.D., Smith, E. and Puck, J.M., Eds. (Oxford University Press, London).

LECCIA, M.T., RICHARD, M.J., FAVIER, A. and BEANI, J.C. (1999). "Zinc protects against ultraviolet A1-induced DNA damage and apoptosis in cultured human fibroblasts," Biol. Trace Elem. Res. **69**, 177–190.

LEE, M.A. (1983). "Coupled hydromagnetic wave excitations and ion acceleration at interplanetary shock waves," J. Geophys. Res. **88**, 6109–6119.

LEE, M.A. (1992). "Particle acceleration in the heliosphere," pages 27 to 44 in *Particle Acceleration in Cosmic Plasmas*, AIP Conference Proceedings, Volume 264, Zank, G.P. and Gaisser, T.K., Eds. (American Institute of Physics, New York).

LEE, M.A. (1999). "Particle acceleration and transport in CME-driven shocks," pages 227 to 234 in *Coronal Mass Ejections,* AGU Monograph 99, Crooker, N. *ET AL*., Eds. (AGU Press, Washington).

LEE, M.A. and RYAN, J.M. (1986). "Time-dependant coronal shock acceleration of energetic solar flare particles," Astrophys. J. **303**, 829–842.

LEITH, J.T., LEWINSKY, B.S., WOODRUFF, K.H., SCHILLING, W.A. and LYMAN, J.T. (1975a). "Tolerance of the spinal cord of rats to irradiation with cyclotron-accelerated helium ions," Cancer **35**, 1692–1700.

LEITH, J.T., WOODRUFF, K.H., LEWINSKY, B.S., LYMAN, J.T. and TOBIAS, C.A. (1975b). "Letter: Tolerance of the spinal cord of rats to irradiation with neon ions," Int. J. Radiat. Biol. Relat. Stud. Phys. Chem. Med. **28**, 393–398.

LEITH, J.T., SCHILLING, W.A., LYMAN, J.T. and HOWARD, J. (1975c). "Comparison of skin responses of mice after single or fractionated exposure to cyclotron-accelerated helium ions and 230 kV x-irradiation," Radiat. Res. **62**, 195–215.

LEITH, J.T., WOODRUFF, K.H. and LYMAN, J.T. (1976). "Early effects of single doses of 375 MeV/nucleon ^{20}neon ions on the skin of mice and hamsters," Radiat. Res. **65**, 440–450.

LEITH, J.T., WOODRUFF, K.H., HOWARD, J., LYMAN, J.T., SMITH, P. and LEWINSKY, B.S. (1977). "Early and late effects of accelerated charged particles on normal tissues," Int. J Radiat. Oncol. Biol. Phys. **3**, 103–108.

LEITH, J.T., DEWYNGAERT, J.K. and GLICKSMAN, A.S. (1981a). "Radiation myelopathy in the rat: An interpretation of dose effect relationships," Int. J. Radiat. Oncol. Biol. Phys. **7**, 1673–1677.

LEITH, J.T., POWERS-RISIUS, P., WOODRUFF, K.H., MCDONALD, M. and HOWARD, J. (1981b). "Response of the skin of hamsters to fractionated irradiation with x rays or accelerated carbon ions," Radiat. Res. **88**, 565–576.

LEITH, J.T., MCDONALD, M., POWERS-RISIUS, P., BLIVEN, S.F. and HOWARD, J. (1982a). "Response of rat spinal cord to single and fractionated doses of accelerated heavy ions," Radiat. Res. **89**, 176–193.

LEITH, J.T., MCDONALD, M. and HOWARD, J. (1982b). "Residual skin damage in rats 1 year after exposure to x rays or accelerated heavy ions," Radiat. Res. **89**, 209–213.

LENARCZYK, M., UENO, A., VANNAIS, D.B., KRAEMER, S., KRONENBERG, A., ROBERTS, J.C., TATSUMI, K., HEI, T.K. and WALDREN, C.A. (2003). "The "pro-drug" Rib-Cys decreases the mutagenicity of high-LET radiation in cultured mammalian cells," Radiat. Res. **160**, 579–583.

LEONARD, A., LEONARD, E.D., GERBER, G.B., CRUTZEN-FAYT, M.C., RICHARD, F., GUEULETTE, J.G. and AKHMATULLINA, N.B. (1998). "No evidence for radiation-induced clastogenic factors after *in vitro* or *in vivo* exposure of human blood," Mutat. Res. **420**, 33–36.

LE ROUX, J.A. and POTGIETER, M.S. (1990). "A time-dependent drift model for the long-term modulation of cosmic rays with special reference to asymmetries with respect to the solar minimum of 1987," Astrophys. J. **361**, 275–282.

LETT, J.T., COX, A.B., KENG, P.C., LEE, A.C., SU, C.M. and BERGTOLD, D.S. (1980). "Late degeneration in rabbit tissues after irradiation by heavy ions," Life Sci. Space Res. **18**, 131–142.

LETT, J.T., KENG, P.C., BERGTOLD, D.S. and HOWARD, J. (1987). "Effects of heavy ions on rabbit tissues: Induction of DNA strand breaks in retinal photoreceptor cells by high doses of radiation," Radiat. Environ. Biophys. **26**, 23–26.

LETT, J.T., LEE, A.C. and COX, A.B. (1991). "Late cataractogenesis in rhesus monkeys irradiated with protons and radiogenic cataract in other species," Radiat. Res. **126**, 147–156.

LEVIN, L.A., GRAGOUDAS, E.S. and LESSELL, S. (2000). "Endothelial cell loss in irradiated optic nerves," Ophthalmology **107**, 370–374.

LEVY, R.P., FABRIKANT, J.I., FRANKEL, K.A., PHILLIPS, M.H. and LYMAN, J.T. (1989). "Stereotactic heavy-charged-particle Bragg peak radiosurgery for the treatment of intracranial arteriovenous malformations in childhood and adolescence," Neurosurgery **24**, 841–852.

LEVY, R.P., FABRIKANT, J.I., FRANKEL, K.A., PHILLIPS, M.H. and LYMAN, J.T. (1990). "Charged-particle radiosurgery of the brain," Neurosurg. Clin. N. Am. **1**, 955–990.

LEVY, R.P., FABRIKANT, J.I., LYMAN, J.T., FRANKEL, K.A., PHILLIPS, M.H., LAWRENCE, J.H. and TOBIAS, C.A. (1992). "Clinical results of stereotactic heavy-charged particle radiosurgery of the pituitary gland," pages 149 to 154 in *Radiosurgery: Baseline and Trends*, Steiner, L., Ed. (Raven Press, New York).

LI, C.Y. and SUNG, F.C. (2003). "Association between occupational exposure to power frequency electromagnetic fields and amyotrophic lateral sclerosis: A review," Am. J. Int. Med. **43**, 212–220.

LI, C.Y., SUNG, F.C. and WU, S.C. (2002). "Risk of cognitive impairment in relation to elevated exposure to electromagnetic fields," J. Occup. Environ. Med. **44**, 66–72.

LIBERTIN, C.R., PANOZZO, J., GROH, K.R., CHANG-LIU, C.M., SCHRECK, S. and WOLOSCHAK, G.E. (1994). "Effects of gamma rays, ultraviolet radiation, sunlight, microwaves and electromagnetic fields on gene expression mediated by human immunodeficiency virus promoter," Radiat. Res. **140**, 91–96.

LIMOLI, C.L., CORCORAN, J.J., MILLIGAN, J.R., WARD, J.F. and MORGAN, W.F. (1999). "Critical target and dose and dose-rate responses for the induction of chromosomal instability by ionizing radiation," Radiat. Res. **151**, 677–685.

LIMOLI, C.L., PONNAIYA, B., CORCORAN, J.J., GIEDZINSKI, E. and MORGAN, W.F. (2000a). "Chromosomal instability induced by heavy ion irradiation," Int. J. Radiat. Biol. **76**, 1599–1606.

LIMOLI, C.L., PONNAIYA, B., CORCORAN, J.J., GIEDZINSKI, E., KAPLAN, M.I., HARTMANN, A. and MORGAN, W.F. (2000b). "Genomic instability induced by high and low LET ionizing radiation," Adv. Space Res. **25**, 2107–2117.

LIMOLI, C.L., GIEDZINSKI, E., ROLA, R., OTSUKA, S., PALMER, T.D. and FIKE, J.R. (2004). "Radiation response of neural precursor cells: Linking cellular sensitivity to cell cycle checkpoints, apoptosis and oxidative stress," Radiat. Res. **161**, 17–27.

LIMOUSE, M., MANIE, S., KONSTANTINOVA, I., FERRUA, B. and SCHAFFAR, L. (1991). "Inhibition of phorbol ester-induced cell activation in microgravity," Exp. Cell Res. **197**, 82–86.

LINFOOT, J.A. (1979). "Heavy ion therapy: Alpha particle therapy of pituitary tumors," pages 245 to 267 in *Recent Advances in the Diagnosis and Treatment of Pituitary Tumors*, Linfoot, J.A., Ed. (Raven Press, New York).

LINGENFELTER, R.E. and HUDSON, H.S. (1980). "Solar particle fluxes and the ancient sun," pages 69 to 79 in *The Ancient Sun*, Pepin, R.O., Eddy, J.E. and Merrill, R.B., Eds. (Pergamon Press, New York).

LINGENFELTER, R.E. and RAMATY, R. (1970). "Astrophysical and geophysical variations in C14 production," pages 513 to 537 in *Proceedings of the 12th Nobel Symposium on Radiocarbon Variations and Absolute Chronology*, Olsson, I.U., Ed. (John Wiley and Sons, New York).

LIPETZ, L.E. (1955). "Electrophysiology of the x-ray phosphene," Radiat. Res. **2**, 306–329.

LITTLE, J.B. (1998). "Radiation-induced genomic instability," Int. J. Radiat. Biol. **74**, 663–671.

LITTLE, J.B. (2003a). "Genomic instability and bystander effects: A historical perspective," Oncogene **22**, 6978–6987.

LITTLE, J.B. (2003b). "Genomic instability and radiation," J. Radiol. Prot. **23**, 173–181.

LITTLE, J.B., NAGASAWA, H., PFENNING, T. and VETROVS, H. (1997). "Radiation-induced genomic instability: Delayed mutagenic and cytogenetic effects of x rays and alpha particles," Radiat. Res. **148**, 299–307.

LITTLEFIELD, L.G., TRAVIS, L.B., SAYER, A.M., VOELZ, G.L. JENSEN, R.H. and BOICE, J.D., JR. (1997). "Cumulative genetic damage in hematopoietic stem cells in a patient with a 40-year exposure to alpha particles emitted by thorium dioxide," Radiat. Res. **148**, 135–144.

LO, E.H. and FABRIKANT, J.I. (1991). "Delayed biologic reactions to stereotactic charged-particle radiosurgery in the human brain," Stereotact. Funct. Neurosurg. **56**, 197–212.

LO, E.H., FRANKEL, K.A., DELAPAZ, R.L., POLJAK, A., WOODRUFF, K.H., BRENNAN, K.M., PHILLIPS, M.H., VALK, P.E., STEINBERG, G.K. and FABRIKANT, J.I. (1989). "Cerebrovascular and metabolic perturbations in delayed heavy charged particle radiation injury," Brain Res. **504**, 168–172.

LO, E.H., DELAPAZ, R.L., FRANKEL, K.A., POLJAK, A., PHILLIPS, M.H., BRENNAN, K.M., WOODRUF, K.H., VALK, P.E., STEINBERG, G.K. and FABRIKANT, J.I. (1991a). "MRI, and PET of delayed

heavy-ion radiation injury in the rabbit brain," Int. J. Radiat. Oncol. Biol. Phys. **20**, 689–696.

LO, E.H., FABRIKANT, J.I., LEVY, R.P., PHILLIPS, M.H., FRANKEL, K.A. and ALPEN, E.L. (1991b). "An experimental compartmental flow model for assessing the hemodynamic response of intracranial arteriovenous malformations to stereotactic radiosurgery," Neurosurgery **28**, 251–259.

LO, E.H., FRANKEL, K.A., STEINBERG, G.K., DELAPAZ, R.L. and FABRIKANT, J.I. (1992). "High-dose single-fraction brain irradiation: MRI, cerebral blood flow, electrophysiological, and histological studies," Int. J. Radiat. Oncol. Biol. Phys. **22**, 47–55.

LOBRICH, M., COOPER, P.K. and RYDBERG, B. (1996). "Non-random distribution of DNA double-strand breaks induced by particle irradiation," Int. J. Radiat. Biol. **70**, 493–503.

LOCKHART, L.H. (1977). "Cytogenetic studies of blood (Experiment M111)," pages 217 to 220 in *Biomedical Results from Skylab*, Johnston, R.S. and Dietlein, L.F., Eds., NASA SP-377 (NASA Center for Aero-Space Information, Hanover, Maryland).

LONGNECKER, D.E., MANNING, F.J. and WORTH, M.H., Eds. (2004). *Review of NASA's Longitudinal Study of Astronaut Health*, Committee on the Longitudinal Study of Astronaut Health, Institute of Medicine (National Academies Press, Washington).

LORIMORE, S.A., KADHIM, M.A., POCOCK, D.A., PAPWORTH, D., STEVENS, D.L., GOODHEAD, D.T. and WRIGHT, E.G. (1998). "Chromosomal instability in the descendants of unirradiated surviving cells after alpha-particle irradiation," Proc. Natl. Acad. Sci. USA **95**, 5730–5733.

LOUCAS, B.D., EBERLE, R.L., DURANTE, M. and CORNFORTH, M.N. (2004). "Complex chromatid-isochromatid exchanges following irradiation with heavy ions?" Cytogenet. Genome Res. **104**, 206–210.

LOWENSTEIN, D.I. (2001). "BNL accelerator-based radiobiology facilities," Phys. Med. **17** (Suppl. 1), 26–29.

MACHLIN, L.J. and BENDICH, A. (1987). "Free radical tissue damage: Protective role of autioxidant nutrients," FASEB J. **1**, 441–445.

MADER, T.H., KOCH, D.D., MANUEL, K., GIBSON, C.R., EFFENHAUSER, R.K. and MUSGRAVE, S. (1999). "Stability of vision during space flight in an astronaut with bilateral intraocular lenses," Am. J. Ophthalmol. **127**, 342–343.

MAMOON, A.M. (1970). *Effects of Ionizing Radiations on Myelin Formation in Rat Brain Cultures*, Ph.D. Thesis (University of California, Berkeley, California).

MANLEY, N.B. (1988). *Cell and Tissue Kinetics of the Subependymal Layer in Mouse Brain Following Heavy Charged Particle Irradiation*, Ph.D. Thesis (University of California, Berkeley).

MANTI, L., JAMALI, M., PRISE, K.M., MICHAEL, B.D. and TROTT, K.R. (1997). "Genomic instability in Chinese hamster cells after exposure to

x rays or alpha particles of different mean linear energy transfer," Radiat. Res. **147**, 22–28.

MAO, X.W., ARCHAMBEAU, J.O., KUBINOVA, L., BOYLE, S., PETERSEN, G. and GROVE, R. (2003). "Quantification of rat retinal growth and vascular population changes after single and split doses of proton irradiation: Translational study using stereology methods," Radiat Res. **160**, 5–13.

MARPLES, B., ADOMAT, H., KOCH, C.J. and SKOV, K.A. (1996). "Response of V79 cells to low doses of x-rays and negative pi-mesons: Clonogenic survival and DNA strand breaks," Int. J. Radiat. Biol. **70**, 429–436.

MARTINS, M.B., SABATIER, L., RICOUL, M., PINTON, A. and DUTRIL-LAUX, B. (1993). "Specific chromosome instability induced by heavy ions: A step towards transformation of human fibroblasts?" Mutat. Res. **285**, 229–237.

MASON, G.M. (1987). "The composition of galactic cosmic rays and solar energetic particles," Rev. Geophys. **25**, 685–696.

MASUMURA, K., KUNIYA, K., KUROBE, T., FUKUOKA, M., YATAGAI, F. and NOHMI, T. (2002). "Heavy-ion-induced mutations in the gpt delta transgenic mouse: Comparison of mutation spectra induced by heavy-ion, x-ray, and gamma-ray radiation," Environ. Mol. Mutagen. **40**, 207–215.

MAUNG, K.M., NORBURY, J.W. and KAHANA, D.E. (1996). "Proportionally off-mass-shell equation for unequal mass systems," J. Phys. G: Nucl. Part. Phys. **22**, 315–320.

MAZUR, J.E., MASON, G.M., KLECKER, B. and MCGUIRE, R.E. (1992). "The energy spectra of solar flare hydrogen, helium, oxygen and iron: Evidence for stochastic acceleration," Astrophys. J. **401**, 398–410.

MCCRACKEN, K.G., DRESCHHOFF, G.A.M., ZELLER, E.J., SMART, D.F. and SHEA, M.A. (2001a). "Solar cosmic ray events for the period 1561–1994: 1. Identification in polar ice, 1561–1950," J. Geophys. Res. **106**, 21585–21598.

MCCRACKEN, K.G., DRESCHHOFF, G.A.M., SMART, D.F. and SHEA, M.A. (2001b). "Solar cosmic ray events for the Period 1561–1994: 2. The Gleissberg periodicity," J. Geophys. Res. **106**, 21599–21609.

MCCRACKEN, K.G., SMART, D.F., SHEA, M.A. and DRESCHHOFF, G.A.M. (2001c). "400 years of large fluence solar proton events," pages 3209 to 3212 in *Proceedings of the 27th International Cosmic Ray Conference* (Copernicus Publications, Kattenburg-Lindau, Germany).

MCDONALD, F.B., MORAAL, H., REINECKE, J.P.L., LAL, N. and MCGUIRE, R.E. (1992), "The cosmic radiation in the heliosphere at successive solar minima," J. Geophys. Res. **97**, 1557–1570.

MCGALE, P. and DARBY, S.C. (2005). "Low doses of ionizing radiation and circulatory diseases: A systematic review of the published epidemiological evidence," Radiat. Res. **163**, 247–257.

MCGUIRE, R.E. and VON ROSENVINGE, T.T. (1984). "The energy spectra of solar energetic particles," Adv. Space Res. **4**, 117–125.

MCGUIRT, W.F., FEEHS, R.S., BOND, G., STRICKLAND, J.L. and MCKINNEY, W.M. (1992). "Irradiation-induced atherosclerosis: A factor in therapeutic planning," Ann. Otol. Rhinol. Laryngol. **101**, 222–228.

MCKIBBEN, R.B. (1987). "Galactic cosmic rays and anomalous components in the heliosphere," Rev. Geophys. **25**, 711–722.

MCKINLAY, A.F., ALLEN, S.G., COX, R., DIMBYLOW, P.J., MANN, S.M., MUIRHEAD, C.R., SAUNDERS, R.D., SIENKIEWICZ, Z.J., STATHER, J.W. and WAINWRIGHT, P.R. (2004). *Review of the Scientific Evidence for Limiting Exposure to Electromagnetic Fields (0-300 GHz)*, Documents of the NRPB, Volume 15, No. 3 (Health Protection Agency, Chilton, Didcot, Oxon, United Kingdom).

MCNAMARA, M.P., BJORNSTAD, K.A., CHANG, P.Y., CHOU, W., LOCKETT, S.J. and BLAKELY, E.A. (2001). "Modulation of lens cell adhesion molecules by particle beams," Phys. Med. **17** (Suppl. 1), 247–248.

MCNULTY, P.J. (1971). "Light flashes produced in the human eye by extremely relativistic muons," Nature **234**, 110.

MCNULTY, P.J., PEASE, V.P. and BOND, V.P. (1975). "Visual sensations induced by Cerenkov radiation," Science **189**, 453–454.

MCNULTY, P.J., PEASE, V.P. and BOND, V.P. (1976). "Muon-induced visual sensations," J. Opt. Soc. Am. **66**, 49–55.

MCNULTY, P.J., PEASE, V.P. and BOND, V.P. (1978). "Visual phenomena induced by relativistic carbon ions with and without Cerenkov radiation," Science **201**, 341–343.

MECK, J.V., REYES, C.J., PEREZ, S.A., GOLDBERGER, A.L. and ZIEGLER, M.G. (2001). "Marked exacerbation of orthostatic intolerance after long- vs. short-duration spaceflight in veteran astronauts," Psychosom. Med. **63**, 865–873.

MEDVEDOVSKY, C. and WORGUL, B.V. (1991). "Neutron effects on the lens," Radiat. Res. **128** (Suppl. 1), S103–S110.

MEDVEDOVSKY, C., WORGUL, B.V., HUANG, Y., BRENNER, D.J., TAO, F., MILLER, J., ZEITLIN, C. and AINSWORTH, E.J. (1994). "The influence of dose, dose-rate and particle fragmentation on cataract induction by energetic iron ions," Adv. Space Res. **14**, 475–482.

MEECHAM, W.J., CHAR, D.H., KROLL, S., CASTRO, J.R. and BLAKELY, E.A. (1994). "Anterior segment complications after helium ion radiation therapy for uveal melanoma. Radiation cataract," Arch. Ophthalmol. **112**, 197–203.

MEHTA, S.K., KAUR, I., GRIMM, E.A., SMID, C., FEEBACK, D.L. and PIERSON, D.L. (2001). "Decreased non-MHC-restricted (CD56+) killer cell cytotoxicity after spaceflight," J. Appl. Physiol. **91**, 1814–1818.

MEHTA, S.K., COHRS, R.J., FORGHANI, B., ZERBE, G., GILDEN, D.H. and PIERSON, D.L. (2004). "Stress-induced subclinical reactivation of varicella zoster virus in astronauts," J. Med. Virol. **72**, 174–179.

MEIER, M.M., CLARK, D.A., GOULDING, C.A., MCCLELLAND, J.B., MORGAN, G.L., MOSS, E.E. and AMIAN, W.B. (1989). "Differential

neutron production cross sections and neutron yields from stopping-length targets for 113-MeV protons," Nucl. Sci. Eng. **102**, 310–321.

MEIER, M.M., AMIAN, W.B., GOULDING, C.A., MORGAN, G.L. and MOSS, C.E. (1992). "Differential neutron-production cross-sections for 256-MeV protons," Nucl. Sci. Eng. **110**, 289–298.

MEINEKE, V., MOEDE, T., GILBERTZ, K.P., MAYERHOFER, A., RING, J., KOHN, F.M. and VAN BEUNINGEN, D. (2002). "Protein kinase inhibitors modulate time-dependent effects of UV and ionizing irradiation on ICAM-1 expression on human hepatoma cells," Int. J. Radiat. Biol. **78**, 577–583.

MEISTRICH, M.L. and SAMUELS, R.C. (1985). "Reduction in sperm levels after testicular irradiation of the mouse: A comparison with man," Radiat. Res. **102**, 138–147.

MERRIAM, G.R., JR. and FOCHT, E.F. (1957). "A clinical study of radiation cataracts and the relationship to dose," Am. J. Roetgenol. Radium Ther. Nucl. Med. **77**, 759–785.

MERRIAM, G.R., JR., WORGUL, B.V., MEDVEDOVSKY, C., ZAIDER, M. and ROSSI, H.H. (1984). "Accelerated heavy particles and the lens. I. Cataractogenic potential," Radiat. Res. **98**, 129–140.

METTING , N.F., ROSSI, H.H., BRABY, L.A., KLIAUGA, P.J., HOWARD, J., ZAIDER, M., SCHIMMERLING, W., WONG, M. and RAPKIN, M. (1988). "Microdosimetry near the trajectory of high-energy heavy ions," Radiat. Res. **116**, 183–195.

METTLER, F.A. and UPTON, A.C. (1995). *Medical Effects of Ionizing Radiation*, 2nd ed. (W.B. Saunders Company, Philadelphia).

MEWALDT, RA. and STONE, E.C. (1989). "Isotope abundances of solar coronal material derived from solar energetic particle measurements," Astrophys. J. **377**, 959–963.

MEWALDT, R.A., CUMMINGS, A.C., ADAMS, J.H., JR, EVENSON, P., FILLIUS, W., JOKIPII, J.R., MCKIBBEN, R.G. and ROBINSON, P.A., JR. (1988). "Toward a descriptive model of galactic cosmic rays in the heliopshere," pages 14 to 32 in *Interplanetary Particle Environment*, JPL Publication 88-28, Feynman, J. and Gabriel, S., Eds. (Center for AeroSpace Information, Hanover, Maryland).

MICKLEY, G.A., BOGO, V., LANDAUER, M.R. and MELE, P.C. (1988). "Current trends in behavioral radiobiology," pages 517 to 536 in *Terrestrial Space Radiation and its Biological Effects*, McCormack, P.D., Swenberg, C.E. and Bucher, H., Eds. (Plenum Press, New York).

MILLER, E.S. and SONNENFELD, G. (1993). "Influence of suspension on the expression of protective immunological memory to murine Listeria monocytogenes infection," J. Leukoc. Biol. **54**, 578–583.

MILLER, E.S. and SONNENFELD, G. (1994). "Influence of antiorthostatic suspension on resistance to murine Listeria monocytogenes infection," J. Leukoc. Biol. **55**, 371–378.

MILLER, T.M. and TOWNSEND, L.W. (2004a). "Double-differential light-ion production cross sections," Radiat. Prot. Dosim. **110**, 57–60.

MILLER, T.M. and TOWNSEND, L.W. (2004b). "Double-differential heavy-ion production cross sections," Radiat. Prot. Dosim. **110**, 53–56.

MILLER, T.M. and TOWNSEND, L.W. (2005). "Comprehensive cross-section database development for generalized three-dimensional radiation transport codes: A status report," Nucl. Sci. Engineering **149**, 65–73.

MILLS, P.J., MECK, J.V.,WATERS, W.W., D'AUNNO, D. and ZIEGLER, M.G. (2001). "Peripheral leukocyte subpopulations and catecholamine levels in astronauts as a function of mission duration," Psychosom. Med. **63**, 886–890.

MITANI, K., HORII, A. and KUBO, T. (2004). "Impaired spatial learning after hypergravity exposure in rats," Brain Res. Cogn. Brain Res. **22**, 94–100.

MIZUMATSU, S., MONJE, M.L., MORHARDT, D.R., ROLA, R., PALMER, T.D. and FIKE, J.R. (2003). "Extreme sensitivity of adult neurogenesis to low doses of x-irradiation," Cancer Res. **63**, 4021–4027.

MOHAN, A.K., HAUPTMANN, M., FREEDMAN, D.M., RON, E., MATANOSKI, G.M., LUBIN, J.H., ALEXANDER, B.H., BOICE, J.D., JR., DOODY, M.M. and LINET, M.S. (2003). "Cancer and other causes of mortality among radiologic technologists in the United States," Int. J. Cancer **103**, 259–267

MOISON, R.M., DOERGA, R., BEIJERSBERGEN, M.J. and VAN HENEGOUWEN, G. (2002). "Increased antioxidant potential of combined topical vitamin E and C against lipid peroxidation of eicosapentaenoic acid in pig skin induced by simulated solar radiation," Int. J. Radiat. Biol. **78**, 1185–1193.

MONOD, J., CHANGEUX, J.P. and JACOB, F. (1963). "Allosteric proteins and cellular control systems," J. Mol. Biol. **6**, 306–329.

MONJE, M.L. and PALMER, T. (2003). "Radiation injury and neurogenesis," Curr. Opin. Neurol. **16**, 129–134.

MONJE, M.L., TODA, H. and PALMER, T.D. (2003). "Inflammatory blockade restores adult hippocampal neurogenesis," Science **302**, 1760–1765.

MOOLGAVKAR, S.H. (1991). "Carcinogenesis models: An overview," Basic Life Sci. **58**, 387–396.

MOOTERI, S.N., PODOLSKI, J.L., DRAB, E.A., SACLARIDES, T.J., ONODA, J.M., KANTAK, S.S. and RUBIN, D.B. (1996). "WR-1065 and radioprotection of vascular endothelial cells. II. Morphology," Radiat. Res. **145**, 217–224.

MOREY, E.R., SABELMAN, E.E., TURNER, R.T. and BAYLINK, D.J. (1979). "A new rat model simulating some aspects of space flight," Physiologist **22**, S23–S24.

MORGAN, W.F. (2003). "Non-targeted and delayed effects of exposure to ionizing radiation: II. Radiation-induced genomic instability and bystander effects *in vivo*, clastogenic factors and transgenerational effects," Radiat. Res. **159**, 581–596.

MORGAN, W.F., HARTMANN, A., LIMOLI, C.L., NAGAR, S. and PONNAIYA, B. (2002). "Bystander effects in radiation-induced genomic instability," Mutat. Res. **504**, 91–100.

MORITA, Y., PEREZ, G.I., PARIS, F., MIRANDA, S.R., EHLEITER, D., HAIMOVITZ-FRIEDMAN, A., FUKS, Z., XIE, Z., REED, J.C., SCHUCHMAN, E.H., KOLESNICK, R.N. and TILLY, J.L. (2000). "Oocyte apoptosis is suppressed by disruption of the acid sphingomyelinase gene or by sphingosine-1-phosphate therapy," Nat. Med. **6**, 1109–1114.

MOTHERSILL, C. and SEYMOUR, C. (1997a). "Medium from irradiated human epithelial cells but not human fibroblasts reduces the clongenic survival of unirradiated cells," Int. J. Radiat. Biol. **71**, 421–427.

MOTHERSILL, C. and SEYMOUR, C. (1997b). "Survival of human epithelial cells irradiated with cobalt 60 as microcolonies or single cells," Int. J. Radiat. Biol. **72**, 597–606.

MOTHERSILL, C. and SEYMOUR, C.B. (1998). "Cell-cell contact during gamma irradiation is not required to induce a bystander effect in normal human keratinocytes: Evidence for release during irradiation of a signal controlling survival into the medium," Radiat. Res. **149**, 256–262.

MOTHERSILL, C. and SEYMOUR, C.B. (2000). "Genomic instability, bystander effects and radiation risks: Implications for development of protection strategies for man and the environment," Radiat. Biol. Radioecol. **40**, 615–620.

MOTHERSILL, C., SEYMOUR, C.B. and JOINER, M.C. (2002). "Relationship between radiation-induced low-dose hypersensitivity and the bystander effect," Radiat. Res. **157**, 526–532.

MOULDER, J.E., ERDRICH, L.S., MALYAPA, R.S., MERRITT, J., PICKARD, W.F. and WIJAYALAXMI. (1999). "Cell phones and cancer: What is the evidence for a connection?" Radiat. Res. **151**, 513–531.

MUEGGE, K., YOUNG, H., RUSCETTI, F. and MIKOVITS, J. (2003). "Epigenetic control during lymphoid development and immune responses: Aberrant regulation, viruses, and cancer," Ann. N.Y. Acad. Sci. **983**, 55–70.

MUSTONEN, R., LINDHOLM, C., TAWN, E.J., SABATIER, L. and SALOMAA, S. (1998). "The incidence of cytogenetically abnormal rogue cells in peripheral blood," Int. J. Radiat. Biol. **74**, 781–785.

NAGANO, J., KONO, S., PRESTON, D.L., MORIWAKI, H., SHARP, G.B., KOYAMA, K. and MABUCHI, K. (2000). "Bladder-cancer incidence in relation to vegetable and fruit consumption: A prospective study of atomic-bomb survivors," Int. J. Cancer **86**, 132–138.

NAGAOKA, S., NAKANO, T., ENDO, S., ONIZUKA, T., KAGAWA, Y., FUJITAKA, K., OHNISHI, K., TAKAHASHI, A. and OHNISHI, T. (1999). "Detection of DNA damages and repair in human culture cells with simulated space radiation," Acta Astronaut **44**, 561–567.

NAGAR, S., SMITH, L.E. and MORGAN, W.F. (2003). "Characterization of a novel epigenetic effect of ionizing radiation: The death-inducing effect," Cancer Res. **63**, 324–328.

NAGASAWA, H. and LITTLE, J.B. (1992). "Induction of sister chromatid exchanges by extremely low doses of alpha-particles," Cancer Res. **52**, 6394–6396.

NAGASAWA, H. and LITTLE, J.B. (1999). "Unexpected sensitivity to the induction of mutations by very low doses of alpha-particle radiation: Evidence for a bystander effect," Radiat. Res. **152**, 552–557.

NARAYANAN, P.K., GOODWIN, E.H. and LEHNERT, B.E. (1997). "Alpha particles initiate biological production of superoxide anions and hydrogen peroxide in human cells," Cancer Res. **57**, 3963–3971.

NARICI, L., BIDOLI, V., CASOLINO, M., DE PASCALE, M.P., FURANO, G., MORSELLI, A., PICOZZA, P., REALI, E., SPARVOLI, R., LICOCCIA, S., ROMAGNOLI, P., TRAVERSA, E., SANNITA, W.G., LOIZZO, A., GALPER, A., KHODAROVICH, A., KOROTKOV, M.G., POPOV, A., VAVILOV, N., AVDEEV, S., SALNITSKII, V.P., SHEVCHENKO, O.I., PETROV, V.P., TRUKHANOV, K.A., BOEZIO, M., BONVICINI, W., VACCHI, A., ZAMPA, N., BATTISTON, R., MAZZENGA, G., RICCI, M., SPILLANTINI, P., CASTELLINI, G., CARLSON, P. and FUGLESANG, C. (2003). "ALTEA: Anomalous long term effects in astronauts. A probe on the influence of cosmic radiation and microgravity on the central nervous system during long flights," Adv. Space Res. **31**, 141–146.

NARICI, L., BELLI, F., BIDOLI, V., CASOLINO, M., DE PASCALE, M.P., DI FINO, L., FURANO, G., MODENA, I., MORSELLI, A., PICOZZA, P., REALI, E., RINALDI, A., RUGGIERI, D., SPARVOLI, R., ZACONTE, V., SANNITA, W.G., CAROZZO, S., LICOCCIA, S., ROMAGNOLI, P., TRAVERSA, E., COTRONEI, V., VAZQUEZ, M.E., MILLER, J., SALNITSKII, V.P., SHEVCHENKO, O.I., PETROV, V.P., TRUKHANOV, K.A., GALPER, A., KHODAROVICH, A., KOROTKOV, M.G., POPOV, A., VAVILOV, N., AVDEEV, S., BOEZIO, M., BONVICINI, W., VACCHI, A., ZAMPA, N., MAZZENGA, G., RICCI, M., SPILLANTINI, P., CASTELLINI, G., VITTORI, R., CARLSON, P., FUGLESANG, C. and SCHARDT, D. (2004). "The ALTEA/ALTEINO projects: Studying functional effects of microgravity and cosmic radiation," Adv. Space Res. **33**, 1352–1357.

NAS/NRC (1973). National Academy of Sciences/National Research Council. *HZE Particle Effects in Manned Space Flight,* Advisory Panel, Committee on Space Medicine, Grahn, D. Ed. (National Academy Press, Washington).

NAS/NRC (1996). National Academy of Sciences/National Research Council. *Radiation Hazards to Crews of Interplanetary Missions*, Task Group on the Biological Effects of Space Radiation, Space Science Board (National Academy Press, Washington).

NAS/NRC (1999). National Academy of Sciences/National Research Council. *Health Effects of Exposure to Radon,* Committee on Health

Risks of Exposure to Radon, Board on Radiation Effects Research (BEIR VI) (National Academy Press, Washington).

NAS/NRC (2006). National Academy of Sciences/National Research Council. *Health Risks from Exposure to Low Levels of Ionizing Radiation: Phase 2,* Committee to Assess Health Risks from Exposure to Low Levels of Ionizing Radiation, Board on Radiation Effects Research (BEIR VII) (National Academy Press, Washington).

NASONOVA, E. and RITTER, S. (2004). "Cytogenetic effects of densely ionising radiation in human lymphocytes: Impact of cell cycle delays," Cytogenet. Genome Res. **104**, 216–220.

NASONOVA, E., GUDOWSKA-NOWAK, E., RITTER, S. and KRAFT, G. (2001). "Analysis of Ar-ion and x-ray-induced chromatin breakage and repair in V79 plateau-phase cells by the premature chromosome condensation technique," Int. J. Radiat. Biol. **77**, 59–70.

NASONOVA, E., FUSSEL, K., BERGER, S., GUDOWSKA-NOWAK, E. and RITTER, S. (2004). "Cell cycle arrest and aberration yield in normal human fibroblasts. I. Effects of x-rays and 195 MeV u^{-1} C ions," Int. J. Radiat. Biol. **80**, 621–634.

NCRP (1980). National Council on Radiation Protection and Measurements. *Influence of Dose and its Distribution in Time on the Dose-Response Relationships for Low-LET Radiations,* NCRP Report No. 64 (National Council on Radiation Protection and Measurements, Bethesda, Maryland).

NCRP (1989). National Council on Radiation Protection and Measurements. *Guidance on Radiation Received in Space Activities,* NCRP Report No. 98 (National Council on Radiation Protection and Measurements, Bethesda, Maryland).

NCRP (1990). National Council on Radiation Protection and Measurements. *The Relative Biological Effectiveness of Radiations of Different Quality*, NCRP Report No. 104 (National Council on Radiation Protection and Measurements, Bethesda, Maryland).

NCRP (1993). National Council on Radiation Protection and Measurements. *Limitation of Exposure to Ionizing Radiation*, NCRP Report No. 116 (National Council on Radiation Protection and Measurements, Bethesda, Maryland).

NCRP (1997). National Council on Radiation Protection and Measurements. *Uncertainties in Fatal Cancer Risk Estimates Used in Radiation Protection*, NCRP Report No. 126 (National Council on Radiation Protection and Measurements, Bethesda, Maryland).

NCRP (2000). National Council on Radiation Protection and Measurements. *Radiation Protection Guidance for Activities in Low-Earth Orbit,* NCRP Report No. 132 (National Council on Radiation Protection and Measurements, Bethesda, Maryland).

NCRP (2001a). National Council on Radiation Protection and Measurements. *Fluence-Based and Microdosimetric Event-Based Methods for Radiation Protection in Space,* NCRP Report No. 137 (National

Council on Radiation Protection and Measurements, Bethesda, Maryland).

NCRP (2001b). National Council on Radiation Protection and Measurements. *Evaluation of the Linear-Nonthreshold Dose-Response Model for Ionizing Radiation,* NCRP Report No. 136 (National Council on Radiation Protection and Measurements, Bethesda, Maryland).

NCRP (2002). National Council on Radiation Protection and Measurements. *Operational Radiation Safety Program for Astronauts in Low-Earth Orbit: A Basic Framework*, NCRP Report No. 142 (National Council on Radiation Protection and Measurements, Bethesda, Maryland).

NCRP (2005). National Council on Radiation Protection and Measurements. *Extrapolation of Radiation-Induced Cancer Risks from Nonhuman Experimental Systems to Humans*, NCRP Report No. 150 (National Council on Radiation Protection and Measurements, Bethesda, Maryland).

NEAL, J.S. and TOWNSEND, L.W. (2001). "Predicting dose-time profiles of solar energetic particle events using Bayesian forecasting methods," IEEE Trans. Nucl. Sci. **48**, 2004–2009.

NEEL, J.V. (1998). "An association, in adult Japanese, between the occurrence of rogue cells among cultured lymphocytes (JC virus activity) and the frequency of "simple" chromosomal damage among the lymphocytes of persons exhibiting these rogue cells," Am. J. Hum. Genet. **63**, 489–497.

NELSON, G.A. and TOFILON, P.J. (2000). *Summary, Introduction, and Charge to the Workshop*, Neuroscience and Radiation Biology Working Group (Universities Space Research Association, Houston, Texas).

NELSON, G.A., SCHUBERT, W.W., KAZARIANS, G.A., RICHARDS, G.F., BENTON, E.V., BENTON, E.R. and HENKE, R. (1994). "Radiation effects in nematodes: Results from IML-1 experiments," Adv. Space Res. **14**, 87–91.

NELSON, G.A., GREEN, L.M., GRIDLEY, D.S., ARCHAMBEAU, J.O. and SLATER, J.M. (2001). "Research activities at the Loma Linda University and Proton Treatment Facility – and overview," Phys. Med. **17** (Suppl. 1), 30–32.

NEUMAYR, A. and THURNHER, B. (1952). "Uber den einfluss lokaler roentgenbestrahlung aud die permeabilitat menschlicher kapillaren," Strahlentherapie **84**, 297.

NEWMAN, H.C., PRISE, K.M., FOLKARD, M. and MICHAEL, B.D. (1997). "DNA double-strand break distributions in x-ray and alpha-particle irradiated V79 cells: Evidence for non-random breakage," Int. J. Radiat. Biol. **71**, 347–363.

NICOGOSSIAN, A.E., HUNTOON, C.L. and POOL, S.L. (1994). *Space Physiology and Medicine* (Lea and Febiger Publishers, Philadelphia).

NIEHS (2002). National Institute of Environmental Health Sciences. *Electric and Magnetic Fields (EMF) Research and Public Information Dissemination (RAPID) Program*, http://www.niehs.nih.gov/emfrapid

(accessed September 2006) (National Institute of Environmental Health Sciences, Research Triangle Park, North Carolina).

NIEMER-TUCKER, M.M., STERK, C.C., DE WOLFF-ROUENDAAL, D., LEE, A.C., LETT, J.T., COX, A., EMMANOUILIDIS-VAN DER SPEK, K., DAVELAAR, J., LAMBOOY, A.C., MOOY, C.M. and BROERSE, J.J. (1999). "Late ophthalmological complications after total body irradiation in non-human primates," Int. J. Radiat. Biol. **75**, 465–472.

NIKJOO, H., UEHARA, S. and BRENNER, D.J. (1997). "Track structure calculations in radiobiology: How can we improve them and what can they do?" pages 3 to 10 in *Microdosimetry: An Interdisciplinary Approach*, Goodhead, D.T., O'Neill, P. and Menzel, H.G., Eds. (Royal Society of Chemistry (Cambridge, United Kingdom).

NIKJOO, H., O'NEILL, P., TERRISSOL, M. and GOODHEAD, D.T. (1999). "Quantitative modelling of DNA damage using Monte Carlo track structure method," Radiat. Environ. Biophys. **38**, 31–38.

NIKJOO, H., KHVOSTUNOV, I.K. and CUCINOTTA, F.A. (2002). "The response of tissue-equivalent proportional counters to heavy ions," Radiat. Res. **157**, 435–445.

NOAA (1993). National Oceanic and Atmospheric Administration. *Products and Services User Guide* (National Oceanic and Atmospheric Administration, U.S. Department of Commerce, Boulder, Colorado).

NOJIMA, K., ANDO, K., FUJIWARA, H. and ANDO, S. (2000). "Effects of carbon ions on primary cultures of mouse brain cells," Adv. Space Res. **25**, 2051–2056.

NOJIMA, K., NAKADAI, T., KOHNO, Y., VAZQUEZ, M.E., YASUDA, N. and NAGAOKA, S. (2004). "Effects of heavy ion on the primary cultures of mouse brain cells," Biol. Sci. Space **18**, 114–115

NOWAK, M.A., KOMAROVA, N.L., SENGUPTA, A., JALLEPALLI, P.V., SHIH, I.M., VOGELSTEIN, B. and LENGAUER, C. (2002). "The role of chromosomal instability in tumor initiation," Proc. Natl. Acad. Sci. USA **99**, 16226–16231.

NUTTING, C., BRADA, M., BRAZIL, L., SIBTAIN, A., SARAN, F., WESTBURY, C., MOORE, A., THOMAS, D.G., TRAISH, D. and ASHLEY, S. (1999). "Radiotherapy in the treatment of benign meningioma of the skull base," J Neurosurg. **90**, 823–827.

NYMMIK, R.A. (1993). "Average energy spectra at peak flux and fluence values in solar cosmic ray events," pages 29 to 32 in *Proceedings of the 23rd International Cosmic Ray Conference* (University of Calgary, Calgary).

NYMMIK, R.A. (1996). "Models describing solar cosmic ray events," Radiat. Meas. **26**, 417–429.

NYMMIK, R.A. (1997). "Space environment (natural and artificial)," in *Probabilistic Model of Fluences and Peak Fluxes in Solar Cosmic Ray*, ISO/AWI 15392 (Moscow State University, Moscow).

NYMMIK, R.A, PANASYUK, M.I., PERVAJA, T.I. and SUSLOV, A.A. (1992), "A model of galactic cosmic ray fluxes," Nucl. Tracks Radiat. Meas. **20**, 427–429.

OBE, G., JOHANNES, I., JOHANNES, C., HALLMAN, K., REITZ, G. and FACIUS, R. (1997). "Chromosomal aberrations in blood lymphocytes of astronauts after long-term space flights," Int. J. Radiat. Biol. **72**, 727–734.

OBE, G., FACIUS, R., REITZ, G., JOHANNES, I. and JOHANNES, C. (1999). "Manned missions to Mars and chromosome damage," Int. J. Radiat. Biol. **75**, 429–433.

OBERDORSTER, G., WHITE, R., RABIN, R., CLARKSON, T., IRONS, R., GARDNER, D., TAYLOR, G.R., SONNENFELD, G. and THOMAS, R. (1994). "Space exploration and toxicology: A new frontier," Fundam. Appl. Toxicol. **22**, 161–171.

OBERHEITMANN, B. (1997). "Whole library-amplification and labelling of human chromosome-specific composite probes for fluorescence *in situ* hybridization (FISH) using PCR," Int. J. Radiat. Biol. **71**, 515–517.

O'BRIEN, K. (2006). "Monte Carlo calculations of spacecraft fluxes," pages 298 to 300 in *14th Biennial Topical Meeting of the Radiation Protection and Shielding Division of the American Nuclear Society* (CD-ROM) (American Nuclear Society, La Grange Park, Illinois).

OGATA, T., TESHIMA, T., KAGAWA, K., HISHIKAWA, Y., TAKAHASHI, Y., KAWAGUCHI, A., SUZUMOTO, Y., NOJIMA, K., FURUSAWA, Y. and MATSUURA, N. (2005). "Particle irradiation suppresses metastatic potential of cancer cells," Cancer Res. **65**, 113–120.

OKADA, S., OKEDA, R., MATSUSHITA, S. and KAWANO, A. (1998). "Histopathological and morphometric study of the late effects of heavy-ion irradiation on the spinal cord of the rat," Radiat. Res. **150**, 304–315.

OLSEN, D.L., BERMAN, B.L., GREINER, D.E., HECKMAN, H.H., LINDSTROM, P.J. and CRAWFORD, H.J. (1983). "Factorization of fragment-production cross sections in relativistic heavy-ion collisions," Phys. Rev. C **28**, 1602–1613.

OMRAN, A.R., SHORE, R.E., MARKOFF, R.A., FRIEDHOFF, A., ALBERT, R.E., BARR, H., DAHLSTROM, W.G. and PASTERNACK, B.S. (1978). "Follow-up study of patients treated by x-ray epilation for tinea capitis: Psychiatric and psychometric evaluation," Am. J. Public Health **68**, 561–567.

O'NEILL, P.M. (2006). "Badhwar-O'Neill galactic cosmic ray model update based on Advanced Composition Explorer (ACE) energy spectra from 1997 to present," Adv. Space Res. **37**, 1727–1733.

OSBORNE, W.Z., PINSKY, L.S. and BAILEY, J.V. (1975). "Apollo light flash investigations," pages 355 to 365 in *Biomedical Results of Apollo,* NASA SP-368, Johnston, R.S., Dietlein, L.F. and Berry, C.A., Eds. (Center for AeroSpace Information, Hanover, Maryland).

OTAKE, M. and SCHULL, W.J. (1990). "Radiation-related posterior lenticular opacities in Hiroshima and Nagasaki atomic bomb survivors based on the DS86 dosimetry system," Radiat. Res. **121**, 3–13.

PADDON-JONES, D., SHEFFIELD-MOORE, M., URBAN, R.J., AARSLAND, A., WOLFE, R.R. and FERRANDO, A.A. (2005). "The catabolic effects of prolonged inactivity and acute hypercortirolemia are offset by dietary supplementation," J. Clin. Endocrinol. Metabl. **90**, 1453–1459.

PAMPFER, S. and STREFFER, C. (1988). "Prenatal death and malformations after irradiation of mouse zygotes with neutrons or x-rays," Teratology **37**, 599–607.

PAMPFER, S., MULLER, W.U. and STREFFER, C. (1992). "Preimplantation growth delay and micronucleus formation after *in vivo* exposure of mouse zygotes to fast neutrons," Radiat. Res. **129**, 88–95.

PAPE, R. and ZAKOVSKY, J. (1954). "The sensitivity of the retina to roentgen rays," Fortschr Geb Rontgenstr Nuklearmed. **80**, 65–71.

PARK, C.C., HENSHALL-POWELL, R.L., ERICKSON, A.C., TALHOUK, R., PARVIN, B., BISSELL, M.J. and BARCELLOS-HOFF, M.H. (2003). "Ionizing radiation induces heritable disruption of epithelial cell interactions," Proc. Natl. Acad. Sci. USA **100**, 10728–10733.

PARKER, E.N. (1965). "The passage of energetic charged particles through the interplanetary space," Planet. Space Sci. **13**, 9–49.

PARSHAD, R., SANFORD, K.K., PRICE, F.M., STEELE, V.E., TARONE, R.E., KELLOFF, G.J. and BOONE, C.W. (1998). "Protective action of plant polyphenols on radiation-induced chromatid breaks in cultured human cells," Anticancer Res. **18**, 3263–3266.

PARSONS, J.L. and TOWNSEND, L.W. (2000). "Interplanetary crew dose rates for the August 1972 solar particle event," Radiat. Res. **153**, 729–733.

PAUNESKU, T., CHANG-LIU, C.M., SHEARIN-JONES, P., WATSON, C., MILTON, J., ORYHON, J., SALBEGO, D., MILOSAVLJEVIC, A. and WOLOSCHAK, G.E. (2000). "Identification of genes regulated by UV/salicylic acid," Int. J. Radiat. Biol. **76**, 189–198.

PECAUT, M.J., NELSON, G.A. and GRIDLEY, D.S. (2001). "Dose and dose rate effects of whole-body gamma-irradiation: I. Lymphocytes and lymphoid organs," In Vivo **15**, 195–208.

PECAUT, M.J., GRIDLEY, D.S., SMITH, A.L. and NELSON, G.A. (2002). "Dose and dose rate effects of whole-body proton-irradiation on lymphocyte blastogenesis and hematological variables: Part II," Immunol. Lett. **80**, 67–73.

PECAUT, M.J., GRIDLEY, D.S. and NELSON, G.A. (2003a). "Long-term effects of low-dose proton radiation on immunity in mice: Shielded vs. Unshielded," Aviat. Space Environ. Med. **74**, 115–124.

PECAUT, M.J., NELSON, G.A., PETERS, L.L., KOSTENUIK, P.J., BATEMAN, T.A., MORONY, S., STODIECK, L.S., LACEY, D.L., SIMSKE, S.J. and GRIDLEY, D.S. (2003b). "Genetic models in applied physiology: Selected contribution: Effects of spaceflight on immunity in the C57BL/6 mouse. I. Immune population distributions," J. Appl. Physiol. **94**, 2085–2094.

PECAUT, M.J., HAERICH, P., MILLER, C.N., SMITH, A.L., ZENDEJAS, E.D. and NELSON, G.A. (2004). "The effects of low-dose, high-LET radiation exposure on three models of behavior in C57BL/6 mice," Radiat. Res. **162**, 148–156.

PECAUT, M.J., DUTTA-ROY, R., SMITH, A.L., JONES, T.A., NELSON, G.A. and GRIDLEY, D.S. (2006). "Acute effects of iron-particle radiation on immunity," *Part I: Population Distributions*, Radiat. Res. **165**, 68–77.

PETERSON, L.E., PEPPER, L.J., HAMM, P.B. and GILBERT, S.L. (1993). "Longitudinal study of astronaut health: Mortality in the years 1959–1991," Radiat. Res. **133**, 257–264.

PHILPOTT, D.E., SAPP, W., MIQUEL, J., KATO, K., CORBETT, R., STEVENSON, J., BLACK, S., LINDSETH, K.A. and BENTON, E.V. (1985). "The effect of high energy (HZE) particle radiation (^{40}Ar) on aging parameters of mouse hippocampus and retina," Scan. Electron Microsc. (Part 3), 1177–1182.

PIERCE, D.A. and PRESTON, D.L. (2000). "Radiation-related cancer risks at low doses among atomic bomb survivors," Radiat. Res. **154**, 178–186.

PIERCE, D.A., SHIMIZU, Y., PRESTON, D.L., VAETH, M. and MABUCHI, K. (1996). "Studies of the mortality of atomic bomb survivors, Report 12, Part I. Cancer: 1950–1990," Radiat. Res. **146**, 1–27.

PINSKY, L.S., OSBORNE, W.Z., BAILEY, J.V., BENSON, R.E and THOMPSON, L.F. (1974). "Light flashes observed by astronauts on Apollo 11 through Apollo 17," Science **183**, 957–959.

PINSKY, L., ANDERSON, V., EMPL, A., LEE, K., SMIRNOV, G., ZAPP, N., FERRARI, A., TSOULOU, K., ROESLER, S., VLACHOUDIS, V., BATTISTONI, G., CAMPANELLA, M., CERUTTI, F., GADIOLI, E., GARZELLI, M.V., MURARO, S., RANCATI, T., SALA, P., BALLARINI, F., OTTOLENGHI, A., PARINI, V., SCANNICCHIO, D., CARBONI, M., PELLICCIONI, M. WILSON, T.N., RANFT, J. and FASSO, A. (2005). "Update on the status of the FLUKA Monte Carlo Transport Code," [online] in the *Proceedings of Conference for Computing in High Energy and Nuclear Physics* (CHEP'04) (European Organization for Nuclear Research, Geneva).

PIRZIO, L.M., FREULET-MARRIERE, M.A., BAI, Y., FOULADI, B., MURNANE, J.P., SABATIER, L. and DESMAZE, C. (2004). "Human fibroblasts expressing htert show remarkable karyotype stability even after exposure to ionizing radiation," Cytogenet. Genome Res. **104**, 87–94.

POTGIETER, M.S. (1995). "The long term modulation of galactic cosmic rays in the heliosphere," Adv. Space Res. **16**(9), 191–203.

POTGIETER, M.S. (1998). "The modulation of galactic cosmic rays in the heliosphere: Theory and models," Space Sci. Rev. **83**, 147–158.

PRASANNA, P.G., KOLANKO, C.J., GERSTENBERG, H.M. and BLAKELY, W.F. (1997). "Premature chromosome condensation assay

for biodosimetry: Studies with fission-neutrons," Health Phys. **72**, 594–600.

PREECE, A.W., IWI, G., DAVIES-SMITH, A., WESNES, K., BUTLER, S., LIM, E. and VAREY, A. (1999). "Effect of a 915-MHz simulated mobile phone signal on cognitive function in man," Int. J. Radiat. Biol. **75**, 447–456.

PREKEGES, J.L. (2003). "Radiation hormesis, or, could all that radiation be good for us?" J. Nucl. Med. Technol. **31**, 11–17.

PRESTON, D.L., KUSUMI, S., TOMONAGA, M., IZUMI, S., RON, E., KURAMOTO, A., KAMADA, N., DOHY, H., MATSUO, T., NONAKA, H., THOMPSON, D.E., SODA, M. and MABUCHI, K. (1994). "Cancer incidence in atomic bomb survivors. Part III. Leukemia, lymphoma and multiple myeloma, 1950–1987," Radiat. Res. **137** (Suppl. 2), S68–S97.

PRESTON, D.L., SHIMIZU, Y., PIERCE, D.A., SUYAMA, A. and MABUCHI, K. (2003). "Studies of mortality of atomic bomb survivors. Report 13: Solid cancer and noncancer disease mortality: 1950–1997," Radiat. Res. **160**, 381–407.

PRESTON, D.L., PIERCE, D.A., SHIMIZU, Y., CULLINGS, H.M., FUJITA, S., FUNAMOTO, S. and KODAMA, K. (2004). "Effect of recent changes in atomic bomb survivor dosimetry on cancer mortality risk estimates," Radiat. Res. **162**, 377–389.

PRISE, K.M., BELYAKOV, O.V., FOLKARD, M. and MICHAEL, B.D. (1998a). "Studies of bystander effects in human fibroblasts using a charged particle microbeam," Int. J. Radiat. Biol. **74**, 793–798.

PRISE, K.M., AHNSTROM, G., BELLI, M., CARLSSON, J., FRANKENBERG, D., KIEFER, J., LOBRICH, M., MICHAEL, B.D., NYGREN, J., SIMONE, G. and STENERLOW, B. (1998b). "A review of DSB induction data for varying quality radiations," Int. J. Radiat. Biol. **74**, 173–184.

PROSS, H.D., KOST, M. and KIEFER, J. (1994). "Repair of radiation induced genetic damage under microgravity," Adv. Space Res. **14**, 125–130.

RABER, J., ROLA, R., LEFEVOUR, A., MORHARDT, D., CURLEY, J., MIZUMATSU, S., VANDENBERG, S.R. and FIKE, J.R. (2004). "Radiation-induced cognitive impairments are associated with changes in indicators of hippocampal neurogenesis," Radiat. Res. **162**, 39–47.

RABIN, B.S. (1982). "The effect of diet on immune responsiveness and aging," Med. Hypotheses **8**, 495–503.

RABIN, B.M., HUNT, W.A. and JOSEPH, J.A. (1989). "An assessment of the behavioral toxicity of high-energy iron particles compared to other qualities of radiation," Radiat. Res. **119**, 113–122.

RABIN, B.M., HUNT, W.H., JOSEPH, J.A., DALTON, T.K. and KANDASAMY, S.B. (1991). "Relationship between linear energy transfer and behavioral toxicity in rats following exposure to protons and heavy particles," Radiat. Res. **128**, 216–221.

RABIN, B.M., HUNT, W.A., WILSON, M.E. and JOSEPH, J.A. (1992). "Emesis in ferrets following exposure to different types of radiation: A dose-response study," Aviat. Space Environ. Med. **63**, 702–705.

RABIN, B.M., JOSEPH, J.A., HUNT, W.A., DALTON, T.B., KANDASAMY, S.B., HARRIS, A.H. and LUDEWIGT, B. (1994). "Behavioral endpoints for radiation injury," Adv. Space Res. **14**, 457–466.

RABIN, B.M., JOSEPH, J.A., SHUKITT-HALE, B. and MCEWEN, J. (2000). "Effects of exposure to heavy particles on a behavior mediated by the dopaminergic system," Adv. Space Res. **25**, 2065–2074.

RABIN, B.M., SHUKITT-HALE, B., SZPRENGIEL, A. and JOSEPH, J.A. (2002). "Effects of heavy particle irradiation and diet on amphetamine- and lithium chloride-induced taste avoidance learning in rats," Brain Res. **953**, 31–36.

RABIN, B.M., BUHLER, L.L., JOSEPH, J.A., SHUKITT-HALE, B. and JENKINS, D.G. (2003a). "Effects of exposure to ^{56}Fe particles or protons on fixed-ratio operant responding in rats," J. Radiat. Res. **43** (Suppl.), S225–S228

RABIN, B.M., JOSEPH, J.A. and SHUKITT-HALE, B. (2003b). "Long-term changes in amphetamine-induced reinforcement and aversion in rats following exposure to ^{56}Fe particle," Adv. Space Res. **31**, 127–133.

RABIN, B.M., JOSEPH, J.A. and SHUKITT-HALE, B. (2005). "Effects of age and diet on the heavy particle-induced disruption of operant responding produced by a ground-based model for exposure to cosmic rays," Brain Res. **1036**, 122–129.

RADFORD, I.R. (1999). "Initiation of ionizing radiation-induced apoptosis: DNA damage-mediated or does ceramide have a role?" Int. J. Radiat. Biol. **75**, 521–528.

RAJU, U., GUMIN, G.J. and TOFILON, P.J. (2000). "Radiation-induced transcription factor activation in the rat cerebral cortex," Int. J. Radiat. Biol. **76**, 1045–1053.

RASTEGAR, N., ECKART, P. and MERTZ, M. (2002). "Radiation-induced cataract in astronauts and cosmonauts," Graefes Arch. Clin. Exp. Ophthalmol. **240**, 543–547.

REAMES, D.V. (1992). "Energetic particle observations and the abundances of elements in the solar corona," pages 315 to 323 in *Coronal Streamers, Coronal Loops, and Coronal and Solar Wind Composition Proceedings of the First SOHO Workshop*, SP-348, Domingo, V., Ed. (European Space Agency, Noordwijk, The Netherlands).

REAMES, D.V. (1995a). "Solar energetic particles: A paradigm shift," Rev. Geophys. **33** (Suppl.), 585–589.

REAMES, D.V. (1995b). "Coronal abundances determined from energetic particles," Adv. Space Res. **15**(7), 41–51.

REAMES, D.V. (1998). "Solar energetic particles: Sampling coronal abundances," Space Sci. Rev. **85**, 327–340.

REAMES, D.V. (1999a). "Particle acceleration at the sun and in the heliosphere," Space Sci. Rev. **90**, 413–491.

REAMES, D.V. (1999b). "Solar energetic particles: Is there time to hide?" Radiat. Meas. **30**, 297–308.

REAMES, D.V. and NG, C.K. (1998). "Streaming-limited intensities of solar energetic particles," Astrophys. J. **504**, 1002–1005.

REAMES, D.V., MEYER, J.P. and VON ROSENVINGE, T.T. (1994). "Energetic particle abundances in impulsive solar flare events," Astrophys. J. (Supp.) **90**, 649–667.

REAMES, D.V., BARBIER, L.M. and NG, C.K. (1996). "The spatial distribution of particles accelerated by coronal mass ejection-driven shocks," Astrophys. J. **466**, 473–486.

REEDY, R.C. (1996). "Constraints on solar particle events from comparisons of recent events and million-year averages," pages 429 to 436 in *Solar Drivers of the Interplanetary and Terrestrial Disturbances*, Conference Series, Vol. 95, Balasubramanian, K.S., Keil, S.L. and Smartt, R.N., Eds. (Astronomical Society of the Pacific, San Francisco).

REES, G.S., TRIKIC, M.Z., WINTHER, J.F., TAWN, E.J., STOVALL, M., OLSEN, J.H., RECHNITZER, C., SCHRODER, H., GULDBERG, P., and BOICE, J.D., JR. (2006). "A pilot study examining germline minisatellite mutations in the offspring of Danish childhood and adolescent cancer survivors treated with radiotherapy," Int. J. Radiat. Biol. **82**, 153–160.

REINHOLD, H.S. and HOPEWELL, J.W. (1980). "Late changes in the architecture of blood vessels of the rat brain after irradiation," Brit. J. Radiol. **53**, 693–696.

REITZ, G., BUCKER, H., FACIUS, R., HORNECK, G., GRAUL, E.H., BERGER, H., RUTHER, W., HEINRICH, W., BEAUJEAN, R., ENGE, W., ALPATOV, A.M., USHAKOV, I.A., ZACHVATKIN, Y.A. and MESLAND, D.A. (1989). "Influence of cosmic radiation and/or microgravity on development of Carausius morosus," Adv. Space Res. **9**, 161–173.

REITZ, G., BUCKER, H., LINDBERG, C., HIENDL, O.C., RUTHER, W., GRAUL, E.H., BEAUJEAN, R., ALPATOV, A.M., USHAKOV, I.A. and ZACHVATKIN, Y. (1992). "Radiation and microgravity effects observed in the insect system Carausius morosus," Nucl. Tracks Radiat. Meas. **20**, 233–239.

REPACHOLI, M.H. (1998). "Low-level exposure to radiofrequency electromagnetic fields: Health effects and research needs," Bioelectromagnetics **19**, 1–19.

RERF (2005). Radiation Effects Research Foundation. *Reassessment of the Atomic Bomb Radiation Dosimetry for Hiroshima and Nagasaki, Dosimetry System 2002 (DS02)*, Young, R.W. and Kerr, G.D., Eds. (Radiation Effects Research Foundation, Hiroshima, Japan).

RERF (2006). Radiation Effects Research Foundation. http://www.rerf.or.jp (accessed September 2006) (Radiation Effects Research Foundation, Hiroshima, Japan).

RICHARDS, T. and BUDINGER, T.F. (1988). "NMR imaging and spectroscopy of the mammalian central nervous system after heavy ion radiation," Radiat. Res. **113**, 79–101.

RICHARDSON, D.B. and WING, S. (1999). "Radiation and mortality of workers at Oak Ridge National Laboratory: Positive associations for doses received at older ages," Environ. Health Perspect. **107**, 649–656.

RICKS, R.C. and LUSHBAUGH, C.C. (1975). *Studies Relative to the Radiosensitivity of Man: Based on Retrospective Evaluations of Therapeutic and Accidental Total-Body Irradiation*, NASA-CR-144439 (Center for AeroSpace Information, Hanover, Maryland).

RIJNKELS, J.M., MOISON, R.M., PODDA, E. and VAN HENEGOUWEN, G.M. (2003). "Photoprotection by antioxidants against UVB-radiation-induced damage in pig skin organ culture," Radiat. Res. **159**, 210–217.

RILEY, A.L. and TUCK, D.L. (1985). "Conditioned taste aversions: A behavioral index of toxicity," Ann. NY Acad. Sci. **443**, 272–292.

RILEY, E.F., LINDGREN, A.L., ANDERSEN, A.L., MILLER, R.C. and AINSWORTH, E.J. (1991). "Relative cataractogenic effects of x rays, fission-spectrum neutrons, and ^{56}Fe particles: A comparison with mitotic effects," Radiat. Res. **125**, 298–305.

RITTER, S., KRAFT-WEYRATHER, W., SCHOLZ, M. and KRAFT, G. (1992). "Induction of chromosome aberrations in mammalian cells after heavy ion exposure," Adv. Space Res. **12**, 119–125.

RITTER, S., NASONOVA, E., SCHOLZ, M., KRAFT-WEYRATHER, W. and KRAFT, G. (1996). "Comparison of chromosomal damage induced by x-rays and Ar ions with an LET of 1840 keV/mm in G_1 V79 cells," Int. J. Radiat. Biol. **69**, 155–166.

RITTER, S., NASONOVA, E. and GUDOWSKA-NOVAK, E. (2002). "Effect of LET on the yield and quality of chromosomal damage in metaphase cells: A time-course study," Int. J. Radiat. Biol. **78**, 191–202.

RODRIGUEZ, A., ALPEN, E.L., DEGUZMAN, R. and PRIOLEAU, J. (1987). "Irradiation of rat thoraco-lumbar spinal cord with fractionated doses of helium and neon ions," pages 162 to 168 in *Proceedings of the 8th International Congress of Radiation Research*, Fielden, E.M., Fowler, J.F., Hendry, J.H. and Scott, D., Eds. (Taylor and Francis, London).

RODRIGUEZ, A., LEVY, R.P. and FABRIKANT, J.I. (1991). "Experimental central nervous system injury after charged-particle irradiation," pages 149 to 182 in *Radiation Injury to the Nervous System*, Gutin, P.H., Leibel, S.A. and Sheline, G.E., Eds. (Raven Press, New York).

ROLA, R., OTSUKA, S., OBENAUS, A., NELSON, G.A., LIMOLI, C.L., VANDENBERG, S.R. and FIKE, J.R. (2004). "Indicators of hippocampal neurogenesis are altered by ^{56}Fe-particle irradiation in a dose-dependent manner," Radiat. Res. **162**, 442–446.

ROLA, R., SARKISSIAN, V., OBENAUS, A., NELSON, G.A., OTSUKA, S., LIMOLI, C.L. and FIKE, J.R. (2005). "High-LET radiation induces inflammation and persistent changes in markers of hippocampal neurogenesis," Radiat. Res. **164**, 556–560.

ROMANO, E., FERRUCCI, L., NICOLAI, F., DERME, V. and DE STEFANO, G.F. (1997). "Increase of chromosomal aberrations induced by ionising radiation in peripheral blood lymphocytes of civil aviation pilots and crew members," Mutat. Res. **377**, 89–93.

RON, E. (1998). "Ionizing radiation and cancer risk: Evidence from epidemiology," Radiat. Res. **150** (Suppl. 5), S30–S41.

RON, E., MODAN, B., FLORO, S., HARKEDAR, I. and GUREWITZ, R. (1982). "Mental function following scalp irradiation during childhood," Am. J. Epidemiol. **116**, 149–160.

RON, E., MODAN, B., BOICE, J.D., JR., ALFANDARY, E., STOVALL, M., CHETRIT, A. and KATZ, L. (1988). "Tumors of the brain and nervous system after radiotherapy in childhood," N. Engl. J. Med. **319**, 1033–1039.

RON, E., LUBIN, J.H., SHORE, R.E., MABUCHI, K., MODAN, B., POTTERN, L.M., SCHNEIDER, A.B., TUCKER, M.A. and BOICE, J.D., JR. (1995). Thyroid cancer after exposure to external radiation: A pooled analysis of seven studies," Radiat. Res. **141**, 259–277.

RONTO, G., BERCES, A., LAMMER, H., COCKELL, C.S., MOLINA-CUBEROS, G.J., PATEL, M.R. and SELSIS, F. (2003). "Solar UV irradiation conditions on the surface of Mars," Photochem. Photobiol. **77**, 34–40.

ROONEY, J.F., STRAUS, S.E., MANNIX, M.L., WOHLENBERG, C.R., BANKS, S., JAGANNATH, S., BRAUER, J.E. and NOTKINS, A.L. (1992). "UV light-induced reactivation of herpes simplex virus type 2 and prevention by acyclovir," J. Infect. Dis. **166**, 500–506.

ROSANDER, K., FRANKEL, K.A., CERDA, H., FABRIKANT, I., LYMAN, J.T. and FABRIKANT, J.I. (1987). "DNA damage in the endothelial cells of the mouse brain after heavy ion irradiation," pages 162 to 168 in *Proceedings of the 8th International Congress of Radiation Research*, Fielden, E.M., Fowler, J.F., Hendry, J.H. and Scott, D., Eds. (Taylor and Francis, London).

ROSE, A., STEFFEN, J.M., MUSACCHIA, X.J., MANDEL, A.D. and SONNENFELD, G. (1984). "Effect of antiorthostatic suspension on interferon-alpha/beta production by the mouse," Proc. Soc. Exp. Biol. Med. **177**, 253–256.

ROSS, W.M., CREIGHTON, M.O. and TREVITHICK, J.R. (1990). "Radiation cataractogenesis induced by neutron or gamma irradiation in the rat lens is reduced by vitamin E," Scanning Microsc. **4**, 641–650.

ROTH, J., BROWN, N., CATTERALL, M. and BEAL, A. (1976). "Effects of fast neutrons on the eye," Br. J. Ophthalmol. **60**, 236–244.

ROZMAN, K.K. and DOULL, J. (2003). "Scientific foundations of hormesis. Part 2. Maturation, strengths, limitations, and possible applications in toxicology, pharmacology, and epidemiology," Crit. Rev. Toxicol. **33**, 451–462.

RUDD, M.E. (1997). "HZE interactions in biological materials," pages 213 to 233 in *Shielding Strategies for Human Space Exploration*, Wilson,

J.W., Miller, J., Konradi, A. and Cucinotta, F.A., Eds., NASA CP 3360 (Center for AeroSpace Information, Hanover, Maryland).

RYDBERG, B. (1996). "Clusters of DNA damage induced by ionizing radiation: Formation of short DNA fragments. II. Experimental detection," Radiat. Res. **145**, 200–209.

RYDBERG, B., LOBRICH, M. and COOPER, P.K. (1994). "DNA double-strand breaks induced by high-energy neon and iron ions in human fibroblasts. I. Pulsed-field gel electrophoresis method," Radiat. Res. **139**, 133–141.

SABATIER, L., FEDORENKO, B.S., GERASIMENKO, V.N., DIUTRILO, B., GOFSHIR, F., FLIURI-ERAR, A., RIKUL, M., MARTEN, L. and REIODU, M. (1995). "Chromosome aberrations in peripheral blood lymphocytes of cosmonauts after long-term space flight," Aviakosm. Ekolog. Med. **29**, 26–29.

SACHER, G.A. and GRAHN, D. (1964). "Survival of mice under duration-of-life exposure to gamma rays, I. The dosage-survival relation and the lethality function," J. Natl. Cancer Inst. **32**, 277–321.

SACHS, R.K., VAN DEN ENGH, G., TRASK, B., YOKOTA, H. and HEARST, J.E. (1995). "A random walk/giant-loop model for interphase chromosomes," Proc. Natl. Acad. Sci. USA **92**, 2710–2714.

SADHAL, S.S., Ed. (2002). "Microgravity transport processes in fluid, thermal, biological and material sciences," Ann. NY Acad. Sci. **974**.

SAFWAT, A. (2000). "The immunobiology of low-dose total-body irradiation: More questions than answers," Radiat. Res. **153**, 599–604.

SAMPSONIDES, D., PAPANASTASSIOK, E., ZAMANI, M., DEBEAUVAIS, M., ADLOFF, J.C., KULAKOV, B.A., KRIVOPUSTOV, M.I. and BUTSEV, V.S. (1995). "Fragmentation cross sections of ^{16}O, ^{24}Mg and ^{32}S projectiles at 3.65 GeV/nucleon," Phys. Rev. C Nucl. Phys. **51**, 3304–3308.

SANKARANARAYANAN, K., CHAKRABORTY, R. and BOERWINKLE, E.A. (1999). "Ionizing radiation and genetic risks. VI. Chronic multifactorial diseases: A review of epidemiological and genetical aspects of coronary heart disease, essential hypertension and diabetes mellitus," Mutat. Res. **436**, 21–57.

SANNITA, W.G., ACQUAVIVA, M., BALL, S.L., BELLI, F., BISTI, S., BIDOLI, V., CAROZZO, S., CASOLINO, M., CUCINOTTA, F., DE PASCALE, M.P., DI FINO, L., DI MARCO, S., MACCARONE, R., MARTELLO, C., MILLER, J., NARICI, L., PEACHEY, N.S., PICOZZA, P., RINALDI, A., RUGGIERI, D., SATURNO, M., SCHARDT, D. and VAZQUEZ, M. (2004). "Effects of heavy ions on visual function and electrophysiology of rodents: The ALTEA-MICE project," Adv. Space Res. **33**, 1347–1351.

SAUNDERS, R.D. (2003). "Rapporteur report: Weak field interactions in the central nervous system," Radiat. Prot. Dosim. **106**, 357–361.

SAWANT, S.G., RANDERS-PEHRSON, G., GEARD, C.R., BRENNER, D.J. and HALL, E.J. (2001). "The bystander effect in radiation oncogenesis:

I. Transformation in C3H 10T1/2 cells *in vitro* can be initiated in the unirradiated neighbors of irradiated cells," Radiat. Res. **155**, 397–401.

SCHATZKIN, A., FREEDMAN, L.S., SCHIFFMAN, M.H. and DAWSEY, S.M. (1990). "Validation of intermediate end points in cancer research," J. Natl. Cancer Inst. **82**, 1746–1752.

SCHATZKIN, A., FREEDMAN, L.S., DORGAN, J., MCSHANE, L.M., SCHIFFIMAN, M.H. and DAWSEY, S.M. (1996). "Surrogate end points in cancer research: A critique," Cancer Epidemiol. Biomarkers Prev. **5**, 947–953.

SCHEID, W., WEBER, J., TRAUT, H. and GABRIEL, H.W. (1993). "Chromosome aberrations induced in the lymphocytes of pilots and stewardesses," Naturwissenschaften **80**, 528–530.

SCHMID, E., SCHLEGEL, D., GULDBAKKE, S., KAPSCH, R.P. and REGULLA, D. (2003). "RBE of nearly monoenergetic neutrons at energies of 36 KeV–14.6 MeV for induction of dicentrics in human lymphocytes," Radiat. Environ. Biophys. **42**, 87–94.

SCHMITT, D.A., HATTON, J.P., EMOND, C., CHAPUT, D., PARIS, H., LEVADE, T., CAZENAVE, J.P. and SCHAFFAR, L. (1996). "The distribution of protein kinase C in human leukocytes is altered in microgravity," FASEB J. **10**, 1627–1634.

SCHNEIDER, U., AGOSTEO, S., PEDRONI, E. and BESSERER, J. (2002). "Secondary neutron dose during proton therapy using spot scanning," Int. J. Radiat. Oncol. Biol. Phys. **53**, 244–251.

SCHULTHEISS, T.E., KUN, L.E., ANG, K.K. and STEPHENS, L.C. (1995). "Radiation response of the central nervous system," Int. J. Radiat. Oncol. Biol. Phys. **31**, 1093–1112.

SCHWARZ, T. (2002). "Photoimmunosuppression," Photodermatol. Photoimmunol. Photomed. **18**, 141–145.

SCOTT, B.R. (2004). "A biological-based model that links genomic instability, bystander effects, and adaptive response," Mutat. Res. **568**, 129–143.

SEDDON, B., COOK, A., GOTHARD, L., SALMON, E., LATUS, K., UNDERWOOD, S.R. and YARNOLD, J. (2002). "Detection of defects in myocardial perfusion imaging in patients with early breast cancer treated with radiotherapy," Radiother. Oncol. **64**, 53–63.

SEED, T.M., INAL, C., DOBSON, M.E., GHOSE, S., HILYARD, E., TOLLE, D. and FRITZ, T.E. (2002a). "Accommodative responses to chronic irradiation: Effects of dose, dose rate, and pharmacological response modifiers," Mil. Med. **167** (Suppl. 2), 82–86.

SEED, T.M., FRITZ, T.E., TOLLE, D.V. and JACKSON, W.E., III (2002b). "Hematopoietic responses under protracted exposures to low daily dose gamma irradiation," Adv. Space Res. **30**, 945–955.

SEMENENKO, V.A., TURNER, J.E. and BORAK, T.B. (2003). "NOREL, a Monte Carlo code for simulating electra tracks in liquid water," Radiat. Environ. Biophys. **42**, 213–217.

SETLOW, R.B., GRIST, E., THOMPSON, K. and WOODHEAD, A.D. (1993). "Wavelengths effective in induction of malignant melanoma," Proc. Natl. Acad. Sci. USA **90**, 6666–6670.

SEYMOUR, C.B. and MOTHERSILL, C. (2000). "Relative contribution of bystander and targeted cell killing to the low-dose region of the radiation dose-response curve," Radiat. Res. **153**, 508–511.

SHAVERS, M.R., CURTIS, S.B., MILLER, J. and SCHIMMERLING, W. (1990). "The fragmentation of 670A MeV neon-20 as a function of depth in water. II. One-generation transport theory," Radiat. Res. **124**, 117–130.

SHAVERS, M.R., CUCINOTTA, F.A. and WILSON, J.W. (2001). "HZETRN: Neutron and proton production in quasi-elastic scattering of GCR heavy ions," Radiat. Meas. **33**, 347–353.

SHAW, G.M. (2001). "Adverse human reproductive outcomes and electromagnetic fields: A brief summary of the epidemiologic literature," Bioelectromagnetics **22** (Suppl. 5), S5–S18.

SHEA, M.A. and SMART, D.F. (1990). "A summary of major solar proton events," Solar Phys. **127**, 297–320.

SHEA, M.A. and SMART, D.F. (1992). "Recent and historical solar proton events," Radiocarbon **34**, 255–262.

SHEA, M.A., SMART, D.F. and DRESCHHOFF, G.A.M. (1999). "Identification of major proton fluence events from nitrates in polar ice cores," Radiat. Meas. **30**, 309–316.

SHIBANUMA, M., KUROKI, T. and NOSE, K. (1991). "Release of H_2O_2 and phosphorylation of 30 kilodalton proteins as early responses of cell cycle-dependent inhibition of DNA synthesis by transforming growth factor beta 1," Cell Growth Differ. **2**, 583–591.

SHIMIZU, Y., PIERCE, D.A., PRESTON, D.L. and MABUCHI, K. (1999). "Studies of the mortality of atomic bomb survivors. Report 12, part II. Noncancer mortality: 1950–1990," Radiat. Res. **152**, 374–389.

SHINN, J.L., JOHN, S., TRIPATHI, R.K., WILSON, J.W., TOWNSEND, L.W. and NORBURY, J.W. (1992). *Fully Energy-Dependent HZETRN (A Galactic Cosmic Ray Transport Code)*, NASA TP-3243 (National Technical Information Service, Springfield, Virginia.)

SHINN, J.L., BADHWAR, G.D., XAPSOS, M.A., CUCINOTTA, F.A. and WILSON, J.W. (1999). "An analysis of energy deposition in a tissue equivalent proportional counter aboard the space shuttle," Radiat. Meas. **30**, 19–28.

SHOT (2006). Space Hardware Optimization Technology, Inc. http://www.shot.com (accessed September 2006) (Space Hardware Optimization Technology, Inc., Greenville, Indiana).

SHUKITT-HALE, B., CASADESUS, G., MCEWEN, J.J., RABIN, B.M. and JOSEPH, J.A. (2000). "Spatial learning and memory deficits induced by exposure to iron-56-particle radiation," Radiat. Res. **154**, 28–33.

SHUKITT-HALE, B., CARADESUS, G., CANTUTI-CASTELVETRI, I., RABIN, B.M. and JOSEPH, J.A. (2003). "Cognitive deficits induced by ^{56}Fe radiation exposure," Adv. Space Res. **31**, 119–126.

SIEBERS, J.V. and SYMONS, J.E. (1997). "Monte Carlo simulations of the NAC proton therapy line," (abstract) Med. Phys. **24**, 1050–1051.

SIGURDSON, A.J. and RON, E. (2004). "Cosmic radiation exposure and cancer risk among flight crew," Cancer Invest. **22**, 743–761.

SIGURDSON, A.J., STOVALL, M., KLEINERMAN, R.A., MAOR, M.H., TAYLOR, M.E., BOICE, J.D., JR. and RON, E. (2002). "Feasibility of assessing the carcinogenicity of neutrons among neutron therapy patients," Radiat. Res. **157**, 483–489.

SIGURDSON, A.J., DOODY, M.M., RAO, R.S. FREEDMAN, D.M., ALEXANDER, B.H., HAUPTMANN, M., MOHAN, A.K., YOSHINAGA, S., HILL, D.A., TARONE, R., MABUCHI, K., RON, E. and LINET, M.S. (2003). "Cancer incidence in the US Radiologic Technologists Health Study, 1983–1998," Cancer **97**, 3080–3089.

SILBERBERG, R. (1966). "Cosmic-ray modulations in the solar system and in interplanetary space," Phys. Rev. **148**, 1247–1259.

SIMONSEN, L.C., CUCINOTTA, F.A., ATWELL, W. and NEALY, J.E. (1993). "Temporal analysis of October 1989 proton flare using computerized anatomical models," Radiat. Res. **133**, 1–11.

SINE, R.C., LEVINE, I.H., JACKSON, W.E., HAWLEY, A.L., PRASANNA, P.G., GRACE, M.B., GOANS, R.E., GREENHILL, R.G. and BLAKELY, W.F. (2001). "Biodosimetry assessment tool: A post-exposure software application for management of radiation accidents," Mil. Med. **166** (Suppl. 12), 85–87.

SKOPEK, T.R., LIBER, H.L., PENMAN, B.W. and THILLY, W.G. (1978). "Isolation of a human lymphoblastoid cell line heterozygous at the thymidine kinase locus: Possibility for a rapid human cell mutation assay," Biochem. Biophys., Res. Commun. **84**, 411–416.

SKOV, K.A. (1999). "Radioresponsiveness at low doses: Hyper-radiosensitivity and increased radioresistance in mammalian cells," Mutat. Res. **430**, 241–253.

SMART, D.F. (1988). "Predicting the arrival times of solar particles," pages 101 to 110 in *Proceedings of the Conference on Interplanetary Particle Environment*, NASA JPL Publication 88-28, Feynman, J. and Gabriel, S., Eds. (Center for AeroSpace Information, Hanover, Maryland).

SMART, D.F. and SHEA, M.A. (1979). "PPS76: A computerized 'event mode' solar proton forecasting technique," pages 406 to 427 in *Solar-Terrestrial Prediction Proceedings, Vol. 1*, Donnelly, R.F., Ed. (Center for AeroSpace Information, Hanover, Maryland).

SMART, D.F. and SHEA, M.A. (1985). "Galactic cosmic radiation and solar energetic particles," pages 6-1 to 6-29 in *Handbook of Geophysics and the Space Environment,* Jursa, A.S., Ed. (Air Force Research Laboratory, Bedford, Massachusetts).

SMART, D.F. and SHEA, M.A. (1991). "A comparison of the magnitude of the 29 September 1989 high energy event with solar cycles 17, 18, and 19 events," pages 101 to 104 in *Proceedings of the 22nd International Cosmic Ray Conference* (Dublin Institute for Advanced Studies, Dublin).

SMART, D.F. and SHEA, M.A. (1992). "Modeling the time-intensity profile of solar flare generated particle fluxes in the inner heliosphere," Adv. Space Res. **12**, 303–312.

SMART, D.F. and SHEA, M.A. (1997). "The >10 MeV peak flux distribution," pages 449 to 452 in *Solar-Terrestrial Predictions-V*, Heckman, G., Maruboshi, K., Shea, M.A., Smart, D.F. and Thompson, R., Eds. (RWC Tokyo, Hiraiso Solar Terrestrial Research Center, Hitachinaka, Ibaraki, Japan).

SMART, D.F. and SHEA, M.A. (2002), "A review of solar proton events during the 22nd solar cycle," Adv. Space Res. **30**, 1033–1044.

SMART, D.F., SHEA, M.A. and FLUCKIGER, E.O. (1999a). "Calculated vertical cutoff rigidities for the International Space Station during magnetically quiet times," pages 394 to 397 in the *Proceedings of the 26th International Cosmic Ray Conference*, Vol. 7, Kieda, D., Salamon, M. and Dingus, B., Eds. (University of Utah, Salt Lake City, Utah).

SMART, D.F., SHEA, M.A., FLUCKIGER, E.O., TYLKA, A.J. and BOBERG, P.R. (1999b). "Calculated vertical cutoff rigidities for the International Space Station during magnetically active times," pages 398 to 401 in the *Proceedings of the 26th International Cosmic Ray Conference*, Vol. 8, Kieda, D., Salamon, M. and Dingus, B., Eds. (University of Utah, Salt Lake City, Utah).

SONNENFELD, G. (1998). "Immune responses in space flight," Int. J. Sports Med. **19** (Suppl. 3), S195–S204.

SONNENFELD, G. (2001). "Extreme environments and the immune system: Effects of spaceflight on immune responses," J. Allergy Clin. Immunol. **107**, 19–20.

SONNENFELD, G. and SHEARER, W.T. (2002). "Immune function during space flight," Nutrition **18**, 899–903.

SONNENFELD, G., MOREY, E.R., WILLIAMS, J.A. and MANDEL, A.D. (1982). "Effect of a simulated weightlessness model on the production of rat interferon," J. Interferon Res. **2**, 467–470.

SPRUILL, M.D., NELSON, D.O., RAMSEY, M.J., NATH, J. and TUCKER, J.D. (2000). "Lifetime persistence and clonality of chromosome aberrations in the peripheral blood of mice acutely exposed to ionizing radiation," Radiat. Res. **153**, 110–121.

STEFFEN, J.M. and MUSACCHIA, X.J. (1986). "Thymic involution in the suspended rat: Adrenal hypertrophy and glucocorticoid receptor content," Aviat. Space Environ. Med. **57**, 162–167.

STEFFEN, J.M., ROBB, R., DOMBROWSKI, M.J., MUSACCHIA, X.J., MANDEL, A.D. and SONNENFELD, G. (1984). "A suspension model for hypokinetic/hypodynamic and antiorthostatic responses in the mouse," Aviat. Space Environ. Med. **55**, 612–616.

STEINBERG, G.K., FABRIKANT, J.I., MARKS, M.P., LEVY, R.P., FRANKEL, K.A., PHILLIPS, M.H., SHUER, L.M. and SILVERBERG, G.D. (1990). "Stereotactic heavy-charged-particle Bragg-peak radiation for intracranial arteriovenous malformations," N. Engl. J. Med. **323**, 96–101.

STERENBORG, H.J. and VAN DER LEUN, J.C. (1990). "Tumorigenesis by a long wavelength UV-A source," Photochem. Photobiol. **51**, 325–330.

STEWART, J.R., FAJARDO, L.F., GILLETTE, S.M. and CONSTING, L.S. (1995). "Radiation injury to the heart," Int. J. Radiat. Oncol. Biol. Phys. **31**, 1205–1211.

STOWE, R.P., MEHTA, S.K., FERRANDO, A.A., FEEBACK, D.L. and PIERSON, D.L. (2001a). "Immune responses and latent herpes virus reactivation in spaceflight," Aviat. Space Environ. Med. **72**, 884–891.

STOWE, R.P., PIERSON, D.L. and BARRETT, A.D. (2001b). "Elevated stress hormone levels relate to Epstein-Barr virus reactivation in astronauts," Psychosom. Med. **63**, 891–895.

STOWE, R.P., SAMS, C.F. and PIERSON, D.L. (2003). "Effects of mission duration on neuroimmune responses in astronauts," Aviat. Space Environ. Med. **74**, 1281–1284.

STRAM, D.O., SPOSTO, R., PRESTON, D., ABRAHAMSON, S., HONDA, T. and AWA, A.A. (1993). "Stable chromosome aberrations among A-bomb survivors: An update," Radiat. Res. **136**, 29–36.

STRAUME, T. and BENDER, M.A. (1997). "Issues in cytogenetic biological dosimetry: Emphasis on radiation environments in space," Radiat. Res. **148** (Suppl. 5), S60–S70.

SUGAHARA, T., NIKAIDO, O. and NIWA, O., Eds. (2002). *Radiation and Homeostasis: Proceedings of the International Symposium* (Elsevier Publishing, New York).

SUIT, H., GOITEIN, M., MUNZENRIDER, J., VERHEY, L., BLITZER, P., GRAGOUDAS, E., KOEHLER, A.M., URIE, M., GENTRY, R., SHIPLEY, W., URANO, M., DUTTENHAVER, J. and WAGNER, M. (1982a). "Evaluation of the clinical applicability of proton beams in definitive fractionated radiation therapy," Int. J. Radiat. Oncol. Biol. Phys. **8**, 2199–2205.

SUIT, H.D., GOITEIN, M., MUNZENRIDER, J., VERHEY, L., DAVIS, K.R., KOEHLER, A., LINGGOOD, R. and OJEMANN, R.G. (1982b). "Definitive radiation therapy for chordoma and chondrosarcoma of the base of the skull and cervical spine," J. Neurosurg. **56**, 377–385.

SUTHERLAND, B.M., BENNETT, P.V., SIDORKINA, O. and LAVAL, J. (2000). "Clustered DNA damages induced in isolated DNA and in human cells by low doses of ionizing radiation," Proc. Natl. Acad. Sci. USA **97**, 103–108.

SUTHERLAND, B.M., BENNETT, P.V., SUTHERLAND, J.C. and LAVAL, J. (2002). "Clustered DNA damages induced by x rays in human cells," Radiat. Res. **157**, 611–616.

SUZUKI, M., PIAO, C., HALL, E.J. and HEI, T.K. (2001). "Cell killing and chromatid damage in primary human bronchial epithelial cells irradiated with accelerated ^{56}Fe ions," Radiat. Res. **155**, 432–439.

TAKAHASHI, A., OHNISHI, K., FUKUI, M., NAKANO, T., YAMAGUCHI, K., NAGAOKA, S. and OHNISHI, T. (1997). "Mutation

frequency of Dictyostelium discoideum spores exposed to the space environment," Biol. Sci. Space **11**, 81–86.

TAKEDA, A., SHIGEMATSU, N., SUZUKI, S., FUJII, M., KAWATA, T., KAWAGUCHI, O., UNO, T., TAKANO, H., KUBO, A. and ITO, H. (1999). "Late retinal complications of radiation therapy for nasal and paranasal malignancies: Relationship between irradiated-dose area and severity," Int. J. Radiat. Oncol. Biol. Phys. **44**, 599–605.

TALAS, M., BATKAI, L., STOGER, I., NAGY, L., HIROS, L., KONSTANTINOVA, I., RYKOVA, M., MOZGOVAYA, I., GUSEVA, O. and KOZHARINOV, V. (1983). "Results of space experiment program "Interferon. I. Production of interferon *in vitro* by human lymphocytes aboard space laboratory Solyut-6 ("Interferon I") and influence of space flight on lymphocyte functions of cosmonauts ("Interferon III")," Acta. Microbiol. Hung. **30**, 53–61.

TALBOTT, E.O., YOUK, A.O., MCHUGH, K.P., SHIRE, J.D., ZHANG, A., MURPHY, B.P. and ENGBERG, R.A. (2000). "Mortality among the residents of the Three Mile Island accident area: 1979–1992," Environ. Health Perspect. **108**, 545–552.

TANG, K.K. (1990). "A nested leaky box model with large leakage time at low rigidities," pages 373 to 376 in *Proceedings of the 21st International Cosmic Ray Conference*, Protheroe, R.J., Ed. (Department of Physics and Mathematical Physics, University of Adelaide, Graphic Services, Northfield, South Australia).

TAO, F., POWERS-RISIUS, P., ALPEN, E.L., MEDVEDOVSKY, C., DAVID, J. and WORGUL, B.V. (1994). "Radiation effects on late cytopathological parameters in the murine lens relative to particle fluence," Adv. Space Res. **14**, 483–491.

TAWN, E.J., WHITEHOUSE, C.A., WINTHER, J.F., CURWEN, G.B., REES, G.S., STOVALL, M., OLSEN, J.H., GULDBERG, P., RECHNITZER, C., SCHRODER, H. and BOICE, J.D., JR. (2005). "Chromosome analysis in childhood cancer survivors and their offspring—no evidence for radiotherapy-induced persistent geomic instability," Mutat. Res. **583**, 198–206.

TWAN, E.J., WHITEHOUSE, C.A. and RIDDELL, A.E. (2006). "FISH chromosome analysis of plutonium workers from the Sellafield Nuclear Facility," Radiat. Res. **165**, 592–597.

TAYLOR, G.R. and JANNEY, R.P. (1992). "*In vivo* testing confirms a blunting of the human cell-mediated immune mechanism during space flight," J. Leukoc. Biol. **51**, 129–132.

TAYLOR, A., JACQUES, P.F., CHYLACK, L.T., JR., HANKINSON, S.E., KHU, P.M., ROGERS, G., FRIEND, J., TUNG, W., WOLFE, J.K., PADHYE, N. and WILLETT, W.C. (2002). "Long-term intake of vitamins and carotenoids and odds of early age-related cortical and posterior subcapsular lens opacities," Am. J. Clin. Nutr. **75**, 540–549.

TENFORDE, T.S. (1996). "Interaction of ELF magnetic fields with living systems," pages 185 to 230 in *Handbook of Biological Effects of*

Electromagnetic Fields, 2nd ed., Polk, C. and Postow, E., Eds. (CRC Press, Boca Raton, Florida).

TENFORDE, T.S. (1998). "Electromagnetic fields and carcinogenesis: An analysis of biological mechanisms," pages 183 to 202 in *Wireless Phones and Health*, Carlo, G.L., Ed. (Kluwer Academic Publishers (Norwell, Massachusetts).

TESTARD, I. and SABATIER, L. (1999). "Biological dosimetry for astronauts: A real challenge," Mutat. Res. **430**, 315–326.

TESTARD, I., RICOUL, M., HOFFSCHIR, F., FLURY-HERARD, A., DUTRILLAUX, B., FEDORENKO, B., GERASIMENKO, V. and SABATIER, L. (1996). "Radiation-induced chromosome damage in astronauts' lymphocytes," Int. J. Radiat. Biol. **70**, 403–411.

TEZELMAN, S., RODRIGUEZ, J.M., SHEN, W., SIPERSTEIN, A.E., DUH, Q.Y. and CLARK, O.H. (1995). "Primary hyperparathyroidism in patients who have received radiation therapy and in patients who have not received radiation therapy," J. Am. Coll. Surg. **180**, 81–87.

THANNICKAL, V.J. and FANBURG, B.L. (1995). "Activation of an H_2O_2-generating NADH oxidase in human lung fibroblasts by transforming growth factor beta 1," J. Biol. Chem. **270**, 30334–30338.

THIERENS, H., VRAL, A., DE RIDDER, L., TOUIL, N., KIRSCH-VOLDERS, M., LAMBERT, V. and LAURENT, C. (1999). "Inter-laboratory comparison of cytogenetic endpoints for the biomonitoring of radiological workers," Int. J. Radiat. Biol. **75**, 23–34.

THOMAS, O., MAHE, M., CAMPION, L., BOURDIN, S., MILPIED, N., BRUNET, G., LISBONA, A., LE MEVEL, A., MOREAU, P., HAROUSSEAU, J. and CUILLIERE, J. (2001). "Long-term complications of total body irradiation in adults," Int. J. Radiat. Oncol. Biol. Phys. **49**, 125–131.

THOMPSON, D.E., MABUCHI, K., RON, E., SODA, M., TOKUNAGA, M., OCHIKUBO, S., SUGIMOTO, S., IKEDA, T., TERASAKI, M., IZUMI, S. and PRESTON, D.L. (1994). "Cancer incidence in atomic bomb survivors. Part II: Solid tumors, 1958–1987," Radiat. Res. **137** (Suppl. 2), S17–S67.

THOMSON, A.B. and WALLACE, W.H. (2002). "Treatment of paediatric Hodgkin's disease. A balance of risks," Eur. J. Cancer **38**, 468–477.

TISELL, L.E., CARLSSON, S., LINDBERG, S. and RAGNHULT, I. (1976). "Autonomous hyperparathyroidism: A possible late complication of neck radiotherapy," Acta Chir. Scand. **142**, 367–373.

TISELL, L.E., CARLSSON, S., FJALLING, M., HANSSON, G., LINDBERG, S., LUNDBERG, L.M. and ODEN, A. (1985). "Hyperparathyroidism subsequent to neck irradiation. Risk factors," Cancer **56**, 1529–1533.

TOBIAS, C.A. (1952). "Radiation hazards in high altitude aviation," J. Aviat. Med. **23**, 345–372.

TOBIAS, C. (1962). "The use of accelerated heavy particles for production of radiolesions and stimulation in the central nervous system," in

Response of the Nervous System to Ionizing Radiation (Academic Press, New York).

TOBIAS, C.A. (1979). "Pituitary radiation: Radiation physics and biology," pages 221 to 243 in *Recent Advances in the Diagnosis and Treatment of Pituitary Tumors*, Linfoot, J.A., Ed. (Raven Press, New York).

TOBIAS, C.A., BUDINGER, T.F. and LYMAN, J.T. (1971). "Radiation-induced light flashes observed by human subjects in fast neutron, x-ray and positive pion beams," Nature **230**, 596–598.

TODD, P. (1993). "Gravity and the mammalian cell," pages 347 to 381 in *Physical Forces and the Mammalian Cell*, Frangos, J.A. and Ives. C., Eds. (Academic Press, New York).

TODD, P., TOBIAS, C. and SILVER, I. (1974). "Current topics in space radiation biology," Chapter 12 in *Space Radiation Biology and Related Topics,* Tobias, C. and Todd, P., Eds. (Academic Press, New York).

TODD, P., PECAUT, M.J. and FLESHNER, M. (1999). "Combined effects of space flight factors and radiation on humans," Mutat. Res. **430**, 211–219.

TOFILON, P.J. and FIKE, J.R. (2000). "The radioresponse of the central nervous system: A dynamic process," Radiat. Res. **153**, 357–370.

TOKUNAGA, M., LAND, C.E. and TOKUOKA, S. (1991). "Follow-up studies of breast cancer incidence among atomic bomb survivors," J. Radiat. Res. (Tokyo) **32** (Suppl.), 201–211.

TOKUNAGA, M., LAND, C.E., TOKUOKA, S., NISHIMORI, I., SODA, M. and AKIBA, S. (1994). "Incidence of female breast cancer among atomic bomb survivors, 1950–1985," Radiat. Res. **138**, 209–223.

TOWNSEND, L.W. and WILSON, J.W. (1986). "Energy-dependent parameterizations of heavy-ion absorption cross sections," Radiat. Res. **106**, 283–287.

TOWNSEND, L.W. and ZAPP, E.N. (1999). "Dose uncertainties for large solar particle events: Input spectra variability and human geometry approximations," Radiat. Meas. **30**, 337–343.

TOWNSEND, L.W., WILSON, J.W., SHINN, J.L. and CURTIS, S.B. (1992). "Human exposure to large solar particle events in space," Adv. Space Res. **12**, 339–348.

TOWNSEND, L.W., CUCINOTTA, F.A., WILSON, J.W. and BAGGA, R. (1994). "Estimates of HZE particle contributions to SPE radiation exposures on interplanetary missions," Adv. Space Res. **14**, 671–673.

TOWNSEND, L.W., JEHRANI, N.H., HINES, J.W. and FORDE, G.M. (1999). *Predicting Astronaut Radiation Doses from Large Solar Particle Events Using Artificial Intelligence*, SAE Technical Papers 1999-01-2172 (Society of Automotive Engineers International, Warrendale, Pennsylvania).

TOWNSEND, L.W., MILLER, T.M. and GABRIEL, T.A. (2002). "Modifications to the HETC radiation transport code for space radiation shielding applications: A status report," in *Proceedings of the 12th Biennial Topical Meeting of the Radiation Protection and Shielding Division* (American Nuclear Society, La Grange Park, Illinois).

TOWNSEND, L.W., STEPHENS, D.L., JR. and HOFF, J.L. (2003). "Carrington flare of 1959 as a prototypical worst case solar energetic particle event," IEEE Trans. Nucl. Sci, **50**(6), 2307.

TOWNSEND, L.W., MILLER, T.M. and GABRIEL, T.A. (2005). "HETC radiation transport code development for cosmic ray shielding applications in space," Radiat. Protect. Dosim. **116**(1–4), 135–139.

TOWNSEND, L.W., STEPHENS, D.L., Jr., HOFF, J.L., ZAPP, E.N., MOUSSA, H.M., MILLER, T.M., CAMPBELL, C.E. and NICHOLS, T.F. (2006). "The Carrington event: Possible doses to crews in space from a comparable event," Adv. Space Res., doi:10.1016/j.asr.2005.01.111, in press.

TRIBBLE, D.L., BARCELLOS-HOFF, M.H., CHU, B.M. and GONG, E.L. (1999). "Ionizing radiation accelerates aortic lesion formation in fat-fed mice *via* SOD-inhabitable processes," Arterioscler. Thromb. Vasc. Biol. **19**, 1387–1392.

TRIBBLE, D.L., KRAUSS, R.M., CHU, B.M., GONG, E.L., KULLGREN, B.R., NAGY, J.O. and LA BELLE, M. (2000). "Increased low density lipoprotein degradation in aorta of irradiated mice is inhibited by preenrichment of low density lipoprotein with alpha-tocopherol," J. Lipid Res. **41**, 1666–1672.

TRIPATHI, R.K., CUCINOTTA, F.A. and WILSON, J.W. (1997). *Universal Parameterization of Absorption Cross Sections*, NASA TP-3621 (NASA Center for AeroSpace Information, Hanover, Maryland).

TRIPATHI, R.K., WILSON, J.W. and CUCINOTTA, F.A. (2001). "Medium modified two-body scattering amplitude from proton-nucleus total cross-sections," Nucl. Instrum. Meth. Phys. Res. B **173**, 391–396.

TRIPATHY, B.C., BROWN, C.S., LEVINE, H.G. and KRIKORIAN, A.D. (1996). "Growth and photosynthetic responses of wheat plants grown in space," Plant Physiol. **110**, 801–806.

TROTT, K.R., JAMALI, M., MANTI, L. and TEIBE, A. (1998). "Manifestations and mechanisms of radiation-induced genomic instability in V-79 Chinese hamster cells," Int. J. Radiat. Biol. **74**, 787–791.

TSUBOI, K., YANG, T.C. and CHEN, D.J. (1992). "Charged-particle mutagenesis. 1. Cytotoxic and mutagenic effects of high-LET charged iron particles on human skin fibroblasts," Radiat. Res. **129**, 171–176.

TUCKER, J.D., MARPLES, B., RAMSEY, M.J. and LUTZE-MANN, L.H. (2004). "Persistence of chromosome aberrations in mice acutely exposed to ^{56}Fe+26 ions," Radiat. Res. **161**, 648–655.

TULL, C.E. (1990). *Relativistic Heavy Ion Fragmentation at HISS*, Ph.D. Thesis, LBL-29718 (University of California, Davis, California).

TURNER, N.D., BRABY, L.A., FORD, J. and LUPTON, J.R. (2002). "Opportunities for nutritional amelioration of radiation-induced cellular damage," Nutrition **18**, 904–912.

TWEED, J., WILSON, J.W. and TRIPATHI, R.K. (2004). "An improved Green's function for ion beam transport," Adv. Space Res. **34**, 1311–1318.

TYLKA, A.J., ADAMS, J.H., JR., BOBERG, P.R., BROWNSTEIN, B., DIETRICH, W.F., FLUECKIGER, E.O., PETERSEN, E.L., SHEA, M.A., SMART, D.F. and SMITH, E.C. (1997a). "CREME96: A revision of the cosmic ray effects on micro-electronics code," IEEE Trans. Nucl. Sci. **44**, 2150–2160.

TYLKA, A.J., DIETRICH, W.F. and BOBERG, P.R. (1997b). "Observations of very high energy solar heavy ions from IMP-8," pages 101 to 104 in the *Proceedings of the 25th International Cosmic Ray Conference* (World Scientific, Hackensack, New Jersey).

TYLKA, A.J., DIETRICH, W.F. and BOBERG, P.R. (1997c). "Probability distributions of high-energy solar-heavy-ion fluxes from IMP-8: 1973–1996," IEEE Trans. Nucl. Sci. **44**, 2140–2149.

UENO, A., VANNAIS, D., LENARCZYK, M. and WALDREN, C.A. (2002). "Ascorbate, added after irradiation, reduces the mutant yield and alters the spectrum of CD59 mutations in A_L cells irradiated with high LET carbon ions," J. Radiat. Res. (Tokyo) **43**, S245–S249.

UNSCEAR (1993). United Nations Scientific Committee on the Effects of Atomic Radiation. *Sources and Effects of Ionizing Radiation*, Publication No. E.94.IX.2 (United Nations Publications, New York).

UNSCEAR (2000). United Nations Scientific Committee on the Effects of Atomic Radiation. *Sources and Effects of Ionizing Radiation* (United Nations Publications, New York).

UPTON, A.C. (2001). "Radiation hormesis: Data and interpretations," Crit. Rev. Toxicol. **31**, 681–695.

URCH, I.H. and GLEESON, L.J. (1972). "Galactic cosmic ray modulation from 1965–1970," Astro. Space Sci. **17**, 426–446.

VAETH, M. and PIERCE, D.A. (1990). "Calculating excess lifetime risk in relative risk models," Environ. Health Perspect. **87**, 83–94.

VANCE, M.M., BAULCH, J.E., RAABE, O.G., WILEY, L.M. and OVERSTREET, J.W. (2002). "Cellular reprogramming in the F3 mouse with paternal F0 radiation history," Int. J. Radiat. Biol. **78**, 513–526.

VAN DEN BELT-DUSEBOUT, A.W., NUVER, J., DE WIT, R., GIETEMA, J.A., TEN BOKKEL HUININK, W.W., RODRIGUS, P.T.R., SCHIMMEL, E.C., ALEMAN, B.M.P. and VAN LEEUWEN, F.E. (2006). "Long-term risk of cardiovascular disease in 5-year survivors of testicular cancer," J. Clin. Oncol. **24**, 467–475.

VAN DYKE, D.C., SIMPSON, M.E., KONEFF, A.A. and TOBIAS, C.A. (1959). "Long term effects of deuteron irradiation of the rat pituitary," Endocrinology **64**, 240–257.

VAN KEMPEN-HARTEVELD, M.L., BELKACEMI, Y., KAL, H.B., LABOPIN, M. and FRASSONI, F. (2002a). "Dose-effect relationship for cataract induction after single-dose total body irradiation and bone marrow transplantation for acute leukemia," Int. J. Radiat. Oncol. Biol. Phys. **52**, 1367–1374.

VAN KEMPEN-HARTEVELD, M.L., STRUIKMANS, H., KAL, H.B., VAN DER TWEEL, I., MOURITS, M.P., VERDONCK, L.F., SCHIPPER, J. and BATTERMANN, J.J. (2002b). "Cataract after total

body irradiation and bone marrow transplantation: Degree of visual impairment," Int. J. Radiat. Oncol. Biol. Phys. **52**, 1375–1380.

VARMA, M.N., PARETZKE, H.G.,BAUM, J.M., LYMAN, J.T. and HOWARD, J. (1976). "Dose as a function of radial distance from a 930 MeV ^{4}He ion beam," pages 75 to 95 in *Proceedings of the Fifth Symposium on Microdosimetry*, Booz, J., Ebert, H.G. and Smith, B.R.G., Eds. (Commission of the European Communities, Luxembourg.)

VAZQUEZ, M.E. and KIRK, E. (2000). "*In vitro* neurotoxic effects of 1 GeV/n iron particles assessed in retinal explants," Adv. Space Res. **25**, 2041–2049.

VERNOS, I., GONZALEZ-JURADO, J., CALLEJA, M. and MARCO, R. (1989). "Microgravity effects on the oogenesis and development of embryos of Drosophila melanogaster laid in the spaceshuttle during the Biorack experiment (ESA)," Int. J. Dev. Biol. **33**, 213–226.

VIGLIANI, M.C., DUYCKAERTS, C., HAUW, J.J., POISSON, M., MAGDELENAT, H. and DELATTRE, J.Y. (1999). "Dementia following treatment of brain tumors with radiotherapy administered alone or in combination with nitrosourea-based chemotherapy: A clinical and pathological study," J. Neurooncol. **41**, 137–149.

VILCHEZ, R.A., MADDEN, C.R., KOZINETZ, C.A., HALVORSON, S.J., WHITE, Z.S., JORGENSEN, J.L., FINCH, C.J. and BUTEL, J.S. (2002). "Association between simian virus 40 and non-Hodgkin lymphoma," Lancet **359**, 817–823.

VILLALOBOS-MOLINA, R., JOSEPH, J.A., RABIN, B.M., KANDASAMY, S.B., DALTON, T.K. and ROTH, G.S. (1994). "Iron-56 irradiation diminishes muscarinic but not α 1-adrenergic-stimulated low-K_m GTPase in rat brain," Radiat. Res. **140**, 382–386.

VIRMANI, R., FARB, A., CARTER, A.J. and JONES, R.M. (1999). "Pathology of radiation-induced coronary artery disease in human and pig," Cardiovas. Radiat. Med. **1**, 98–101.

VOSS, E.W., JR. (1984). "Prolonged weightlessness and humoral immunity," Science **225**, 214–215.

VUNJAK-NOVAKOVIC, G., SEARBY, N., DE LUIS, J. and FREED, L.E. (2002). "Microgravity studies of cells and tissues," Ann. N.Y. Acad. Sci. **974**, 504–517.

WALDREN, C., VANNAIS, D., DRABEK, R., GUSTAFSON, D., KRAEMER, S., LENARCZYK, M., KRONENBERG, A., HEI, T. and UENO, A. (1998). "Analysis of mutant quantity and quality in human-hamster hybrid AL and AL-179 cells exposed to ^{137}Cs-gamma or HZE-Fe ions," Adv. Space Res. **22**, 579–585.

WALDREN, C.A., VANNAIS, D.B. and UENO, A.M. (2004). "A role for long-lived radicals (LLR) in radiation-induced mutation and persistent chromosomal instability: Counteraction by ascorbate and RibCys but not DMSO," Mutat. Res. **551**, 255–265.

WANG, J.A., FAN, S., YUAN, R.Q., MA, Y.X., MENG, Q., GOLDBERG, I.D. and ROSEN, E.M. (1999). "Ultraviolet radiation down-regulates

expression of the cell-cycle inhibitor p21WAF1/CIP1 in human cancer cells independently of p53," Int. J. Radiat. Biol. **75**, 301–316.

WARD, J.F. (1994). "The complexity of DNA damage: Relevance to biological consequences," Int. J. Radiat. Biol. **66**, 427–432.

WARFIELD, M.E., SCHNEIDKRAUT, M.J., RAMWELL, P.W. and KOT, P.A. (1990). "WR2721 ameliorates the radiation-induced depression in reactivity of rat abdominal aorta to U46619," Radiat. Res. **121**, 63–66.

WEAVER, V.M., PETERSEN, O.W., WANG, F., LARABELL, C.A., BRIAND, P., DAMSKY, C. and BISSELL, M.J. (1997). "Reversion of the malignant phenotype of human breast cells in three-dimensional culture and *in vivo* by integrin blocking antibodies," J. Cell Biol. **137**, 231–245.

WEBBER, W.R. and YUSHAK, S.M. (1979). *The Energy Spectra of Cosmic Ray Iron Nuclei and the Predicted Intensity Variation During the Solar Cycle with Applications for the Intensity Observed by a Magnetospheric Satellite*, AFGL-TR-80-0056 (Air Force Geophysics Laboratory, Hanscom Air Force Base, Massachusetts).

WEBBER, W.R., SOUTHOUL, A., FERRANDO, P. and GUPTA, M. (1990a). "The source charge and isotopic abundances of cosmic rays with Z=9–16: A study using new fragmentation cross sections," Astrophys. J. **348**, 611–620.

WEBBER, W.R., KISH, J.C. and SCHRIER, D.A. (1990b). "Individual isotopic fragmentation cross sections of relativistic nuclei in hydrogen, helium, and carbon targets," Phys. Rev. C Nucl. Phys. **41**, 547–565.

WEISS, J.F. and LANDAUER, M.R. (2003). "Protection against ionizing radiation by antioxidant nutrients and phytochemicals," Toxicology **189**, 1–20.

WEST, S.K., DUNCAN, D.D., MUNOZ, B., RUBIN, G.S., FRIED, L.P., BANDEEN-ROCHE, K. and SCHEIN, O.D. (1998). "Sunlight exposure and risk of lens opacities in a population-based study: The Salisbury Eye Evaluation project," J. Am. Med. Assoc. **280**, 714–718.

WESTFALL, G.D., WILSON, L.W., LINDSTROM, P.J., CRAWFORD, H.J., GREINER, D.E. and HECKMAN, H.H. (1979). "Fragmentation of relativistic ^{56}Fe," Phys. Rev. C **19**, 1309–1323.

WHALEY, J.M. and LITTLE, J.B. (1990). "Molecular characterization of hprt mutants induced by low- and high-LET radiations in human cells," Mutat. Res. **243**, 35–45.

WIESE, C., GAUNY, S.S., LIU, W.C., CHERBONNEL-LASSERRE, C.L. and KRONENBERG, A. (2001). "Different mechanisms of radiation-induced loss of heterozygosity in two human lymphoid cell lines from a single donor," Cancer Res. **61**, 1129–1137.

WIGG, D.R., MURRAY, R.M. and KOSCHEL, K. (1982) "Tolerance of the central nervous system to photon irradiation: Endocrine complications," Acta Radiol. Oncol. **21**, 49–60.

WILEY, L.M., VAN BEEK, M.E. and RAABE, O.G. (1994). "Embryonic effects transmitted by male mice irradiated with 512 MeV/u ^{56}Fe nuclei," Radiat. Res. **138**, 373–385.

WILKINSON, D.C., SHEA, M.A. and SMART, D.F. (2000). "A case history of solar and galactic space weather effects on the geosynchronous communication satellite TDRS-1," Adv. Space Res. **26**, 27–30.

WILLIAMS, G.R. and LETT, J.T. (1994). "Effects of ^{40}Ar and ^{56}Fe ions on retinal photoreceptor cells of the rabbit: Implications for manned missions to Mars," Adv. Space Res. **14**, 217–220.

WILLIAMS, G.R. and LETT, J.T. (1996). "Damage to the photoreceptor cells of the rabbit retina from ^{56}Fe ions: Effect of age at exposure," Adv. Space Res. **18**, 55–58.

WILSON, J.W., KHANDELWAL, G.S., SHINN, J.L., NEALY, J.E., TOWNSEND, L.W. and CUCINOTTA, F.A. (1990). *Simplified Model for Solar Cosmic Ray Exposure in Manned Earth Orbital Flights*, NASA TM-4182 (Center for AeroSpace Information, Hanover, Maryland).

WILSON, J.W., TOWNSEND, L.W., SCHIMMERLING, W., KHANDELWAL, G.S., KHAN, F., NEALY, J.E., CUCINOTTA, F.A., SIMONSEN, L.C., SHINN, J.L. and NORBURY, J.W. (1991). "Application to space exploration," Chapter 12, pages 459 to 517 in *Transport Methods and Interactions for Space Radiation*, NASA-RP-1257 (Langley Research Center, Hampton, Virginia).

WILSON, J.W., KIM, M., SCHIMMERLING, W., BADAVI, F.F., THIBEAULT, S., CUCINOTTA, F.A., SHINN, J. and KIEFER, R. (1995a). "Issues in space radiation protection: Galactic cosmic rays," Health Phys. **68**, 50–58.

WILSON, J.W., TRIPATHI, R.K., CUCINOTTA, F.A., SHINN, J.L., BADAVI, F.F., CHUN, S.Y., NORBURY, J.W., ZEITLIN, C.J., HEILBRONN, L. and MILLER, J. (1995b). *NUCFRG2: An Evaluation of the Semiempirical Nuclear Fragmentation Database*, NASA TP 3533 (Center for AeroSpace Information, Hanover, Maryland).

WILSON, J.W., MILLER, J., KONRADI. A. and CUCINOTTA, F.A., Eds. (1997a). *Shielding Strategies for Human Space Exploration,* NASA CP 3360 (Center for AeroSpace Information, Hanover, Maryland).

WILSON, J.W., SIMONSEN, L.C., SHINN, J.L., DUBEY, R.R., JORDAN, W. and KIM, M. (1997b). *Radiation Analysis for the Human Lunar Return Mission,* NASA TP 3622 (Center for AeroSpace Information, Hanover, Maryland).

WILSON, J.W., CUCINOTTA, F.A., SHINN, J.L. , SIMONSEN, L.C., DUBEY, R.R., JORDAN, W.R., JONES, T.D., CHANG, C.K. and KIM, M.Y. (1999). "Shielding from solar particle event exposures in deep space," Radiat. Meas. **30**, 361–382.

WILSON, J.W., CUCINOTTA, F.A., MILLER, J., SHINN, J.L., THIBEAULT, S.A., SINGLETERRY, R.C., SIMONSEN, L.C. and KIM, M.H. (2001). "Approach and issues related to shield material design to protect astronauts from space radiation," Mater. Design **22**, 541–554.

WOLF, G., PIEPER, R. and OBE, G. (1999a). "Chromosomal alterations in peripheral lymphocytes of female cabin attendants," Int. J. Radiat. Biol. **75**, 829–836.

WOLF, G., OBE, G. and BERGAU, L. (1999b). "Cytogenetic investigations in flight personnel," Radiat. Prot. Dosim. **86**, 275–278.

WOLFF, S. (1998). "The adaptive response in radiobiology: Evolving insights and implications," Environ. Health Perspect. **106** (Suppl. 1), 277–283.

WOLOSCHAK, G.E. and CHANG-LIU, C.M. (1990). "Differential modulation of specific gene expression following high- and low-LET radiations," Radiat. Res. **124**, 183–187.

WONG, M., SCHIMMERLING, W., PHILLIPS, M.H., LUDEWIGT, B.A., LANDIS, D.A., WALTON, J.T. and CURTIS, S.B. (1990). "The multiple Coulomb scattering of very heavy charged particles," Med. Phys. **17**, 163–171.

WONG, F.L., YAMADA, M., SASAKI, H., KODAMA, K. and HOSODA, Y. (1999). "Effects of radiation on the longitudinal trends of total serum cholesterol levels in the atomic bomb survivors," Radiat. Res. **151**, 736–746.

WOOD, D.H., YOCHMOWITZ, M.G., HARDY, K.A. and SALMON, Y.L. (1986). "Occurrence of brain tumors in rhesus monkeys exposed to 55-MeV protons," Adv. Space Res. **6**, 213–216.

WOOD, D., COX, A., HARDY, K., SALMON, Y. and TROTTER, R. (1994). "Head and neck tumors after energetic proton irradiation in rats," Adv. Space Res. **14**, 681–684.

WOODRUFF, K.H., LYMAN, J.T., LAWRENCE, J.H., TOBIAS, C.A., BORN, J.L. and FABRIKANT, J.I. (1984). "Delayed sequelae after pituitary irradiation," Hum. Pathol. **15**, 48–54.

WORGUL, B.V. (1986). "Cataract analysis and the assessment of radiation risk in space," Adv. Space Res. **6**, 285–293.

WORGUL, B.V., BRENNER, D.J., MEDVEDOVSKY, C., MERRIAM, G.R., JR. and HUANG, Y. (1993). "Accelerated heavy particles and the lens. VII: The cataractogenic potential of 450 MeV/amu iron ions," Invest. Ophthalmol. Vis. Sci. **34**, 184–193.

WORGUL, B.V., MEDVEDOVSKY, C., HUANG, Y., MARINO, S.A., RANDERS-PEHRSON, G. and BRENNER, D.J. (1996). "Quantitative assessment of the cataractogenic potential of very low doses of neutrons," Radiat. Res. **145**, 343–349.

WORGUL, B.V., SMILENOV, L., BRENNER, D.J., JUNK, A., ZHOU, W. and HALL, E.J. (2002). "ATM heterozygous mice are more sensitive to radiation-induced cataracts than are their wild-type counterparts," Proc. Natl. Acad. Sci. USA **99**, 9836–9839.

WRIGHT, E.G. (1998). "Radiation-induced genomic instability in haemopoietic cells," Int. J. Radiat. Biol. **74**, 681–687.

WU, B., MEDVEDOVSKY, C. and WORGUL, B.V. (1994). "Non-subjective cataract analysis and its application in space radiation risk assessment," Adv. Space Res. **14**, 493–500.

WU, H., DURANTE, M., GEORGE, K. and YANG, T.C. (1997). "Induction of chromosome aberrations in human cells by charged particles," Radiat. Res. **148** (Suppl. 5), S102–S107.

WU, H., DURANTE, M., FURUSAWA, Y., GEORGE, K., KAWATA, T. and CUCINOTTA, F.A. (2003). "M-FISH analysis of chromosome aberrations in human fibroblasts exposed to energetic iron ions *in vitro*," Adv. Space Res. **31**, 1537–1542.

WULF, H., KRAFT-WEYRATHER, W., MILTENBURGER, H.G., BLAKELY, E.A., TOBIAS, C.A. and KRAFT, G. (1985). "Heavy-ion effects on mammalian cells: Inactivation measurements with different cell lines," Radiat. Res. **8** (Suppl.), S122–S134.

XAPSOS, M.A., SUMMERS, G.P., SHAPIRO, P. and BURKE, E.A. (1996). "New techniques for predicting solar proton fluences for radiation effects applications," IEEE Trans. Nucl. Sci. **43**, 2772–2777.

XAPSOS, M.A., BARTH, J.L., STASSINOPOULOS, E.G., MESSENGER, S.R, WALTERS, R.J., SUMMERS, G.P. and BURKE, E.A. (2000). "Characterizing solar proton energy spectra for radiation effects applications," IEEE Trans. Nucl. Sci. **47**, 2218–2223.

YAAR, I., RON, E., MODAN, B., RINOTT, Y., YAAR, M. and MODAN, M. (1982). "Long-lasting cerebral functional changes following moderate dose x-radiation treatment to the scalp in childhood: An electroencephalographic power spectral study," J. Neurol. Neurosurg. Psychiatry **45**, 166–169.

YANG, T.C. (1999). "Proton radiobiology and uncertainties," Radiat. Meas. **30**, 383–392.

YANG, V.V. and AINSWORTH, E.J. (1982). "Late effects of heavy charged particles on the fine structure of the mouse coronary artery," Radiat. Res. **91**, 135–144.

YANG, V.C. and AINSWORTH, E.J. (1987). "A histological study on the cataractogenic effects of heavy charged particles," Proc. Natl. Sci. Counc. Repub. China B **11**, 18–28.

YANG, T.C. and TOBIAS, C.A. (1984). "Effects of heavy ion radiation on the brain vascular system and embryonic development," Adv. Space Res. **4**, 239–245.

YANG, V.V., STEARNER, S.P. and AINSWORTH, E.J. (1978). "Late ultrastructural changes in the mouse coronary arteries and aorta after fission neutron or ^{60}Co gamma irradiation," Radiat. Res. **74**, 436–456.

YANG, T.C.H., TOBIAS, C.A., BLAKELY, E.A., CRAISE, L.M., MADFES, I.S., PEREZ, C. and HOWARD, J. (1980). "Enhancement effects of high-energy neon particles on the viral transformation of mouse C3H1OT1/2 cells *in vitro*," Radiat. Res. **81**, 208–223.

YANG, T.C., CRAISE, L.M., MEI, M.T. and TOBIAS, C.A. (1985). "Neoplastic cell transformation by heavy charged particles," Radiat. Res. **8** (Suppl.), S177–S187.

YANG, T.C., MEI, M., GEORGE, K.A. and CRAISE, L.M. (1996). "DNA damage and repair in oncogenic transformation by heavy ion radiation," Adv. Space Res. **18**, 149–158.

YANG, T.C., GEORGE, K., JOHNSON, A.S., DURANTE, M. and FEDORENKO, B.S. (1997). "Biodosimetry results from space flight Mir-18," Radiat. Res. **148** (Suppl. 5), S17–S23.

YANG, T.C., CRAISE, L.M. and RAJU, M.R. (2000). "Oncogenic transformation of mammalian cells by ultrasoft x-rays and alpha particles," Adv. Space Res. **25**, 2123–2130.

YANG, F., STENOIEN, D.L., STRITTMATTER, E.F., WANG, J., DING, L., LIPTON, M.S., MONROE, M.E., NICORA, C.D., GRISTENKO, M.A., TANG, K., FANG, R., ADKINS, J.N., CAMP, D.G., II, CHEN, D.J. and SMITH, R.D. (2006). "Phosphoproteome profiling of human skin fibroblast cells in response to low- and high-dose irradiation," J. Proteome Res. **5**, 1252–1260.

YASUDA, H., BADHWAR, G.D., KOMIYAMA, T. and FUJITAKA, K. (2000). "Effective dose equivalent on the ninth Shuttle-Mir mission (STS-91)," Radiat. Res. **154**, 705–713.

YATAGAI, F., SAITO, T., TAKAHASHI, A., FUJIE, A., NAGAOKA, S., SATO, M. and OHNISHI, T. (2000). "rpsL mutation induction after space flight on MIR," Mutat. Res. **453**, 1–4.

YIN, L., MORITA, A. and TSUJI, T. (2001). "Skin aging induced by ultraviolet exposure and tobacco smoking: Evidence from epidemiological and molecular studies," Photodermatol. Photoimmunol. Photomed. **17**, 178–183.

YIN, E., NELSON, D.O., COLEMAN, M.A., PETERSON, L.E. and WYROBEK, A.J. (2003). "Gene expression changes in mouse brain after exposure to low-dose ionizing radiation," Int. J. Radiat. Biol. **79**, 759–775.

YONEHARA, S., BRENNER, A.V., KISHIKAWA, M., INSKIP, P.D., PRESTON, D.L., RON, E., MABUCHI K. and TOKUOKA, S. (2004). "Clinical and epidemiologic characteristics of first primary tumors of the central nervous system and related organs among atomic bomb survivors in Hiroshima and Nagasaki, 1958–1995," Cancer **101**, 1644–1654.

YOSHINAGA, S., MABUCHI, K., SIGURDSON, A.J., DOODY, M.M. and RON, E. (2004). "Cancer risks among radiologists and radiologic technologists: Review of epidemiologic studies," Radiology **233**, 313–321.

YUHAS, J.M. (1979). "Differential protection of normal and malignant tissues against the cytotoxic effects of mechlorethamine," Cancer Treat. Rep. **63**, 971–976.

YUHAS, J.M. (1980). "Active versus passive absorption kinetics as the basis for selective protection of normal tissues by S-2-(3-aminopropylamino)-ethylphosphorothioic acid," Cancer Res. **40**, 1519–1524.

ZEEB, H., BLETTNER, M., LANGNER, I., HAMMER, G.P., BALLARD, T.J., SANTAQUILANI, M., GUNDESTRUP, M., STORM, H., HALDORSEN, T., TVETEN, U., HAMMAR, N., LINNERSJO, A., VELONAKIS, E., TZONOU, A., AUVINEN, A., PUKKALA, E., RAFNSSON, V. and HRAFNKELSSON, J. (2003). "Mortality from cancer and other causes among airline cabin attendants in Europe: A collaborative cohort study in eight countries," Am. J. Epidemiol. **158**, 35–46.

ZEITLIN, C., HEILBRONN, L., MILLER, J., RADEMACHER, S.E., BORAK, T., CARTER, T.R., FRANKEL, K.A., SCHIMMERLING, W. and STRONACH, C.D. (1997). Heavy fragment production cross sections from 1.05 GeV/nucleon ^{56}Fe in C, Al, Cu, Pb, and CH_2 targets," Phys. Review C Nucl. Phys. **56**, 388–397.

ZEITLIN, C., FUKUMURA, A., HEILBRONN, L., IWATA, Y., MILLER, J. and MURAKAMI, T. (2001). "Fragmentation cross sections of 600 MeV/nucleon ^{20}Ne on elemental targets," Phys. Review C **64**, 24902.

ZEITLIN, C., HEILBRONN, L., MILLER, J., FUKUMURA, A., IWATA, Y. and MURAKAMI, T. (2002). *Charge-Changing and Fragment Production Cross Sections of ^{28}Si on Elemental Targets from 400 MeV/nucleon to 1200 MeV/nucleon*, LBNL-47655 (Lawrence Berkeley National Laboratory, Berkeley, California).

ZEITLIN, C., CLEGHORN, T., CUCINOTTA, F.A., SAGANTI, P., ANDERSEN, V., LEE, K., PINSKY, L., ATWELL, W., TURNER, R. and BADHWAR, G. (2004). "Overview of the Martian radiation environment experiment," Adv. Space Res. **33**(12), 2204–2210.

ZELLER, E.J. and DRESCHHOFF, G.A.M. (1995). "Anomalous nitrate concentrations in polar ice cores – Do they result from solar particle injections into the polar atmosphere?" Geophys. Res. Lett. **22**, 2521–2524.

ZHOU, H., RANDERS-PEHRSON, G., WALDREN, C.A., VANNAIS, D., HALL, E.J. and HEI, T.K. (2000). "Induction of a bystander mutagenic effect of alpha particles in mammalian cells," Proc. Natl. Acad. Sci. USA **97**, 2099–2104.

ZHOU, H., RANDERS-PEHRSON, G., WALDREN, C.A. and HEI, T.K. (2004). "Radiation-induced bystander effect and adaptive response in mammalian cells," Adv. Space Res. **34**, 1368–1372.

ZIEGLER, M.G. and MECK, J.V. (2001). "Physical and psychological challenges of space travel: An overview," Psychosom. Med. **63**, 859–861.

ZIERHUT, D., LOHR, F., SCHRAUBE, P., HUBER, P., WENZ, F., HAAS, R., FEHRENTZ, D., FLENTJE, M., HUNSTEIN, W. and WANNENMACHER, M. (2000). "Cataract incidence after total-body irradiation," Int. J. Radiat. Oncol. Biol. Phys. **46**, 131–135.

ZMUDZKA, B.Z., MILLER, S.A., JACOBS, M.E. and BEER, J.Z. (1996). "Medical UV exposures and HIV activation," Photochem. Photobiol. **64**, 246–253.

ZUTTER, M.M., SANTORO, S.A., STAATZ, W.D. and TSUNG, Y.L. (1995). "Re-expression of the alpha 2 beta 1 integrin abrogates the malignant phenotype of breast carcinoma cells," Proc. Natl. Acad. Sci. USA **92**, 7411–7415.

The NCRP

The National Council on Radiation Protection and Measurements is a non-profit corporation chartered by Congress in 1964 to:

1. Collect, analyze, develop and disseminate in the public interest information and recommendations about (a) protection against radiation and (b) radiation measurements, quantities and units, particularly those concerned with radiation protection.
2. Provide a means by which organizations concerned with the scientific and related aspects of radiation protection and of radiation quantities, units and measurements may cooperate for effective utilization of their combined resources, and to stimulate the work of such organizations.
3. Develop basic concepts about radiation quantities, units and measurements, about the application of these concepts, and about radiation protection.
4. Cooperate with the International Commission on Radiological Protection, the International Commission on Radiation Units and Measurements, and other national and international organizations, governmental and private, concerned with radiation quantities, units and measurements and with radiation protection.

The Council is the successor to the unincorporated association of scientists known as the National Committee on Radiation Protection and Measurements and was formed to carry on the work begun by the Committee in 1929.

The participants in the Council's work are the Council members and members of scientific and administrative committees. Council members are selected solely on the basis of their scientific expertise and serve as individuals, not as representatives of any particular organization. The scientific committees, composed of experts having detailed knowledge and competence in the particular area of the committee's interest, draft proposed recommendations. These are then submitted to the full membership of the Council for careful review and approval before being published.

The following comprise the current officers and membership of the Council:

Officers

President	Thomas S. Tenforde
Senior Vice President	Kenneth R. Kase
Secretary and Treasurer	David A. Schauer
Assistant Secretary	Michael F. McBride

Members

John F. Ahearne
Sally A. Amundson
Benjamin R. Archer
Mary M. Austin-Seymour
Steven M. Becker
Joel S. Bedford
Eleanor A. Blakely
William F. Blakely
John D. Boice, Jr.
Wesley E. Bolch
Thomas B. Borak
Andre Bouville
Leslie A. Braby
David J. Brenner
James A. Brink
Antone L. Brooks
Jerrold T. Bushberg
John F. Cardella
Stephanie K. Carlson
Polly Y. Chang
S.Y. Chen
Kelly L. Classic
Mary E. Clark
Michael L. Corradini
J. Donald Cossairt
Allen G. Croff
Francis A. Cucinotta
Paul M. DeLuca
David A. Eastmond
Stephen A. Feig
John R. Frazier
Donald P. Frush
Thomas F. Gesell
Robert L. Goldberg
Andrew J. Grosovsky
Raymond A. Guilmette
Roger W. Harms
Kathryn Held
John W. Hirshfeld, Jr.
F. Owen Hoffman
Roger W. Howell
Kenneth R. Kase
Ann R. Kennedy
William E. Kennedy, Jr.
David C. Kocher
Ritsuko Komaki
Amy Kronenberg
Susan M. Langhorst
Edwin M. Leidholdt
Howard L. Liber
James C. Lin
Jill A. Lipoti
John B. Little
Paul A. Locke
Jay H. Lubin
C. Douglas Maynard
Debra McBaugh
Cynthia H. McCollough
Barbara J. McNeil
Fred A. Mettler, Jr.
Charles W. Miller
Donald L. Miller
Jack Miller
Kenneth L. Miller
William H. Miller
William F. Morgan
David S. Myers
Bruce A. Napier
Gregory A. Nelson
Carl J. Paperiello
R. Julian Preston
Jerome C. Puskin
Allan C.B. Richardson
Henry D. Royal
Michael T. Ryan
Jonathan M. Samet
Thomas M. Seed
Stephen M. Seltzer
Roy E. Shore
Edward A. Sickles
Steven L. Simon
Paul Slovic
Christopher G. Soares
Daniel J. Strom
Thomas S. Tenforde
Julie E.K. Timins
Richard E. Toohey
Lawrence W. Townsend
Lois B. Travis
Fong Y. Tsai
Richard J. Vetter
Chris G. Whipple
Stuart C. White
J. Frank Wilson
Susan D. Wiltshire
Gayle E. Woloschak
Shiao Y. Woo
Andrew J. Wyrobek
Marco A. Zaider
Pasquale D. Zanzonico

Honorary Members

Warren K. Sinclair, *President Emeritus;* Charles B. Meinhold, *President Emeritus*
S. James Adelstein, *Honorary Vice President*
W. Roger Ney, *Executive Director Emeritus*
William M. Beckner, *Executive Director Emeritus*

Seymour Abrahamson
Lynn R. Anspaugh
John A. Auxier
William J. Bair
Harold L. Beck
Bruce B. Boecker
Victor P. Bond
Robert L. Brent
Reynold F. Brown
Melvin C. Carter
Randall S. Caswell
Frederick P. Cowan
James F. Crow
Gerald D. Dodd
Sarah S. Donaldson
William P. Dornsife
Patricia W. Durbin
Keith F. Eckerman
Thomas S. Ely
Richard F. Foster
R.J. Michael Fry
Ethel S. Gilbert
Joel E. Gray
Robert O. Gorson
Arthur W. Guy
Eric J. Hall
Naomi H. Harley
William R. Hendee
Donald G. Jacobs
Bernd Kahn
Charles E. Land
Roger O. McClellan
Dade W. Moeller
A. Alan Moghissi
Wesley L. Nyborg
John W. Poston, Sr.
Andrew K. Poznanski
Genevieve S. Roessler
Marvin Rosenstein
Lawrence N. Rothenberg
Eugene L. Saenger
William J. Schull
John E. Till
Robert L. Ullrich
Arthur C. Upton
F. Ward Whicker
Marvin C. Ziskin

Lauriston S. Taylor Lecturers

Robert L. Brent (2006) *Fifty Years of Scientific Investigation: The Importance of Scholarship and the Influence of Politics and Controversy*
John B. Little (2005) *Nontargeted Effects of Radiation: Implications for Low-Dose Exposures*
Abel J. Gonzalez (2004) *Radiation Protection in the Aftermath of a Terrorist Attack Involving Exposure to Ionizing Radiation*
Charles B. Meinhold (2003) *The Evolution of Radiation Protection: From Erythema to Genetic Risks to Risks of Cancer to ?*
R. Julian Preston (2002) *Developing Mechanistic Data for Incorporation into Cancer Risk Assessment: Old Problems and New Approaches*
Wesley L. Nyborg (2001) *Assuring the Safety of Medical Diagnostic Ultrasound*
S. James Adelstein (2000) *Administered Radioactivity: Unde Venimus Quoque Imus*
Naomi H. Harley (1999) *Back to Background*
Eric J. Hall (1998) *From Chimney Sweeps to Astronauts: Cancer Risks in the Workplace*
William J. Bair (1997) *Radionuclides in the Body: Meeting the Challenge!*
Seymour Abrahamson (1996) *70 Years of Radiation Genetics: Fruit Flies, Mice and Humans*
Albrecht Kellerer (1995) *Certainty and Uncertainty in Radiation Protection*
R.J. Michael Fry (1994) *Mice, Myths and Men*
Warren K. Sinclair (1993) *Science, Radiation Protection and the NCRP*
Edward W. Webster (1992) *Dose and Risk in Diagnostic Radiology: How Big? How Little?*
Victor P. Bond (1991) *When is a Dose Not a Dose?*
J. Newell Stannard (1990) *Radiation Protection and the Internal Emitter Saga*
Arthur C. Upton (1989) *Radiobiology and Radiation Protection: The Past Century and Prospects for the Future*
Bo Lindell (1988) *How Safe is Safe Enough?*
Seymour Jablon (1987) *How to be Quantitative about Radiation Risk Estimates*
Herman P. Schwan (1986) *Biological Effects of Non-ionizing Radiations: Cellular Properties and Interactions*
John H. Harley (1985) *Truth (and Beauty) in Radiation Measurement*
Harald H. Rossi (1984) *Limitation and Assessment in Radiation Protection*
Merril Eisenbud (1983) *The Human Environment—Past, Present and Future*
Eugene L. Saenger (1982) *Ethics, Trade-Offs and Medical Radiation*
James F. Crow (1981) *How Well Can We Assess Genetic Risk? Not Very*
Harold O. Wyckoff (1980) *From "Quantity of Radiation" and "Dose" to "Exposure" and "Absorbed Dose"—An Historical Review*
Hymer L. Friedell (1979) *Radiation Protection—Concepts and Trade Offs*
Sir Edward Pochin (1978) *Why be Quantitative about Radiation Risk Estimates?*
Herbert M. Parker (1977) *The Squares of the Natural Numbers in Radiation Protection*

Currently, the following committees are actively engaged in formulating recommendations:

Program Area Committee 1: Basic Criteria, Epidemiology, Radiobiology, and Risk
- SC 1-8 Risk to Thyroid from Ionizing Radiation
- SC 1-13 Impact of Individual Susceptibility and Previous Radiation Exposure on Radiation Risk for Astronauts
- SC 1-15 Radiation Safety in NASA Lunar Missions
- SC 85 Risk of Lung Cancer from Radon

Program Area Committee 2: Operational Radiation Safety
- SC 46-17 Radiation Protection in Educational Institutions

Program Area Committee 3: Nonionizing Radiation
- SC 89-5 Study and Critical Evaluation of Radiofrequency Exposure Guidelines

Program Area Committee 4: Radiation Protection in Medicine
- SC 4-1 Management of Persons Contaminated with Radionuclides
- SC 4-2 Population Monitoring and Decontamination Following a Nuclear/Radiological Incident
- SC 91-1 Precautions in the Management of Patients Who Have Received Therapeutic Amounts of Radionuclides

Program Area Committee 5: Environmental Radiation and Radioactive Waste Issues
- SC 64-22 Design of Effective Effluent and Environmental Monitoring Programs
- SC 64-23 Cesium in the Environment

Program Area Committee 6: Radiation Measurements and Dosimetry
- SC 6-1 Uncertainties in the Measurement and Dosimetry of External Radiation Sources
- SC 6-2 Radiation Exposure of the U.S. Population
- SC 6-3 Uncertainties in Internal Radiation Dosimetry
- SC 6-4 Fundamental Principles of Dose Reconstruction
- SC 57-17 Radionuclide Dosimetry Models for Wounds

Advisory Committee 1: Public Policy and Risk Communication

In recognition of its responsibility to facilitate and stimulate cooperation among organizations concerned with the scientific and related aspects of radiation protection and measurement, the Council has created a category of NCRP Collaborating Organizations. Organizations or groups of organizations that are national or international in scope and are concerned with scientific problems involving radiation quantities, units, measurements and effects, or radiation protection may be admitted to collaborating status by the Council. Collaborating Organizations provide a means by which NCRP can gain input into its activities from a wider segment of society. At the same time, the relationships with the Collaborating Organizations facilitate wider dissemination of information about the Council's activities, interests and concerns. Collaborating Organizations have the opportunity to comment on draft reports (at the time that these are submitted to the members of the Council). This is intended to capitalize on the fact that Collaborating Organizations are in an excellent position to both contribute to the identification of what needs to be treated in NCRP reports and to identify problems that might result from proposed recommenda-

tions. The present Collaborating Organizations with which NCRP maintains liaison are as follows:

American Academy of Dermatology
American Academy of Environmental Engineers
American Academy of Health Physics
American Association of Physicists in Medicine
American College of Medical Physics
American College of Nuclear Physicians
American College of Occupational and Environmental Medicine
American College of Radiology
American Conference of Governmental Industrial Hygienists
American Dental Association
American Industrial Hygiene Association
American Institute of Ultrasound in Medicine
American Medical Association
American Nuclear Society
American Pharmaceutical Association
American Podiatric Medical Association
American Public Health Association
American Radium Society
American Roentgen Ray Society
American Society for Therapeutic Radiology and Oncology
American Society of Emergency Radiology
American Society of Health-System Pharmacists
American Society of Radiologic Technologists
Association of Educators in Radiological Sciences, Inc.
Association of University Radiologists
Bioelectromagnetics Society
Campus Radiation Safety Officers
College of American Pathologists
Conference of Radiation Control Program Directors, Inc.
Council on Radionuclides and Radiopharmaceuticals
Defense Threat Reduction Agency
Electric Power Research Institute
Federal Communications Commission
Federal Emergency Management Agency
Genetics Society of America
Health Physics Society
Institute of Electrical and Electronics Engineers, Inc.
Institute of Nuclear Power Operations
International Brotherhood of Electrical Workers
National Aeronautics and Space Administration
National Association of Environmental Professionals
National Center for Environmental Health/Agency for Toxic Substances
National Electrical Manufacturers Association
National Institute for Occupational Safety and Health
National Institute of Standards and Technology
Nuclear Energy Institute
Office of Science and Technology Policy
Paper, Allied-Industrial, Chemical and Energy Workers
International Union

Product Stewardship Institute
Radiation Research Society
Radiological Society of North America
Society for Risk Analysis
Society of Chairmen of Academic Radiology Departments
Society of Nuclear Medicine
Society of Radiologists in Ultrasound
Society of Skeletal Radiology
U.S. Air Force
U.S. Army
U.S. Coast Guard
U.S. Department of Energy
U.S. Department of Housing and Urban Development
U.S. Department of Labor
U.S. Department of Transportation
U.S. Environmental Protection Agency
U.S. Navy
U.S. Nuclear Regulatory Commission
U.S. Public Health Service
Utility Workers Union of America

NCRP has found its relationships with these organizations to be extremely valuable to continued progress in its program.

Another aspect of the cooperative efforts of NCRP relates to the Special Liaison relationships established with various governmental organizations that have an interest in radiation protection and measurements. This liaison relationship provides: (1) an opportunity for participating organizations to designate an individual to provide liaison between the organization and NCRP; (2) that the individual designated will receive copies of draft NCRP reports (at the time that these are submitted to the members of the Council) with an invitation to comment, but not vote; and (3) that new NCRP efforts might be discussed with liaison individuals as appropriate, so that they might have an opportunity to make suggestions on new studies and related matters. The following organizations participate in the Special Liaison Program:

Australian Radiation Laboratory
Bundesamt fur Strahlenschutz (Germany)
Canadian Nuclear Safety Commission
Central Laboratory for Radiological Protection (Poland)
China Institute for Radiation Protection
Commonwealth Scientific Instrumentation Research Organization (Australia)
European Commission
Health Council of the Netherlands
Institut de Radioprotection et de Surete Nucleaire
International Commission on Non-ionizing Radiation Protection
International Commission on Radiation Units and Measurements
Japan Radiation Council
Korea Institute of Nuclear Safety
National Radiological Protection Board (United Kingdom)
Russian Scientific Commission on Radiation Protection
South African Forum for Radiation Protection

World Association of Nuclear Operations
World Health Organization, Radiation and Environmental Health

NCRP values highly the participation of these organizations in the Special Liaison Program.

The Council also benefits significantly from the relationships established pursuant to the Corporate Sponsor's Program. The program facilitates the interchange of information and ideas and corporate sponsors provide valuable fiscal support for the Council's program. This developing program currently includes the following Corporate Sponsors:

Duke Energy Corporation
GE Healthcare
Global Dosimetry Solutions, Inc.
Landauer, Inc.
Nuclear Energy Institute

The Council's activities have been made possible by the voluntary contribution of time and effort by its members and participants and the generous support of the following organizations:

3M Health Physics Services
Agfa Corporation
Alfred P. Sloan Foundation
Alliance of American Insurers
American Academy of Dermatology
American Academy of Health Physics
American Academy of Oral and Maxillofacial Radiology
American Association of Physicists in Medicine
American Cancer Society
American College of Medical Physics
American College of Nuclear Physicians
American College of Occupational and Environmental Medicine
American College of Radiology
American College of Radiology Foundation
American Dental Association
American Healthcare Radiology Administrators
American Industrial Hygiene Association
American Insurance Services Group
American Medical Association
American Nuclear Society
American Osteopathic College of Radiology
American Podiatric Medical Association
American Public Health Association
American Radium Society
American Roentgen Ray Society
American Society of Radiologic Technologists
American Society for Therapeutic Radiology and Oncology
American Veterinary Medical Association
American Veterinary Radiology Society

Association of Educators in Radiological Sciences, Inc.
Association of University Radiologists
Battelle Memorial Institute
Canberra Industries, Inc.
Chem Nuclear Systems
Center for Devices and Radiological Health
College of American Pathologists
Committee on Interagency Radiation Research and Policy Coordination
Commonwealth Edison
Commonwealth of Pennsylvania
Consolidated Edison
Consumers Power Company
Council on Radionuclides and Radiopharmaceuticals
Defense Nuclear Agency
Defense Threat Reduction Agency
Eastman Kodak Company
Edison Electric Institute
Edward Mallinckrodt, Jr. Foundation
EG&G Idaho, Inc.
Electric Power Research Institute
Electromagnetic Energy Association
Federal Emergency Management Agency
Florida Institute of Phosphate Research
Florida Power Corporation
Fuji Medical Systems, U.S.A., Inc.
Genetics Society of America
Global Dosimetry Solutions
Health Effects Research Foundation (Japan)
Health Physics Society
ICN Biomedicals, Inc.
Institute of Nuclear Power Operations
James Picker Foundation
Martin Marietta Corporation
Motorola Foundation
National Aeronautics and Space Administration
National Association of Photographic Manufacturers
National Cancer Institute
National Electrical Manufacturers Association
National Institute of Standards and Technology
New York Power Authority
Philips Medical Systems
Picker International
Public Service Electric and Gas Company
Radiation Research Society
Radiological Society of North America
Richard Lounsbery Foundation
Sandia National Laboratory
Siemens Medical Systems, Inc.
Society of Nuclear Medicine
Society of Pediatric Radiology
Southern California Edison Company
U.S. Department of Energy

U.S. Department of Labor
U.S. Environmental Protection Agency
U.S. Navy
U.S. Nuclear Regulatory Commission
Victoreen, Inc.
Westinghouse Electric Corporation

Initial funds for publication of NCRP reports were provided by a grant from the James Picker Foundation.

NCRP seeks to promulgate information and recommendations based on leading scientific judgment on matters of radiation protection and measurement and to foster cooperation among organizations concerned with these matters. These efforts are intended to serve the public interest and the Council welcomes comments and suggestions on its reports or activities.

NCRP Publications

NCRP publications can be obtained online in both hard- and soft-copy (downloadable PDF) formats at http://NCRPpublications.org. Professional societies can arrange for discounts for their members by contacting NCRP. Additional information on NCRP publications may be obtained from the NCRP website (http://NCRPonline.org) or by telephone (800-229-2652, ext. 25) and fax (301-907-8768). The mailing address is:

NCRP Publications
7910 Woodmont Avenue
Suite 400
Bethesda, MD 20814-3095

Abstracts of NCRP reports published since 1980, abstracts of all NCRP commentaries, and the text of all NCRP statements are available at the NCRP website. Currently available publications are listed below.

NCRP Reports

No.	Title
8	*Control and Removal of Radioactive Contamination in Laboratories* (1951)
22	*Maximum Permissible Body Burdens and Maximum Permissible Concentrations of Radionuclides in Air and in Water for Occupational Exposure* (1959) [includes Addendum 1 issued in August 1963]
25	*Measurement of Absorbed Dose of Neutrons, and of Mixtures of Neutrons and Gamma Rays* (1961)
27	*Stopping Powers for Use with Cavity Chambers* (1961)
30	*Safe Handling of Radioactive Materials* (1964)
32	*Radiation Protection in Educational Institutions* (1966)
35	*Dental X-Ray Protection* (1970)
36	*Radiation Protection in Veterinary Medicine* (1970)
37	*Precautions in the Management of Patients Who Have Received Therapeutic Amounts of Radionuclides* (1970)
38	*Protection Against Neutron Radiation* (1971)
40	*Protection Against Radiation from Brachytherapy Sources* (1972)
41	*Specification of Gamma-Ray Brachytherapy Sources* (1974)
42	*Radiological Factors Affecting Decision-Making in a Nuclear Attack* (1974)
44	*Krypton-85 in the Atmosphere—Accumulation, Biological Significance, and Control Technology* (1975)
46	*Alpha-Emitting Particles in Lungs* (1975)
47	*Tritium Measurement Techniques* (1976)

49 *Structural Shielding Design and Evaluation for Medical Use of X Rays and Gamma Rays of Energies Up to 10 MeV* (1976)
50 *Environmental Radiation Measurements* (1976)
52 *Cesium-137 from the Environment to Man: Metabolism and Dose* (1977)
54 *Medical Radiation Exposure of Pregnant and Potentially Pregnant Women* (1977)
55 *Protection of the Thyroid Gland in the Event of Releases of Radioiodine* (1977)
57 *Instrumentation and Monitoring Methods for Radiation Protection* (1978)
58 *A Handbook of Radioactivity Measurements Procedures*, 2nd ed. (1985)
60 *Physical, Chemical, and Biological Properties of Radiocerium Relevant to Radiation Protection Guidelines* (1978)
61 *Radiation Safety Training Criteria for Industrial Radiography* (1978)
62 *Tritium in the Environment* (1979)
63 *Tritium and Other Radionuclide Labeled Organic Compounds Incorporated in Genetic Material* (1979)
64 *Influence of Dose and Its Distribution in Time on Dose-Response Relationships for Low-LET Radiations* (1980)
65 *Management of Persons Accidentally Contaminated with Radionuclides* (1980)
67 *Radiofrequency Electromagnetic Fields—Properties, Quantities and Units, Biophysical Interaction, and Measurements* (1981)
68 *Radiation Protection in Pediatric Radiology* (1981)
69 *Dosimetry of X-Ray and Gamma-Ray Beams for Radiation Therapy in the Energy Range 10 keV to 50 MeV* (1981)
70 *Nuclear Medicine—Factors Influencing the Choice and Use of Radionuclides in Diagnosis and Therapy* (1982)
72 *Radiation Protection and Measurement for Low-Voltage Neutron Generators* (1983)
73 *Protection in Nuclear Medicine and Ultrasound Diagnostic Procedures in Children* (1983)
74 *Biological Effects of Ultrasound: Mechanisms and Clinical Implications* (1983)
75 *Iodine-129: Evaluation of Releases from Nuclear Power Generation* (1983)
76 *Radiological Assessment: Predicting the Transport, Bioaccumulation, and Uptake by Man of Radionuclides Released to the Environment* (1984)
77 *Exposures from the Uranium Series with Emphasis on Radon and Its Daughters* (1984)
78 *Evaluation of Occupational and Environmental Exposures to Radon and Radon Daughters in the United States* (1984)
79 *Neutron Contamination from Medical Electron Accelerators* (1984)
80 *Induction of Thyroid Cancer by Ionizing Radiation* (1985)
81 *Carbon-14 in the Environment* (1985)
82 *SI Units in Radiation Protection and Measurements* (1985)
83 *The Experimental Basis for Absorbed-Dose Calculations in Medical Uses of Radionuclides* (1985)
84 *General Concepts for the Dosimetry of Internally Deposited Radionuclides* (1985)

86 *Biological Effects and Exposure Criteria for Radiofrequency Electromagnetic Fields* (1986)
87 *Use of Bioassay Procedures for Assessment of Internal Radionuclide Deposition* (1987)
88 *Radiation Alarms and Access Control Systems* (1986)
89 *Genetic Effects from Internally Deposited Radionuclides* (1987)
90 *Neptunium: Radiation Protection Guidelines* (1988)
92 *Public Radiation Exposure from Nuclear Power Generation in the United States* (1987)
93 *Ionizing Radiation Exposure of the Population of the United States* (1987)
94 *Exposure of the Population in the United States and Canada from Natural Background Radiation* (1987)
95 *Radiation Exposure of the U.S. Population from Consumer Products and Miscellaneous Sources* (1987)
96 *Comparative Carcinogenicity of Ionizing Radiation and Chemicals* (1989)
97 *Measurement of Radon and Radon Daughters in Air* (1988)
99 *Quality Assurance for Diagnostic Imaging* (1988)
100 *Exposure of the U.S. Population from Diagnostic Medical Radiation* (1989)
101 *Exposure of the U.S. Population from Occupational Radiation* (1989)
102 *Medical X-Ray, Electron Beam and Gamma-Ray Protection for Energies Up to 50 MeV (Equipment Design, Performance and Use)* (1989)
103 *Control of Radon in Houses* (1989)
104 *The Relative Biological Effectiveness of Radiations of Different Quality* (1990)
105 *Radiation Protection for Medical and Allied Health Personnel* (1989)
106 *Limit for Exposure to "Hot Particles" on the Skin* (1989)
107 *Implementation of the Principle of As Low As Reasonably Achievable (ALARA) for Medical and Dental Personnel* (1990)
108 *Conceptual Basis for Calculations of Absorbed-Dose Distributions* (1991)
109 *Effects of Ionizing Radiation on Aquatic Organisms* (1991)
110 *Some Aspects of Strontium Radiobiology* (1991)
111 *Developing Radiation Emergency Plans for Academic, Medical or Industrial Facilities* (1991)
112 *Calibration of Survey Instruments Used in Radiation Protection for the Assessment of Ionizing Radiation Fields and Radioactive Surface Contamination* (1991)
113 *Exposure Criteria for Medical Diagnostic Ultrasound: I. Criteria Based on Thermal Mechanisms* (1992)
114 *Maintaining Radiation Protection Records* (1992)
115 *Risk Estimates for Radiation Protection* (1993)
116 *Limitation of Exposure to Ionizing Radiation* (1993)
117 *Research Needs for Radiation Protection* (1993)
118 *Radiation Protection in the Mineral Extraction Industry* (1993)
119 *A Practical Guide to the Determination of Human Exposure to Radiofrequency Fields* (1993)
120 *Dose Control at Nuclear Power Plants* (1994)
121 *Principles and Application of Collective Dose in Radiation Protection* (1995)

122 *Use of Personal Monitors to Estimate Effective Dose Equivalent and Effective Dose to Workers for External Exposure to Low-LET Radiation* (1995)
123 *Screening Models for Releases of Radionuclides to Atmosphere, Surface Water, and Ground* (1996)
124 *Sources and Magnitude of Occupational and Public Exposures from Nuclear Medicine Procedures* (1996)
125 *Deposition, Retention and Dosimetry of Inhaled Radioactive Substances* (1997)
126 *Uncertainties in Fatal Cancer Risk Estimates Used in Radiation Protection* (1997)
127 *Operational Radiation Safety Program* (1998)
128 *Radionuclide Exposure of the Embryo/Fetus* (1998)
129 *Recommended Screening Limits for Contaminated Surface Soil and Review of Factors Relevant to Site-Specific Studies* (1999)
130 *Biological Effects and Exposure Limits for "Hot Particles"* (1999)
131 *Scientific Basis for Evaluating the Risks to Populations from Space Applications of Plutonium* (2001)
132 *Radiation Protection Guidance for Activities in Low-Earth Orbit* (2000)
133 *Radiation Protection for Procedures Performed Outside the Radiology Department* (2000)
134 *Operational Radiation Safety Training* (2000)
135 *Liver Cancer Risk from Internally-Deposited Radionuclides* (2001)
136 *Evaluation of the Linear-Nonthreshold Dose-Response Model for Ionizing Radiation* (2001)
137 *Fluence-Based and Microdosimetric Event-Based Methods for Radiation Protection in Space* (2001)
138 *Management of Terrorist Events Involving Radioactive Material* (2001)
139 *Risk-Based Classification of Radioactive and Hazardous Chemical Wastes* (2002)
140 *Exposure Criteria for Medical Diagnostic Ultrasound: II. Criteria Based on all Known Mechanisms* (2002)
141 *Managing Potentially Radioactive Scrap Metal* (2002)
142 *Operational Radiation Safety Program for Astronauts in Low-Earth Orbit: A Basic Framework* (2002)
143 *Management Techniques for Laboratories and Other Small Institutional Generators to Minimize Off-Site Disposal of Low-Level Radioactive Waste* (2003)
144 *Radiation Protection for Particle Accelerator Facilities* (2003)
145 *Radiation Protection in Dentistry* (2003)
146 *Approaches to Risk Management in Remediation of Radioactively Contaminated Sites* (2004)
147 *Structural Shielding Design for Medical X-Ray Imaging Facilities* (2004)
148 *Radiation Protection in Veterinary Medicine* (2004)
149 *A Guide to Mammography and Other Breast Imaging Procedures* (2004)
150 *Extrapolation of Radiation-Induced Cancer Risks from Nonhuman Experimental Systems to Humans* (2005)
151 *Structural Shielding Design and Evaluation for Megavoltage X- and Gamma-Ray Radiotherapy Facilities* (2005)

152 *Performance Assessment of Near-Surface Facilities for Disposal of Low-Level Radioactive Waste* (2005)
153 *Information Needed to Make Radiation Protection Recommendations for Space Missions Beyond Low-Earth Orbit* (2006)

Binders for NCRP reports are available. Two sizes make it possible to collect into small binders the "old series" of reports (NCRP Reports Nos. 8–30) and into large binders the more recent publications (NCRP Reports Nos. 32–153). Each binder will accommodate from five to seven reports. The binders carry the identification "NCRP Reports" and come with label holders which permit the user to attach labels showing the reports contained in each binder.

The following bound sets of NCRP reports are also available:

Volume I. NCRP Reports Nos. 8, 22
Volume II. NCRP Reports Nos. 23, 25, 27, 30
Volume III. NCRP Reports Nos. 32, 35, 36, 37
Volume IV. NCRP Reports Nos. 38, 40, 41
Volume V. NCRP Reports Nos. 42, 44, 46
Volume VI. NCRP Reports Nos. 47, 49, 50, 51
Volume VII. NCRP Reports Nos. 52, 53, 54, 55, 57
Volume VIII. NCRP Report No. 58
Volume IX. NCRP Reports Nos. 59, 60, 61, 62, 63
Volume X. NCRP Reports Nos. 64, 65, 66, 67
Volume XI. NCRP Reports Nos. 68, 69, 70, 71, 72
Volume XII. NCRP Reports Nos. 73, 74, 75, 76
Volume XIII. NCRP Reports Nos. 77, 78, 79, 80
Volume XIV. NCRP Reports Nos. 81, 82, 83, 84, 85
Volume XV. NCRP Reports Nos. 86, 87, 88, 89
Volume XVI. NCRP Reports Nos. 90, 91, 92, 93
Volume XVII. NCRP Reports Nos. 94, 95, 96, 97
Volume XVIII. NCRP Reports Nos. 98, 99, 100
Volume XIX. NCRP Reports Nos. 101, 102, 103, 104
Volume XX. NCRP Reports Nos. 105, 106, 107, 108
Volume XXI. NCRP Reports Nos. 109, 110, 111
Volume XXII. NCRP Reports Nos. 112, 113, 114
Volume XXIII. NCRP Reports Nos. 115, 116, 117, 118
Volume XXIV. NCRP Reports Nos. 119, 120, 121, 122
Volume XXV. NCRP Report No. 123I and 123II
Volume XXVI. NCRP Reports Nos. 124, 125, 126, 127
Volume XXVII. NCRP Reports Nos. 128, 129, 130
Volume XXVIII. NCRP Reports Nos. 131, 132, 133
Volume XXIX. NCRP Reports Nos. 134, 135, 136, 137
Volume XXX. NCRP Reports Nos. 138, 139
Volume XXXI. NCRP Report No. 140
Volume XXXII. NCRP Reports Nos. 141, 142, 143
Volume XXXIII. NCRP Report No. 144
Volume XXXIV. NCRP Reports Nos. 145, 146, 147
Volume XXXV. NCRP Reports Nos. 148, 149

(Titles of the individual reports contained in each volume are given previously.)

NCRP Commentaries

No.	Title
1	*Krypton-85 in the Atmosphere—With Specific Reference to the Public Health Significance of the Proposed Controlled Release at Three Mile Island* (1980)
4	*Guidelines for the Release of Waste Water from Nuclear Facilities with Special Reference to the Public Health Significance of the Proposed Release of Treated Waste Waters at Three Mile Island* (1987)
5	*Review of the Publication, Living Without Landfills* (1989)
6	*Radon Exposure of the U.S. Population—Status of the Problem (1991)*
7	*Misadministration of Radioactive Material in Medicine—Scientific Background* (1991)
8	*Uncertainty in NCRP Screening Models Relating to Atmospheric Transport, Deposition and Uptake by Humans* (1993)
9	*Considerations Regarding the Unintended Radiation Exposure of the Embryo, Fetus or Nursing Child* (1994)
10	*Advising the Public about Radiation Emergencies: A Document for Public Comment* (1994)
11	*Dose Limits for Individuals Who Receive Exposure from Radionuclide Therapy Patients* (1995)
12	*Radiation Exposure and High-Altitude Flight* (1995)
13	*An Introduction to Efficacy in Diagnostic Radiology and Nuclear Medicine (Justification of Medical Radiation Exposure)* (1995)
14	*A Guide for Uncertainty Analysis in Dose and Risk Assessments Related to Environmental Contamination* (1996)
15	*Evaluating the Reliability of Biokinetic and Dosimetric Models and Parameters Used to Assess Individual Doses for Risk Assessment Purposes* (1998)
16	*Screening of Humans for Security Purposes Using Ionizing Radiation Scanning Systems* (2003)
17	*Pulsed Fast Neutron Analysis System Used in Security Surveillance* (2003)
18	*Biological Effects of Modulated Radiofrequency Fields* (2003)
19	*Key Elements of Preparing Emergency Responders for Nuclear and Radiological Terrorism* (2005)

Proceedings of the Annual Meeting

No.	Title
1	*Perceptions of Risk,* Proceedings of the Fifteenth Annual Meeting held on March 14-15, 1979 (including Taylor Lecture No. 3) (1980)
3	*Critical Issues in Setting Radiation Dose Limits*, Proceedings of the Seventeenth Annual Meeting held on April 8-9, 1981 (including Taylor Lecture No. 5) (1982)
4	*Radiation Protection and New Medical Diagnostic Approaches,* Proceedings of the Eighteenth Annual Meeting held on April 6-7, 1982 (including Taylor Lecture No. 6) (1983)

5 *Environmental Radioactivity,* Proceedings of the Nineteenth Annual Meeting held on April 6-7, 1983 (including Taylor Lecture No. 7) (1983)
6 *Some Issues Important in Developing Basic Radiation Protection Recommendations*, Proceedings of the Twentieth Annual Meeting held on April 4-5, 1984 (including Taylor Lecture No. 8) (1985)
7 *Radioactive Waste*, Proceedings of the Twenty-first Annual Meeting held on April 3-4, 1985 (including Taylor Lecture No. 9)(1986)
8 *Nonionizing Electromagnetic Radiations and Ultrasound,* Proceedings of the Twenty-second Annual Meeting held on April 2-3, 1986 (including Taylor Lecture No. 10) (1988)
9 *New Dosimetry at Hiroshima and Nagasaki and Its Implications for Risk Estimates*, Proceedings of the Twenty-third Annual Meeting held on April 8-9, 1987 (including Taylor Lecture No. 11) (1988)
10 *Radon*, Proceedings of the Twenty-fourth Annual Meeting held on March 30-31, 1988 (including Taylor Lecture No. 12) (1989)
11 *Radiation Protection Today—The NCRP at Sixty Years*, Proceedings of the Twenty-fifth Annual Meeting held on April 5-6, 1989 (including Taylor Lecture No. 13) (1990)
12 *Health and Ecological Implications of Radioactively Contaminated Environments*, Proceedings of the Twenty-sixth Annual Meeting held on April 4-5, 1990 (including Taylor Lecture No. 14) (1991)
13 *Genes, Cancer and Radiation Protection,* Proceedings of the Twenty-seventh Annual Meeting held on April 3-4, 1991 (including Taylor Lecture No. 15) (1992)
14 *Radiation Protection in Medicine,* Proceedings of the Twenty-eighth Annual Meeting held on April 1-2, 1992 (including Taylor Lecture No. 16) (1993)
15 *Radiation Science and Societal Decision Making,* Proceedings of the Twenty-ninth Annual Meeting held on April 7-8, 1993 (including Taylor Lecture No. 17) (1994)
16 *Extremely-Low-Frequency Electromagnetic Fields: Issues in Biological Effects and Public Health*, Proceedings of the Thirtieth Annual Meeting held on April 6-7, 1994 (not published).
17 *Environmental Dose Reconstruction and Risk Implications,* Proceedings of the Thirty-first Annual Meeting held on April 12-13, 1995 (including Taylor Lecture No. 19) (1996)
18 *Implications of New Data on Radiation Cancer Risk*, Proceedings of the Thirty-second Annual Meeting held on April 3-4, 1996 (including Taylor Lecture No. 20) (1997)
19 *The Effects of Pre- and Postconception Exposure to Radiation*, Proceedings of the Thirty-third Annual Meeting held on April 2-3, 1997, Teratology **59**, 181–317 (1999)
20 *Cosmic Radiation Exposure of Airline Crews, Passengers and Astronauts*, Proceedings of the Thirty-fourth Annual Meeting held on April 1-2, 1998, Health Phys. **79**, 466–613 (2000)
21 *Radiation Protection in Medicine: Contemporary Issues*, Proceedings of the Thirty-fifth Annual Meeting held on April 7-8, 1999 (including Taylor Lecture No. 23) (1999)
22 *Ionizing Radiation Science and Protection in the 21st Century,* Proceedings of the Thirty-sixth Annual Meeting held on April 5-6, 2000, Health Phys. **80**, 317–402 (2001)
23 *Fallout from Atmospheric Nuclear Tests—Impact on Science and Society,* Proceedings of the Thirty-seventh Annual Meeting held on April 4-5, 2001, Health Phys. **82**, 573–748 (2002)

24 *Where the New Biology Meets Epidemiology: Impact on Radiation Risk Estimates*, Proceedings of the Thirty-eighth Annual Meeting held on April 10-11, 2002, Health Phys. **85**, 1–108 (2003)
25 *Radiation Protection at the Beginning of the 21st Century–A Look Forward*, Proceedings of the Thirty-ninth Annual Meeting held on April 9–10, 2003, Health Phys. **87**, 237–319 (2004)
26 *Advances in Consequence Management for Radiological Terrorism Events*, Proceedings of the Fortieth Annual Meeting held on April 14–15, 2004, Health Phys. **89**, 415–588 (2005)
27 *Managing the Disposition of Low-Activity Radioactive Materials*, Proceedings of the Forty-first Annual Meeting held on March 30–31, 2005, Health Phys. **91**, 413–536 (2006)

Lauriston S. Taylor Lectures

No. Title

1 *The Squares of the Natural Numbers in Radiation Protection by* Herbert M. Parker (1977)
2 *Why be Quantitative about Radiation Risk Estimates?* by Sir Edward Pochin (1978)
3 *Radiation Protection—Concepts and Trade Offs* by Hymer L. Friedell (1979) [available also in *Perceptions of Risk*, see above]
4 *From "Quantity of Radiation" and "Dose" to "Exposure" and "Absorbed Dose"—An Historical Review* by Harold O. Wyckoff (1980)
5 *How Well Can We Assess Genetic Risk? Not Very* by James F. Crow (1981) [available also in *Critical Issues in Setting Radiation Dose Limits*, see above]
6 *Ethics, Trade-offs and Medical Radiation* by Eugene L. Saenger (1982) [available also in *Radiation Protection and New Medical Diagnostic Approaches*, see above]
7 *The Human Environment—Past, Present and Future* by Merril Eisenbud (1983) [available also in *Environmental Radioactivity*, see above]
8 *Limitation and Assessment in Radiation Protection* by Harald H. Rossi (1984) [available also in *Some Issues Important in Developing Basic Radiation Protection Recommendations*, see above]
9 *Truth (and Beauty) in Radiation Measurement* by John H. Harley (1985) [available also in *Radioactive Waste*, see above]
10 *Biological Effects of Non-ionizing Radiations: Cellular Properties and Interactions* by Herman P. Schwan (1987) [available also in *Nonionizing Electromagnetic Radiations and Ultrasound*, see above]
11 *How to be Quantitative about Radiation Risk Estimates* by Seymour Jablon (1988) [available also in *New Dosimetry at Hiroshima and Nagasaki and its Implications for Risk Estimates*, see above]
12 *How Safe is Safe Enough?* by Bo Lindell (1988) [available also in *Radon*, see above]
13 *Radiobiology and Radiation Protection: The Past Century and Prospects for the Future* by Arthur C. Upton (1989) [available also in *Radiation Protection Today*, see above]
14 *Radiation Protection and the Internal Emitter Saga* by J. Newell Stannard (1990) [available also in *Health and Ecological Implications of Radioactively Contaminated Environments*, see above]
15 *When is a Dose Not a Dose?* by Victor P. Bond (1992) [available also in *Genes, Cancer and Radiation Protection*, see above]

16 *Dose and Risk in Diagnostic Radiology: How Big? How Little?* by Edward W. Webster (1992) [available also in *Radiation Protection in Medicine*, see above]

17 *Science, Radiation Protection and the NCRP* by Warren K. Sinclair (1993) [available also in *Radiation Science and Societal Decision Making,* see above]

18 *Mice, Myths and Men* by R.J. Michael Fry (1995)

19 *Certainty and Uncertainty in Radiation Research* by Albrecht M. Kellerer. Health Phys. **69**, 446–453 (1995)

20 *70 Years of Radiation Genetics: Fruit Flies, Mice and Humans* by Seymour Abrahamson. Health Phys. **71**, 624–633 (1996)

21 *Radionuclides in the Body: Meeting the Challenge* by William J. Bair. Health Phys. **73**, 423–432 (1997)

22 *From Chimney Sweeps to Astronauts: Cancer Risks in the Work Place* by Eric J. Hall. Health Phys. **75**, 357–366 (1998)

23 *Back to Background: Natural Radiation and Radioactivity Exposed* by Naomi H. Harley. Health Phys. **79**, 121–128 (2000)

24 *Administered Radioactivity: Unde Venimus Quoque Imus* by S. James Adelstein. Health Phys. **80**, 317–324 (2001)

25 *Assuring the Safety of Medical Diagnostic Ultrasound* by Wesley L. Nyborg. Health Phys. **82**, 578–587 (2002)

26 *Developing Mechanistic Data for Incorporation into Cancer and Genetic Risk Assessments: Old Problems and New Approaches* by R. Julian Preston. Health Phys. **85**, 4–12 (2003)

27 *The Evolution of Radiation Protection–From Erythema to Genetic Risks to Risks of Cancer to ?* by Charles B. Meinhold, Health Phys. **87**, 240–248 (2004)

28 *Radiation Protection in the Aftermath of a Terrorist Attack Involving Exposure to Ionizing Radiation* by Abel J. Gonzalez, Health Phys. **89**, 418–446 (2005)

29 *Nontargeted Effects of Radiation: Implications for Low Dose Exposures* by John B. Little, Health Phys. **91**, 416–426 (2006)

Symposium Proceedings

No. Title

1 *The Control of Exposure of the Public to Ionizing Radiation in the Event of Accident or Attack*, Proceedings of a Symposium held April 27-29, 1981 (1982)

2 *Radioactive and Mixed Waste—Risk as a Basis for Waste Classification,* Proceedings of a Symposium held November 9, 1994 (1995)

3 *Acceptability of Risk from Radiation—Application to Human Space Flight,* Proceedings of a Symposium held May 29, 1996 (1997)

4 *21st Century Biodosimetry: Quantifying the Past and Predicting the Future*, Proceedings of a Symposium held February 22, 2001, Radiat. Prot. Dosim. **97***(*1), (2001)

5 *National Conference on Dose Reduction in CT, with an Emphasis on Pediatric Patients*, Summary of a Symposium held November 6-7, 2002, Am. J. Roentgenol. **181**(2), 321–339 (2003)

NCRP Statements

No.	Title
1	"Blood Counts, Statement of the National Committee on Radiation Protection," Radiology **63**, 428 (1954)
2	"Statements on Maximum Permissible Dose from Television Receivers and Maximum Permissible Dose to the Skin of the Whole Body," Am. J. Roentgenol., Radium Ther. and Nucl. Med. **84**, 152 (1960) and Radiology **75**, 122 (1960)
3	*X-Ray Protection Standards for Home Television Receivers, Interim Statement of the National Council on Radiation Protection and Measurements* (1968)
4	*Specification of Units of Natural Uranium and Natural Thorium, Statement of the National Council on Radiation Protection and Measurements* (1973)
5	*NCRP Statement on Dose Limit for Neutrons* (1980)
6	*Control of Air Emissions of Radionuclides* (1984)
7	*The Probability That a Particular Malignancy May Have Been Caused by a Specified Irradiation* (1992)
8	*The Application of ALARA for Occupational Exposures* (1999)
9	*Extension of the Skin Dose Limit for Hot Particles to Other External Sources of Skin Irradiation* (2001)
10	*Recent Applications of the NCRP Public Dose Limit Recommendation for Ionizing Radiation* (2004)

Other Documents

The following documents were published outside of the NCRP report, commentary and statement series:

Somatic Radiation Dose for the General Population, Report of the Ad Hoc Committee of the National Council on Radiation Protection and Measurements, 6 May 1959, Science **131** (3399), February 19, 482–486 (1960)

Dose Effect Modifying Factors in Radiation Protection, Report of Subcommittee M-4 (Relative Biological Effectiveness) of the National Council on Radiation Protection and Measurements, Report BNL 50073 (T-471) (1967) Brookhaven National Laboratory (National Technical Information Service, Springfield, Virginia)

Residential Radon Exposure and Lung Cancer Risk: Commentary on Cohen's County-Based Study, Health Phys. **87**(6), 656–658 (2004)

Index